UNIVERSITÉ DE NEUCHÂTEL

Synthesis of Calix[4]pyrrolidine, Calix[m]tetrahydrofuran[n]pyrrolidine (m+n=4) and Similar Macrocyclic Systems - Elucidation of the Hydrogenation Sequence and Factors Influencing the Stereoselectivity

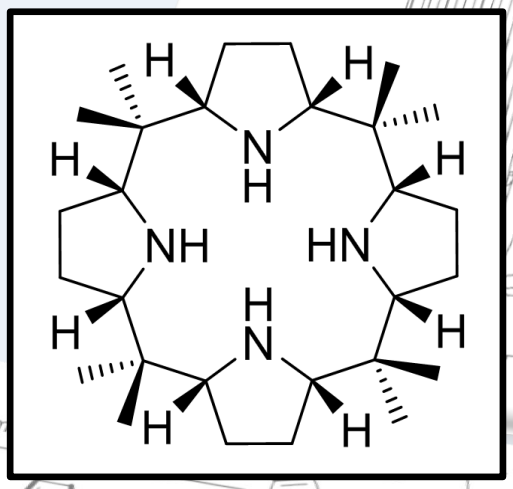

Thèse présentée à la faculté des Sciences de l'Université de Neuchâtel
pour l'obtention du titre de Docteur ès Sciences
par

Guillaume JOURNOT

Chimiste diplômé de l'Université de Haute Alsace
Mai 2012

UNIVERSITÉ DE
NEUCHÂTEL

FACULTE DES SCIENCES
Secrétariat-Décanat de la faculté
Rue Emile-Argand 11
CH-2000 Neuchâtel

IMPRIMATUR POUR LA THESE

Synthesis of Calix[4]pyrrolidine, Calix[m]tetrahydrofuran[n]pyrrolidine and Similar Macrocyclic Systems-Elucidation of the Hydrogenation Sequence and Factors Influencing the Stereoselectivity

Guillaume JOURNOT

UNIVERSITE DE NEUCHATEL

FACULTE DES SCIENCES

La Faculté des sciences de l'Université de Neuchâtel,
sur le rapport des membres du jury

MM. Reinhard Neier (directeur de thèse),
Robert Deschenaux, Université de Neuchâtel
Andreas Pfaltz, Université de Bâle

autorise l'impression de la présente thèse.

Neuchâtel, le 22 mai 2012

Le doyen :
P. Kropf

Téléphone : +41 32 718 21 00 E-mail : secretariat.sciences@unine.ch www.unine.ch/sciences

Ce travail a été effectué de septembre 2008 à avril 2012 à l'institut de Chimie de l'Université de Neuchâtel sous la direction du Prof. Reinhard Neier. Je tiens vraiment à le remercier pour m'avoir offert l'opportunité de travailler au sein d'un groupe de recherche si stimulant, sur un sujet de thèse extrêmement intéressant et fructueux, pour sa disponibilité et sa gentillesse. Merci pour la confiance que tu m'as accordé dès les premiers jours, pour la liberté d'action que tu m'as offerte et merci d'avoir toujours su me guider et me soutenir dans mes choix. Finalement, merci pour toutes les discussions que l'ont a partagées, plus intéressantes les unes que les autres, pour tes conseils si précieux…

J'adresse mes sincères remerciements aux Prof. Andreas Pfaltz et Prof. Robert Deschenaux qui ont pris part à mon jury de thèse et pris le temps de lire et de corriger mon manuscrit.

Je remercie particulièrement le Prof. Helen Stoekli-Evans pour les nombreuses structures au rayon X élucidées, pour sa patience et sa gentillesse.

Je remercie également toutes les personnes avec lesquelles j'ai eu la chance de travailler sur mon projet, le Dr. Christophe Letondor, Dr. Andrea Gualandi, Dr. Frédéric Bruyneel, Dr Claudio Dalvit et Lionel Burri.

Mes remerciements s'adressent également à tous les membres de notre groupe, Dr. Damien Thevenet, Dr. Anca Pordea, Dr. Christophe Letondor, Dr. Andrea Gualandi, Dr. Frédéric Bruyneel, Christian Invernizzi, Christelle Schenk, Inga Kholod-Zaitseva, Dr. Maria Kolympadi, Dr. Ana-Maria Buciumas, Bjorn Bastürk, Lionel Burri et Lucia Cerisoli.

Je remercie les membres du service analytique facultaire : Dr. Armelle Vallat (spectrométrie de masse) et le Dr. Julien Furrer et Dr. Claudio Dalvit (spectroscopie RMN). Merci pour leur efficacité et leurs analyses indispensables à la chimie organique de synthèse.

Je remercie particulièrement les personnes qui ont fait que ces années passées à Neuchâtel resterons gravé en moi : Saltimbanque, Larson le pervers, Bucheron l'Alsacien, l'Italien (le Mont Blanc…), Mr. Thevent (une faute ?), Mr Synthol dit José le beau gosse, Luyen, Chris, Cyril et Cyrille, Anne-Flore, Christelle, Anca, Khosrow, Mika, Pipo, Jordi, Ha. Merci votre amitié, pour tous ces moments passés au Cerf, au Cercle national (la fondue !!!!), les repas à Champreveyre, au resto Chinois, toutes les parties d'échecs, les tennis et surtout à la salle de

fit… Je tiens à remercier tous mes potes de Mulhouse city, Georgy, Best, Yass, Jojo, Matt, Fan, Chris, Damien, Bo-gosse, Taylor, Couzin, Franki, Marco, Guigui… Je remercie les personnes qui m'ont fait découvrir la recherche et m'ont donnés la passion de la chimie, sans lesquelles je ne serai pas la actuellement : Prof. Céline Tarnus, Dr. Albert Defoin et Dr. Joseph Schoepfer.

Mes pensées vont également à tous les autres doctorants, post-doc et membres du personnel. Ce travail a été soutenu financièrement par l'Etat de Neuchâtel.

Un grand merci à ma famille pour m'avoir toujours soutenu dans mes choix et encouragé dans les moments difficiles, en particulier mes parents Gabrielle et Jacques, mes trois sœurs Anne, Claire et Sophie, et finalement Mathieu.

Finalement, je remercie du fond du cœur mon ange, Julie, pour son amour et son soutien.

A Julie,

A mes parents,

A mes sœurs,

"A scientist in his laboratory is not a mere technician: he is also a child confronting natural phenomena that impress him as though they were fairy tales"

(Marie Curie)

Keywords:

Calix[4]pyrrole, mesooctamethylporphyrinogen, hydrogenation, reduction, pyrrole, furan, heterocycle, macrocycle, ligand.

Abbreviation:

aq. : aqueous
atm.: atmosphrere
cat. : catalytic
TLC : Thin layer chromatography
GC: gas chromatography
ESI : Electron Spray Ionization
h : hour (s)
min.: minute (s)
HR-MS : High
Resolution Mass Spectroscopy
IR : infra-red
ppm : parts per million
NMR : Nuclear Magnetic Resonance
Rf : retention factor
rt: room temperature
DI: diastereoselective induction
SM: starting material
PBG. Porphobilinogen
Uro III: uroporphirinogen III
PpIX: protoporphyrin IX
NCP: N-confused porphyrins
NCCP: N-confused calix[4]pyrrole
IS: internal standard

The abbreviations of chemical reagents have been written according to the description done by Daub et al.[1]

Summary:

The first *meso*-octaalkylporphyrinogen (calix[4]pyrrole) was synthesized by Baeyer more than 120 years ago, mixing pyrrole and acetone in the presence of an acid. We have performed a thorough study of the catalytic hydrogenation of calix[4]pyrrole **1**, by using common as well as novel heterogeneous catalysts based on transition metals (Pd, Rh, Ru) supported on solid matrices. Another investigation concerning the hydrogenation reaction was performed using twelve different macrocyclic substrates. Different factors were tested, which might influence the stereoselectivity during the hydrogenation process and therefore the number of diastereomers obtained. One of the macrocycles synthesized, offers interesting perspectives for the development of novel catalysts. In this context, we investigated the reactivity and the modification of this macrocycle. A thorough study of the nucleophilic properties and a kinetic study allow the discovery the factors that influence the reactivity of these macrocycles.

Table of Contents

Chapter 1

INTRODUCTION

1. INTRODUCTION

Context

« What I cannot create, I do not understand ». (Richard Feynman on his blackboard on his death date, 1988)

The success of chemists disclosing more and more complex structures of vital natural products and their activity changed profoundly our understanding of important biological processes. In parallel, a huge effort went into synthesizing and discovering new, "purely synthetic" pharmaceutics as new efficient drug candidates. The scientific question driving all these efforts is the understanding of the biological world: how are all these beautiful structures functioning? When and how did these structures evolve? And the final challenge: are we capable of deducing the "rules" so as to design new active structures on the drawing board?

From its inception, organic chemistry has always been intimately linked to our understanding of the processes of life. The development of organic chemistry can be traced back to the isolation, detection and structure determination of important active natural products. For more than one hundred years, the determination of the structures of natural products was one of the fundamental activities, which determined the progress of organic chemistry and in parallel of our understanding of the fundamental processes of life (Figure 1). The experimental approach, and to some extent the importance of the classic natural products chemistry, changed with the arrival of efficient spectroscopic methods. The "art" of natural product determination by chemical degradation and correlation was replaced by a more systematic analytical approach.

Substituting the tedious process of chemical structure determination by spectroscopic measurements allowed much faster progress and gave a higher degree of certainty to the proposed structures.[2]

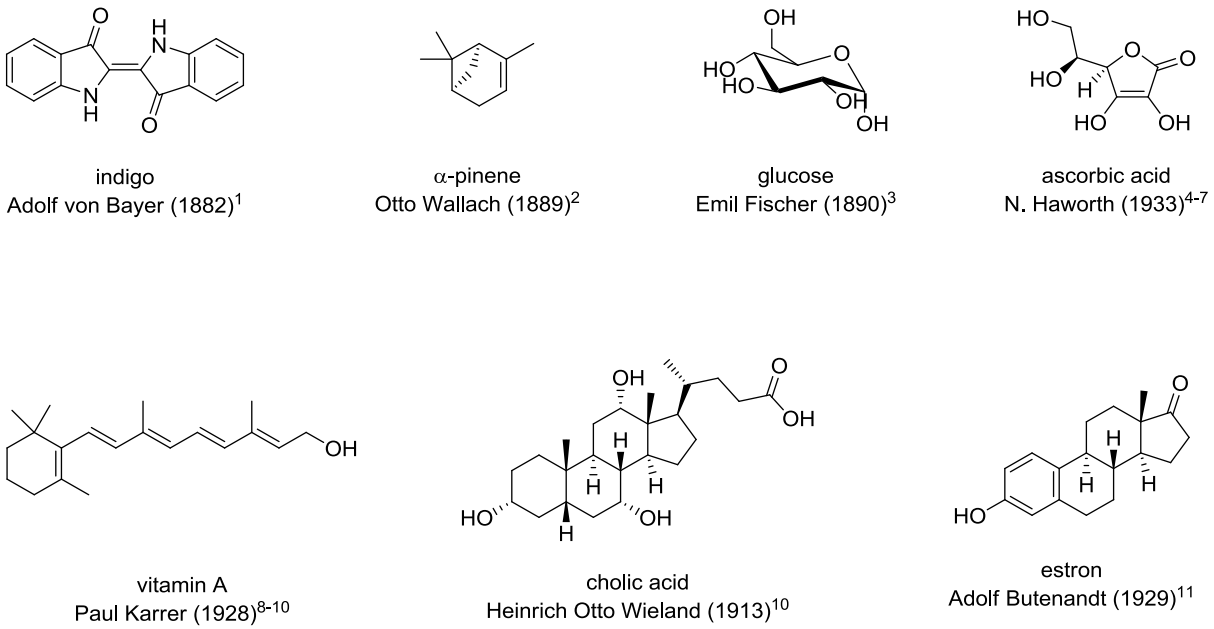

Figure 1. Natural products isolated and fully described using exclusively a chemical approach.[3-13]

However, structure determinations based on spectroscopy cannot furnish information on the reactivity or the chemistry of a new natural product. Before the advent of spectroscopic methods, this information was gradually accumulated during the process of chemical structure determination. The analytical part of a modern natural products project has been highly automatized. The goal is to achieve an efficient high-throughput and a database driven identification of the isolated structures. Chemical manipulations are often limited to the preparation of the samples. These developments of modern analytical technology have induced a radical change. The inherent connection between chemical and biological reactivity and structure determination has been lost. Libraries of natural products have been determined without having acquired knowledge about the use and the properties of the structures. In this respect, natural products chemistry has become more similar to medicinal chemistry. Both approaches can be described as a search of biological activities starting from a library of compounds. The difference being that in natural products chemistry, the library of compounds

is isolated from natural sources, whereas in medicinal chemistry the library is synthesized by chemists or machines.

Bioorganic chemistry has become an important complement to the analytical approach, trying to fill the gap between a library of compounds and its activity, either of the individual compounds or of a mix of compounds.[2, 14-16] In a broader sense, the main challenge for chemistry has stayed the same over the years, independent of the instruments and methods available. The challenge of chemistry has been and will, for the foreseeable future, be: discover and describe the structural laws of life. Compiling the design principles and understanding the correlations between chemical structures and their functions should enable us to design, from scratch, new active compounds on the drawing board.

2. «PIGMENTS OF LIFE»

Many important processes of life like the transport of electron, oxygen, ion and photosynthesis depend on the presence of metal complexes of specific macrocyclic ligands.[17-25] These metal complexes have been called «pigments of life», thereby indicating the fundamental roles played by these metal complexes (Figure 2).[26-33]

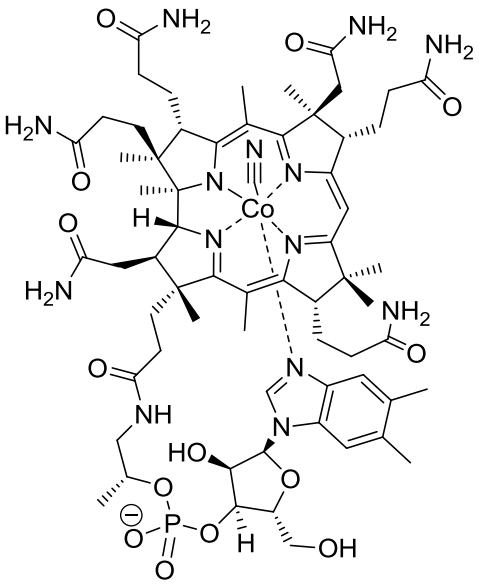

vitamin B_{12}
isomerisation/methyl transfer

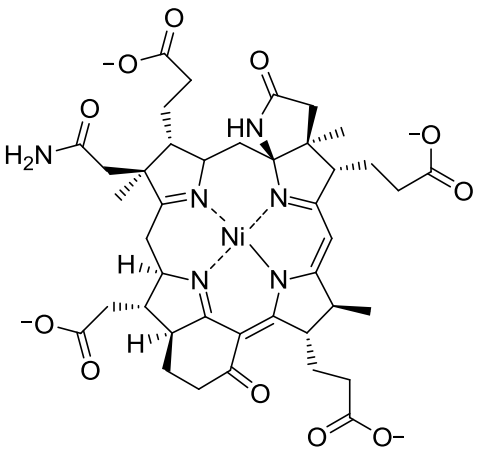

factor F430
methanogenesis

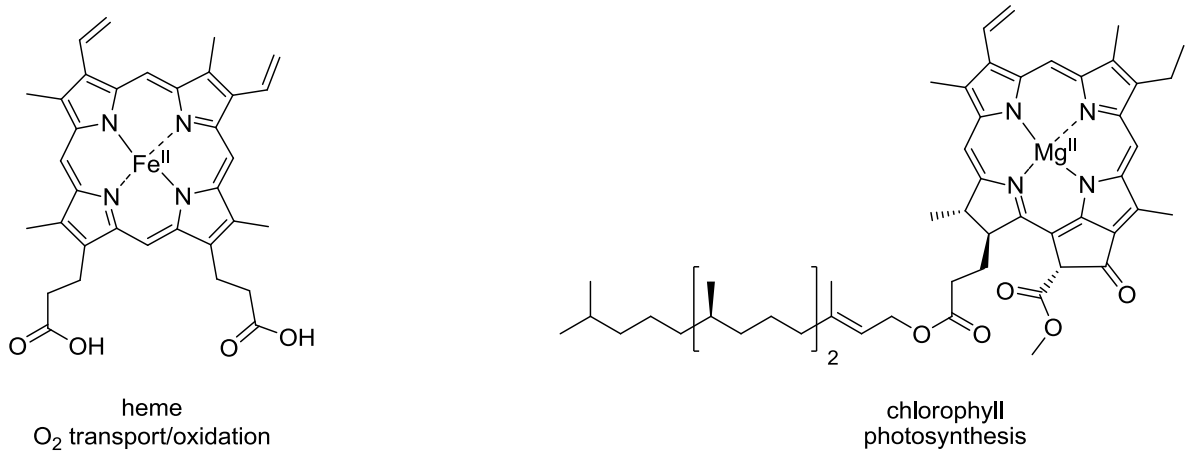

Figure 2. The structures of four «pigments of life» and the processes they perform.

The macrocycle of the «pigments of life» is formed in two elegant and efficient condensation reactions.[34-37] Uroporphyrinogen III is the last common intermediate in the biosynthesis of the «pigments of life» (Scheme 1). The first step is the condensation of two molecules of δ-aminolevulinic acid (δ-ALA) forming one molecule of porphobilinogen (PBG), which is catalyzed by a single enzyme.[32, 33, 38-41] The second transformation, where 4 molecules of PBG are condensed to the macrocyclic uroporphyrinogen III (Uro III), requires the presence of two enzymes working in sequence.[28, 30, 31] The first enzyme the porphobilinogen deaminase catalyzes the oligomerization to a linear precursor. The second enzyme the uropophyrinogen III synthase cyclizes the linear precursor and concomitantly inverts the D-ring. Finally, it is worth mentioning that the formation of uroporphyrinogens from PBG has been imitated in the test tube just by heating an acidic solution of PBG.[42-49]

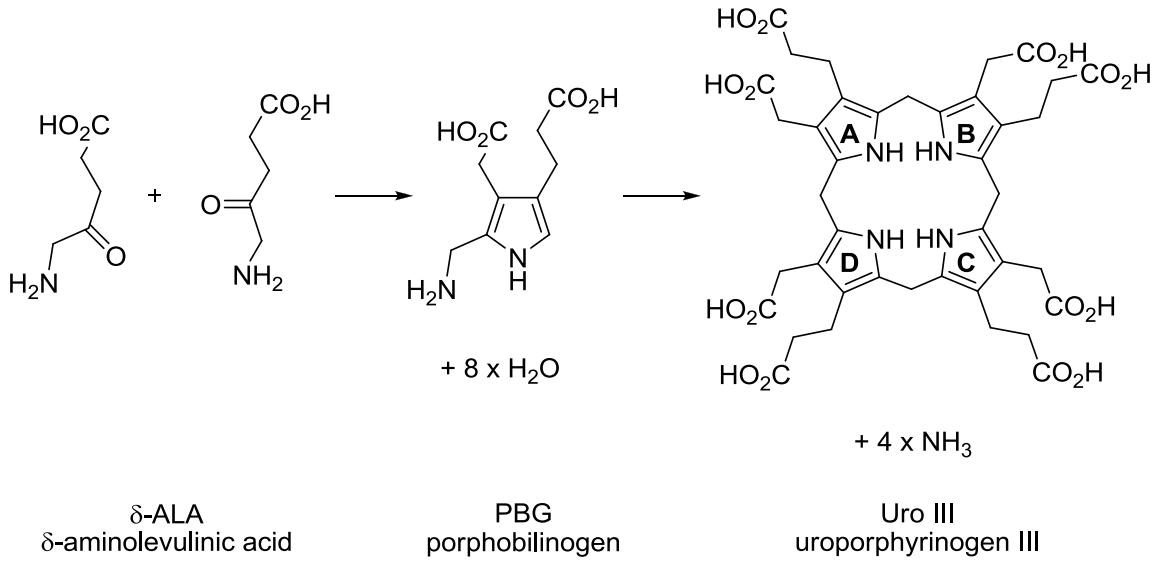

Scheme 1. The biosynthetic path to uroporphyrinogen III (Uro III)

The uroporphyrinogen chromophore, the first macrocyclic structure of the biosynthesis, does not easily form Werner complexes with transition metals. Forcing conditions have to be applied to achieve the incorporation of metals into the macrocyclic structures and often further transformations are induced under these conditions.[50-56] Most of the natural tetrapyrrolic macrocycles derived from uroporphyrinogen III acquire the capacity to complex metals by oxidizing the chromophore part of the ligand and by simultaneously tautomerizing the double bonds of the chromophore (see Figure 3).[15, 57-61] Vitamin B_{12} and factor F430 are exceptions as their chromophore are formed by reductive processes starting from Uro III. The four nitrogen atoms of the pyrrole rings in the uroporphyrinogens are arranged in a pre-structured array, but the free electron pairs are not available for complexation as they are part of the aromatic heterocyclic pyrrole rings. The oxidation of an urophorphyrinogen chromophore is a process thermodynamically favored by the creation of conjugated aromatic system. For the organisms biosynthesizing the «pigments of life», it is of advantage that uroporphyrinogen III does not capture metal ions. The presence of "unwanted" and potentially dangerous metal complexes can, thus, be avoided. It is a question of precaution to create the highly coloured and reactive «pigments of life» only where and when they are needed. A way to circumvent these "protective measures" is used in photodynamic therapy, where large quantities of the unwanted protoporphyrin IX are accumulated (PpIX).[62, 63]

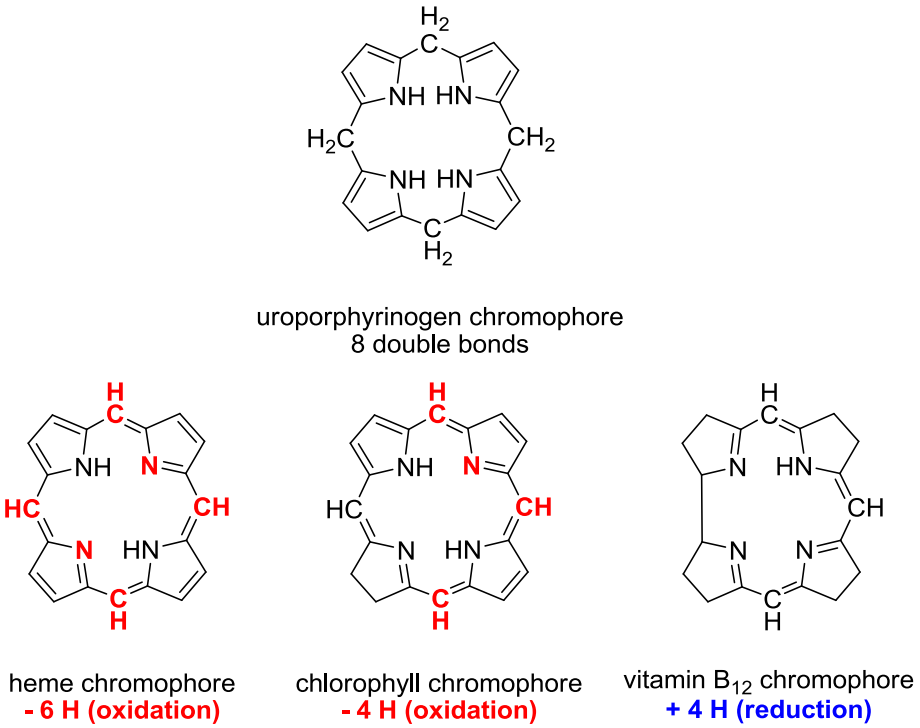

Figure 3. Change of the oxidation state during the transformation of Uro III into the chromophores of important tetrapyrrolic macrocycles.

3. SYNTHETIC NITROGEN CONTAINING MACROCYCLES

Synthetic nitrogen-containing macrocycles like triazacyclononanes, cyclens, cyclams and obviously non-natural porphyrins have been reported in the past (Figure 4). The structures of the synthetic ligands are characterized by short aliphatic chains of two or three methylene groups linking three or four nitrogen atoms. The cyclams and the porphyrins share the same "distance" between the two pairs of nitrogen atoms: a linker composed of three carbon atoms. The other two pairs are connected by a shorter ethylene linker (Figure 4). The chemical, catalytic and structural properties of these synthetic systems have been studied thoroughly.[64-66] Metal complexes of aza-macrocycles and their derivatives have been applied as sensors, contrast agents, in the detection and in the destruction of cancer cells or as oxidation and bleaching catalysts.[67-76] Azamacrocycles are of great importance for the studies of the mechanism of enzyme catalyzed reactions. Spectacular results have been obtained in experiments using simpler artificial systems to mimic the active site of elusive enzyme processes. The quest for high-valent iron or manganese oxo species is an important example of this type of studies.[73, 74, 76, 77] Other metal complexes were synthesized to obtain very useful transformations like selective oxidation of small hydrocarbons as methane, ethane or propane.[73, 78] The properties of the metal complexes of macrocyclic porphyrins have been compared to those of linear chelating ligands like salens and their derivatives.[79-81] White and coll. have beautifully demonstrated that rigidifying a linear tetradentate ligand restrains the geometry of the metal complex to one single conformation leading to a more stable metal complex and thereby to a more efficient catalyst (Figure 5a).[82] In another example Ready and Jacobsen have improved the catalytic activity of a linear salen derivative by transforming it to a macrocyclic analogue (Figure 5b).[83]

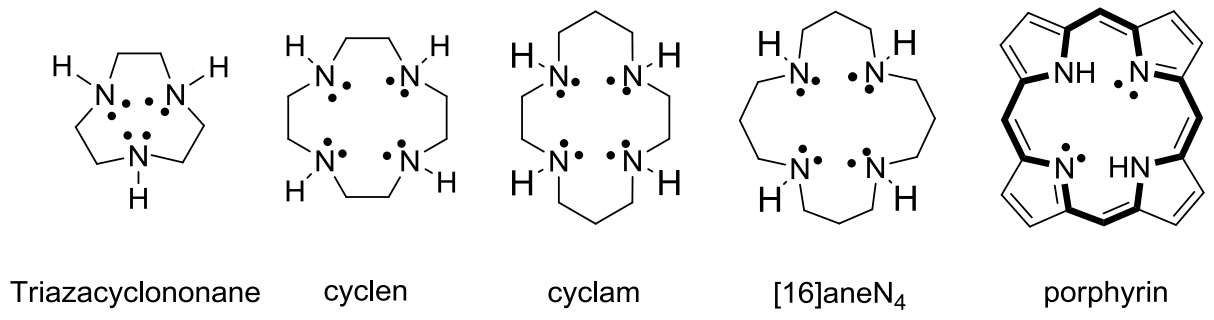

Figure 4. Classes of synthetically studied azamacrocycles

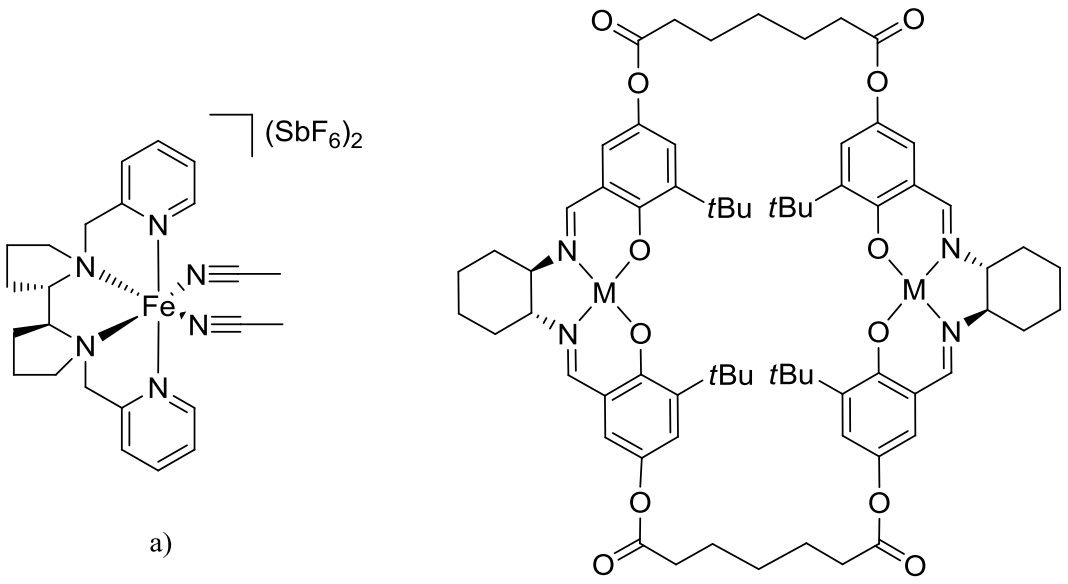

a) b)

Figure 5. a) The example of White; b) the example of Jacobsen

4. BRIDGED AZAMACROCYCLES

Cyclens and cyclams can be formally obtained by macrocyclization of linear oligomer type precursors. Adding additional bridges to these azamacrocycles induces topological constraints and enhances the high complex stability. Reducing the conformational space available to macrocyclic ligands has been conceptionally pioneered by Jean-Marie Lehn in his seminal work on cryptands.[84-86] For synthetic reasons, the additional bridge is often introduced between the nitrogen atoms (Figure 6a, 6b and 7). The availability of methriol as starting material allowed an easy synthetic access to the macrobicycles of the type illustrated in Figure 6c. Bridged or "strapped" porphyrins have been synthesized with the goal to imitate the properties of natural heme containing enzymes and proteins. A huge effort has been dedicated to the synthesis of such macrobicycles and to studies of the properties of their metal complexes, especially in the context of mimicking the reversible binding of dioxygen to iron complexes.

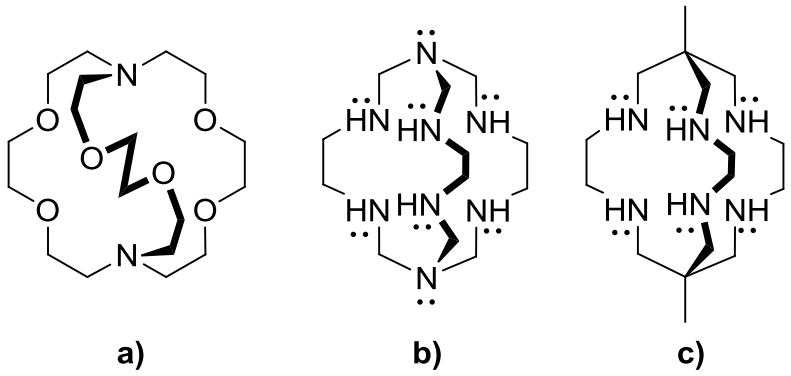

Figure 6. Bridged or "strapped" azamacrocycles **a)** Lehn's cryptand; **b)** a clathorochelate also called sepulchrate; **c)** ligand obtained by a template-directed synthesis using ethylene diamine, formaldehyde and propionaldehyde.[87-89]

Numerous examples and variations have been reported in the literature. Only a few examples will be shown illustrating the structures, which have been made available.[90, 91] The synthetic strategies limited and directed the design of the structures synthesized. The typical approaches to such macrobicycles were: 1) The direct synthesis where a pre-existing cyclen or a cyclam is modified by alkylation or acylation; 2) The template-directed synthesis where a metal complex pre-arranges the precursor for the macrocyclization reaction; 3) The protection/deprotection approach, where the cyclization is effected step by step using protective groups to assure the selectivity; 4) The condensation approach, where a multicyclic hemiaminal is formed which is then reductively opened to leave a bridge in the molecule. Approach 1) suffers from the typical low yields observed for the macrocyclization reactions. Approach 2) is efficient but not very flexible. Approach 3) is often long and complicated. Approach 4) is mechanistically complex but often leads to good results as far as efficiency and yield are concerned. In conclusion the synthetic methodologies available determine the structures, which can be studied and also the design of the structures proposed. Even if a specific compound is available by one of the strategies mentioned, its use is severely hampered if the length of the synthesis or the low overall yield is prohibitive for a systematic use of the desired compound for further physicochemical and biomimetic studies. Easiness and efficiency of a synthetic access to a desirable structure are crucial for the progress in science and understanding.

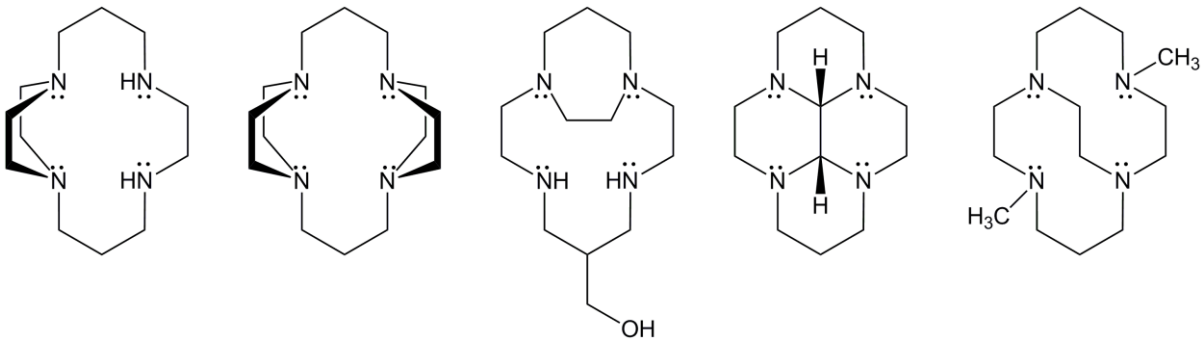

Figure 7. Typical bridged or "strapped" structures reported and studied

5. CALIX[4]PYRROLE

Adolf von Baeyer and his group were the first to isolate the *meso*-octaalkylporphyrinogen **1** more than 120 years ago by mixing pyrrole and acetone in the presence of a mineral acid (Scheme 2).[92] This reaction was an extension of the systematic studies in von Baeyer's group on condensation reactions using phenol and formaldehyde. Von Baeyer called the compound "acetonepyrrole". The easiness of the reaction and especially of the isolation are remarkable. The product of the condensation between pyrrole and acetone precipitates out of the solution in pure, crystalline form. Despite these important factors, favoring the characterization and identification of the new material, the structure determination proved to be tedious. It took a very long time until the structure of the compound was firmly established using a degradation approach.

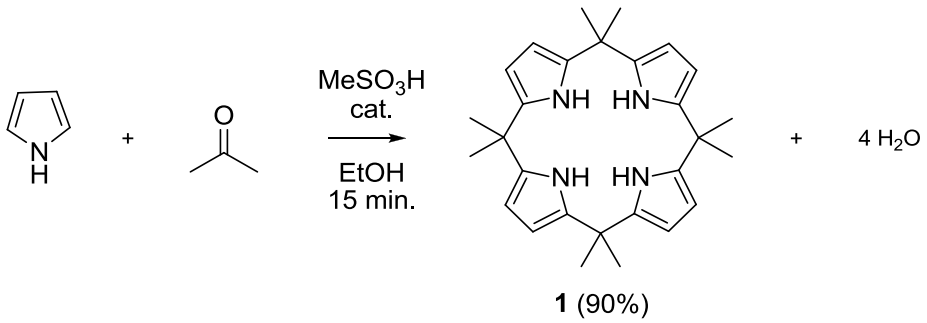

Scheme 2. Synthesis of calix[4]pyrroles[92]

Chelintzev et al. were the first to propose the correct structure in 1916.[93] Hans Fischer gave it the name α, β, γ, δ-octamethylporphinogen. This name suggested the close structural similarity of this compound to the porphyrins. It almost took forty years until Rothemund could definitively prove in 1955 the α,α'-linkage between the pyrrole rings included in the

macrocyclic structure.[94] Another forty years later, the X-ray structure determination of this compound revealed the alternating conformations of the pyrrole rings in the solid state,[95] where vicinal pyrrole rings were pointing in opposite directions. The pyrrole rings opposite to each other were nearly parallel forming a cavity. One pair of hydrogen bonds is pointing up and the other pair of hydrogen bonds is pointing down if the disk of the macrocycle is aligned horizontally. The X-ray crystal structures of these macrocycles binding anions like fluoride and chloride disclosed a significant change in the conformation of the macrocycle.[95] In this halogenide binding complexes all the NH were directing towards the anion, adopting a cone like conformation similar to that observed for calixarenes (Figure 8).[56]

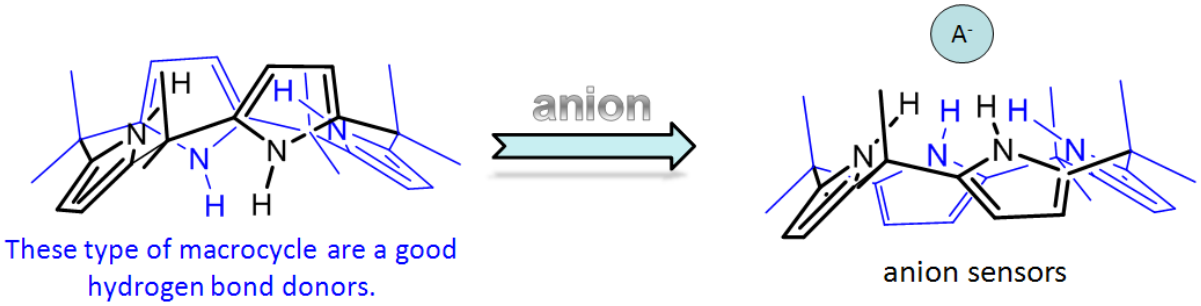

Figure 8. Change in the conformation of calix[4]pyrrole in the presence of an anion.

Based on this observation and on the similarity of the Rothemund procedure[94] for the synthesis of calixarenes with the von Baeyer procedure, it was proposed to change the name of these macrocycles once again from *meso*-octaalkylporphyrinogen to "calix[4]pyrroles".[95] The *meso*-octaalkylporphyrinogen is not *bona fide* precursors of porphyrins, an observation which legitimizes the proposed name change.

The calix[4]pyrroles were intensively studied for their capacity to function as anion sensor via the formation of four pyrrole NH-anion hydrogen bonds.[96] Two different approaches have been used to quantify the presence of halogenides using calix[4]pyrrole based sensor. Fluorescent groups have been introduced onto the ligand, for example the synthesis of calix[4]pyrrole-anthracene by coupling a calix[4]pyrrole mono-acid, prepared from calix[4]pyrrole, with different aminoanthracene to afford the conjugated conpounds.[97] The second approach is based on the competitive replacement of para-nitrophenolate by halogenides. The color change of the complexes versus the free para-nitrophenolate is used for sensing.[98] Using fluorescence as a method of quantification has been more intensively studied and gives simple and very effective colorimetric halide sensor systems.[98, 99]

In contrast to typical Werner type complexes, the nitrogen lone pairs of calix[4]pyrroles are part of the aromatic π system of the pyrrole ring and are, therefore not available for complexation of metal species. The metallation of calix[4]pyrroles to give the tetra-anion allows the introduction of metal ions (Scheme 3).[100] This procedure is experimentally challenging and requires the use of strong bases and strict exclusion of oxygen and water.

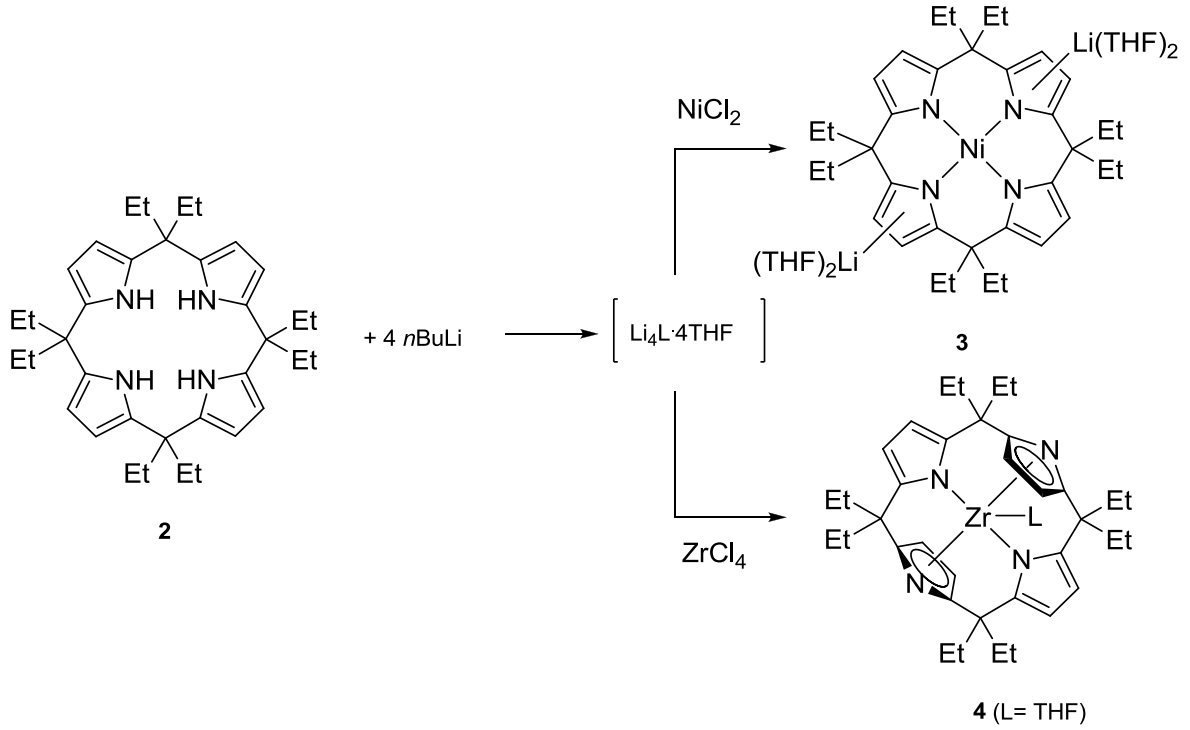

Scheme 3. Synthesis of the tetraanion of calix[4]pyrrole and its transformation into metal complexes described by Jubb et al.[100]

To sum up, calix[4]pyrroles have been known for a long time and are very easy to obtain and to isolate. Their chemistry has attracted attention only in the nineties, when the anion binding of the calix[4]pyrroles has been detected in the group of Sessler.[95, 101, 102] This anion binding capacity can be attributed to the four directed H-bonds they are forming. During the same period the capacity of the calix[4]pyrroles to form metal complexes has been studied starting from the tetraanion by the group of Floriani.[54, 56, 100, 103] The transformation of these metal complexes is complicated. The reactivity differs from the one observed with the porphyrins, which form Werner complexes with great ease. The calix[4]pyrroles are very poor ligands, because the lone pairs of the four pyrrole rings are involved in the heteroaromatic ring and thereby the lone pairs are not available for metal binding.

6. MOTIVATION

The analysis of the reported reactivity of calix[4]pyrroles led to the question of whether or not the completely hydrogenated macrocycle can be obtained and what would be the chemical characteristics of this saturated system. The lone pairs of the completely saturated macrocycle should become available for metal binding (Figure 9).

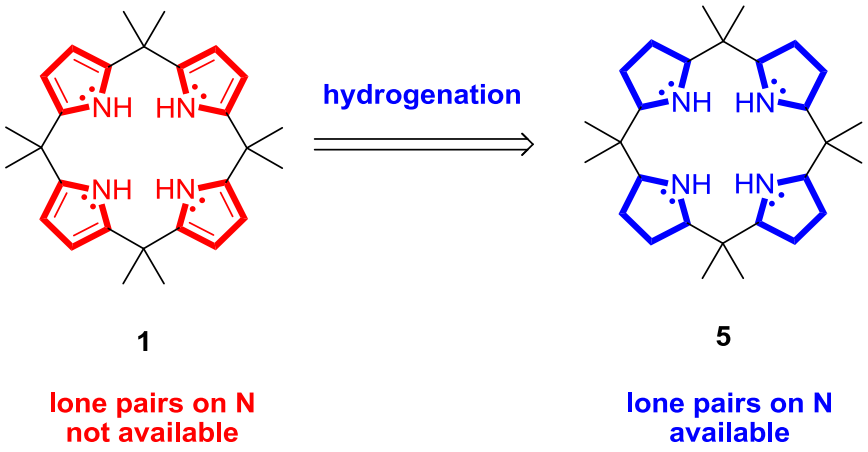

Figure 9. Proposed hydrogenation of calix[4]pyrroles and the expected change in metal binding characteristics

A second topological correlation can be envisaged, if one compares the proposed totally reduced calix[4]pyrroles with the simple ligand having the same connectivity linking the nitrogen atoms to each other. The fully flexible ligand and its metal binding properties have been thoroughly studied (Figure 9). Bridged or "strapped" versions of this ligand have been extensively examined. Typically, the bridges were introduced between the nitrogen atoms, for the easiness of the synthesis. In some cases, the bridge connects opposite sides of the macrocycle. The synthesis of this type of macrocycle often starts with methriol as starting material leading to a macrobicyclic structure. We did not find reports on structures, where the additional cycles were added "externally" or in an "exocyclic" fashion to the basic macrocyclic structure. As in the cases reported in the literature, where the introduction of a bridge (="endocyclic" ring formation) reduces the conformational flexibility, the addition of "exocyclic" rings will stiffen the skeleton and should thereby increase the thermodynamic stability of the metal complexes.

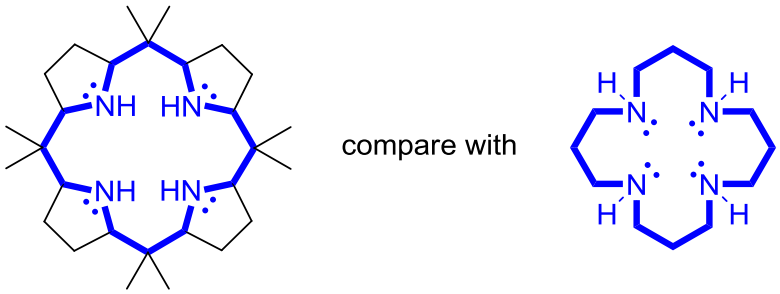

5

Figure 10. Comparison of the totally reduced calix[4]pyrroles with the fully flexible ligand connecting the nitrogen atoms with propylene linkers

In contrast to most bridged ligands published so far, the pentacyclic structure **5** possesses eight stereogenic centers. Due to the symmetry of the ligand, not all combinations of the relative configuration of the eight stereogenic centers lead to separate diastereoisomers. If this would be the case, a total of 256 stereoisomers should be obtainable. A total of 45 different stereoisomers of compound **5** can be drawn.[104] The influence of the relative configuration of a specific stereoisomer of **5** on its capacity to act as a ligand for metal atoms is difficult to predict. If the structures with the constitution of **5** become synthetically available, the correlation between metal binding and the relative configuration of the stereogenic centers of the ligand can be studied. The proposed ligand **5** has symmetry properties, which resemble those of Nonactin a natural ligand for potassium. The tetrameric macrolide possesses an unusual S_4 symmetry. Recent studies show that this specific relative configuration is a more efficient potassium cation binder than other optical pure artificial isomers synthesized for comparison purposes.[105] Studies of the stereoisomers of **5** could contribute to our understanding of the influence of the relative configuration of the ligand on metal binding and complex stability.

7. KNOWN HYDROGENATIONS OF HETEROCYCLIC CALIX[4]ARENES

All the three simple homo heterocyclic calix[4]arenes (containing four identical aromatic heterocycles) are known: calix[4]furan **6**, calix[4]pyrrole **1** and the calix[4]thiophene **8** (Figure 11). The synthetic access to the macrocycles **6** and **1** is easy, *via* the procedure pioneered by von Baeyer. The fully substituted calix[4]thiophene **8** is more difficult to obtain and the reported yields are low.[94] The group of Vogel developed a method where the

calix[4]furan **6** could be converted into the calix[4]thiophene **8** using hydrogen sulfide under acidic conditions.[106-109] A recent publication reports on the efficient synthesis of highly substituted calix[4]furans and calix[4]thiophenes adding a heteroaryllithium compound to ketones and treating the products with *N*-iodosuccinimide to achieve the condensation to the macrocycle.[110, 111]

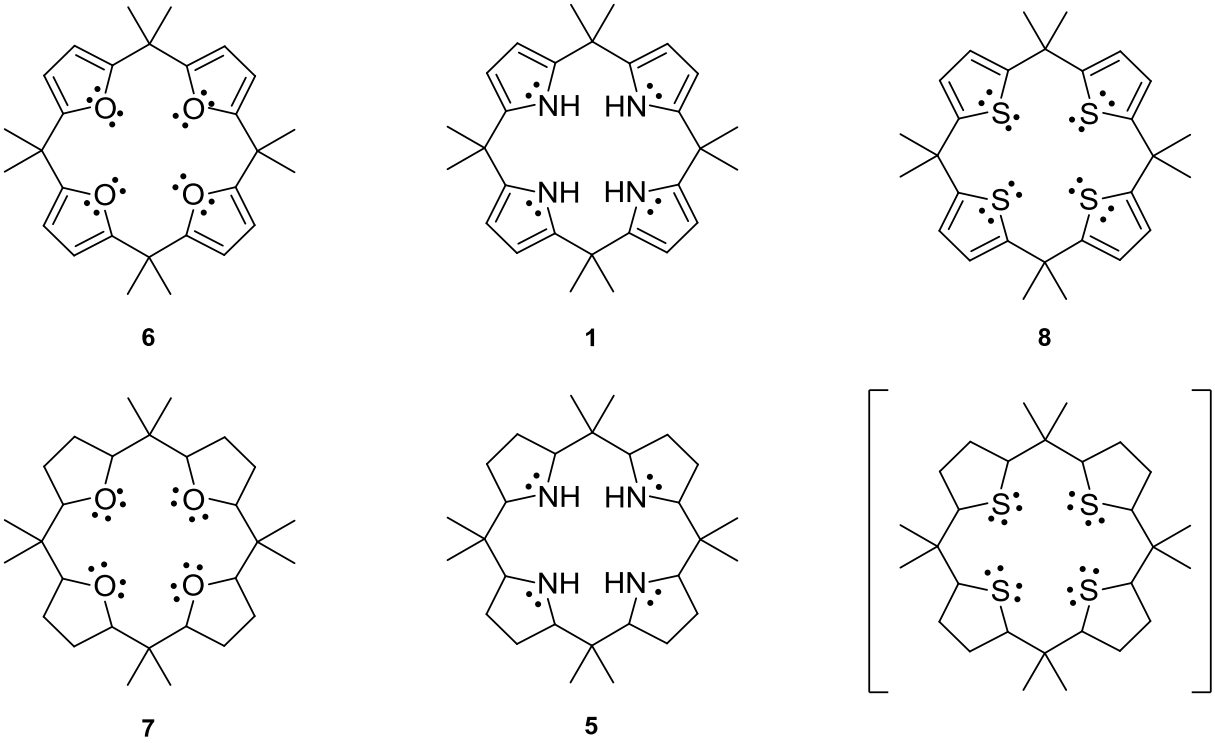

Figure 11. The heterocyclic calix[4]arenes: calix[4]furan **6**, calix[4]pyrrole **1** and calix[4]thiophene **8** their totally reduced counterparts: calix[4]tetrahydrofuran **7** and calix[4]pyrrolidine **5**

The synthetically easiest way to obtain the reduced macrocycles is the exhaustive hydrogenation of the corresponding heterocyclic calix[4]arenes. In principle, the reduced compounds **5** and **7** should be available in two simple synthetic steps: 1) acid catalyzed condensation of the five membered heterocycle with acetone followed by 2) heterogeneous catalytic hydrogenation. Only the transformation of the calix[4]furan **6** to the calix[4]tetrahydrofuran **7** has been reported in the literature before our own studies.

8. HYDROGENATION OF CALIX[4]FURAN 6

The synthesis of calix[4]furan **6**, the starting material for the heterogenous reduction, was first described by Ackman et al. in 1955, [110, 112-114] almost 80 years after the first publication of von Baeyer describing the synthesis of calix[4]pyrrole **1**. Historically the first preparation of a calix[4]furan had already been reported in 1906 by Hale et al.,[115] when they treated ethyl 2-furoate with ethyl magnesium iodide. Based on the limited analytical data available at that time, they incorrectly proposed 2-(pent-2-en-3-yl)furan as the structure of the product obtained (Scheme 4).

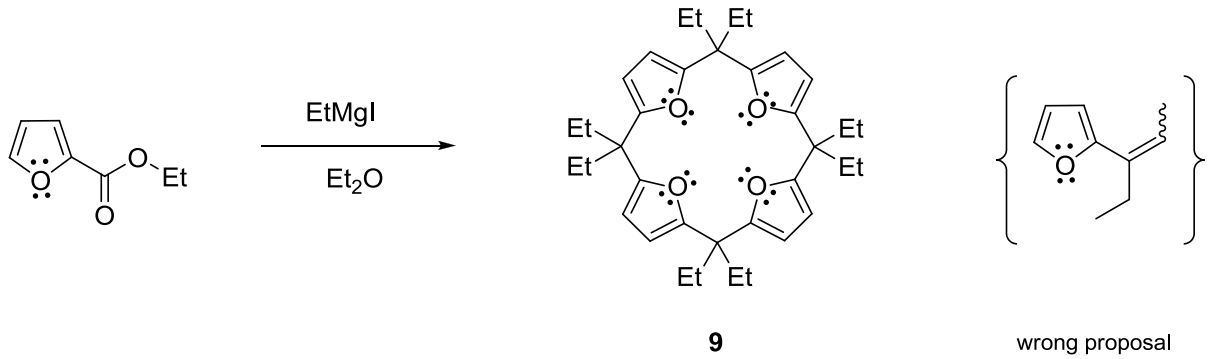

Scheme 4. First historic synthesis of calix[4]furan **9** in 1906 with the wrong structure assignment.[115]

The reaction conditions in 1955 and later are similar to the conditions used for the synthesis of calix[4]pyrrole **1**, however the yields are generally lower (Scheme 5). The best conditions reported are using a large excess of $LiClO_4$ to accelerate the reaction.[116, 117] In 1985, de Sousa Healy and Rest published a systematic study of the role of metal salts in the macrocycle synthesis by furan-ketone condensation.[118] Alkaline-earth metal salts gave **6** in generally good yields, typically between 14 and 32% for $Ca(ClO_4)_2$. The salts of transition metals like chromium, manganese, iron, cobalt, nickel, copper and zinc gave good to excellent yields, situated between 12 and 33% of the macrocycle **6**. In all cases the best yields were obtained when perchlorate was used as the anion. They also studied the influence of the type and amount of acid, the amount of water present and the reaction time. The authors also studied the complexation of the macrocycle **6** with the metal salts used. In contrast to the publications of Chastrette, the authors came to the conclusion that the template effect was not the major factor for the outcome of the condensation. They preferred to attribute the increase of yield to the pH change induced in the presence of the metal salts.

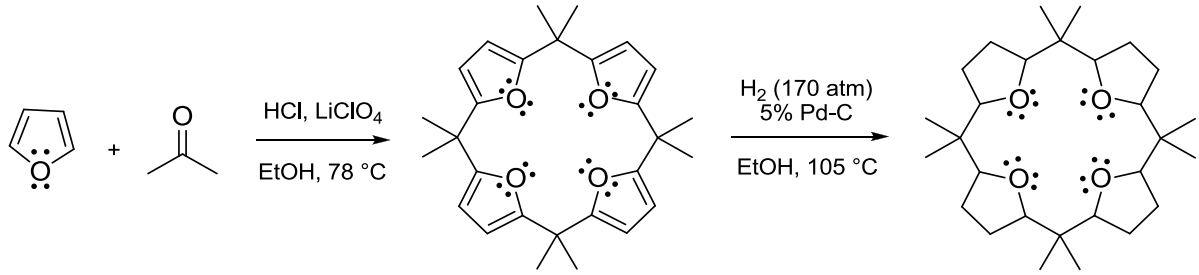

Scheme 5. Synthesis and catalytic hydrogenation of calix[4]furan **6**[116, 117]

The recent report by Lee et al. [110] described the efficient synthesis of sterically demanding calix[4]furans e.g. **10** and calix[4]thiophenes, which were so far not accessible (Scheme 6). The method is based on the selective direct C-H metallation of furan in the α-position followed by a reaction with a ketone as electrophile. The benzylic alcohol obtained is not isolated but converted into arylalkenes by dehydratation. The arylalkenes were tetra-cyclized with the aid of iodonium ion from *N*-iodosuccinimide. The catalytic hydrogenation of the calix[4]furan **6** was first reported by Kobuke et al. in 1976,[119] who made a systematic study of the transport capacities of macrocyclic tetrahydrofuran-containing structures through liquid membranes. Kobuke et al. used ruthenium on carbon as catalyst and had to apply 120 atm H_2-pressure and 190 °C for 6 h obtaining 73% yield of the totally reduced macrocycle **7**.

Slightly different conditions for the reduction were reported by Rest et al. in 1976,[120] by Chastrette[117] and by Wiegers and Smith.[111] When palladium on carbon was used as catalyst, the pressure needed for the reduction varied from 110 atm to 170 atm at a temperature of 105 °C. The yields reported were consistently between 57 and 72%.

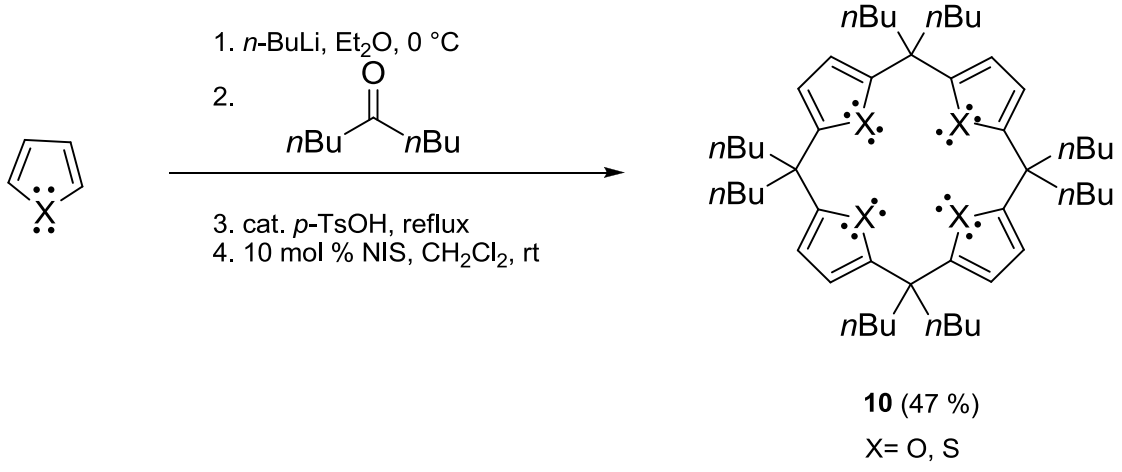

Scheme 6. Synthesis of calix[4]furan **10** (X = O) or of calix[4]thiophene (X = S)**.** [110]

Contrary to the previous authors, de Sousa Healy and Rest[118] were not able to carry out the reduction in ethanol. Using THF as solvent, Raney Ni as catalyst and similar conditions of pressure and temperature as those reported by previous authors, they isolated and separated a mixture consisting of 38% of the totally reduced macrocycle **7** and 18% of the half-reduced compound **11**, isolated by successive crystallization (Scheme 7).

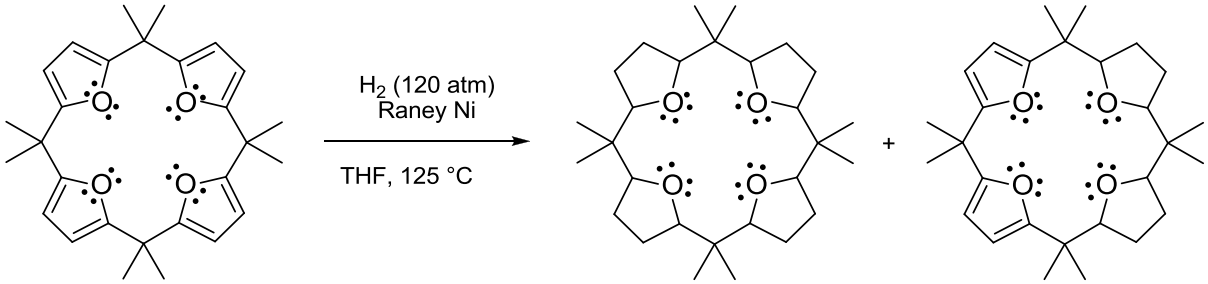

6 **7** (38 %) **11** (18 %)

Scheme 7. Heterogenous catalytic hydrogenation of calix[4]furan **6** with Raney Ni yielding the calix[4]tetrahydrofuran **7** and the calix[2]furan[2]tetrahydrofuran **11** according to de Sousa Healy and Rest.[118]

In the publication by Van Beylen et al.,[104, 121], which appeared the same year, the authors reported the successful hydrogenation under considerably milder conditions. Hydrogenation was successful at room temperature and under atmospheric H_2 pressure (Scheme 8).

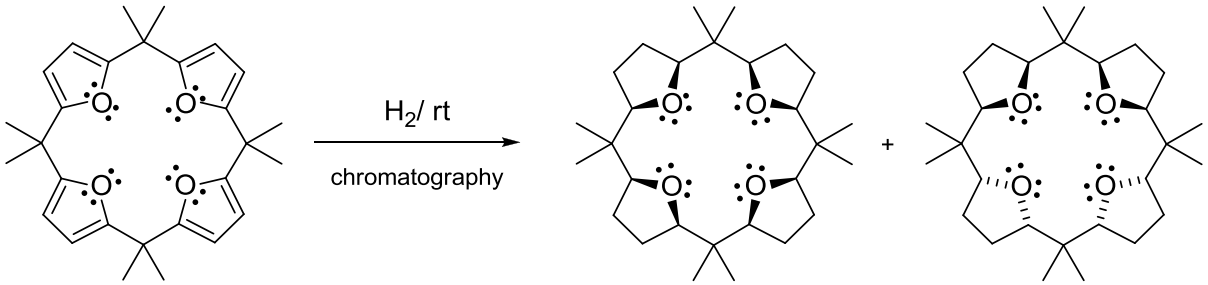

6 **7a** (49 %) **7b** (14 %)

Scheme 8. Hydrogenation of the macrocycle **6** under mild conditions and separation of the two diastereoisomers according to van Beylen.[104]

Under these conditions, at least two different disastereoisomers were formed. The authors could separate the two diastereoisomers **7a** and **7b** in a 70:30 ratio. Both diastereoisomers crystallized and their structures in the solid were determined by X-ray diffraction. Characterization of the two diastereoisomers by additional analytical and spectroscopic data and the detailed experimental description are, unfortunately, missing. Ten years later, the authors described a detailed spectrophotometric study of the metal complexation of these two new ligands, without giving more details describing the ligands.[122]

9. THE STRUCTURES AND PROPERTIES OF THE CALIX[4]TETRAHYDROFURANS 7

The interest in the calix[4]tetrahydrofurans **7** was stimulated by the discovery of the crown ethers by Pedersen, Cram and Lehn.[86] An additional stimulus came from the discovery of the capability of Nonactin to form complexes with alkali cations, showing a remarkable preference for potassium over sodium ions (Figure 12).[123]

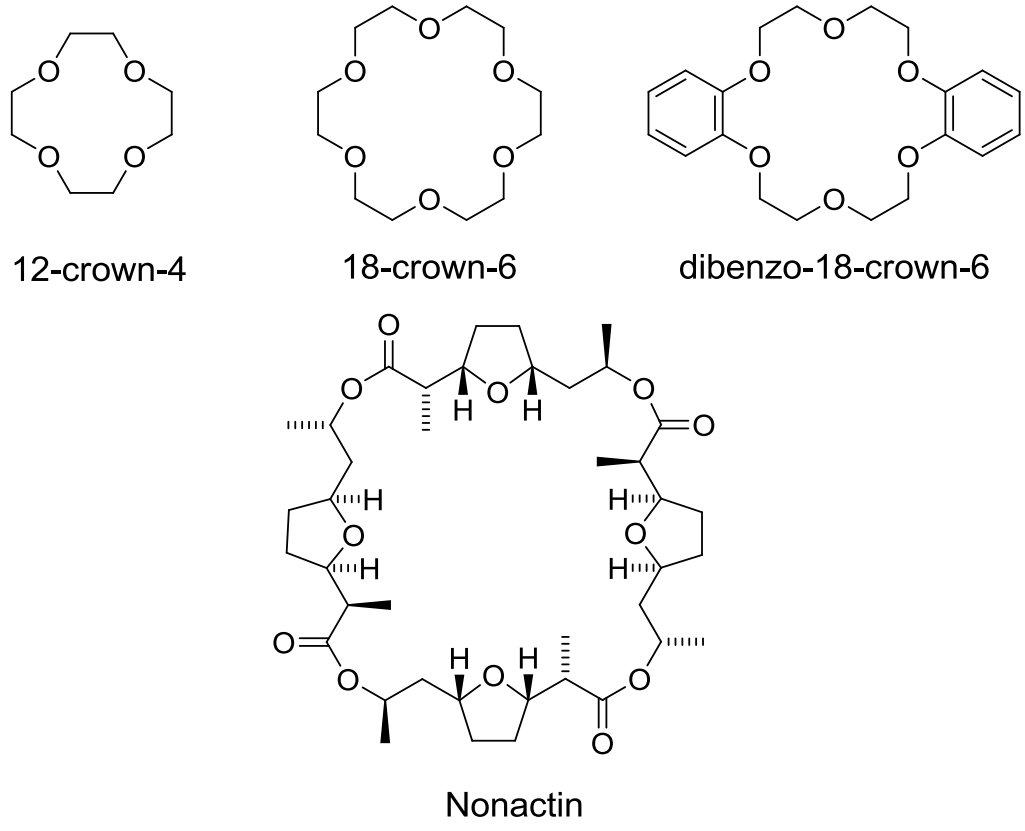

Figure 12. Typical synthetic crown ethers and Nonactin, a complex natural ionophore, serving as inspiration for the hydrogenation of calix[4]furans.[123]

The X-ray structures of the two diastereoisomers **7a** and **7b** were reported by von Beylen et al. (Scheme 8 and Figure 13).[104, 121] The conformations of compounds **7a** and **7b** resemble each other and are quite similar to the conformations found in the unsaturated heterocyclic calix[4]arenes, calix[4]furan **6** and calix[4]pyrrole **1**, namely a 1,3-alternate conformation.[121] A dramatic change of conformation is observed when the lithium picrate complex of the macrocycle **7a** is studied. The complex crystallized from a mixture of lithium picrate and the calix[4]furan **6** in chlorobenzene containing a small amount of THF. The four oxygen atoms of the furan rings are almost in a planar arrangement. The metal binding changes the overall appearance of the macrocycle. The global form of the macrocycle becomes bowl shaped. The central lithium cation is in a position slightly out of the plane deviating towards the picrate, which is in binding distance (Figure 14). The bowl shape creates two distinctively different faces: a concave face limited by the four axial methyl groups and a convex face opened to the solvent. As a consequence of the overall shape of the macrocycle, four of the methyl groups are in equatorial positions whereas the other four methyl groups are in axial positions forming a tight cleft seriously restraining the access to the metal atom.

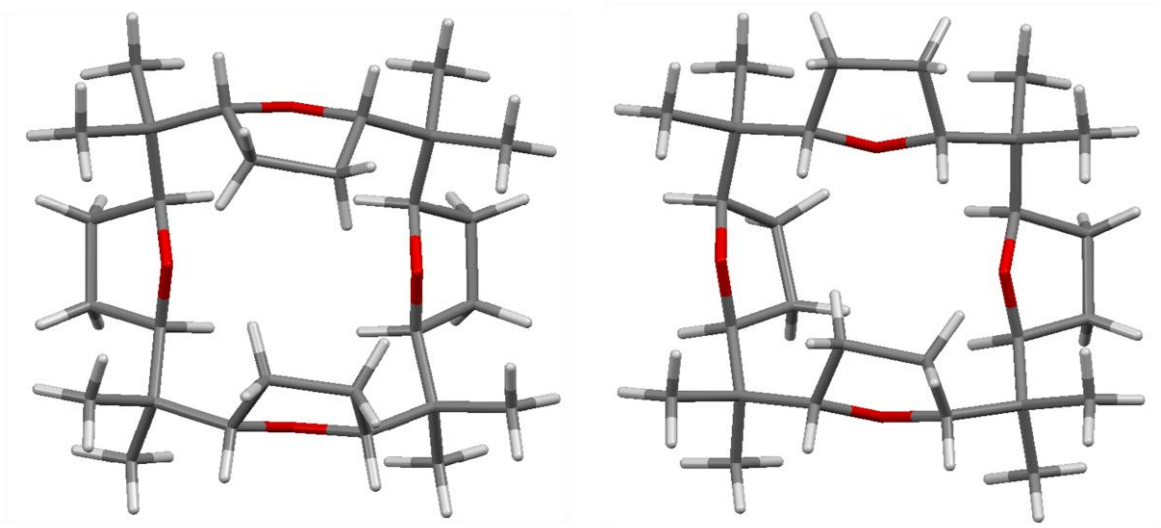

Isomer **7a** Isomer **7b**

Figure 13. Molecular structures of isomers **7a** and **7b.**[121]

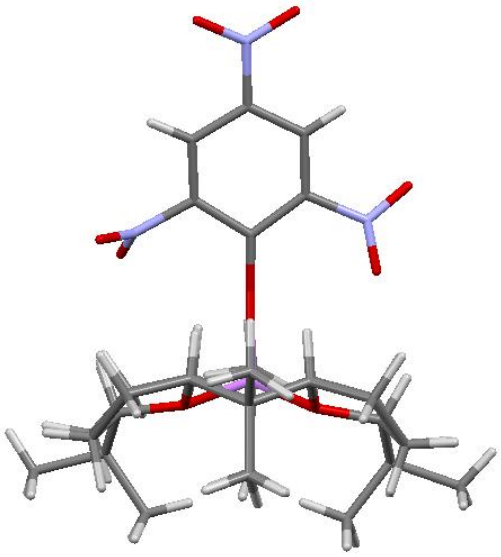

Figure 14. Molecular structure of lithium picrate complex of isomer **7a**[121]

The early studies of Kobuke et al. showed that the reduced calix[4]tetrahydrofuran **7** was capable of extracting alkali metal cations into organic media, typically chloroform.[121] Lithium and sodium picrates could be extracted from aqueous to the chloroform phase using the macrocycle **7**. Transport rates through liquid membranes were determined as well. The selectivity measured in transport rates was fastest for sodium cations with a 2 : 1 preference compared to lithium cations and at least a 6 : 1 preference compared to the transport rate of potassium cations. Wiegers and Smith isolated the complex formed by the mixing of one equivalent of $LiAlH_4$ and one equivalent of calix[4]tetrahydrofuran **7** in THF.[111] They obtained a crystalline complex, which was characterized by its CHN analysis, compatible with a complex containing one equivalent of THF. Using increasing quantities of the calix[4]tetrahydrofuran **7** in the presence of $LiAlH_4$ for the reduction of camphor, decreased the rate of the reduction. The influence of the macrocycle **7** on the reduction was, however, moderate compared to the influence of cryptands, which stopped the reduction completely.[124-126] De Sousa, Healy and Rest observed characteristic changes in the NMR signals on the complex formation between calix[4]tetrahydrofuran **7** and lithium salts, like LiI, LiSCN and $LiClO_4$. Van Beylen et al. determined the rate of complex formation and the binding constants separately for the two diastereoisomers **7a** and **7b**.[122] Spectrophotometric studies showed that both diastereoisomers formed complexes with lithium picrate in different solvents like THF, tetrahydropyran, dioxane, diethyl ether or chlorobenzene. The complex formation was slow for both diastereoisomers. The authors attribute the sluggishness of this process to the

importance of the conformational changes needed for the complex formation. The complexes formed from the all *cis*-diastereoisomer **7a** were considerably more stable than the complexes formed from **7b**. The small changes in the position of the absorption band on complexation are compatible with the presence of a stretched contact ion pair. For the complex with the other diastereoisomer **7b** more important bathochromic shifts are observed. This is compatible with the formation of a solvent-separated ion pair.

10. HYDROGENATION OF CALIX[4]PYRROLE

To the best of our knowledge, only one report on the hydrogenation of calix[4]pyrrole **1** was published in 1955 before our own work published in 2009 (Scheme 9).[94] The goal of the study by Rothemund and Gage was to ascertain the structure of calix[4]pyrrole **1** called acetonepyrrole at the time. The conditions used for the hydrogenation were extremely harsh. The objective of this transformation was securing the position of the linkage connecting the neighboring pyrrole rings into the macrocycle. The main result of this degradation experiment was the proof of the position of the links in the 2 and 5 positions of the pyrrole exclusively. Almost 70 % of the bridging atoms were accounted for.

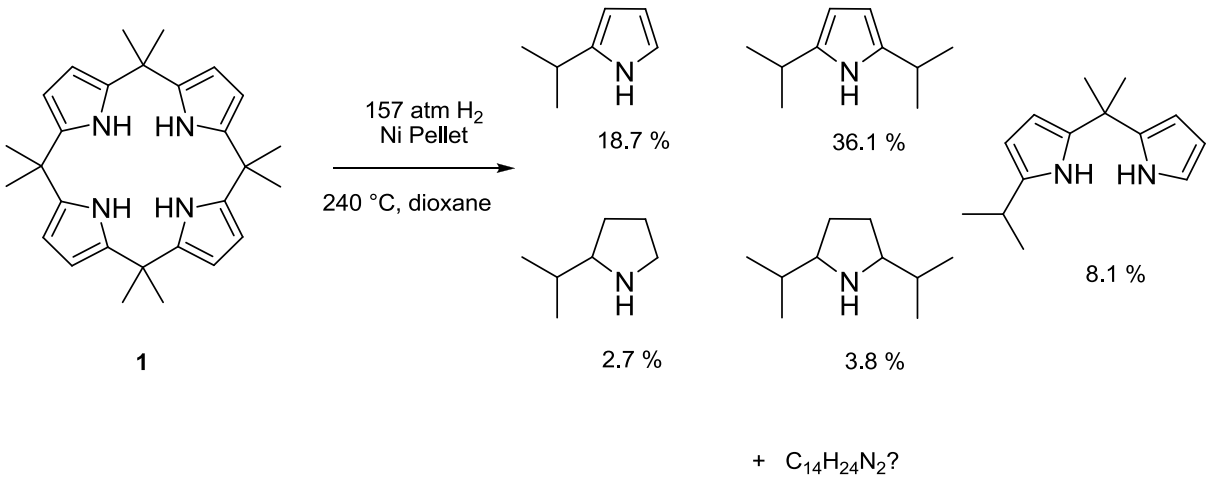

Scheme 9. Results of the heterogenous catalytic hydrogenation of calix[4]pyrrole **1**[94]

11. CONCLUSIONS

The publication of Rothemund and Gale is the only experiment reported in the literature describing trials to hydrogenate calix[4]pyrrole **1**. It is therefore the only valuable source of information if one is interested in the hydrogenation process. Three types of conclusions can be drawn from the described experiments: 1) Experimental conditions for a successful hydrogenation; 2) Difficulty of the hydrogenation of alkyl substituted pyrrole rings; 3) Relative rate of hydrogenation of pyrrole rings compared to the rate of the benzylic hydrogenation.

The first conclusion concerns the experimental conditions. The extreme harshness of the hydrogenation conditions is striking. In a second hydrogenation experiment, the authors use even higher pressures and only a slightly lower temperature: 204 atm H_2 at 215 °C. Under these strenuous conditions, it is somewhat of a surprise that the material balance is relatively good. To account for 69.4% of the bridging atoms is an excellent experimental result considering the aggressive conditions used and the difficulty of the separation process. The authors used only distillation and acid base extractions. The good material balance is clearly a testimony for the quality of the experimental work of the authors.

The second conclusion concerns the inherent difficulty to reduce dialkyl substituted pyrroles. The process must be quite difficult at least under the conditions described by the authors. The experimental conditions are extreme. Pressure and temperature are at the limit of what can be reasonably and safely implemented in a typical laboratory. It is worth mentioning that the authors used similarly strenuous conditions for the hydrogenation of the 2-isopropylpyrrole and for the 2,5-diisopropylpyrrole to the corresponding 2-isopropyl-pyrrolidine and the 2,5-diisopropyl-pyrrolidine (Scheme 10). The goal of these hydrogenations was to prove the structures of the compounds that were obtained by degradation by an independent synthetic approach. Obviously, the hydrogention of simple alkyl substituted pyrroles as well as the hydrogenation of calix[4]pyrrole require very harsh conditions. One can rationalize these extreme conditions by the difficulty to reduce an electron rich heterocycle and by the steric hindrance imposed by the substituents at positions 2 and 5. The temperatures and pressures needed for the hydrogenation remain a surprise, if one compares the heats of hydrogenation for furan (14.9 kcal/mol), pyrrole (17.1 kcal/mol) and thiophene (18.5 kcal/mol).[127] The estimates for the resonance energies of furan (16.3 kcal/mol), pyrrole (21.5 kcal/mol) and thiophene (29.2 kcal/mol) derived from the energy of combustion indicate a more important thermodynamic difference than the figures reported for the hydrogenation. The considerable

differences in the resonance energy might be compatible with the differences observed for the hydrogenation.[128]

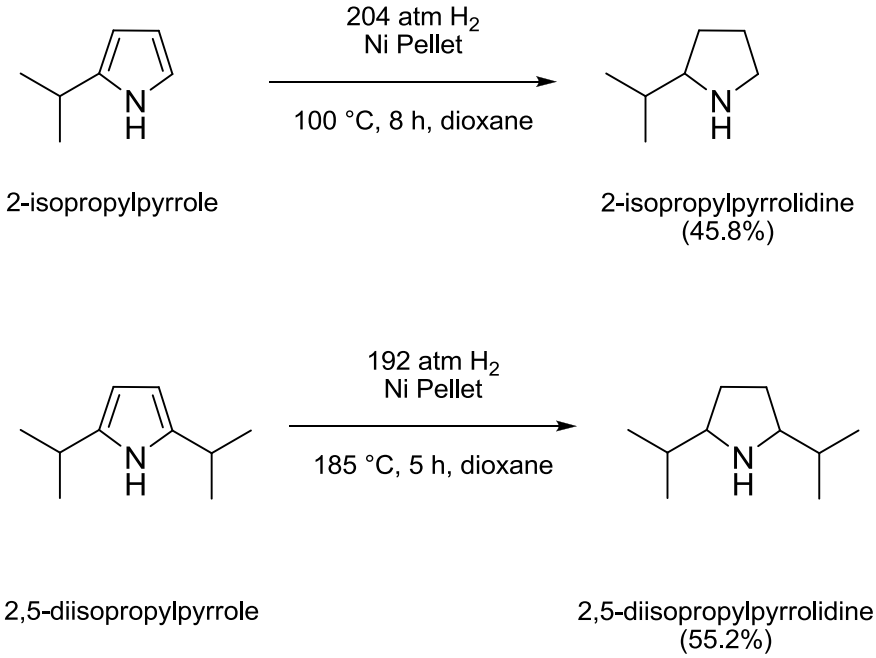

Scheme 10. The synthesis of the 2-isopropylpyrrolidine and 2,5-diisopropylpyrrolidine by hydrogenation[94]

The last conclusion concerns the relative rate of hydrogenation of the pyrrole rings compared to the rate of the benzylic hydrogenolysis. Rothemund and Gale isolated and identified only ring opened products. One has to mention, however, that they report some supposed decomposition during their first distillation, which might be due to the presence of oligomeric or macrocyclic products: 23.6 % of the material was present as charred residue, not distillable under the conditions used by the authors. More conclusive is the observation that the relative amount of the pyrrolic degradation products isolated is about ten times as high as the amount of the totally hydrogenated corresponding pyrrolidines (Scheme 9). This observation is compatible with a considerably faster benzylic hydrogenolysis than the hydrogenation of the aromatic pyrrole rings. Even in the dipyrromethane type compound (Scheme 9) the two pyrrole rings are fully aromatic. The amount of the dipyrromethane type compound is almost a factor of eight smaller than the amount of monocyclic compounds isolated under these hydrogenation conditions. Also, this observation is consistent with a kinetically faster benzylic hydrogenolysis.

To sum up: Harsh conditions are needed for a successful hydrogenation of calix[4]pyrroles. The reasons for these extreme conditions are not easily rationalized based on the thermodynamic data available. Under the conditions applied the benzylic hydrogenolysis seems to be kinetically faster than the hydrogenation of the pyrrole rings. The challenge is therefore to find experimental conditions where the ring opening and thereby the benzylic hydrogenolysis is slowed down and/or to find conditions where the hydrogenation of the pyrrole rings is sufficiently accelerated to allow the isolation of the reduced macrocycle.

Chapter 2

SYNTHESIS OF CALIX[4]PYRROLIDINE

Abstract

The first *meso*-octaalkylporphyrinogen (calix[4]pyrrole) was synthesized by Baeyer more than 120 years ago, mixing pyrrole and acetone in the presence of an acid.[92] First proposed by Chelintzev et al., the correct structure was definitively proven by Rothemund in 1955,[93, 94] followed forty years later by the X-ray analysis.[95] This macrocycle could be obtained in gram scale and in very good yield.

We have performed a thorough study of the catalytic hydrogenation of calix[4]pyrrole **1**, by using common as well as novel heterogeneous catalysts based on transition metals (Pd, Rh, Ru) supported on solid matrices[129]. During our studies, we were able to isolate and identify two half-hydrogenated products, **12a** and **12b**. A single, all-*cis*, fully hydrogenated compound **13** could be obtained in low yields only under drastic reaction conditions (100 atm of hydrogen pressure at 100 °C in acetic acid) (Scheme 11). Gas chromatographic analysis of the heterogeneously catalyzed hydrogenation reactions of calix[4]pyrrole **1** allowed to determine the composition of the reaction mixtures. The relative configuration of the three products has been unequivocally determined by single crystal X-ray diffraction.[129, 130]

The reduced calix[4]pyrrole **13** reacts smoothly with transition metals to form new organometallic complexes with a large range of transition metals. The manganese complex has shown to possess interesting catalytic activity for oxidation processes.[131]

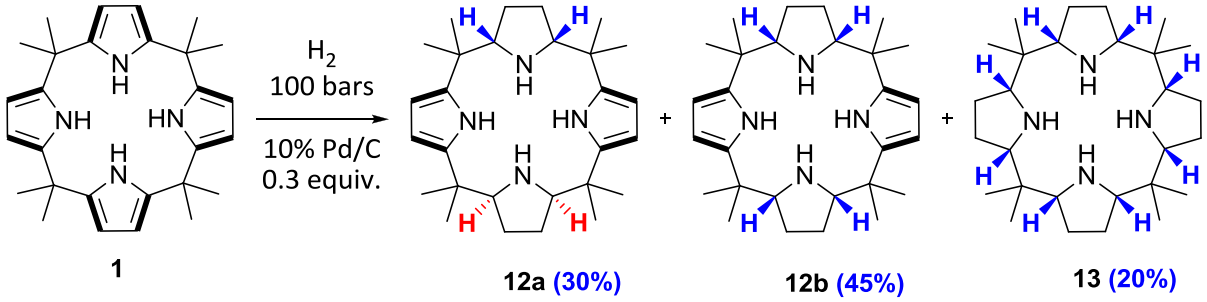

Scheme 11. Catalytic hydrogenation of calix[4]pyrrole **1**

The macrocycle **12b** also has the ability to form metal complexes (NMR investigation still under progress). Recently, we have been able to find conditions for the achievement of the complete reduction of macrocycle **13** starting from compound **12b**. The mechanism involved is not fully understood yet and is still under investigation.

1. INTRODUCTION

Many vital biological processes depend on the presence of macrocyclic metal prophyrin complexes. The electron transport by cytochrome c, the transport of oxygen by myoglobin or hemoglobin and most important (of all) the photosynthesis by chlorophylls are fundamental processes of life.[17-19, 132, 133] These complexes are, therefore, known as "the pigments of life" and are formed by condensation reactions of comparatively simple starting materials [34-37] in an early step of the biosynthetic pathway.[34, 36]

In view of their exceptional properties, the synthesis of porphyrins became a keenly contested research field and attracted wide attention. Numerous efforts have been made to create other synthetic nitrogen-containing macrocycles, such as triazacyclononanes, cyclens, cyclams and non-natural porphyrins and their chemical, catalytic and structural properties have been thoroughly studied.[64-66] The metal complexes of these ligands and their derivatives have found interesting applications as sensors, as contrast agents, in the detection and destruction of cancer cells and as oxidation and bleaching catalysts.[67-69] The scientific and economic importance of enantioselective catalytic processes combined with the challenges of developing "green", selective and efficient alternatives for traditional synthetic transformation has led to a large number of studies on catalysis. Synthetic nitrogen containing macrocycles have found many applications as catalysts e.g. in oxidation reactions.[70-76] There are two major mutually fertilizing approaches for these studies. In the first approach, one tries to understand the function and mechanism of enzyme catalyzed reactions by mimicking, with much simpler artificial systems, the active site. These studies have led to the quest for high-valent iron or manganese oxo species.[73, 74, 76, 77] In the second approach, one tries to obtain challenging but inherently very useful transformations like selective oxidation of small hydrocarbons like methane, ethane or propane, based on our understanding of the natural catalytic processes.[73, 78]

The cyclams and the porphyrins share the same "distance" between the two pairs of nitrogen atoms: a linker composed of three carbon atoms (Scheme 1). It is well known that rigidifying a linear tetradentate ligand restrains the geometry of the metal complex to one single conformation, leading to a more stable metal complex and thereby to a more efficient catalyst.[82, 83] Therefore, the fully flexible cyclam ligand and its metal binding properties have been intensively studied, as well as the bridged or "strapped" versions of this ligand.[87, 88, 90, 134]

We did not find reports on structures, where the additional cycles were added "externally" or in an "exocyclic" fashion to the basic macrocyclic structure in order to rigidify the skeleton.

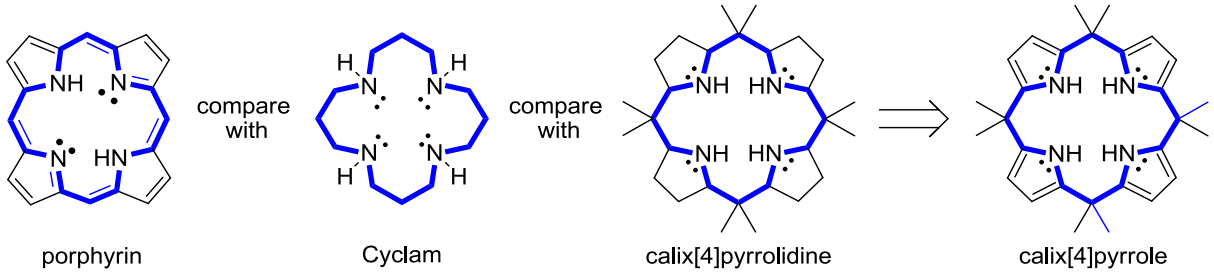

Figure 15. Comparison between the fully reduced calix[4]pyrrole, cyclam and porphyrin

In this context, we envisaged the synthesis of such a rigidified molecule, the calix[4]pyrrolidine presented in Figure 15 and the study of its metal binding properties. This new ligand could be obtained in a single hydrogenation step starting from the easily synthesized calix[4]pyrrole. In contrast to typical Werner type complexes, the nitrogen lone pairs of calix[4]pyrroles are part of the aromatic system of the pyrrole ring and are therefore not available for complexation of metal species. The analysis of the reported reactivity of calix[4]pyrroles led to the question: can the completely hydrogenated macrocycle be obtained and what would be the chemical characteristics of this saturated system? The lone pairs of the completely saturated macrocycle should become available for metal binding.

2. FIRST RESULTS ON HYDROGENATION OF CALIX[4]PYRROLE IN OUR GROUP (VALERIA BLANGY)

2.1. First success

To the best of our knowledge, the controlled reduction of calix[4]pyrrole (**1**) has never been reported before the publication of our own work. We embarked on a systematic research program with the aim of developing methods for the reduction of calix[4]pyrrole (**1**)[135]. We avoided conditions known to facilitate ring opening processes. As the synthesis of the macrocycle **1** is catalyzed by the presence of strong acids, we reasoned that the acidic reaction conditions leading to the macrocycle should also be able to open the macrocyclic structure. We therefore chose neutral conditions. Based on the reports of Lunn,[136] we tested Raney Nickel W_2 as catalyst, in a THF as solvent. Using freshly prepared Raney Nickel, we isolated unreacted starting material applying temperatures up to 120 °C and hydrogen pressures up to 100 atm. Applying temperatures of 150 °C to 220 °C and pressures finally reaching 150 atm,

partial destruction of the macrocycle **1** was observed, without any hint at the formation of a reduction product. Trials to hydrogenate the macrocycle **1** in ethanol with Pd/C also yielded solely recovered starting material. Following a literature precedence, we used Rh/C and acetic acid as solvent as reported in the publication.[137] To our surprise, no hydrogenation but also no destruction of the starting material occurred using conditions going up to 70 atm and 65 °C. Using a stronger acid, such as trifluoroacetic acid, led to the complete destruction of the macrocycle **1**. Using acetic acid as solvent for the hydrogenation may transform small amounts of the pyrrole rings into the protonated imminium form, destroying the aromaticity and thereby facilitating the hydrogenation. Even if these series of hydrogenations using Rh/C as catalyst did not achieve our goal, they paved the way to new experimental conditions. The recovery of the starting material proved that protonating conditions can be applied to the calix[4]pyrrole **1**, avoiding the detrimental ring opening reaction, at least to a large extend. We started testing hydrogenation using acetic acid either as additive or as solvent. This change of strategy induced the discovery of the first reduction process of the macrocycle **1**.[135] Using either mixtures of acetic acid in ethanol or pure acetic acid as solvent and catalysts like Pd/C, Rh/C, PdO, PtO_2 and $Pd/BaSO_4$ partial reduction of the macrocycle **1** could be observed. The hydrogen pressure for these reactions varied slightly between 80 atm and 90 atm and the temperatures used were between 50°C and 70°C. Using higher temperatures under these conditions led to a decrease in the isolated yield, which we attributed to an increase in the rate of the ring opening reaction.

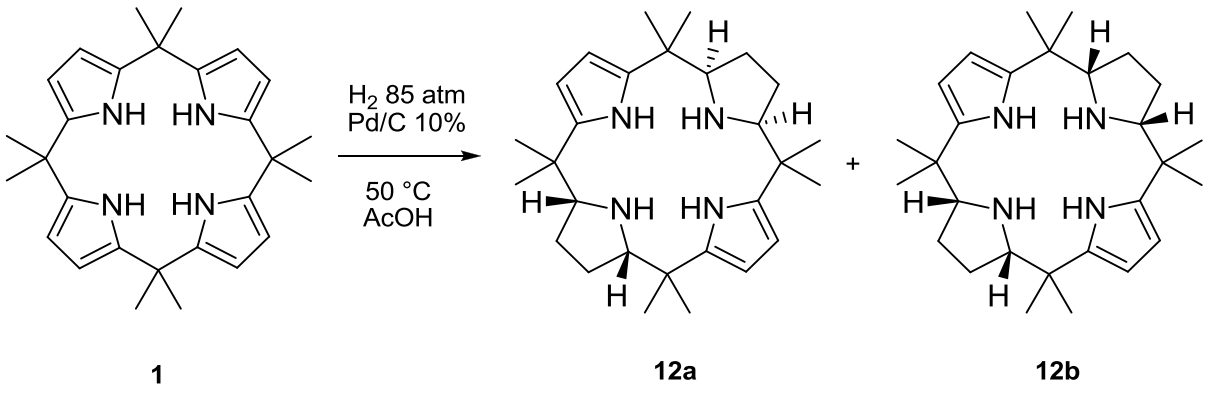

Scheme 12. Catalytic hydrogenation of calix[4]pyrrole **1** yielding a mixture of the diastereoisomers of **12a** and **12b** in 81% combined yield

Based on these observations, we preceded to a first optimization of the hydrogenation conditions. The hydrogenation of calix[4]pyrrole under 85 atm of hydrogen with a catalytic amount of palladium on charcoal (13 mol% Pd compared to the macrocycle **1**) in acetic acid

as solvent at 50°C for 16 hours, provided a mixture of two diastereoisomers of the half-reduced form of the macrocycle **12a** and **12b** (Scheme 12).[138] The structures were rigorously assigned based on spectroscopic data and finally with the help of X-ray analysis of the crystals.[130] As in the case of the hydrogenation of the calix[4]furan, only two of the seven possible stereoisomers were identified and characterized, namely **12a** and **12b**.

2.2. First isolation of the totally reduced calix[4]pyrrolidine 13

The only known reduction of a heterocyclic calix[4]arene, the hydrogenation of calix[4]furan, gave the completely saturated macrocycle (Scheme 8).[121] In contrast to these reports in the literature, the hydrogenation of calix[4]pyrrole **1** gave in our hands the partially reduced macrocyclic structure **12**. The initial attempts to achieve complete saturation of the calix[4]pyrrole macrocycle failed; no traces of a completely hydrogenated product could be detected. The degradation of the macrocycle was observed when temperatures higher than 150 °C were used. Increasing the hydrogen pressure to 150 atm with the same temperature, also led to degradation. By varying the type of catalyst (Raney nickel, rhodium on alumina, platinum on carbon, palladium oxide), the solvent (THF, EtOH/AcOH, dioxane, dioxane/AcOH, MeOH) or changing the quantities and the type of acid added (TFA, HCl, HBr) either no reaction occurred or only degradation was observed. After a long, fruitless period, we were able to observe the product of the total reduction of calix[4]pyrrole for the first time. We had to use harsh but carefully adapted conditions for the catalytic hydrogenation.[130]. Under these conditions, the calix[4]pyrrole **1** was transformed mostly into the partially reduced macrocycles **12a** and **12b**. Only a very small amount of the totally reduced product **13** could be isolated (initial yields were below 5 %) (Scheme 13).

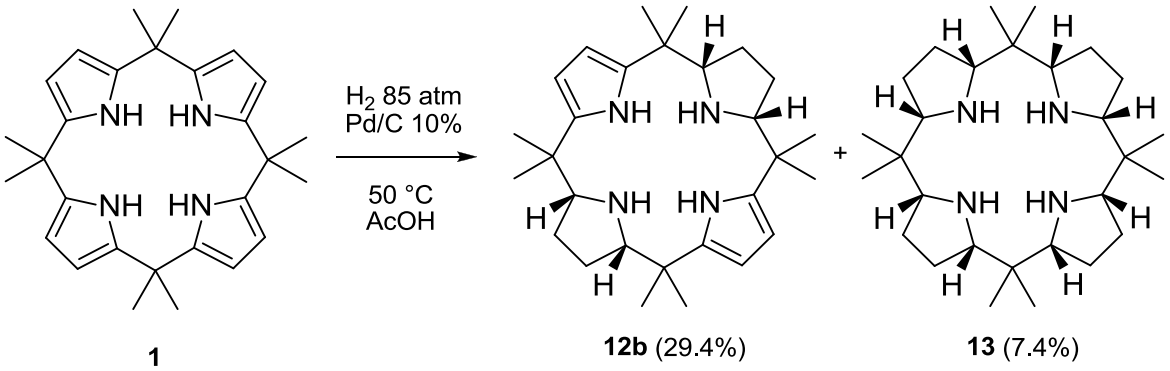

1 **12b** (29.4%) **13** (7.4%)

Scheme 13. Catalytic hydrogenation of calix[4]pyrrole (**1**) leading to the partially reduced macrocycle **12a** as the major product and to small amount of the macrocycle **13**

In a first intensive effort, we optimized the isolation of the new macrocycle **13** and fully characterized its structure. As mentioned before, using temperatures considerably above 100 °C, inevitably led to the destruction of the material. More surprising for us, was the fact that increasing the pressure to 150 atm also lead to the degradation of calix[4]pyrrole **1**. At this stage, the conditions for the reduction could not be varied and the yield of the totally reduced macrocycle **13** seemed to be limited to a value between 5% and 10%. We were clearly in the regime of a formation (yields below 20%) and not of a "real" synthesis. We, therefore, concentrated our efforts on obtaining reproducible reaction conditions and a reasonably easy isolation procedure. As a consequence of this first optimization, the following harsh conditions were systematically applied to create sufficient quantities of the macrocycle **13** for further studies: 100 atm of hydrogen in pure acetic acid at 100°C for 24 h using 10% palladium on charcoal.

2.3. Hydrogenation of the structurally different calix[4]pyrroles 14 and 15

In order to check if our conditions could be successfully applied to other calix[4]pyrroles, we tested the calix[4]pyrroles **14** and **15**. We were able to isolate the partially reduced products **16a**, **16b** and **17a** and **17b** in similar yields as for the simpler calix[4]pyrrole **1** (Scheme 13). The recovery of characterized material was, relatively poor. We attributed this to the sensitivity of the macrocycles **14** and **15** to the acidic reaction. Only 22% combined yield of **16a** and **16b** were recovered from the calix[4]pyrrole **14**. The amount of the half-reduced macrocycles **17a** and **17b** was slightly better when starting from compound **15**. A total of 30.6% could be isolated. Degradation of the starting material largely accounted for the remaining percentage. In both cases, the all-*cis* compounds **16a** and **16a** were, again, the major products of the hydrogenation, with a diastereomeric ratio of: **16a** : **16b** = 84 : 16 and **17a** : **17b** = 64 : 36.

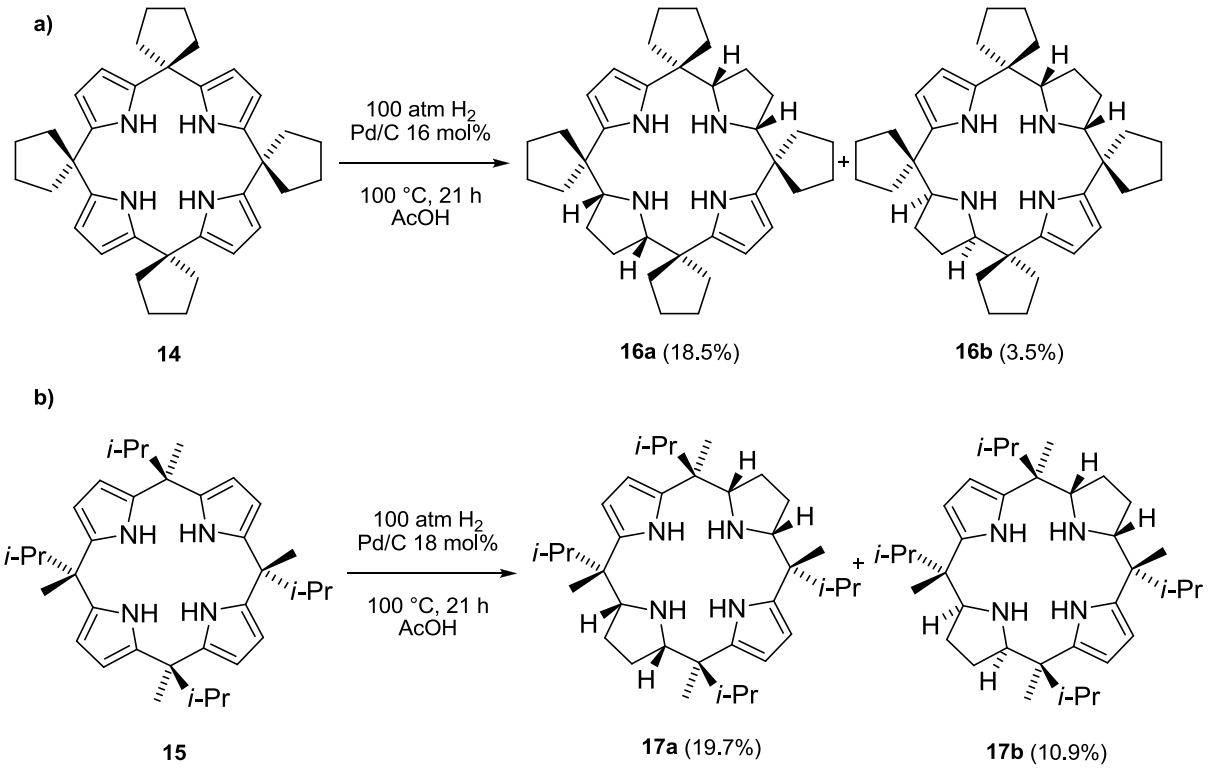

Scheme 14. Catalytic hydrogenation of meso-tetraspirocyclopentylporphyrinogen (**14**) and 5, 10, 15, 20-tetraisobutyl-5, 10, 15, 20-tetramethylporphyrinogen (**15**)

2.4. Complexation of calix[4]pyrrolidine (made Dr. Valeria Blangy)

Having the ligand **13** in our hands, complexation studies were undertaken using Cu^{2+} as the first metal. Spectrophotometric studies immediately indicated the formation of the copper complex **18** (Figure 16).

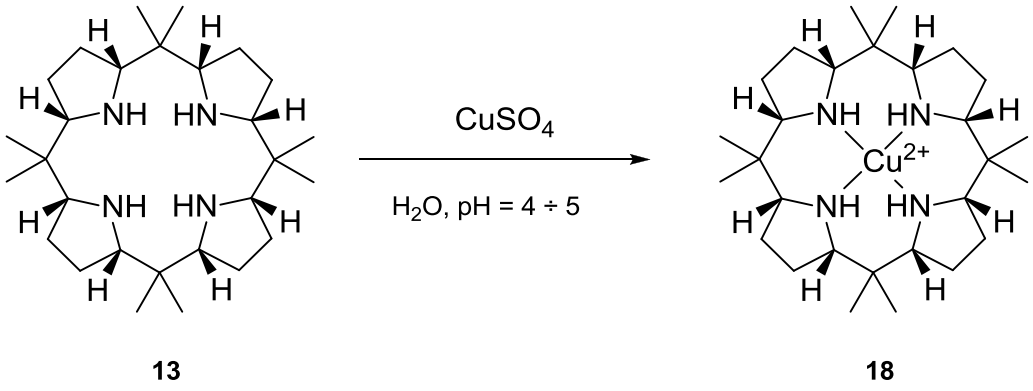

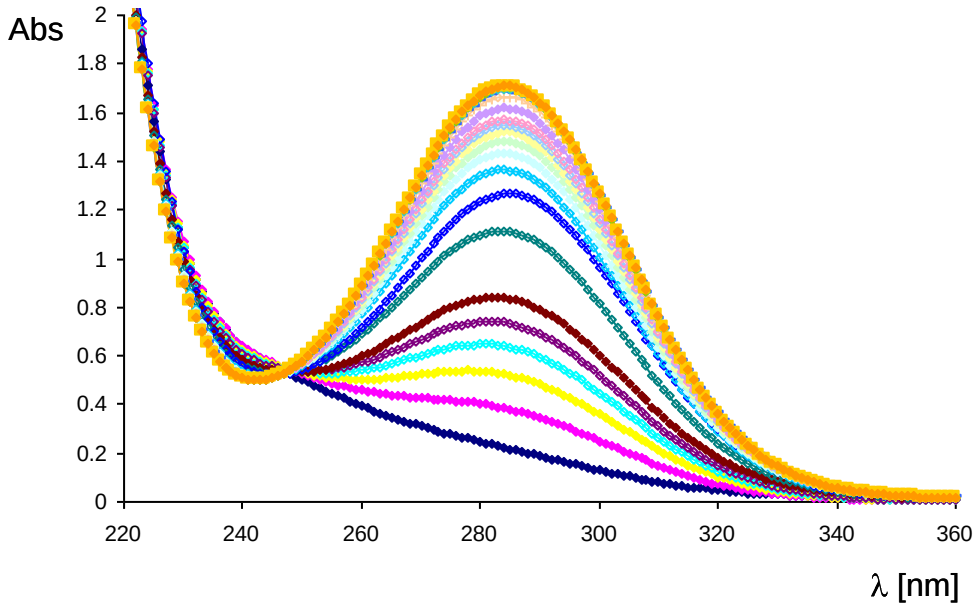

Figure 16. Complexation of **13** in an aqueous solution of $CuSO_4$ at pH = 4.5 and rt using equimolar concentrations of Cu^{2+} and **13** of 2 10^{-4} mol/L

The complexation is a relatively slow process with a second order constant of 48 mol^{-1} min^{-1}. The observed isosbestic point is in accordance with a process where only the starting materials and the product can be observed. No intermediate is detectable under those conditions. The chloride of the copper complex **18** crystallized and the X-ray structure of this complex was the first of a series of metal complexes studied in our group (Figure 17).

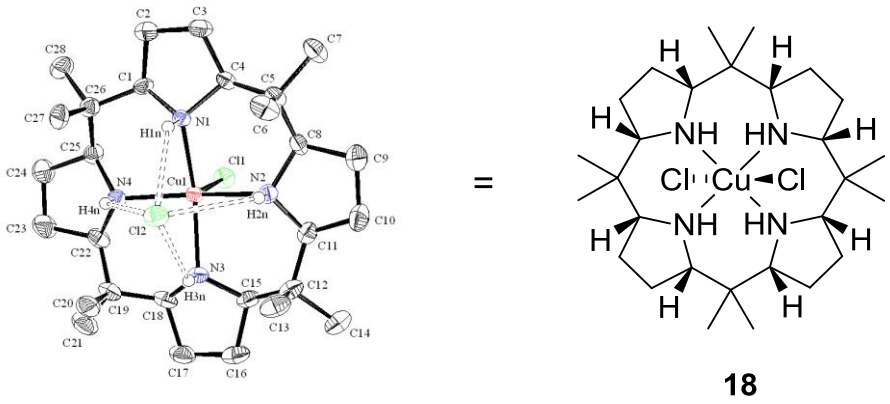

Figure 17. The X-ray structure of the copper complex **18** determined by Dr. Lydia Karmazin-Brelot working with the group of Professor Helen Stoeckli-Evans[130]

The structure of complex **18** proved to be prototypical for all the metal complexes, whose structures have been determined so far. The metal sits in the center of the macrocycle bound to the lone pairs of the four pyrrolidine nitrogen atoms. The coordination sphere of the metal is a distorted octahedron. One of the chlorides is in binding distance to the copper (2.4320(9) Å). The second chloride is kept in place by four hydrogen bonds to the N-H bonds of the pyrrolidine rings. The four N-H bonds form a sort of picket fence. The two faces of the macrocycle **18** are clearly differentiated in all the complexes we have studied so far.[129, 130]

After the characterization of the Cu(II) complex **18** the analogous Mn(II) complex **19** could also be characterized (Figure 18). The comparison of the edge-on view of the free ligand **13** and the Mn(II) complex **19** show that only minimal geometric and conformational changes are induced by the metal complex formation. One of the chlorides is directly bound to the Mn(II) whereas the other chloride is held in place with four hydrogen bonds. The two faces of the metal complex **19** are clearly differentiated. Preliminary experiments showed that manganese complexes of our ligand can function as a catalyst for epoxidation reactions on olefins. A detailed study of the scope and limitation of the epoxidation reaction, the influence of additives and preliminary studies on the mechanism has been recently published.[2]

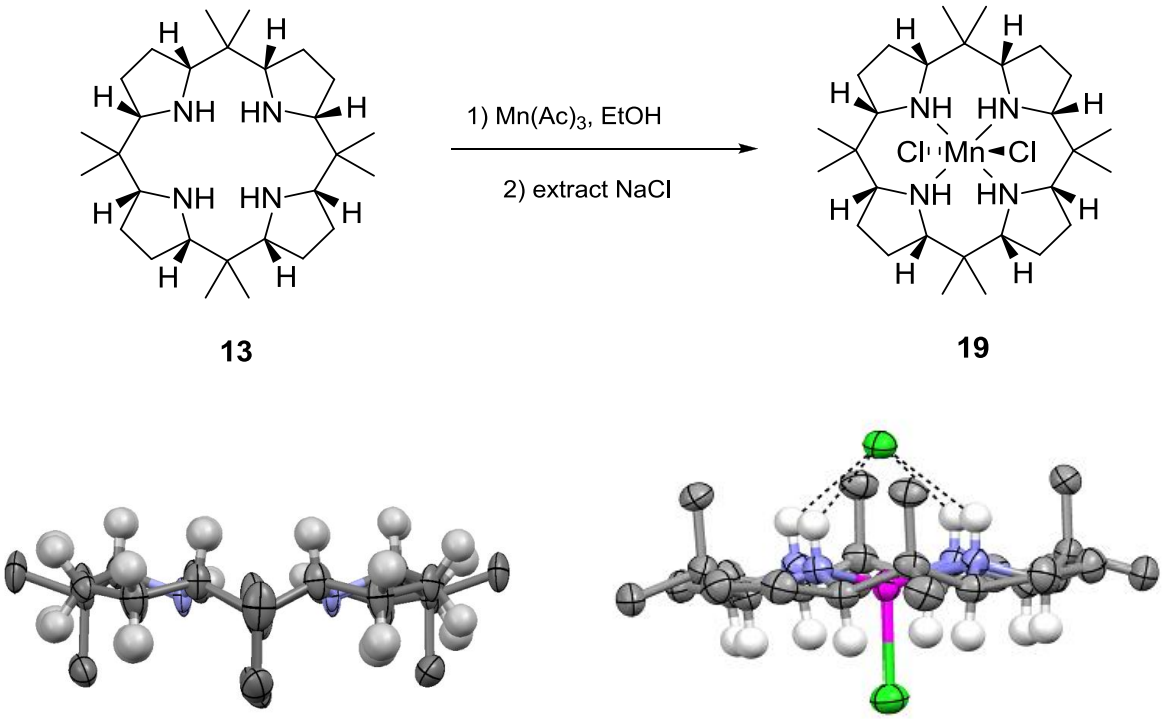

Figure 18. The synthesis of the Mn(II) complex **19** and its X-ray structure

3. HYDROGENATION OF CALIX[4]PYRROLE

A thorough study of the catalytic hydrogenation of calix[4]pyrrole **1** has been performed, using common as well as novel heterogeneous catalysts based on transition metals (Pd, Rh, Ru) supported on solid matrices (carbon, graphite, alumina) (Scheme 15). During our studies, we were able to isolate and identify two novel half-hydrogenated products, **12a** and **12c**, although the yield of the fully hydrogenated product **13** could not be improved. It is noteworthy that no other diastereoisomers of compound **13** were detected in the crude reaction mixtures.

Before starting the screening of the hydrogenation catalysts under different experimental conditions (solvent, temperature), we developed an easy and fast analytical protocol that allowed the qualitative and quantitative determination of the composition of the reaction mixtures. The GC analysis using the internal standard methodology proved to be the best tool:[22] *n*-eicosane was used as the internal standard (IS), which was added in exact amounts into each reaction mixture before running the hydrogenation.

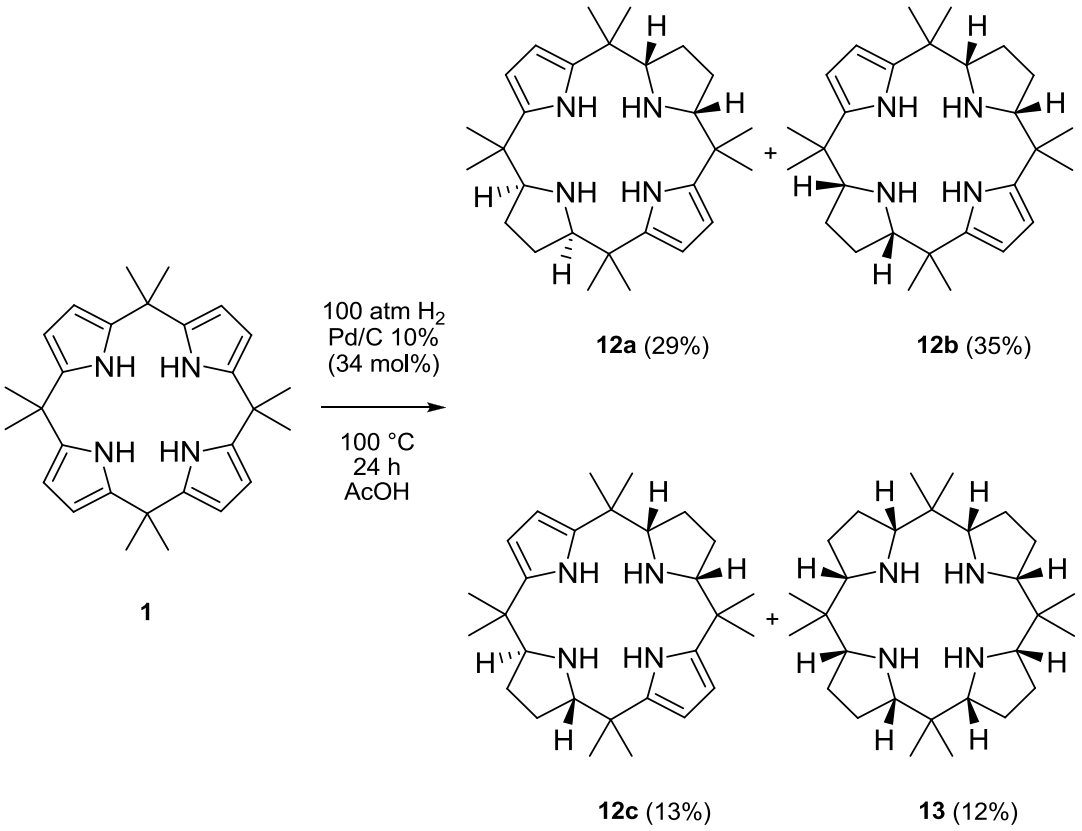

Scheme 15. Optimized catalytic hydrogenation of **1** giving the products **12a-c** and **13**

The method of isolation of the four products coming from the hydrogenation of calix[4]pyrrole **1** in large scale is presented Figure 19.

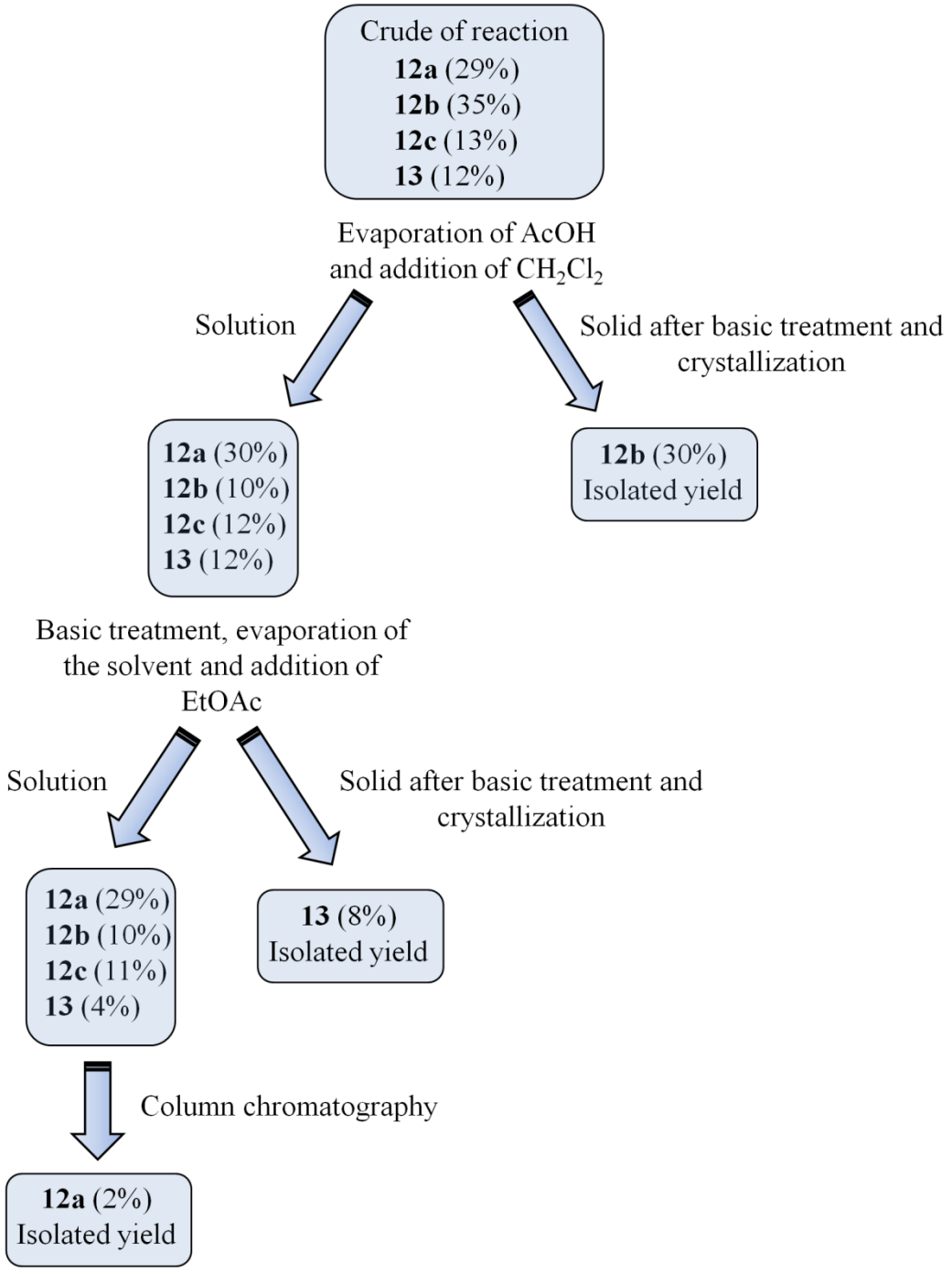

Figure 19. General description of the successive steps for the isolation of the four products

3.1. Calibration curve for control of hydrogenation reactions (made by Dr. Andrea Gualandi)

A series of solutions containing **12b**, **13** (2 mM each) and *n*-eicosane (internal standard, IS) in known amounts and variable ratios were prepared in CH_2Cl_2 by mixing different volume of standard solutions of **12b**, **13** and IS. Each solution (2 µL) was injected in GC (Agilent 6850A GC-system, column HP-1, length 3 m, I.D. 0.32 mm, film 0.25µm) by using the following temperature gradient: initial temperature 220 °C, 2 min., then heating 5 °C/min. up to 300 °C, further 6 min. at 300 °C). Calibration plots (Table 2, Figure 20) were prepared reporting the ratio (mmoles of IS)/(mmoles of **12b** or **13**) *vs.* the ratio (peak areas of IS)/(peak areas of **12b** or **13**).

Table 1. Retention time of different compounds in the reaction mixture.

Compound	Retention Time (min.)
n-eicosane	4.5
1	11.3
12a	15.9
12b	16.5
12c	17.3
13	19.4

Table 2. Data for the preparation of calibration plot.

mmol IS/ mmol **12b**	mmol IS/ mmol **13**	Area IS	Area **12b**	Area **13**	Area IS/ Area **12b**	Area IS/ Area **13**
4.14	4.72	2069.1	272.0	266.3	7.61	7.77
2.76	3.15	1389.0	286.3	270.5	4.85	5.13
1.72	1.97	876.0	341.0	268.0	2.57	3.27
1.52	1.73	708.9	325.8	252.8	2.18	2.80
1.10	1.26	515.5	367.5	294.9	1.40	1.75
0.83	0.94	378.5	320.3	270.7	1.18	1.40
0.62	0.71	192.7	292.5	198.7	0.66	0.97
0.55	0.63	167.1	320.6	268.8	0.52	0.62
0.28	0.31	56.0	322.4	255.7	0.17	0.22

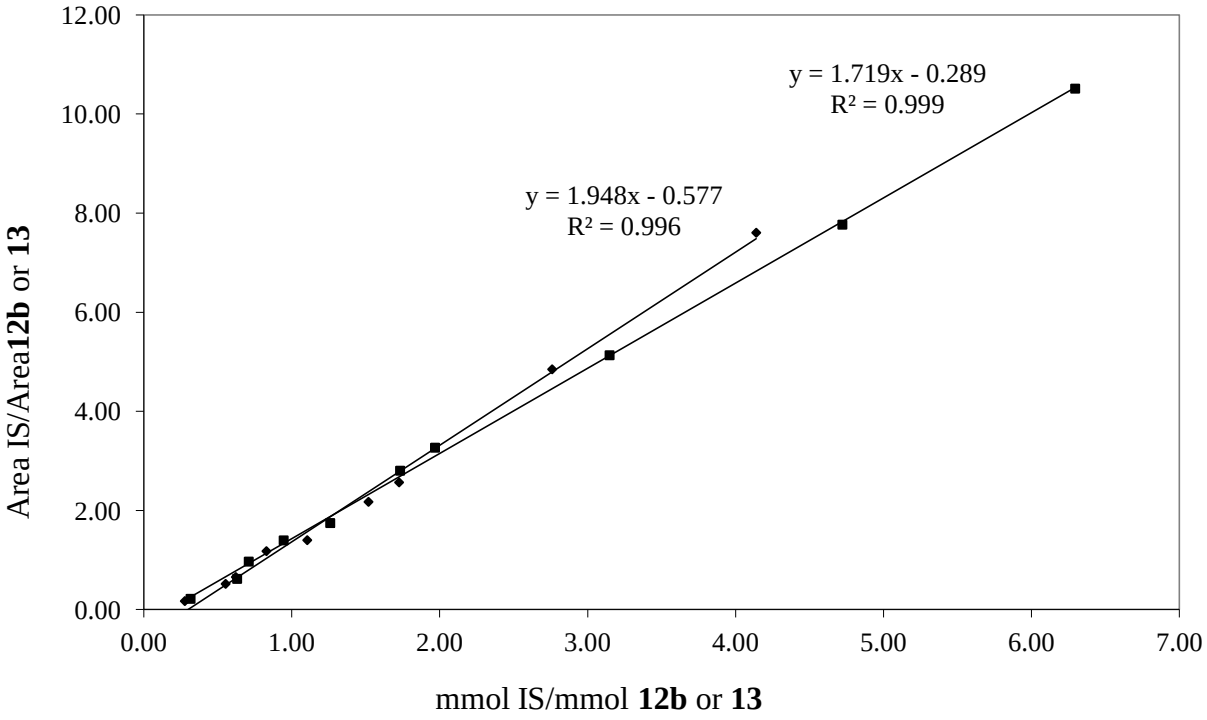

Figure 20. Calibration plot of the reduced compounds **12b** (■) and **13** (◆) referred to *n*-eicoesane (IS).

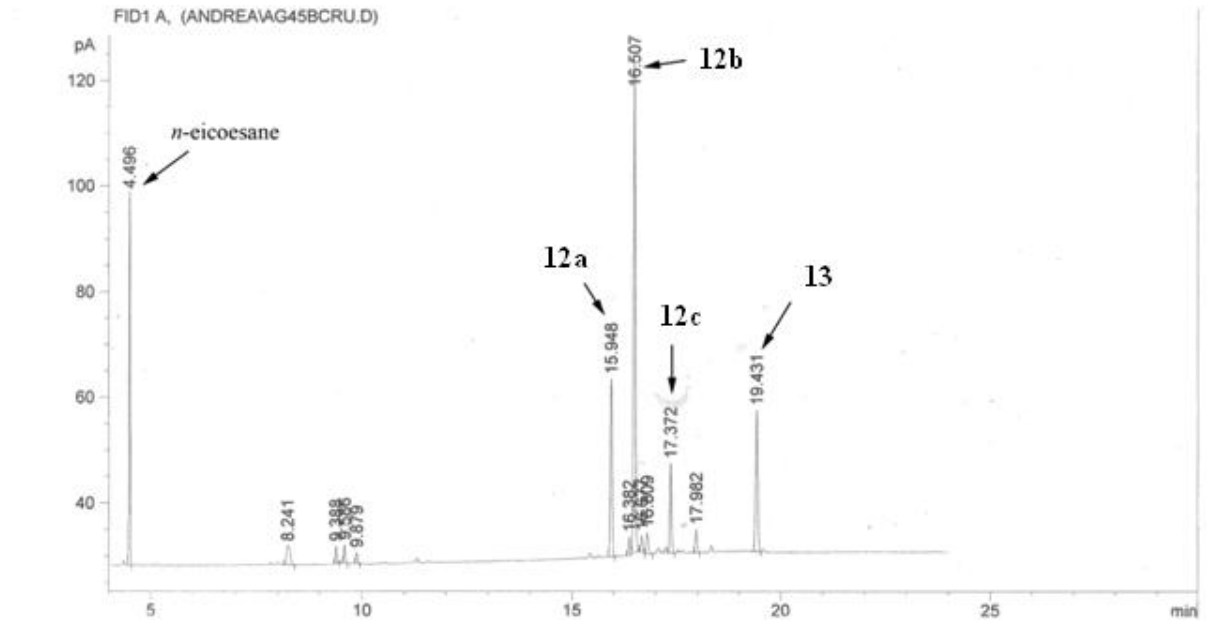

Figure 21. Copy of GC chromatogram of hydrogenation reaction.

Injection of a sample from the crude reaction mixture, obtained after basic treatment, gave the composition of the four characterized products. For the calculations we assumed that the products **12a**, **12b** and **12c** posses the same response factor. The amounts of the half-hydrogenated products **12a-c** and fully hydrogenated product **13** were calculated using the following equation:

$$mmol_{\mathbf{2}} = \frac{1.948 \cdot mmol_{\mathrm{IS}}}{\frac{Area_{\mathrm{IS}}}{Area_{\mathbf{12b}}} - 0.577}$$

$$mmol_{\mathbf{3}} = \frac{1.719 \cdot mmol_{\mathrm{IS}}}{\frac{Area_{IS}}{Area_{\mathbf{13}}} - 0.289}$$

A test reaction was performed to check the accuracy of the method. The products **12b** and **13** were isolated as described in the following Figure 21. After separation of the solid (**12b** or **13**), the solid was weighed and the residual amount of **12b** or **13** in the mother liquor was calculated by GC analysis using the IS methodology. For each compound the sum of the weighed amount and the residual amount in solution was very close to the yield calculated by GC analysis determined from the crude reaction product.

Dr. Andrea Gualandi developed this GC method based on the unconventional reverse response factor (IS)/(X) and the yield calculated during this study have been done respect to this choice.

3.2. Results and discussion

GC-MS analysis of the reaction mixtures allowed us to detect the formation of four major compounds: according to their molecular weight, three of them were diastereoisomers of the half-reduced product **12**, and one was the fully reduced compound **13** (Scheme 15). The diastereoisomers **12a** and **12c** of the half-reduced product, previously not detected, could be isolated in a pure form and characterized.

3.2.1. Screening of heterogeneous-catalyst (this work is the result of the common effort with Dr. Andrea Gualandi)

Table 3. Catalytic hydrogenations of calix[4]pyrrole **1**.[a]

Entry	Catalyst[b]	**12a**/**12b**/**12c**[b]	**13**[b]
1	10% Pd/C	25/40/14	16
2	10% Pd/C[c]	23/35/11	12
3	10% Pd/C[d]	29 (2)[e]/35 (24)[e]/13	12 (8)[e]
4	5% Rh/Al_2O_3	40/33/11	8
5	$C_{24}Rh$	43/31/12	9
6	$C_{24}Ru$	36/39/19[f]	5
7	$C_{16}Pd$	27/34/17	6
8	10% Pd/C	39/45/5[g]	12
9	10% Pd/C[h]	40/47/9	0
10	10% Pd/C[i]	26/36/15	16
12	5% Pd/C[j]	25/40/12	7
13	5% Pd/C[k]	17/25/14	18

[a] The reactions were performed in an autoclave on a 0.47 mmol scale in acetic acid (5 mL) at 100 °C for 24 h under 100 atm of H_2 pressure using a catalyst loading of 34 mol% of metal. [b] Yields (%) were calculated by GC analysis using the internal standard methodology. [c] Catalyst loading: 17% mol of metal. [d] The reaction was performed on a 4.70 mmol scale. [e] Isolated yield. [f] Traces of **1** were detected. [g] The reaction was performed for 24h, then 34 mol% of catalyst was re-added and the reaction was let another 24h. [h] The reaction was performed 4 times more diluted. [i] Pd/C source: Aldrich/basis; [j] Pd/C source: Evonik/eggshell oxidic (50% wet); [k] Pd/C source: Evonik/uniform oxidic (50% wet).

The crude reaction mixture obtained performing hydrogenation of **1** (0.47 mmol) in the previously described conditions (34% of 10% Pd/C, AcOH, 100 atm of H_2 pressure, 100 °C) was first analyzed. The three diastereoisomers **12a-c** (in order of GC elution) where compound **12b** was the prevalent one, were detected with a total yield of 79%, together with the fully reduced compound **13** which was formed in 16% yield (Table 3, entry 1). Reducing the relative amount of the catalyst to a 17 mol% (metal loading), resulted in a lower yield of both products **12** and **13**, which were formed with comparable ratio and diastereoselectivity (Table 3, entry 2).

Then hydrogenation under the former conditions was carried out in a larger scale (4.7 mmol of **1**) allowing the isolation of all the reaction products, which were formed with a similar

ratio as compared to the small scale reaction (Table 3, entry 3). The acetate salt of **12b**, precipitated from the crude mixture after evaporation of the solvent and addition of dichloromethane. The free-base **12b**, was obtained in 24% yield by treatment with aq. NaOH. Crystallization from ethyl acetate gave pure **12b** in 23% yield. Compound **12c**, featuring one *cis*- and one *trans*-2,5-disubstituted pyrrolidine rings, was isolated from impure **12b** by column chromatography (Al_2O_3, CH_2Cl_2/MeOH/Et_3N, 95/4.5/0.5) and by repeated recrystallizations in EtOAc. However, we have recently discovered a mistake we made on the characterisation of compound **12c**. Compound **12c** is actually a reduced form of an impurity present in calix[4]pyrrole **1** (see complete analyses and explanation in Chapter 2, 3.5.). Starting with a pure calix[4]pyrrole, we isolated only two products from the half-reduction of **1**, such as compound **12a** and compound **12b**.

Product **13** was recovered in 8% yield from the dichloromethane mother liquor after aq. Na_2CO_3 treatment, solvent evaporation and addition of ethyl acetate. This caused separation of **13** as an insoluble solid, whereas compound **12a** was isolated from the mother liquor as a solid by solvent evaporation and column chromatography (Al_2O_3) of the residue. Compound **12a** was purified by crystallization (EtOAc) and the relative configuration of the stereocenters was determined by an X-ray diffraction study.

Having identified and isolated all the products, which have been detected by GC and GC-MS analysis, we started the screening of different catalysts under the same experimental conditions, aiming to increase the relative amount of the fully reduced product **13**. The use of commercially available 5% Rh/Al_2O_3 in the same conditions resulted in a slight increase in the total yield of the partially reduced products **12a-b** and a concomitant fall of the yield of the totally reduced product **13** (Table 3, entry 4). Moreover, inversion of the diastereoselectivity occurred in the formation of the partially reduced products **12**, in favour of the diastereoisomer **12a**.

Professor Diego Savoia has been involved in the past years in the preparation of highly active zero-valent transition metals dispersed on graphite by reduction of the metal salt with potassium graphite C_8K, an intercalation compound of graphite.[139] Recently, rhodium on graphite ($C_{24}Rh$) was prepared and used as a catalyst for the hydrogenation of aromatic compounds, including pyrrole derivatives.[140, 141] When this catalyst was applied to the hydrogenation of calixpyrrole **1**, a slightly increased yield of **12** (86%) and almost the same diastereoselectivity were observed, but the amount of **13** did not increase significantly (Table 3, entry 5). Then we prepared a new catalyst, $C_{24}Ru$, in 97% yield by reduction of anhydrous $RuCl_3$ with 3 equivalents of C_8K. $C_{24}Ru$ showed a comparable activity and **12a** and **12b** were

mainly obtained in almost the same amounts (Table 3, entry 6). We observed that palladium on graphite, $C_{16}Pd$,[142] was slightly less effective than 10% Pd/C for the complete reduction of **1** to **13** (Table 3, entry 7). The increase of reaction time (2 x 24h) and amount of catalyst (64 mol%) did not afford significant changes in the ratio of the four products. Under high dilution conditions the totally hydrogenated product **13** was not detected but the reaction produced a good yield of compound **12a** and **12b** (Table 3, entry 9). We finally investigated the activity of palladium on charcoal from different providers. No significant changes on the yield of the totally reduced **13** were observed, the yield of partially reduced compounds **12** were similar to the ones observed with the other catalysts.

In conclusion, palladium on charcoal 10% remained the cheapest and best catalyst and we could obtain up to 16 % of the totally reduced calix[4]pyrrolidine **13**, which doubled the yield compared to our earlier experiments. Using the optimal conditions, such as of 10% Pd/C (0.36 equiv.), acetic acid as solvent at 100°C for 24h, we carried out the hydrogenation on a gram scale. Taking advantage of the difference in solubility and pH behavior or the products of the hydrogenation, we developed a method of separating the products by successive crystallization and thereby minimizing the use of chromatography for the separation.

3.2.2. Screening of the reaction media

3.2.2.1. Results

Then we changed the reaction medium. For this study, we selected the three catalysts (10% Pd/C, $C_{24}Rh$, 5% Rh/Al_2O_3) that gave the best results in the previously adopted experimental conditions (Table 2). At first, we wished to determine the effect of the acidity of the medium using the Pd/C catalyst, other experimental conditions remaining unchanged. We performed the hydrogenation with 10% Pd/C as the catalyst in 95:5 mixtures of acetic/sulphuric acids and acetic/trifluoroacetic acids. In both cases, no hydrogenation product was formed, (perhaps because of catalyst deactivation) and the starting compound **1** was not quantitatively recovered (Table 4, entries 1 and 2). No transformation was also observed in neat trifluoroacetic acid (TFA) at 70 °C using either Pd/C or Rh/Al_2O_3 (Table 4, entries 3 and 4), whereas the use of $C_{24}Rh$ in the latter conditions gave selectively **12b** in 55% yield (Table 4, entry 5).

On the other hand, in a 1:1 tetrahydrofuran-acetic acid mixture at 55 °C the formation of both the half-reduced products **12a-c** and the totally hydrogenated product **13** was observed using

either one of the three catalysts (Table 2, entries 6-8). Similar results were obtained in 1:1 methanol/acetic acid mixture (Table 4, entries 9-11). However, the total yields of the reduced products and the diastereoselectivities for compounds **12** were low in all cases. It is surprising that compound **13** was obtained in higher yield in the less acidic medium and at lower temperatures.

The poor solubility of **1** and/or **12** in the solvent mixtures is probably responsible for the low yields obtained. The choice of the solvent appears to be crucial to achieve satisfactory results. Surprisingly, we noticed that performing the reaction with Pd/C in 80:20 acetic acid-water mixture at 100°C generated compounds **12a** and **12b** with pleasing 36 and 57% yields, respectively. Finally, only small quantities of **12b** were observed then the reaction was performed in acetone and using tartaric acid as acid (Table 4, entry 13)

Table 4. Catalytic hydrogenations of calix[4]pyrrole **1** in different media.[a]

Entry	Catalyst	Solvent/Additive	*T* (°C)	**12a**/**12b**/**12c** [b]	**3**[b]
1	10% Pd/C	AcOH/H_2SO_4 (95/5)	100	-[c]	-
2	10% Pd/C	AcOH/TFA (95/5)	100	-[c]	-
3	10% Pd/C	TFA	70	-[c]	-
4	5% Rh/Al_2O_3	TFA	70	-[c]	-
5	$C_{24}Rh$	TFA	70	0/55/0	-
6	10% Pd/C	THF/AcOH (1:1)	55	16/26/9[d]	6
7	5% Rh/Al_2O_3	THF/AcOH (1:1)	55	32/20/8[e]	4
8	$C_{24}Rh$	THF/AcOH (1:1)	55	23/14/11[e]	0.4
9	10% Pd/C	MeOH/AcOH (1:1)	55	18/17/4[d]	2
10	5% Rh/Al_2O_3	MeOH/AcOH (1:1)	55	21/12/5[e]	-
11	$C_{24}Rh$	MeOH/AcOH (1:1)	55	9/5/3[e]	-
12	10% Pd/C	AcOH/H_2O (8/2)	100	36/57/0[e]	-
13	10% Pd/C	Acetone/Tartaric ac.	25	13/0/0[e]	-

[a] The reactions were performed in an autoclave using a catalyst loading of 34 mol% of metal under 100 atm of H_2 pressure for 24 h. [b] Yields (%) were calculated by GC analysis using the internal standard methodology. [c] Decomposition of the starting material **1** was observed. [d] Traces of **1** were detected. [e] Starting material **1** largely accounted for the remaining percentage.

Kuwano and co-workers reported the enantioselective catalytic hydrogenation of *N*-Boc-pyrroles to pyrrolidines using chiral homogeneous ruthenium catalyst.[143] Our attempt to

hydrogenate the calix[4]pyrrole **1** by the analogous ruthenium-based procedure without chiral ligands was unsuccessful.

3.2.2.2. Discussion

Summarizing our results, acetic acid remains the best solvent for the hydrogenation of calix[4]pyrrole **1**. It is important to note that the calix[4]pyrrole **1** is extremely sensitive to acid. Traces of acid, for instance traces of HCl in deuterated chloroform, inevitably led to degradation. However, the use of acid (or at least catalytic amounts of acid) is needed to achieve the hydrogenation of our heterocycles. We were directly confronted to the following paradox: we needed to use conditions for the hydrogenation of macrocycle **1** under which the starting material is not stable. Our only chance was to bet on the relative rate of the two competing reactions: if the hydrogenation was faster than the degradation the reduction would be possible. However, the problem of mixing all reagents before the introduction of hydrogen pressure remained; we would systematically lose a part of the starting material. We were, finally, very pleased to find acetic acid for the hydrogenation of **1**. Using this acid as solvent avoided the problems described above thanks to the following reasons: 1) At room temperature, calix[4]pyrrole **1** is not soluble in acetic acid or the solubilization is very slow. Therefore compound **1** is stable enough as suspension in this solution and no degradation occurred before the introduction of H_2 pressure. 2) When we started the reaction, we first introduced the pressure of H_2 and then increased the temperature. Increasing the temperature led to the solubilisation of the macrocycle **1** and then, competition between the acid catalyzed degradation and the acid catalyzed hydrogenation occurred. Under optimized conditions the yields are around 95%. The hydrogenation reaction has therefore to be faster than the degradation (Scheme 16).

The use of stronger acids than acetic acid inevitably involved the problems described above which led to the degradation of **1**. To rationalize our experiments we came to the following conclusions: 1) If we partially solubilize **1** (with a strong acid for instance) before the introduction of the hydrogen (*i.e.* during the preparation of the reaction) the degradation of the starting material was observed; 2) During the reaction process the hydrogenation of the macrocycle **1** has to be faster than the degradation if we can isolate reduction products.

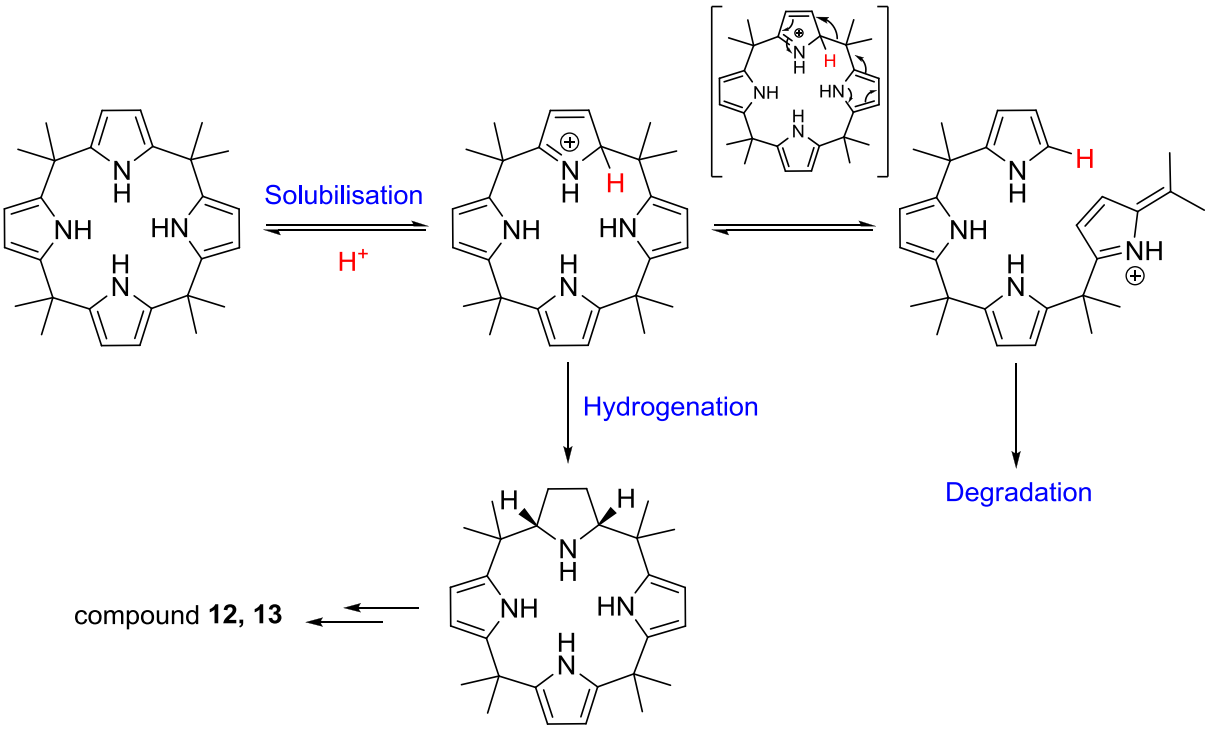

Scheme 16. Degradation versus hydrogenation of calix[4]pyrrole **1**.

The success of the reduction of **1** in acetic acid was largely due to the relative rates under the reaction conditions favoring the hydrogenation versus degradation. As the degradation occurred quickly in acetic acid in the absence of hydrogen, hydrogenation must be faster than the degradation processes. If this is true the "standard" reaction time of 24 hours was much too long. For this reason, we then decided to systematically study the degradation of calix[4]pyrrole **1** in acetic acid at 100°C (*i.e.* best condition of hydrogenation). This investigation gave us valuable information for a further optimization of the hydrogenation time.

3.2.3. Degradation of calix[4]pyrrole

3.2.3.1. Results

This investigation was made to test the stability of the macrocycle **1** under the standard condition of hydrogenation. To characterize the stability of **1** we will determine the reaction rate for the degradation. We will compare this rate with the reaction time used for the hydrogenation of **1**. With these data we can then optimize the time of the reaction.

3.2.3.1.1. Calibration curve

We measured first the calibration curve required to quantify the starting material in GC. The experimental procedure was similar to the one described previously: a solution containing **1** and *n*-eicosane (internal standard, IS) in known amounts and variable ratios were prepared in CH_2Cl_2 by mixing different volumes of standard solutions of **1** and IS. Each solution (1 μL) was injected in GC by using the following temperature gradient: initial temperature 220 °C, 2 min., then heating 5 °C/min. up to 300 °C, further 6 min. at 300 °C). The calibration plot (Table 5, Figure 22) was prepared reporting the ratio (mmoles of **1**)/(mmoles of IS) (x axis) *vs.* the ratio (peak areas of **1**) /(peak areas of IS) (y axis).

Table 5. Data for the preparation of calibration plot.

mmol C20	mmol calix	C20/calix	A C20	A calix	$A_{C20}/A_{\mathbf{1}}$
0.0708	0.0058	0.082	1235.66	88.59	0.072
0.0354	0.0058	0.165	1299.21	207.91	0.160
0.0283	0.0058	0.206	943.12	185.04	0.196
0.0177	0.0058	0.330	854.01	267.46	0.313
0.0088	0.0058	0.659	622.00	335.48	0.539
0.0053	0.0058	1.099	512.00	523.77	1.023
0.0035	0.0058	1.648	311.18	456.64	1.467

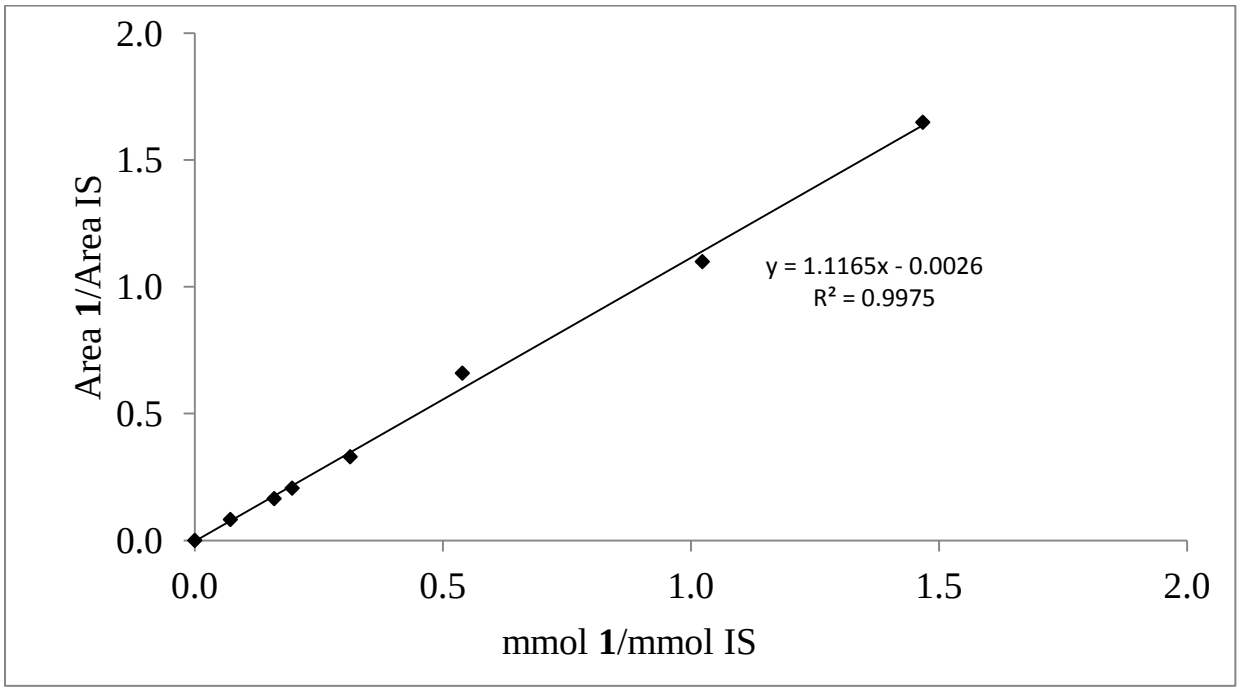

Figure 22. Calibration plot of the reduced compounds **1** (■) referred to *n*-eicoesane (IS).

3.2.3.1.2. Monitoring of the degradation of calix[4]pyrrole **1**

The degradation of calix[4]pyrrole **1** was investigated with the described GC method using *n*-eicosane as the internal standard (IS). The reaction was performed in acetic acid at 100°C in a two-necked flask with a condenser. When the solution reaches the right temperature (100 °C) we start the experiment with time t=0. We take samples at time t, which are injected in the GC after basic treatment followed by filtration on Millipore filter. Using our calibration curve we transformed the GC signal into the amount of compound **1**. The remaining amount of substance **1** in solution was calculated using the following equation:

$$n_{\mathbf{1}} = n_{IS}.\, x$$

where:

$$x = \frac{A_{\mathbf{1}}}{A_{IS}.\, 1.116} + \frac{0.002}{1.116}$$

with A_{IS} is the area of the internal standard.

3.2.3.1.3. Reaction order

The degradation of calix[4]pyrrole **1** is certainly a complex process. The first steps in this process are probably intermediates of the type described in Scheme 17.

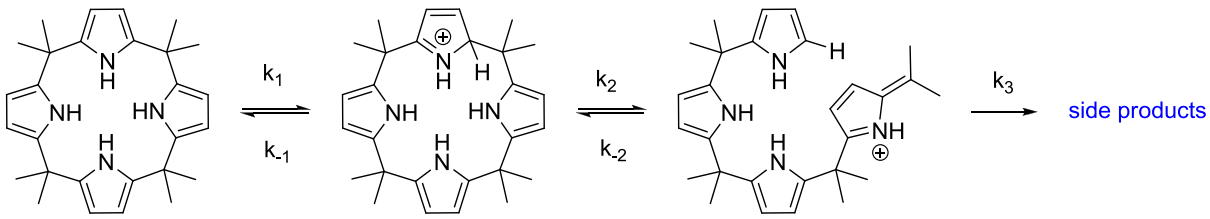

Scheme 17. Mechanism of the degradation of calix[4]pyrrole **1**

The protonation of compound **1** after solubilization gives the intermediate **II**. This intermediate is in equilibrium with its ring opened form **III**. Then the intermediate **III** can react in different ways: 1) react with another molecule; 2) continue to be degraded in smaller units (mechanism similar to the retrosynthesis of **1**); 3) intramolecular reaction to come back to **II**. The determination of the reaction order is therefore not obvious; however, some approximations can simplify this problem.

First approximation: we can suppose that the quench during the workup is fast. Therefore, the quantity of **1** measure in GC experiment corresponds to the quantities of **I** and **II**. In our scheme the side products are represented by **III** and **IV**.

Second approximation: $k_3 >> k_{-2}$ means that the rate limiting step of the degradation is the ring opening. The rate of degradation can then be written as:

$$V_{degradation} = d[\mathbf{III}]/dt = k_2\,[\mathbf{II}]$$

Third approximation: the equilibrium between **I** to **II** is very fast:

$$[\mathbf{II}] = K.\,[\mathbf{I}].\,[H^+]$$

So:

$$V_{degradation} = k_2.\,K.\,[\mathbf{I}]\,[H^+]$$

The reaction was performed in pure acetic acid and therefore the concentration of H^+ is constant, we obtained a pseudo-first order reaction, which can be simplified:

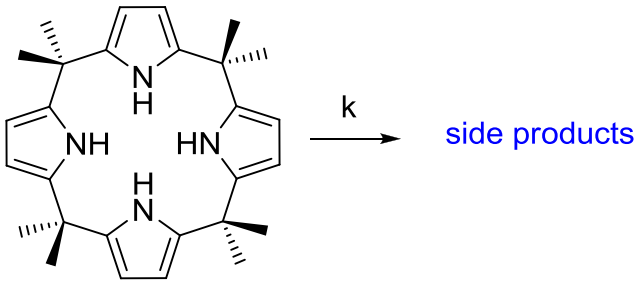

the degradation rate is written $V_{degradation} = k[\mathbf{I}]$; where $k = k_2.k_1.[H^+]$

In conclusion, the degradation rate should be proportional to the concentration of calix[4]pyrrole **1** (a pseudo first order reaction).

3.2.3.1.4. Degradation of calix[4]pyrrole **1** in acetic acid at a concentration of 0.023 M

The reaction has been performed using calix[4]pyrrole (0.202 g) in acetic acid (0.023 M). The result of the degradation experiment is documented in Table 6 and Figure 23. In Figure 23 the amount of substance reaming in solution (%) *vs.* the time (minute) is plotted.

Table 6. Data for the preparation of the degradation plot.

time (min)	A_{C20}	A_{calix}	mmol $_{Calix}$	Normalized
0	36.9	231.9	0.000260	100
5	17.2	93.0	0.000240	92
10	13.0	68.7	0.000237	91
20	22.7	115.2	0.000232	89
30	15.5	75.0	0.000225	86
40	17.9	84.1	0.000222	85
180	18.5	72.8	0.000199	76
240	15.9	57.2	0.000188	72
300	7.67	25.4	0.000178	68
360	14.3	43.1	0.000167	64

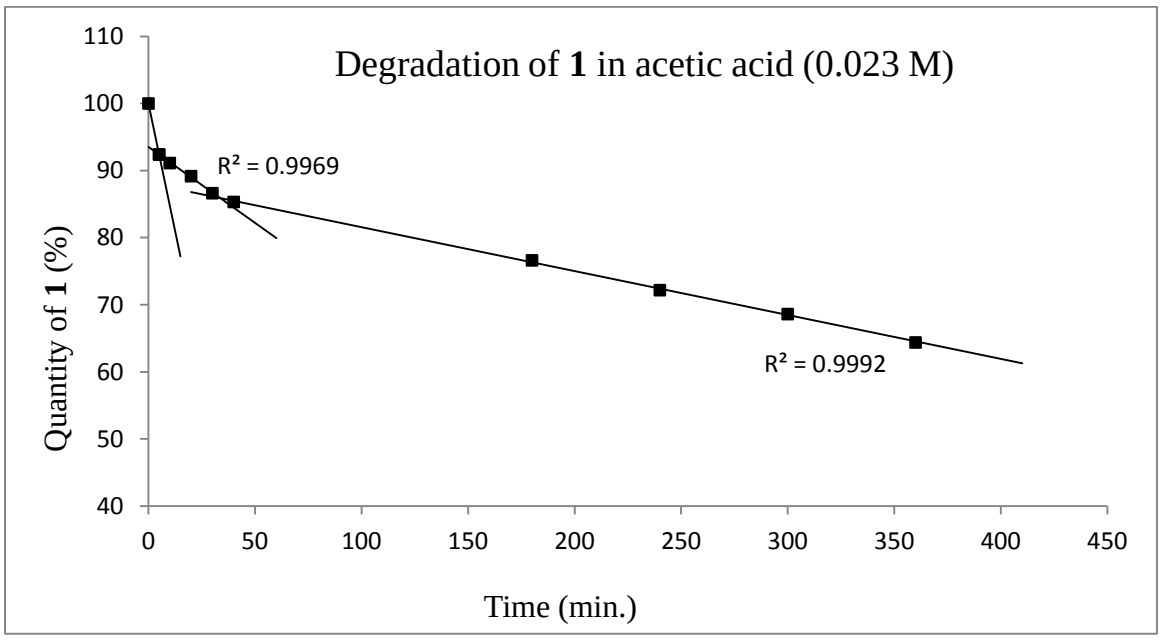

Figure 23. Degradation curve of the calix[4]pyrrole in acetic acid (0.023 M) at 100°C.

The graphic obtained from ln [**1**] according to the time was not linear. The shape resulting plot is by far the expected plot for a first or a pseudo-first order reaction. For this reason we decided to present only "the results observed" (the quantities of starting material according to the time) without any treatment. The degradation seems to be much more complicated than expected. The reaction rate is not related to the concentration of **1** in solution.

The plot can be divided in three parts and the three different slopes observed, are directed related to their reaction rate. Nevertheless, considering these surprising results, we wished to

vary the concentration in order to confirm the previous results, obtain more information on the reaction or maybe find other kinds of results.

3.2.3.1.5. Degradation of calix[4]pyrrole **1** in acetic acid at a concentration of 0.011 M

The second reaction has been performed using calix[4]pyrrole (0.102 g) in a more diluted media at a concentration of 0.011 M. The experimental results are documented in Table 7 and Figure 24.

Table 7. Data for the preparation of the degradation plot.

time (min)	A_{C20}	A_{calix}	mmol $_{Calix}$	Normalized
0	66.5	339.9	0.000256	100
10	70.4	243.4	0.000202	78
20	71.3	238.4	0.000197	77
30	65.1	212.2	0.000194	75
40	76.5	246.4	0.000192	75
50	73.3	227.7	0.000188	73
60	67.7	207.9	0.000186	73
90	77.3	211.4	0.000172	67
110	69.0	177.6	0.000164	64
120	57.7	144.5	0.000161	63
190	72.3	157.6	0.000146	57
270	65.1	125.8	0.000133	52
300	66.5	339.9	0.000127	49
370	70.4	243.4	0.000113	44
420	71.3	238.4	0.000103	40
490	65.1	212.2	0.000088	34

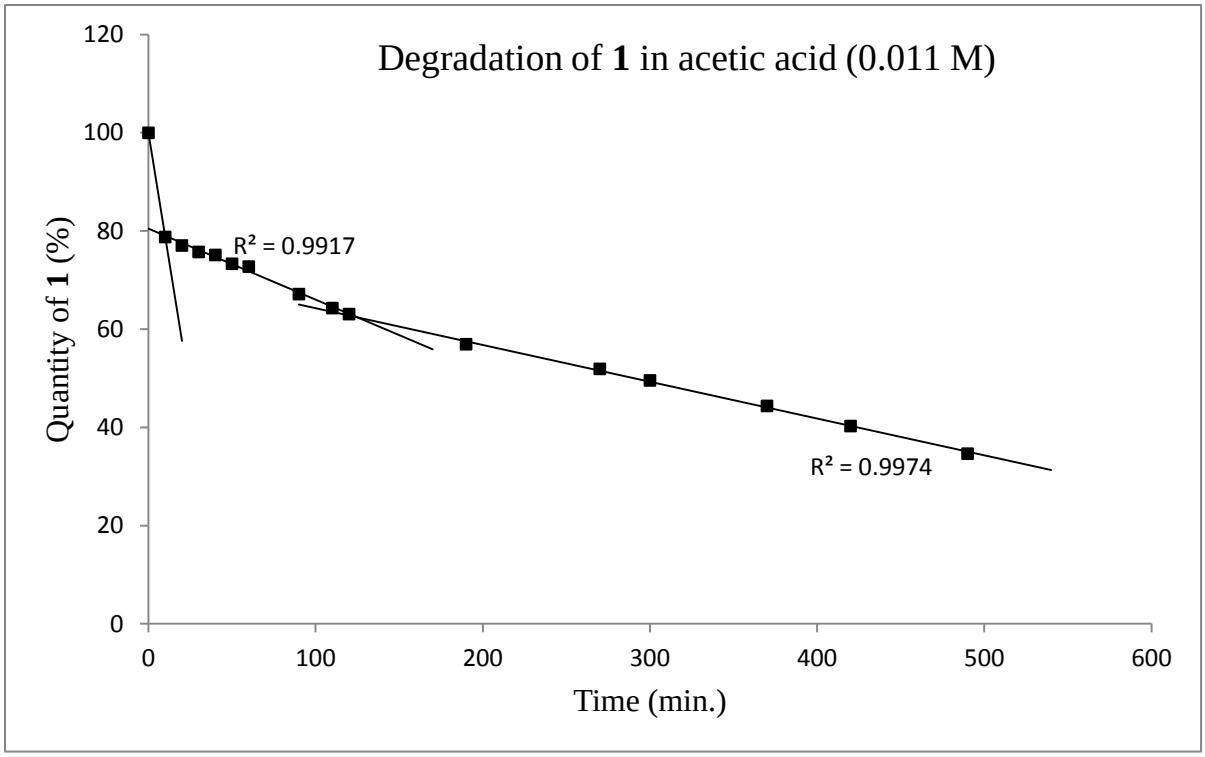

Figure 24. Degradation curve of the calix[4]pyrrole in acetic acid (0.011 M) at 100°C.

The rate of the degradation is considerably higher. At high concentration (= 0.0.23 M) the amount of starting material converted after 5 hours was 32% (=68% of starting material **1** still present), whereas in the experiment using a more diluted solution (= 0.011 M) 51% (49% of starting material **1** detected) after 5 hours.

3.2.3.2. Discussion

The degradation of **1** cannot be reduced as a simple reaction with a simple pseudo-first order kinetics. The process is concentration dependent. Higher concentrations protect the starting material against degradation, by a mechanism, which is not evident at this point. We have to assume a change in mechanism as a function of the concentration. We decided not to pursue the mechanistic studies at this point. At this stage these results are interesting and useful for the further optimization of the hydrogenation of compound **1**. As described above, we know that the hydrogenation has to be faster than the degradation. Our studies of the degradation clearly show that we should lose 11% or 23% of the starting material in the first 20 minutes. Under our optimized conditions we recovered 90 to 95% of the starting material as a mixture of products. We can therefore conclude that the hydrogenation reaction is a fast process, and that the reaction time for this reaction should be considerably shorter than the 24 hours we

used under our standard conditions. We decided to optimize the reaction time.

3.2.4. Final optimization

Considering the previous results on the degradation of calix[4]pyrrole **1**, which had shown that the hydrogenation is faster that the degradation, we assumed that the hydrogenation time can be shortened. All the previous reactions were performed during 24 hours according to procedure reported by Valeria Blangy. We decided to optimize the reaction time and then the amount of palladium on charcoal which is supposed to influence the kinetic of the hydrogenation.
The following investigation has been done using a pure calix[4]pyrrole **1** (99% GC) as starting material.

For this investigation, we wished to determine the optimal reaction time and the smallest amount of catalyst possible to perform the reaction (Table 8).

Table 8. Final optimization of the catalytic hydrogenations of calix[4]pyrrole **1**[a]

Entry	Catalyst	Cat. (mol%)	Time (h)	Conversion of **1**	**12a**/**12b** [b]	**13**[b]
1	10% Pd/C	0.36	4	100	36/50	8
2	10% Pd/C	0.16	2	100	34/48	10
3	10% Pd/C	0.16	1	100	31/43[c]	1
4	10% Pd/C	0.08	1	100	23/33[c]	1
5	10% Pd/C	0.04	1	90	23/26[c] [d]	0.5

[a] The reactions were performed in an autoclave using AcOH (5mL) as solvent, 100 bars of H_2, at 100°C. [b] Yields (%) were calculated by GC analysis using the internal standard methodology. [c] Side products were observed coming from the degradation of **1**. [d] A new product has been identified with 25% yield (see text).

We first started our study by decreasing the reaction time by a factor 6. The hydrogenation of compound **1** using acetic acid as solvent, 36 mol% of Pd/C 10% at 100°C for 4h afforded the half-reduced compound **12a** and **12b** and the totally reduced compound **13** with an overall yield of 94% (Table 8, entry 1). The remaining percentage was attributed to unidentified side products. Total consumption of the starting material was observed and the yield obtained for the hydrogenation of **1** was similar that those performed during 24h. We were pleased to observed similar results even by decreasing the reaction time to 2h and decreasing the amount

of palladium by 16 mol% affording 92% overall yield (Table 8, entry 2). Unfortunately, by decreasing the reaction time to 1h, formation of side products was observed in the crude reaction mixture (GC) and the hydrogenated products **12** and **13** were obtained with 75% yield (Table 8, entry 3). The formation of side products might be explained by the following hypothesis: when we stop the reaction after one hour of reaction the remaining starting material is completely solubilised. To lower the temperature of the autoclave needs time (almost two hours). Under these conditions the degradation of the remaining solubilised starting material **1** might be faster than hydrogenation creating the side products visible in GC. It is worth noting that only 1% of the totally reduced compound **13** was observed, it means that the formation of this products is slower than the formation of half-reduced compounds. This observation will be analysed thoroughly in the next chapter (Chapter 2, 4.1.).

In order to control the influence of decreasing the amount of palladium catalyst, we performed the reaction with 8 mol% of Pd/C 10% during 1h (Table 8, entry 4). The reaction was so slow to produce large quantities of side products. The compounds **12** and **13** were obtained with 57% overall yield. It is interesting to note that by decreasing the quantity of palladium by a factor of 2, the reaction rate is still acceptable regarding the yield of compound **12** and **13**. Finally we decreased the quantity of palladium to 4 mol%. We performed the reaction for 1h in order to avoid the total consumption of the starting material with the hope to be able to observe an intermediate (Table 8, entry 5). Under these circumstances, we were able to avoid the total consumption of **1** and we were pleased to observe a new product with 25% yield. This compound has been characterized by GC-MS but not isolated. The MS of this compound is compatible with the structure **20** (Figure 25). If the proposed structure is correct **20** would be an intermediate in the formation of compound **12** and **13**.

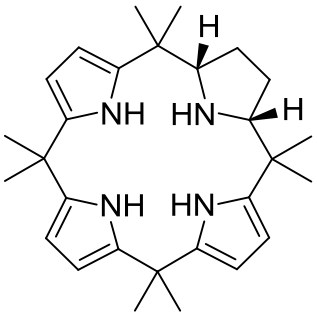

20

Figure 25. Intermediate compound **20** in the catalytic hydrogenation of calix[4]pyrrole **1**.

3.3. Studies and discussion of the mechanism

At this stage a series of questions arose:

1) Why is the hydrogenation stopping at the stage of the bis-reduced macrocycles of type **12**?
2) Why did we identify only the alternating bis-reduced macrocycles of type **12**? In all our products, the pyrrolidine rings and the pyrrole rings alternate. We have found no signs of products where the two pyrrolidine rings are contiguous.
3) Why is the yield of the totally reduced macrocycle **13** so low?
4) Are the partially reduced macrocycles of type **12** intermediates on the way to the totally reduced macrocycle **13**? Or, alternatively, is the compound **13** formed in a different sequence and if this is the case, what is the sequence?

We suggest the following mechanistic hypothesis for the hydrogenation of the calix[4]pyrrole **1**, which rationalizes most of the questions and remarks mentioned above. As the presence of acetic acid is compulsory for a successful hydrogenation, we assume that the reduction is starting from the small quantity of protonated calix[4]pyrrole **I** (Scheme 18). The protonation of one of the pyrrole rings destroys the aromaticity of the heterocycle and creates an electron poor π-system, avoiding the necessity to reduce an electron rich pyrrole. If this assumption is correct, the central intermediate for the hydrogenation is the protonated form **I**. The central intermediate **I** should be amenable to efficient hydrogenation giving an intermediate of the structure **II**. Alternatively, the hypothetical intermediate **I** can undergo ring opening to give the intermediate **III**. This reaction is the reverse reaction to the final step in the synthesis of calix[4]pyrrole **1**. In contrast to the hydrogenation process forming **II**, the ring opening will be reversible. However, it is highly probable that an intermediate of type **III** will form a plethora of side reactions: further degradation, condensation and/or reduction processes on ring opened linear compounds. Assuming this tentative mechanistic proposal to be accurate, the challenge of the hydrogenation is to ensure, that the hydrogenation of the central intermediate **I** is faster than the side reactions that become accessible by ring opening to form **III**. In view of this hypothesis, the reaction conditions applied and the difficulties of the process make perfect sense. High hydrogen pressures are needed to speed up the hydrogenation. Increasing the temperature too much favors the ring opening process as the entropy is increased and leads to degradation. Our results of the experiments with reduced reaction time are also compatible with this hypothesis. If this analysis is true the

hydrogenation process is a walk on razor's edge between the need to increase the rate of the desired hydrogenation and the necessity to avoid the ring opening process leading to uncontrolled destruction.

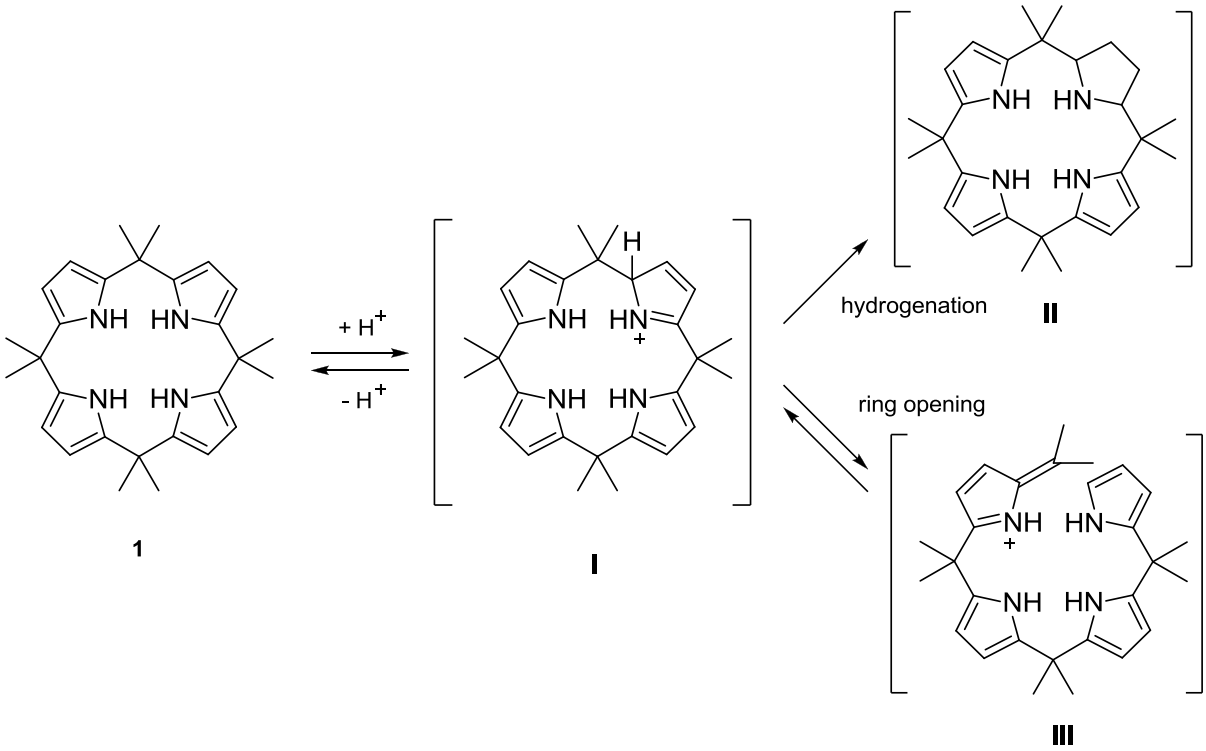

Scheme 18. Proposed first steps of the catalytic hydrogenation of calix[4]pyrrole **1**

If the hydrogenation process of the pyrroles requires initial protonation, we can rationalize the isolation of the partially reduced macrocycles of type **12** and give a tentative answer to questions 1 and 2 (Scheme 19). The protonation of the macrocycle **12** leads to an intermediate of type **IV**. This intermediate **IV** is "protected" against ring opening, or at least the ring opening reaction is considerably slower than the ring opening of compounds where at least one of the neighbors is a pyrrole ring like in **I** or in **VI**. The major postulated pathway to destruction is no longer accessible for compound **12**. If intermediates of the type **V** should be present, the situation would be completely different. If the intermediate **V** is protonated to form **VI**, this protonated form is still amenable to ring opening and thereby to destruction *via* compound **VII**. For simplicity's sake, we have omitted the protonations of the pyrrolidine rings at this point in our discussion (Scheme 19). As a consequence of this proposal, the isolation of the partially reduced macrocycle of type **7** can be interpreted as the isolation of the most stable regioisomer under the acidic reaction conditions.

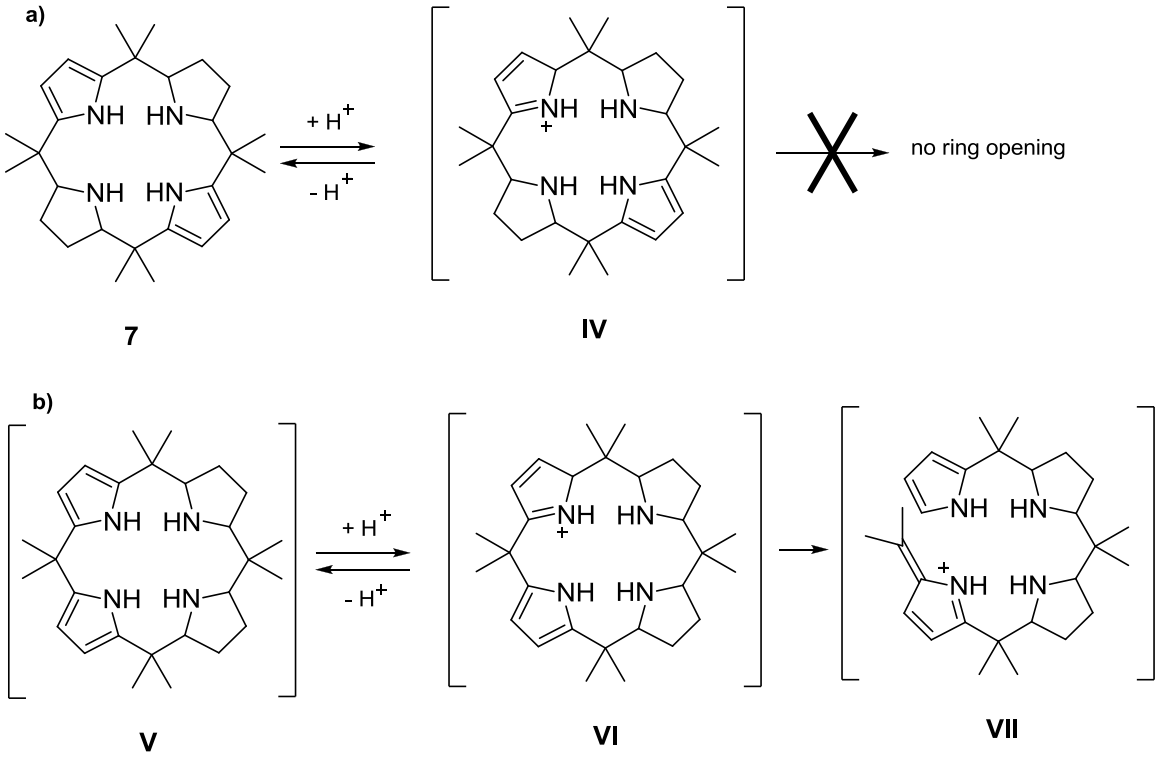

Scheme 19. a) Tentative mechanistic proposal for the hydrogenation from the partially reduced macrocycle **12**. **b)** Protonation of the proposed intermediate **V** forming the intermediate **VI**. This protonated intermediate can undergo a ring opening process to an intermediate of type **VII** or it can be hydrogenated. For simplicity reasons, the probable protonation of the pyrrolidine nitrogens has been omitted.

The hydrogenation of the calix[4]pyrrole **1** transforms a neutral compound into a dibasic macrocycle of the type **12** and into a tetrabasic macrocycle of the type **13**. The partially and totally reduced macrocycles will be present in their *N*-protonated form under the reaction conditions (Scheme 20).

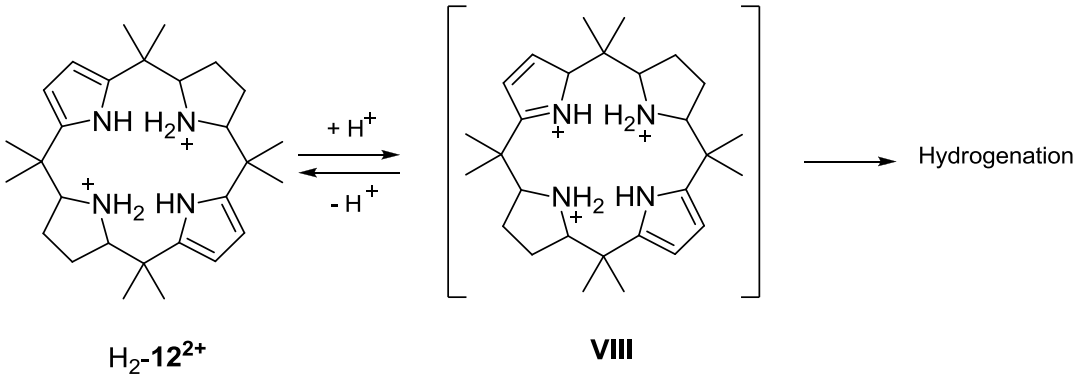

Scheme 20. Postulated mechanism for the hydrogenation, taking into account protonation of **12**

For each pyrrole ring, which is hydrogenated, a positive charge is created by protonation of the formed pyrrolidine. The hydrogenation of **12** would demand the additional protonation of one of the two remaining pyrrole rings of a molecule which is already bis protonated (**12** + $2H)^{2+}$ (Scheme 20). As a consequence of this hypothesis, the reduction of the calix[4]pyrrole **1** would become more difficult as the hydrogenation is progressing: in the first reduction, one has to protonate a pyrrole starting from the neutral compound **1** whereas in the last hydrogenation, one would need to protonate a pyrrole starting from a trication. The mechanistic hypothesis predicts therefore that the hydrogenation becomes more and more difficult. This rationale is at least a partial answer to question 3.

On the whole our simplified mechanistic proposal for the sequence is compatible with most of the observations and has lead us to optimize the reaction conditions.

3.4. The X-ray structures of calix[2]pyrrole[2]pyrrolidine 12a and 12b and of the calix[4]pyrrolidine 13

3.4.1. Formal description of compound 12a and compound 13

Compound **12a** crystallized with three independent molecules per asymmetric unit.[144] In one of the molecules, the pyrrolidine rings occupy two alternative positions. However, the overall structures of the three independent molecules are very similar (Figure 26).

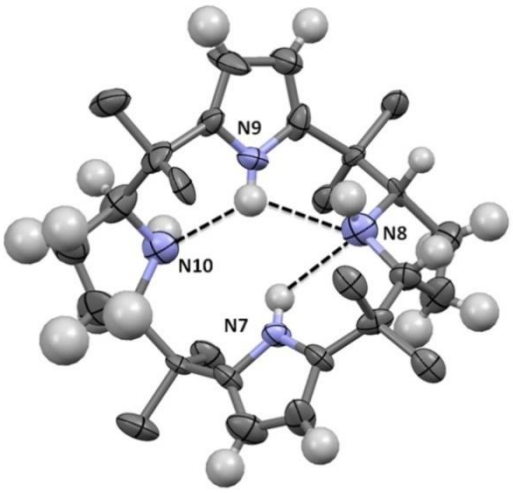

Figure 26. Molecular structure of one of the independent molecules of compound **12a**,[144] with the thermal ellipsoids draw at the 50% of probability level (hydrogen on CH_3 are omit for clarity). N-H…N hydrogen bonds are shown as black dotted lines.

The adjacent N…N distances are also similar, with three distances being shorter [2.687(12) – 2.893(13) Å] than the fourth [3.174(12) – 3.246(11) Å]. Three intramolecular hydrogen bonds between the pyrrolic N-H bond and the lone pair of one of the neighbouring pyrrolidines are present. One hydrogen bond is a single hydrogen bond (between N7-H and N18) whereas the two other hydrogen bonds are bifurcated (N9-H to N18 and N10). The hydrogen bonds fix the relative positions of the adjacent pyrrole ring compared to the neighbouring pyrrolidine ring and define two planes; the pyrrole rings are inclined to one another by 69.4(6) - 71.2(6)˚, and the best mean-planes of the pyrrolidine rings are inclined to one another by 26.0(9) – 26.8(6)º. The pyrrolidine rings have twisted conformations leading to alternating positions of the quaternary carbons. Two of the quaternary carbons are situated above the average plane of the macrocycle and the other two are situated below. The position of the quasi-axial methyl groups is also alternating; two above the plane and two below. Compound **12b** was described previously[130, 145] and possesses crystallographic C_2 symmetry. There the pyrrole rings are inclined to one another by 71.3(1)˚ however, the pyrrolidine rings have twisted conformations and their best mean-planes are inclined to one another by 85(2)˚. In the macrocycle of **12b** there are two short [2.802(16) Å] and two long [3.1174(17) Å] adjacent N…N distances. This is compatible with two pairs of hydrogen bonds.

The X-ray structure analyses of various metal complexes of compound **13** have been reported previously.[130, 145] The crystal structure of compound **13** obtained by crystallization from slow evaporation of a solution of **13** in chloroform is shown in Figure 27.

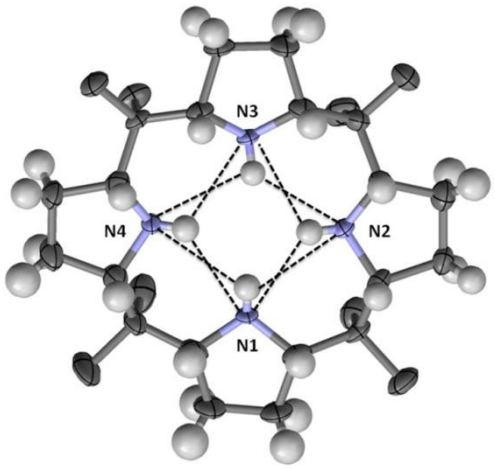

Figure 27. Molecular structure of compound **13**, with thermal ellipsoids draw at the 50% of probability level (hydrogen on CH_3 are omitted for clarity). N-H…N hydrogen bonds are shown as black dotted lines.

The molecule in the crystal has pseudo C_2 symmetry rather than C_4.[144] The compound presents an average plane defined by the four nitrogen atoms. All the NH groups point towards the same point slightly above the average plane of the macrocycle, on the same side as the H-C-N hydrogen atoms. Four of the eight methyl groups bonded to *meso* carbons are arranged in quasi-axial position, whereas the four others point away from the macrocycles in a quasi-equatorial position. Two opposite pyrrolidine rings, involving atoms N2 and N4, have envelope conformations with the nitrogen at the flap, whereas the other two pyrrolidine rings, involving atoms N1 and N3, have twisted conformations. Here the adjacent N···N distances vary much less, between 2.999(4) – 3.109(4) Å and eight hydrogen bonds are present. It is noteworthy that the free ligand presents a conformation similar to that observed in the metal complexes except for the NH groups: in the metal complexes the NH hydrogens are in quasi-axial positions and on the opposite side with respect to H-C-N hydrogen atoms.

3.4.2. Number of possible stereoisomers

The partially reduced calix[2]pyrrole[2]pyrrolidine possesses 4 stereogenic centers. The maximum number of possible stereoisomers should be 16. Due to the high symmetry of the compound, only 7 different stereoisomers exist: 3 *meso* compounds (**12a**, **12b** and **12e**) and 2 pairs of enantiomers (**12c**, ent-**12c**, **12d** and ent-**12d**) (Figure 28).

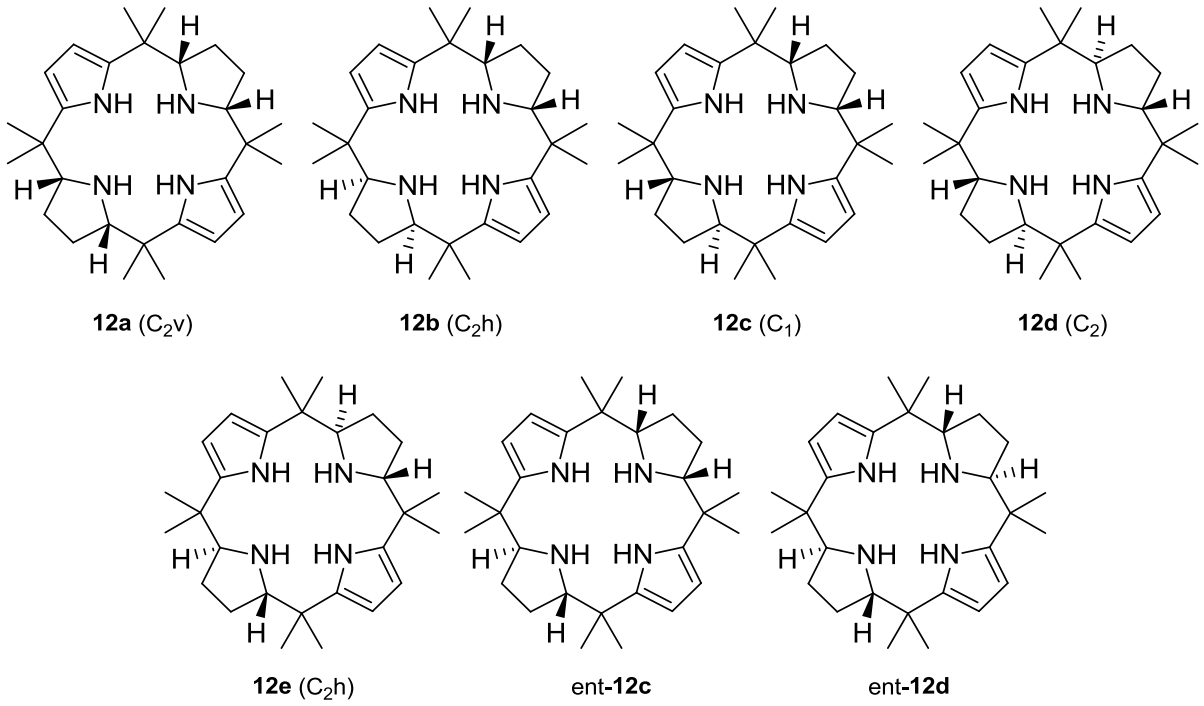

Figure 28. The seven possible stereoisomers of **12** with their point groups

So far, we have only been able to isolate and characterize two stereoisomeric structures: the two *meso* structures **12a** and **12b**. The calix[4]pyrrolidine **13** possesses eight carbon atoms with four different substituents. The maximum number of stereoisomers is therefore 256. Only 45 stereoisomers can exist as has already been mentioned by van Beylen.[121] As in the case of the hydrogenation of the calix[4]furan, only one of the 45 possible stereoisomers of the totally reduced macrocycle **1** was identified and characterized namely **13** (Figure 29).

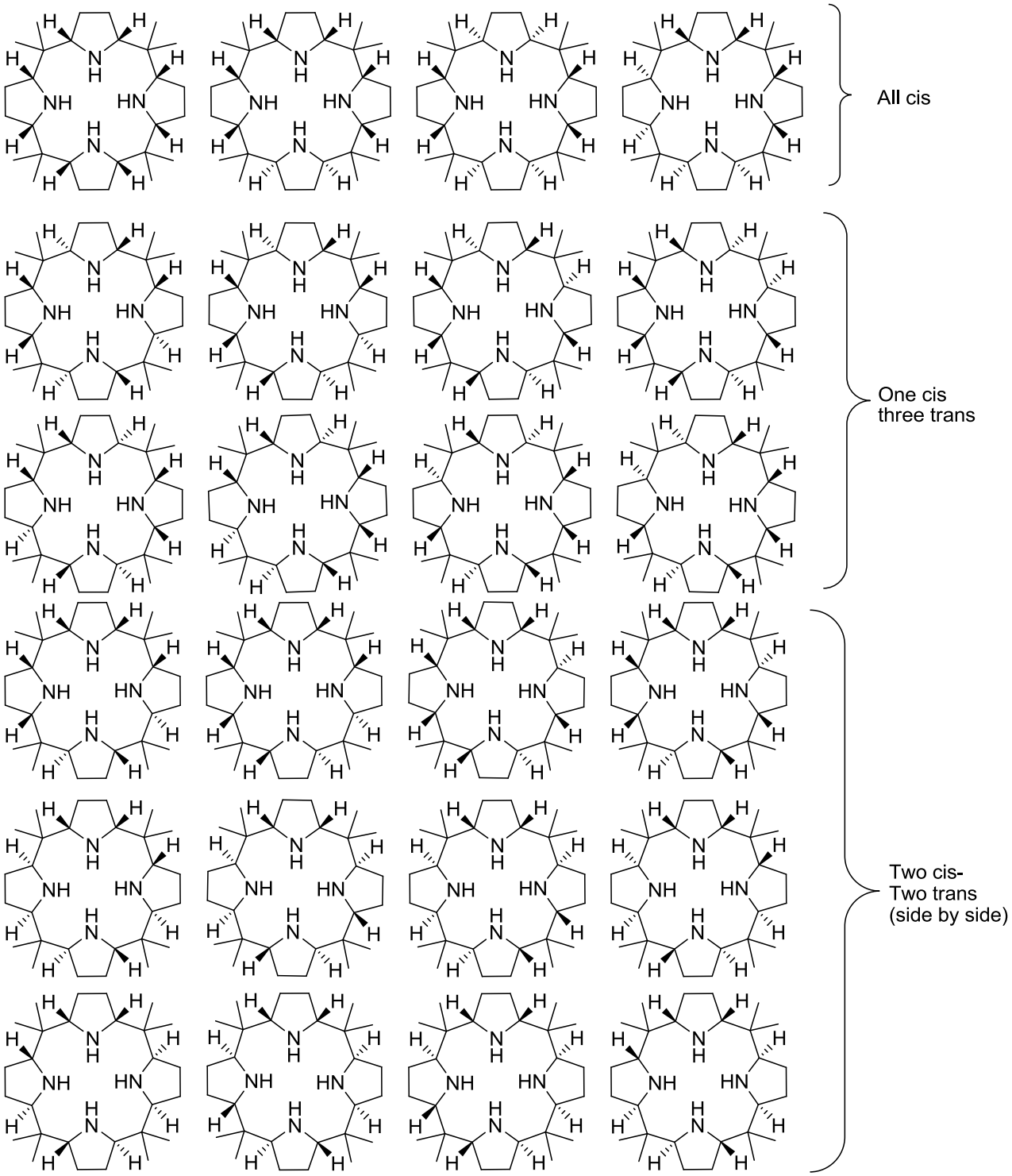

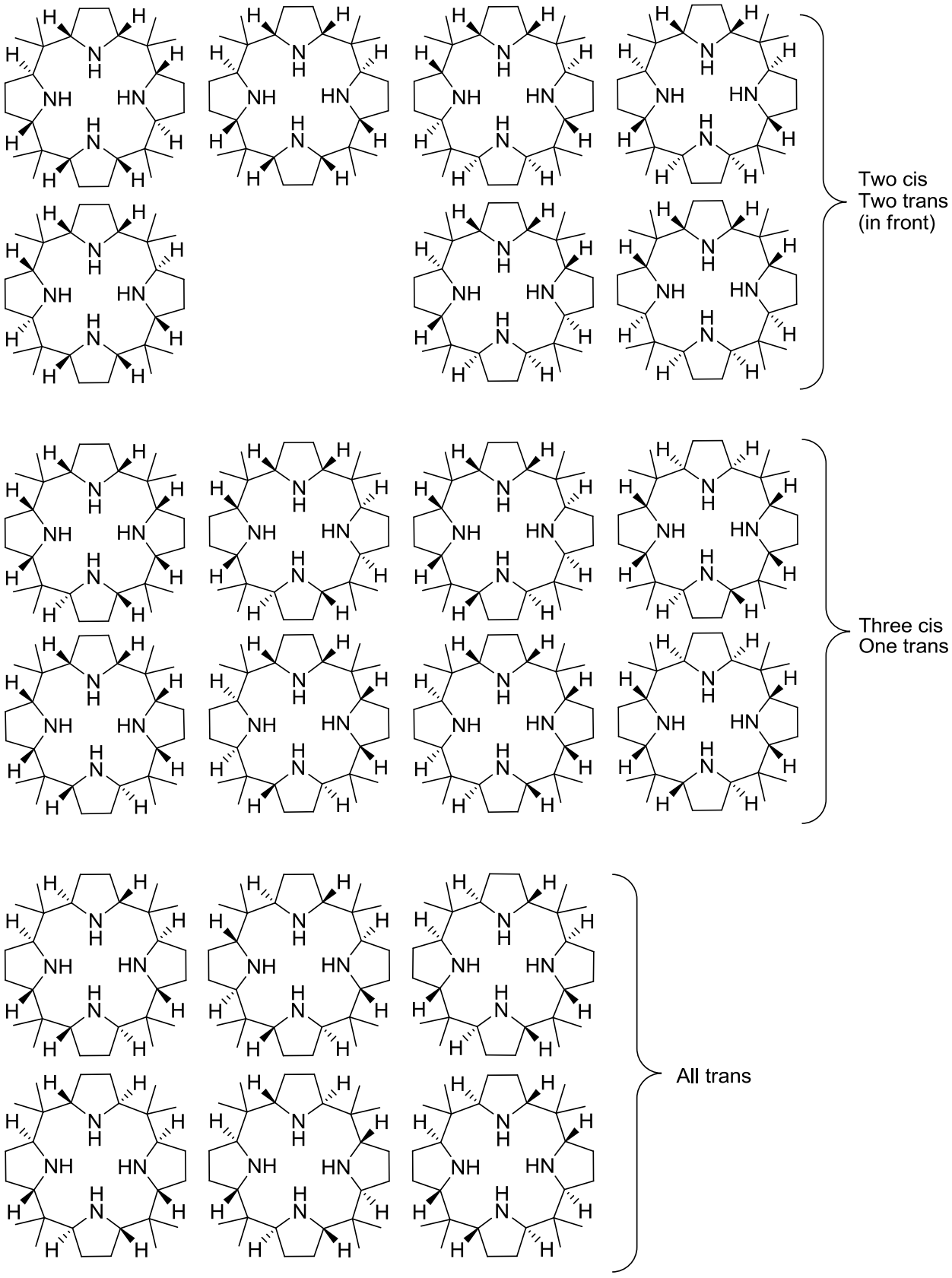

Figure 29. The 45 possible stereoisomers of the calix[4]pyrrolidine **13**

3.4.3. Discussion of the structures of calix[2]pyrrole[2]pyrrolidine 12a and 12b

To ascertain the structures deduced from the spectroscopic data of the two partially reduced macrocycles **12a** and **12b**, the determination of the structures in the solid state by X-ray diffraction was essential (Figure 30).[129, 130] Due to the high symmetry of these two *meso*-compounds the unequivocal assignment of the structures based on spectroscopic data only was delicate. The result of the X-ray diffraction enabled us to attribute the relative configurations, but more importantly, the structures gave important hints to understand the properties of the calix[2]pyrrole[2]pyrrolidine structures **12a** and **12b**.

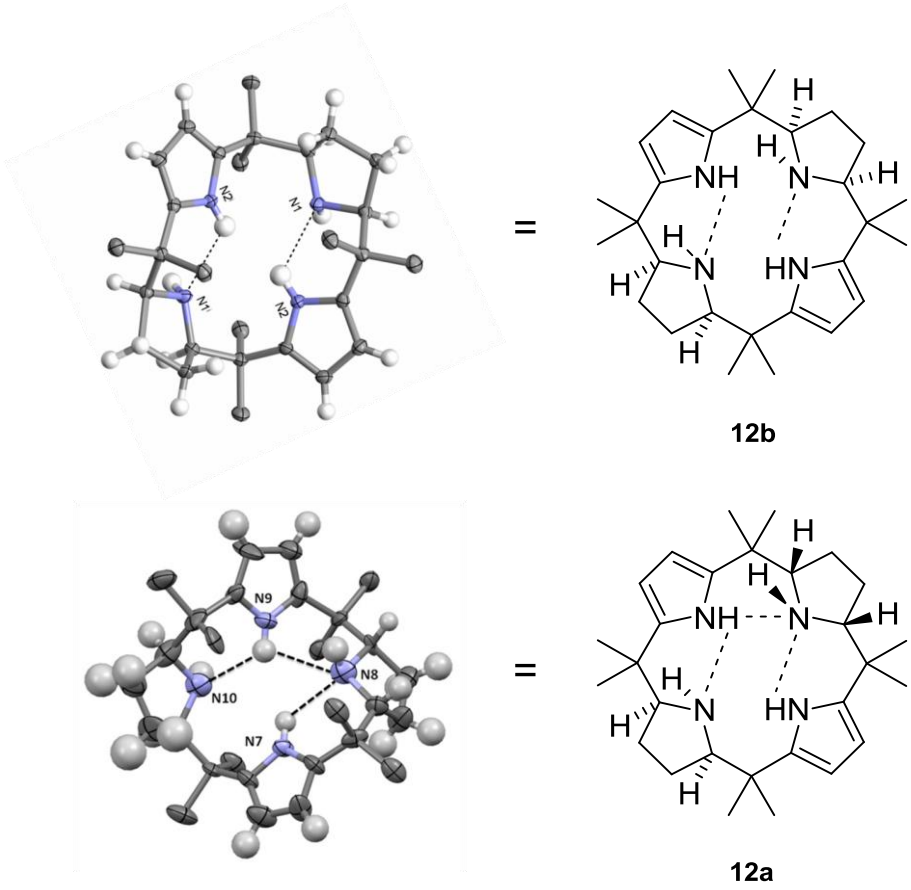

Figure 30. Solid state structures of the macrocycles **12a** and **12b** determined by X-ray diffraction[129, 130]

Both structures are characterized by a tight hydrogen bond network in the center, connecting the pyrrole N-H with the lone pair of the neighboring pyrrolidine nitrogen. In the case of **12a**, the network is a two by two network, where one pyrrole N-H is bound to one of the pyrrolidine neighbors, whereas the second pyrrole N-H is linked to the other pyrrolidine neighbor. The hydrogen bond network of **12b** is more complicated. One pyrrole forms two

hydrogen bonds to the two neighboring pyrrolidine rings. The bifurcated hydrogen bond emanating from this pyrrole is almost symmetric. In both macrocycles, the hydrogen bond network forms an inner core, which fixes the conformation and thereby the properties of the molecules. The N-H from the two pyrrolidine rings in **12a** are directed towards the same face of the macrocycle, whereas in **12b** the N-H bonds of the pyrrolidine rings are pointing in opposite directions. The structures are very tight and access to the inner core, without breaking the hydrogen bond network, is not easy. This fixed inner core determines by a sort of conformational coupling the arrangement at the outside of the macrocycles. For both molecules four of the eight methyl groups are arranged in a *quasi* equatorial position, whereas the four other methyl groups are arranged in pairs in *quasi* axial positions: two methyl groups are up and two methyl groups are down.

3.4.4. Discussion on the structure of calix[4]pyrrolidine 13

The structure determination of the calix[4]pyrrolidine **13** from the spectral data alone was easier. The high symmetry of the compound led to an extremely simple ^{1}H- and ^{13}C-NMR spectrum. These spectra together with the MS and the high-resolution MS did not leave any doubts about the structure. Crystallization proved to be difficult, but finally good crystals could be obtained (Figure 31).[129]

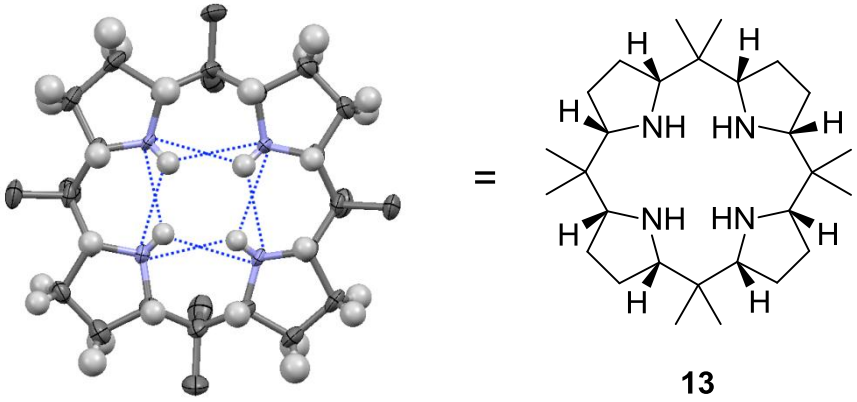

Figure 31. The X-ray structure of the calix[4]pyrrolidine **13**[129]

The solid state structure reflects the beauty of the symmetrical chemical structure **13**. Once again the nitrogen atoms and the N-H bonds form a tight inner core. Due to the symmetry of the molecule, this inner core is C_4 symmetric. The arrangement of the methyl groups also reflects this C_4 symmetry. Therefore 4 out of the 8 methyl groups are *quasi* equatorial. The

other 4 methyl groups are *quasi* axial, but in contrast to the macrocycles **12a** and **12b** the 4 axial methyl groups are pointing all to the same face of the disk-like compound.

Looking at the molecule from the edge reveals additional, remarkable structural aspects of the calix[4]pyrrolidine **13** (Figure 32). The macrocycle **13** has a disk-like overall shape, creating two half spaces: one face is characterized by the four hydrogen bonded to the pyrrolidine nitrogen and the other face is forming a shallow cleft limited by the four *quasi* axial methyl groups. The four lone pairs of the nitrogen are arranged in an almost perfect square, directed towards the center of the macrocycle **1**. If one compares the structure of the calix[4]pyrrolidine **13** with the structure of a porphyrin the similarities and differences of the two systems are striking.

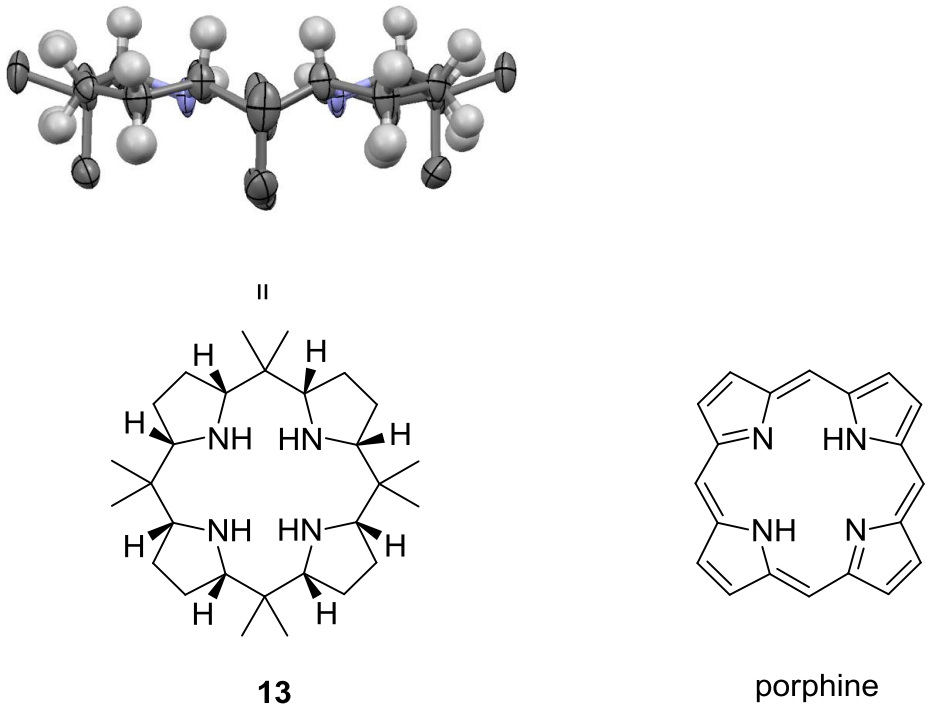

Figure 32. The solid state structure of **13** seen from the edge in comparison with the generic porphine structure.[129]

The porphyrins are flat systems. The two faces of the disk-like molecule are identical. The porphyrins are characterized by an arrangement of four nitrogen atoms in a flat and square arrangement perfectly aligned for complex formation. The N-H bonds in the ligand are in the plane of the disk and engaged in an efficient network. The tautomerism allows quick exchange of the positions of the H-atoms. The ligand has to be deprotonated twice for the formation of metal complexes; thereby the H-bond donation is lost when a metal complex is formed. The porphyrins offer four lone pairs for an efficient σ-interaction with the metal. The

aromatic 18 electron aromatic π-system offers the opportunity for π-back donation. The electronic properties on the metal can be tuned *via* the π-system of the ligand.

The macrocycle **13** has a disk-like overall shape as well. The four nitrogen atoms are in a flat and square arrangement, well aligned for complex formation. The two faces of the disk are clearly differentiated: one face is characterized by the N-H bonds directing away from the disk, the other face is characterized by a shallow cleft formed by the four axial methyl groups. However the four N-H bonds are orthogonal to the plane of the disk. The ligand can complex metals without deprotonation, therefore the H-bond donating property remains intact when a metal complex is formed.

In summary, our ligand **13** is geometrically very similar to the porphyrins, but electronically very different. The ligand **13** has inherently two different faces and should be highly resistant to oxidation or other side reactions in view of the fact that the ligand **13** is completely saturated.

3.5. Correction

We have recently discovered that the tentative structure attribution of one of the hydrogenation products has to be corrected. The attribution was based on the fact that the NMR spectra showed the absence of any element of symmetry. The previous structure attribution for compound **12c** is incorrect! We discovered that the starting material used for the investigation of the hydrogenation of macrocycle **1** was not pure. The GC analysis of the starting material revealed the presence of 10% of an impurity. This impurity has been isolated and characterized as the *N*-confused calix[4]pyrrole **21**.[146] The catalytic hydrogenation of this *N*-confused macrocycle afforded the described compound **12c** (Scheme 21).

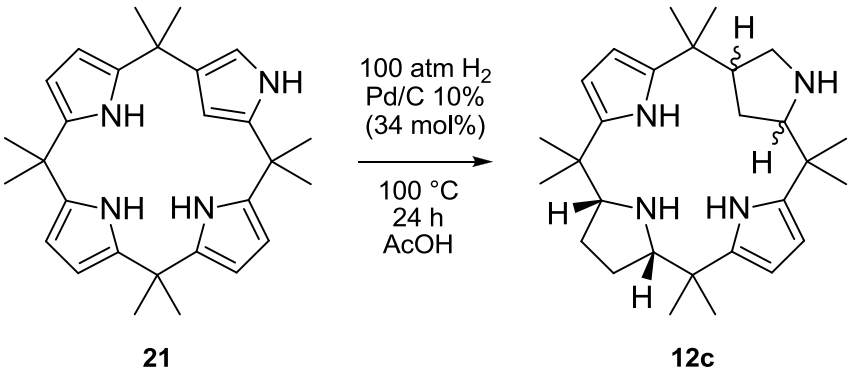

Scheme 21. Catalytic hydrogenation of *N*-confused calixpyrrole **21**

Compound **12c** was isolated and characterized from the catalytic hydrogenation of the N-confused calix[4]pyrrole **21**. The GC spectra and the NMR analysis of this compound were in agreement with those performed previously. Full characterization of this compound is in progress.

3.6. Summary

GC analyses allowed to follow the progress of the heterogeneously catalyzed hydrogenation reactions of calix[4]pyrrole **1**. As a function of the reduction conditions, one to three different reduction products could be isolated. Two of them, **12a** and **12b**, were diastereoisomers of the partially reduced compound and displayed alternating pyrrole and pyrrolidine rings. Compound **12a**, which had not been detected during previous work, has been isolated and its relative configuration has been assigned through single-crystal X-ray diffraction (**12a**). A single, all-*cis*, fully hydrogenated compound **13** could be obtained in low yields only under drastic reaction conditions (100 atm of hydrogen pressure at 100°C in acetic acid). The relative configuration of compound **13** has been unequivocally assigned by X-ray diffraction analysis. Attempts to considerably increase the yield of the saturated compound **13** using a variety of common as well as novel heterogeneous catalysts under diverse reaction conditions were unsuccessful. However, the half-hydrogenated compounds **12a** and **12b** could be obtained in increased overall yield (87%) in an approximately 2:3 ratio by employing the same catalyst in an 80:20 AcOH/H_2O mixture, all other experimental conditions being identical. Besides, **12b** was selectively obtained in 55% GC yield using rhodium-graphite, $C_{24}Rh$, in trifluoroacetic acid at 70°C under a hydrogen pressure of 100 atm. Given all the results, the best condition to perform the hydrogenation of calix[4]pyrrole **1** is the following: acetic acid as solvent (C_1=0.1 M), 16 mol% of Pd/C 10%, 100 atm. of H_2 for 4 hours at 100°C.

The tentative structure attribution of compound **12c** had to be corrected. Compound **12c** is the reduced form of the *N*-confused calix[4]pyrrole **21** present in the starting material as impurity.

4. HYDROGENATION OF CALIX[2]PYRROLE[2]PYRROLIDINE 12B

4.1. Theoretical analysis

As one of the first ways of trying to improve the yield of the reduction to the totally reduced compound **13**, we tried to achieve the total reduction of compounds of type **12**. Using pure **12b** as starting material and submitting it to identical hydrogenation conditions as the ones which allow us to obtain small quantities of **13** starting from the calix[4]pyrrole **1.** We have not been able to obtain evidence for the formation of the totally reduced macrocycle **13** starting from the partially reduced compounds **12**. Given this result, it is safe to assume that the half-reduced calix[4]pyrrole **12b** is not an intermediate in the formation of compound **13** in the reaction starting from calix[4]pyrrole **1**. Considering this information we can present the following hypothetical mechanistic sequence of the formation of compound **13** under standard reaction conditions starting from **1** (Scheme 22).

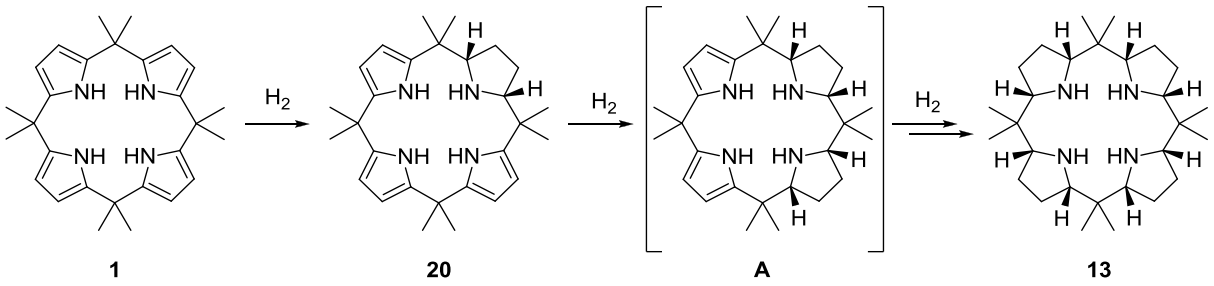

Scheme 22. Mechanism of the formation of the totally reduced macrocycle **13**

Compound **A** has never been observed so far. We assume that compound **A** is an extremely reactive species towards further hydrogenation. On the whole, the proportion of the totally reduced macrocycle compared to the half reduced is around 10%. This observation is compatible with the proposal that the hydrogenation of the pyrrole opposite to the reduced pyrrolidine ring of compound **20** is easier to hydrogenate than the neighboring pyrrole ring. In the solution compound **20** is present as its protonated form. The protonation of the pyrrole opposite to the pyrrolidine ring is likely easier and thereby slightly favored due to the repulsion of the positive charges. If our hypothesis is correct the reaction giving **A** starting from **20** must be highly *cis*-stereoselective. Finally those observations allow to tentatively

propose a complete mechanistic sequence for the hydrogenation process (Scheme 23). A consequence of the mechanistic proposal is that we can attribute relative rates to the different steps of the sequence. Compound **20** could only be isolated by stopping the reaction before the complete conversion of the starting material. Reaction giving compound **20** is thereby considered as a fast reaction.

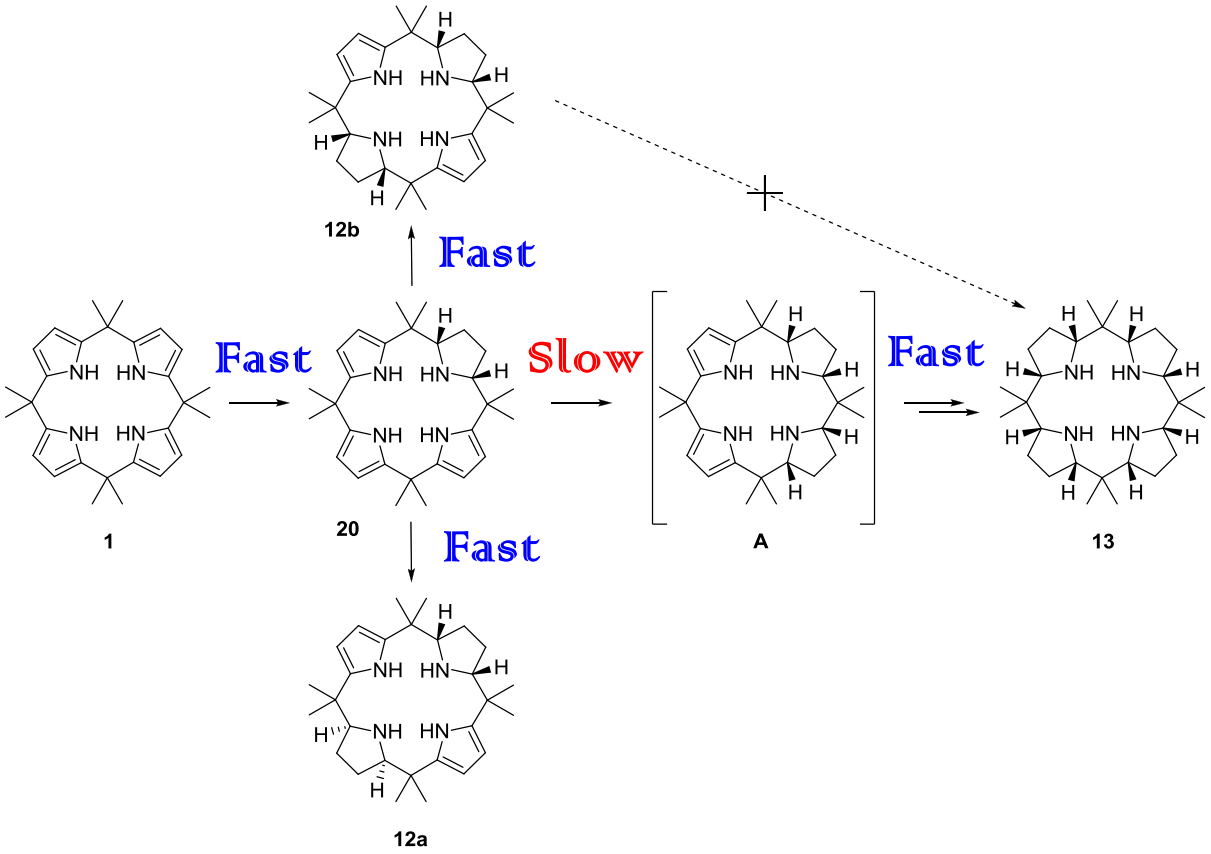

Scheme 23. Sequence of the hydrogenation of calix[4]pyrrole **1**

Under the standard conditions, the hydrogenation of compound **1** giving compound **12** and **13** favors the formation of half-reduced compound **12** by a factor of 10. Therefore the reaction giving both stereoisomers **12a** and **12b** must be faster than the one giving **13**. Despite the number of experiments we did, we were not able to observe compound **A**; the transformation into compound **A** must therefore be slower than the formation giving **13**. This transformation should therefore be the rate limiting step of the reaction. The mechanistic hypothesis presented in Scheme 23 is compatible with the lack of success to increase the yield of the fully reduced **13**. The sequence rationalizes also the fact that we obtain only one single diastereiosomer **13** of the fully reduced macrocycle. This is in marked contrast to the reduction of calix[4]furan, where two stereoisomers of the completely reduced form were

isolated and characterized. The only possibility left to improve the yield of **13** is by pushing the reduction from **12b**. These analyses could also explain the ratio 6/4 obtained for products outcome (see Chapter 3, 3.1.1.1.), the reduction of calix[4]furan favored the isomer **7a** (Scheme 24).

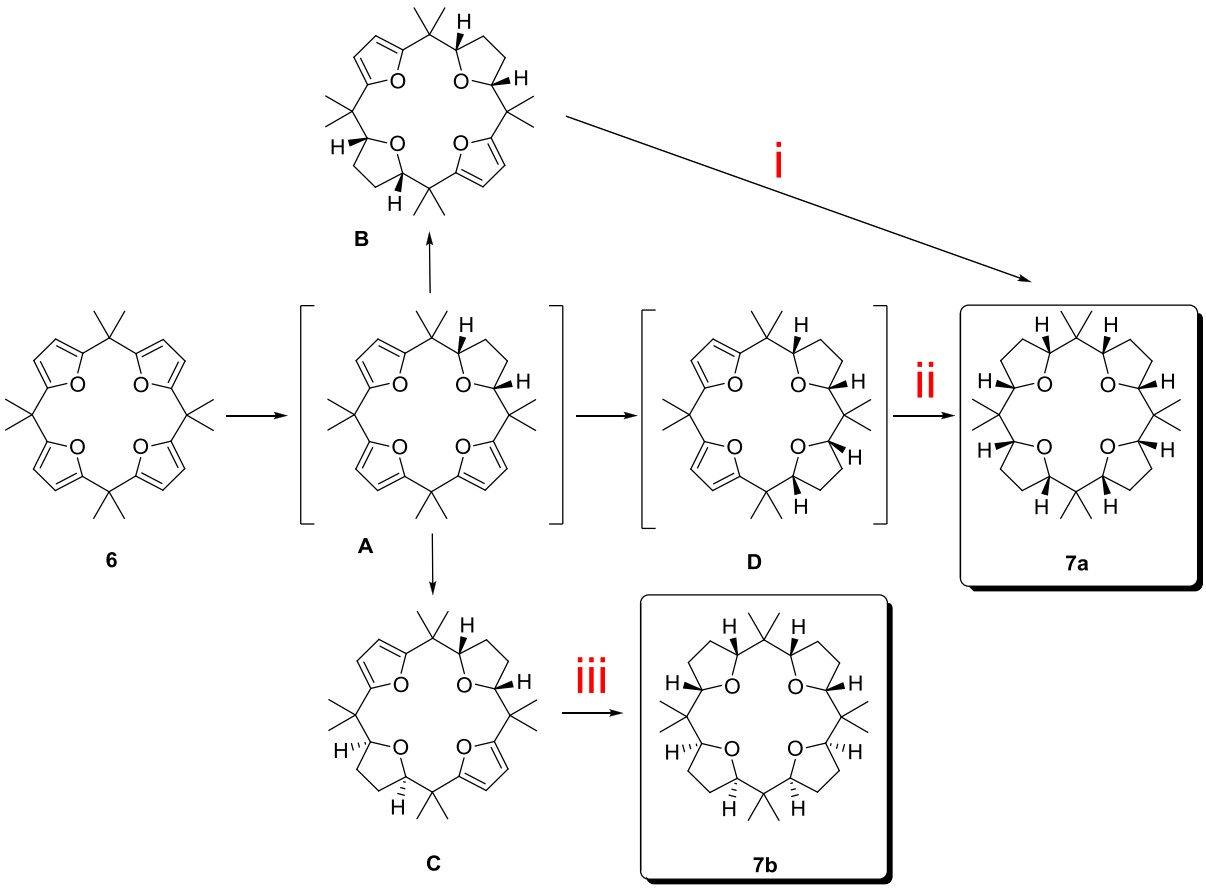

Scheme 24. Sequence of the hydrogenation of calix[4]furan 6

If the reaction rate starting from **A** and giving neither **B** and **C**, nor **D** is comparable to the hydrogenation of calix[4]pyrrole, compound **7a** comes from the reaction i and ii and is thereby present in the reaction crude in a higher amount, compared to **7b**. Following this analysis the hydrogenation of **12b** would give the fully reduced macrocycle **13** and the reduction of **12a** would give a new saturated compound with the same relative configuration than **7b**.

4.2. Attempts to hydrogenate compound 12b

4.2.1. Variations of the catalysts

During this long process, we achieved one encouraging result. Using a specific sample of palladium on carbon from Fluka, we were able to hydrogenate small but reproducible quantities of macrocycle **12b** to the fully reduced macrocycle **13** (results obtained by Dr. Andrea Gualandi). When we had to order a new batch of the "same" palladium catalyst from the same provider, the reduction did not work anymore. Confronted with this irreproducibility, we wished to analyze the influence of different palladium catalyst on the hydrogenation of the half reduced **12b**. So far, we have not been able to identify the factors, which allow the hydrogenation of **12b** to take place or that prevent the hydrogenation. The studies of this important fact are still intensively ongoing.

For this investigation on the variation of the catalyst we varied the following parameter: the catalyst provider, the catalyst loading, the type of the solid matrix, the pH of the catalyst and the procedure for synthesizing the catalyst. A selection of the results of the hydrogenation attempts of compound **12b** over different catalysts is presented in Table 8.

Table 8. Catalytic hydrogenation of calix[2]pyrrole[2]pyrrolidine **12b**.[a]

Entry	Catalyst	Provider/Type	**13**
1	10% Pd/C	Aldrich/basis (75990)	-
2	10% Pd/C	Fluka/basis (75990)	-
3	5% Pd/C	Aldrich/basis (75992)	-
4	10% Pd/C	Strem/reduced, dry powder (46-1900)	-
5	5% Pd/C	Strem/reduced, dry powder (461890)	-
6	5% Pd/C	Strem/eggshell, reduced (50% wet), evonik E5	-
7	20% Pd/C	Strem/(Pearlman) unreduced (50% wet) (461707)	-
8	30% Pd/C	Aldrich/basis (407305)	-
9	0.6% Pd/C	Strem/50% wet (46-1710)	-
10	0.5% Pd/Al_2O_3	Stream/reduced, dry (46-1920)	-
11	1% Pd/SiO_2	Strem/supported on polyethylenimine (46-2087)	-
12	5% Rh/Al_2O_3	Aldrich/powder (212857)	-
13	$C_{24}Rh$	Diego Savoia catalyst	-

Entry	Catalyst	Provider/Type	**13**
14	5% Pd/C	Evonik (sample from industry)	-
15	5% Pd/C	Evonik (sample from industry)	-
16	5% Pd/C	Evonik (sample from industry)	-
17	5% Pd/C	Evonik (sample from industry)	-

[a] The reactions were performed in an autoclave using 36 mol% of catalyst, 100 bars of H_2, at 100°C for 12 h.

In all cases, no conversion of the starting material was observed over any catalyst applied, even under the harsh condition of hydrogenation such as acetic acid as solvent, 100 bars of H_2, 100°C for 12h.

4.2.2. Variation of the acids

Our tentative mechanistic proposal attributes a considerable importance to the protonation state of the intermediates. So we changed the strength of the acid used for the hydrogenation trials starting from **12**. Influences modifying the quantity of palladium, the temperature, the pressure and the type of acid have been investigated (Table 9).

Table 9. Catalytic hydrogenation of calix[2]pyrrole[2]pyrrolidine **12b**.[a]

Entry	Pd (mol%)	Solvent	Acid	H_2 (bars)	T (°C)	**13**
1	34	AcOH	AcOH	100	100	-
2	34	AcOH	AcOH	100	150	-[b]
3	34	AcOH	AcOH	150	100	-[b]
4	7	AcOH	AcOH	100	100	-
5	34	AcOH	AcOH /TFA (8/2)	100	100	-
6	34	AcOH	AcOH /H_2SO_4 (8/2)	100	100	-
7	34	AcOH	AcOH /BF_3OET_2	100	100	-
8	34	Isopropanol	BF_3OET_2	100	65	-
9	34	AcOH/HCl (1/1)	AcOH/HCl (1/1)	100	100	-
10	34	TFA	TFA	100	65	-
11	34	HCl	HCl	100	50	-

[a] The reactions were performed in an autoclave using a Pd/C 10% from Aldrich for 12 h. [b] Degradation of the starting material has been observed.

The standard condition of hydrogenation has been described Table 9, entry 1 as reference. We started the study by increasing the temperature to 150°C (Table 9, entry 2), unfortunately only traces of degradation of the starting material has been observed. Similar results have been observed when we performed the reaction under higher pressure of hydrogen, 150 atm (Table 9, entry 3). The limits between no reaction and degradation were similar to those observed for the initial process (temperatures of 150 °C and higher, and hydrogen pressure of 150 atm). Increasing the amount of catalyst to 0.7 equivalent led to a disappointing result (Table 9, entry 4). The use of a large range of acid has been investigated (Table 9, entry 5-11). Unfortunately, even using HCl as solvent for the reaction, no trace of the totally reduced product **13** was detected and starting material was completely recovered. We were extremely surprised regarding the stability of the compound **12b** under this extremely harsh acidic condition. Under these condition the steel of the autoclave was attacked, resulting in a beautiful green color of the solution probably due to the presence of dissolved Ni^{2+}. Attempts to hydogenate compound **12b** under strong acidic conditions failed. As our macrocycles are only stable under these conditions in the presence of H_2, we cannot test if the pyrroles are protonated under these conditions.

To sum up, using the standard conditions, no degradation but also no transformation was observed. The partially reduced macrocycle **12b** proved to be quite stable, but also very resistant to further reduction. As a consequence of these experiments we can exclude **12b** as an intermediate on the way to the totally reduced compound **13** at least with the catalysts we are using now. We cannot exclude **12b** as an intermediate for the special sample of palladium catalyst we used in the above mentioned series of experiments.

4.2.3. Decrease the pKa of the pyrrolidine rings in compound 12b

Based on our mechanistic hypothesis indicating that the hydrogenation should become more and more difficult as we progress in the reduction process, because of the two protonated pyrrolidine rings, we decided to decrease the pKa of the nitrogen by transforming the secondary amine into an amide. The pKa of the protonated acetylated pyrrolidine will be in the same range than the pKa of the pyrrolinium and then the pyrrole should be easier to protonate under acidic condition. For this reason we synthesized the mono and bis-acetylated derivatives of compound **12b**, compound **22** and **23** respectively (Figure 33). The detailed studies of the syntheses and the properties of these new compounds are described in Chapter 4.

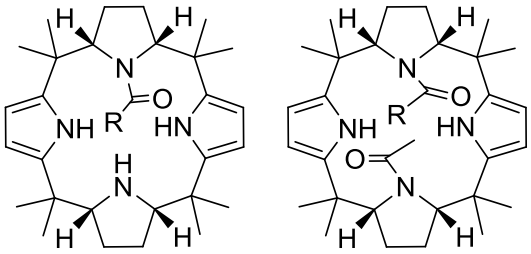

22 **23**

Figure 33. Mono and bis-acylated version of macrocycle **12b**

The catalytic hydrogenation of amide **22** and **23** have been carried out using the standard conditions, 36 mol% of Pd/C 10%, 100 bars of H_2, in acetic acid at 100°C for 24 h. In both reactions we recovered the starting material unchanged. As previously observed for compound **12b**, both compound **22** and **23** are extremely stable under these harsh conditions as no traces of degradation have been observed.

4.2.4. Is the pyrrole really not protonated under strong acidic conditions??

Owing to those previous unsuccessful results, we decided to investigate the protonation of the bis-reduced compound **12b** in deuterated acetic acid at 100°C. Assuming that protonation of pyrroles is a very fast equilibrium process and that a third protonation is possible, a deuterated acidic medium would lead to complete exchange of the pyrroles protons by deuterium (Scheme 25).

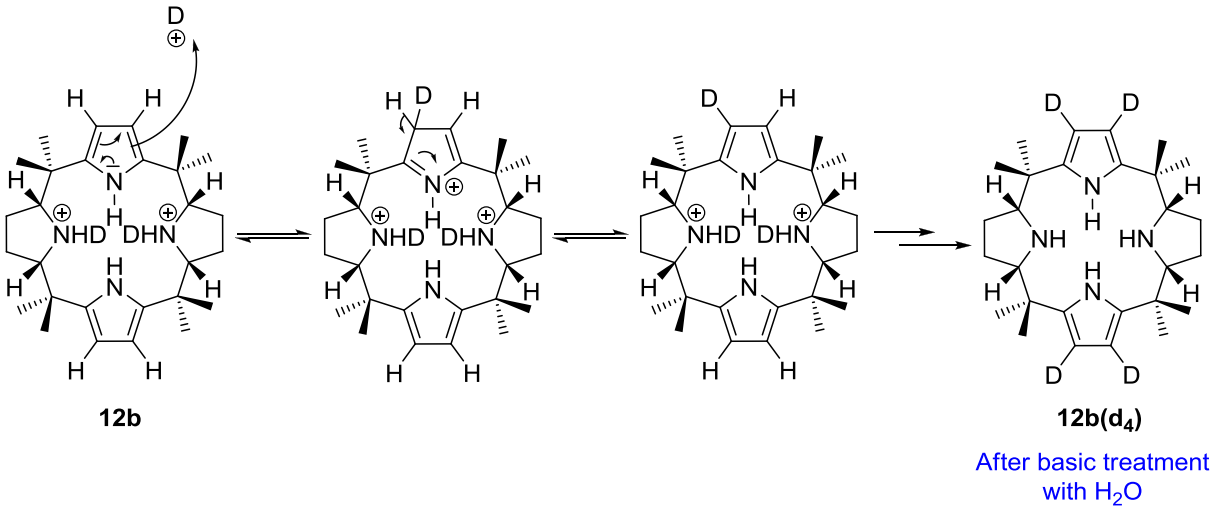

Scheme 25. Deuterium/hydrogen exchange of macrocycle **12b** in deuterated acetic acid.

A basic treatment at the end should replace the N-D of the pyrrole and pyrrolidine rings to N-H. The resulting macrocycle should possess four deuterium in the pyrrolic position (compound **12b(d$_4$)** scheme 25). The MS peak of the molecular ion should therefore show spectra mass shift by 4 unities: M(**12b**)+1=437 g.mol^{-1} where M(**12b(d$_4$)**)+1 = 441 g.mol^{-1}.

Compound **12b** has been solubilized in CH_3COOD and heated at 100°C for 4 hours. The resulting MS spectrum after a basic workup of the reaction is presented Figure 33.

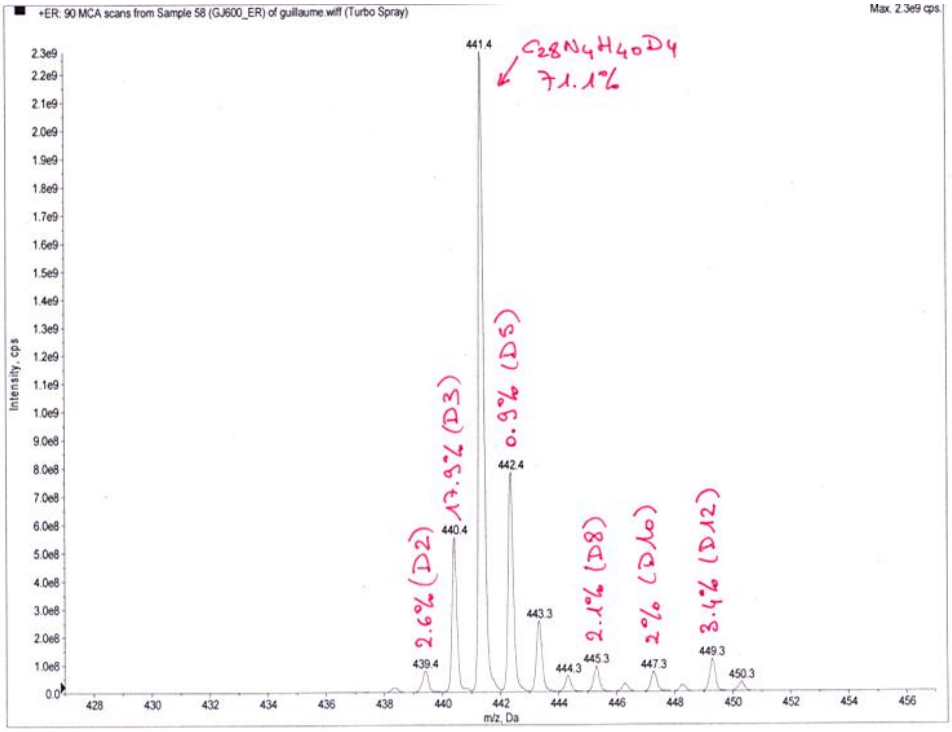

Figure 33. MS spectra of compound **12b** after a treatment by CH_3COOD.

The major product obtained (71.1%) was the macrocycle containing four deuteriums M+1=441 g.mol^{-1}. This MS result is compatible with the hypothesis that the deuterium has been incorporated in the pyrrolic β-positions (position 3 and 4). This assumption is correct if we have been able to completely exchange the N-D to N-H during the basic workup in water. The ^{1}H-NMR spectrum confirmed these hypotheses: the N-H of the pyrrole and pyrrolidine rings are clearly visible and only minute intensities can be detected for the pyrrolic hydrogens. As a conclusion the protonation of pyrroles under our experimental conditions is possible even when the two pyrrolidine rings are already protonated. The creation of a third charge on the macrocycle **12b** in acidic condition seems to be feasible. This result is a strong indication that the protonation or the strength of the acidic medium is not the reason for the failure to achieve the hydrogenation of compound **12b**.

4.3. Breakthrough: it is possible to push the reduction of compound 12b into 13!

4.3.1. The discovery

After three years of "intensive" work, having tried in a common effort with Dr. Andrea Gualandi several hundred different conditions we were finally able to achieve a reproducible and repeatable conversion of the half reduced compound **12b** into the fully reduced **13.**

Analyzing all the data we could exclude many possible explanations for our failure to develop an efficient procedure for the total reduction. The arguments which we can exclude as reasons for this failure are: steric effects due to the presence of four quaternary centers, difficulties with the protonation, insufficient rate of hydrogenation due to too small hydrogen pressure. Despite this rather disappointing situation we knew that reduction from compounds of type **12** to the totally reduced macrocycle of type **13** was possible. Our results had shown that the catalyst was the key element. Using a specific batch of Fluka catalyst we had been able to achieve this elusive transformation. We could think of three reasons: 1) the efficiency of the catalyst was due to the disposition of palladium on the matrix. 2) The matrix had a special morphology. 3) An impurity was the key of this success. We have no way too distinguish between these three possible elements and what is worth we have no criteria in hand to analyze our catalysts for the presence of one or several of these elements. Independent on the precise reason for our results, the other catalysts tested should contain the key elements also, but may be in insufficient quantities. We therefore decided to increase the amount of catalyst to increase the amount of the key element, which made the hydrogenation of **12** possible.

Having tried so many different types of catalysts, the only one variation, which has not been explored systematically and thoroughly, was the amount of catalyst. The only one trial to succeed the hydrogenation of **12b** by increasing the amount of catalyst of 34 mol% to 70 mol% failed. We then decided to carry out the reaction with stoechiometric amounts of catalyst. First, the hydrogenation of **12b** was performed with one equivalent of palladium (Table 10, entry 1). We were extremely pleased to see the conversion of 32% of the starting material into the totally reduced macrocycle **13**.

Table 10. Catalytic hydrogenation of calix[2]pyrrole[2]pyrrolidine **12b**.[a]

Entry	Pd (equiv.)	Conversion of **12b**[b]
1	1	32
2	2.5	41
3	3.5	53
4	4.5	51
5	5.5	60
6	7.5	72
7	9.5	**100/75**[c]

[a] The reactions were performed in an autoclave using Pd/C 10% from Aldrich, AcOH as solvent, 100 bars of H_2 at 100°C. [b] Conversions (%) were calculated by GC. [c] Isolated yield (%).

Systematically increasing the amount of catalyst we finally observed a full conversion of the starting material using 9.5 equivalents of palladium and obtained an isolated yield of 75% (Table 10, Entry 7). Under these extreme conditions side reactions were scarce (one of whom was in majority ~20% GC). The breakthrough was achieved! Once we had a procedure for full conversion in our had we decided to perform a study of the scope and limitations of the methods by varying pressure, solvent, acid and catalyst loading and the matrix, always keeping a large excess of catalyst (Table 11).

Table 11. Stoechiometric hydrogenation of calix[2]pyrrole[2]pyrrolidine **12b**.[a]

Entry	Catalyst	Solvent	Acid	H_2 (bars)	**13**[b]
1	Pd/C 10%	AcOH	AcOH	100	41
2	Pd/C 10%	AcOH	AcOH	120	41
3	Pd/C 10%	AcOH	AcOH	70	-
4	Pd/C 10%	AcOH/H_2O (1/1)	AcOH	100	16
5	Pd/C 10%	AcOH	AcOH/HCl (1/1)	100	-
6	Pd/Carbon 10%	AcOH	AcOH	100	48
7	Pd/C 5%	AcOH	AcOH	100	65
8	Pd/C 30%	AcOH	AcOH	100	15
9	Présat.Pd/C 10%	AcOH	AcOH	100	55

[a] The reactions were performed in 0.1 mmol scale (0.01 M) an autoclave using 2.5 equiv. of catalyst, AcOH as solvent at 100°C. [b] Conversions (%) were calculated by GC.

For our investigation we used 2.5 equivalent of Pd/C 10% as reference conditions (Table 11, entry). We studied the effect of the H_2 pressure on the conversion first. Increasing the pressure

to 120 bars afforded the same conversion, 41%, than the reference reaction using 100 bars (Table 11, entry 2). For a partial conversion the reaction needed at least 100 bars. Decreasing the pressure to 70 bars no transformation was observed (Table 11, entry 3). Diluting the acetic acid with water led to a dramatic decrease of conversion (Table 11, entry 4). No conversion was observed when we used a mixture of AcOH/HCl to perform the reaction (Table 11, entry 5). The reaction media is a crucial factor in the success of the hydrogenation. To test the influence of the matrix of the catalyst we compared the efficiency of palladium on carbon 10% instead of palladium on charcoal 10%. Interestingly, an improvement of the conversion was observed using this catalyst (Table 11, entry 6). This result comforted our guess that the matrix is decisive element for the success of the hydrogenation. For the next two experiments we used Pd/C with different loadings (Table 11, entry 7 and 8). Decreasing the loading of palladium (Pd/C 5%) therefore increasing the quantity of matrix gave a considerably improved yield of the transformation 65% (Table 11, entry 7). In order to keep the quantity of palladium constant (2.5 equiv.) we had to increase the amount of catalyst (=catalyst plus its matrix) accordingly. Using a highly loaded catalyst decreased the amount of matrix and therefore the yield of the reaction decreased to 15% (Table 11, entry 8). Finally, a presaturated catalyst (presaturation under 50 bars of hydrogen) has been tested (Table 11, entry 9). This treatment increased the activity of the catalyst and therefore the reaction reached 55% conversion.

The simplest hypothesis to rationalize these results is the following: the catalyst is “poisoned” or blocked during the reaction and the number of free and active centers limits the transformation. The active sites of the catalyst are blocked either by the intermediates and the products of the reaction or by some other compounds present, so the catalyst loses its catalytic activity for this process. The result of the experiment using presaturated catalyst is not compatible with the presence of an impurity coming either from the solvent or from the catalyst and its matrix. Despite our concentrated efforts to identify the so far missing key element responsible for the success of the hydrogenation has not been identified. Intensive work aiming to answer this question is under progress.

After three years, we found a key to experimentally solve this thorny problem. We arrived at this solution guided first by our mechanistic understanding. The successful experimental procedure is however based on a new mechanism that is still unknown at the moment. However this advance will allow us to explore new territory and hopefully discover the jewel enclosed behind the door.

4.3.2. Scope of this discovery

Despite the fact that we do not understand why the key works, we can now explore the scope of this discovery. The first idea was obviously to apply the successful condition to the hydrogenation of the other isomers, compound **12a**. The catalytic hydrogenation of macrocycle **12a** is described scheme 26.

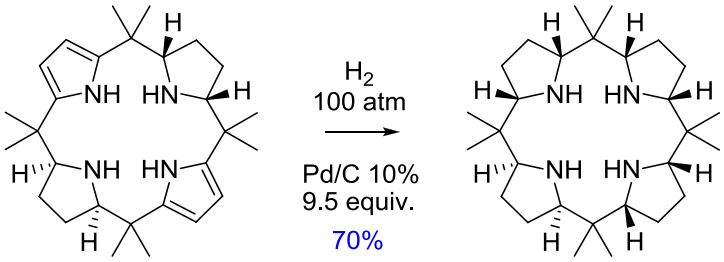

Scheme 26. Hydrogenation of compound **12a**

The hydrogenation of compound **12a** afforded a new diastereoisomer of the totally reduced calix[4]pyrrole, compound **24**. This reaction was highly stereoselective, only one diastereoisomer was observed! Crystals of compound **24** were obtained, but unfortunately they were not good enough for the X-ray diffraction analysis. However, the stereochemistry of **24** could be attributed by NMR analysis! The two possible isomers with their symmetry are represented Figure 34.

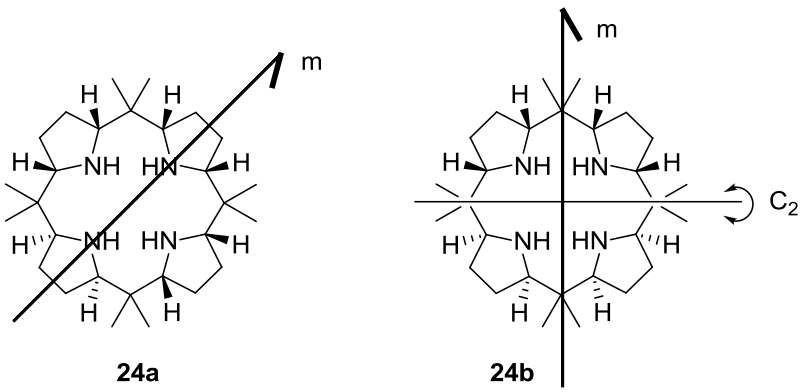

Figure 34. The two possible isomers compound **24a** and **24b.**

We clearly see that compound **24b** belongs to a higher symmetry group than **24a**. Compound **24b** possesses a plane of symmetry m and a C_2 axis, where compound **24a** only possesses a

plane *m*. As a consequence, the ^{1}H-NMR spectra should only show two different peaks for the methyl groups of compound **24b**. However we observed four different ones on the ^{1}H-NMR spectra of the isolated product from the hydrogenation of compound **12a**. We therefore deduced that we have obtained the macrocycle with the structure **24a**. The hydrogens added during hydrogenations of the two pyrrole rings in the macrocycle have been coming from the same side of the macrocycle.

We applied the new conditions for the hydrogenation to the other obvious substrate, calix[4]pyrrole **1** itself. The hydrogenation of calix[4]pyrrole was carried out with 10 equivalents of Pd/C 10% in a diluted media C = 0.01 M (Scheme 27).

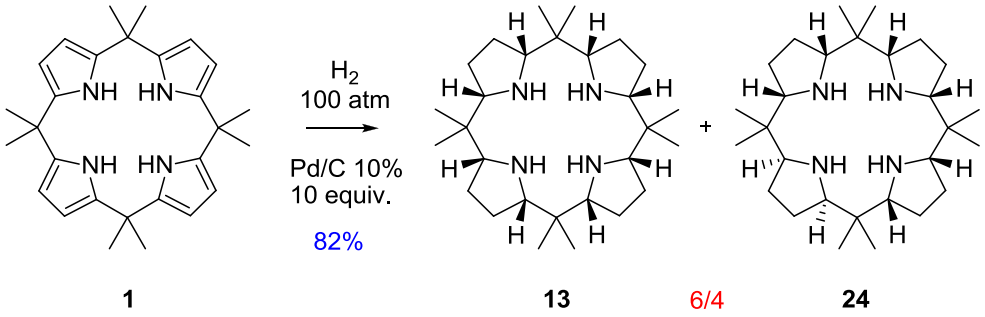

Scheme 27. Hydrogenation of calix[4]pyrrole

We were pleased to observe, as expected, only two products compound **24a** and **13**. The two isomers **13** and **24a** were obtained with the following ratio: 60/40. This ratio is due to the formation of the intermediates of type **A** shown in scheme 22. The mechanism for the hydrogenation of the macrocycle **1** should therefore follow a similar pathway as the hydrogenation of calix[4]furan (see Figure 24). It is interesting to note that we obtained two diastereoisomers of the completely reduced products, like in the hydrogenation of calix[4]furan, but the relative configuration of the minor product for the two heterocyclic calixarenes (Figure 35).

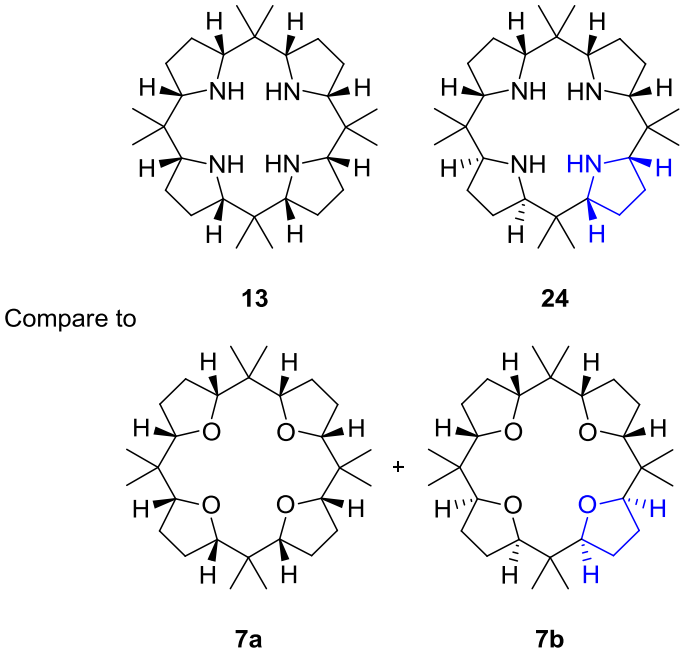

Figure 35. Comparison between the stereochemistry of products issue to the hydrogenation of calix[4]pyrrole and calix[4]furan.

This highly surprising difference has been the base of a thorough study of the stereoselectivity of the hydrogenation of a wide variety of heterocyclic calixarenes presented in the next chapter.

5. SYNTHESIS OF NEW CALIX[4]PYRROLES AND THEIR HYDROGENATION

Since the first anion binding properties of calix[4]pyrrole discovered in 1996, numerous efforts have been done to improve its anion binding affinity and enhance the selectivity. Those thorough studies have led to a multitude of new calix[4]pyrrole derivatives and therefore to the development of new methodology to synthesize them. Among those various recipes, variations modifying the ketone remain the most powerful method to synthesize libraries of different derivatives of the parent macrocycle. The [2+2] condensation emerged as one of the most efficient way to synthesize derivatives with different substituents on the meso-positions. With our methodology for the complete hydrogenation in hand we were interested to apply our hydrogenation procedure to the synthesis of new suitably modified calix[4]pyrroles to afford interesting ligands.

5.1. Synthesis of new calix[4]pyrrole: modification of one meso-substituents

5.1.1. Context

In organo-metallic chemistry and especially for heme and non-heme chemistry, adding external axial ligands (often thiolate and imidazole) is a well-known method to stabilize and increase the catalytic activity of metal-complexes.[147-153] Recently new metal complexes with intramolecular axial ligand attracted particular attention due to their capacity to stabilize high oxidation states of iron. The aim of these studies was to mimic the active site of Cytochrome P450 like enzymes using a modified porphyrins and cyclams as surrogate for the active cofactor (respectively a) and b) Figure 36).[73, 154]

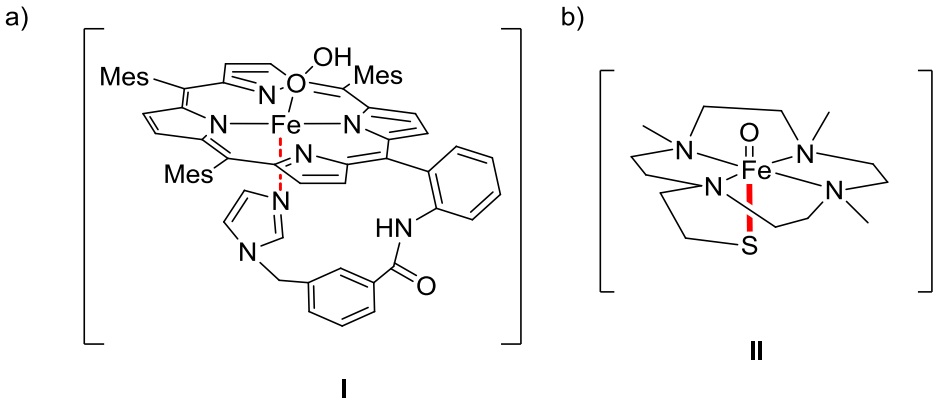

Figure 36. Active iron-oxo species stabilized by intramolecular axial ligand

In the first case, the formation the highly reactive intermediate **I** was only possible when the axial imidazole ligand was present.[154] In the second case, the rigidity of the ligand framework stabilized the thiolate under strongly oxidizing conditions. The thiolate bound to the iron center was to a large extend responsible for the successful stabilization of the oxo-Fe(IV) complex **II**.[73]

In a recent paper, our group described the interesting catalytic activity for oxidation processes of a manganese complex formed with the totally reduced calix[4]pyrrole, the calix[4]pyrrolidine.[155] Sulfur additives were used as apical ligands and increased the catalytic activity of the complex through a postulated intermediate of type **I** was postulated (Figure 37, a)). Our basic idea was to synthesize a new ligand which could provide a square pyramidal $N4(X)_{apical}$ complex and therefore rigidify the framework to increase the catalytic activity of

the manganese complex (Figure 37, b)).

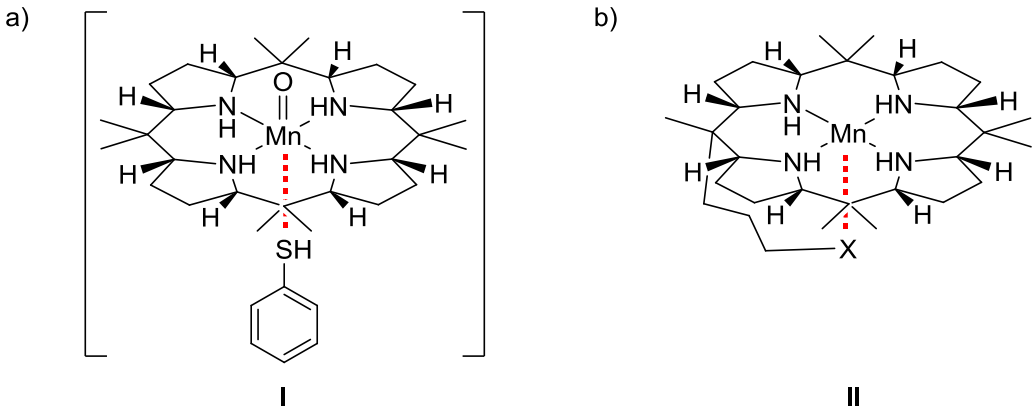

Figure 37.

The synthesis of the ligand type **II** as shown in Figure 37 can be achieved starting with a calix[4]pyrrole modified in one of the meso position. The hydrogenation of of the corresponding precursor macrocycle would also be very interesting. The two faces of the calix[4]pyrrole precursor are not any more identical so the hydrogenation should become stereoselective due to the steric hindrance created by the additional substituent.

5.1.2. Synthesis

As the Rothemund condensation[94] proceeds in a stepwise sequence to form the meso-octamethylcalix[4]pyrrole, we wondered if the use of two different ketones in 4 to 1 ratio could afford the searched for derivative of calix[4]pyrrole with one different meso-substituent. If this approach has to be successful we have to assume that the reactivity of both ketones are similar and that we obtain products determined by the statistical reactions between the two starting materials. We decided to perform the reaction with acetone and the commercially available 5-hydroxy-2-pentanone because the alcohol can easily be functionalized. We carried out the synthesis of the modified calix[4]pyrrole derivative using pyrrole (4 equiv.), acetone (1 equiv.) and 5-hydroxy-2-pentanone (1.1 equiv.) catalyzed by methanesulfonic acid (0.077 equiv.) in ethanol at room temperature (Scheme 28).

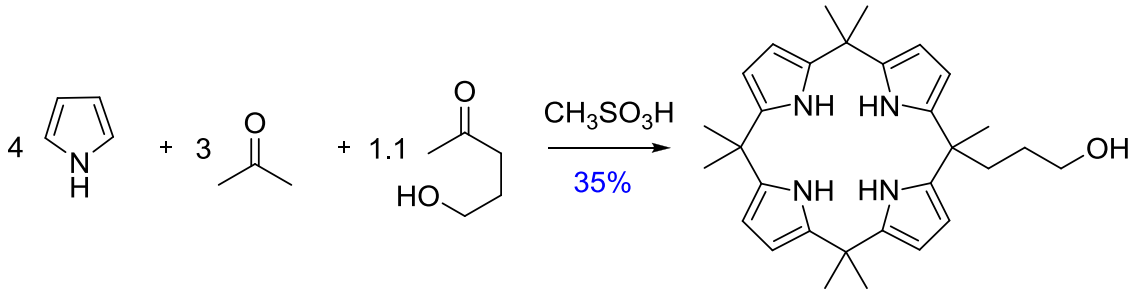

25

Scheme 28. Synthesis of a calix[4]pyrrole derivative, compound **25**

Happily, our efforts along these lines were indeed successful. The driving force during the synthesis of calix[4]pyrrole is the precipitation of the macrocycle, it is the major reason explaining the excellent yield obtained. In our case the product precipitates as well and we were able to isolate and characterized the macrocycle **25** in 35% yield after chromatography. The ratio between compound **25** and the regular calix[4]pyrrole **1** is about 65/35 in the precipitate with almost 10% of side products (GC analysis). A noteworthy aspect of the present reaction is the large amounts of side products detected (50%) in the solution before the filtration; however the purification by column chromatography is relatively easy after filtration. We then discovered that the macrocycle **25** was quite soluble in ethanol and therefore we decided to survey the use of different solvents. Unfortunately, the use of isopropanol, acetonitrile or nitromethane led to disappointing results where the quantities of side products reached 75%. In order to isolate the larger quantity of macrocycle **25**, the reaction mixtures had to be partially evaporated at the end of the reaction and then filtered without additional washing. Attempts to increase the ratio between **25** and **1** failed, even after a long investigation modifying the ratio between the starting ketones did not lead to improved yields of the new macrocylce **25**. In order to gain access to large quantity of macrocycle **25** for a future hydrogenation, the reaction had to be performed in multigram scale (20 g of pyrrole). In this case again the isolation of compound **25** gave a 35% yield.

5.1.3. Hydrogenation of macrocycle 25

The catalytic hydrogenation of macrocycle **25** has been performed under standard conditions described previously for calix[4]pyrrole, 0.36 equiv. of Pd/C 10%, 100 bars of H_2 in acetic acid at 100 °C for 12h. The reaction has been performed several times, affording every time

an extremely complex mixture of products (at least 6 different N-$H_{pyrrole}$). The ^{1}H-NMR spectra of the crude of reaction is presented Figure 38.

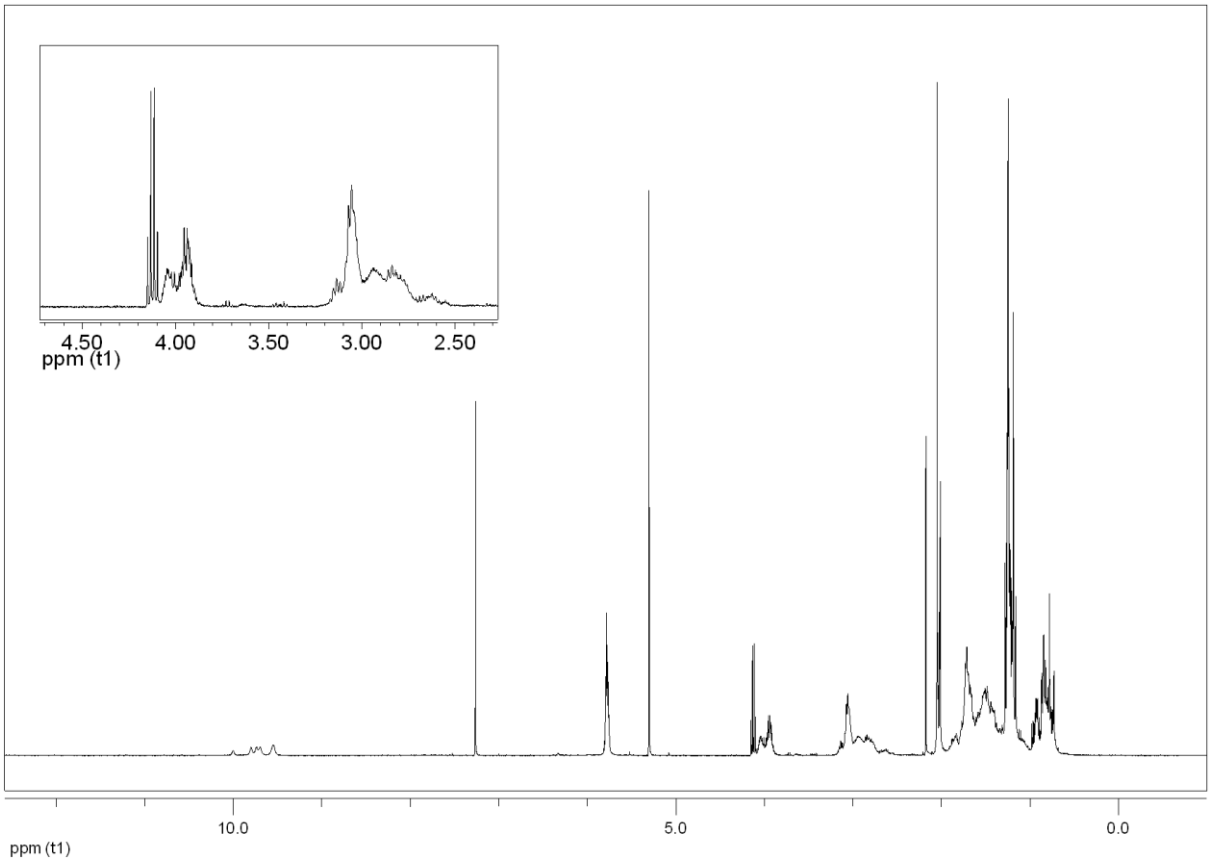

Figure 38. ^{1}H-NMR spectra of the reaction crude of the catalytic hydrogenation of **25**

However the complexity of ^{1}H-NMR spectra had to be expected. Even if we assume that the hydrogenation takes place with high stereoselectivity only forming *cis*-products mixtures of products will be obtained. The totally symetric calix[4]pyrrole gave two stereomers. If we use the mono-substituted calix[4]pyrrole derivative **25** eight *cis*-stereomers would be obtained in this case (Figure 39).

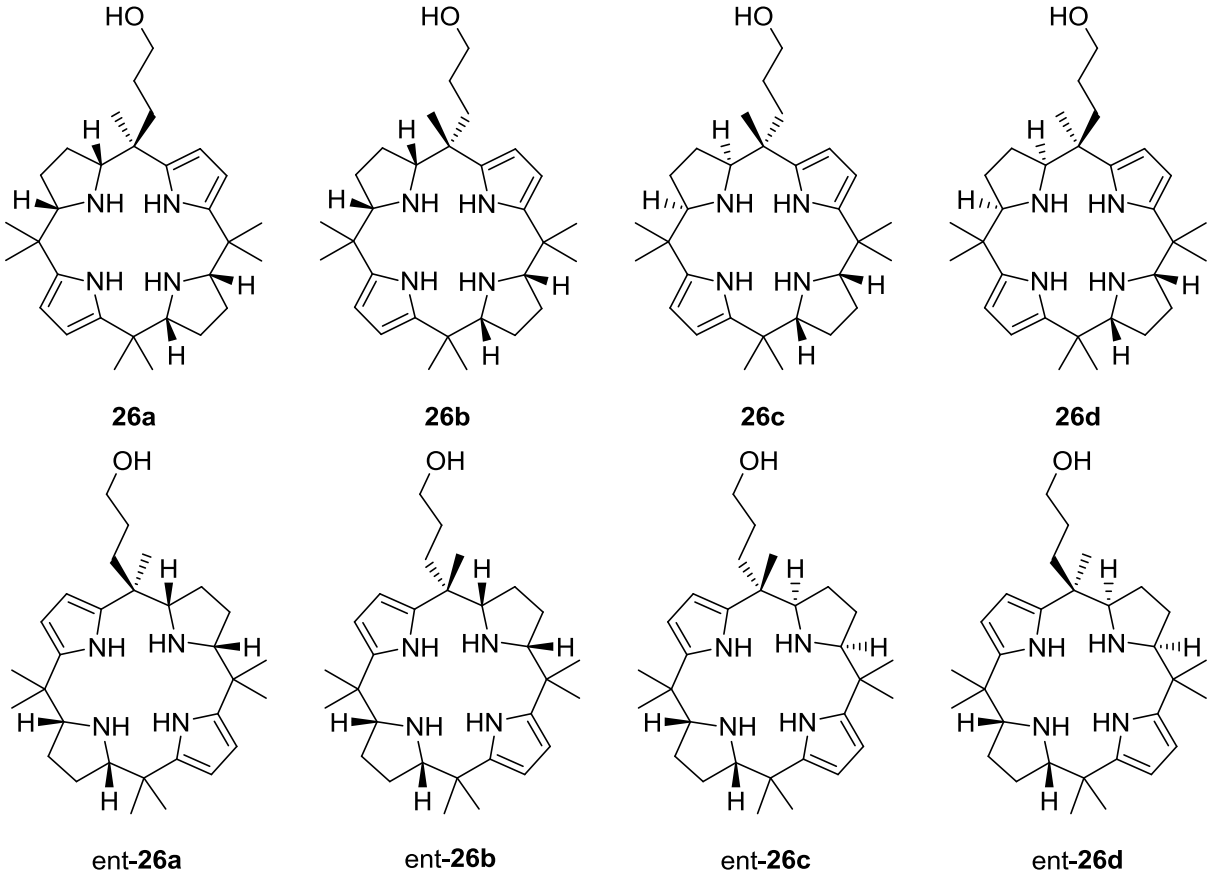

Figure 39. The eight possible cis-stereomers of **26**

Contrary to calix[4]pyrrole, the half-reduction of **25** created only chiral compounds because of the asymmetric meso-carbon. Moreover, because of the two different faces of the formed macrocycles **25,** the hydrogenation of pyrroles could take place on both faces, doubling the number of possible stereoisomers obtainable. The ^{1}H-NMR spectra are compatible with a mixture containing several diastereoisomers (maximum of eight compounds).

Unfortunately, because of time constraints and the complexity of the reaction mixture, the thorough analysis of the crude as well as isolation of products have not been achieved yet. The transformation of a symmetric compound to eight chiral products in a single step was extremely interesting and deserves to be thoroughly analyzed.

It is also interesting to analyze the possible structures which could be obtained after the complete reduction of macrocycle **25**. In view of the results obtained for the hydrogenation of calix[2]pyrrole[2]pyrrolidine **12a** and **12b** previously described and the analysis of the half-

reduction of macrocycle **25**, we should be able to predict the possible structures, which can be obtained for a complete reduction of **25** (Figure 40).

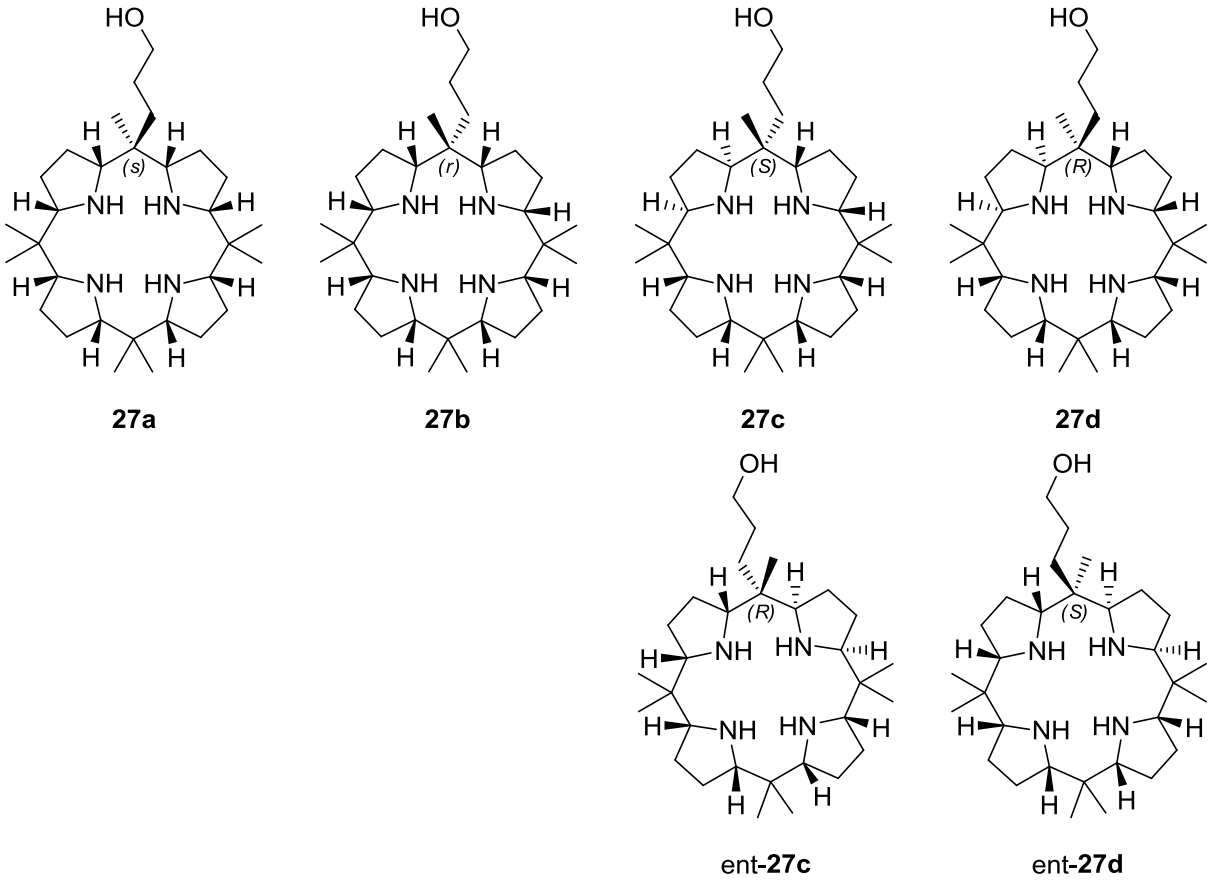

Figure 40. Prediction of the possible stereomers obtained after the complete hydrogenation of **25**

The total reduction of **25** should afford six stereoisomers. Two of them are meso compounds (**27a** and **27b**), the other are chiral (**27a**, **27b**, ent-**27c** and ent-**27d**). The achievement of the complete hydrogenation of the macrocycle **25** would lead in a single step to a collection of highly interesting ligands for metal complexation.

5.2. Synthesis of new calix[4]pyrrole: modification of two meso-substituents

In view of the interesting results described above, we sought to increase the symmetry by adding an additional substituent in another meso-position. The typical Rothemund

condensation with acetone and the 5-hydroxy-2-pentanone in equal quantities should give a complex mixture of products. We consequently decided to use the [2+2] methodology already described for the synthesis of strapped calix[4]pyrrole.[156-159]

5.2.1. Synthesis

We started this investigation by the synthesis of dipyrromethane **28**. The condensation between pyrrole (7.3 equiv.) and 5-hydroxy-2-pentanone (1 equiv.) catalyzed by TFA (0.1 equiv.) without additional solvent provided compound **28** in almost 64% yield (Scheme 29).

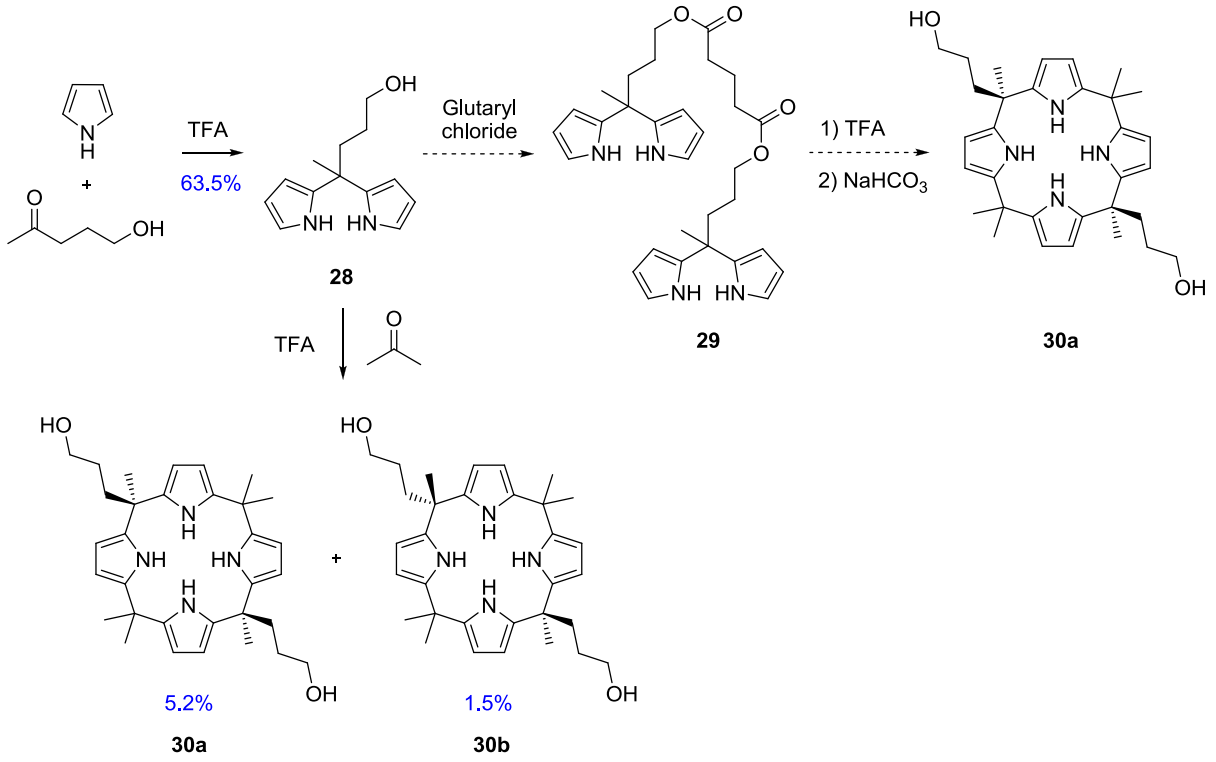

Scheme 29. Synthesis of new calix[4]pyrrole **30a** and **30b**

We were pleased to successfully grow single crystals of compound **28** by slow evaporation of a solution of **28** in CH_2Cl_2. The X-ray diffraction analysis and the complete description of compound **28** will be described in a later chapter (Chapter 2, 5.3).

The direct [2+2] condensation has been tried by Christophe Letondor, a former Post-Doc in our group, gave the two products **30a** and **30b** in very low yield. In view of those poor yields and the difficulties he had during the purification, we decided to proceed via the linear bis-

dipyrromethane **29** and to perform an intramolecular condensation. We then decided to control the location of the alcohol on the same face of the macrocycle by linking the two dipyrromethane **28**. We synthesized a "strapped" calix[4]pyrrole which should allow us to release the two alcohols at the end of the synthetic sequence. We directed our attention toward the synthesis of compound **29**. We wished to applied the methodology developed by Lee et al[160] for the synthesis of strapped calix[4]pyrrole to the synthesis of **30a** via the bis-dipyrromethane **29**. First trials were promising; however this synthetic route has not been explored thoroughly due to a lack of time. The catalytic hydrogenation of **30a** has not been achieved yet, but we can postulate on the number of half and totally reduced compounds possible to be obtained after the partial or total hydrogenation of **30a** (respectively Figure 41 a) and b)).

a)

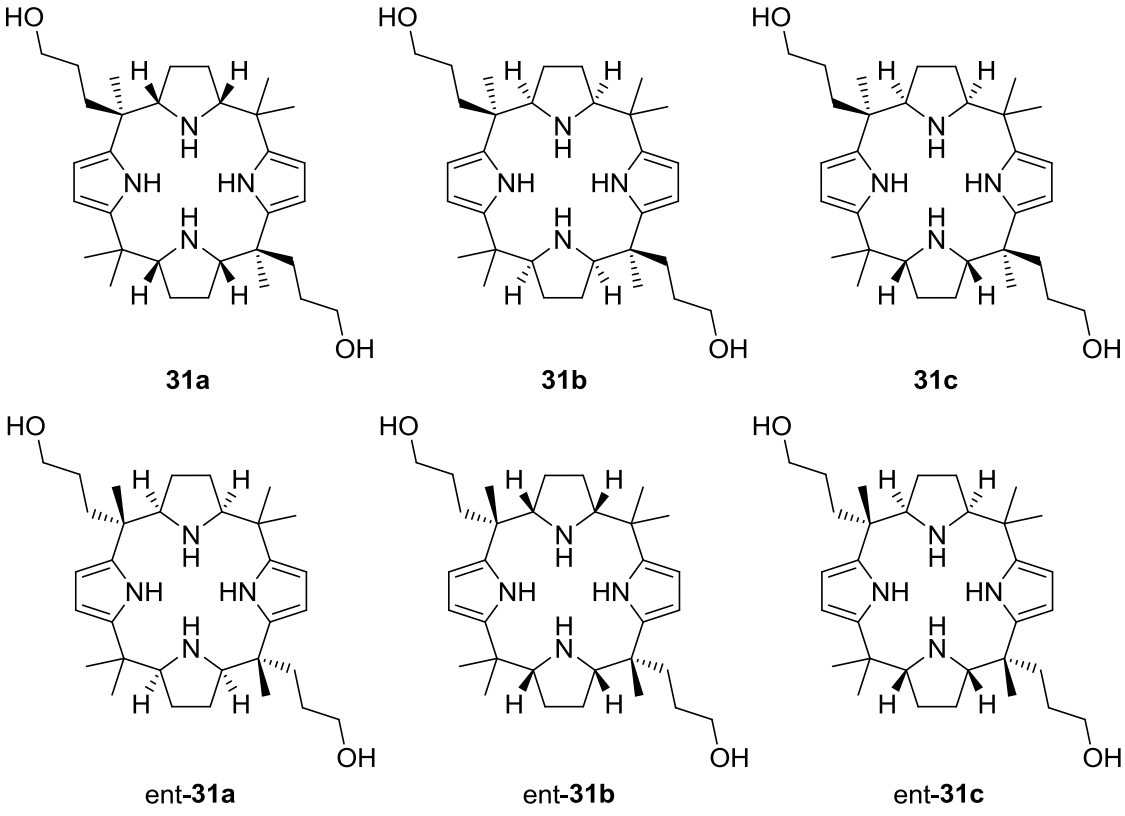

b)

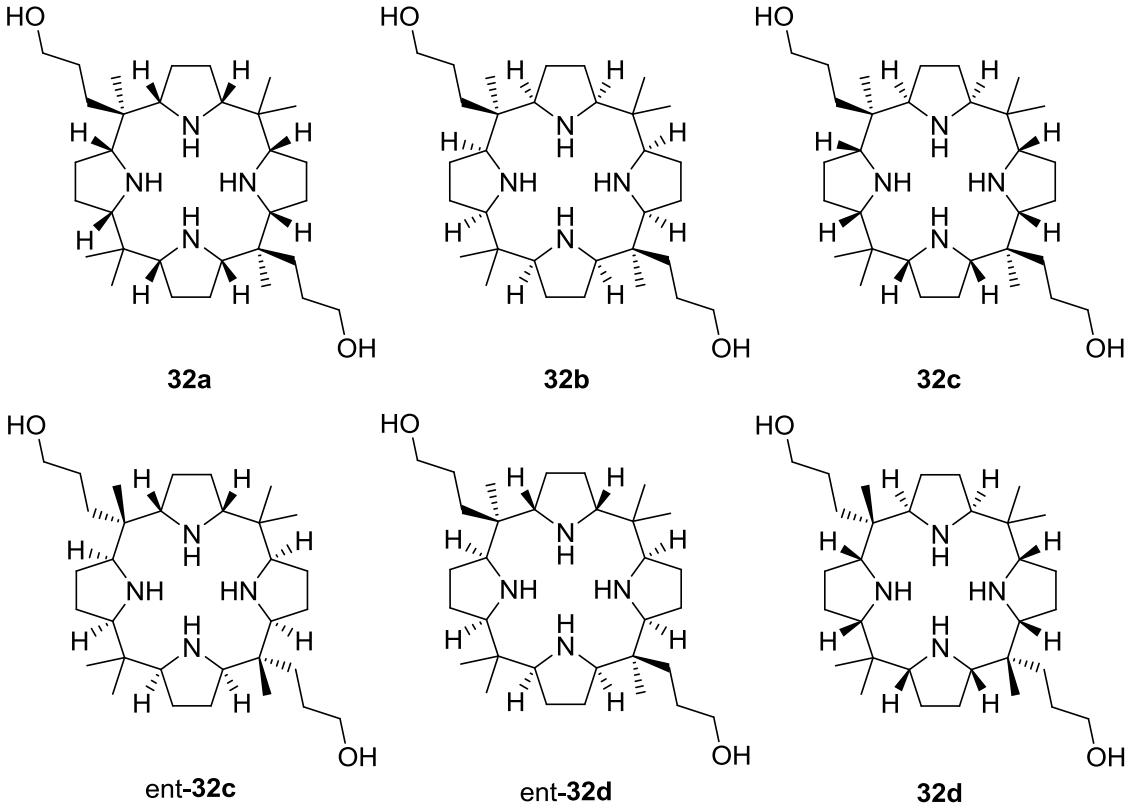

Figure 41. Prediction of the possible stereomers obtained after the partial (a) and complete (b) hydrogenation of **30a**

Always assuming that only cis-hydrogenation occurs, six chiral macrocycles should be obtained for the half reduction of **30a** against eight for the partial reduction of **25**. This is explained by the additional element of symmetry of **30a** (C_2 and mirror plane m) compared to **25** (possessing only one mirror plane m). Therefore only one pair of enantiomers can be written for the half-reduced **32** where *cis*-pyrrolidine are on the two different faces. Six stereomers could be obtained for the complete reduction of **30a**, two meso-compounds and two pairs of enantiomers.

5.3. Description of the molecular structure of compound 28

The 4,4-Bis(1H-pyrrol-2-yl)pentanol is described in our work as compound **28** and its structure is published in Acta Cryst. E.[161] Suitable crystals of compound **28** have been successfully obtained for an X-ray diffraction analysis. Compound **28** crystallized in the chiral

monoclinic space group *P*21. The pyrrole rings are inclined to one another by 62.30 (11) °, and the propanol chain is in the extended conformation. In the crystal, the two pyrrole NH atoms are involved in intermolecular N-H···O hydrogen bonds, leading to the formation of a helical arrangement propagating in [010] plane. An interesting feature of the crystal structure is the absence of any conventional hydrogen bonds involving the hydroxyl H-atom. There is, however, a short intermolecular O-H···π interaction involving one of the pyrrole rings (Figure 42 and 43).

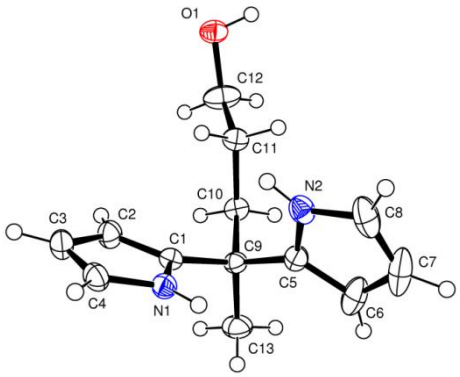

Figure 42. A view of the molecular structure of compound **28**, with the displacement ellipsoids drawn at the 50% probability level.

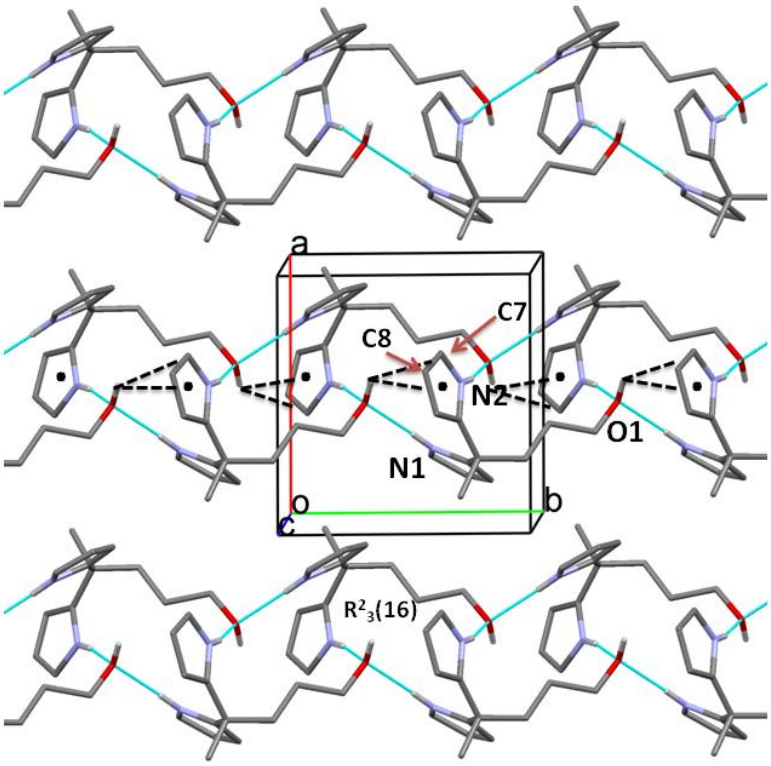

Figure 43. A view, along the *a* axis, of the crystal packing of compound **28**. The N-H···O

hydrogen bonds are shown as dotted cyan lines and the O-H···π interactions are shown as dotted black lines (for clarity these interactions are shown for only one of the helices; see Table 12 for details).

The structure of compound **28** is shown in Figure 42, and the geometrical parameters are given in the experimental part. This achiral compound crystallized in the chiral monoclinic space group *P*21. In the 5 compounds of dipyrromethane structure located in the CSD this angle varies between 68.5 to 89.6 °. In the crystal, the molecules are linked by conventional N-H···N intermolecular hydrogen bonds leading to the formation of helical chains propagating in [010] (Figure 43 and Table 12). The basic unitary hydrogen bonding graph set can be described by a 2-donor, 3-acceptor *R*2 3(16) ring, while the basic binary graph set is a C(8) chain. This gives an extended notation of C(8)[*R*2 3(16)]. A fuller hydrogen bonding graph set analysis can be obtained using Mercury. It can be considered to involve either the C7═C8 bond (centroid = *Cg*1) with an O-H···π angle of *ca* 135.0°, or a weaker interaction involving the pyrrole ring (N2,C5—C8; centroid = *Cg*2), with an O-H···π angle of only *ca* 114.0° (these data were obtained using the program Mercury). Footnote for Table 12: *Cg*1 = centroid of bond C7═C8; *Cg*2 = centroid of pyrrole ring N1,C5—C8.

Table 12.

Hydrogen-bond geometry (Å, °)

D—H···*A*	*D*—H	H···*A*	*D*···*A*	*D*—H···*A*
N1—H1*N*···O1^{i}	0.88 (2)	2.05 (2)	2.9238 (18)	174.3 (19)
N2—H2*N*···O1^{ii}	0.90 (2)	2.06 (2)	2.9529 (18)	171.5 (19)
O1—H1*O*···*Cg*1^{iii}	0.87 (3)	2.53	3.20	135.0
O1—H1*O*···*Cg*2^{iii}	0.87 (3)	2.64	3.10	114.0

Symmetry codes: (i) *x*, *y*−1, *z*; (ii) −*x*+1, *y*−1/2, −*z*+2; (iii) *x*, *y*+1, *z*. *Cg*1 and *Cg*2 are the centroids of the C7=C8 bond and the N2/C5–C8 pyrrole ring, respectively.

5.4. Conclusion

Two new calix[4]pyrroles **25** and **30a** have been isolated and characterized. The catalytic hydrogenation of those macrocycles needs to be investigated more thoroughly because the products were obtained as mixtures of diastereoisomers. It will certainly be interesting to determine the selectivity of this process and to study the properties of the different

stereoisomers. However, those macrocycles were not subjected to the successful condition found previously for the complete reduction of calix[4]pyrrole **1**. The complete reduction of calix[4]pyrrole **25** and **30a** should afford numerous highly valuable ligands capable to form metal complexes.

6. CONCLUSION

The synthesis of calix[4]pyrrolidine **13** by catalytic hydrogenation of calix[4]pyrrole **1** has been achieved. We have developed a reproducible procedure which allows the isolation of two diastereoisomers **12a** and **12b** of the partially reduced macrocycle and the calix[4]pyrrolidine **13** in large scale. GC analyses of the mixtures, obtained following heterogeneously catalyzed hydrogenation reactions of calix[4]pyrrole **1**, have allowed determining the product composition. Compound **12a**, which had not been detected during previous work, has been isolated and its relative configuration has been assigned through single-crystal X-ray diffraction. A single, all-*cis*, fully hydrogenated compound **13** could be obtained in low yields only under drastic reaction conditions (100 atm of hydrogen pressure at 100°C in acetic acid). The relative configuration of compound **13** has been unequivocally assigned by X-ray diffraction analysis. The yield of the totally reduced calix[4]pyrrolidine **13** has first been more than doubled since we isolated this compound for the first time, and can now be obtained in high yields starting from the half reduced compound **12b**. To our huge satisfaction a reproducible procedure for the complete reduction of calix[4]pyrrole has been developed recently. This reaction provided only two fully reduced products, compound **13**, already isolated from our previous work, and a new isomer of the fully reduced macrocycle, compound **24**. Despite our intensive efforts, the reasons for the use of a huge excess of catalyst to perform the complete hydrogenation of **12b** or calix[4]pyrrole **1** have not been elucidated yet. We still intensively work on this project, always with the aim of, maybe, one day discovering or creating a new catalyst system. This discovery opens a new route in the fascinating world of calix[4]pyrrole chemistry

Chapter 3

SYNTHESIS AND HYDROGENATION OF CALIX[M]FURAN[N]PYRROLE (M+N=4)

Abstract

Complete mechanistic understanding of heterogeneous catalytic hydrogenation processes remains a challenging problem. The details of mechanistic sequence, the influence of the substrate and the source of *cis*-stereoselectivity are often only purely understood By increasing the number of heterocycles in a substrate molecule, we increase the number of possible diastereomers obtained after hydrogenation. However, the hydrogenation of calix[4]furan[104] and of calix[4]pyrrole[129, 130, 162] are known to afford only two isomers out of 45 possible probably due to their limited degree of conformational freedom. A thorough investigation of the hydrogenation reaction was performed using twelve different macrocyclic substrates (Scheme 30).

Different factors were tested, which might influence the stereoselectivity during the hydrogenation process and therefore the number of diastereomers obtained: 1) The number of pyrroles (n) and furans (m) contained in different substrates of the generic class described by calix[m]furan[n]pyrrole (m+n=4) (for instance the calix[3]furan[1]pyrrole). 2) In the case of m=n, the position of the two different cycles (i.e. alternating or neighboring positions). 3) The replacement of pyrrole(s) or furan(s) by their reduced analogues (this modification created dramatic changes in the electronic properties and incorporated three-dimensional information into the starting materials). 4) The replacement of pyrrole by non-cyclic chains, which had a great impact on the flexibility respectively the rigidity of the macrocycles. All the macrocycles were synthesized via novel syntheses. The 38 products have been fully

characterized and their relative configuration determined by X-ray analysis (15 selected structures). As a consequence of this work, the probable sequence of the catalytic hydrogenation of calix[4]pyrrole was revealed. This conclusion could be drawn based on the identification of intermediates and the unequivocal determination of the relative configuration of these model compounds for the hydrogenation sequence.

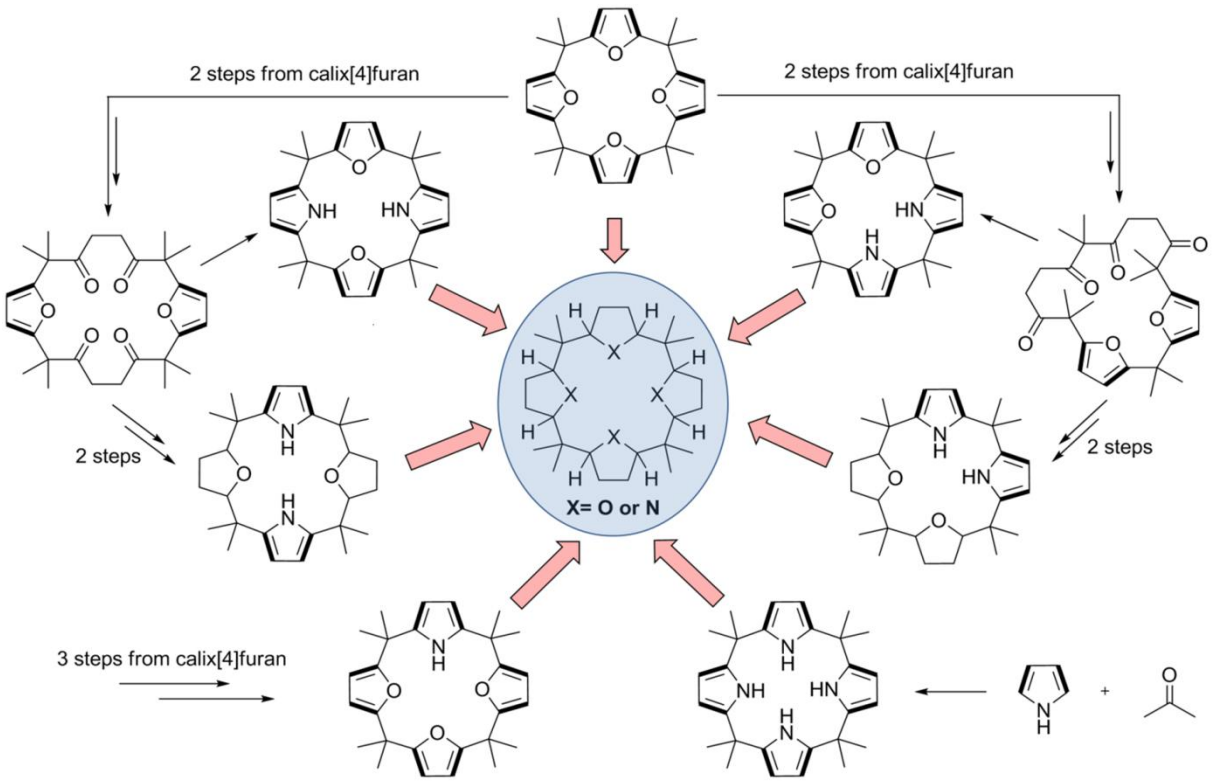

Scheme 30. Catalytic hydrogenation of various macrocycles.

Context

The total reduction by catalytic hydrogenation of calix[4]pyrrole **1** was extremely difficult to achieve. Finding suitable conditions to perform the complete reduction of **1** took me almost three years. During those years, only the half reduction was possible in good yields. Confronted to repeated failures to obtained the calix[4]pyrrolidine in acceptable yield, we started to seek a way to bypass the problem. We thought about replacing pyrroles by an isoelectronic heterocycle, which would be easier to reduce, e.g. the furan ring. We wished to selectively replace pyrroles in calix[4]pyrrole by one, two or three furan rings in order to facilitate the complete reduction of the macrocycle and obtain information on the sequence of the hydrogenation process. Using our knowledge about the reduction process we postulated a probable sequence of the calix[4]pyrrole hydrogenation (see Scheme 23 in Chapter 2). One of the conclusions we came up with was that partially reduced macrocycles containing two adjacent pyrroles were easier to reduce than macrocycles containing two pyrroles in opposite position of each other. Replacing selectively pyrroles by furan in those positions would create valuable stable model compounds. We reasoned that studying the hydrogenation behavior of these model compounds should allow us to validate the hypothetical sequence.

It was during this study that we discovered impressive differences in the diastereoselectivity of the hydrogenation depending on the type of starting material used. We decided to analyze systematically the influence of the structure of the starting material on the diastereoselectivity of hydrogenation of our macrocycles. The hydrogenation of mixed macrocycles forming a structural continuum between calix[4]pyrrole on one end of the spectrum and calix[4]furan and on the other extreme might provide us with a collection of interesting data. We speculated that these data may allow us to improve our understanding not only of the specific sequence of events occurring during the heterogeneous catalytic hydrogenation of our substrates, but that we might also detect more general trends in these important class of transformations.

1. INTRODUCTION

The term “asymmetric induction” could be divided into three major categories: 1) the external asymmetric induction: the chiral information is obtained from an external source, most of the time from a chiral catalyst or ligand (catalytic processes). This is probably the most powerful and efficient method for asymmetric syntheses. 2) the relayed asymmetric induction: the source of chirality comes from so called “chiral auxiliaries” (stoechimetric processes). This strategy involves at least three steps. Two of the three steps are needed to add before the asymmetric induction and to remove the auxiliary after the crucial step. 3) the internal asymmetric induction: the information, source of chirality, is located in a stereogenic center present in the molecule (all type of reactions). Most of the time, the molecules used are obtained from the “chiral pool”, such as enantiopure natural products.

The internal asymmetric induction is a perfect illustration of the strong link between the structure of a molecule and its reactivity. Emil Fischer was the first to recognize the importance of the strong connection between 3D structure of molecules and their properties especially in a biological and medicinal environment. Emil Fischer enlarged his concept to a key-lock picture in order to paraphrase the action of enzymes, nature’s superbe catalysts. Based on the concepts developed by Fischer Cram and Elhafez[163] analyzed nucleophilic additions to carbonyls possessing a stereogenic center near to the reactive part of the molecule. They proposed the “Cram’s rule” in order to describe the process and to predict the outcome of the diastereoselective addition. The presence of a stereogenic center in a molecule will induce the chirality of the adjacent carbon created during the transformation. The approach proposed by Cram is mainly based on the analysis of the steric hindrance of the substituents present at the stereogenic center. Other models and rules have been developed later (Felkin-Anh model, for instance) improving and generalizing the pioneering concepts proposed in Cram’s rule.[164]

Most of the asymmetric inductions described in literature are performed in homogeneous media using homogeneous catalyst. Many of the methods developed by the chemists can applied for a multitude of substrates and surprisingly also for many different reactions. This is one of the big advantages of the chemical approach compared to the biochemical approach, where scope is almost always a problem. Huge efforts have gone into the development of heterogeneous catalysis with the aim to combine the lessons learned from homogenous catalysis with the advantages of having a solid catalyst in a separate phase. Heterogeneous

catalysts are easily separated from the reaction mixture. The recycling of the catalyst is straight forward and the amount of metal traces in the products are minimized, an argument of utmost importance in the synthesis of drug molecules. The heterogeneous catalysts for asymmetric reaction could be classified into three categories:[165] 1) catalysts made from the binding of homogeneous catalysts to a solid heterogeneous matrix; 2) modification of heterogeneous catalysts by adsorption of chiral molecules; **3) <u>achiral catalysts which could provide asymmetric reactions because of its interaction with chiral substrates.</u>**

The diastereoselective heterogeneous catalysis via achiral catalysts remains an extremely attractive field of research dominated by hydrogenation reaction.[166, 167] The reactions are based on the interaction of achiral catalysts, such as Pd/C, Rh/C or Raney-Ni, with substrates using the electronic affinity between the metal, its matrix and the organic molecule. As in homogenous catalysis steric repulsion plays the role of a counterbalancing factor (Figure 44).

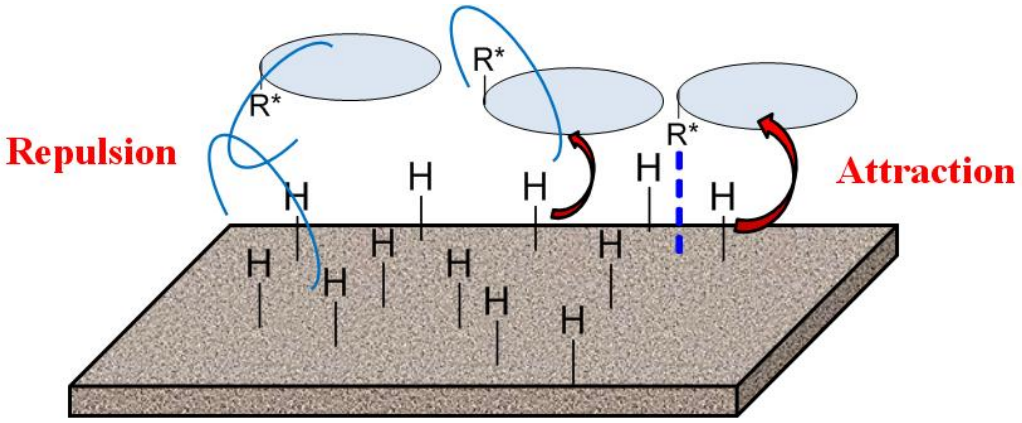

Figure 44. Interaction between heterogeneous catalyst and chiral substrates.

These interactions allow a diastereotopic face differentiation and therefore are involved in the face selective hydrogenation. Compounds with a small degree of freedom are often preferred and give better results. One of the relevant examples in this context is the selective hydrogenation of α-pinene into cis-pinane (Scheme 31).[168, 169]

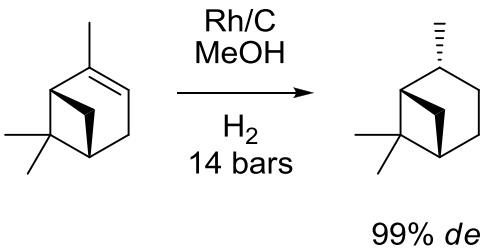

Scheme 31. Diastereoselective hydrogenation of α-pinene

The steric hindrance of the bicyclic ring provides an excellent diastereoselective excess. Heteroatoms like nitrogen or oxygen are also known to influence the diastereoselectivity of the hydrogenation via interaction with the surface of the catalyst. A good illustration is the reduction of (S,E)-2-butylidenecyclopentanol where the alcohol interacts with the catalyst to form a reduced compound with high diastereoselective excess (Scheme 32).[170]

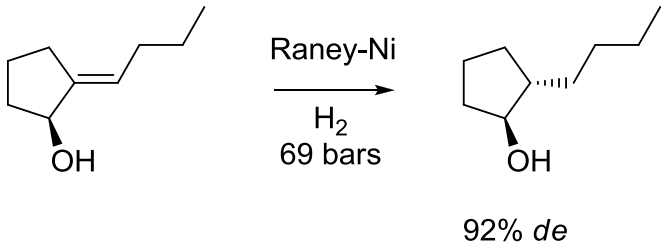

Scheme 32. Diastereoselective hydrogenation of (S,E)-2-butylidenecyclopentanol

The interaction between the substrate and the catalyst is extremely dependent on the polarity of the solvent. For instance, the authors observed that a very polar solvent like DMF reverses the diastereoselectivity of the reaction.
Chiral auxiliaries could also be used to induce the diastereoselectivity of the hydrogenation. This method has very often been used for the preparation of amino-acids,[171-176] and carried out with oxazolidinone, proline or derivatives for the selective reduction of double bonds[177] or aromatics.[178-182]

In our work, we wished to determine what kind of factors are involved in the induction of the diastereoselectivity during the hydrogenation of macrocycles of the type calix[4]heterocycles. The reduction of calix[4]furan to the corresponding saturated compound has been known for a long time, however no investigation had been done on the source of the diastereoselectivity. We decided to perform a systematic investigation modifying the rigidity of the macrocycles, the nature of heteroatoms and their positions in the macrocycle, the oxidation state of the five membered rings and the relative configuration of the connections between the reduced five membered rings of the macrocycle. The initial goal was to mimic the sequence of the hydrogenation process. The second goal was to detect the factors influencing the diastereoselectivity of the heterogeneous catalytic hydrogenation process on macrocyclic molecules with restricted conformational freedom, based on a relatively simple construction principle.

For review on this topic see:
M. Heitbaum, F. Glorius, I. Escher, *Angew. Chem. Int. Ed*. **2006**, *45*, 4732.
and especially substrate-directable reactions see:
A. H. Hoveyda, D. A. Evans, G. C. Fu, *Chem. Rev*. **1993**, *93*, 1307.

2. CONFIRMATION OF THE HYDROGENATION SEQUENCE

2.1. Our basic idea

The Scheme 22 of Chapter 2 describes our mechanistic hypothesis for the hydrogenation process. The central argument of our hypothesis is that compound **12d** is much easier to reduce than compound **12b** (Scheme 33). To confirm this assumption, we were confronted to three problems: 1) compound **12d** has never been isolated so far and its rational synthesis would be extremely difficult to achieve; 2) compound **12b** has been obtained but at that time we were not able to achieve the hydrogenation of **12b**; 3) compound **12d** and **12b** come from the same starting material. As we could not control the reaction we were not able to change the conditions in such a way to obtain the selective formation of **12d**. For these reasons, we thought that replacing compounds **12b** and **12d** respectively by compounds **33** and **34** might give us important information on the hydrogenation process.

Compound **33** and **34** would be readily obtained from respectively compound **35** and **36**. Assuming that the furan rings in the macrocycle are still easier to reduce than the pyrrole rings in the macrocycle, we should be able to control the site of the first hydrogenation and obtain **33** or **34** selectively. To test this approach we have to control the position of the furan rings in the unsaturated macrocycle. Moreover, we would have a great opportunity to probe the difference in the diastereoselective induction of THF compared to pyrrolidine rings during the hydrogenation. We therefore concentrated our efforts toward the synthesis of compound **35** and **36**.

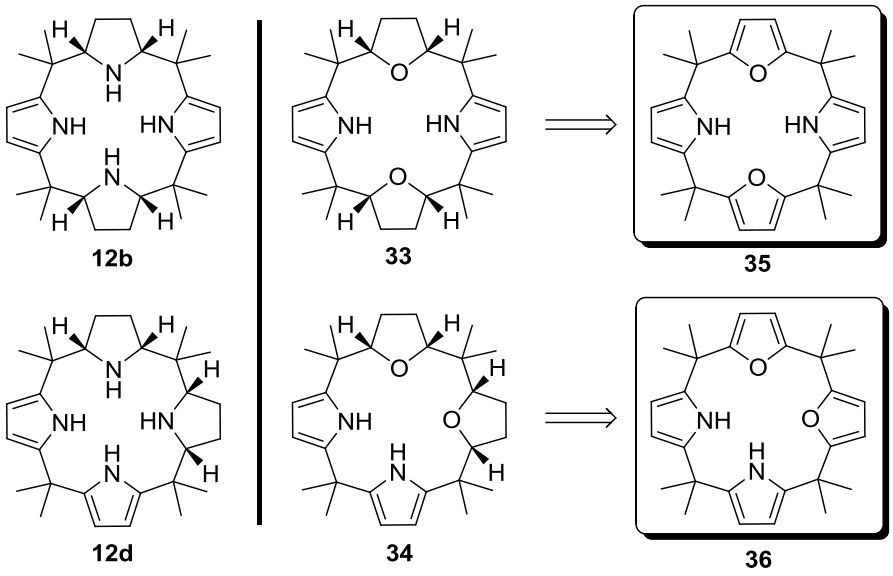

Scheme 33. Basic idea of our new project with the goal to mimic the sequence of the hydrogenation process

2.2. Synthesis of macrocycle 35 and 36

2.2.1. Introduction

The calix[2]furan[2]pyrrole **35** and **36** have already been described in literature. They have been synthesized for the first time by French et al in 1958.[183] Their basic approach was to use a [2+2] condensation of dipyrromethanes (Scheme 34).

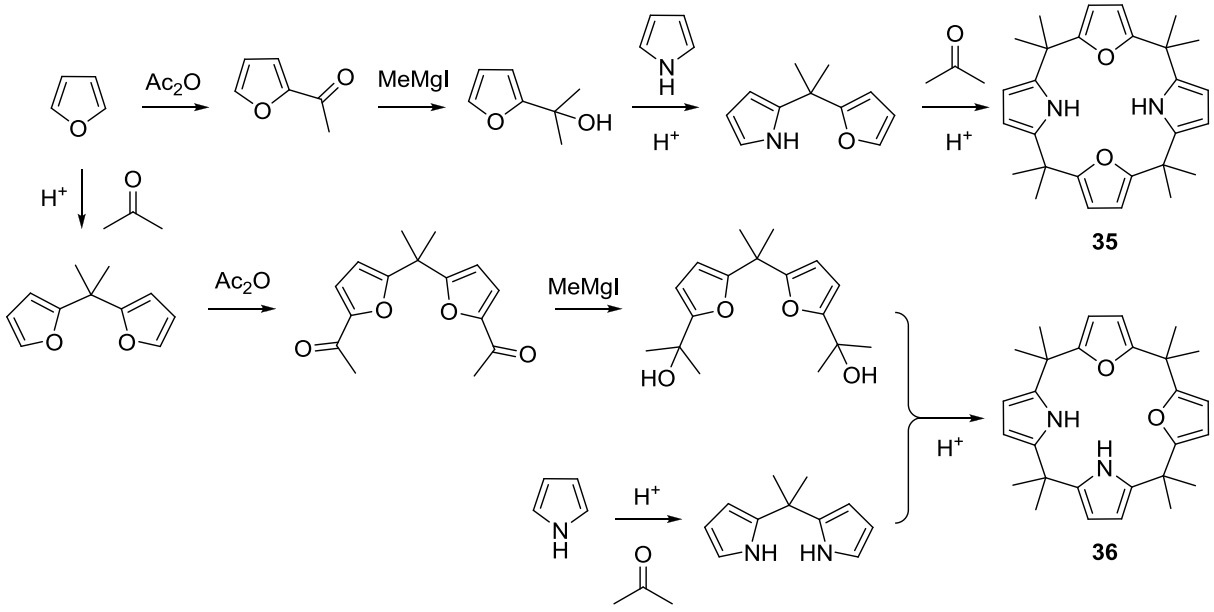

Scheme 34. Synthesis of macrocycle **33** and **34** by French et al[183]

Following this extremely long synthetic pathway, calix[2]furan[2]pyrrole **35** and **36** were synthesized in very poor yields (1-4%). This paper was followed a few years later by an investigation on their potential application as ligands.[184] Another approach appeared at the beginning of the 21th century, based on the "3+1" condensation only applicable for the synthesis of compound **33** (Scheme 35).[185]

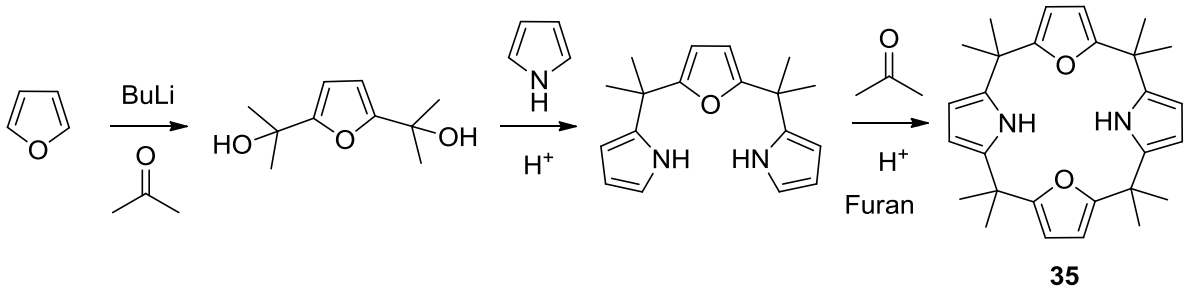

35

Scheme 35. Synthesis of macrocycle **35** by Lee et al.[185]

Following this strategy, macrocycle **35** was obtained in almost 20% yield. The major drawback of this approach is that only a limited number of other calix[m]furan[n]pyrrole (m+n=4) are accessible. Surprisingly, only few studies of their anion binding abilities have been reported so far.[186-189] The difficulty of their syntheses coupled to the low yield is probably the reason for this lack of scientific interest. The synthetic pathway offered by French and al, is the only route available for the synthesis of all four possible calix[m]furan[n]pyrroles (m+n=4).

2.2.2. Our synthetic approach

In order to gain access to appropriate quantities of compound **35** and **36** for our investigation, we decided to use another strategy. This pathway has to allow the synthesis of the four regioisomers of calix[m]furan[n]pyrroles (m+n=4). It should produce acceptable overall yields of the final product and minimizes the number of steps. We based our strategy on two reactions: 1) the pioneer work of by LeGoff et al[190] in the early 80's on the selective oxidative ring opening of calix[4]furan by *m*CPBA. They described the selective formation of mono-, bis- tri- or tetra-α,β-insaturated-1,4-diketones according to the number of equivalent of *m*CPBA added. 2) The Paal-Knorr synthesis of pyrrole, successfully applied for the synthesis of calix[m]furan[n]pyrrole (m+n=6).[191] Using this pathway, we would gain access to the four possible calix[m]furan[n]pyrroles (m+n=4) starting from the easy available calix[4]furan (Scheme 36).

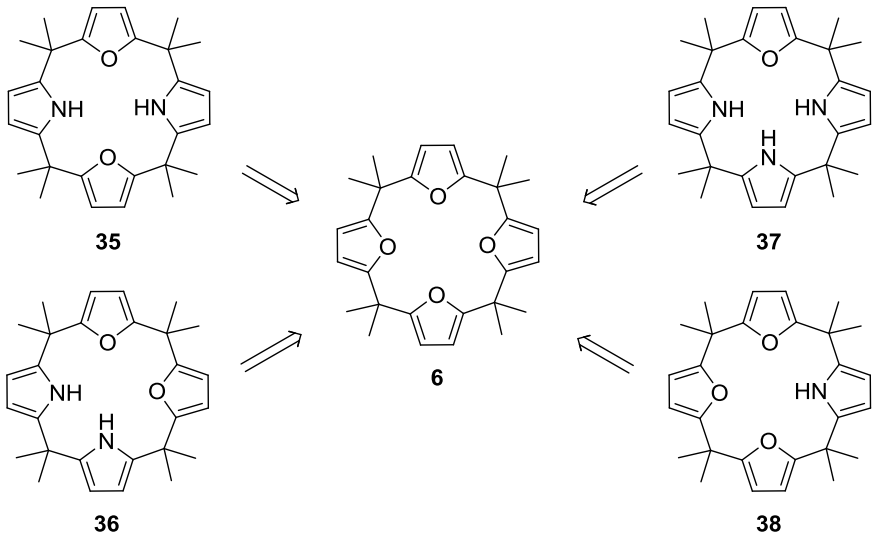

Scheme 36. General retrosynthesis of calix[m]furan[n]pyrroles (m+n=4)

We started our investigation by the synthesis of calix[4]furan in large scale, our starting material for the synthesis of macrocycle **35** and **36**. We used an experimental procedure described by Jurczak et al.[192] in 2000 which should potentially afford calix[4]furan with 70% yield. The condensation between furan and acetone in dioxane using sulfuric acid afforded calix[4]furan in 30% yield in our case (Scheme 37).

The oxidative ring opening of **6** was carried out with 2.2 equivalent of *m*CPBA in cold $CHCl_3$. This reaction provided three different products: two di-ring-opened enediones **39** and **40** and one tri-ring-opened unsaturated hexaketone **41**. Compound **39** and **40** were obtained as a mixture, after column chromatography in 45/55 ratio respectively and 60% yield. Compound **41** has been isolated after column chromatography with 28% yield. In their experimental part, French et al. succeeded in isolating each product by column chromatography, however, following their condition, we were not able to separate compound **39** and **40**. Nevertheless, we wished to continue with the mixture in the aim to separate them in a later step. The mixture of **39** and **40** was submitted to the reduction of the α,β-unsaturated ketones using zinc dust and acetic acid at 100°C to provide compound **42** and **43** in 92% yield after chromatography. Unfortunately the separation by column chromatography of the regioisomers was still impossible at that time. When trying to perform the next step from the mixture of isomers, we realized that only one of the two compounds, compound **43,** was soluble in the solvent used for the reaction.

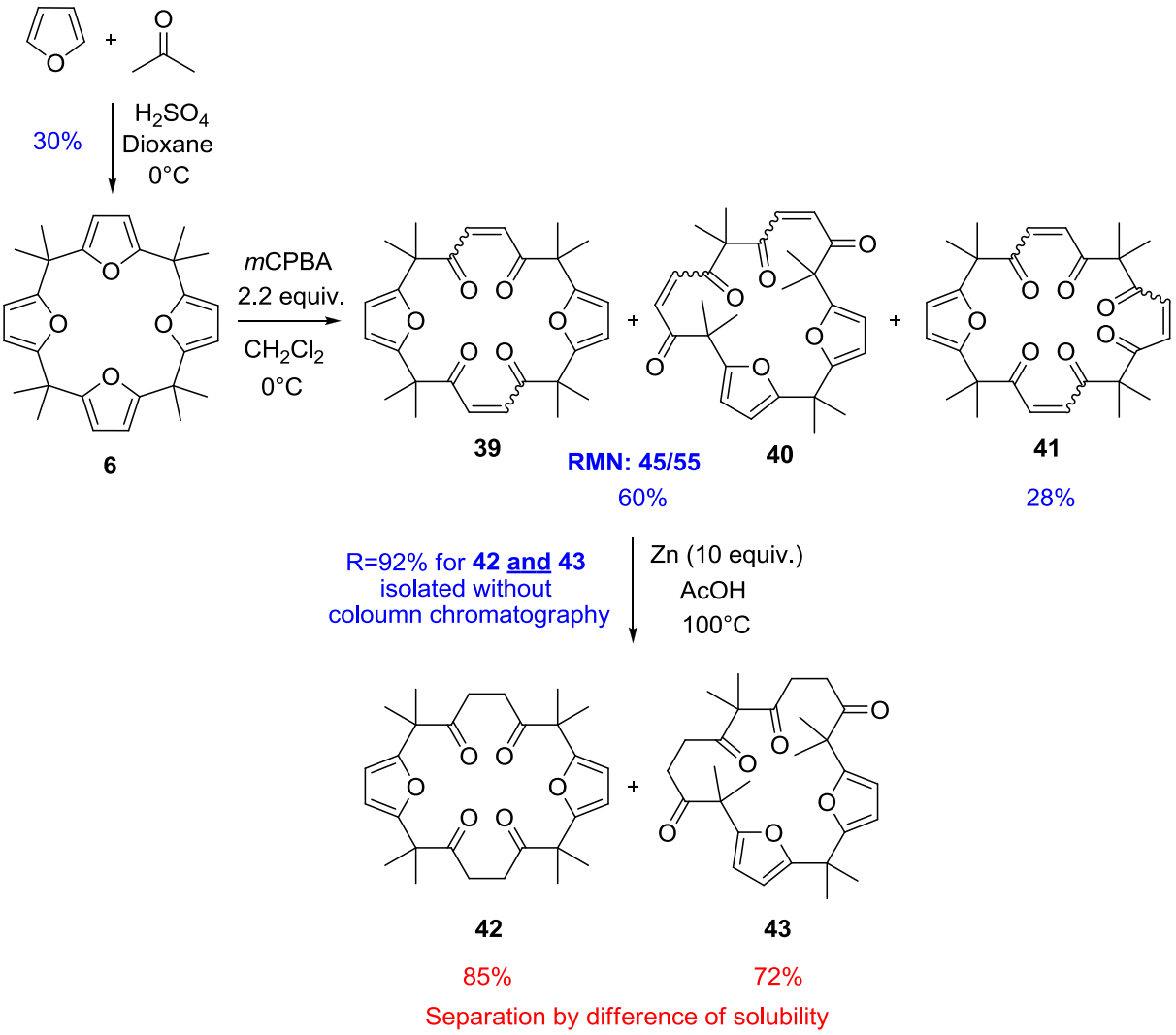

Scheme 37. Synthesis of bis-2,4-diketones **42** and **43**

Thanks to this difference of solubility, we were able to separate the regioisomers by successive washing with 80°C ethanol. We finally isolated the reduced tetraketone **42** and **43** with respectively 85 and 72% yields. The next step is the formation of pyrroles by Paal-Knorr reaction. This reaction had never been applied to tetraketone **42** and **43** so far, and a special effort had to be done to optimize the conditions, especially for **42**. The synthesis of calix[2]furan[2]pyrrole **35** was carried out using 5 equiv. of ammonium acetate as source of ammoniac in a mixture of EtOH/$CHCl_3$ (1/1) at 60°C over night (a, Scheme 38). After evaporation of chloroform, we were able to filter off compound **35** in 84% yield (>99%, GC).

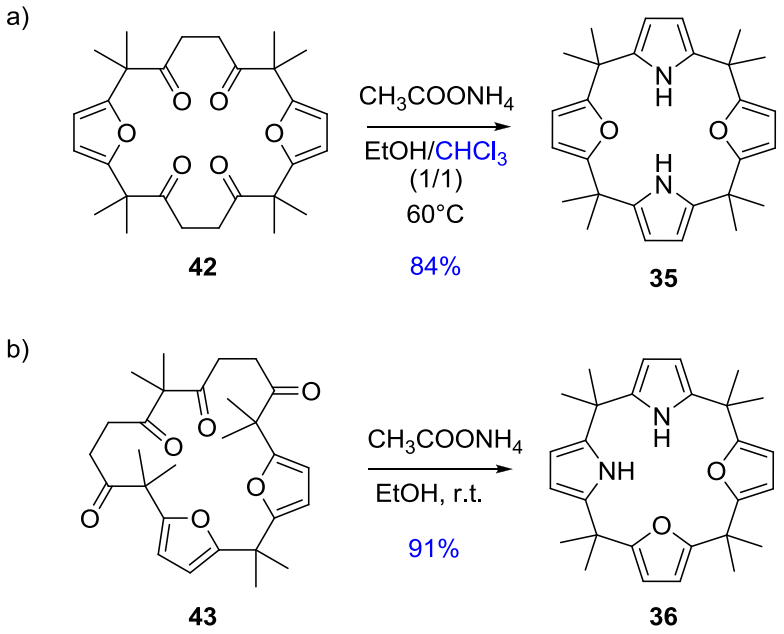

Scheme 38. Synthesis of calix[2]furan[2]pyrrole **35** and **36** via Paal-Knorr reaction

The reduced tetraketone **43** smoothly reacts with ammonium acetate, in ethanol at room temperature to afford after filtration the calix[2]furan[2]pyrrole **36** with 91% yield (b, Scheme 36). The two unsaturated macrocycles **35** and **36** were characterized by NMR and HRMS spectroscopy. We were pleased to successfully grow single mono-crystals of both compounds as well. The X-ray diffraction analyses of macrocycle **35** and **36** are shown in Figure 45 and 46 respectively.

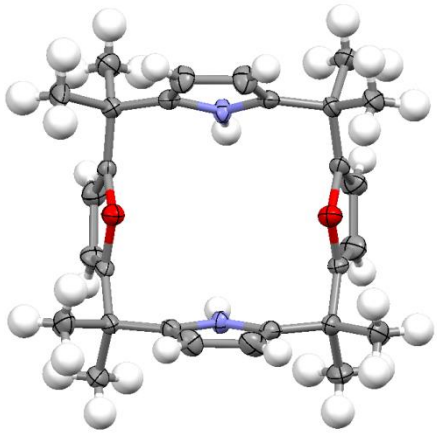

Figure 45. Molecular structure of compound **35**, with the displacement ellipsoids drawn at the 30% probability level

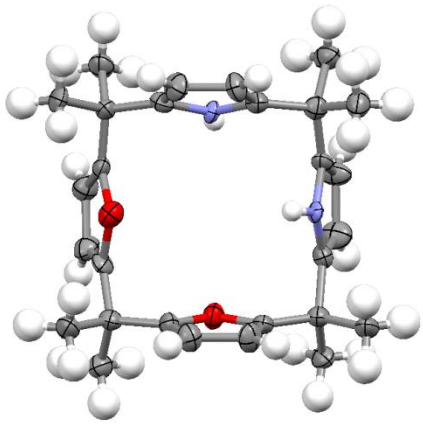

Figure 46. Molecular structure of compound **36**, with the displacement ellipsoids drawn at the 50% probability level

The X-ray structure analysis of compound **35** and **36** revealed the alternating conformations of the pyrrole and furan rings in the solid state. For both compounds, rings opposite each other are in almost parallel plans which form a very nice cavity. The two structures are extremely similar to the crystalline structure of calix[4]pyrrole previously described.
Finally, calix[2]furan[2]pyrrole **35** and **36** were obtained with 43 and 40% overall yield respectively, starting from calix[4]furan, in three easy and efficient steps. Moreover, compound **41** which has been produced during the ring opening of calix[4]furan will be used in a further investigation, that increases the efficiency of the synthetic pathway.

2.3. Hydrogenation of macrocycle 35 and 36

General remark: We systematicaly indicate the diastereoselectivity by the ratio of the diastereomeric products (d.r., normalized to 100).[193]

2.3.1. Hydrogenation of 35

We submitted the macrocycle **35** to the optimized hydrogenation condition developed previously for calix[4]pyrrole. We carried out the reduction of **35** using 0.3 equiv. of Pd/C 10%, 100 bars of H_2 in acetic acid as solvent at 100°C for 24 h (Scheme 39).

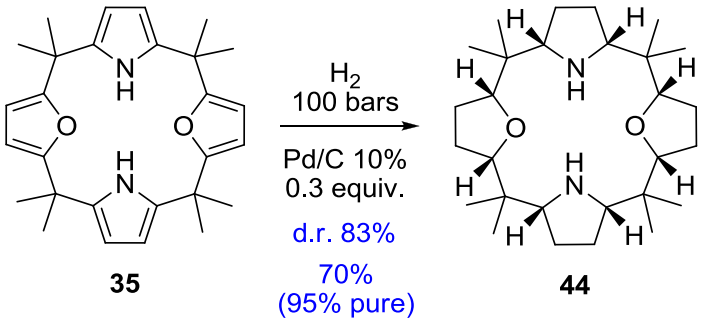

Scheme 39. Catalytic hydrogenation of calix[2]furan[2]pyrrole **35**

We were surprised to detect in the GC analysis only one major product (d.r. ~83%) in the crude together with 3 other side products. After a recrystallization in EtOAc, we removed a large amount of side products, to provide the product in 84% purity. After successive recrystallizations trying to remove the impurity (probably another isomer of **44**) we obtained the totally saturated macrocycle **44** with 70% yield, 95% pure. The relative configuration of

the reduced macrocycle is exclusively based on NMR spectroscopy analysis. We could later confirm its relative configuration by X-ray diffraction crystallography (Figure 47).

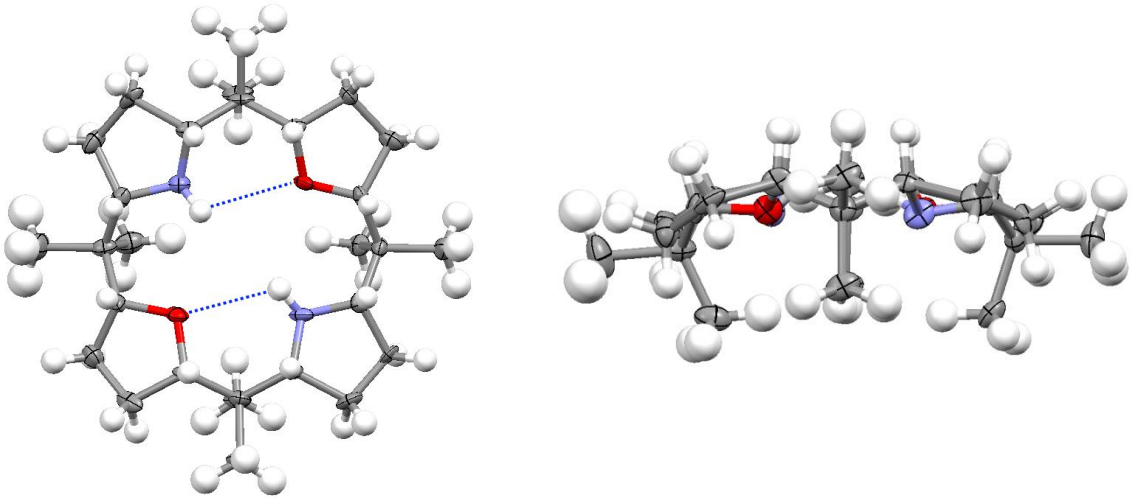

Figure 47. Molecular structure of compound **44**, with the displacement ellipsoids drawn at the 30% probability level. N-H···O hydrogen bonds are shown as blue dotted lines.

Hydrogens α to heteroatoms are all on the same face of the macrocycle. The four heterocyclic rings form a slightly distorted plane. Four of the eight methyl groups are in quasi axial position and the other in quasi equatorial position. The structure of **44** is very similar to the structure of calix[4]pyrrolidine illustrated previously.

We then wished to probe the influence of the hydrogen pressure during the reduction of compound **35**. We decided to test if we could observe a complete conversion even at low pressure or if applying a reduced hydrogen pressure would allow observing intermediates on the way to the fully reduced macrocycle. The hydrogenation of **35** was carried out using 0.3 equiv. of Pd/C 10%, 27 bars of H_2 in acetic acid as solvent at 100°C for 24h (Scheme 40).

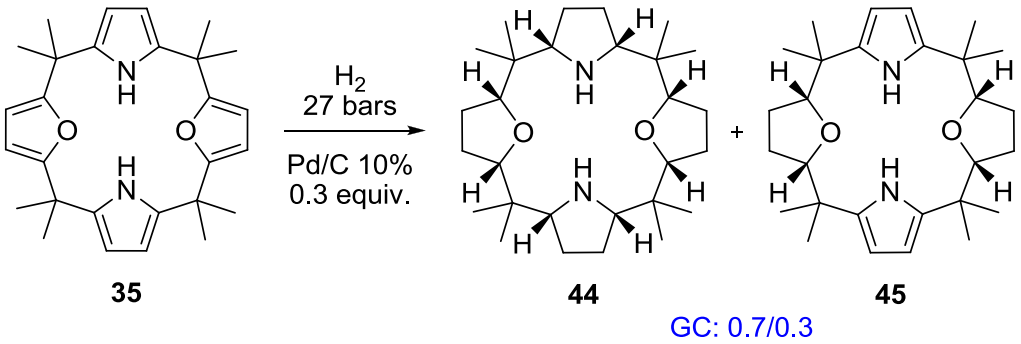

Scheme 40. Catalytic hydrogenation of calix[2]furan[2]pyrrole **35**

The consumption of **35** under this condition was complete. However, we discovered a new minor product together with compound **44** in a 0.7/0.3 ratio. This new reduced macrocycle was then characterized as the half reduced macrocycle **45**. So, we decided to check with different pressure of H_2 in order to determine if compound **45** was an intermediate in the formation of the completely reduced compound **45**. The amount of conversion of compound **45** into compound **44** as a function of the variation of the hydrogen pressure is presented (Figure 48).

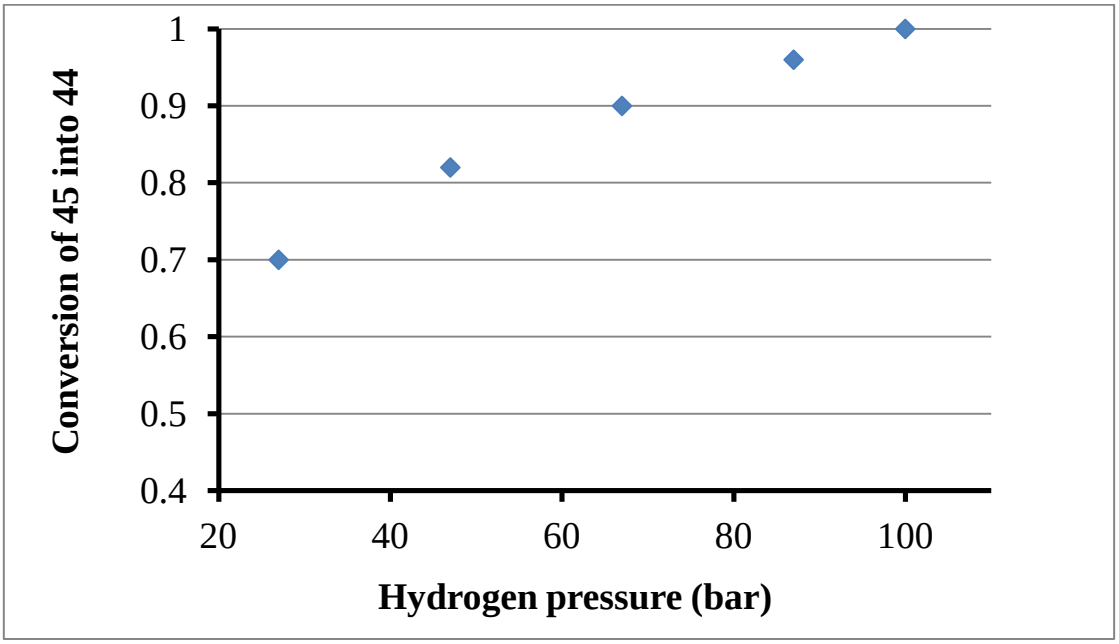

Figure 48. Conversion of compound **45** into **44** according to the hydrogen pressure

The quantities of compound **45** decrease with the increase the H_2 pressure. These observations proof that compound **45** is an intermediate on the way to the formation of **44**. This result means that the hydrogenation to the half reduced macrocycle **45** is relatively easy, happening already under reduced pressure. The next step the transformation of **45** into the fully reduced macrocycle **44** is considerably more difficult and needs higher pressure.

2.3.2. Hydrogenation of 36

As next step we analyzed the behavior of the unsaturated macrocycle **36**. First, we decided to test the hydrogenation under the same conditions than previously described for **35**. We carried out the reduction of compound **36** under the 100 bars of H_2 (Scheme 41).

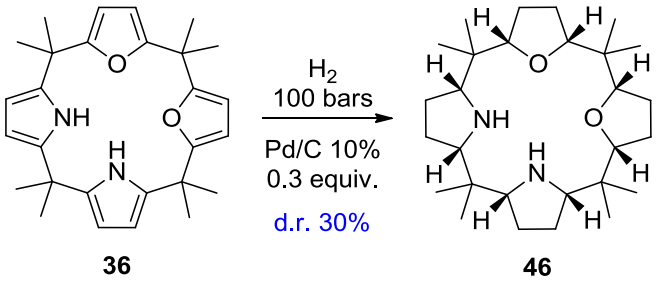

Scheme 41. Catalytic hydrogenation of calix[2]furan[2]pyrrole **36**

Surprisingly, the catalytic hydrogenation of **36** afforded a multitude of products containing a major product in up to 30% yield as determined in the GC. The isolation of the major product was extremely difficult. After a first recrystallization, we performed two chromatographic separations on columns. By this tedious procedure we obtained the fully saturated macrocycle **46** with 15 % yield in ~80% purity. We were not able to completely purify this compound and therefore the full characterization could not be achieved in a satisfactory quality. The major product was characterized by GCMS and HRMS. The relative configuration has been successfully attributed by X-ray diffraction analysis of the sample containing the major product (80%). The molecular structure of compound **46** is shown figure 49.

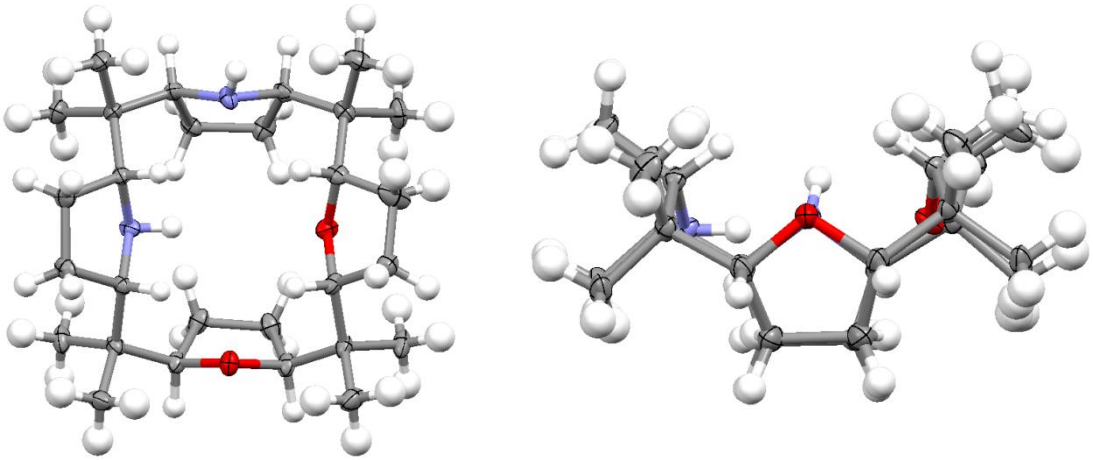

Figure 49. Molecular structure of compound **46**, with the displacement ellipsoids drawn at the 30% probability level.

The structure of **46** in the solid is very interesting, it significantly differs from the molecular structure of **44**. The molecule is not plane and forms a kind of cavity with the rings on opposite sides of the macrocycle almost parallel. The molecular structure of **46** is very close

to the structure of calix[4]furan described in Chapter I. No hydrogen bonds have been detected. The almost planar conformation of **44** can therefore be attributed to its hydrogen bond networks.

If the mechanistic hypothesis described in the beginning of this chapter is correct, the complete hydrogenation of **36** should be easier than the hydrogenation of compound **35**. We tested the influence of a low hydrogen pressure on the reduction of **36**. The hydrogenation of **36** could be successfully achieved using two different pressures: 50 and 15 bars. The hydrogenation carried out with 50 bars gives essentially the same results than the one performed at 100 bars. The GC of the crude reaction mixture presents a multitude of products and a major one (d.r. ~30%). The hydrogenation carried out at 15 bars gave again a similar result. The GCMS of the crude showed the presence of a small amount of the half reduced macrocycle. It is very interesting to note that even at low hydrogen pressure the reduction of the macrocycle **36** and therefore the hydrogenation of the half reduced macrocycle **34** is easy to achieve. The conditions needed for the hydrogenation of **35** (clearly more than 27 atm) are more strenuous than the conditions which are sufficient for a quasi complete hydrogenation of **36** (15 atm are sufficient).

Assuming that the general behavior of macrocycle **12b** and **12d** (Scheme 30) is closely related to macrocycle **33** and **34**, therefore compound **12d** must be much easier to reduce than compound **12b**. The hydrogenation sequence of calix[4]pyrrole **1** described scheme 22 Chapter 2 has been mimicked and the proposed sequence is compatible with the results obtained from the furan analogues! The question arises: why are two pyrroles in opposite position in a macrocycle of the type calix[4]heterocycle more difficult to be reduced than two neighboring pyrroles?

If we summarize the products of the hydrogenation of calix[4]pyrrole **1**, calix[4]furan **6** and calix[2]furan[2]pyrrole **35** and **36** in term of diastereoselectivity, we obtained the following: 1) the complete hydrogenation of calix[4]pyrrole affords two diastereoisomers of the fully reduced macrocycles from 45 stereoisomers possible; 2) the complete hydrogenation of calix[4]furan affords two diastereoisomers as well. One of the diastereoisomers is different from the one obtained with calix[4]pyrrole; 3) the complete hydrogenation of calix[2]furan[2]pyrrole **35** only affords one major diastereoisomer (80%); 4) the complete hydrogenation of calix[2]furan[2]pyrrole **36** affords one major diastereoisomer (30%) and lot

of minor isomers (70%). These results lead to the following question: what are the factors influencing the strength of the diastereoselective induction of these types of macrocycles during the hydrogenation process? It is well known that hydrogenation of double bonds, pyrroles or furans takes place with high *cis*-stereoselectivity. In our molecules we observe another type of diastereoselective induction. In the reduction of our macrocycles two distinct diastereoselectivty processes must occur to give one or two diastereomer with almost complete selectivity: 1) the *cis*-hydrogenation of the five membered rings; 2) the influence of reduced heterocycles on the ring-face discrimination for the next *cis*-hydrogenation of a neighbouring ring or of a ring situated opposite to the first saturated ring. The 3D structure of the macrocycle, its rigidity or the nature of heteroatoms and their position must have a direct impact on the diastereoselective induction observed. For this reason, we decided to investigate experimentally the influence of the major factors on the diastereoselectivity observed in the hydrogenation process.

3. INVESTIGATION ON FACTORS INFLUENCING THE DIASTEREO-SELECTIVITY OF THE HYDROGENATION OF DIFFERENT MACROCYCLES

To clarify the content of this chapter, we decided to separate the results for each class of compounds into two subchapters: the first chapter treating the syntheses and hydrogenation, and the second chapter discussing the stereoselectivity of the hydrogenation process.

3.1. Results

3.1.1. Synthesis and hydrogenation of unsaturated macrocycles type calix[4]heterocycle

For this investigation some of the macrocycles were already synthesized, calix[4]pyrrole **1**, calix[4]furan **6**, calix[2]furan[2]pyrrole **35** and **36**. The complete hydrogenations of compound **1**, **35** and **36** have been described in the previous chapter. However, the complete reduction of calix[4]furan **6** already described in literature, has never been done in our group. For this reason we decided to repeat the catalytic hydrogenation of calix[4]furan in order to

have a serious of comparable results done under experimental conditions, which are as similar as possible.

3.1.1.1. Reduction of calix[4]furan **6**

The first reduction of calix[4]furan has been reported by Van Beylen et al.[121] in 1985. The hydrogenation provides two different diastereoisomers of the saturated macrocycle. The authors were able to separate the two diastereoisomers **7a** and **7b** in a 70:30 ratio. Characterization of the two diastereoisomers has been done only by X-ray diffraction analysis, other additional analytical and spectroscopic data and the detailed experimental description are missing. The HRMS, IR and especially the complete analysis of the NMR spectrum has not been reported so far.

We carried out the hydrogenation of calix[4]furan under the optimized condition used for calix[4]pyrrole using 100 bars of H_2, Pd/C 10% in acetic acid for 24h at 100°C (Scheme 42).

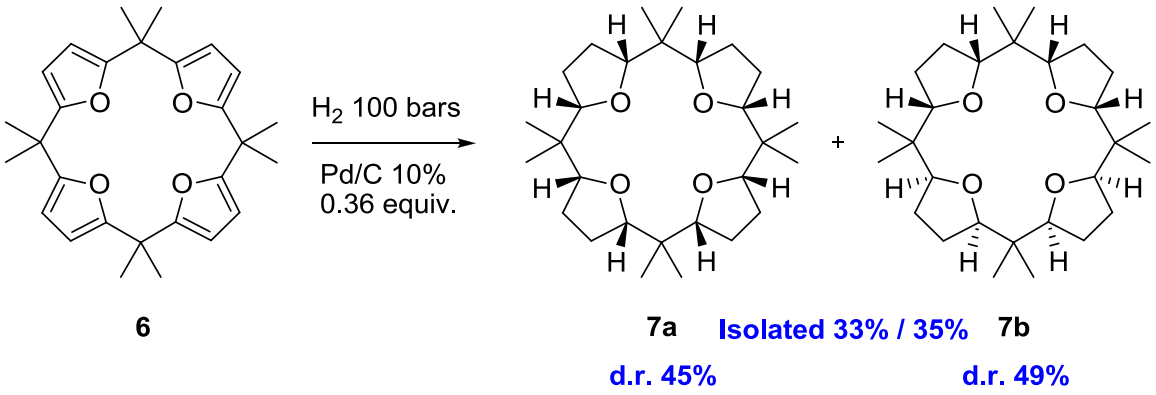

Scheme 42. Catalytic hydrogenation of calix[4]furan **6**

After treatment, the crude reaction mixture was simply washed with cold ethanol. The purity of the crude product analyzed by GC was astonishing: two major products in 49:45 ratio in favor of **7b** were visible together with a small impurity (6%) (Figure 50). Surprisingly, we obtained more of compound **7b** than compound **7a**. Van Beylen et al. reported a 30:70 ratio in favor of compound **7a**.

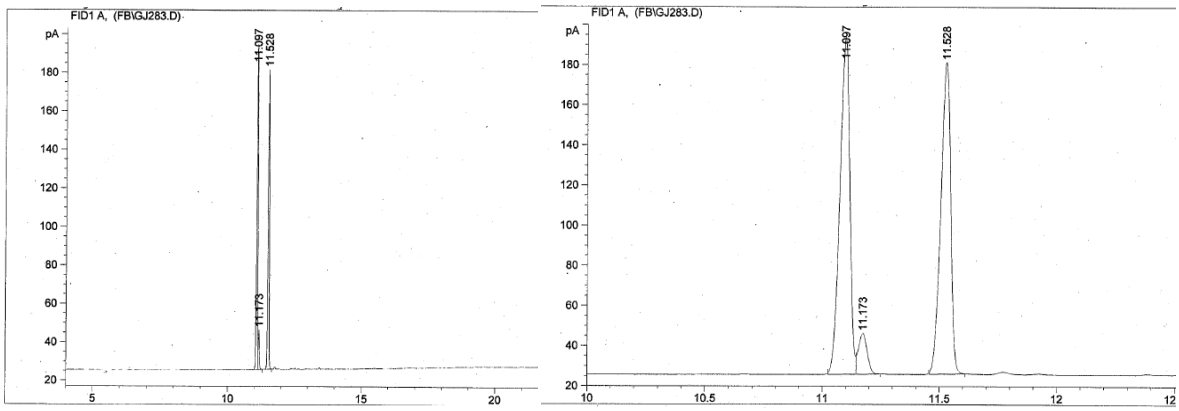

Figure 50. GC spectra from the crude of the hydrogenation of calix[4]furan **6**

After column chromatography we were able to isolate compound **7a** and **7b** with 33 and 35% respectively. The ^{1}H-NMR spectra of the two macrocycles presented puzzling shape.

3.1.1.1.1. Characterization of compound **7a**

The ^{1}H-NMR spectrum of compound **7a** is shown Figure 51.

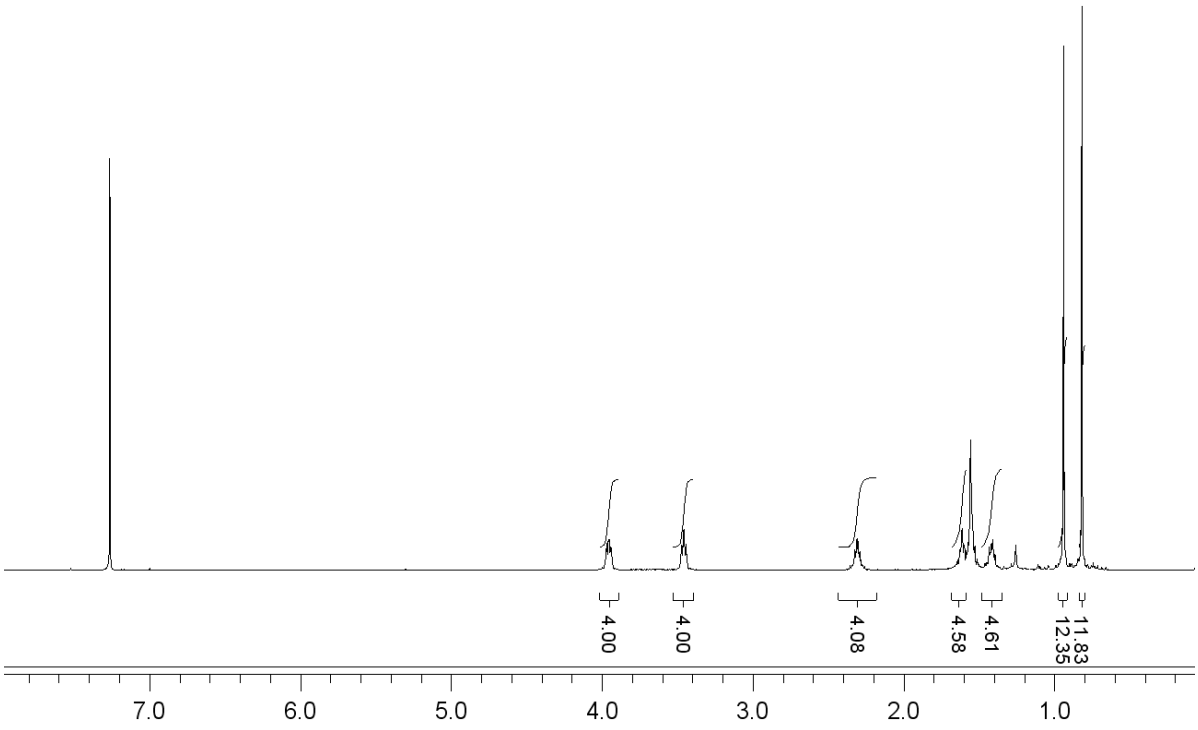

Figure 51. ^{1}H-NMR spectrum of compound **7a**

We were extremely surprised by the ^{1}H-NMR spectrum, which displayed two distinct peaks for the hydrogen in α-position of oxygen. Considering the C_4 axis of molecule **7a** we should have detected only one peak in this region. It means that the molecule lost a part of its symmetry. It is known that the stable conformations of molecules in solution could often be related to their molecular structure in the solid state. In order to analyze the solid structure of **7a**, we successfully grew a single mono-crystal suitable for X-ray diffraction analysis. The molecular structure of compound **7a** is shown Figure 52.

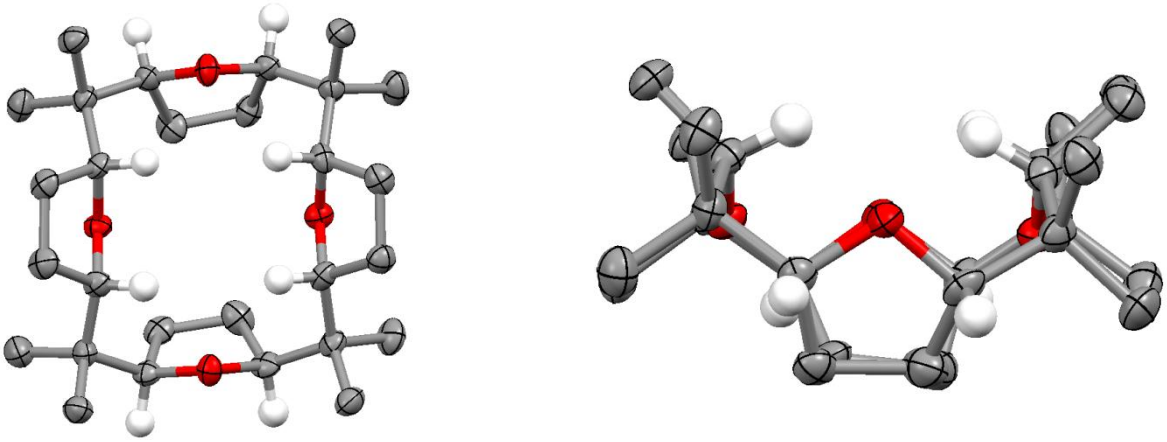

Figure 52. Molecular structure of compound **7a**, with the displacement ellipsoids drawn at the 50% probability level (hydrogen on CH_3 are omit for clarity).

The structure is distorted and forms a cavity where two THF molecules sitting in opposite positions are turned inside the cavity and the two others are turned toward the outside. The four oxygen atoms are almost in the same plane. The THF rings are present in distinct pairs in the solid state structure of compound **7a**. The structure normally written with a C_4 axis (point group symmetry C_{4v}) became a structure with a lower point group symmetry (C_{2v}) (Figure 53).

The structural conformation of **7a bis** has been drawn following the structure of compound **7a** in the solid state. We can clearly see that molecule **7a bis** belongs to the point group symmetry C_{2v}. If the conformational flip (=exchange process) is slow the two different types of protons in the α-position of the oxygen can be observed at different shift values.

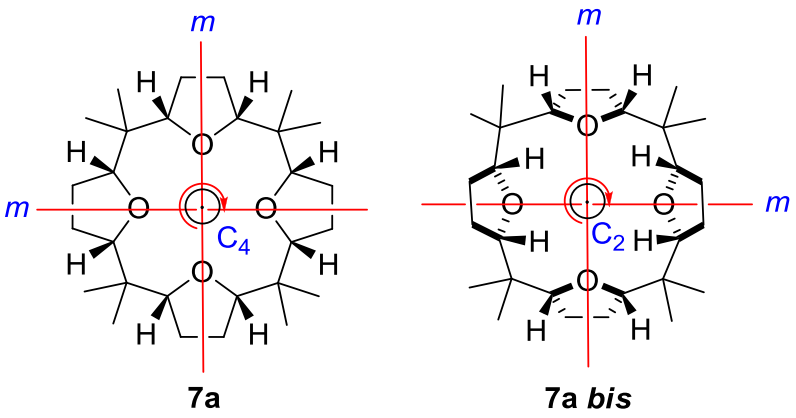

Figure 53. Comparison between the two different ways to write compound **7a**. The expected averaged conformation **7a** and the real conformation in the solid state **7a bis**, which has to be responsible for the unusual NMR signals

Assuming that the structure of **7a** in the solid state is the major conformer in the solution (visible at the NMR time scale), we can easily explain its ^{1}H-NMR spectrum. The full characterization by NMR spectroscopy has to be based on the structure drawing **7a bis**. The complete interpretation of the spectrum is presented in the experimental part Chapter 7. The spectrum has never been reported so far for whatever reasons.

3.1.1.1.2. Characterization of compound **7a**

Subsequently we performed the ^{1}H-NMR spectrum of compound **7b** (Figure 54)

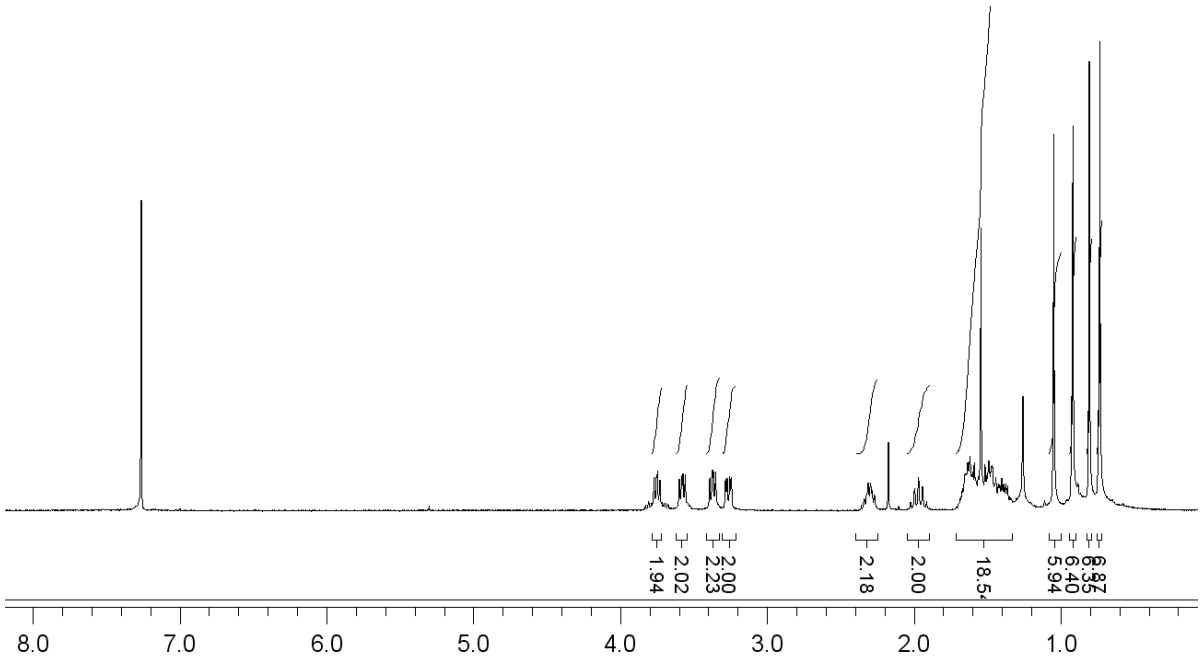

Figure 54. ^{1}H-NMR spectrum of compound **7b**

We were also surprised by the ^{1}H-NMR spectrum, which displayed four distinct peaks for the hydrogens in the α-position of the oxygens. Considering the point symmetry C_{2h} of the molecule **7b** we should have detected only two peaks in this region. Once again this molecule must have lost one of its elements of symmetry and must therefore be present in conformations of lower point symmetry than the one deduced from structure. We were able to obtain suitable crystals to determine the molecular structure of compound **7b** by X-ray diffraction analysis (Figure 55).

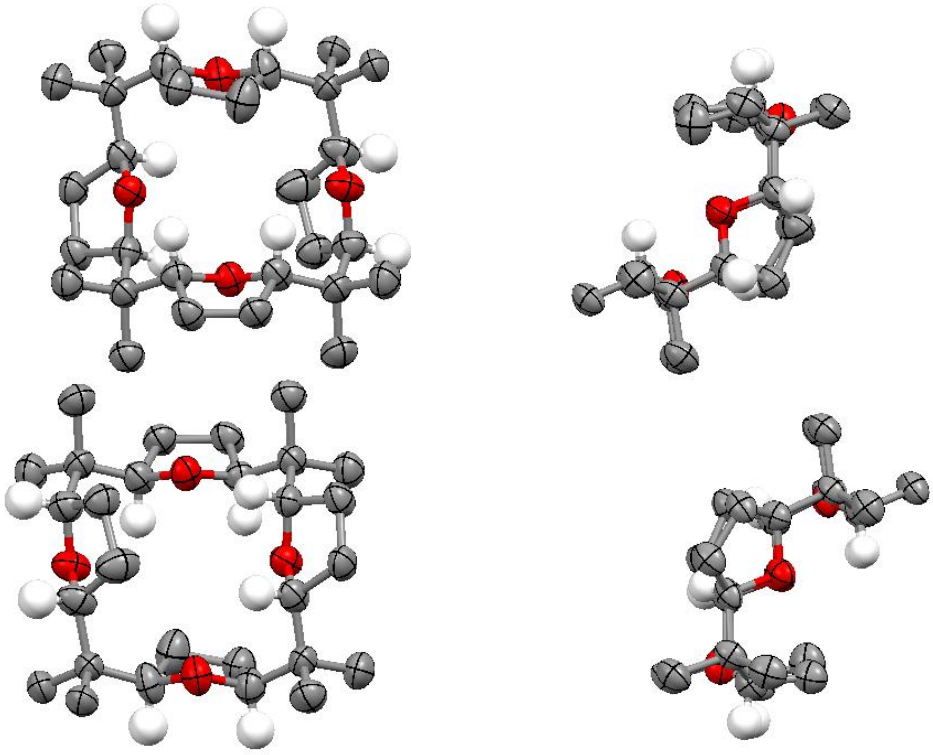

Figure 55. Molecular structure of the two enantiomer of compound **7b** along two different views, with the displacement ellipsoids drawn at the 50% probability level (hydrogen on CH_3 are omit for clarity).

The macrocycle **7b** crystallized as a racemate. Two enantiomers crystallize side by side. The conformation of the macrocycle is best described looking at the two pairs of THF rings, which are in opposite position. The two THF rings in opposite position are arranged in almost parallel plains pointing towards the same direction. As a consequence of this conformation the protons α to the THF oxygen are pointing towards the inside of the macrocycle in one THF ring and towards the outside of the macrocycle for the other THF ring (Figure 56).

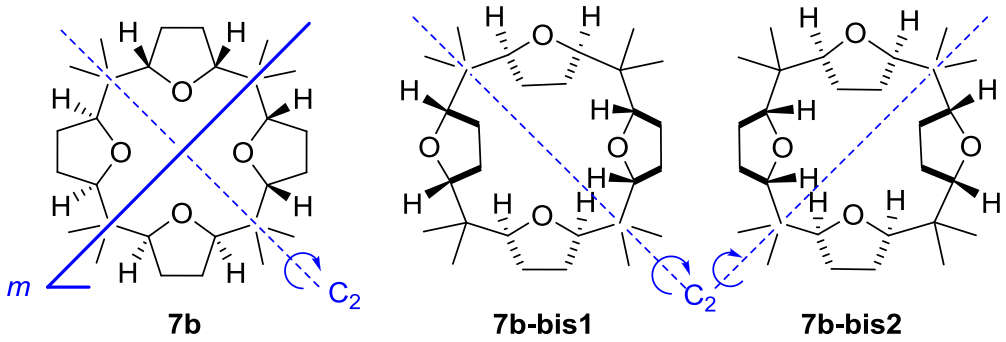

Figure 56. The structures of compound **7b**. The structure of **7b** showing the highest possible point symmetry. The two enantiomers of **7b bis1** and **7b bis2** as detected in the solid state

In view of the ^{1}H NMR spectrum compound **7b** does not show the highest possible point symmetry as we expected. The implicit assumption for obtaining the spectrum reflecting the highest possible point symmetry is that the rotation around all single bonds not involved in a small ring is fast compared to the NMR measuring time. Obviously this assumption is not true for compound **7b**, which leads to the observation of **7b** in a stable conformation of lower point symmetry. Based on the structure in the solid state we can fully interpret the NMR spectrum of **7b**. The complete attribution of the ^{1}H and ^{13}C NMR spectrum is presented in the experimental part. The peaks in the ^{1}H-NMR spectrum are well resolved. The exchange process between the two enantiomeric conformers has to be very slow. It will be very interesting to carry out a study of the dynamic NMR behavior to determine the rate of the exchange process.

The complete characterization of both calix[4]tetrahydrofuran **7a** and **7b** was challenging and has lead to unexpected results. We accomplished this difficult analysis associating NMR spectra and X-ray diffraction to decrypt and to fully interpret the NMR spectra.

3.1.1.2. Synthesis and reduction of calix[3]furan[1]pyrrole **48**

The synthesis of calix[3]furan[1]pyrrole **48** was carried out using the same synthetic pathway than previously described for compound **35** and **36**. We started the synthesis by the oxidative ring opening of the starting material, the calix[4]furan **6** (Scheme 43).

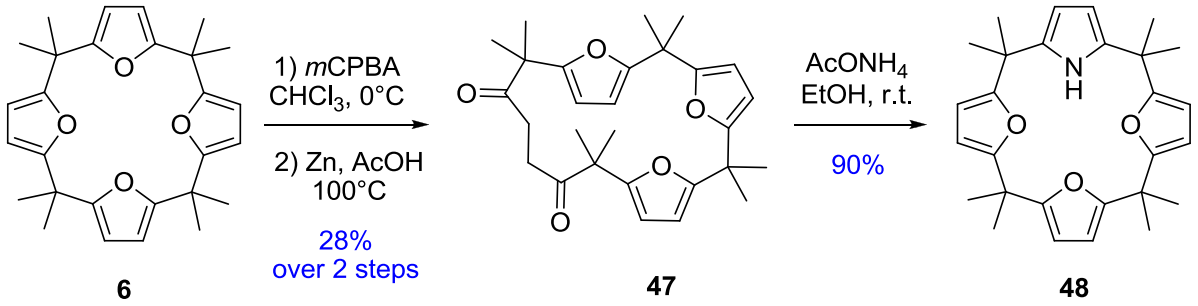

Scheme 43. Synthesis of calix[3]furan[1]pyrrole **48**

This reaction has been done using 1.2 equiv. of mCPBA in chloroform at 0°C. The quantity of mCPBA used is directly related to number of rings opened. This reaction obviously affords a non-negligible number of side products from the multiple opening. The reduction of the double bond was performed directly after a simple workup of the reaction. The two consecutive steps afforded the macrocycle **47** in 28% overall yield after chromatography. The ring closing reaction to pyrrole was carried out very smoothly at room temperature to engender calix[3]furan[1]pyrrole **48** in 90% after a simple filtration, in a high purity. We submitted this unsaturated macrocycle to the optimized conditions of hydrogenation. The reduction of **48** under 100 bars of H_2, Pd/C 10% in acetic acid at 100°C, gave only one diastereoisomer of the fully reduced macrocycle, the calix[3]THF[1]pyrrolidine **49** (Scheme 44).

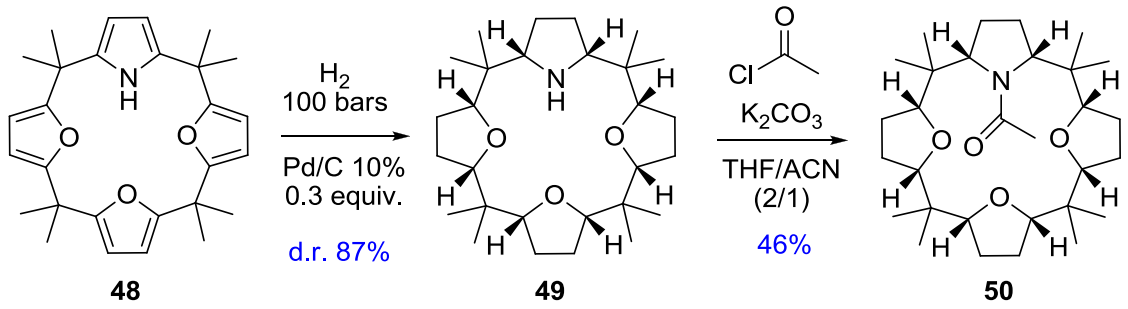

Scheme 44. Synthesis of calix[3]THF[1]pyrrolidine **49** and its acetilation

The reaction was again highly diastereoselective (d.r. 87%). The fully reduced compound **49** was obtained after a recrystallization in ethanol with 78% yield (>97% pure). We then successfully crystallized the product and performed an X-ray diffraction analysis. Unfortunately, we were not able to differentiate the nitrogen from the oxygen in the macrocycle. We suppose the reason is that compound **49** piles up in the crystal, doing a 90°

turn each time. So, we were forced to modify the macrocycle in order to get crystal structure of a compound where nitrogen and oxygen are better differentiated. We chose to acylate the amine with acetyl chloride. The reaction was carried out using an optimized condition which will be described in the next Chapter, using K_2CO_3 as base in a mixture of THF/ACN 2/1 at room temperature (Scheme 39). After purification with column chromatography we obtained, a modest 46% yield of the acetylated macrocycle **50**. The structure of **50** has been determined by X-ray diffraction analysis (Figure 57).

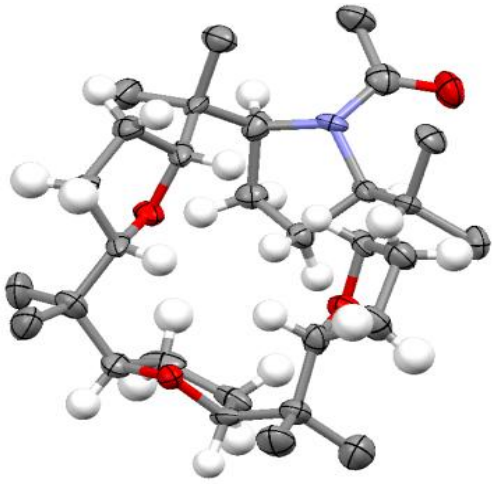

Figure 57. Molecular structure of compound **50**, with the displacement ellipsoids drawn at the 50% probability level (hydrogen on CH_3 are omit for clarity).

The hydrogens α to the heteroatoms on the same face of the macrocycle. Due to the steric hindrance introduced by substituent on nitrogen the acylated pyrrolidine ring points toward the outside of the macrocyclic ring.

For compound **50** we expected a broad ^{1}H-NMR spectrum due to the usually slow rotation around the amide bond. To our surprise the spectrum was very well defined. The observation of well defined NMR peaks can be interpreted as the consequence of a fast rotation or as the presence of one major conformer under an extremely slow exchange regime. As the amide rotation in similar macrocycles has been shown to be slow (see Chapter 4) the first hypothesis is improbable. We therefore assume the "freezing" out of one major conformer. This might be due to the conformational coupling of two relatively slow processes: the amide rotation and the ring flip. A complete dynamic NMR analysis of **50** has to be done to fully characterize the process.

3.1.2. New synthetic routes starting from compound 41, 42 and 43

3.1.2.1. Synthesis of macrocycle **56** starting with compound **41**

We started the synthesis of compound **56** from compound **41** obtained from the oxidative ring opening of calix[4]furan **6**. First, we reduced the three double bonds of the macrocycle by adding zinc dust in a warm solution of **41** in acetic acid. The reduction provides the hexaketone **51** in quantitative yield without purification (Scheme 45). Paal-Knorr reaction on compound **51** provides, surprisingly, only the unsaturated macrocycle **36** in 60% yield. No traces of compound **52** have been detected. This reaction has been repeated three times giving the same result.

Subsequently, we decided to reduce the furan ring first and then to close the three diketones into pyrrole rings. The catalytic hydrogenation of compound **51** was carried out using 40 bars of H_2, Pd/C 10% in acetic acid at 50°C. The reduction of **51** provided the corresponding compound **53** in 93% yield. An important aspect during this reaction is the control of the temperature. Above 50°C the 1,4 diketones, reacts with the acid to afford products from the Paal-Knorr reaction, the synthesis of furans. Having tried the reaction at 100°C, the fully reduced calix[4]THF **7a** and **7b** were isolated as major products. We could selectively synthesize the mono- or the tri-pyrrole adapting the reaction temperature. The Paal-Knorr reaction carried out using ammonium acetate in ethanol at 80°C provided the macrocycle **54** in 78% yield after purification. The hydrogenation of **54** generated a mixture of reduced compounds where half reduced macrocycles were the major components. The mixed compound **54** showed a similar behavior than calix[4]pyrrole **1**. The same reaction was performed at room temperature. After 48 h the racemate **55** could be isolated in 42% yield. Unreacted starting material accounted for the remaining material according to the GC analysis. Only one regioisomer was formed under these conditions. If the three pairs of 1,4-diketones would have a similar reactivity the formation of only one pyrrole ring should give a mixture of two regioisomers in a 2:1 ratio. The macrocycle containing one THF ring seems to provide a high preference for the preferential reaction at only one type of the 1,4-diketones.

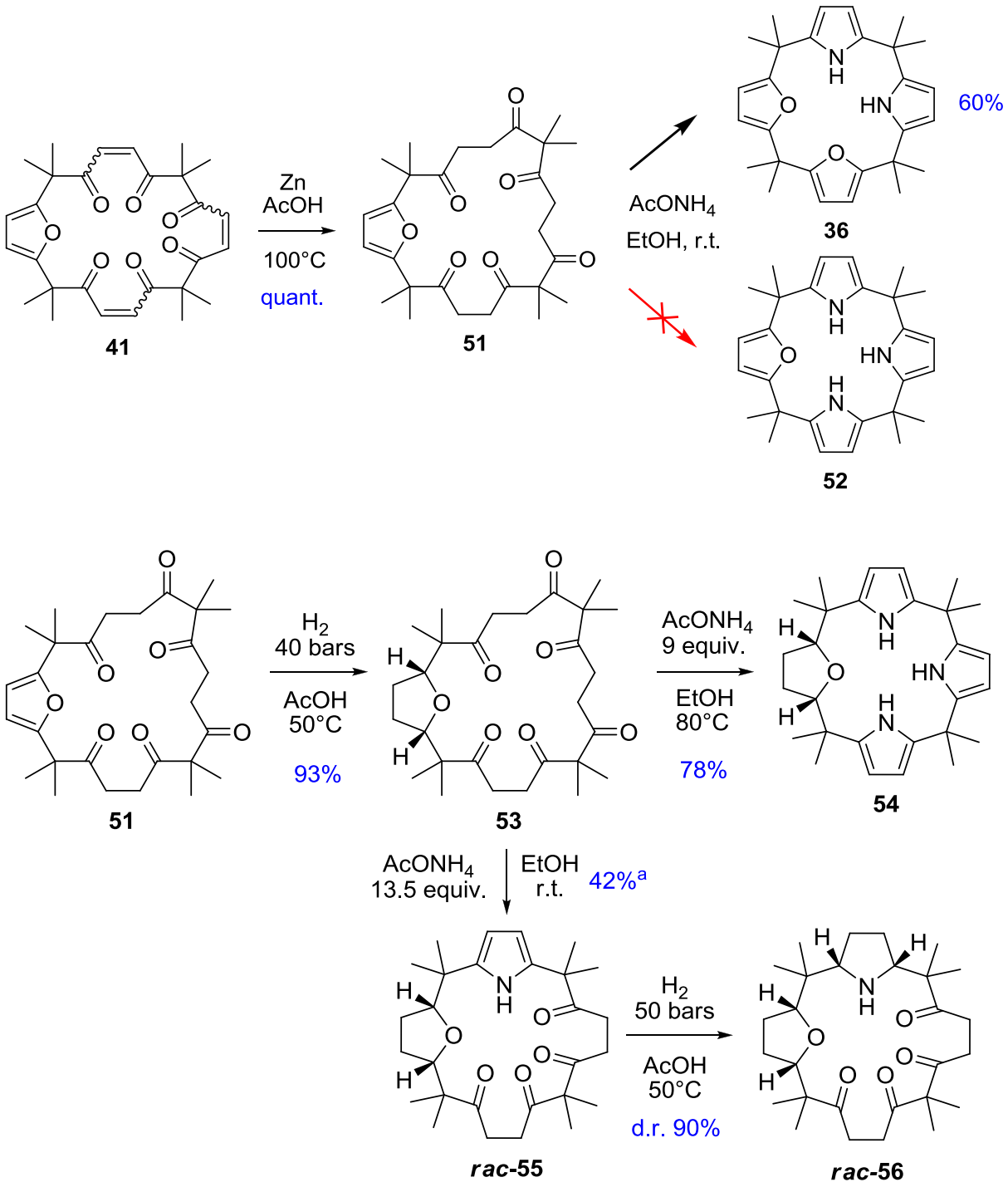

Scheme 45. Synthesis of macrocycle **56**

We carried out the hydrogenation of compound **55** to test the diastereoselectivity of a pyrrole ring influenced by a neighboring THF ring. The reduction of **55** should afford two diastereomers. The catalytic hydrogenation of compound **55** was performed with 50 bars of

H_2 at 50°C to avoid side reactions. We obtained only one major product (d.r. 90%), the racemic compound **56** in 92% yield and in 85% purity after recrystallization in ethanol. Despite an intensive effort to obtain this compound in higher purity we were not able to improve the quality of this compound. The reduction was also diastereoselective, only one of the two possible diastereomers was obtained (Figure 58).

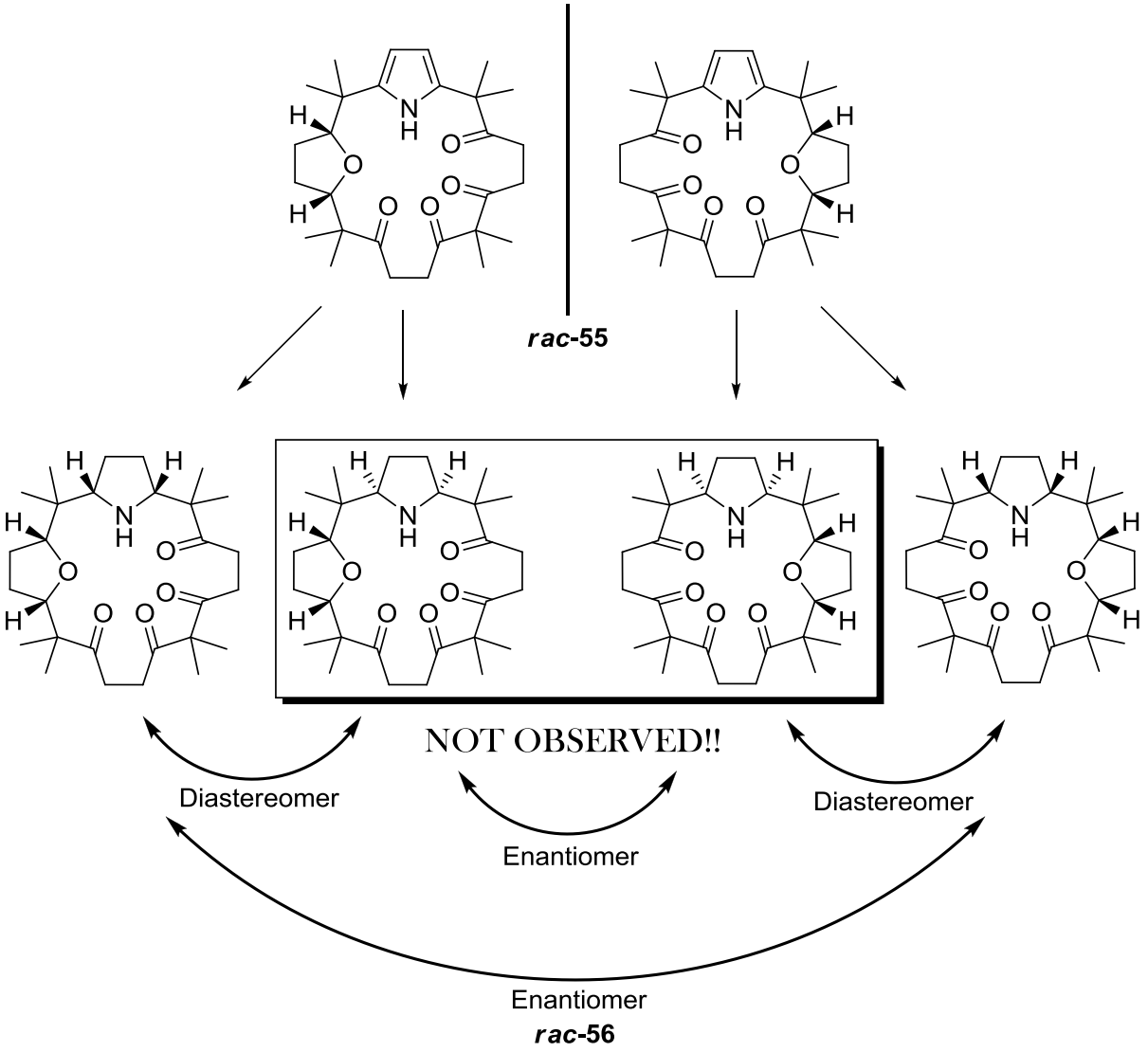

Figure 58. Diastereoselective hydrogenation of ***rac*-55**

The relative configuration of ***rac*-56** has been successfully confirmed by X-ray diffraction analysis. The molecular structure of ***rac*-56** is illustrated Figure 59.

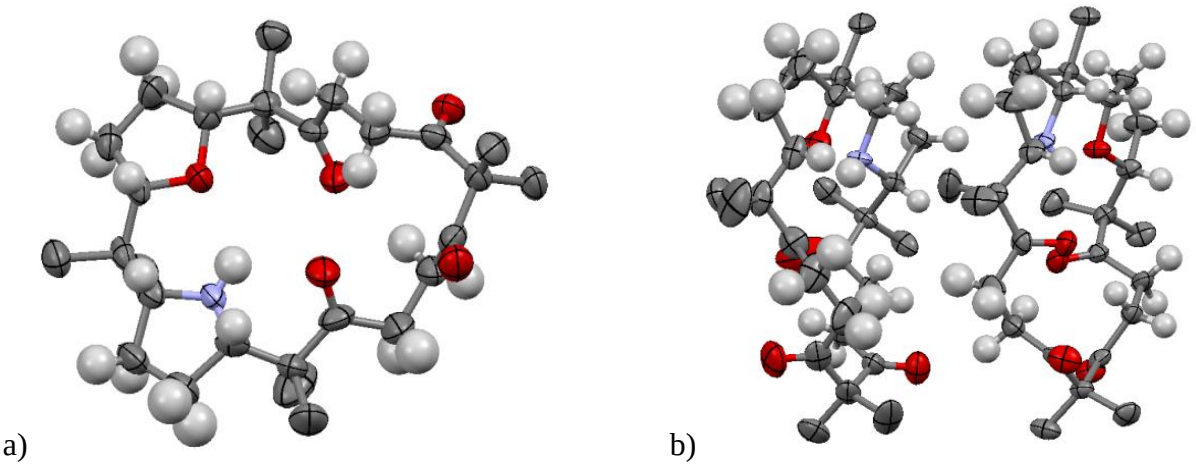

a) b)

Figure 59. a) Molecular structure of one enantiomer of compound ***rac*-56**, b) Molecular structure of the two enantiomers of compound ***rac*-56** in the crystal packing. The displacement ellipsoids are drawn at the 50% probability level (hydrogen on CH_3 are omitted for clarity).

The two enantiomers of compound ***rac*-56** are present in the crystal. All our trials to transform the racemate **56** by a Paal-Knorr reaction into the corresponding rigid macrocycle failed.

3.1.2.2. Synthesis of calix[2]THF[2]pyrrolidine **44**, **60a** and **60b** starting from compound **42**

During the reduction of macrocycle **35** we found that compound **33** was an intermediate. In view this observed diastereoselectivity, we couldn't have direct access to the other diastereoisomer of **33** by direct hydrogenation (Figure 60). We decided to attempt an independent synthesis of the diastereoisomer of **33** in order to analyze its hydrogenation behavior.

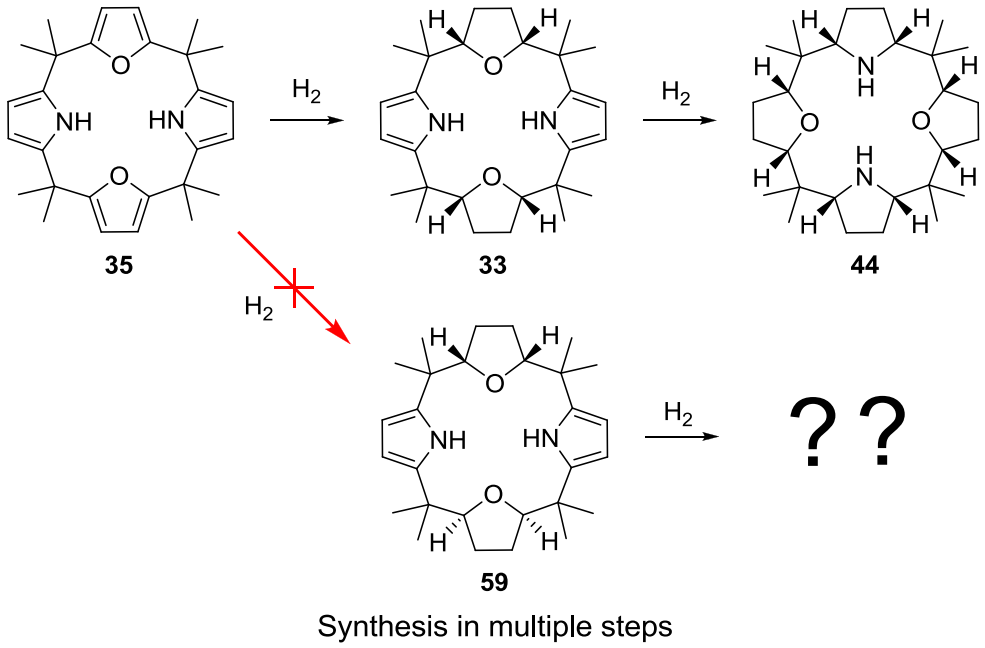

Figure 60. Illustration of our basic idea to embellish this project

Using a rational synthesis to build compound **59**, we would have the opportunity to probe the influence of the rigidity of macrocycle and the stereochemistry of the heterocycles on their diaseteroselective induction during the hydrogenation.

We started the synthesis from compound **42** already described (see above). The catalytic hydrogenation of **42** under 40 bars of H_2 and run at 50°C provided the two possible diastereoisomers **58a** and **58b** in 36 and 38% yield respectively, after purification (Scheme 46).

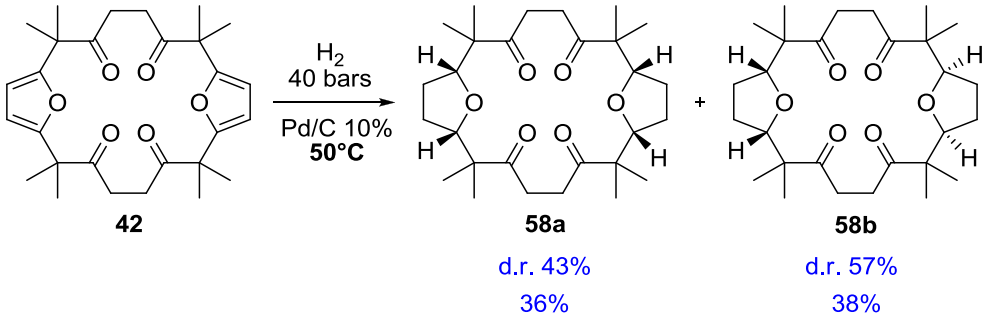

Scheme 46. Catalytic hydrogenation compound **42**

The reaction was performed at 50°C in order to avoid the formation of furan as side reaction. The GC of the crude reaction mixture shows about 10% impurities and the two products with

very similar retention times. The two isomers were obtained in 43/57 ratio in favor of compound **58b** (GC). The reaction has been reproduced two times. The product ratios were different: 2nd trial ratio: **58a**/**58b** = 53/47 and 3rd trial ratio: **58a**/**58b** = 66/34. The change in the product ratios is not huge. We do not know at the moment the factors influencing this product ratio. We were not able to separate the two isomers by chromatography. Purification of the mixture from the impurities by column chromatography was relatively easy (Silica, 99/1 CH_2Cl_2/MeOH). After a intensive effort, we found the conditions to isolate each isomer. Compound **58a** is considerably more soluble in warm ethyl acetate than **58b**. After a simple wash under this condition we isolated compound **58a** with 89.5% purity and **58b** with 86% purity (starting from the mixture obtained from the 3rd trial). After successive crystallizations in ethanol or ethyl acetate respectively we were able to isolate compound **58a** and **58b** in >91% and >95% purity. The relative configuration cannot be attributed by NMR spectroscopy and therefore we needed a crystal structure of one of the products to attribute the structures with confidence. We have successfully grown a suitable mono-crystal of compound **58a** and determined its molecular structure by X-ray diffraction analysis (Figure 61).

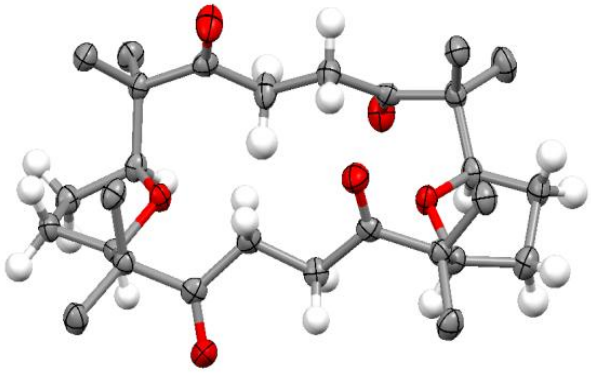

Figure 61. Molecular structure of compound **58a**, with the displacement ellipsoids drawn at the 50% probability level (hydrogen on CH_3 are omit for clarity).

Protons 2 and 5 of the two THF rings are pointing toward the same face of the macrocycle. The hydrogenation of the two rings is almost non diastereoselective: The configuration of one ring does not influence the hydrogenation of the second ring

We then continue the synthesis of **33** by introducing the two pyrroles via the Paal-Knorr reaction starting from **58a** (Scheme 47).

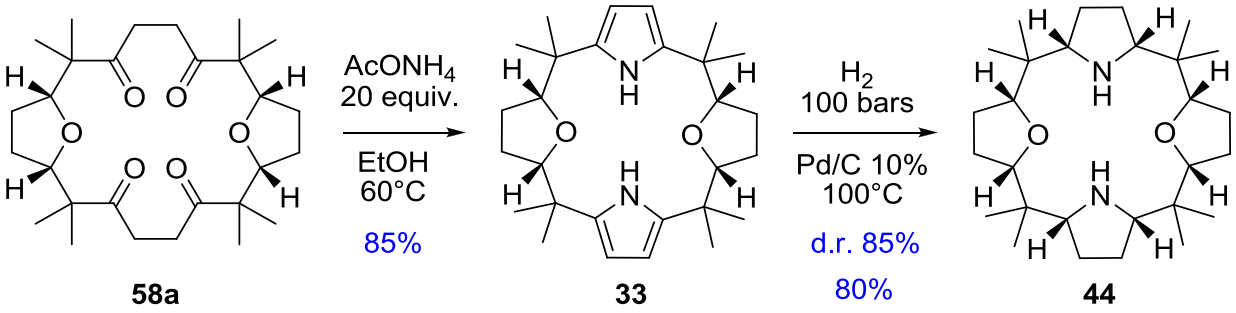

Scheme 47. Synthesis of macrocycle **44** started from compound **58a**

We performed the reaction with **58a** (d.r. 75%). Only compound **33** precipitated during the reaction. After a simple filtration compound **33** was obtained in 85% yield in >98% purity (yield based on the quantity of **58a** pure in the starting material). The catalytic hydrogenation of compound **33** was carried out under our standard conditions to afford compound **44** in 80% yield, 95% pure after two recrystallizations in ethanol.

We did the same synthetic sequence starting from compound **58b**. The pyrrole syntheses via Paal-Knorr reaction from **58b** afford the corresponding compound **59** (Scheme 48).

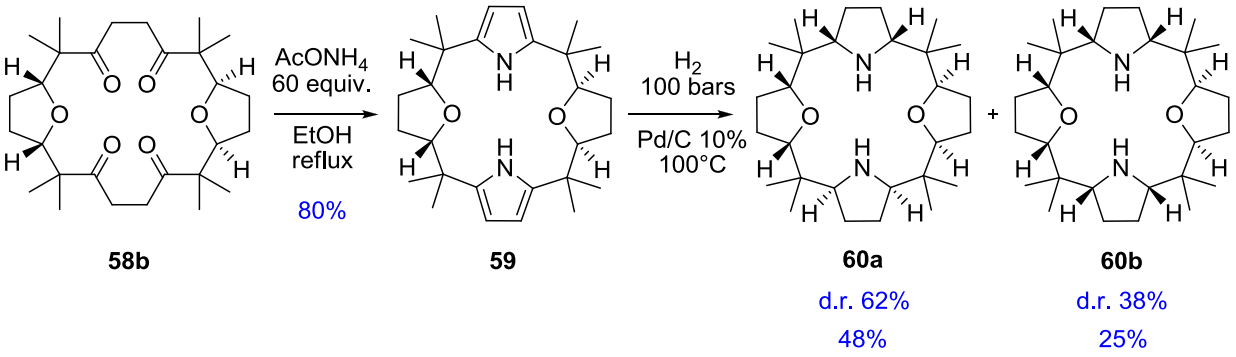

Scheme 48. Synthesis of fully saturated macrocycles **60a** and **60b**

We performed the reaction with **58b** (d.r. = 91). Compound **59** was isolated after basic treatment. The purification of **59** was not trivial, it was impossible to separate compound **59** from the small amount of **33** present by chromatography. We finally succeeded in purifying compound **59** by successive recrystallizations in ethanol and obtained 80% yield with >98% purity after 10 recrystallizations. We therefore obtained high quality crystals of **59** and made the X-ray diffraction analysis. This gives us the opportunity to control the relative

configuration of the molecule and also obtain important information on the structure itself. The structure of **59** is presented Figure 62.

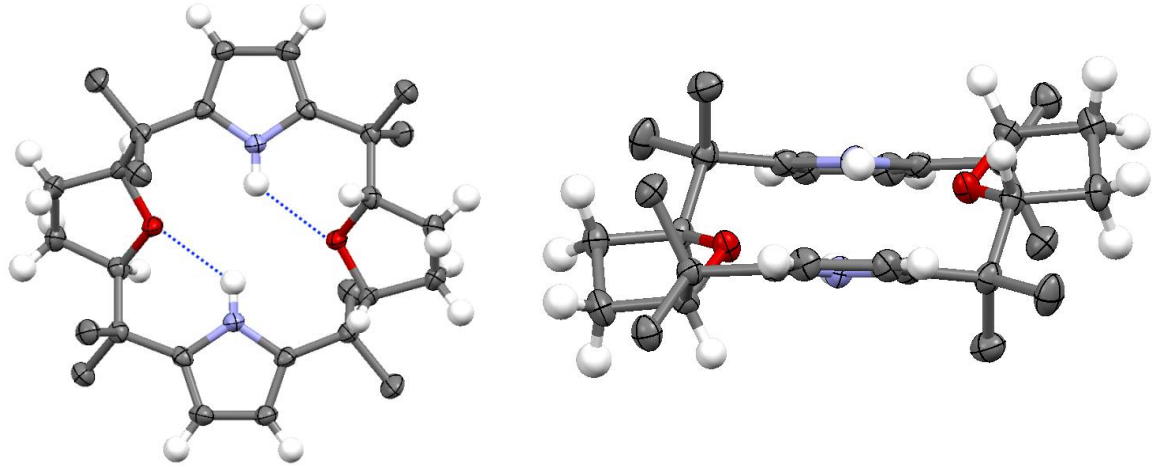

Figure 62. Molecular structure of compound **59** along two different views, with the displacement ellipsoids drawn at the 50% probability level (hydrogen on CH_3, are omitted for clarity). N-H···O hydrogen bonds are shown as blue dotted lines.

The molecular structure of **59** is distorted. Each pyrrole forms a hydrogen bond with its neighboring THF ring and thereby fixes the relative arrangements of the pairs formed by one THF ring and one pyrrolidine ring. The pyrrolidine rings of the two pairs are almost parallel to each other. We tested the hydrogenation of **59** and characterized the products. The reduction of **59** was carried out under standard conditions (Scheme 46). Two major products were present in the crude reaction mixture (GC: ~87%; d.r. 60/40). The GCMS confirmed that the two products are actually diastereoisomers. We successfully found a condition, which allowed the separation of the two products by column chromatography (see experimental part). We obtained the fully saturated compound **60a** in 48% yield and 94% purity after chromatography and a recrystallization from a mixture of EtOH/EtOAc. The separation was tedious as the impurities co-eluted with the product during the chromatography. Repeated recrystallization allowed removing the impurities. Compound **60b** was obtained with 25% yield in 92% purity. The NMR spectrum did not allow attributing the configuration of the molecule. We depended on X-ray analysis once again. We successfully get suitable crystals of **60a** and **60b**. The molecular structure of calix[2]THF[2]pyrrolidine **60a** and **60b** as determined by X-ray diffraction analyses are shown in Figures 63 and 64 respectively.

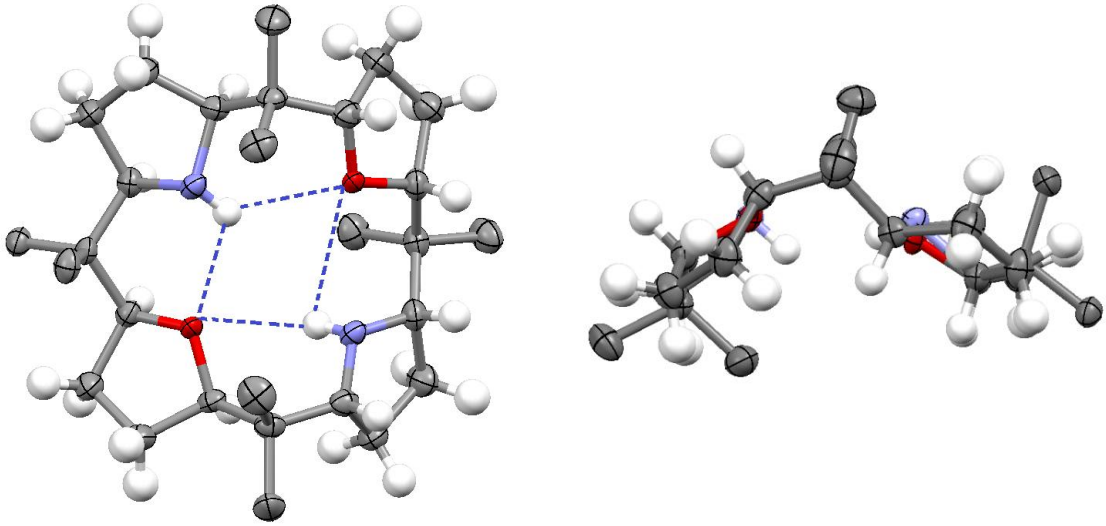

Figure 63. Molecular structure of compound **60a** along two different views, with the displacement ellipsoids drawn at the 50% probability level (hydrogen on CH_3 are omitted for clarity). N-H···O hydrogen bonds are shown as blue dotted lines.

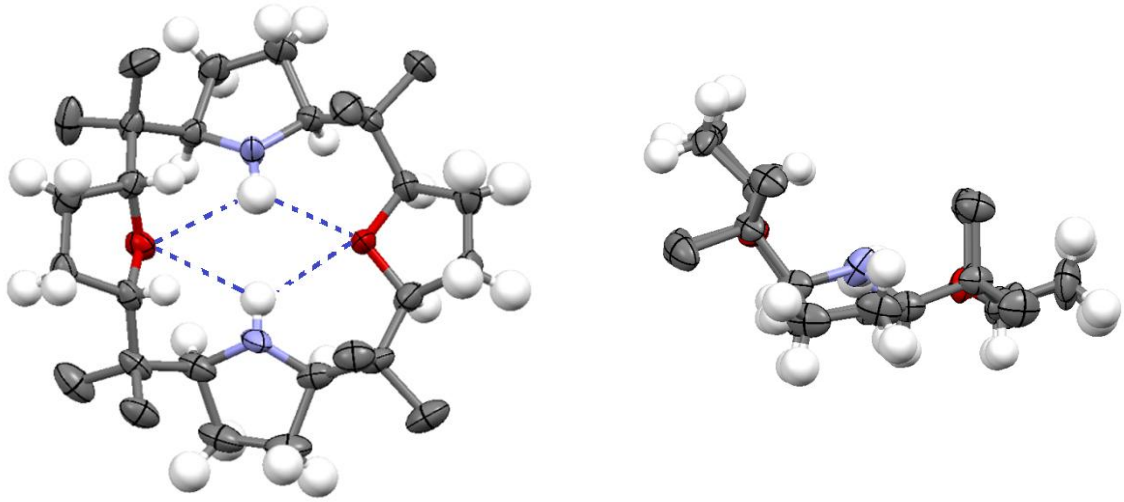

Figure 64. Molecular structure of compound **60b** along two different views, with the displacement ellipsoids drawn at the 50% probability level (hydrogen on CH_3 are omitted for clarity). N-H···O hydrogen bonds are shown as blue dotted lines.

The molecular structure of compound **60a** shows for the macrocycle a stair-like arrangement. The pyrrolidine and THF ring having their α protons pointing toward the same face of the macrocycle, are almost in the same plane. The molecular structure of compound **60b** shows a V-shaped arrangement. The three heterocyclic rings which have their α protons pointing

toward the same face, are also in the same plane. The plane formed by the last THF rings is almost orthogonal.

We concentrated our efforts on reproducing the same approach, starting from compound **43**

3.1.2.3. Synthesis of calix[2]THF[2]pyrrolidine 46 and *rac*-64 starting from compound 43

We started this synthesis from the compound **43** described previously. The catalytic hydrogenation of **43** was carried out with 40 bars of H_2, Pd/C 10% at 50°C. The reduction provided the two possible diastereoisomers **61a** and **61b** in respectively 26 and 38% yield, after purification (Scheme 49).

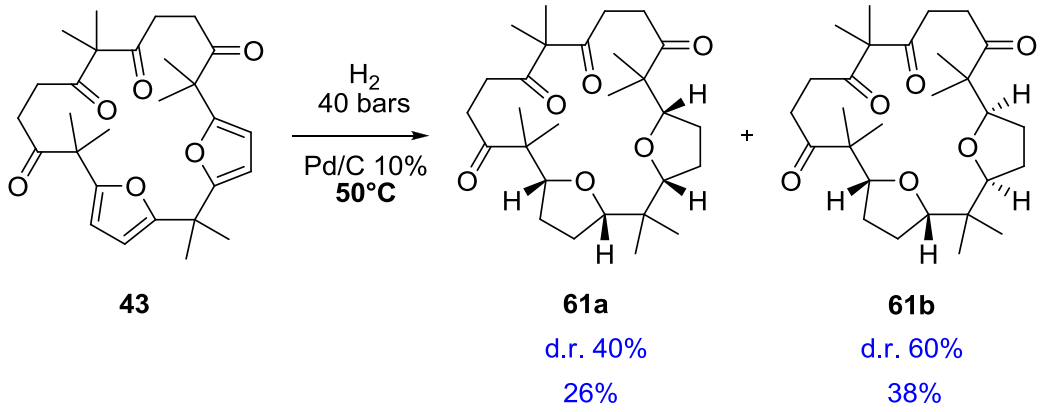

Scheme 49. Catalytic hydrogenation compound **43**

The hydrogenation of **43** provided a mixture of the two possible diastereoisomers in 4/6 ratio in favor of compound **61b**. This reaction has been performed twice and gave similar results in term of d.r. and yield. The reaction is slightly diastereoselective. The purification of the two products has been difficult to achieve. First, we began by a column chromatography (silica, 98/2 CH_2Cl_2/EtOAc) in order to separate the two product from the impurities. Then, a second column was done (Aluminum oxide, 92/8 cyclohexane/EtOAc) to isolate each product. Finally, we recrystallized compound **61a** and **61b** in a mixture of EtOH/EtOAc 1:1 provided **61a** in 26% yield in 96% purity and compound **61b** with 38% yield and in 97% purity. The determination of the relative configuration of both compounds was not possible by RNM spectroscopy and we therefore tried to crystallize one of them. We were successful in getting suitable crystals of compound **61b** for the X-ray analysis. The molecular structure of the macrocycle **61b** is illustrated in Figure 65.

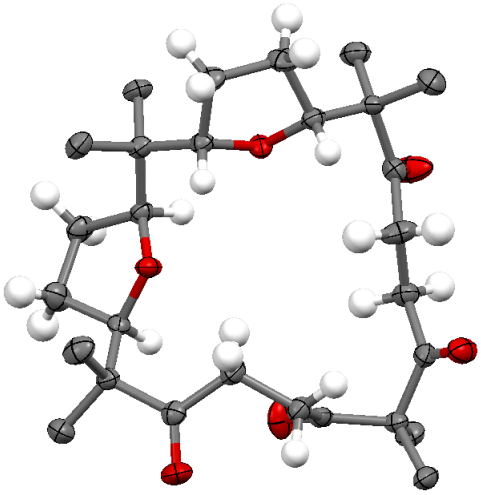

Figure 65. Molecular structure of compound **61b**, with the displacement ellipsoids drawn at the 50% probability level (hydrogen on CH_3 are omitted for clarity).

The protons 2 and 5 of the THF rings of compound **61b** are pointing toward different faces of the macrocycle. Having established the relative configuration of compound **61a** and **61b**, we then concentrated our effort toward the pyrrole synthesis via the Paal-Knorr reaction followed by the reduction of the corresponding product.

We started by the Paal-Knorr pyrrole synthesis on **61a**. The reaction was carried out using 35 equivalent of ammonium acetate in ethanol at 80°C and provided the macrocycle **62** in 70% yields in 97% purity (Scheme 50).

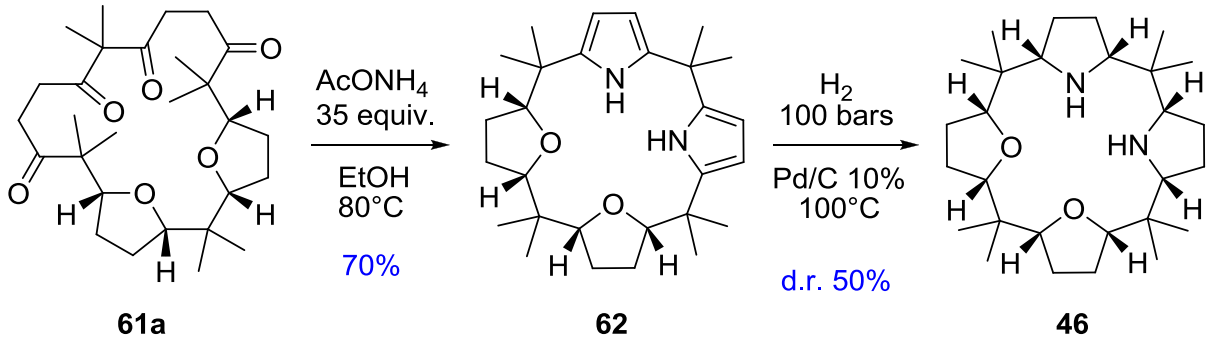

Scheme 50. Synthesis of the fully saturated macrocycles **46**

The product **62** seemed to precipitate partially during the reaction. It was isolated after the column chromatography of the crude reaction mixture. Compound **62** was recovered with over 79% yields after chromatography but with only 90% purity. A second purification by

recrystallization in ethanol provided **62** in good purity. This recrystallization allowed us to get suitable crystals for the X-ray diffraction analysis. The molecular structure of **62** is illustrated Figure 66.

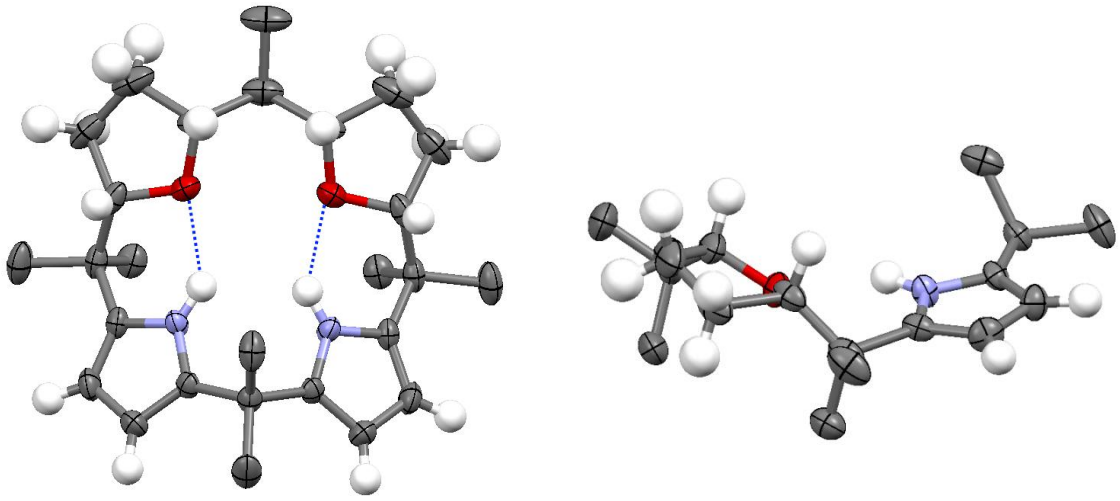

Figure 66. Molecular structure of compound **62** along two different views, with the displacement ellipsoids drawn at the 50% probability level (hydrogen on CH_3 are omitted for clarity). N-H···O hydrogen bonds are shown as blue dotted lines.

Compound **62** is perfectly symmetric and is almost planar. Two hydrogen bonds between N-H and the oxygen of THF rings fix the relative positions of the two pairs of five membered rings and the arrangement of the macrocycle.

Hydrogenation of compound **62** was carried out following our standard conditions and afforded only one major isomer, the calix[2]THF[2]pyrrolidine **46** in diastereoisomeric ratio of 50%. The hydrogenation of **62** gave approximately result very similar to the result obtained for the hydrogenation of **36**. Attempts to purify the macrocycle were all unsuccessful.

Finally, we reproduced the same synthetic route starting from compound **61b**. Compound **64** was synthesized via Paal-Knorr reaction with 86% yield (Scheme 49).

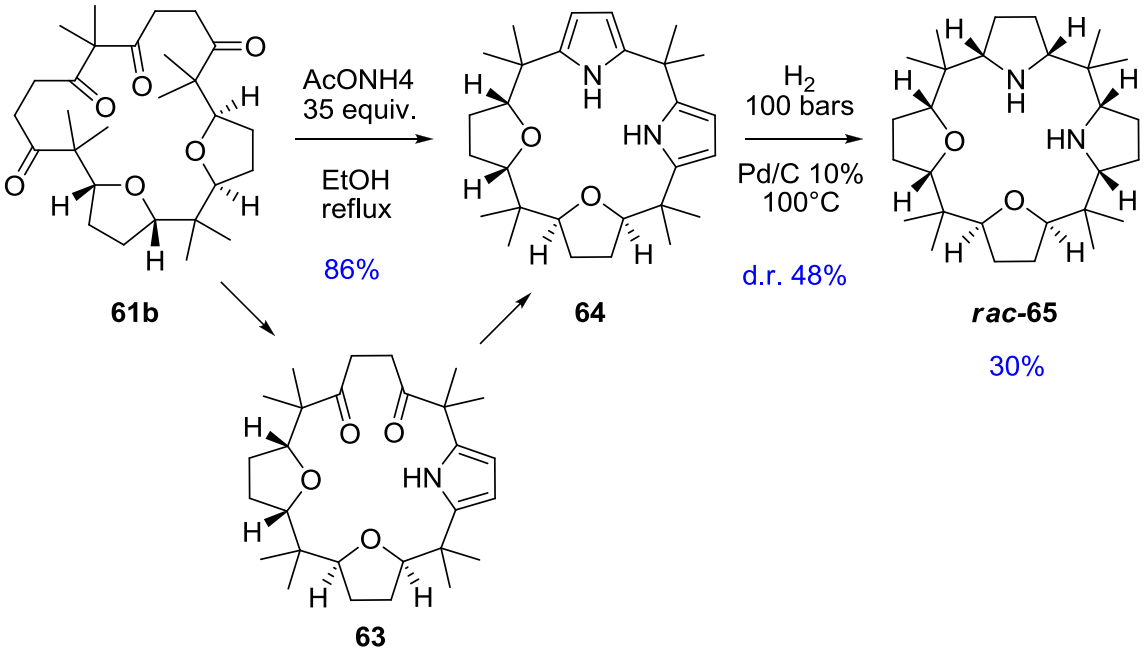

Scheme 51. Synthesis of fully saturated macrocycles ***rac*-65**

The reaction was slow enough that we were able to isolate and characterize compound **63**, an intermediate in the reaction with only one pyrrole formed. Compound **64** was isolated from the crude reaction mixture and purified by filtration on a small pad of silica. This purification led to 86% yield **64** and >98% purity. Then the reduction of **64** by hydrogenation under standard conditions provided the racemic compound **65** in 30% yield after chromatography (Scheme 49). The reaction was diastereoselective (d.r. 48%). Surprisingly, the ^{1}H-NMR spectrum of **65** displayed eight different protons in the region of α-H of the reduced heterocyclic rings. The product as observed by NMR has to be chiral. We wished to secure the structure via X-ray analysis. We successfully grew suitable mono-crystals of **65**. Its relative configuration was confirmed though X-ray diffraction analysis. The molecular structure of calix[2]THF[2]pyrrolidine **65** is presented Figure 67.

The molecular structure of **65** is very similar to structure of calix[4]THF where the conformation of the five membered rings is alternating up/down. The four heteroatoms are almost in the same plane and the molecule forms a nice cavity.

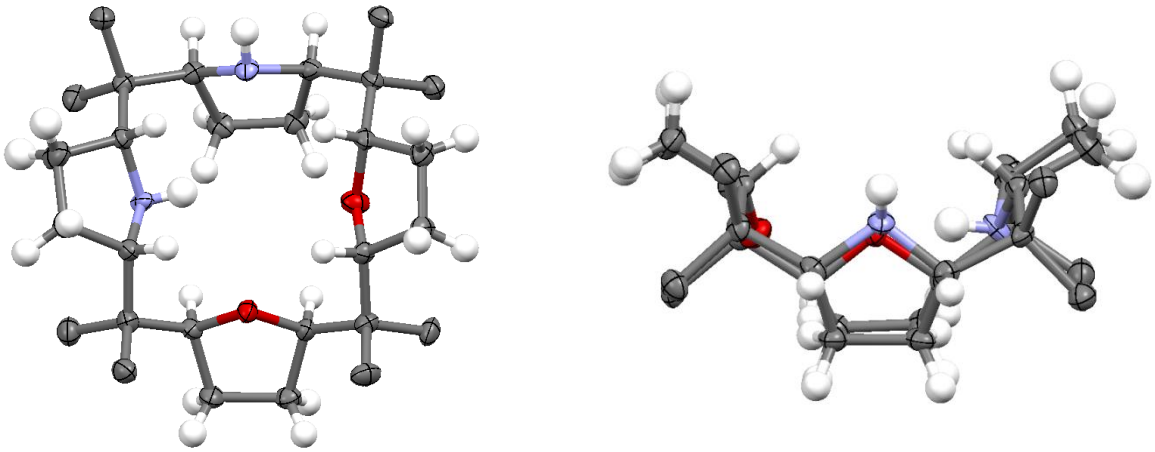

Figure 67. Molecular structure of compound **65** along two different views, with the displacement ellipsoids drawn at the 50% probability level (hydrogen on CH_3 are omitted for clarity).

As a result of our effort we have obtained a panel of structurally related macrocycle whose hydrogenation has been studied with the goal to decipher the diastereoselectivity of this process.

3.1.3. Synthesis of calix[2]pyridine[2]pyrrole

We wished to stay in the same logic and synthesize a derivative of calix[4]pyrrole which would be easier to reduce by hydrogenation. We concluded that the insertion of a pyridine into the macrocycle would enhance propensity of the hydrogenation because pyridines are known to be easily reduced. Mixed macrocycles of the type calix[m]pyridine[n]pyrrole (m+n=4) have already been synthesized in the past. In 1998, Sessler et al.[194] described a method to convert calix[4]pyrrole into a calix[m]pyridine[n]pyrrole (m+n=4) derivative by reaction of dichlorocarbene with pyrrole. The major drawback of this method was the formation of a multitude of isomers due to the presence of a chlorine after the ring expansion. Indeed, the chlorine could be in position 3 or 5 of the pyridine. Later, Dycker et al.[195] described a rational synthesis of *meso*-octa*p*-methoxybenzylcalix[2]pyridine[2]pyrrole by Friedel-Crafts reaction. Based on this work, we wished to synthesize the simple *meso*-octamethylcalix[2]pyridine[2]pyrrole **66** starting from dimethyl pyridine-2,6-dicarboxylate (Scheme 52).

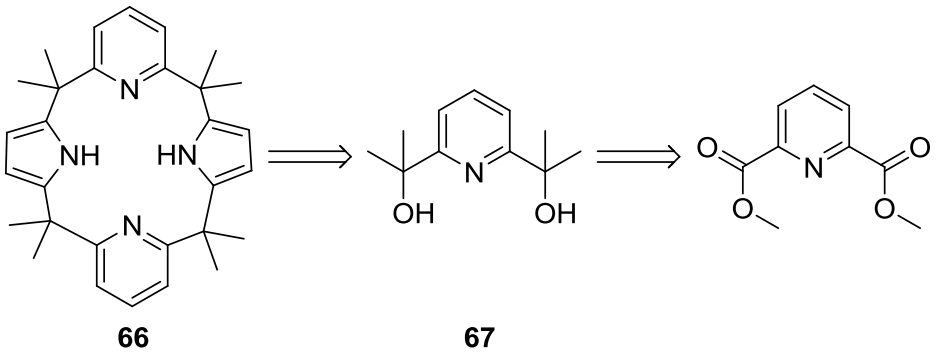

66 **67**

Scheme 52. Retrosynthesis of *meso*-octamethylcalix[2]pyridine[2]pyrrole **66**

We started with the synthesis of the building block **67** following the procedure described by Butsch et al.[196] (Scheme 53). The reaction carried out with 4.4 equivalent of MeLi in THF at -78°C, provided compound **67** with 65% yield after chromatography.

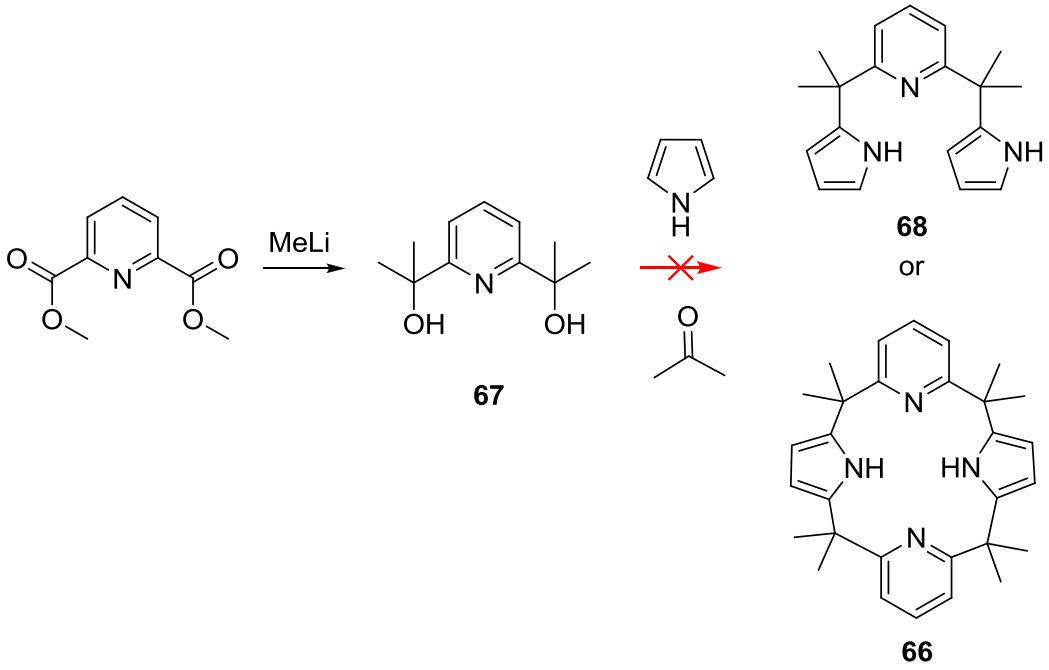

Scheme 53. Attempts to synthesized the macrocycle **66**

The next step is the Friedel-Crafts alkylation of pyrrole to cyclize directly **67** into macrocycle **66** or simply get the intermediate **68** which would easily give **66**. Similar syntheses were successfully performed by Sessler et al.[197] in which the pyridine was replaced by a benzene ring. Despite numerous variations of the reaction conditions, the formation of **68** or **66** has never been observed. The difficulty to obtain the active intermediate in the presence of the protonated pyridine ring may be the reason for this failure. All the trials are summarized in table 13.

Table 13.

Entry	equiv. pyrrole	Solvent	Acid	equiv. acid	Temperature (°C)	Concentration (M)
1	0.9	CH_2Cl_2	CH_3SO_3H	1	r.t.	0.051
2	0.9	EtOH	CH_3SO_3H	1	r.t.	0.051
3	4	CH_2Cl_2	CH_3SO_3H	1	r.t.	0.025
4	4	CH_2Cl_2	CH_3SO_3H	1	65	0.175
5	8	CH_2Cl_2	CH_3SO_3H	2	r.t.	0.175
6	8	EtOH	CH_3SO_3H	2	r.t.	0.175
7	8	EtOH	CH_3SO_3H	4	r.t.	0.175
8	16	EtOH	CH_3SO_3H	2	r.t.	0.175
9	0.9	EtOH	*p*TSA	0.5	r.t.	0.051
10	0.9	EtOH	*p*TSA	0.5	80	0.051
11	4	CH_2Cl_2	*p*TSA	0.5	r.t.	0.35
12	50	CH_2Cl_2	*p*TSA	50	r.t.	0.35
13	4	CH_2Cl_2	TFA	1	r.t.	0.175
14	4	CH_2Cl_2+EtOH	HCl	1	r.t.	0.087
15	4	CH_2Cl_2+EtOH	HCl	1	65	0.087
16	4	CH_2Cl_2+EtOH	HCl	5	r.t.	0.087
17	0.9	CH_2Cl_2	$BF_3O(Et)_2$	2	r.t.	0.0051
18	0.9	CH_3CN	$BF_3O(Et)_2$	4	r.t.	0.051

Different parameters were modified: 1) the polarity of the solvent; 2) the number of equivalents of pyrrole; 3) the type of acid (Brønsted (mineral, organic), Lewis); 3) the number of equivalents of acid; 4) the temperature; 5) the concentration. Unfortunately, no traces of products were detected. The starting material was most of the time recovered (NMR). Using methansulfonic acid led to a crude of reaction much more dark than using *p*-toluenesulfonic (probably polymers of pyrroles seeing the dark color of the crude). If we assume that the reaction goes through a carbocation intermediate, the effect of the aromatic ring will be crucial. The compound used by Butsch et al.[196] forms a much more stabile carbocation in the benzylic position of three aromatic rings. The same is true for the molecule with a benzene ring described by Sessler et al..[197]

Subsequently, we studied the hydrogenation of compound **67**. We carried out the hydrogenation of compound **67** using 50 bars of H_2, Pd/C 10% in a 1:1 mixture of methanol and acetic acid at 50°C for the night (Scheme 54).

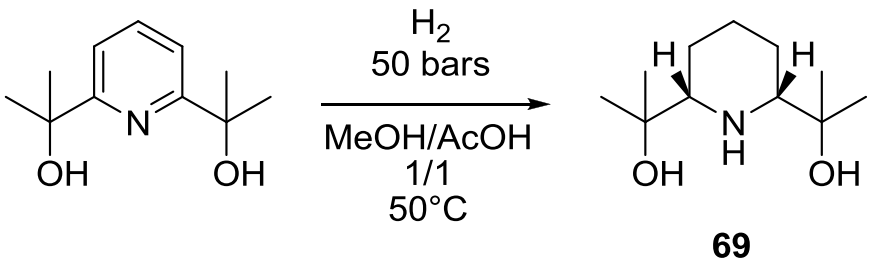

69

Scheme 54. Catalytic hydrogenation of compound **67**

The product **69** was isolated with 96% yield and >98% purity (LCMS) without purification. We successfully grew a mono-crystal suitable for X-ray diffraction analysis by slow evaporation of a solution of **69** in CH_2Cl_2. The molecular structure of the piperidine ring **69** is shown Figure 68 and will be fully described in the annex.

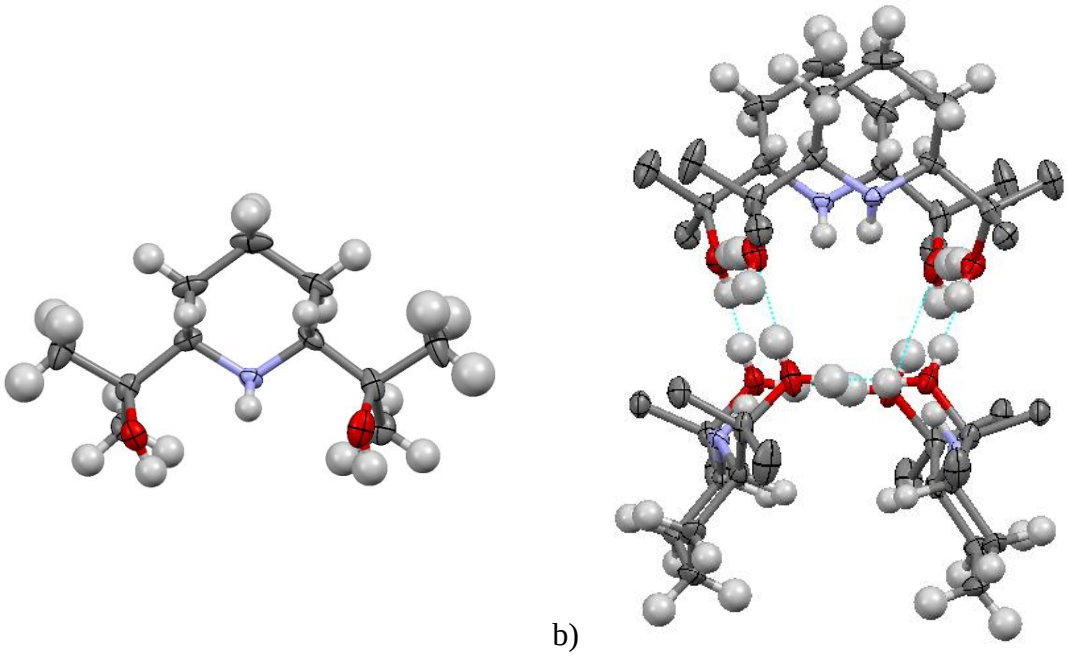

a) b)

Figure 68. a) Molecular structure of compound **69.** b) Tetramers of compound **69** in the crystal packing. The displacement ellipsoids are drawn at the 30% probability level (b: hydrogen on CH_3 are omitted for clarity).

The synthesis of compound **66** could not be achieved on the lines presented above. The hydrogenation of the pyridine ring gave an interesting result as a sort of "compensation" for the time invested on the synthesis of **66**.

The summary of all the reactions performed is given in a single scheme in order to present the essential results (Scheme 55).

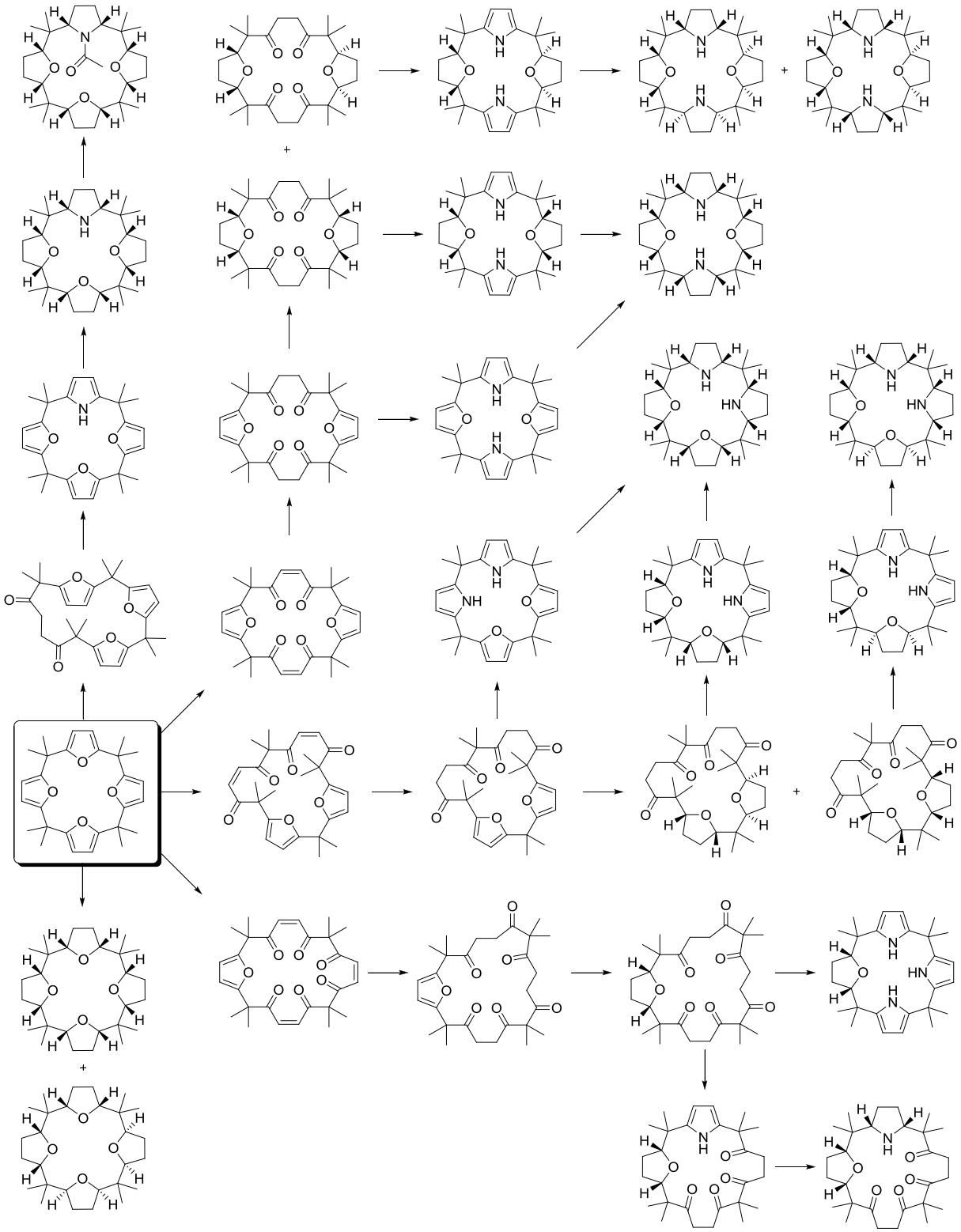

Scheme 55. Sum of the previous “Results” part

4. DISCUSSION

This part focuses on the comparison between the relative configurations of the products obtained by heterogeneous catalytic hydrogenation and thereby on the stereochemistry for this process. The relative configuration of the starting materials is also discussed in order to have a save starting point for our mechanistic discussions. We will probe: 1) the influence of heteroatoms (N or O) and their location in the macrocycle; 2) the influence of the relative configuration of the macrocycle used as starting material; 3) the influence of the rigidity of the macrocycles. The macrocycles studied possess four reducible rings, so four separate hydrogenation steps and concomitantly four separate processes influencing the diasteroselectivity have to be discussed. However, all starting materials are symmetric, having at least a C_2 axis. Therefore we have to discuss only three diastereoselective steps. In the interest of clarity, we will separate the discussion of each step.

For our discussion we use the following simplifications: 1) we assumed that the hydrogenation of the five membered heterocycles took place only with *cis*-stereoselectivity; 2) Compounds were not labeled (only the reaction).

Remarks: Intermediates (in bracket) were not isolated and they were written according to the relative configuration of the final product. In the case of a racemate, only one enantiomer was written.

4.1. Influence of one reduced heterocycle in the macrocycle on the hydrogenation

We start the analysis from macrocycles where only one heterocycle was reduced. We analyze the relative configuration of the products after the hydrogenation of another ring. The results of all the reactions studied are presented in Scheme 56.

4.1.1. Influence of the rigidity of the macrocycle on the diastereoselectivity of the hydrogenation

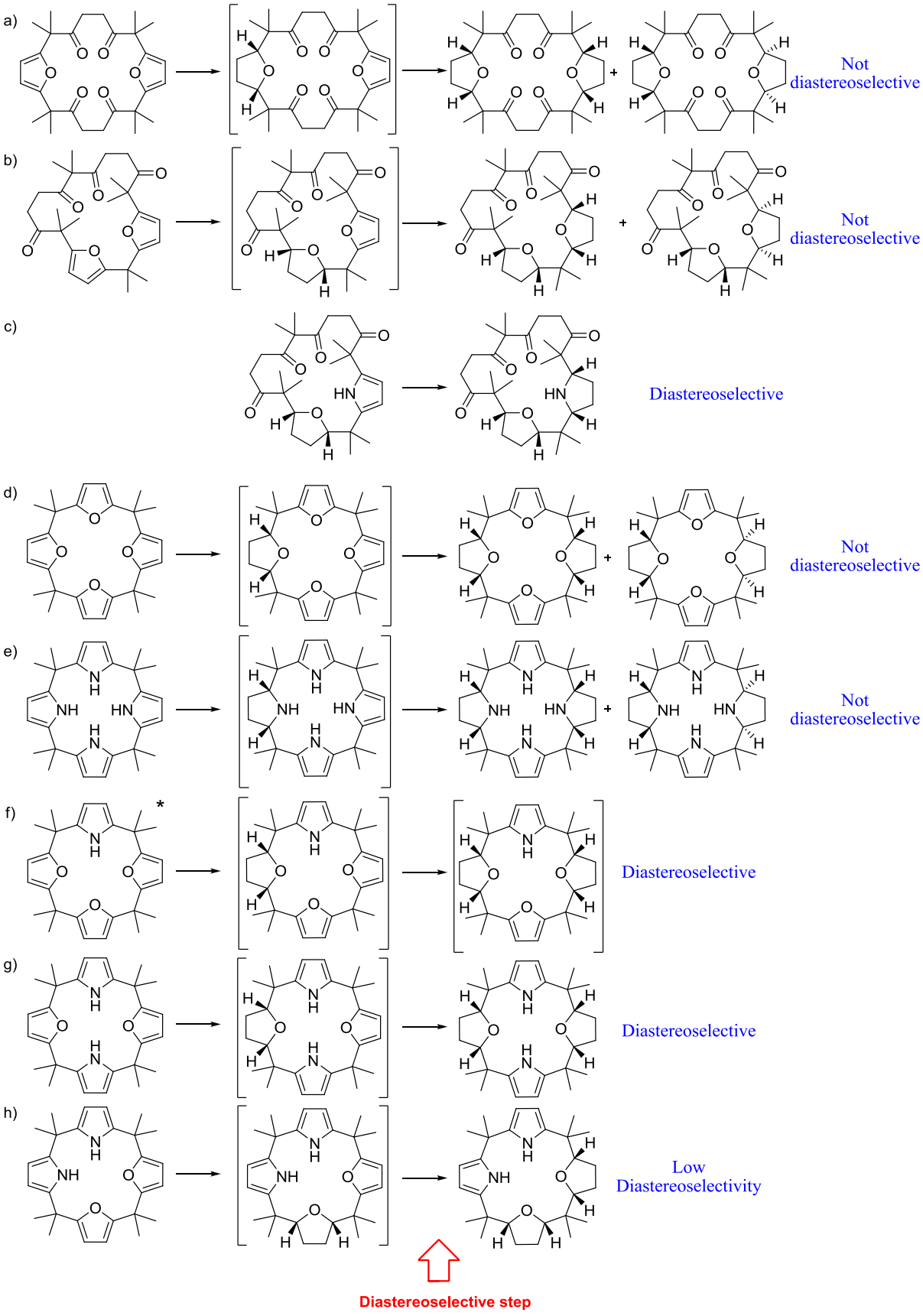

Scheme 56. Influence of one reduced heterocycle in the molecule. *Mechanism extracted from the hydrogenation of compound **48** (Scheme 44)

Flexible macrocycles lead to diastereoselective reactions (reaction **c**, Scheme 56) or non diastereoselective reaction (reaction **a** and **b**, Scheme 56). Rigid starting materials yielded only one diastereoisomer in some cases (reaction **f**-**h**, Scheme 56) as they formed the two possible diastereoisomers in other cases (reaction **d** and **e**, Scheme 56). If we compare the hydrogenation of a furan ring in opposite position to a preexisting THF, we come to the following conclusions: 1) in a flexible macrocycle the hydrogenation is not diastereoselective (reaction **a**, Scheme 56); 2) in rigid macrocycles the reduction can be either non diastereoselective (reaction **d**, Scheme 56) or diastereoselective (reaction **f** and **g**, Scheme 56). The only difference between those rigid macrocycles is the replacement of furan(s) by pyrrole(s). Hydrogen bonding between furan and pyrrole seems to be involved the diastereoselectivity observed.

In conclusion, the rigidity of our macrocycles is not a decisive factor inducing the diastereoselectivity of the hydrogenation. In order to understand the DI observed in some cases, we have to explore the influence of other parameters. The interaction (probably H-bonds) between the reduced heterocycle and another heterocycle seems to be the key.

4.1.2. Influence of heteroatoms in macrocycles

Despite the high degree of freedom of the macrocycles used in the reactions **a**, **b** and **c**, we observed a DI when a pyrrole ring is next to one THF ring (reaction **c** compared to reaction **b**, Scheme 56). The THF ring alone or together with a furan ring, in flexible macrocycles does not induce a diastereoselective hydrogenation (reaction **b**, Scheme 56). However the combination of the THF and a pyrrole ring leads to a diastereoselective reaction. We conclude that the THF and the pyrrole interact together so that the catalyst delivers the hydrogen only to one face of the macrocycle. This interaction seems to be also involved in the DI observed with rigid macrocycles (reaction **f**-**h**, Scheme 56). If we compare the starting materials in the reaction **d** and **f**, we observe that: one reaction is diastereoselective (**f**) and the other is not (**d**). In this case again, replacing one furan ring by a pyrrole is sufficient to induce diastereoselectivity.

In the case of a THF ring beside a furan, no DI was observed (reaction **d**, Scheme 56). We reached the same conclusion when a pyrrolidine is next to a pyrrole; no DI was observed (reaction **e**, Scheme 56). We note that the DI is higher when a furan is in opposite position to a THF (reaction **g**, Scheme 56) compared to the case where a pyrrole is in opposite position to a THF (reaction **h**, Scheme 56).

4.2. Influence of two reduced heterocycles on the hydrogenation of the macrocycles

In this part, no matter if the two reduced heterocycles of the starting material are either in opposition or side by side in the macrocycle, they have to have the same stereochemistry, for instance (2*S*, 5*R*). Otherwise, the molecule would possess a C_2 axis and the first hydrogenation leads to a unique intermediate diastereoisomer.

4.2.1. Two hydrogenated heterocycles in opposite positions

This part will be devoted to the analysis of two reduced heterocycles in opposite positions in the macrocycle. Only the first step of each reaction has to be considered (Scheme 57).

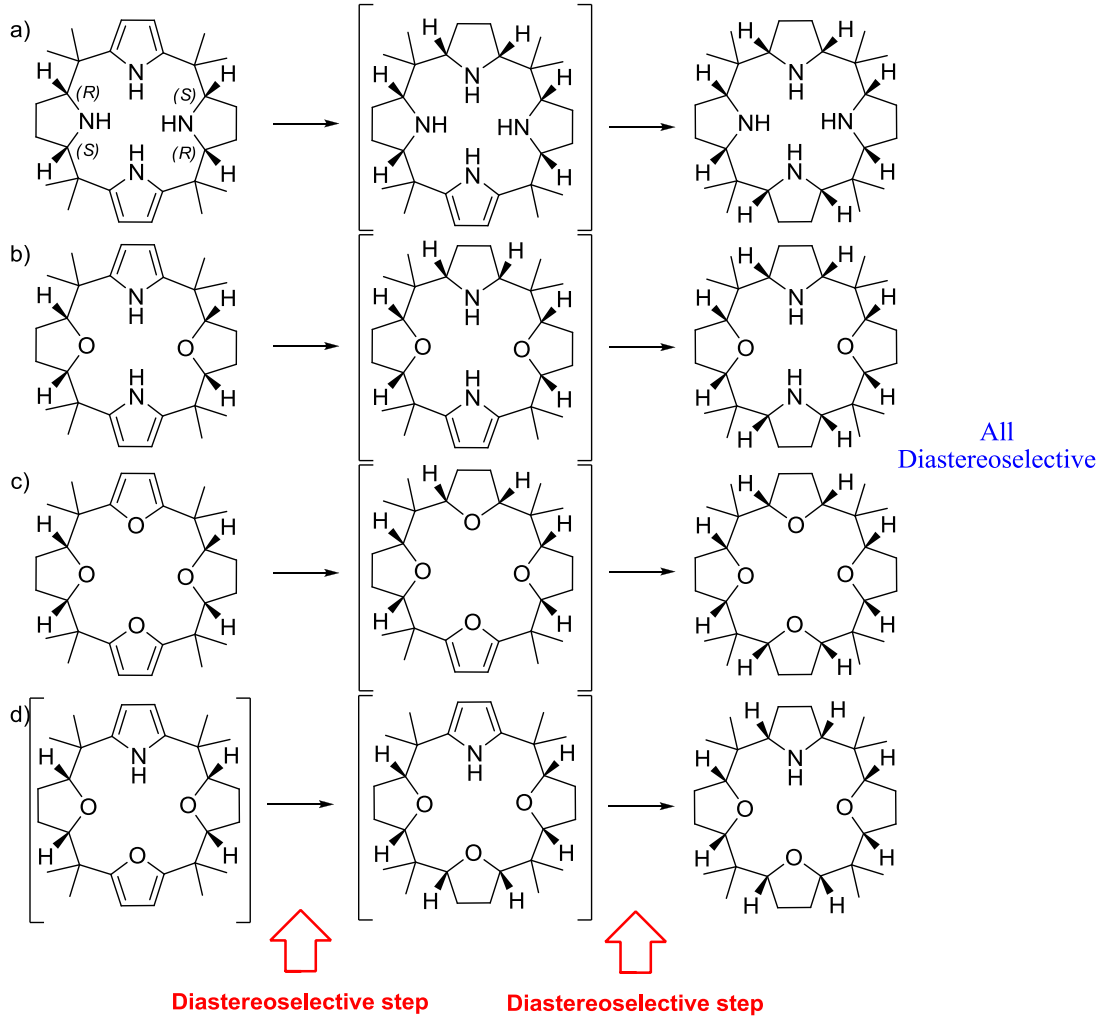

Scheme 57. Influence of two reduced heterocycles on the diastereoselectivity of the hydrogenation of the macrocycles.

In these cases, furans or pyrroles in the molecule do not seem to affect the diastereoselectivity of the reaction. The two reduced heterocycles being in opposite positions (which have the same relative configuration (2*S*, 5*R*)) are probably the source of the DI observed. If it is true, the saturated rings (with high electronic density) have a strong interaction with the catalyst, perhaps a partial chelation of the metal. We previously saw that the combination of a THF and furan ring was not favorable to induce a good diasteroselectivity (reaction **d**, Scheme 56). To have two saturated rings situated in opposite position is obviously a determining factor. Combining this arrangement with the influence of THF-pyrrole pair previously observed, should boost the diastereoselectivity for the reactions **b** and **d** Scheme 57.

4.2.2. Influence of two reduced, neighbouring five membered rings on the diastereoselectivity of the hydrogenation process

This part will be devoted to the analysis of the hydrogenation of macrocycles having two reduced neighbouring heterocycles. Only the first step of each reaction has to be considered (Scheme 58).

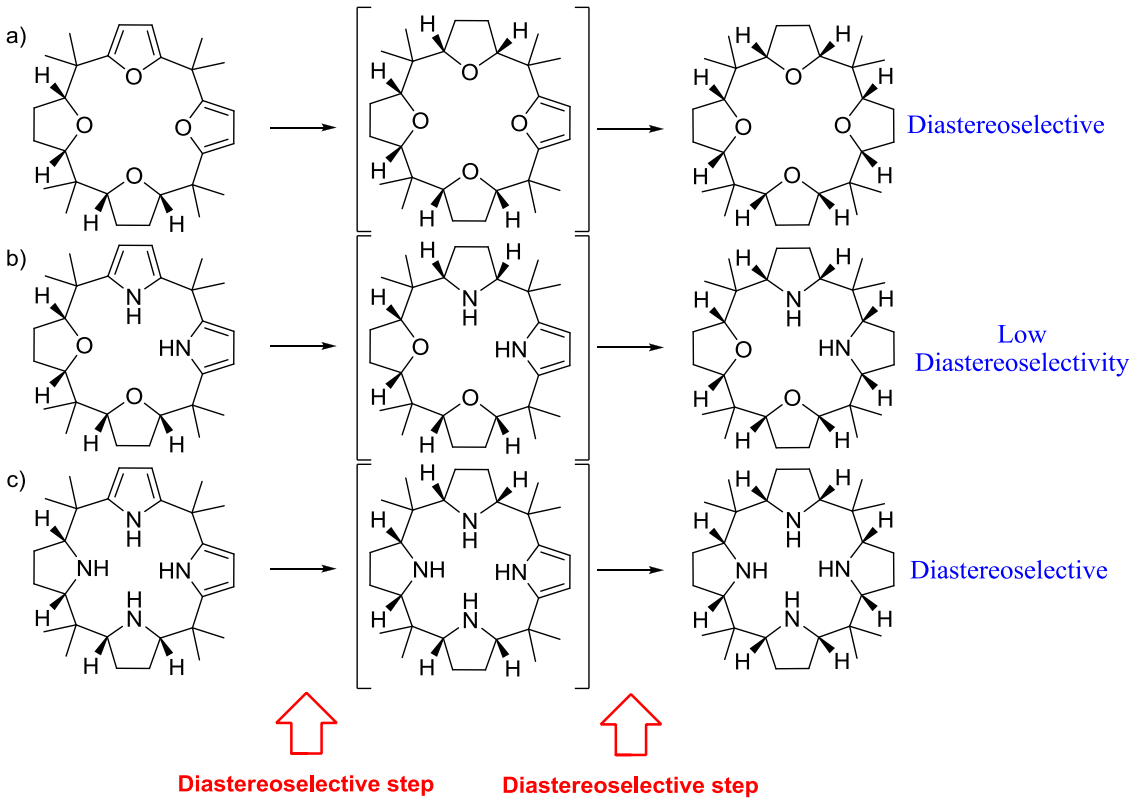

Scheme 58. Influence of two reduced heterocycles in the molecule.

Again, we observed a favorable influence of the two saturated heterocycles on the outcome (=diastereoselectivity) of the hydrogenation. The low diastereoselectivity of reaction **b** is somewhat of a surprise in view of the good diasteroselectivities induced by furan-pyrrole pairs. In a summery the three reactions reported in Scheme 58 show the diastereoselectivity expected...

4.3. Influence on the diastereoselectivity of the hydrogenation of macrocycles containing three reduced heterocycles

This part will be devoted to the analysis of the influence on the diastereoselectivity of the hydrogenation of the macrocycle containing three reduced heterocycles. Only the second step of reactions described Scheme 57 and 58 has to be considered, as well as the second steps in the following reactions Scheme 59).

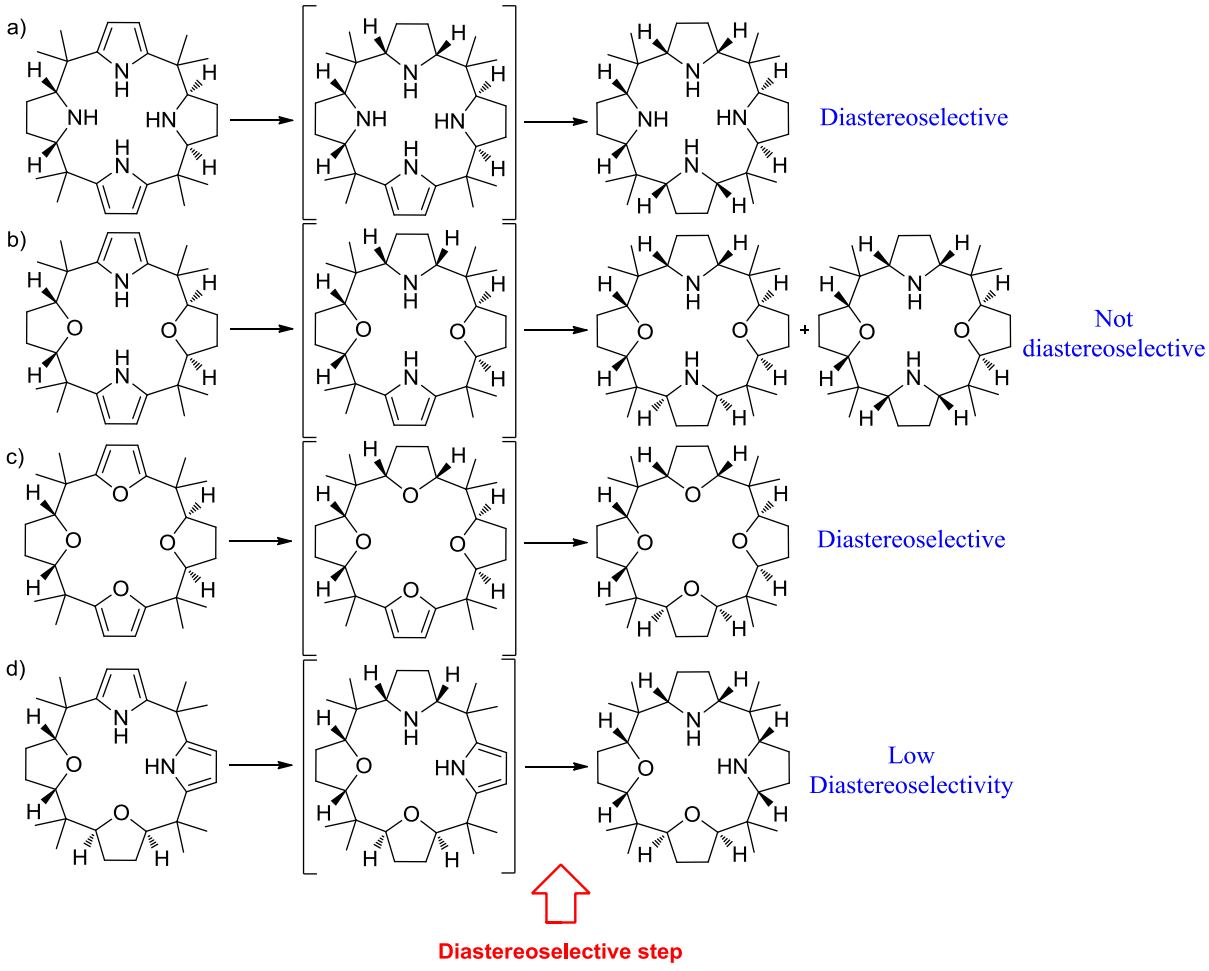

Scheme 59. Influence of three reduced heterocycles in the molecule.

The first hydrogenation leads to a unique intermediate diastereoisomer. The diastereoselectivity of the process as observed in the final product is therefore exclusively the consequence of the second hydrogenation step. The intermediates have been drawn in Scheme 59 to help to understand the stereochemistry of the process (= correlation between the starting material (the not isolated intermediate) and the final product).

In view of the results of the second hydrogenation steps illustrated in Scheme 56 and 57, three reduced heterocycles with the same stereochemistry (2*S*, 5*R*), strongly induce a diastereoselectivity for the next steps. Considering that, all the reaction are diastereoselective and all the intermediates (which are the "starting materials" for the step determining the diastereoselectivity) have the same relative configuration, we cannot say for certain that it is the three saturated rings which are involved in the DI and not two.

However, we could extract this information from the hydrogenation of macrocycles which have three saturated heterocycles with different configuration (Scheme 59). If we compare the two reactions **a**, Scheme 57 and Scheme 59, one realizes that the presence of the two pyrrolidine rings with the same relative configuration induces high DI for the third as well as for the fourth hydrogenation.

The THF and the pyrrolidine next to each other, with the same relative configuration, are inducing a DI only in the case **c**, Scheme 58. The interaction between a pyrrole and a pyrrolidine as next neighbor seems to be a major factor (see next paragraph).

Comparing reaction **b**, Scheme 57 and reaction **b**, Scheme 59, leads to an interesting conclusion. In the reaction **b** Scheme 59, the pyrrole has two THF rings as neighbors, which are pointing toward different faces of the macrocycle. This arrangement leads to a non-diastereoselective reaction, probably due to two different conformers in solution as a consequence of a hydrogen bond between pyrrole with a furan or the other.

A similar situation is present for reaction **a**, Scheme 58 and reaction **c**, Scheme 59. Despite the change in the relative configuration of one of the three THF rings an excellent DI is observed in this case.

4.4. Conclusion and perspectives

Based on the results available we can analyze the trends without having already the full picture:

- The rigidity of these types of macrocycles is not relevant and compulsory for a high DI.
- The combination of a THF and a pyrrole directs hydrogenation of the macrocycle towards a specific face. This combination induces a stereoselectivity
- Two hydrogenated rings in opposite position of the macrocycle with the same relative configuration also induce a high diastereoselectivity.
- Three reduced heterocycles with the same diastereoselectivity induces the hydrogenation of the last heterocycles from the same face.

This investigation could be completed by the hydrogenation of other macrocycles. For instance, replacing furan or pyrrole by thiophen or pyridine rings could be interesting. The synthesis and reduction of novel macrocycles could also be very interesting (but they are very challenging to synthesize) (Figure 69):

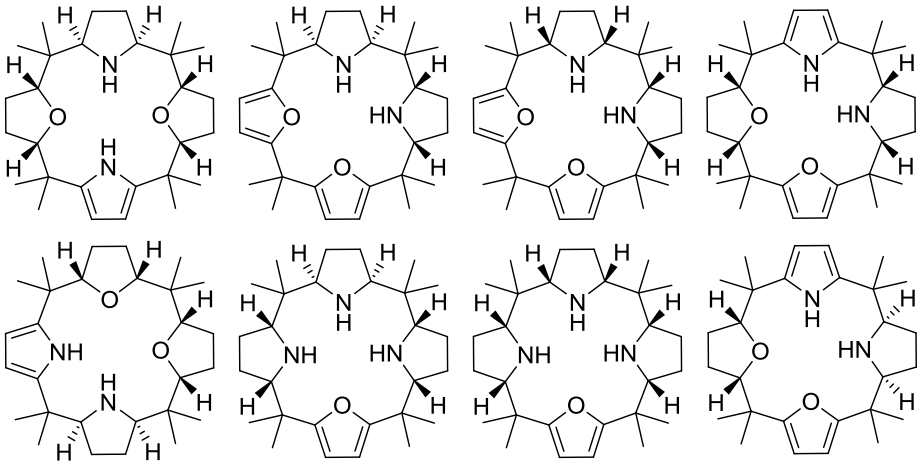

Figure 69. Novel interesting macrocycles for this investigation

5. CONCLUSION

A thorough investigation aiming at the discovery of relevant factors influencing or inducing diastereoselectivity of the hydrogenation was done. This study involved the analysis of the hydrogenation products of twelve different macrocyclic substrates. The syntheses of those macrocycles were based on a novel strategy starting from calix[4]furan. During this investigation, 28 products (18 of whom are novel molecules) were fully characterized and for

relevant cases, their relative configurations were determined by X-ray analysis (15 selected structures). Remarkably selective hydrogenations were successfully realized.

As a consequence of this work, the sequence of the catalytic hydrogenation of calix[4]pyrrole was revealed and the discovery of interesting diastereoselective induction effects of our macrocycles was made.

We realized that, small changes in the macrocyclic structure led to completely different behavior of these molecules during the. The complete understanding of the hydrogenation process remains a very challenging problem.

6. ANNEX

6.1. Description of compound 69

Terpyridine and its derivatives are prototypical ligands of the pincer type family,[198, 199] which have been widely used in coordination chemistry.[200] The metal complexes obtained from pincer ligands are conformationally restricted and often thermodynamically highly stable.[200, 201] The bis-benzylic alcohols of 2,6-disubstituted pyridines belonging to this class of ligands can be easily transformed.[196, 202-209] The modification of these ligands by the hydrogenation of the pyridine ring installs chirality into the structure and increases the basicity and the strength of the ligand. In contrast to the 2,6-pyridinedicarboxylic acids and its derivatives, which have been extensively used, studies on the corresponding tridentate ONO-piperidine ligands containing the bis alcohols have been very rare so far.

The structure of 2,2'-[(2S*,6R*)-Piperidine-2,6-diyl]dipropan-2-ol named compound **69** in the result part, is public and visible in Acta cryst. E.[210] In compound **69**, $C_{11}H_{23}NO_2$, the piperidine ring has a chair conformation. The two hydroxy H atoms are disordered over two positions with fixed occupancy ratios of 0.57:0.43 and 0.63:0.37. In the molecule, there are two short N-H···O interactions. In the crystal, four symmetry-related molecules are linked by O-H···O hydrogen bonds to form a cage-like arrangement, centered about the point of intersection of three twofold axes. These cages stack along the [100] direction.

The molecular structure of the title molecule is illustrated in Figure 70. The geometric parameters are very similar to those found for *cis*-(piperidine-2,6-diyl)dimethanol.[211] The

piperidine ring has a chair conformation, with atoms N1 and C4 being displaced from the plane through atoms C2/C3/C5/C6 by 0.667 (2) and -0.662 (3) Å, respectively.

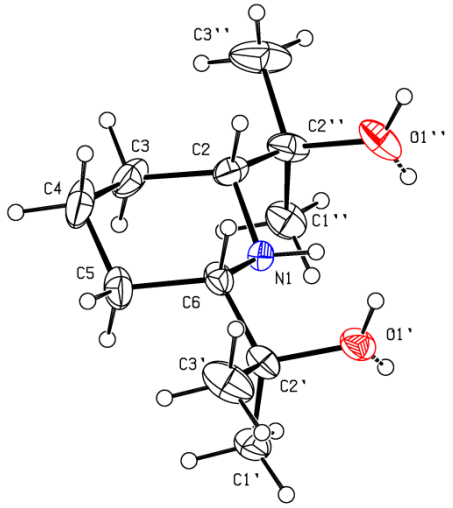

Figure 70. A view of the molecular structure of **69**, with displacement ellipsoids drawn at the 30% probability level. (The O···H dashed lines indicate the positions of the minor components of the hydroxyl H atoms.)

In the molecule the amine (N1) H atom is involved in two short interactions with the hydroxyl O atoms, O1′ and O1″ (Table 14). The hydroxyl H atoms are each disordered over two positions, H1A/H1B and H1C/H1D. Their occupancies were initially refined before being fixed at 0.57/0.43 and 0.63/0.37, respectively. The ^{1}H NMR signal for the hydroxyl H atoms [δ 2.88 (bs, 2 H, OH)] is a broad singlet, which indicates some fluxionality of these protons in solution.

Table 14.

Hydrogen-bond geometry (Å, °)

D—H···A	D—H	H···A	D···A	D—H···A
N1—H1N···O1’	0.84 (3)	2.38 (3)	2.792 (3)	111 (2)
N1—H1N···O1’’	0.84 (3)	2.43 (3)	2.814 (3)	109(2)
O1’—H1A···O1’’^{i}	0.82	1.99	2.805	169
O1’—H1B···O1’^{ii}	0.83	1.99	2.807	167
O1’’—H1C···O1’^{i}	0.82	2.00	2.805	171
O1’’—H1D··· O1’’^{iii}	0.83	2.03	2.762	148

Symmetry codes: (i) *x*, -*y*+1/4, -*z*+1/4; (ii) −*x*+5/4, -*y*+1/4, *z*; (iii) −*x*+*5/4*, *y*, -*z*+1/4.

In the crystal, four symmetry related molecules are linked by O−H· · · O hydrogen bonds to form a cage-like arrangement, centered about the point of intersection of three 2-fold axes (Figure 71). These cages are arranged in stacks along direction [100], as shown in Figure 72.

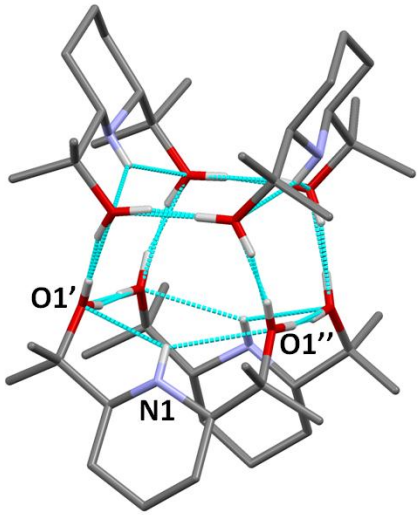

Figure 71. A view of the hydrogen bonded cage formed by four symmetry related molecules of **69**. The C-bound H atoms have been omitted for clarity. The O−H· · · O and N−H· · · O hydrogen bonds are shown as dashed cyan lines (see Table 14 for details).

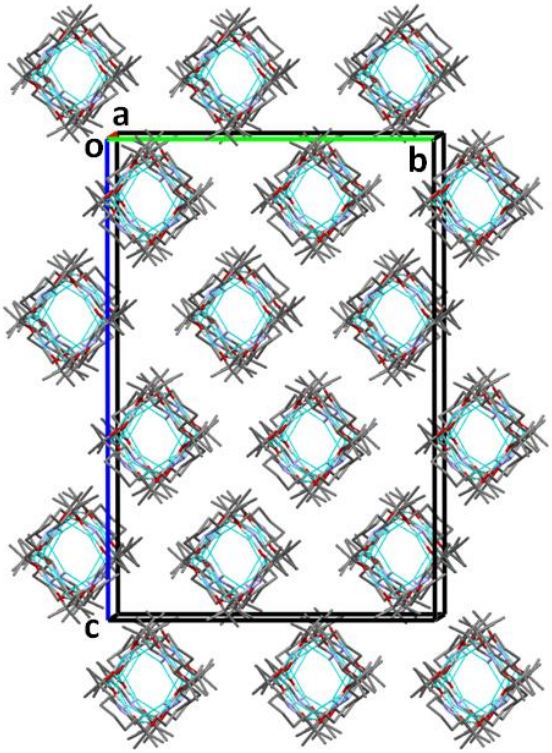

Figure 72. A view along the *a* axis of the crystal packing of **69**. The C-bound H atoms have been omitted for clarity. The O−H· · · O and N−H· · · O hydrogen bonds are shown as dashed cyan lines (see Table 14 for details).

Chapter 4

MODIFICATION OF CALIX[2]PYRROLIDINE[2]PYRROLE

Abstract

One of the major challenges for the scientific community is the reduction of the energy consumption and of the waste production. In chemistry catalysts offer tremendous opportunities to reach these goals. The development of metal-containing or of exclusively organic catalysts has been keenly investigated. The macrocycle **12b** offers interesting perspectives for the development of novel catalysts. The metal binding properties but also the closely connected arrays of pyrrole and pyrrolidine rings are interesting features, which makes these macrocycles suitable for catalyst development. In this context, we investigated the reactivity and the modification of this macrocycle.

Introducing chirality by easily available α-amino acids or small peptides, is one of the recipes applied successfully in the field of enantioselective catalysis.[212-219] In spite of the wealth of methodologies available, N-acylation of macrocycle **12b** revealed to be unexpectedly tricky. We propose that the tight hydrogen bond network of the compound **12b** is responsible for the remarkable reactivity and selectivity pattern. To address this problem, we developed new conditions for a successful mono or bis-N-acylation of compound **12b** by a series of acyl chloride and amino-acids (Scheme 60). A thorough study of the nucleophilic properties and a kinetic study allow the discovery the factors that influence the reactivity of these macrocycles.

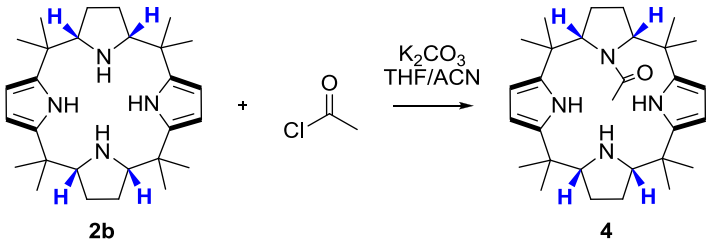

Scheme 60. N-acylation of the calix[2]pyrrole[2]pyrrolidine **12b**.

The structures of the mono and the bis-acetylated products were elucidated by X-ray analysis and led to surprising results. Two conformations in the liquid state at low temperature were observed with products acylated by small acyl chlorides. This “ring flip” was fully characterized with different NMR spectroscopic methods.

1. INTRODUCTION

Molecules belonging to a point group of "high" symmetry have always attracted the attention of chemists for esthetical motives but also for synthetic efficiency.[94, 112, 220-223] Calix[4]pyrroles belong to the class of highly symmetric macrocycles, whose efficient synthesis reflects the symmetry of the final product.[92, 94] The ease of access coupled with the beauty of the structure has created an increasing fascination and in parallel a growing activity for the chemistry of calix[4]pyrroles, initiated by the group of Sessler.[101, 224-231] Most of the growing activities focused on variations of the calix[4]pyrrole basic structure. The goals of these scientific activities were multiple and ranged from curiosity to the improvement of the application as sensor molecule.[101, 224-231] Both types of research have led to an impressive collection of new structural variants.[160, 229, 232-243] Many of the newly synthesized molecules possess unexpected and unpredicted properties, which are often independent of the goals initially motivating the beginning of a research program. One of the intellectually appealing aspects of working with highly symmetric molecules relies on the opportunity to break the symmetry by simple chemical transformations at a later stage of the synthesis. With this single symmetry breaking operation, one creates efficiently, structurally and stereochemically more complex molecules from simple, symmetric starting materials (Figure 73).

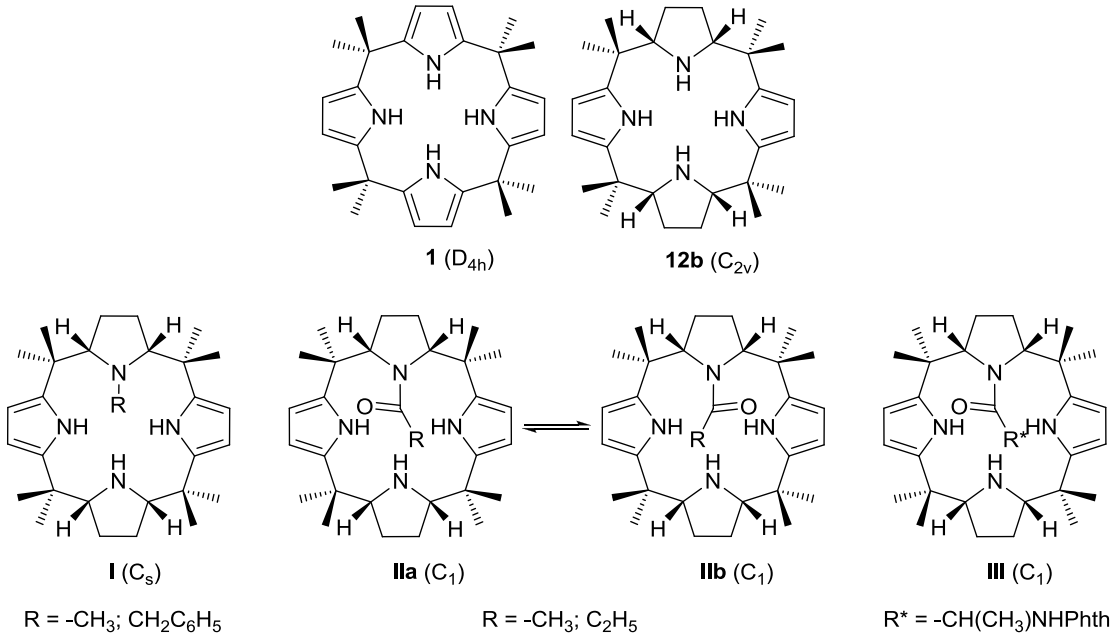

Figure 73. Calix[4]pyrrole (**1**), Calix[2]pyrrolidine[2]pyrrole (**12b**) and simple derivatives thereof of the types **I**, **II** and **III** and their corresponding point groups

We were intrigued by the possibility to monofunctionalize the C_{2h} symmetric bis-hydrogenated macrocycle **12b** by a simple acylation reaction, thereby making a novel class of chiral macrocycles available. The attraction of this standard transformation relies on the fact that we create a unique array of a basic pyrrolidine and two hydrogen bond donating pyrrole rings in a stereochemically complex environment. We decided to study the simple modification of the half hydrogenated calix[2]pyrrolidine[2]pyrrole **12b** by amide formation using achiral aliphatic and aromatic acids and α-amino acids as typical chiral derivatizing agent. We expected that the amide formation of the pyrrolidine rings should be an easy and simple transformation. To obtain selectively the mono-amide might however pose problems. We expected that the bis-amidation might be an unwanted and difficult to control side reaction. The easy and reliable amidation process was chosen,[244-246] because we intended to synthesize a family of derivatives by a simple and efficient process. The goal of our project was to study the properties of these novel and unique macrocycles with the hope of discovering interesting chemical and catalytic activities.

Aside from the ease and the elegance of the synthetic access, the attraction of the calix[2]pyrrolidine[2]pyrrole is its high symmetry and the unique array of basic pyrrolidine rings linked to hydrogen bond donating pyrrole rings. The hydrogen bond donating capacities of calix[4]pyrroles are well documented and represent the principal property of calix[4]pyrroles used and studied so far. Replacing two pyrrole rings of calix[4]pyrroles by two hydrogenated pyrrolidine rings as in calix[2]pyrrolidine[2]pyrrole, should induce a switch in the chemical and physical properties of the molecule. The two pyrrolidine nitrogens are good hydrogen bond acceptors, keeping the capacity to function as H-bond donors. The interplay between the two pyrroles as good hydrogen bond donors and the two pyrrolidines as good hydrogen bond acceptors in a confined geometry should lead to strong interactions within the cavity of the macrocycle. The X-ray structures of the two stereoisomers of the half-hydrogenated compounds **12a** and **12b** showed in each case an intramolecular hydrogen bond network in the central cavity of the macrocycle. This H-bond network structured and fixed the conformation of the relatively flexible macrocyclic ligand. Analyzing a series of X-ray structures of different isomers with the goal to identify and to characterize hydrogen bonds is a widely used approach. This approach is systematically used in the analysis of X-ray structures of proteins. In enzymes hydrogen bonds found in the active site or between the protein and small molecules are used as key information for the understanding of the functioning of the enzyme. The analysis of hydrogen bonds is one of the crucial points for planning drugs interacting specifically with a given enzyme.[247-249] In this approach the

presence of hydrogen bonds in the solid state is often taken as a valid hint for the presence of similar hydrogen bonds in solution. There are different difficulties associated with this type of extrapolation from the solid state to the behavior in solution. The crystal packing influences the conformation of the individual molecules in the unit cell and even more importantly, the relative position of molecules in the crystal, strongly depends on the packing forces. The extrapolation of the data obtained from the crystal (mainly the distances between the two hydrogen bonded atoms and bond angle around the hydrogen atom towards the two electronegative atoms) are difficult to extrapolate to thermodynamic and kinetic data of the specific hydrogen bond in solution. In most cases additional information, thermodynamic measurements and/or NMR studies are needed to obtain information on the thermodynamic and kinetic properties of specific hydrogen bonds.[250, 251] In the case of the calix[2]pyrrolidine[2]pyrrole, neither good model compounds nor relevant comparison data were available at the start of our studies. An additional difficulty for the interpretation of the X-ray of our new structures is the macrocycle itself, whose restricted conformational mobility will certainly influence the arrangement of our compounds in the solid state as well as in solution. The calix[2]pyrrolidine[2]pyrrole possesses 8 carbon-carbon simple bonds, which can rotate relatively freely. The two pyrrolidine rings are characterized by a relatively flat conformational surface, which makes many different ring conformations easily accessible.[252, 253]

2. ACYLATION OF CALIX[2]PYRROLE[2]PYRROLIDINE

2.1. Results

2.1.1. Acylation of calix[2]pyrrole[2]pyrrolidine 12b

We intended to introduce selectively one amino acids and small peptides unto the calix[2]pyrrole[2]pyrrolidine **12b** in order to create chiral scaffolds containing the combination of two hydrogen bond donating pyrroles and a basic amine. To the best of our knowledge the mono- or bis-acylation of this kind of macrocycle has never been achieved so far. To optimize the reagents and the conditions for the mono- or bis-acylation, we started the investigation by the straightforward acylation of **12b** with acetyl chloride. Our first trials

using standard conditions failed. Using THF as solvent to obtain a homogenous reaction mixture, we tested different organic bases without success. A large amount in the crude of reaction mixture was attributed to the starting material and the strong orange color suggested the formation of unidentified side reactions. We decided to test the simple model compound **71** obtained by partial hydrogenation of the readily available dipyrromethane **70** (Scheme 61).[254-256]

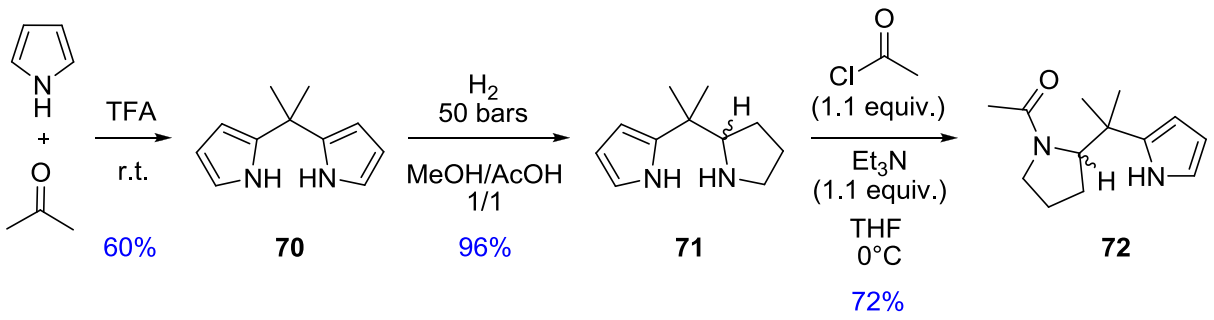

Scheme 61. Synthesis of the model compound **6**.

The partial hydrogenation of **70** under 50 atm of H_2 afforded our racemic model compound **71**.[257] Under the condition previously tried with **12b**, the model compound **71** was smoothly transformed in 72% yield to the amide **72** (Scheme 61). We successfully crystallized compound **70**, **71** and **72** and performed X-ray diffraction analysis for each of them. Their molecular structures which are described in the Annex present interesting properties. The compounds **70** and **71** can be considered as models for the H-bonding and conformational behavior of the central structural element of the calix[4]pyrroles and calix[2]pyrrole[2]pyrrolidine. The spatial arrangement of the two heterocyclic rings linked by the quaternary carbon atom can be studied, without the restrictions imposed by the macrocycle.

The crude product was yellowish and had to be purified by column chromatography suggesting that side reactions are competing with the wanted acetylation.[258-262] We focused on identifying the suitable base for the acylation of **12b** and a series of base have been tried (Scheme 62). The reactions were performed with two equivalents of acetyl chloride and two equivalents of base in order to get the bis-acylated macrocycle. A first positive result was obtained, when the macrocycle **12b** was reacted with 2.1 equivalent of acetyl chloride in THF without base. After 15 minutes a precipitate appears. The precipitate was filtered off after 1 h. It exclusively contained the mono-protonated form of the macrocycle **12b** as shown by the

NMR spectrum. From the mother liquor, we solely isolated the mono-acylated macrocycle **7** and a small amount of starting material in ~50% yields (Scheme 62, condition c). The high selectivity for the mono-acetylation came as a surprise to us. Usually one has to use protecting group strategies for the selective mono-acylation of symmetric diamines.[263-271] Trials to push the reaction towards bis-acetylation were unsuccessful. The success of the acetylation of the macrocycle **12b** crucially depended on the type of base used: homogenous organic bases like DBU, DABCO, DMAP, and pyridine or potassium *tert*-butoxide failed to produce the product (Scheme 62, condition a). Acetylation of the macrocycle **12b** using the conditions applied to the bicyclic compound **71** led to the mono-acetylated derivative **73** in 60% isolated yield (Scheme 62, condition b). Only Et_3N worked well as base, but the reaction stopped at the state of the mono-acylated product **73**. Under the conditions tested, we could not detect any trace of the bis-acetylated product.

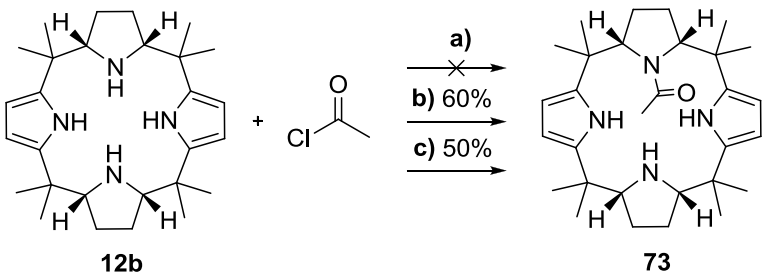

Scheme 62. Acylation of calix[2]pyrrole[2]pyrrolidine **12b** with acetyl chloride. Reagents and conditions: (a) acetyl chloride 2.1 equiv., THF, DMAP or Pyridine or DBU or DABCO or *t*-ButOK, -78°C to 0°C; (b) THF, Et_3N 2.1 equiv., r.t. ; (c) THF, 1h, r.t.

We assume that the organic bases react with acetyl chloride forming reactive intermediates, like ketenes, which lead to side products. In order to avoid these types of side reactions, we tested the use of weak inorganic bases under conditions, where they are only partially soluble in the reaction medium. The suitable base was K_2CO_3 because of its basicity and its partial solubility in ACN. We then developed a new condition for the acylation, using 2.1 equiv. of acetyl chloride, 2.1 equiv. of K_2CO_3 in mixture of THF/ACN (2/1). Happily, our efforts along these lines were indeed successful, and we were pleased to see the acylation of compound **2b** with this optimized condition afforded the amide **7** in quantitative yield (Scheme 63).

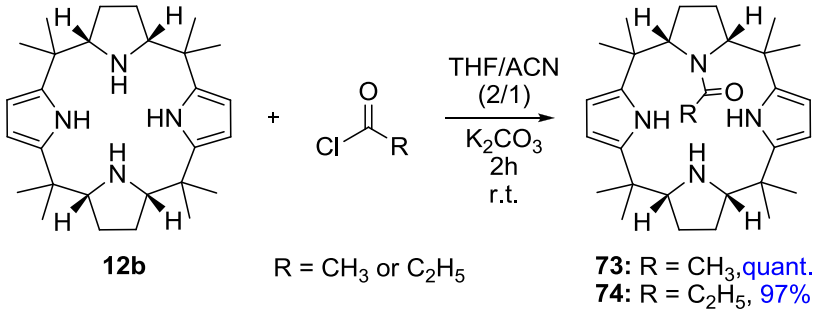

Scheme 63. Acylation of calix[2]pyrrole[2]pyrrolidine **12b** with acetyl chloride and propionyl chloride

The selective mono-acylation has been obtained without traces of the bis-acylated product. This reaction has been repeated with propionyl chloride as acylating reagent affording the amide **74** in 97% yield (Scheme 63). The products **73** and **74** were isolated without column chromatography and characterized by NMR and mass spectroscopy. The NMR spectra at room temperature showed broad signals due to slow exchange between different conformations. The NMR spectra at 60 °C are compatible with a molecule showing C_S symmetry due to fast exchange. Lowering the temperature to room temperature shows considerable line broadening. Lowering the temperature to -64 °C shows well-resolved signals for the macrocycle **73** with a point symmetry C_1. The signals became sharp due to the slow exchange between the two amide conformers. Additional signals start to appear attributed to the presence of an additional conformer, which was not identified initially. Compound **73** gave nice crystal from ethanol suitable for X-ray diffraction. Crystals of **74** were obtained from a slow evaporation of a solution of **74** in CH_2Cl_2. Under our optimized conditions using two equivalents of acid chloride and two equivalents of potassium carbonate in an ACN/THF mixture of 1/2 the acylation product **72** could be isolated pure in preparative yields of up to 96% without chromatography. Our optimized conditions were identical to the reaction conditions published by Li Zhang et al. during our own work.[272]

We were not able to detect small quantities of the doubly acylated product even by considerably increasing the reaction time, the number of equivalents of acetyl chloride and the temperature. The failure to detect the formation of a doubly acylated product under a variety of exploratory conditions finally pushed us to use the harsh conditions developed by Floriani and co-worker.[100] Treating the mono-acylated compounds **73** and **74** with three equiv. of butyl lithium at -80 °C should lead by deprotonation to the tri-anion (Scheme 64). The solution

containing the tri-anion was quenched with one equiv of acetyl chloride, giving after a cumbersome chromatographic purification, very low yields of the bis-acetyl compounds **75** and **76** in 7% respectively 12% isolated yield.

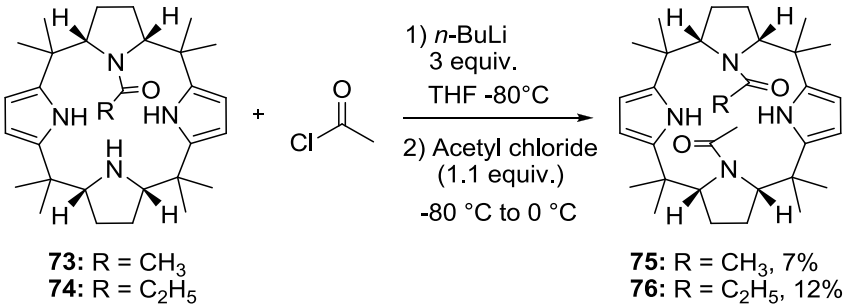

Scheme 64. Acylation of the totally deprotonated form of compounds **73** and **74** by acetyl chloride

The two products were fully characterized by NMR and mass spectroscopy. The ^{1}H-NMR spectrum of the bis-acetylated macrocycle **75** was expected show two different conformers due to the slow rotation around the two amide bonds: a C_2-symmetric conformer and a C_S-symmetric conformer. The ^{1}H-NMR spectrum of compound **75** recorded at low temperature shows only the signals of one present in solution.

The structure of compound **75** was determined by X-ray diffraction. The molecular structure in the solid state of **75** showed only the C_2-symmetric conformer. Finally we were pleased to obtain only the selective mono-acylation so easily, avoiding numerous efforts of protection/deprotection steps.

2.1.2. Scope and limitations

We decided to test the scope and limitations of our protocol. We used 2.1 equivalents of the electrophiles, 2.1 equivalents of K_2CO_3 in the solvent mixture THF/ACN (2/1) at room temperature for two hours (Table 15). This work is the result of the common effort with Dr. Frédéric Bruyneel, labeled in the table by a "*".

Table 15. Scope of the acylation of macrocycle **12b** by different electrophiles.[a]

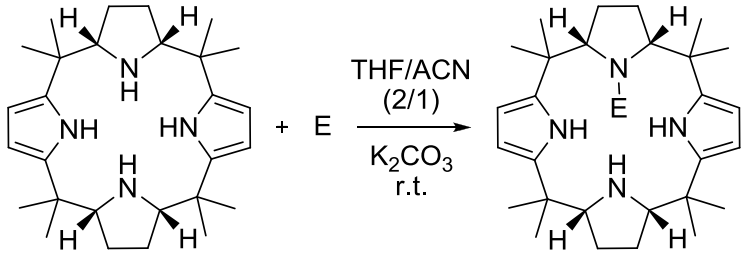

12b

Entry	Electrophile	Products	Yield[b] (%)
1		**73**	quant.[c]
2		**74**	97[c]
3	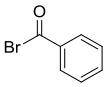	**77**	quant. [c]
4*		**78**	99[c]
5*	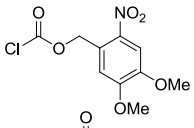	**79**	99[c]
6*	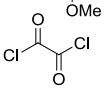	-	nd[d]
7		-	nd [d]
8	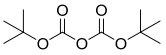	-	nd [d]
9	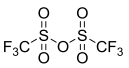	-	nd [d]
10		-	nd [d]
11*	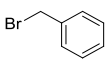	**80**	10[d]
12	CH_3I	**81**	60[d, e]

[a] The reactions were performed using 0.46 mmol of starting material, K_2CO_3 (2.1 equiv.), electrophile 2.1 equiv., in a solvent mixture THF/ACN (2/1) at r.t. for 2 h. [b] Isolated yields. [c] Isolated without chromatography. [d] Starting material could be recovered unchanged. [e] Reaction time 40 h.

Using the strong electrophile, benzoyl bromide (Table 15, entry 3), we observed only the selective mono-acylation in high yield. The reaction of **12b** with methyl and 6-nitroveratryl chloroformate (Table 15, entry 4 and 5) gave compounds **78** and **79** without chromatography in excellent yields and good purity. To our surprise **12b** did not react with oxalyl chloride, acetic anhydride, di-*tert*-butyl dicarbonate, trifluoromethanesulfonic anhydride and methane sulfonyl chloride (Table 15, entry 6-10). The alkylation with methyl iodide and benzyl bromide worked under our conditions but was quite sluggish (Table 15, entry 11 and 12). After two hours a disappointing yield of 10% of compound **80** was obtained. The alkylation by methyl iodine needed 40 hours until the complete consumption of the starting material affording 60% of compound **81**. Under our conditions the reactions seems to be limited to acyl halide and chloroformates giving the mono-substituted products exclusively. The reaction with alkylhalides and benzyl halides was sluggish.

2.1.3. Introducing amino-acids

Introducing commercially available α-amino acids or small peptides onto an easily accessible molecule installs chirality and allows creating a diverse set of analogues. Introducing easily available α-amino-acids or small peptides on easily accessible molecule, is one of the recipes applied successfully in the field of enantioselective catalysis to inset chirality.[212-219] We hoped to apply one of the mild methods developed for peptide coupling. We started our studies with the acylation of **12b** by *N*-carboxybenzyl-glycine activated by HOBt[273-276] and HBTU[277-280] first under standard conditions reported in the literature. Our effort acylating **12b** with those reagents were unsuccessful, despite many variations of conditions such as Et_3N (2 equiv.) in DMF for 3 hours at 0°C[281], 50°C or 100°C, Et_3N (2 equiv.) in DMF for 24 hours at 0°C, potassium carbonate (2 equiv.) in ACN and THF (2/1) for 4 hours at 0°C. The following coupling reagents were tested unfortunately without success: carbodiimide reagents, DCC and DIC,[258, 282, 283] the combination DCC/HOBt[284] as well as phosphonium reagent, PyBOP.[285] We resigned to use acyl chloride for the activation of glycine,[246] despite the many side-reactions known to occur with this harsh activation: formation of ketene or of oxazolone intermediates (carbamate protection)[286]. Treatment of *N*-carboxybenzyl-glycine by thionyl chloride in CH_2Cl_2 for 4 hours at room temperature afforded the corresponding acyl chloride 95% yield.[287] The product was used directly without purification for the next step under our optimized condition (Scheme 65). No product was detected under these conditions.

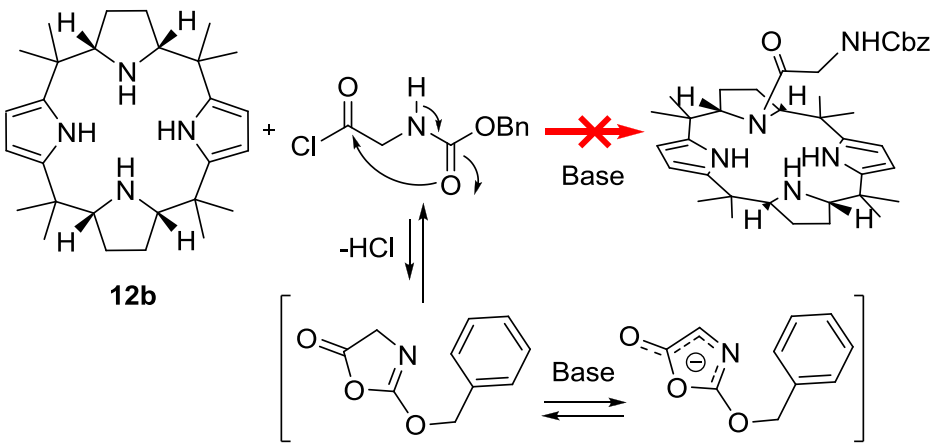

Scheme 65. Acylation of macrocycle **12b** by N-carboxybenzyl-glycinoyl chloride

Replacing the *Boc* group by phtalimide [288] should avoid oxazolone formation. The readily prepared *N*-phtalimide-glycinoyl chloride **82** could successfully be used for the acylation reaction giving compound **83** in 70% yield after 4h (Scheme 66).

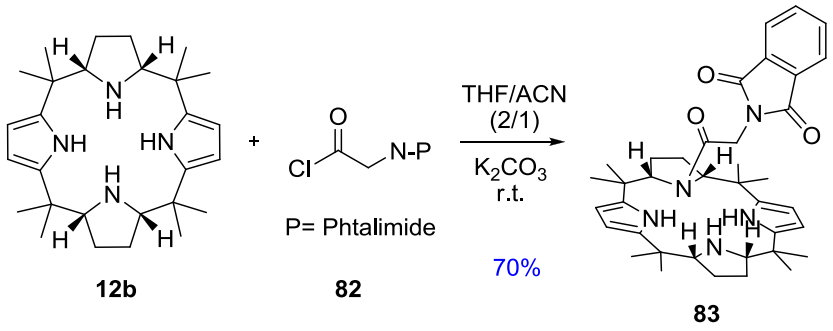

Scheme 66. Acylation of macrocycle **12b** by N-phtalimide-glycinoyl chloride **82**

The synthesis of *N*-phtalimide-valine **84** was carried out by reacting the commercially available phtalic anhydride with valine, with 99% yield (Scheme 67). The acyl chloride **85** was readily prepared in 99% yield. The acylation of the macrocycle **12b** with the freshly prepared acyl chloride **85** afforded the product **86** in 70% yield (Scheme 67).

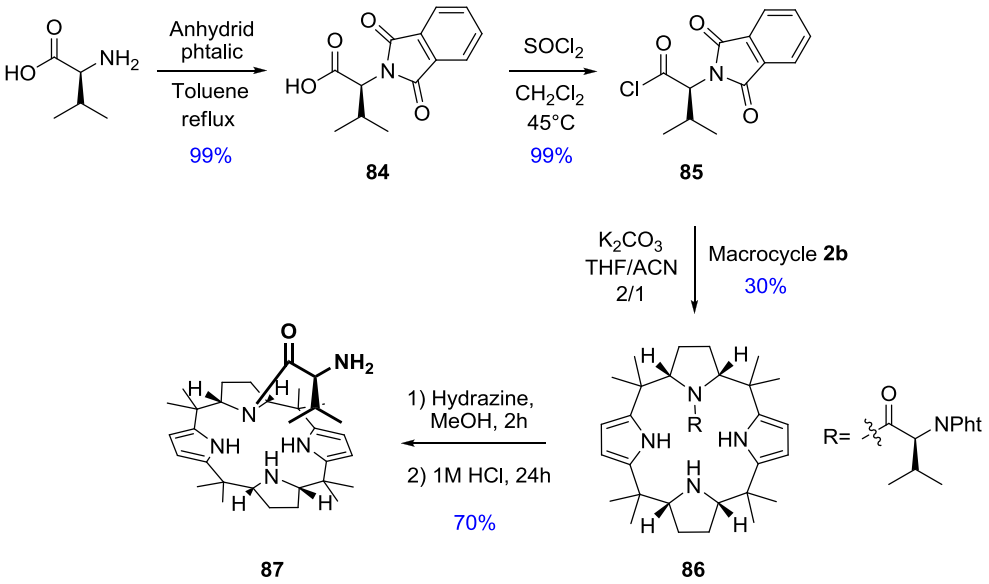

Scheme 67. Acylation of macrocycle **12b** by *N*-phtalimide-valinoyl chloride **85**.

The rate of the reactions with the acyl chlorides of the α-amino acids is slow, which increases the risk of racemization. To test the propensity for racemization under our conditions we examined the reaction between *N*-phtalimide-glycinoyl chloride **85** with the chiral amine (*R*)-(-)-2-methylpyrrolidine (Scheme 68).

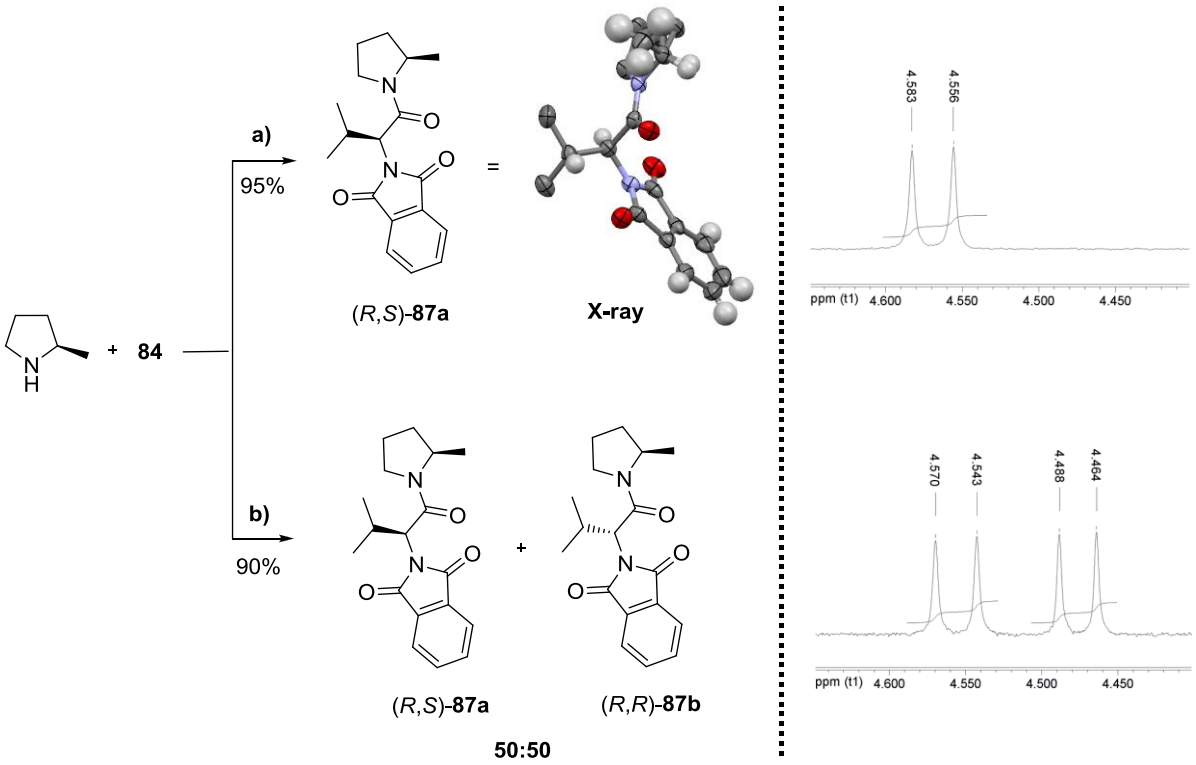

Scheme 68. (Left) Examination of possible racemization under our optimized condition. Molecular structure of compound (*R*,*S*)-**87a** with the thermal ellipsoids drawn at the 50%

probability level. (Right) Selected region of the ^{1}H-NMR spectrum of **87a** and the mixture of diastereoisomers (*R*,*S*)-**87a** and (*R*,*R*)-**87b**. Reagents and conditions: (a) (i) CH_2Cl_2, $SOCl_2$, 2h, 45°C; (ii) THF/ACN (2/1), K_2CO_3, 2h, r.t. (b) DMF, PyBOP, Et_3N, 2h, r.t.

Using our conditions (Scheme 68, method a) the enantiomerically pure product (*R*,*S*)-**87a** was obtained in 95% overall yield. The ^{1}H-NMR spectrums showed only the signals for one a single diastereomer. In contrast complete racemization occurred using the coupling reagent PyBOP together with Et_3N (Scheme 68, way b) as documented by the ^{1}H-NMR spectrums. The pure enantiomer (*R*,*S*)-**87a** crystallized and the X-ray diffraction analysis confirmed our previous analysis.

2.1.4. Kinetic study

The unusual reactivity pattern of our transformation induced us to characterize the reaction further by carrying out a Hammett study. We choose five differently substituted benzoyl chlorides using the optimized conditions. The reactions have been performed in parallel (Table 16).

Table 16. Reactions Performed for Hammett Study

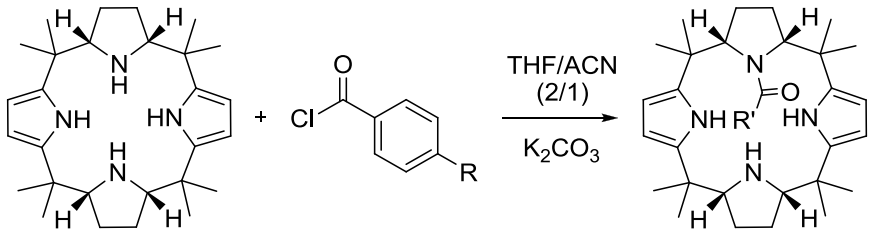

12b **77, 88-91**

Entry	k (L.mol^{-1}s^{-1})	R	Sigma	Products	Yields (%)
1	4.6 10^{-4}	-NO_2	0.77	**88**	57[b]/81[c]
2	1.9 10^{-4}	-Cl	0.22	**89**	75.6[c]
3	1.3 10^{-4}	-H	0	**77**	61.3[c]
4	1.0 10^{-4}	-Me	-0.17	**90**	54.3[c]
5	9.3 10^{-5}	-OMe	-0.26	**91**	49[c]

[a] The reactions were performed on 0.46 mmol scale of starting material, K_2CO_3 (2.1 equiv.), acyl halide 2 equiv., in a mixture of THF/ACN 2/1 at r.t. for 2h. [b] Reaction made during 0.5h. [c] Isolated yield after column chromatography. Starting material largely accounted for the remaining percentage.

We obtained an approximation for the reaction rate from the relative amount of product formed after 2 h reaction time. In the case of the *p*-nitrobenzoyl chloride we measured the % transformation after 30 min because the conversion was total after 2 h. All products were preparatively isolated, fully characterized and their crystal structures determined (see annex). To simplify the analysis we assumed a pseudo-first order kinetics for our process (see experimental part).

The resulting Hammett plot based on our data is displayed in Figure 74. This plot is linear over the domain tested showing a positive ρ value (ρ = 0.682) and good correlation coefficient (R^2= 0.998).

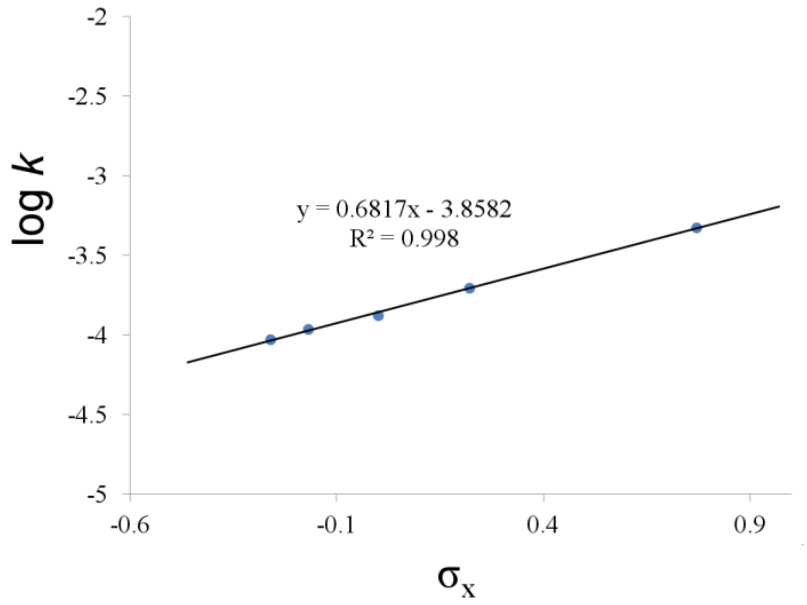

Figure 74. Hammett plot for reaction of various *para*-substituted benzoyl chlorides with calix[2]pyrrole[2]pyrrolidine **12b**. The identity of points is given table 2.

2.1.5. Dynamic NMR investigation and conformational analysis

The following paragraphs reports the result of the NMR studies undertaken by Dr. Claudio Dalvit and Dr. Julien Furrer. The detailed NMR analysis and the simulations have been done exclusively by Dr. Claudio Dalvit. We thank both Dr. Dalvit and Dr. Furrer for this fruitful collaboration and for sharing their experience and their results with us.

The NMR spectra at r.t. of **73** and **75** are broad due to the slow rotation around the amide bond. Heating to 65 °C gave spectra with sharp lines, which was fully compatible with the structures proposed. At 205 K the spectrum of compound **73** shows splitting of the signals due to the slow rotation around the amide bond. Due to the slow exchange the NMR spectrum of compound **73** shows separate signals for each proton or group of protons of different type according to the point group symmetry C_S of the conformer (Figure 75). This is valid also for compound **75**, despite its C_2 symmetry.

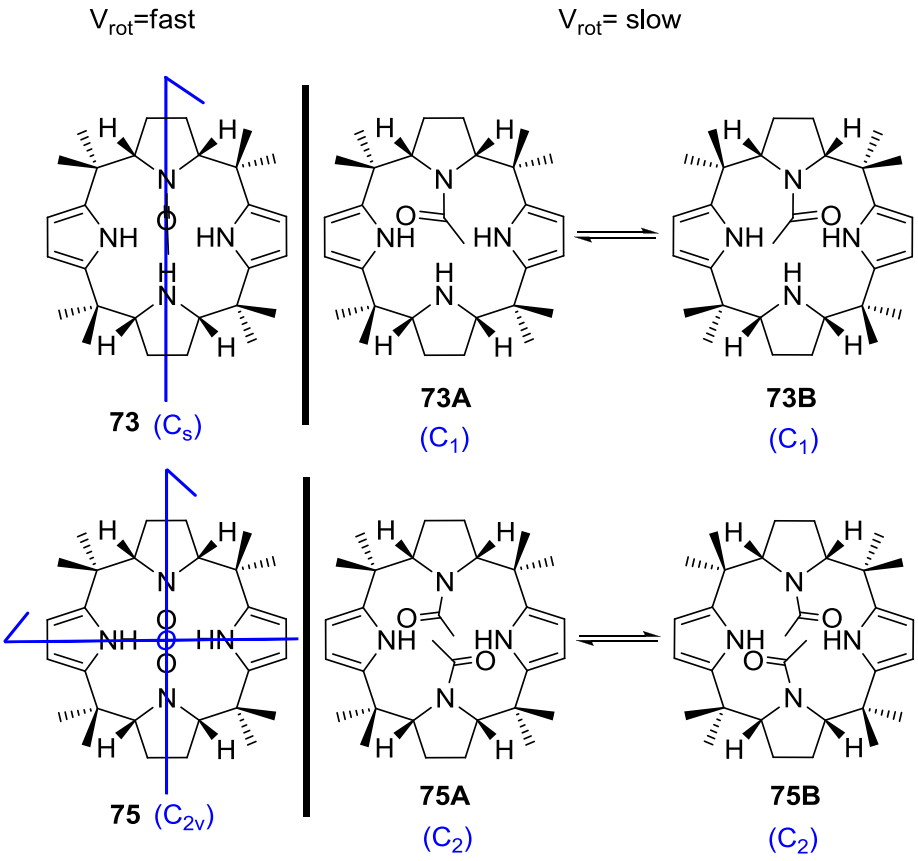

Figure 75. Representation of the average conformation (fast exchange) of **73** and **75**. At slow exchange two conformers **73A**, **73B** and **75A** and **75B** and for **75** the enantiomeric conformers should be observable in solution.

The slow rotation around the amide bond leads to an exchange between the two enantiomeric conformers **73A** and **73B**. In the case of **75** we should observe the exchange between two diastereoisomeric conformers and the slow exchange between the enantiomeric conformations of each diastereoisomer.

2.1.5.1. Conformational analysisThe ^{1}H NMR spectrum of **73** in chloroform exhibits distinct signals for every proton at 209 K. The spectrum displays small additional peaks in a 1:0.14 ratio, clearly visible in the N-H area of pyrrole (Figure 76). The full spectrum is presented in the annex.

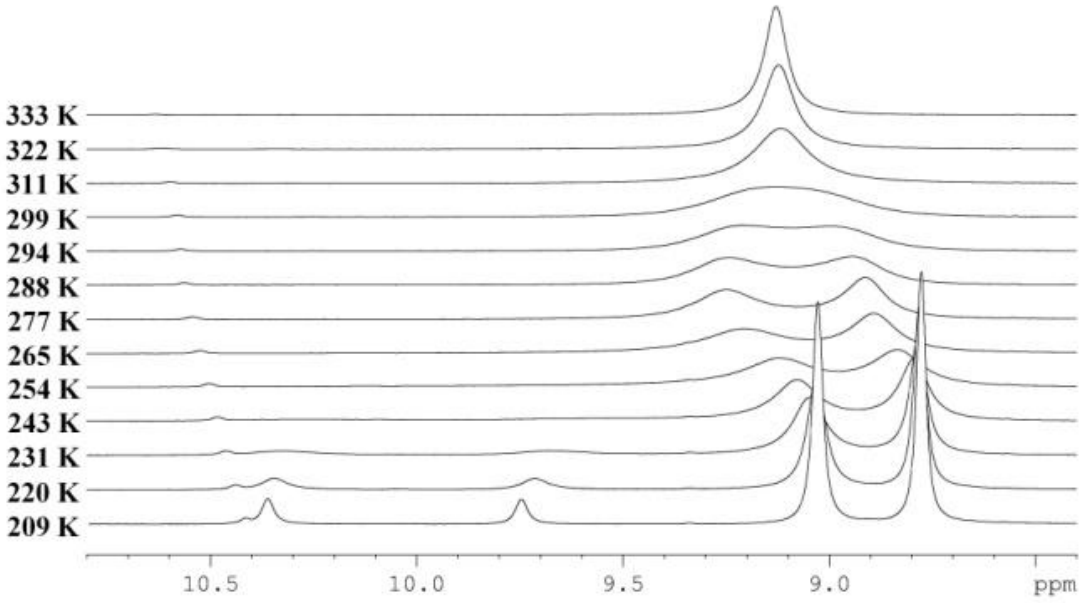

Figure 76. Dynamic NMR spectra of compound **73** over a 124 °c range of temperature. Only the spectral region of the pyrrolic N-H is shown

At 209 K the region between 8 and 11 ppm shows a total of four peaks: two major peaks around 9 ppm and two smaller peaks at 9.7 and 10.4 ppm for the signals the pyrrole N-H protons. Rising the temperature the two major N-H peaks start to coalesce ($T_{coalescence}$ = 311K) into a single peak that sharpens as the temperature increase further. For the minor component an up field shift and line broadening are observed which strongly suggests that compound **73** is present in another not yet identified conformation. To test this assumption, we performed 2D-ROESY experiments at variable temperature in dichloromethane. Figure 77 displays 2D-ROESY of the N-H region of pyrrole at 180K and 224K (Copies of the full spectra can be found in the annex).

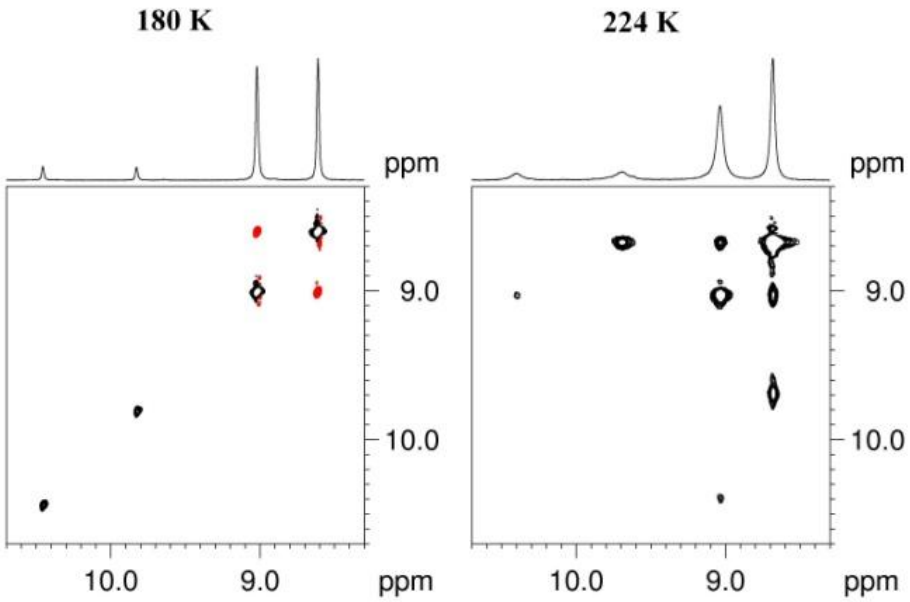

Figure 77. 2D-ROESY experiment of compound **73** recorded at two different temperatures in $CdCl_3$. Cross peaks are in red and exchange in black

The ROSY spectrum in $CDCl_3$ as solvent recorded at 224 K clearly shows the characteristic features of a two-site chemical exchange process (amide rotation: **73A** to **73B**, unidentified additional conformational change: **73a** to **73A** and **73b** to **73B**). Another 2D-ROESY experiment has been performed in chloroform at 204 K in order to characterize peaks of the minor conformation. At this temperature the not yet identified exchange **73a** to **73A** and **73b** to **73B** was still fast, whereas the exchange rate for the amide rotation **73A** to **73B** was slow on the NMR scale. At 180 K all exchange processes are slow on the NMR time scale. The 2D-ROESY spectrum recorded at this temperature gave us the opportunity to elucidate the structure of the other conformation of **73**. Cross peaks between protons of the minor conformer were meticulously analyzed. Relevant cross peaks between H(23) with H(2) and H(16) (in their minor conformation) were the key for our analysis. (Figure 78 and 79).

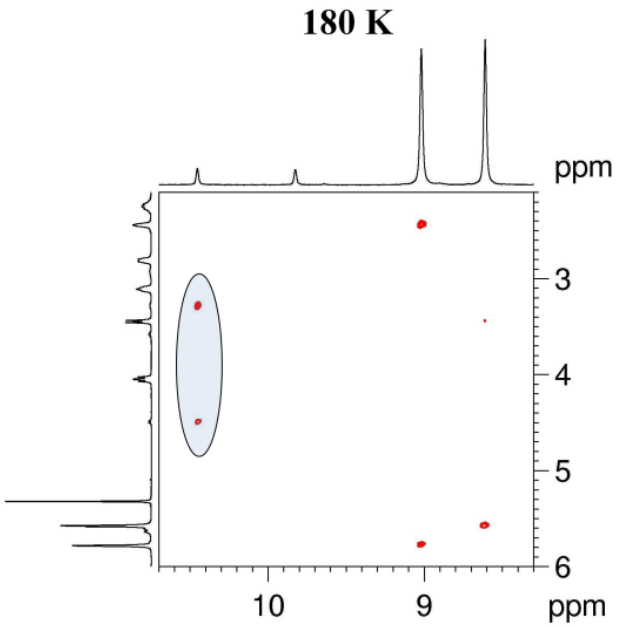

Figure 78. 2D-ROESY spectrum of compound **73** recorded at 180 K. Cross peaks are in red

We asserted that the new conformer came from a ring flip, the amide passing through the macrocycle (Figure 79). This result was extremely surprising, the very robust H-bonds between pyrrole and pyrrolidine described previously have to be broken, and then the acetamide to squeeze through the interior of the macrocycle. Despite the fact that we have only rotations around the exocyclic C-C single bonds the process obviously is highly hindered.

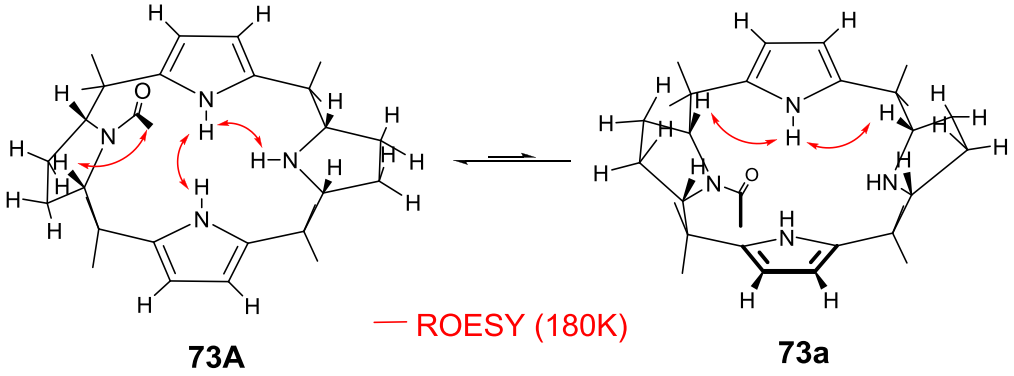

Figure 79. The interpretation of the ROESY of compound **73** in solution at 180 K, where the amide rotation and the ring flip are slow processes.

The ^{1}H-NMR spectra of **73** dissolved in different solvents were compared with each other to observe the influence of the solvent-polarity on the populations of different conformers. The following differences in population (comparing the ring-flipped conformer with the "standard" conformer) were observed: CD_2Cl_2 (13%) > $CDCl_3$ (9%) > THF-d_8 (3%). Increasing the polarity of solvent decreased the population of **73a** and **73b**. The same behavior (ring flip) has been observed for compounds **74** and **78**. However, it is interesting to note that compounds **75** and **76** did not present signs of a ring flipped conformer. More surprising is the fact, that we do not see the other diastereomeric conformer due to the slow rotation of the amide bond. The full ^{1}H-NMR spectrum of **75** recorded at variable temperatures is reproduced in the annex.

2.1.5.2. Dynamic NMR

Due the slow rotation around the amide bond in compound **73**, the chemically inequivalent N-H protons of the two pyrrole show temperature dependent signals. The NMR spectra were recorded at variable temperatures to probe the kinetic and thermodynamic parameters of this process. As we observe in parallel two exchange processes (the rotation of the amide bond and the ring-flip) at similar temperature a full line shape analysis has been performed. Rate constants (k) at different temperatures were extracted to fit the experimental spectra with the MEXICO program. The MeOH method was used for the NMR temperature calibration.[289]

Figure 80 shows the expanded downfield region of the ^{1}H spectra recorded at temperatures varying from 209 K to 294 K for compound **73** dissolved in CD_2Cl_2 along with the corresponding simulated spectra.

The major resonances in this spectral region originated from the NH of the two pyrroles differentiated due to the slow amide rotation. The minor resonances are attributed to the ring-flipped conformation, also showing two signals due to the slow amide. The spectra were simulated using two different exchange rates: one for the ring-flip process **a→A** and **b→B** and the other for the amide rotation **A** to **B** (the exchange between a and b is not visible). An additional line-broadening was applied to resonance **A** in order to simulate closely the experimental spectra. This broadening of resonance **A** could originate from another exchange mechanism which was not considered in the simulation and which we have not been able to identify. An expanded region of the spectra with the signals of the pyrrolic NH of the minor component along with the simulated spectra is reported in the annex.

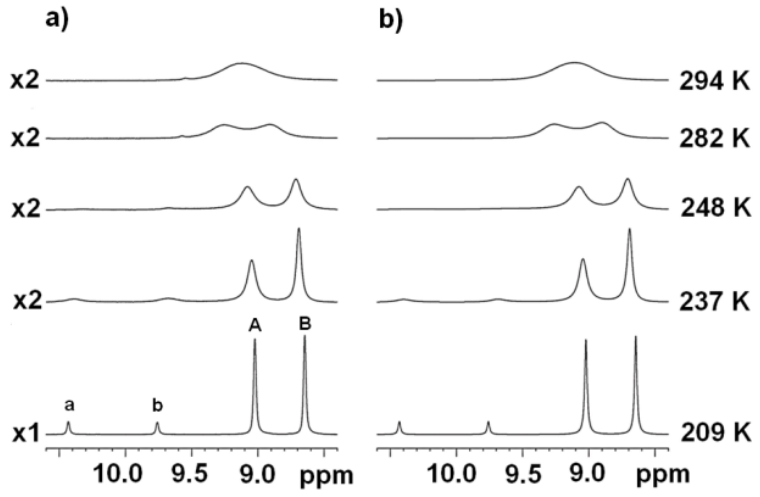

Figure 80. Dynamic NMR spectra of compound **73** over a 85°C range of temperature. (a) Only the spectral region of the pyrrolic N-H is shown. (b) Results of the fitting procedure simulation

Figure 81 shows the expanded upfield region of the ^{1}H NMR spectra recorded at temperatures from 243 K to 344 K for compound **75** dissolved in chloroform along with the corresponding simulated spectra. The spectra with the four methyl group resonances were simulated using the same exchange rate between resonances A and A' than between resonances B and B' (Figure 81). The simulated spectra closely imitate the experimental spectra. The only difference is the presence of small impurities recognizable in Figure 81.

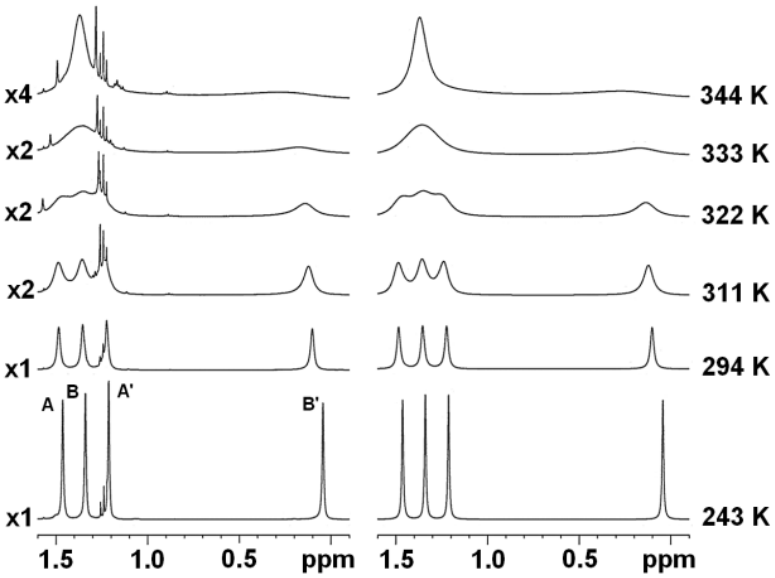

Figure 81. Dynamic NMR spectra of compound **75** over the temperature 243 K to 344 K. (a) Only the spectral region of part of the methyl signals is shown. (b) Results of the procedure simulation

The conformers due to the rotation of the amide bond in the two molecules **73** and **75** are equally populated in solution. The conformers associated with the ring flip in compound **73** have widely different populations as can be seen in Figure 80. The ratio of the standard ring flip conformation to the ring flipped conformation [A]/[a] = [B]/[b] = K_{Aa} = K_{Bb} = 0.13 (see spectrum in Figure 80). The free energy difference ΔG^o between the two conformers associated to the ring flip can be obtained applying the equation:

$$\Delta G^o = -RTlnK_{Aa} \qquad (3)$$

The free energy difference at 209 K corresponds to 0.85 kcal/mol for the conformer A preferred or "standard" conformation in solution.

The energy barriers due to the bond rotation and ring flip are calculated using transition state theory. The exchange rate k is related to the enthalpy $\Delta H^{\ddagger}$ and entropy $\Delta S^{\ddagger}$ of activation according to the equation:

$$k = \frac{K_B T}{h} e^{\Delta S^{\ddagger}/R} e^{\Delta H^{\ddagger}/RT} \qquad (4)$$

where *h* is the Planck's constant, K_B is the Boltzmann constant, T is the absolute temperature and R is the gas constant. The $\Delta H^{\ddagger}$ and $\Delta S^{\ddagger}$ values can be obtained from equation (5) by a linear regression of the ln(k/T) against 1/T data according to the Eyring equation:

$$\ln\left(\frac{k}{T}\right) = -\frac{\Delta H^{\ddagger}}{RT} - \ln\left(\frac{K_B}{h}\right) + \frac{\Delta S^{\ddagger}}{R} \qquad (5)$$

The result of the linear regression are shown in Figure 82. For the compound **73** the Eyring plots for the amide rotation process and for the ring flip process are shown. For compound **75** only one exchange process has been observed as presented in Figure 82.

The slope in these graphs corresponds to $\Delta H^{\ddagger}/R$ and the intercept corresponds to ln(k/T) + $\Delta S^{\ddagger}/R$. The enthalpy and entropy difference respectively $\Delta H^{\ddagger}$ and $\Delta S^{\ddagger}$ values for the different exchange mechanisms in the two molecules extracted from the best fit of the graphs in Figure 80 and 81 are reported in Table 17.

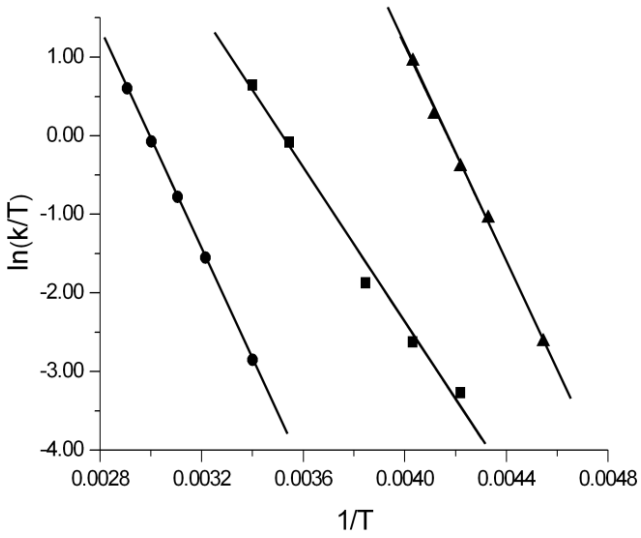

Figure 82. Eyring plot of tis/trans isomerization process of compound **73** (■) and **75** (•), and down/up process of **73** (▲)

The Gibbs free activation energy $\Delta G^{\ddagger}$ derived from the equation

$$\Delta G^{\ddagger} = \Delta H^{\ddagger} - T\Delta S^{\ddagger} \qquad (6)$$

is also reported in Table 17 for two different temperatures.

Table 17. Thermodynamic Parameters for the cis/trans Isomerization of **73** and **75**, and the Ring Flip of **73**

Mechanism	$\Delta H^{\ddagger}$ (kcal/mol)	$\Delta S^{\ddagger}$ (cal/mol.K)	$\Delta G^{\ddagger}$ at 233K (kcal/mol)	$\Delta G^{\ddagger}$ at 293K (kcal/mol)
Cis/Trans **73**	9.78 ± 0.58	-12.83 ± 2.20	12.77	13.54
Down/Up **73**	13.58 ± 0.32	+9.35 ± 1.33	11.40	10.84
Cis/Trans **75**	13.88 ± 0.02	-5.66 ± 0.07	15.20	15.54

2.2. Discussion

2.2.1. Kinetic study

The mechanisms of acyl transfer processes have been intensively studied (selected ref.).[99, 290-298] The fundamental questions in the context of acyl transfer reactions are: determining the

sequence of events and the stability of the intermediate(s), establishing the rate determining step and deducing the influence of the starting material, the reagent and the solvent on the mechanism. A stepwise mechanism with a tetrahedral intermediate is usually admitted for acyl transfer when this intermediate has a significant lifetime. When the tetrahedral intermediate is too unstable the reaction passes via a single step mechanism.[299] The preliminary kinetic studies performed probed the mechanism of the acylation depending on the nucleophilicity of acylating agent **12b**. The Hammett plots for the *para*-substituted benzoyl chlorides (Figure 74) showed a linear behavior over the moderate domain of tested compounds (ρ = 0.682, R^2= 0.998). The rate of the reaction is slow. The positive ρ-value indicates that an electron-withdrawing influence the rate of the acylation as one would expect it from the standard mechanism. The linearity is compatible with a mechanism, where no change in the rate determining state (RDS) is observed. According to these observations and the small ρ value obtained, we proposed that the reactions proceed via a concerted mechanism[290, 300] (Scheme 69). This conclusion is comforted by the suggestion of concerted mechanisms for reactions involving acyl halides[301-307] and especially aminolysis,[301, 302] analyzed to be similar than solvolysis mechanism of acyl halides.[308-310] Aminolysis of esters[295, 297, 311] and a recent investigation on hydrolysis of acyl chlorides[312] also supports this conclusion.

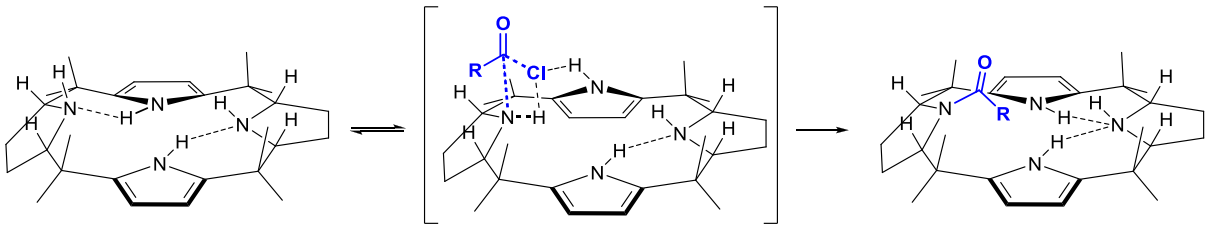

Scheme 69. Possible transition state for acylation of **12b** with acyl chlorides and chloroformates

This concerted mechanism perfectly explains the special reactivity observed for **12b** over the range of tested electrophiles. The steric hindrance and the moderate nucleophilicity of the amine of **12b** allow only concerted and fast non-reversible reactions. The very slow reaction rate may explain why, in our early investigations, attempts to modify this macrocycle via well-described acylation processes with organic bases failed. The bases used are more reactive than **12b** and therefore react with acyl chloride first opening the door to side reactions, (e.g. the well-known formation of ketene). However the combination of acyl

chloride and base, like DMAP,[313] is known to afford an activate ester,[314] which remains an extremely electrophilic species and should react with **12b**. It may be that the series of proton transfer needed is happening within the frame of the macrocycle during this process. If this is the case the type of leaving group might play a major role. As it is well known that pyrrolic N-H bonds form very strong hydrogen bonds with chlorides, this might help the expulsion of the leaving group. Choosing K_2CO_3 as base was important because this base does not form a homogenous solution, so the concentration of the base in the solution is small and controlled. However the carbonate is able to trap HCl and/or deprotonate compound **12b** which had trapped HCl. Under these heterogeneous conditions the acylation using the acid chloride of amino-acids could be performed avoiding racemization.

The pyrrolidine rings of **12b** are very poor nucleophiles probably due to the tight hydrogen bond network installed within the macrocycle (see the following chapter). The X-ray structure shows also that the access to the lone pairs of the basic nitrogens is sterically hindered. The acylation reaction is therefore very slow and reaction conditions were needed where a highly activated electrophile could used without giving access to side reactions like the ketene formation. Using organic homogenous bases lead to problems. The use of carbonate in a two phase system avoided the side reactions, diminished the basicity of the solution and allowed selective mono-acylation.

2.2.2. Structural analysis

First introduced by Pauling,[315] hydrogen bonding has been largely studied for its key role in chemical and the biological processes.[316-321] One has to mention the impressive activation effect of hydrogen bonding in enzyme catalysis.[322-325] The opposite, the deactivation of reactions due to hydrogen bonding on a strong acceptor has been poorly described.[326] In an earlier work, we have shown the X-ray analysis of calix[2]pyrrole[2]pyrrolidine **12b** where the pyrrole pyrrolidine pairs are forming two tight hydrogen bonds. In view of the unusual sluggish acylation of the macrocycle **12b** towards acylation we postulate that the tight hydrogen bond networks are responsible for the remarkable low reactivity of calix[2]pyrrole[2]pyrrolidine **12b**. The hydrogen bonds partially deactivate the nucleophilicity and the modify basicity of the molecule!

2.2.2.1. Compound **71**

As reported we studied the acylation of compound **71** as model compound containing the same array of a pyrrole and an adjacent pyrrolidine ring as in our macrocycles The X-ray diffraction analysis of **71** revealed a self assembling motif forming a dimeric structure by intermolecular hydrogen bonding network between the pyrrolidine and pyrrole rings of the two molecules forming the dimeric structure. The resulting dimer shares the same hydrogen bond networks than **12b** and presents a very similar conformation (Figure 83). Compound **71** can be considered as an open model for the macrocycle **12b**.

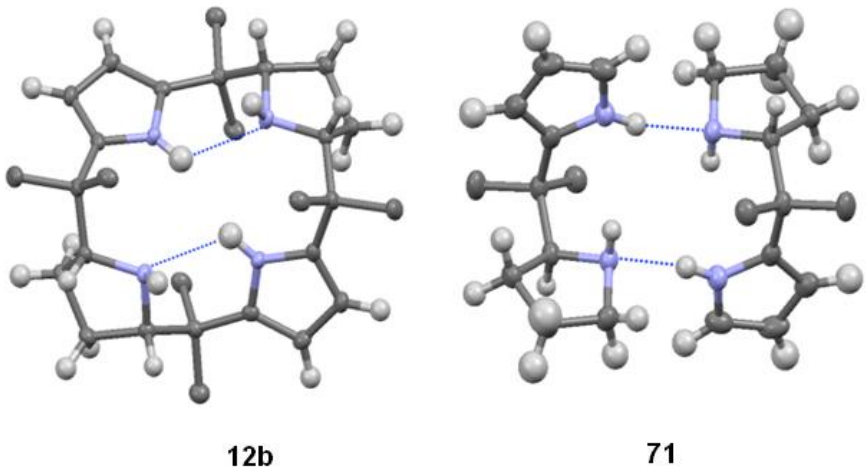

Figure 83. Molecular structure of compound **12b** and the dimer of compound **71** with the thermal ellipsoids drawn at the 50% probability level (the hydrogen atoms of the *meso*-CH_3 groups are omitted for clarity). N-H···N hydrogen bonds are shown as dashed lines.

Both molecules present two N-H···N bonds between the nitrogen of pyrrolidine and the hydrogen of the pyrrole rings. In the case of compound **71**, the intermolecular H-bonds have a much smaller influence on its reactivity compared to the intramolecular H-bonds of **12b**. The breaking of the H-bonds in **71** is entropically favored. On top of that the access to basic nitrogen is quasi unperturbed once the hydrogen bonds are broken, whereas the basic nitrogen is still confined within the macrocycle for compound **12b**. The dramatic decrease in the reaction rate and therefore the increased probability of side reactions between bases and acyl chlorides is compatible with these arguments derived from the X-ray structures.

2.2.2.2. Compound **73** and **74**

When we first encountered the experimental difficulty to obtain acylated products we asked our self the question, if acylation might create sterically highly unfavorable compounds. We were able to successfully grow single crystals of mono-acylated compound **73** and **74** by recrystallization in ethanol. The X-ray diffraction analysis of compound **73** and **74** are shown Figure 84.

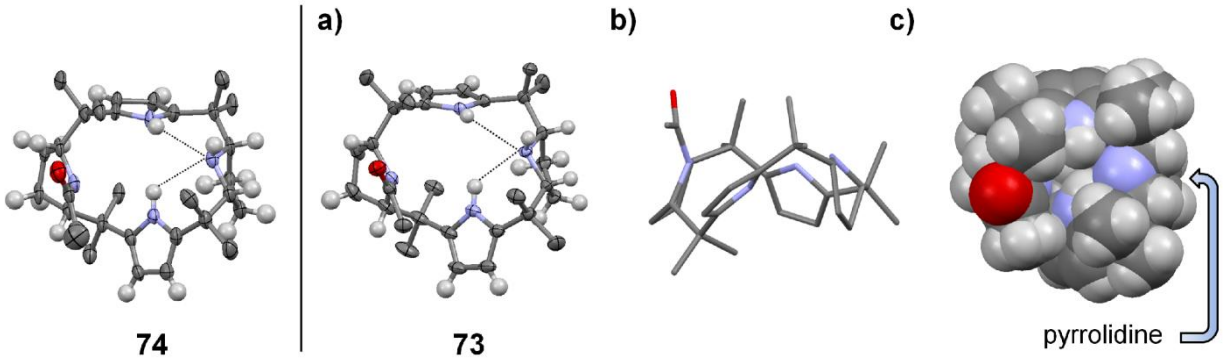

Figure 84. Molecular structure of one enantiomer of compound **74** the thermal ellipsoids drawn at the 50% probability level (the hydrogen atoms of the *meso*-CH_3 and acetyl groups are omitted for clarity). N-H···N hydrogen bonds are shown as dashed lines; a) Molecular structure of one enantiomer of compound **73** the thermal ellipsoids drawn at the 50% probability level (the hydrogen atoms of the *meso*-CH_3 and acetyl groups are omitted for clarity). N-H···N hydrogen bonds are shown as dashed lines; b) Molecular structure of compound **73** drawn with capped stick style (all the hydrogen atoms are omitted for clarity); c) Molecular structure of compound **73** drawn with spacefilling model (the hydrogen atom of the pyrrolidine is omitted for clarity).

The two structures of compound **73** and **74** are very similar. The two enantiomeric conformers of both compounds are present in their respective crystals. The unsubstituted pyrrolidine forms two strong bifurcated H-bonds to the adjacent pyrroles (Figure a) of Figure 84). The two pyrroles are pointing toward the lone pair of the pyrrolidine with a distance between H(11)-N(17) and H(23)-N(17) of 2.35 and 2.55 Å respectively. Due to this strong hydrogen bond network the methyl 26 is fixed in a conformation near to the pyrrole ring opposite. This conformational blocked arrangement puts the hydrogens of the methyl group 26 into the cone of the aromatic pyrrole ring explaining its highly unusual chemical shift at 0 ppm due to shielding effect of the heteroaromatic ring. The distance between one of the hydrogens of

methyl 26 (the closer) and the carbon 22 of pyrrole is 2.69 Å. To confirm that we can use the structure of **7** at low temperature in the crystal as good starting point for the conformational behavior in solution we measured the ROESY spectrum. The data of the ROESY spectrum are compatible with the conformation determined in the X-ray structure. In contrast to the free ligand the acylated pyrrolidine ring and the unsubstituted pyrrolidine ring are in an almost parallel arrangement. The two pyrrolidines and one of the pyrroles form a nice cavity, whereas the last pyrrole ring is directing inside the cavity (b, Figure 84). The spacefilling model shows that the macrocycle adopts and extremely compact conformation (c, Figure 84). The acetyl group is pointing outward avoiding the steric hindrance caused by the methyl groups. The N-H bond of the nitrogen of the unsubstituted pyrrolidine is directed to the outside of the macrocycle. The two adjacent methyl groups next to the pyrrolidine ring are creating a rather hindered environment. Due to the hydrogen bonding with the two pyrrole rings the lone pair of the nitrogen is deeply buried within the inner part of the macrocycle. The observed tight arrangement must be remarkably stable; otherwise we cannot explain the absence of any bis-acylation product when we tried to transform **73** and **74** further using standard methods. We have no thermodynamic data to characterize the strength of the hydrogen bonds. The tight H-bonds must increase the energy of activation for the second acylation sufficiently to inhibit completely the second acylation, which is a remarkable observation.

2.2.2.3. Compound **75**

Once we had realized that the reactivity of the partially reduced macrocycle **12b** was extremely low and unusual we tried to apply the recipe developed in the Floriani group for pushing the reactivity of calix[4]pyrroles. We intended to deprotonate the macrocycle **73** completely using three equivalents of butyl lithium. The reaction of the formally formed trianion should follow the rule: “last out first in”. We were aware of the danger of side reactions due to the use of butyl lithium which can and will react with amide bonds. Despite this drastic, non ideal reaction conditions we could isolate a small amount of the bis-acylated product **75**. We successfully crystallized compound **75** by slow evaporation of a solution in dichloromethane (Figure 85).

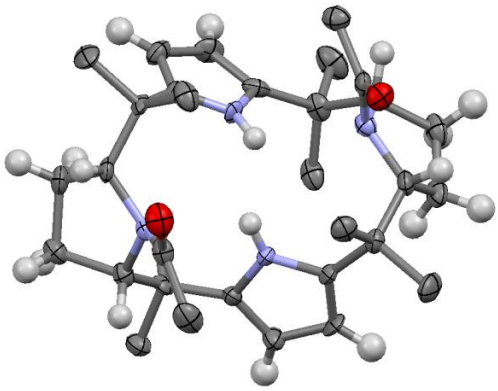

Figure 85. Molecular structure of one enantiomer of compound **75** the thermal ellipsoids drawn at the 50% probability level (the hydrogen atoms of the *meso*-CH_3 and acetyl groups are omitted for clarity).

The two enantiomeric conformations are present in the crystal. The molecule shows a highly compact conformation. Both acylated pyrrolidine rings define planes which are almost parallel. Methyl 26 and 30 are in the cone of their pyrrole rings opposite to them exposing them to the shielding effect of the heteroaromatic ring. The conformation in the solid state is with the solution state conformation determined via NMR at low temperature. The ^{1}H-NMR spectrum of compound **75** at 218K displays a peak at 0 ppm for those two methyl groups.
The spectrum of compound **75** shows only the signals for one of the two possible diastereoisomeric conformers (Figure 86).

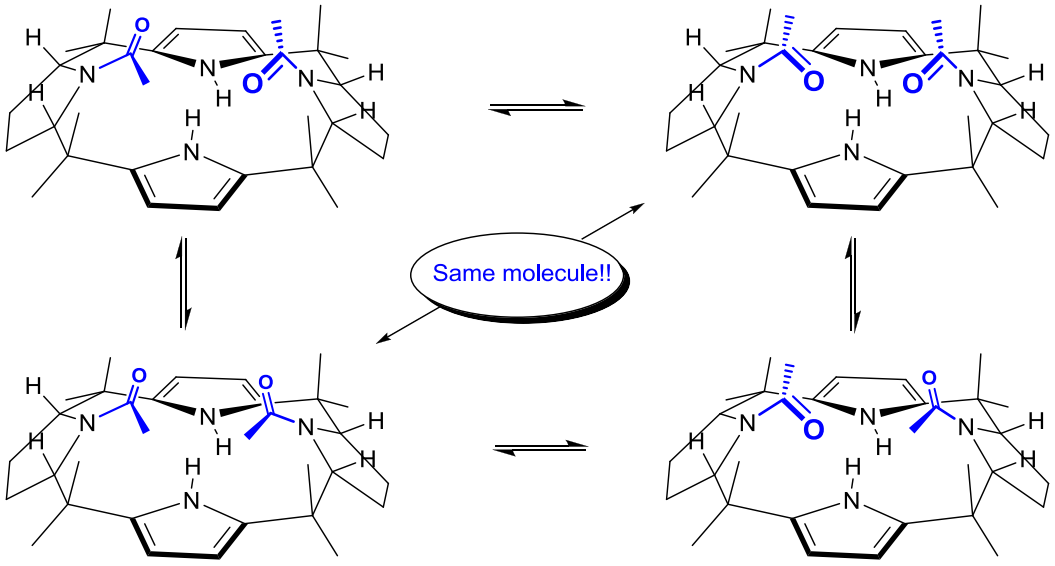

Figure 86. The different theoretically possible conformers of the macrocycle **75** due to the slow rotation around the two amide bonds

The analysis of the spectra recorded at low temperature showed no evidence for the presence of a second diastereoisomeric conformer. The ^{1}H-NMR spectrum showed one well resolved signal for the two CH_3 groups of the acetamides. To explain this observation there are only two hypotheses possible. A) the rotation around the two amides is so fast that even at 209 K we are under the conditions of fast exchange; B) one of the diastereoisomeric conformations corresponding either to the C_S or the C_2 symmetry point group molecules is not observed or is present at extremely low proportions. We think that hypothesis A) is highly improbable, we therefore assume hypothesis B). Two problems remain: 1) which is the conformer we observe and 2) how to explain the process of double exchange (concomitant rotation around both amide bonds). For the question 1) we assume that the C_2 conformer observed in the crystal is also the conformer observed in solution. The remaining problem is how to explain the simultaneous rotations of the two amides, a highly unusual behavior! The kinetic data give a first hint. The $\Delta H^{\ddagger}$ value of **75** is more than 40% bigger than $\Delta H^{\ddagger}$ for **73**. In contrast the $\Delta S^{\ddagger}$ value of **73** is juste 40% of the $\Delta S^{\ddagger}$ value of **75**. Both $\Delta S^{\ddagger}$ values are negative, which means an increase in the order going through the transition state. The differences in these kinetic parameters are significant in view of the fact, that we observe two similar processes: rotation around an amide bond between an acetyl group and a pyrrolidine nitrogen. The difference can be attributed to a change in the process. The data are not showing a doubling of the $\Delta H^{\ddagger}$ value, which we would have to expect, if the two rotations would be completely independent of each other and had nevertheless to occur simultaneously. The major problem is to explain, why such a simultaneous amide rotation should happen. The careful analysis of the X-ray structure of **75** provided us with a reasonable hypothesis (Figure 87).

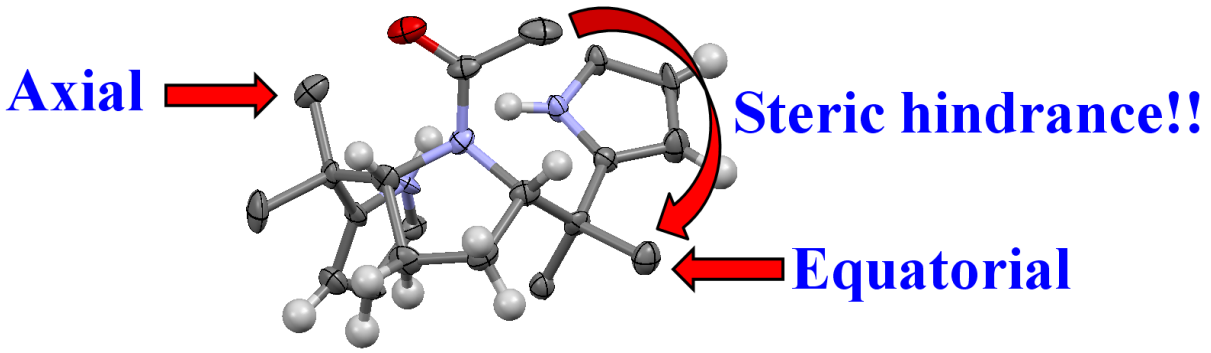

Figure 87. Part of the molecular structure of **75** where only half of the molecule is drawn in the interest of clarity

The X-ray structures show that the methyl of acetyl is arranged in such a way that it is directed toward the quaternary center leaving an opening on the side of the acetyl group. The methyl group which is on the same side of the macrocycle as the acetyl group is in an equatorial position. The methyl group of the other quaternary center is close to the oxygen of the acetyl group and is in axially oriented. If one turns around the macrocycle the next CH_3 group bonded to the next quaternary center has to be in equatorial position and the last CH_3 finds itself by consequence one in axial position (Figure 88).

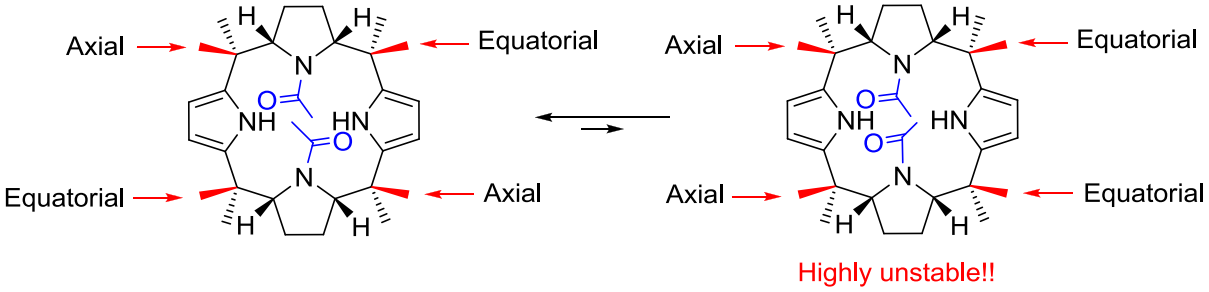

Figure 88. Determination of the axial or equatorial position of the methyl groups

We have an alternation of axial and equatorial methyl groups on one side of the macrocycle. The steric interaction of the methyl of the acetamide fixes the conformation of BOTH acetamide groups due to the conformational link described above. If one acetamide rotates, it distorts the macrocyclic structure due to this conformational link. The methyl groups, which were axial, become equatorial and vice versa. This switch of the axial and equatorial positions of the methyl groups bonded to the quaternary carbon might lead to a forced rotation of the second amide function. The analysis of the molecular structure of **75** has brought us to propose a concerted rotation. If we follow our hypothesis the total process should be composed of two amide rotations concomitant to a macrocycle inversion. The barrier of activation should be considerably higher than for one rotation. The DNMR show us that the experimental $\Delta H^{\ddagger}$ value is only 40% higher than for the single. This is very puzzling. More detailed analysis has to be done to characterize this process completely

In contrast to compound **73** we have no indication for a ring flip reaction. With the results available we cannot exclude that the ring flip occurs, although we think that this process is extremely improbable.

The partial double bond character of the amide C-N bond is the important factor influencing the height of the rotational barriers. Ohwada et al. suggested in their pioneering work that the deviation of the amide planarity would lead to a reduction of its double bond character and therefore the deviation from planarity should have a direct impact on the rotational barrier. We determined the deviation from planarity of the two acetamides **73** and **75**. The planarity of the amide nitrogen can be represented using the two angle parameters (θ and α) available from the X-ray structure of **73** and **75**. θ is the sum of the three angles around the nitrogen (θ=360° for a flat nitrogen) and α is the angle between the plan of the pyrrolidine ring and the N-CO bond (α=180° for sp^2 and 125° for sp^3). Angle parameters extracted from the X-ray structure of compound **73** and **75** are shown in table 18.

Table 18. Selected Crystal Structural Data of mono and bis-Acylated Macrocycles **73** and **75**

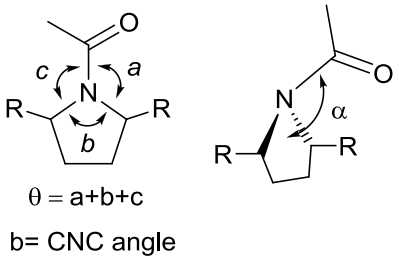

Compound	CNC (deg)	θ (deg)	α(deg)	N-C bond(Å)
73	111.4	345.1	142.5	1.381
75	112.3	345.1	141.0	1.385

We observe a significant pyramidalization of the nitrogen atom of compound **73** and **75**. Deviation out of the plane for amide **73** and **75** reaches 37.5° and 39° respectively. The consequence of this deviation is as expected a longer N-CO bond (see Ohwada et al.).[327] The large pyramidalization of the amide in both compounds **73** and **75** should have a significant influence on their rotational barrier. Both barriers would be expected to be significantly smaller than usual amide rotation barriers. Comparing the $\Delta G^{\ddagger}$ values of **73** with 9.78 kcal/mole to the known barrier of acetamide 15 $kcal.mol^{-1}$ shows a significant decrease in the barrier height.[328] The barrier for **75** with a $\Delta G^{\ddagger}$ value of 13.88 kcal/mol is nearer to the barrier of acetamide, but the process is more complex in **75** and can therefore not be directly compared with simple amide rotations.

2.2.3. Dynamic NMR investigation / conformational analysis

The dynamic of the amide rotation has been extensively studied by NMR spectroscopy over the last decades due to its highly important role in biology, especially for the structure and dynamic determination of proteins. The mechanism of the ring flip was confirmed by the dynamic NMR performed on the ring flip, which has been really productive. We found that the ring flip dynamic has positive entropy. It means that, the Gibbs free energy of activation decrease with the increase of temperature. This result is in accordance with the hypothesis linking the height of the barrier of activation directly with the energy necessary to break the two hydrogen bonds. Increasing the temperature helps to break the hydrogen bonds, the entropy of this specific process must be positive (figure 89).

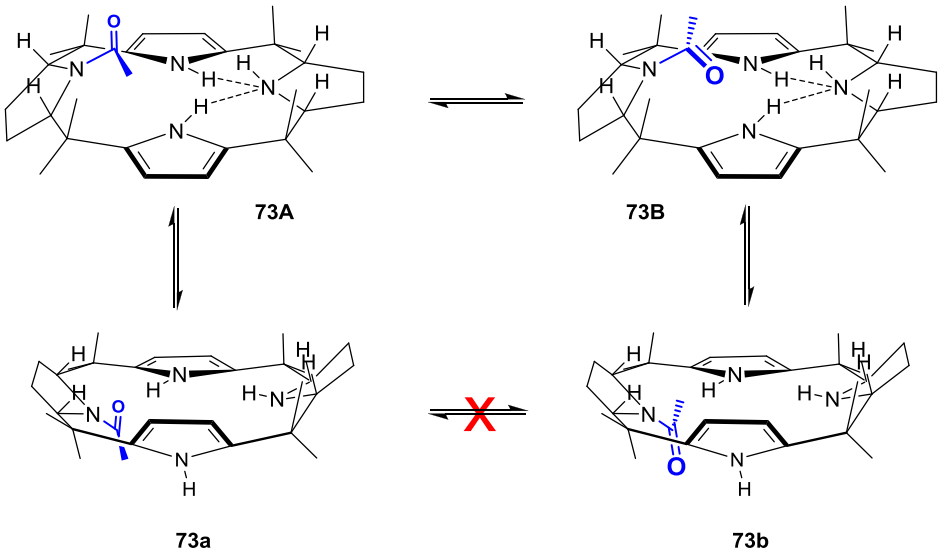

Figure 89. Different conformers of compound **73**. The transition A→a is only possible by breaking the hydrogen bonds

The ROESY recorded at 224 K did not show an exchange between the two ring flipped conformers **73a** and **73b**. This means that the conformers **73a** and **73b** once formed through a ring flip reaction do not exchange position via the rotation around the amide bond. This life time of the two separate rotamers must be higher than the life time of **73a** due to the ring flip reaction.

3. FORMATION OF ORGANOMETALLIC COMPLEX

The calix[2]pyrrole[2]pyrrolidine **12b** presents the characteristic features of ligands suitable to form organometallic complexes. We have previously described different metal complexes from the fully reduced macrocycle **13** where metals were held by four strong dative bonds. The macrocycle **12b** displays the same characteristics with its two pyrrolidine rings. The two pyrroles could potentially be deprotonated to for two additional covalent bonds with a metal. Interestingly metal complexes of **12b** would be closely related to metal complexes of porphyrins sharing the same size and the same type of chelation to metals, two dative and two covalent bonds (Figure 90).

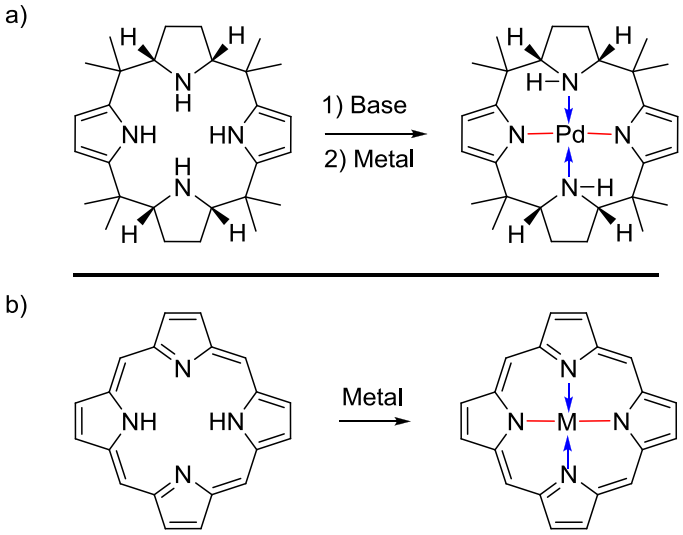

Figure 90. Complexation similarity between macrocycle **12b** (a) and porphine (b). Covalent bonds are in red and dative in blue

Considering their high similarity and the extraordinary range of applications of porphyrin complexes in chemistry, probing the ability of **12b** to form metal complexes should lead to interesting results. We decided to investigate the synthesis of metal complexes from compound **12b**.

3.1. First results

We tried to apply the successful conditions already developed for the synthesis of metal complexes from compound **13** for the investigation starting with compound **12b**. First, we wished to use different salts of copper and iron without any addition of organic base. We observed strong color changes indicating that the reactions (complexations) occurred. We tried for a long time to characterize the products obtained. As no complexes of this type are known we concentrated our efforts on obtaining crystals suitable for X-ray diffraction analyses. However our efforts were unsuccessful. Mass spectroscopy always showed peaks and isotope distributions compatible with metal chelation. The UV-visible spectra suggested that some interactions with the metal has occurred, but we were unable to obtain sufficient information to make a structure proposition (Figure 91).

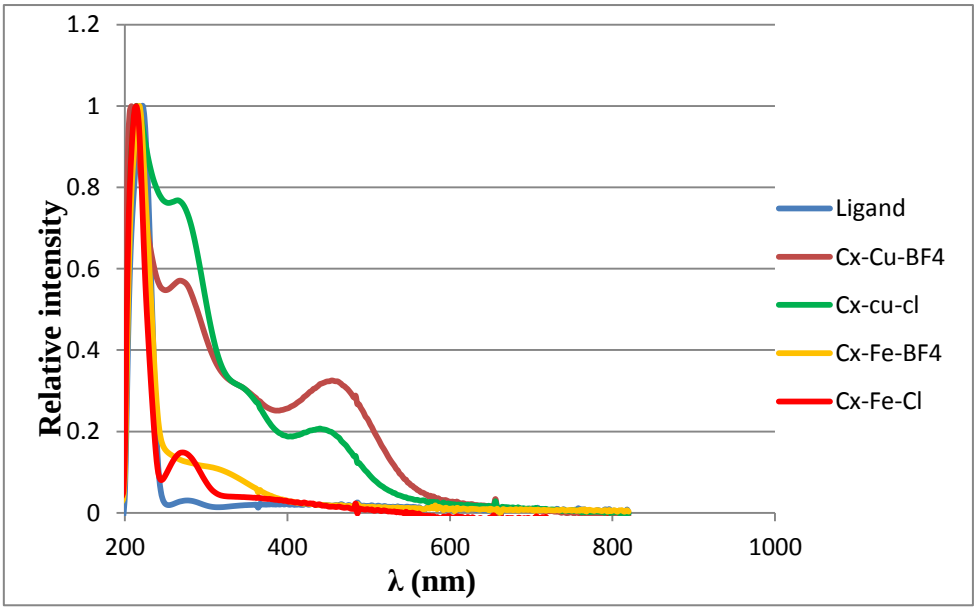

Figure 91. UV-visible spectra of different metal complexes of compound **12b**

The characterization of those metal complexes is extremely difficult as it is not possible to obtain a characterization via NMR spectroscopy. For this reason we decided to study the complexation of non-paramagnetic metal.

3.2. Results and discussion

For the studies of the complexation with a non-paramagnetic metal we choose palladium. Palladium acetate is soluble in chloroform where compound **12b** is highly soluble as well. We prepared a solution of **12b** in $CDCl_3$ (0.5mL, 0.02 M) and added 1 equivalent of palladium acetate in $CDCl_3$ (0.2 mL) in "open tube" (without inert atm.). We followed the complexation of compound **12b** by NMR at 50 °C (Figure 92).

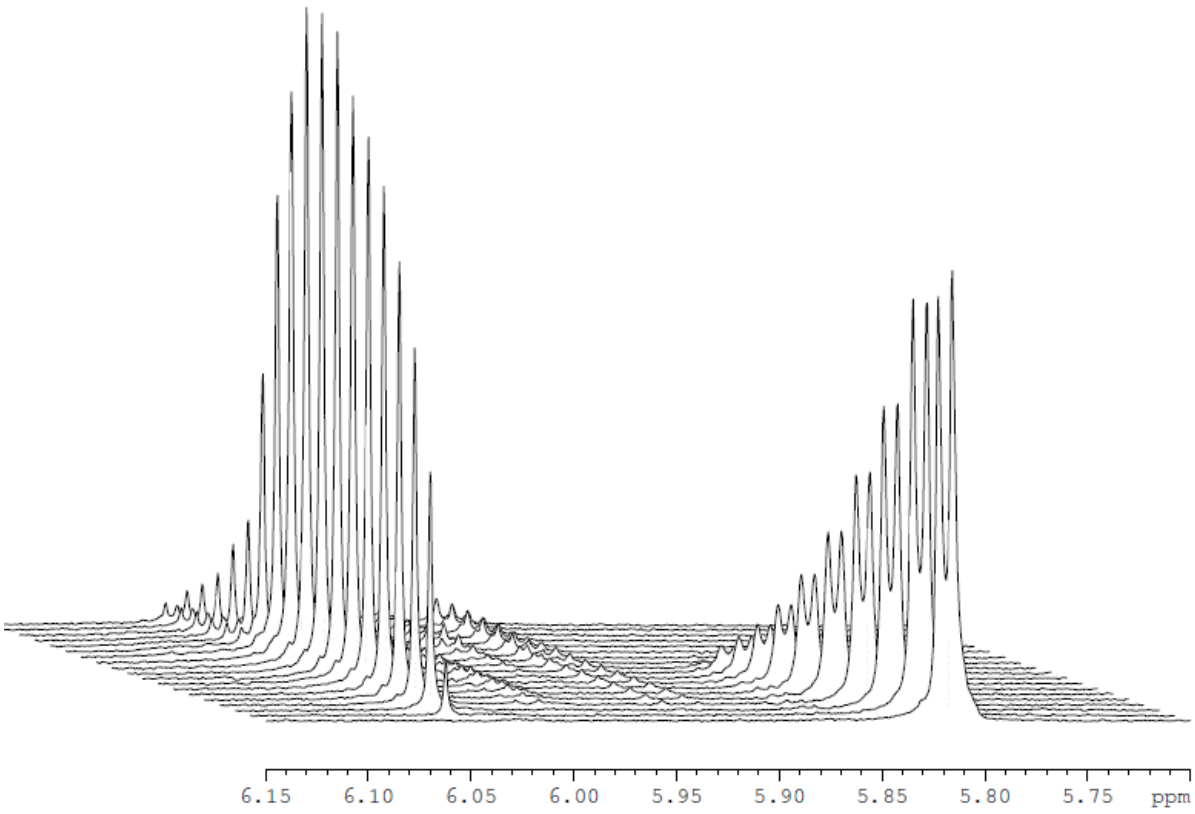

Figure 92. Superposition of ^{1}H-NMR spectrum according to the time recorded at 50°C in $CDCl_3$. Only the spectral region of pyrrole is shown

The ^{1}H-NMR spectrum of compound **12b** is characterized by a doublet located at 5.81 ppm which corresponds to the pyrrolic C-H. At time t=0 only the doublet is present in the pyrrolic region. After just a few minutes at 50°C, a singlet located around 6.06 ppm starts to appear and grows with time. On the contrary, the doublet of the pyrrolic C-H of **12b** decreases proportionally. This trend continues until the complete consumption of the starting material. We decided to let the reaction go further, and were extremely surprised to see the diminution

of the singlet intensity and the apparition of new additional peaks. Obviously two consecutive reactions occur. The spectra of the first phase suggest the formation of a symmetric complex in view of the symmetrical ^{1}H-NMR spectrum. The second transformation leads to a molecule which has lost its high symmetry. We further analyzed the metal complex by MS spectroscopy (see below). If we analys the proton spectra carefully, we observe the formation of the second complex already before the total consumption of the starting material. The change of the relative concentrations of the starting material and the two complexes as function of time is shown in Figure 93.

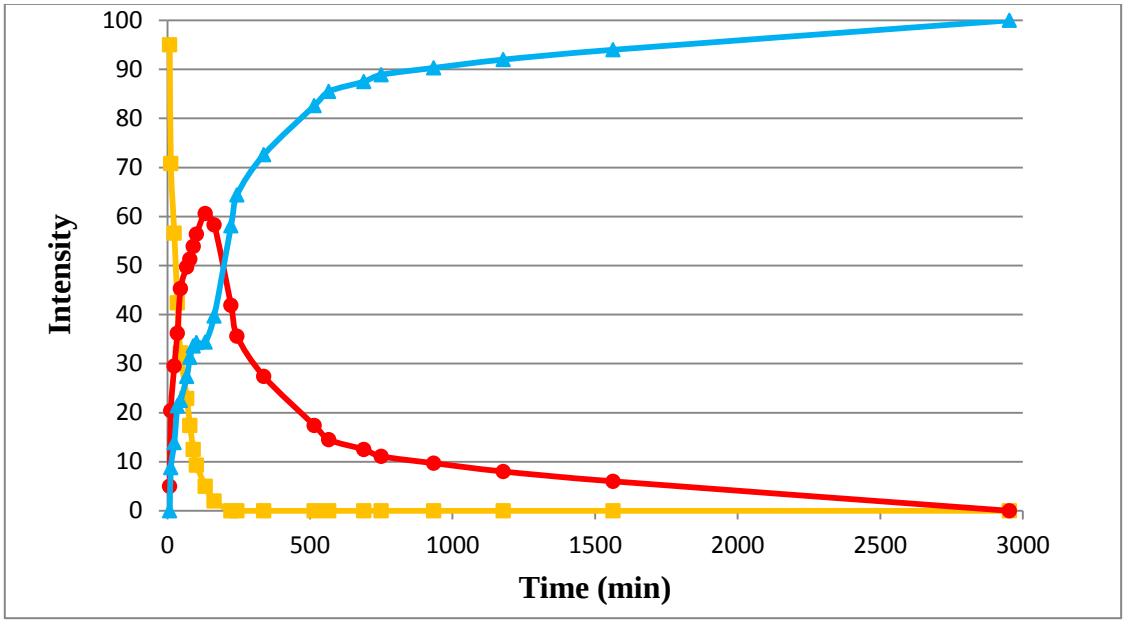

Figure 93. Relative concentrations of the starting material and the two products as a function of the reaction time. Orange (■): compound **12b**, red (●): first symmetrical complex, blue (▲): the second chiral complex.

During the NMR monitoring we took out samples at different times, to analyze them by mass spectroscopy. The first sample has been taken after the consumption of 50% of the starting material and another at the end of the two reactions. The MS analysis of both sample are respectively named spectrum A and spectrum B. The first one (spectrum A) displays a peak at 437 g.mol^{-1} corresponding to the starting material (M+1) and three other peaks at 541, 557 and 573 g.mol^{-1} showing the isotope distribution characteristic of palladium (zoom, Figure 94).

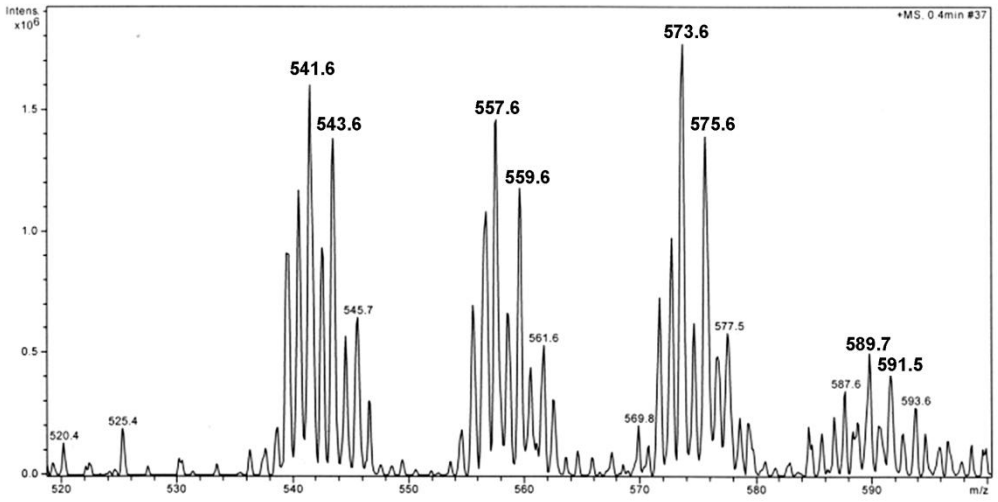

Figure 94. Zoom of the MS spectrum A

The second spectrum B shows only a major molecular peak at 557 g.mol^{-1} and small at 573 and 589 g.mol^{-1}.

We conclude that the mass 541 corresponds to the symmetrical complex and 557 to the second less symmetric product. The molecular weight 541 g.mol^{-1} is compatible with a neutral complex between compound **12b** and palladium where the metal is held by two covalent bonds and probably two dative ones (Scheme 70):

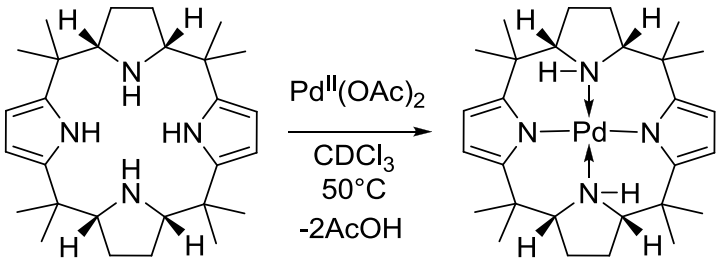

Scheme 70. Postulated formation of the palladium complex **92** of compound **12b**

The molecular weight 540 g.mol^{-1} corresponds to the molecular weight of the starting material having lost two hydrogen atoms plus one palladium. The two acetates must deprotonate the hydrogen atoms of the pyrroles to give two molecules of acetic acid. The molecular weight 557 g.mol^{-1} corresponds to the same structure +16. This is compatible with the addition of one oxygen atom, suggesting that an oxidation has occurred. The molecular weight 573 g.mol^{-1}

corresponds to the first structure + 32, which would correspond to the addition of two oxygen atoms.

We then decided to repeat this reaction under inert atmosphere to avoid oxidation. We mixed compound **12b** with palladium acetate in $CDCl_3$ under argon, sealed the NMR tube and followed the complexation of compound **12b** by NMR at 50 °C (Figure 95).

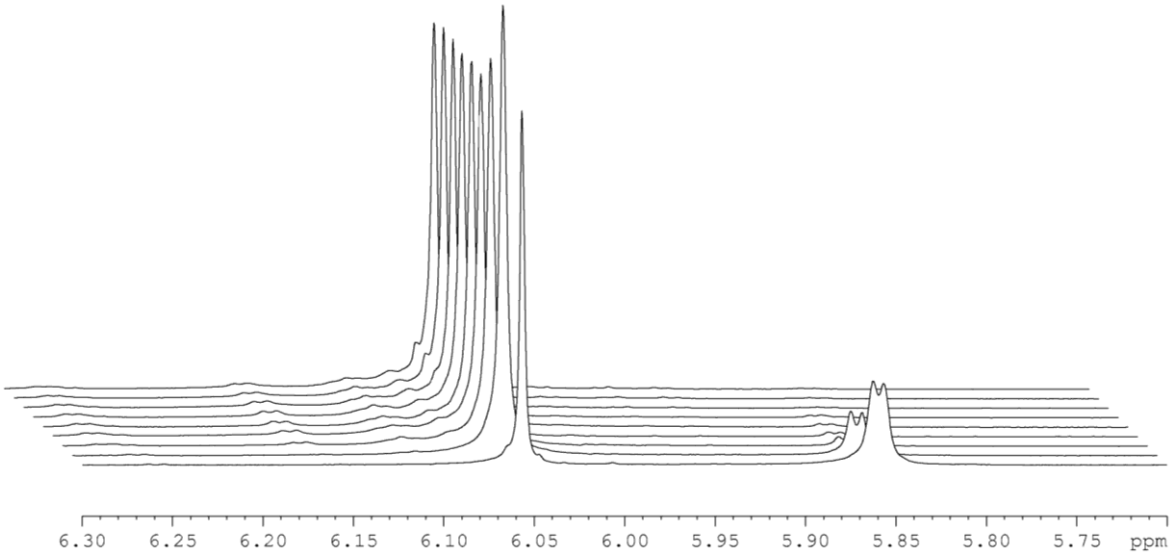

Figure 95. Superposition of ^{1}H-NMR spectrum according to the time recorded at 50°C in $CDCl_3$ under inert atmosphere. Only the region of pyrrole protons is shown

Avoiding oxygen the reaction stops after the total consumption of the starting material **12b**. Several indications confirm the symmetrical structure described in Figure 70 for the palladium complex **92**: 1) the disappearing of the pyrrolic N-H in the ^{1}H-NMR spectrum; 2) the pyrrolic doublet of the starting material is converted into a singlet (no more coupling between the pyrrolic C-H and N-H); 3) the apparition of a peak at 2.1 ppm corresponding to CH_3COOH. Regarding the last aspect, normally acetate anions, pKa around 4.8, are not able to deprotonate pyrroles, pKa around 23. In order that this proton transfer can occur the complex formation must be thermodynamically favorable to compensate for the pKa difference.

We then opened the tube and observed the transformation of our first complex into the second complex. There are two possibilities to explain the phenomena observed. 1) the complex **32** is

extremely sensitive toward oxygen and starts to be attacked in the presence of air. We favor the second hypothesis; 2) the oxygen might form an extremely reactive intermediate (may be an oxo species). This unknown intermediate starts to oxdize the complex **32**. An oxo or μ-oxo- palladium complex might be the reactive intermediate responsible for the oxidation process.

We need further investigations to determine the structure of the oxidized complex and its mode of action. Ideally we should be able to crystallize the symmetrical and the second less symmetrical complex. We obviously hope to be able to characterize the sequence in order to gain insight into this exciting series of transformations.

4. CONCLUSION

The modification of calix[2]pyrrolidine[2]pyrrole via a acylation reaction was studied. We developed a successful experimental methodology for the selective mono- and bis-acylation of **12b**. Finding suitable conditions for the acylation of the macrocycle was very challenging and led to interesting results. The improvement of the condition of acylation was achieved using a model compound. The acylation could be achieved in good yield using only an inorganic base (K_2CO_3), which avoided side reactions with the electrophiles. The selective mono-acylation came is probably a consequence of the strong hydrogen bond networks in the acylated compound. We, then, successfully applied our knowledge for the introduction of amino-acids under non racemizing condition. The structures of the mono- and the bis-acetylated products were elucidated by X-ray analysis. A conformational analysis was performed by NMR spectroscopy together with X-ray diffraction analysis of the structures in the crystal. The NMR studies led to the discovery of a ring flip conformer of **73** visible only at low temperature. Kinetic and thermodynamic parameters of the amide rotation of compound **73** and **75** and the ring-flip of **73** were extracted from line fitting experiments.

5. ANNEX

5.1. Description of molecular structure of dipyrromethane 70

Compound **70**, $C_{11}H_{14}N_2$, crystallized with two independent molecules (A and B) in the asymmetric unit. The two molecules differ only slightly, with the pyrrole rings being inclined to one another at a dihedral angle of 87.67 (8)° in molecule A and 88.09 (7)° in molecule B. In the crystal, there are no classical hydrogen bonds, but the two pyrrole NH groups of one molecule are involved in N-H···π interactions with the pyrrole rings of the other molecule. In this manner, a compact box-like arrangement of the two independent molecules is formed. The molecular structure of the dipyrromethane **70** is shown Figure 96

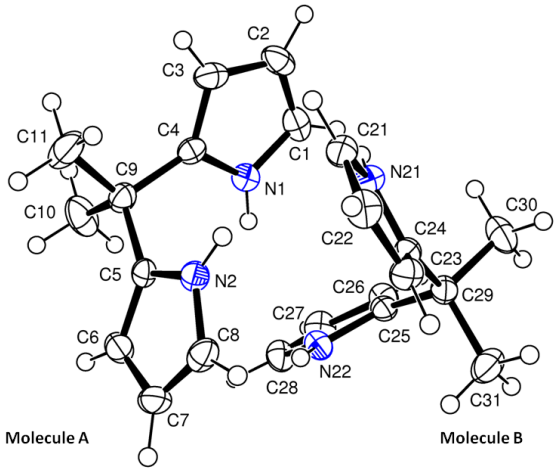

Figure 96. View of the molecular structure of the two independent molecules (A and B) of compound **70**, with the displacement ellipsoids drawn at the 50% probability level.

In the crystal the molecules are linked by N-H···π interactions involving the pyrrole NH H-atoms of molecule A, for example, with the pyrrole rings of molecule B, and vice-*versa* (see Table 19 for details). This leads to the formation of a compact box-like arrangement of the two molecules, as shown in Figure 97. Again this arrangement is similar to that in the crystal of the diethyl analogue.

Table 19. *N-H···π* interactions [Å, °]

D	H	Centroid	N-H	H···*Cg*	D···*Cg*	N-H···*Cg*
N1	H1N	*Cg*4	0.86 (2)	2.534 (17)	3.2190 (12)	137.4 (14)
N2	H2N	*Cg*3	0.86 (2)	2.591 (17)	3.2425 (12)	133.7 (13)
N21	H21N	*Cg*1	0.86 (2)	2.523 (16)	3.1925 (12)	133.9 (12)
N22	H22N	*Cg*2	0.86 (2)	2.610 (17)	3.2440 (12)	131.3 (13)

*Cg*1 = centroid of ring N1,C1—C4, *Cg*2 = centroid of ring N2,C5—C8, *Cg*3 = centroid of ring N21,C15—C18, *Cg*4 = centroid of ring N22, C25—C28.

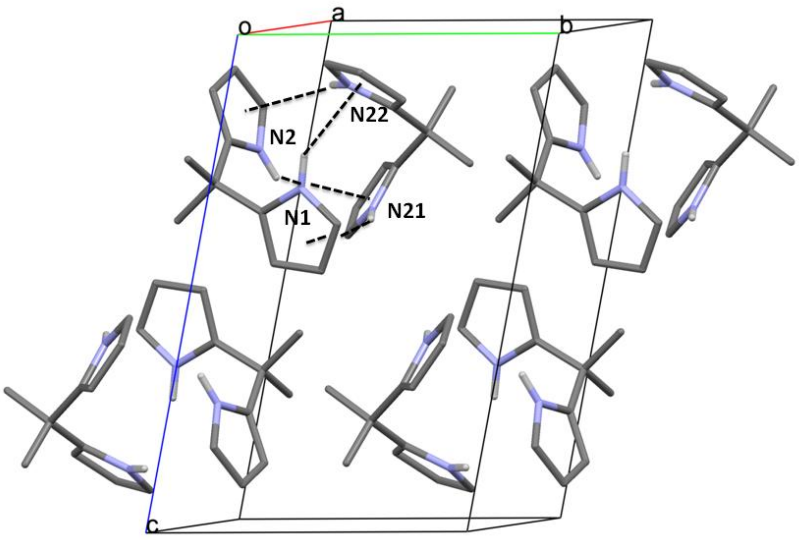

Figure 97. View, along the *a* axis, of the crystal packing of the title compound. The N-H···π interactions are shown as dotted black lines for one of the box-like arrangements of the two independent molecules (see Table 19 for details).

5.2. Description of molecular structure of compound 71 and 72

Compound **71** crystallizes with two independent molecules (A and B) in the asymmetric unit (Figure 98, left). An AUTO-FIT diagram (Figure 98, right; Spek, 2009) of inverted molecule B on molecule A illustrates the small difference in the conformation of the two molecules. The best weighted and unit-weight r.m.s. fit parameters are only 0.032 and 0.035 Å, respectively, for the 13 non-H fitted atoms. In molecule A, the pyrrolidine ring has a twist conformation on bond C4-N1, while in molecule B the twist is on the corresponding bond C24-N3. In both molecules, the mean planes of the pyrrole and pyrrolidine rings are almost perpendicular to one another; the dihedral angles are 89.99 (11)° and 89.35 (10)° in molecules A and B, respectively.

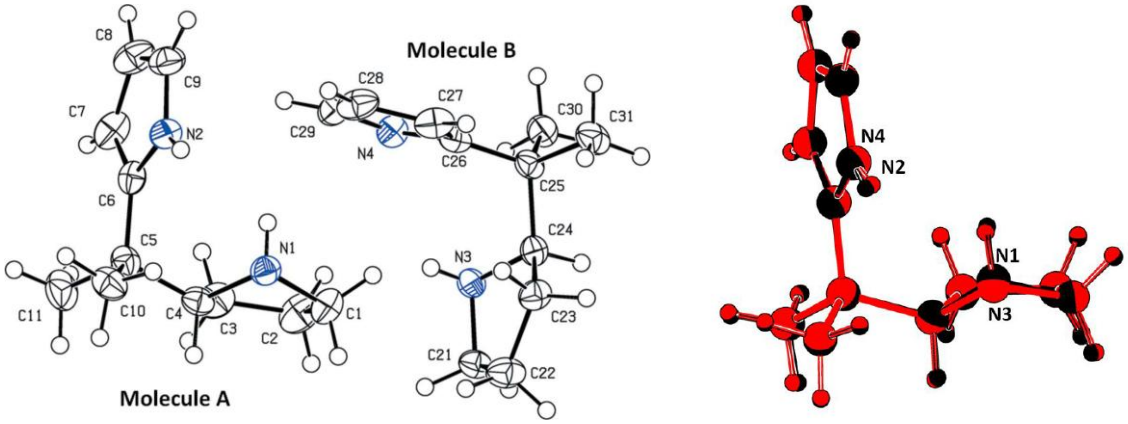

Figure 98. (Left) The structures of the two independent molecules (A and B) of **71**, showing the atom-numbering schemes. Displacement ellipsoids are drawn at the 50% probability level. (Right) A view of the fit of molecule B (red in the electronic version of the paper) inverted on molecule A (black) of **71**.

In the crystal structure of **71**, the individual independent molecules are linked via N-H···N hydrogen bonds to form inversion dimers (Table 20 and Figure 99). These dimers can be described by an R22 (12) graph-set motif. Each dimer is composed solely of A or B molecules.

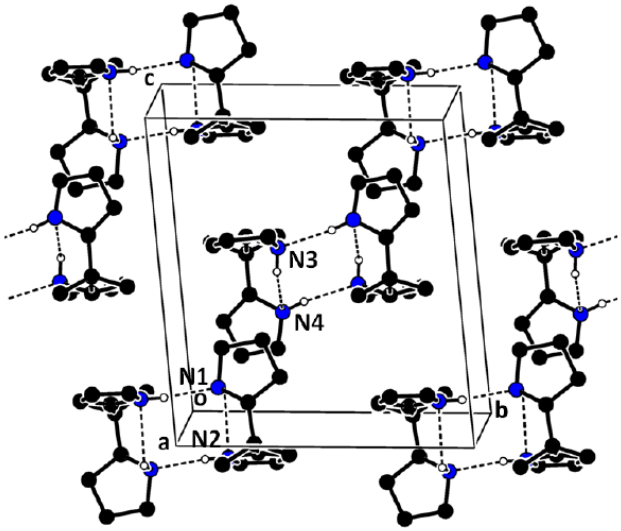

Figure 99. A view, along the a axis, of the crystal packing of **71**, showing the formation of the N-H···N hydrogen-bonded (dashed lines) inversion dimers. C-bound H atoms have been omitted for clarity

Table 20. Hydrogen-bond geometry (Å , °) for **71**.

D—H···A	D-H	H···A	D···A	D-H···A
N2-H2N···N1^{i}	0.905 (19)	2.04 (2)	2.9254 (18)	166.2 (17)
N4-H4N···N3^{ii}	0.873 (16)	2.092 (16)	2.9533 (19)	169.3 (16)

Symmetry codes: (i) -x + 1;-y;-z; (ii) -x + 1;-y + 1;-z + 1.

The crystal structure of **71** can be compared with that of the compound **70**, which also crystallizes with two independent molecules per asymmetric unit. There too the two pyrrole rings are almost perpendicular to one another, with dihedral angles of 87.67 (8)° and 88.09 (7)° in the two independent molecules. However, the crystal packing in **70** is quite different to that of **71**, with the two independent molecules being linked not by N-H···N hydrogen bonds but by N-H··π interactions.

The molecular structure of **72** is shown in Figure 100 (left). Here, the amide-substituted pyrrolidine ring also has a twist conformation, but this time on the C3-C4 bond. The mean plane of the pyrrole ring is inclined to the mean plane of the pyrrolidine ring by only 13.42 (10)°, compared with these planes being nearly perpendicular to one another in both independent molecules of **70** and **71**. In the crystal structure of **72**, molecules are linked via N- H···O hydrogen bonds to form inversion dimers (Table 21 and Figure 100, right), which can be described by an R22 (16) graph-set motif. It has therefore been shown that, under the conditions used, it was finally possible to reduce partially bis(pyrrole) **70** to **71** and to transform this partially reduced bis(pyrrole) into its amide derivative, **72**. These protocols have been used subsequently to modify partially reduced calix[4]pyrroles by introducing amides on the pyrrolidine rings.

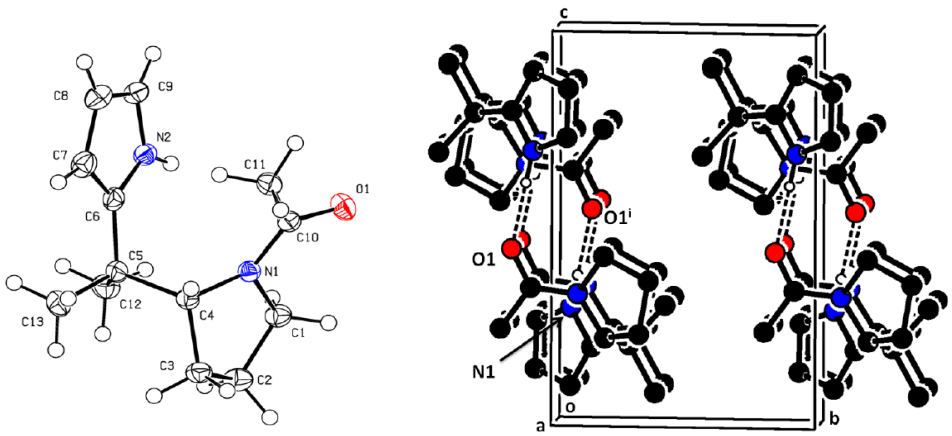

Figure 100. (Left) The molecular structure of **72**, showing the atom-numbering scheme. Displacement ellipsoids are drawn at the 50% probability level. (Right) The A view, along the

a axis, of the crystal packing of **72**, showing the formation of the N-H···O hydrogen-bonded (dashed lines) inversion dimers. C-bound H atoms have been omitted for clarity

Table 21. Hydrogen-bond geometry (Å , °) for **72**.

D—H···A	D-H	H···A	D···A	D-H···A
N2-H2N···O1^{i}	0.95 (2)	1.93 (2)	2.8751 (18)	175 (2)

Symmetry codes: (i) -x + 2;-y;-z+1

5.3. Molecular structure of macrocycle 75, 88-91

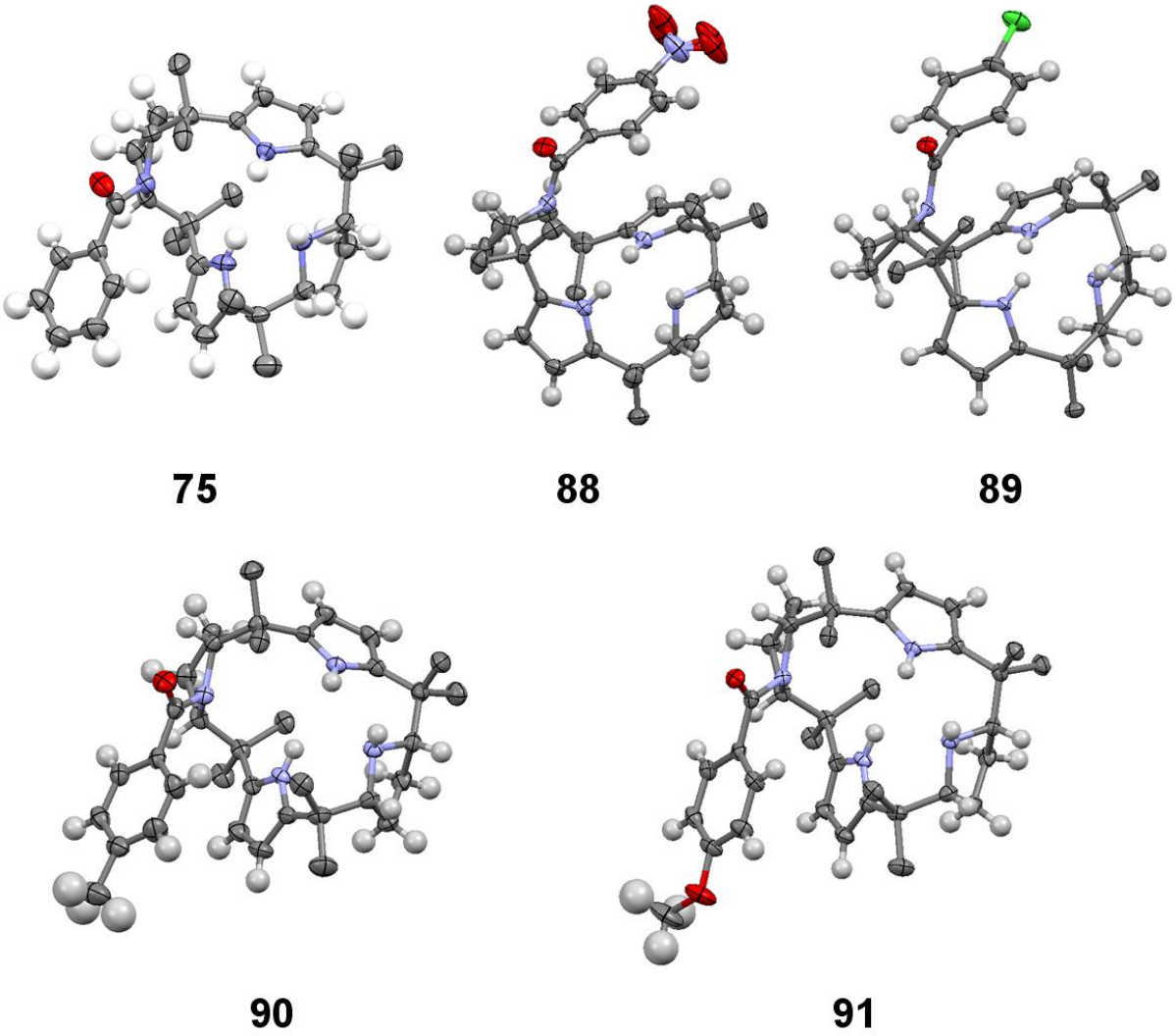

Figure 101. Molecular structure of one enantiomer of compound **75, 88, 89, 90** and **91** the thermal ellipsoids drawn at the 50% probability level (the hydrogen atoms of the *meso*-CH_3 and acetyl groups are omitted for clarity).

5.4. ^{1}H NMR spectrum of compound 73 recorded at variable temperature

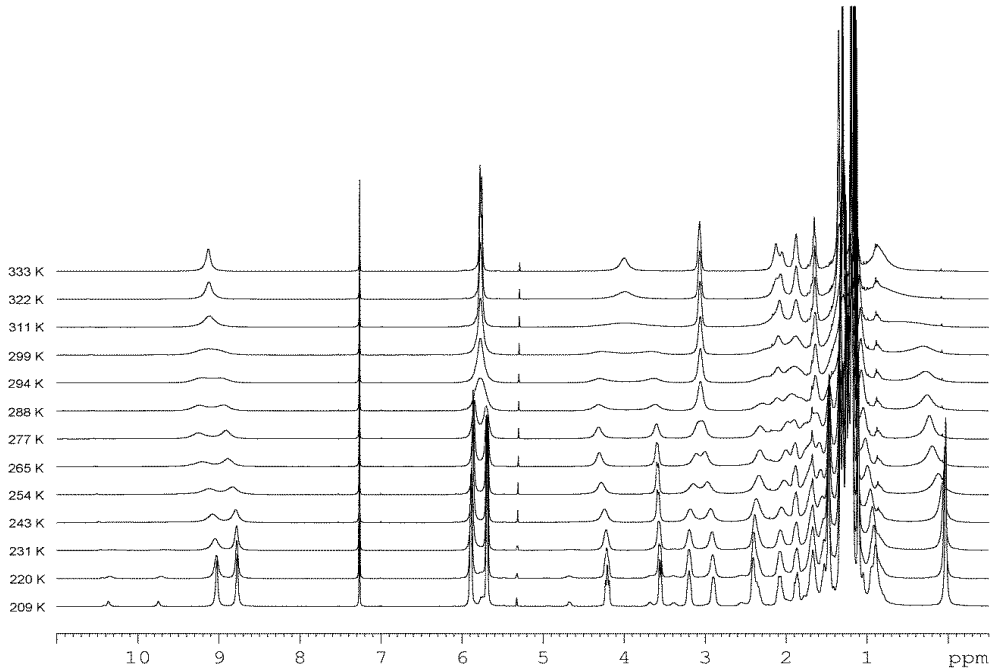

Figure 102. Dynamic NMR spectra of compound **73** in $CDCl_3$ over a 124 °C range of temperature. Full spectrum

5.5. ^{1}H NMR spectrum of compound 75 recorded at variable temperature

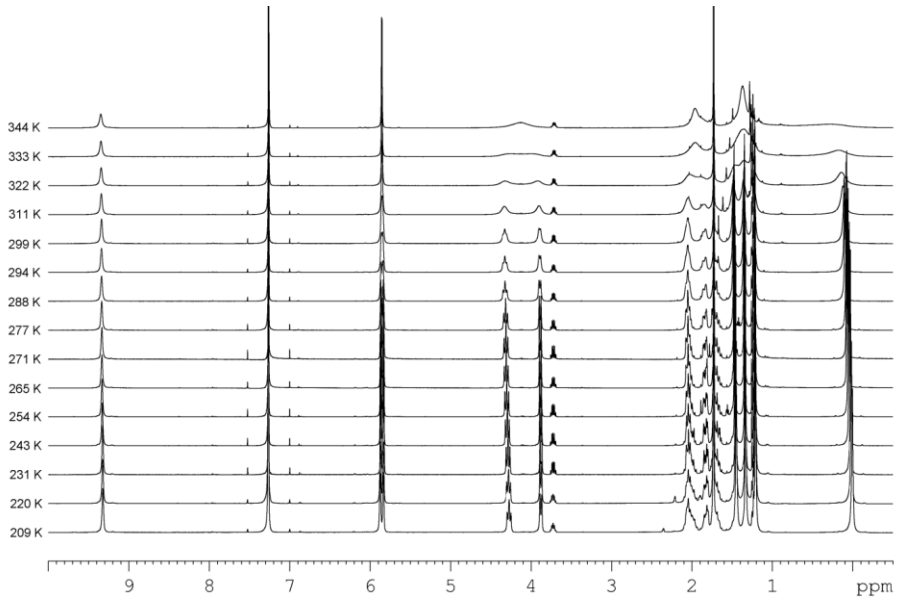

Figure 103. Dynamic NMR spectra of compound **75** in $CDCl_3$ over a 135 °C range of temperature. Full spectrum

5.6. 2D-ROESY analysis of compound 73

We have first determined the dynamic exchange processes in the macrocycle **73**. A 2D-ROESY has been performed at room temperature; however the exchange rate was too high for a relevant analysis. We then have performed the same experience at 244 K.

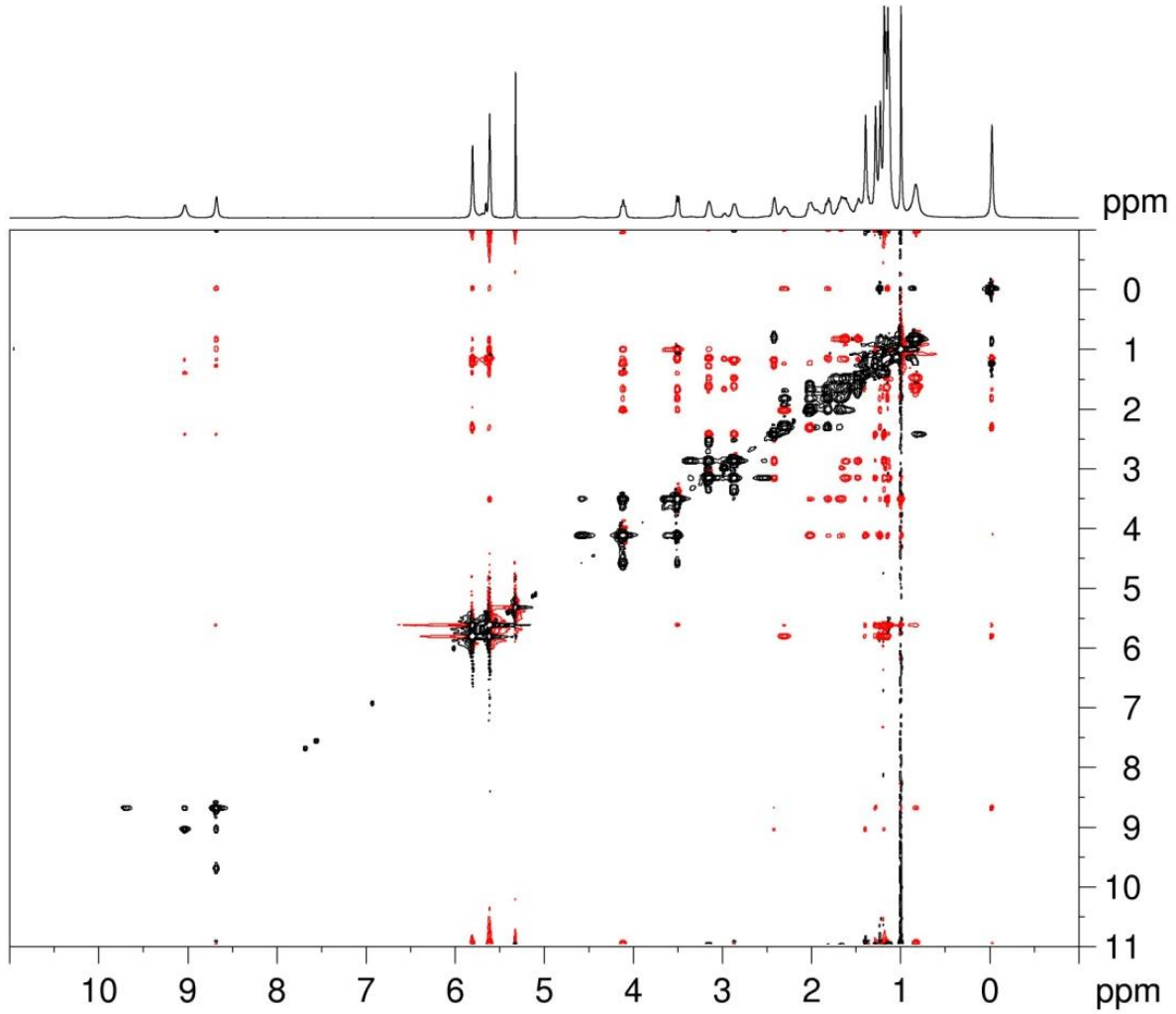

Figure 104. 2D-ROESY experiment of compound **73**, recorded at 244 K and solved in CD_2Cl_2

The spectrum displays the characteristic features of a two-site chemical exchange process. When, we wished to perform the same experiment where one of those two processes was off. We found that at 204 K the rotation rate of the amide rotation was too law for the NMR time scale, therefore only one exchange process was visible, the ring flip. This experiment was very useful to characterize proton coming from the minor conformation of compound **73**.

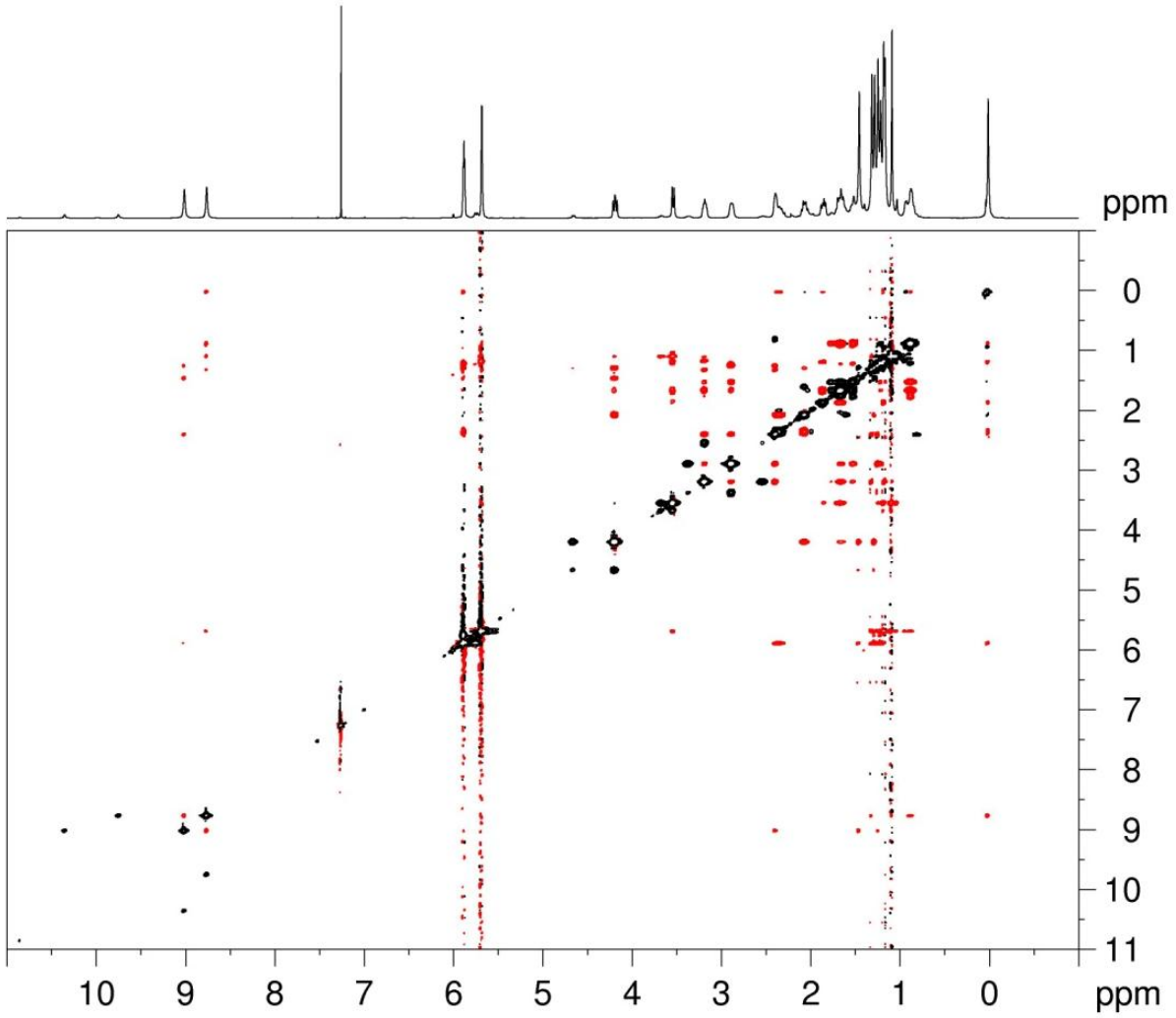

Figure 105. 2D-ROESY experiment of compound **7**, recorded at 204 K and solved in $CDCl_3$

We finally wished to perform the experiment where no one of the two processes was active. We found that a 180 K both processes rate were too slow and recorded by NMR like freeze molecules. Neither the cis/trans isomerization process nor up/down switch process were active. This spectrum was useful to analyze the conformation of the minor conformer of compound **73**.

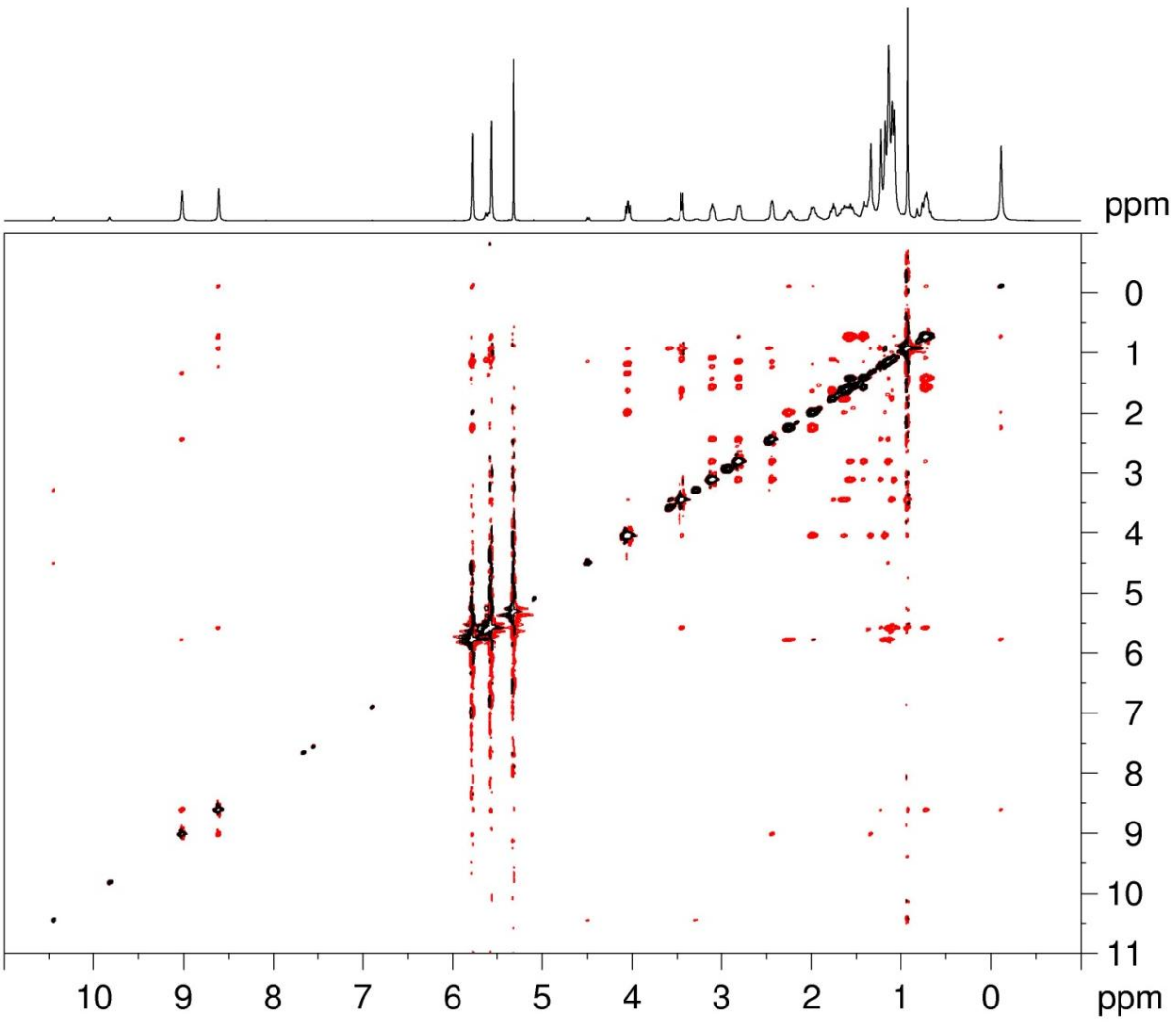

Figure 106. 2D-ROESY of compound **73** recorded at 180 K and solved in CD_2Cl_2

Chapter 5

SYNTHESIS OF N-CONFUSED DIPYRROMETHANE

Abstract

The Rothenmund type condensation of dimethoxycarbonylpyrrol with acetone mainly produces the α,β' linked dipyrromethane, a building block for the synthesis of N-confused macrocycles. We have based our study on the directing effect of Electron-withdrawing (EWG) groups (methyl ester) on pyrrole, which enhances the β-selectivity in electrophilic substitution reactions (Scheme 71). The influences of the reaction conditions on the regioselectivity of the process are reported. The X-ray structures of the α,α', α,β' and the β,β' linked dipyrromethanes show an interesting discrimination of the structurally different types of H-bonds (Figure 107).

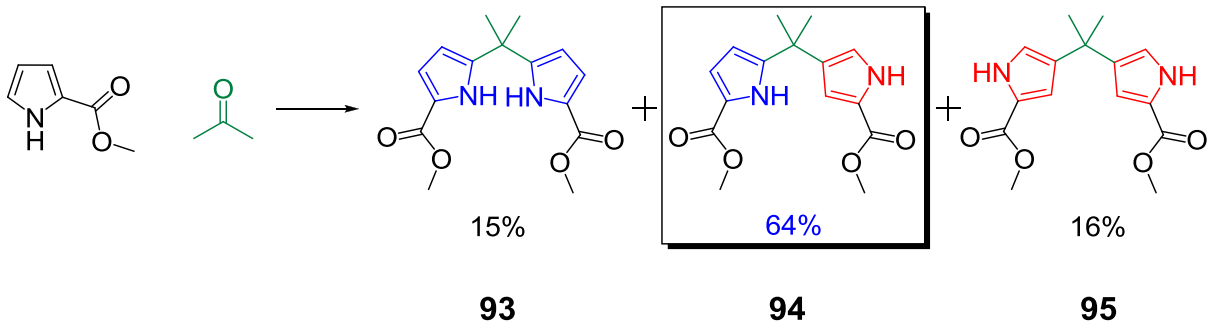

Scheme 71. Synthesis of the N-confused dipyrromethane **94**

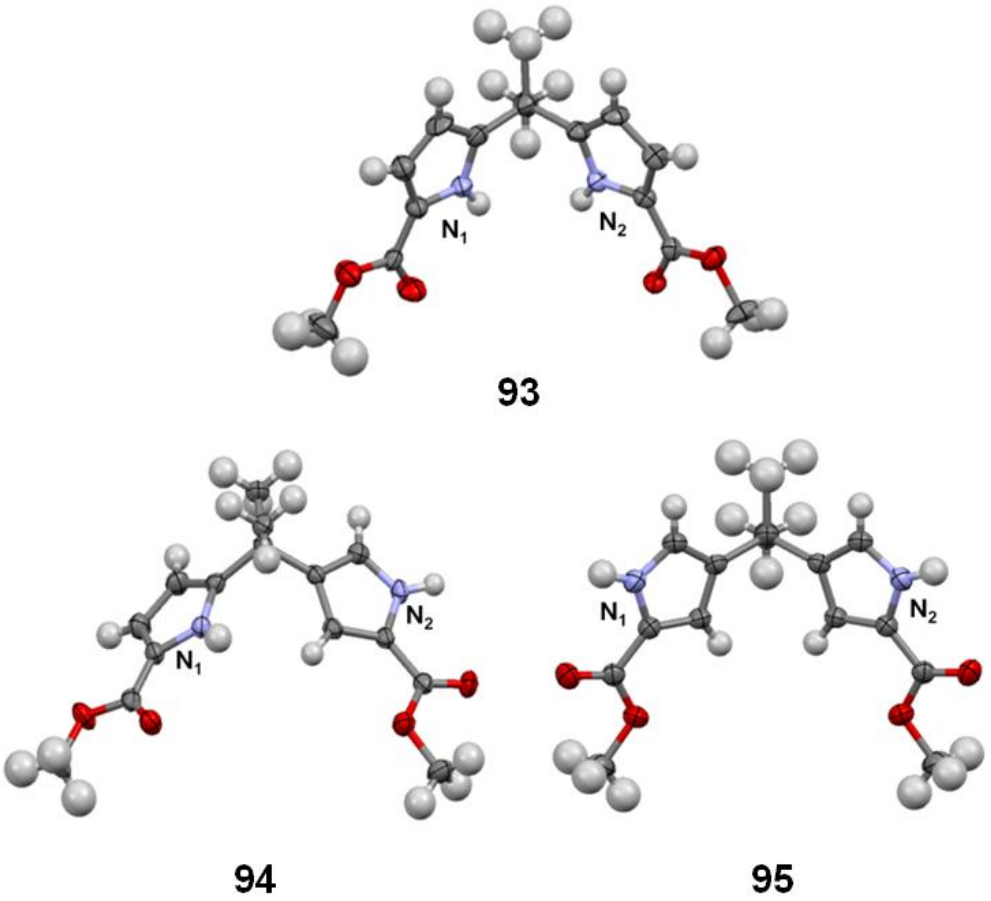

Figure 107. Molecular structure of compounds **1a**, **2** and **3** with the thermal ellipsoids drawn at the 30% probability level

1. QUICK OVERVIEW

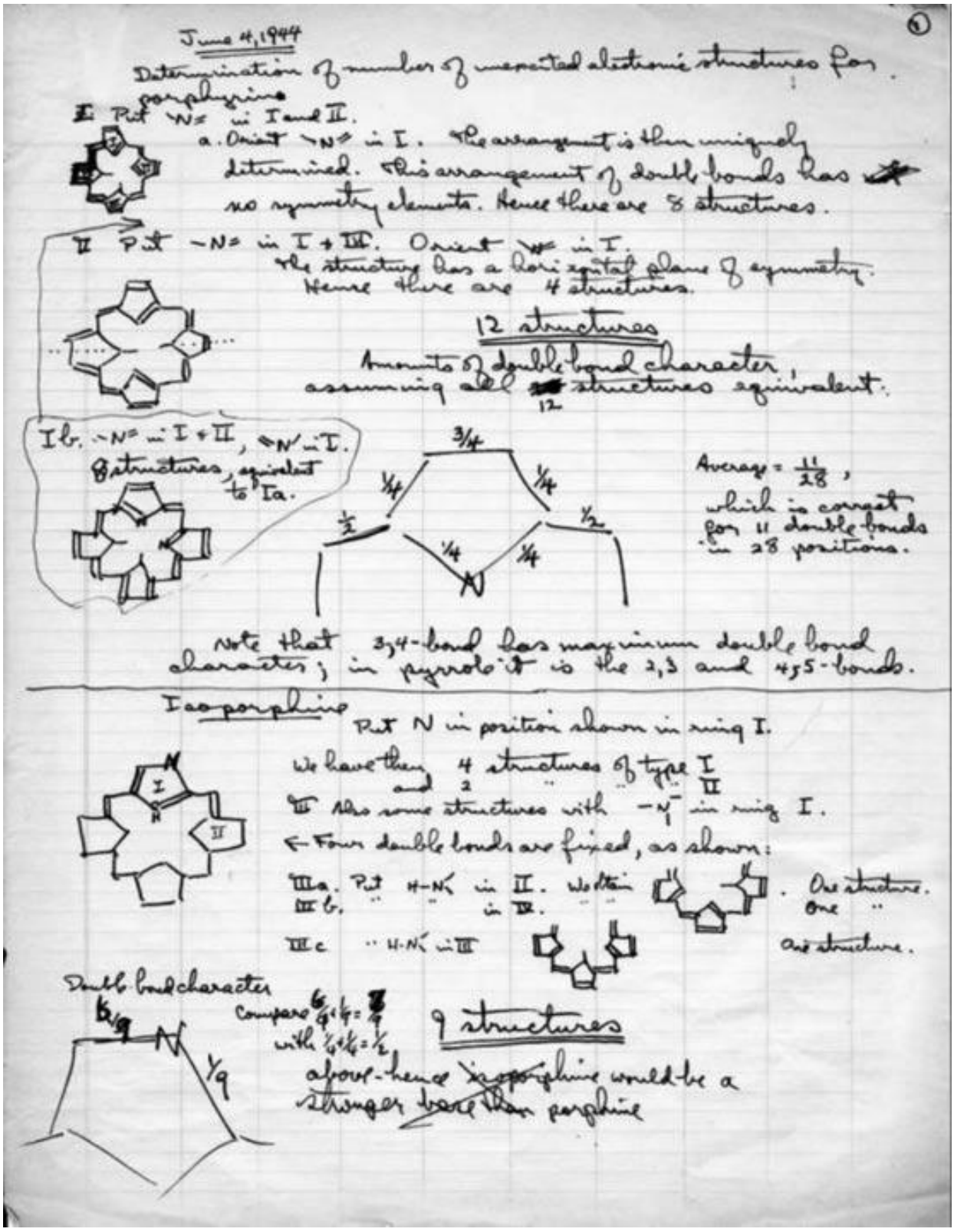

Figure 108. Page from the notebook of Pauling. (source: Ava Helen and Linus Pauling Papers, Oregon State University Special collection)[329]

The well-known colloquial term “N-confusion” was invented in 1940 by one of the most famous chemist of modern time, Linus Pauling. He made significant contributions to almost every area of chemistry. His taste for structure and molecular binding especially in biology and biochemistry led him to enrich largely the field of porphyrin chemistry. He was very interested in the fundamental structure and therefore the electronic aspect of this “pigment of life”. It was during the Second World War that Pauling conceptualized the structure and electronic aspect of isomeric forms of porphyrins (Figure 108)[329]. Pauling tried to determine the stability of porphyrin containing one or more “extroverted” pyrrole rings which he called isoporphyrins. The nitrogen of the “extroverted” pyrrole is actually located on the outside of the macrocycle.

Fifty years later, the first isolation and characterization of a porphyrin containing one “extroverted” pyrrole ring emerged. This isomer of porphyrins was described in two publications by Furuta et al.[330] and Latos-Grażyński and coworkers[331] in early 1994. Furuta was then the first to use the name “N-confused porphyrin” to describe this isomer where one pyrrole is connected via C2 and C4 positions. Both groups described the formation of this isomer as a side product obtained in very low yield during the synthesis of porphyrins via the acid catalyzed Rothmund condensation[220] (Scheme 72).

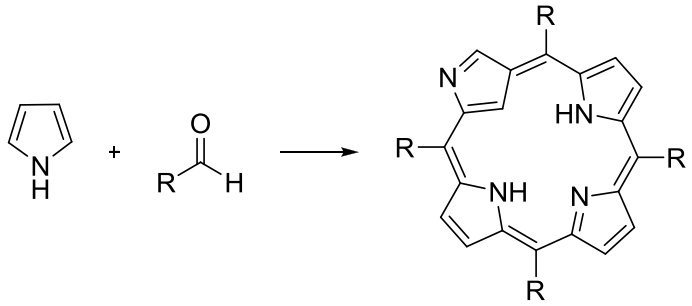

Scheme 72. Synthesis of N-confused porphyrins by Furuta et al.[330] and Latos-Grażyński and coworkers[331]

Five years later, in 1999, Dehaen and coworkers detailed the first systematic effort to synthesized the N-confused calix[4]pyrrole.[146] The structural determination of the N-confused octamethylcalix[4]pyrrole and derivatives by X-ray diffraction analysis has “recently” been described by Azenbacher and coworkers in 2006.[238]

Since the end of the twentieth century the investigation on those N-confused porphyrins (NCP) as well as calix[4]pyrroles (NCCP) became extremely popular for two major reasons: 1) They keep their fundamental and original properties, for instance coordination with metals for NCP and anion binding for NCCP. 2) **Above all**, the easiness of their modification due to reactive C2, C4 and N of NCP and the highly reactive free α-position of the confused pyrrole in NCCP. For those reasons, Furuta and coworkers wrote in a review dealing with NCP,[332] a releaing sentence: "*creation from the confusion*" which perfectly described the potential of these novel macrocycles.

The α-free position of pyrrole in NCCP allows easy access to a multitude of possible reactions which are not feasible with the regular calix[4]pyrrole. For instance the easy synthesis of chromogenic sensor starting with NCCP as revealed by the pioneer work of Dehaen[333] and Azenbacher[238] and coworkers (Figure 109), where the same type of modification of calix[4]pyrrole generates an extremely complex mixture of products.[237]

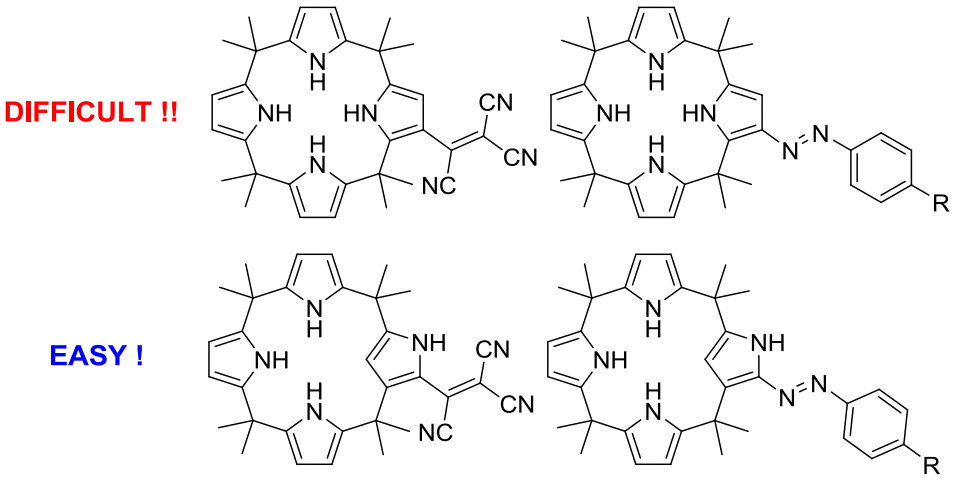

Figure 109. Structure of chromogenic sensors starting with calix[4]pyrrole and NCCP.

Porphyrin is by far the most extensively studied macrocycle in chemistry and biology because of its multiple attractive properties and especially the formation of very stable metal complexes. It is normal that its isomers, the NCP, attract also much attention. The NCP has by far been more studied than any other N-confused macrocycles. The reasons for this focused interest are the easiness of its modification and the facility to form new metal complexes, like in regular porphyrins.

The confused pyrrole ring in NCP has a much higher reactivity than the three remaining pyrroles and than the pyrroles in regular porphyrins. The modification of NCP is also simple to achieve and opens the access to a wide variety of derivatives. Here are some selected functionalizations of NCP: (a) nitration[334] and hydroxylation,[335] (b) halogenations[336, 337] and coupling reactions,[338] (c) acylation,[339-341] (d) cycloaddition, (e) synthesis of N-fused porphyrins[336, 337] (Scheme 73).

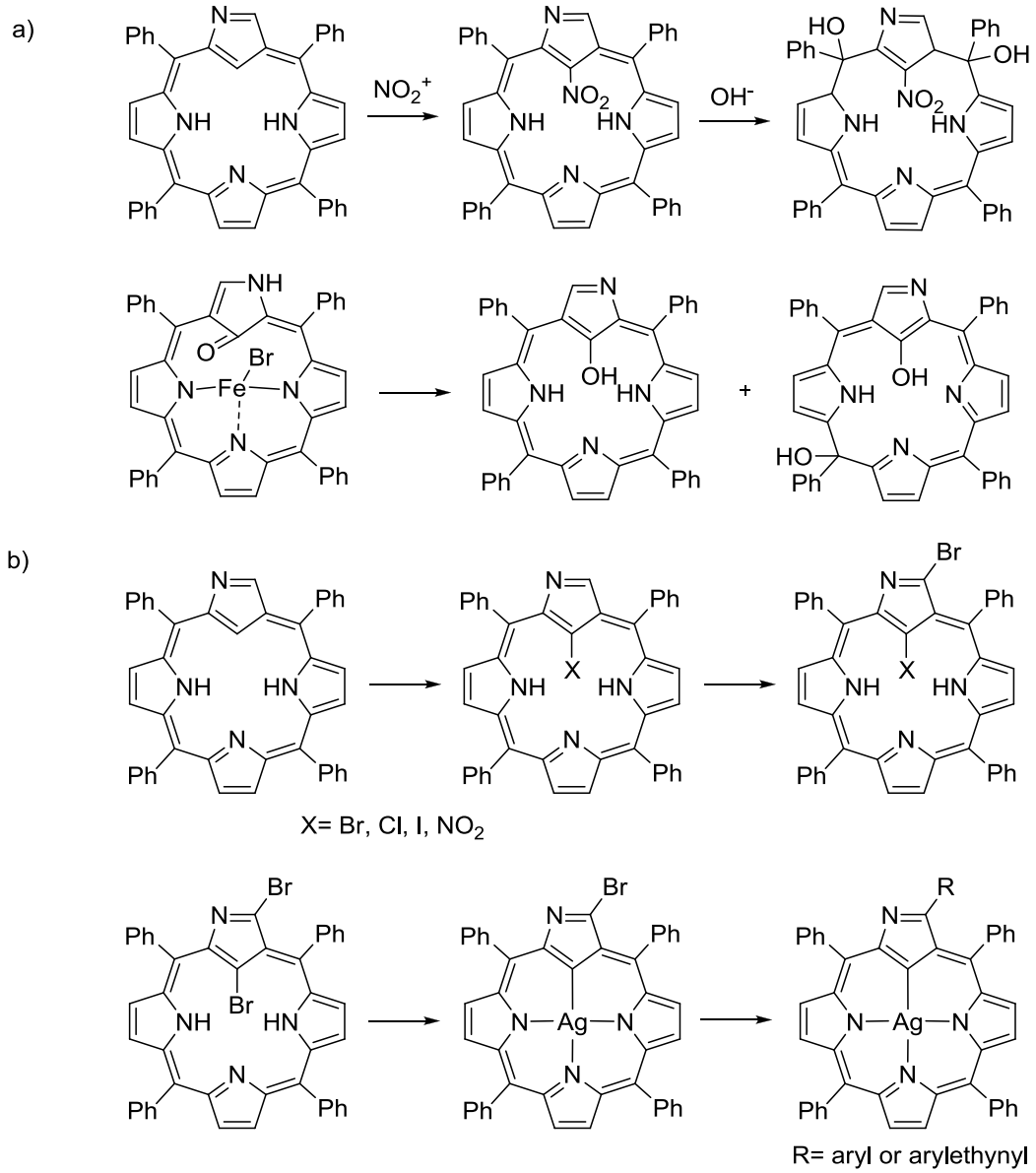

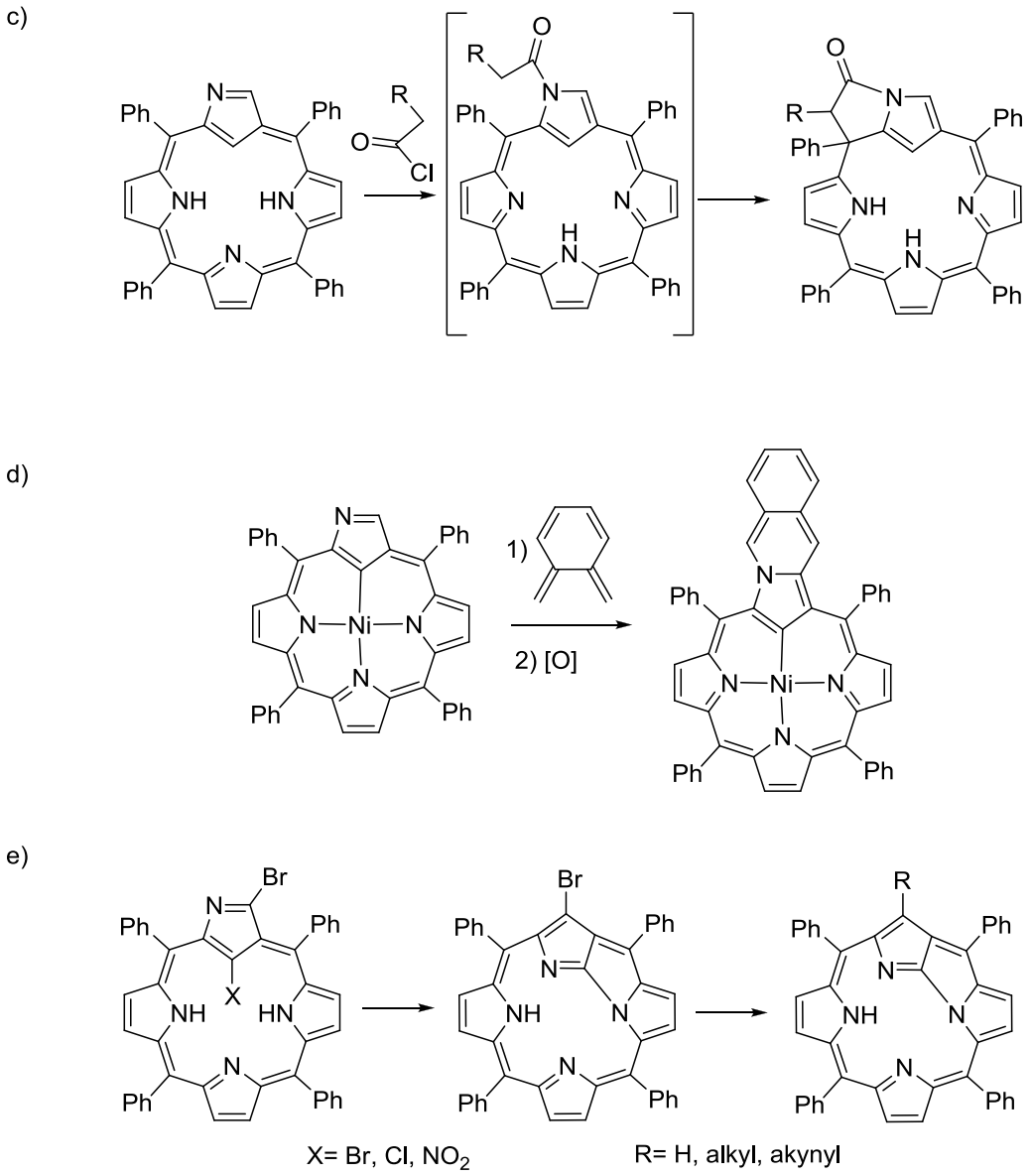

Scheme 73. Functionalizations of NCP

Considering their interest, the quantities of NCP obtained as side product of the "normal" porphyrin synthesis were not satisfactory. Chemists applied the successful building-block methods developed for porphyrin synthesis to the synthesis of NCP. Using the stepwise syntheses MacDonald-type [2 + 2] and [3 + 1] condensation, gave many possibilities to synthesize numerous NCP derivatives (Scheme 74).

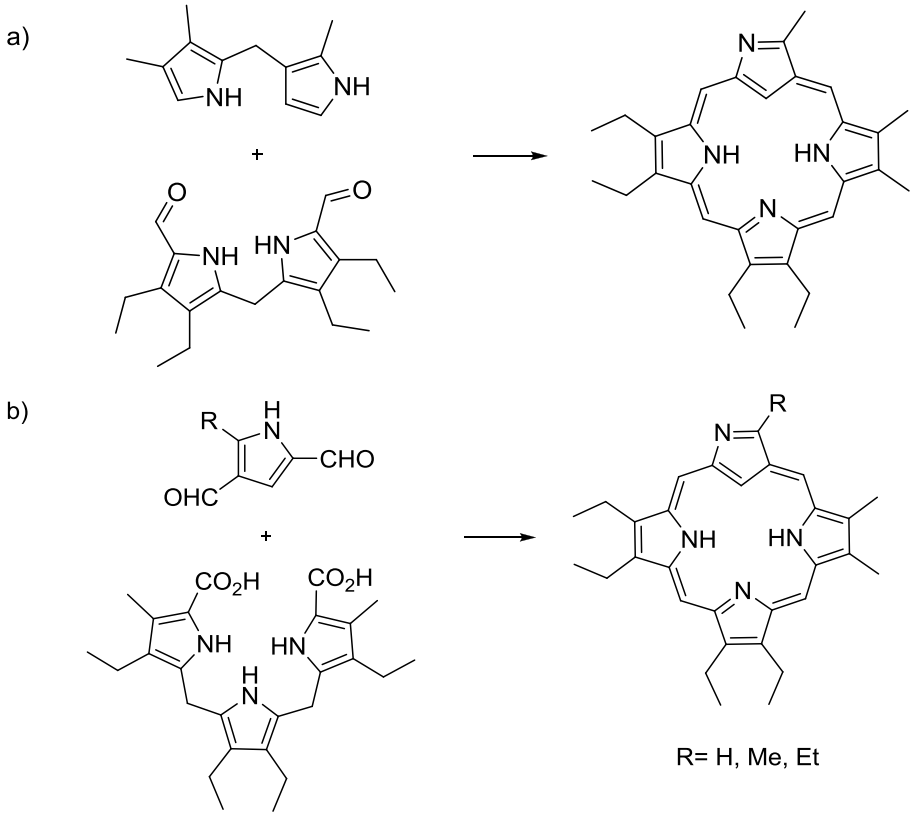

Scheme 74. Syntheses of N-confused porphyrins from MacDonald type (a) [2 + 2][342] and (b) [3 + 1][343] condensation.

From the synthetic point of view, [2 + 2] reactions are favored because the starting materials, dipyrromethanes, are much easier to synthesize than tripyrromethane. This method implies the synthesis of N-confused dipyrromethane which is still poorly described and often obtained with low yields because multi-step synthesis are often needed. This lack of knowledge how to synthesize N-confused dipyrromethane is a challenge, which has to be taken up by the synthetic chemists.

For recent reviews on N-confused macrocycles see:
Toganoh, M.; Furuta, H. *Chem. Commun*. **2012**, *48*, 937; Anzenbacher, P.; Nishiyabu, R.; Palacios, M. A. *Coord. Chem. Rev.* **2006**, *250*, 2929; Senge, M. O. *Angew. Chem. Int. Ed.* **2011**, *50*, 4272; Srinivasan, A.; Furuta, H. *Acc. Chem. Res*. **2005**, *38*, 10; H. Furuta, H. Maeda and A. Osuka, *Chem. Commun.*, **2002**, 1795.

2. INTRODUCTION

The three important classical transformations of pyrroles, the Mannich reaction, the Vilsmeier-Haak reaction and the Rothenmund condensation leading to porphyrins are all electrophilic aromatic substitution reactions showing a high α-regioselectivity. The isolation and characterization of the so called *N*-confused porphyrins at the end of the last century was a spectacular finding. It attracted the attention of the synthetic community to the feasibility of obtaining β-substituted pyrroles via electrophilic substitution reactions. The discovery of products obtained by reaction at the β-position is largely due to the development of efficient and sensitive analytical methods. In the past, the existence of a competition between α- and β-reactivity has been largely ignored and the products of β-substitution have probably been often discarded as unwanted side products. The new findings and the more careful modern studies show that the regioselectivity is essentially in favour of the α-position, while only minor amounts of the β-products are formed. Reversing the selectivity of these reactions towards β-reactivity remains a real challenge. To develop conditions for selectively obtaining either α- or β-substituted pyrroles is of synthetic importance. Substituted pyrrole containing active ingredients has been part of important drug molecules. At the same time, the chemistry of tetrapyrrolic macrocycles has regained importance in material science, catalysis and in the synthesis of new structural variants of this class of compounds.

For the rational and efficient synthesis of *N*-confused macrocycles, controlling the regioselectivity of the electrophilic aromatic substitution process is a central factor. For a rational synthesis of *N*-confused tetrapyrrolic macrocycles one needs good methods of synthesizing mono- (α,β'-linked) or bis-confused (β,β'-linked) dipyrromethane as building blocks (Figure 110).[342, 344-350]

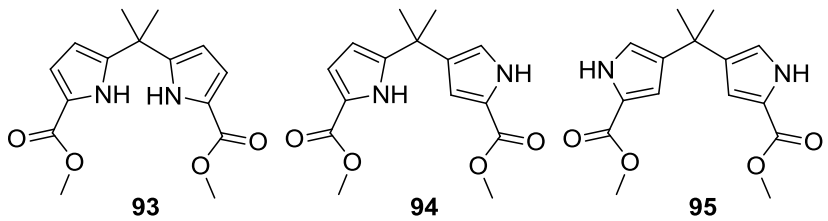

Figure 110. α,β-linked dipyrromethane **94** and its regioisomers (α,α'-linked **93** and β,β'-linked **95** dipyrromethane).

Only few syntheses of confused dipyrromethanes have been described so far. Confused dipyrromethanes or confused macrocycles have generally been isolated as minor side products only.[146, 238, 330, 331, 351-354] Three main strategies exist for the synthesis of *N*-confused dipyrromethanes: 1) Selective syntheses via multiple steps starting from a reactive species in the β-position of the pyrrole precursor[355, 356] 2) Avoiding the α-substitution by using an α,α'-substituted pyrrole as starting material[342, 357] or by introducing a bulky protecting group on the nitrogen[346, 358] 3) Introducing an electron-withdrawing group on the pyrrole in order to change its electronic properties.[359, 360] These strategies involve multiple steps and usually lead to poor yields. To the best of our knowledge, syntheses of *N*-confused dipyrromethane starting from an α-free pyrrole in a single step have not been reported so far. We decided to explore a method to obtain the *N*-confused dipyrromethane **94** in a single step and good yield.

3. MATERIALS AND METHODS

In this part, we investigated the influence of the conditions on the ratio between the different regioisomers by GC analyses. GC measurements were carried out using an Agilent 6850A, column Agilent Technologies (Part Number 19091Z-413E, Length (m): 30; Diam. (mm): 0.320; film (µm): 0.25).

GC method used (injection volume (µL): 1; Inlet Temp. (°C): 280; Inlet Pres. (PSI): 10.32; Flow (mL/min.): 45.6; Detector Temp (°C): 280; Flow (mL/min.): H_2: 40.0, Air: 450, N_2: 45):

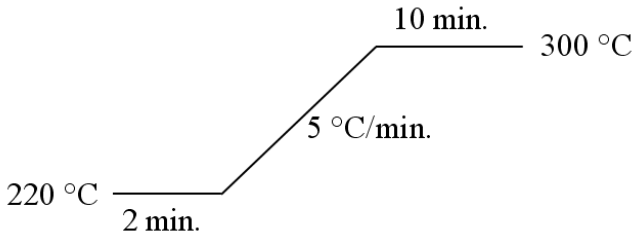

4. SYNTHESIS OF DIPYRROMETHANE 93, 94 AND 95

The directing effect in pyrroles has been first described by Sonnet.[361] Electron-withdrawing (EWG) groups enhance the β-selectivity in electrophilic substitution reactions. Using the

iminium salt of the 2-formylpyrrole, Sonnet prepared β-halogenated pyrroles with high regioselectivity (Scheme 75).

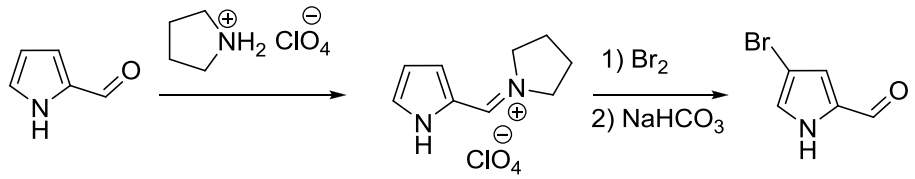

Scheme 75. Synthesis of β-halogenated pyrrole by Sonnet

Based on his work, Dolphin and coworkers[359] have recently reported the synthesis of β,β'-linked dipyrromethane using the same iminium salt as a strong EWG (Scheme 76).

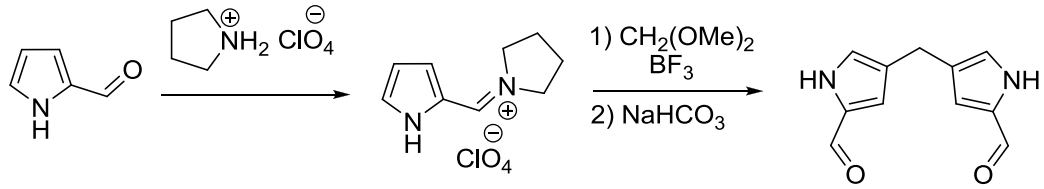

Scheme 76. Synthesis of β,β'-linked diformyldipyrromethane by Dolphin and coworkers

Using a weaker EWG, Sonnet isolated a mixture of α- and β-substituted products. Taking this observation into account, we decided to study the commercially available methyl 2-pyrrolecarboxylate **96** as starting material. If compound **96** should show no selectivity in the condensation of **96** with acetone, a statistical mixture of the three possible dipyrromethanes **93** : **94** : **95** = 25% : 50% : 25% should be obtained.

The condensation of **96** needed relatively high quantities of acid to proceed with a reasonable rate and in a decent conversion as determined by GC. Despite the high concentration of acid needed, no formation of black degradation products was observed. These observations are in accordance with the deactivating effect of the ester group. Already, in one of our early non-optimized trials, we detected only three products by GC. The three products were isolated and characterized. In a later preparative trial, we used an optimized procedure for the condensation of methyl 2-pyrrolecarboxylate **96** and acetone (10 equivalents) at room temperature for 40 min, using 10 equivalents of methanesulfonic acid (Scheme 77).

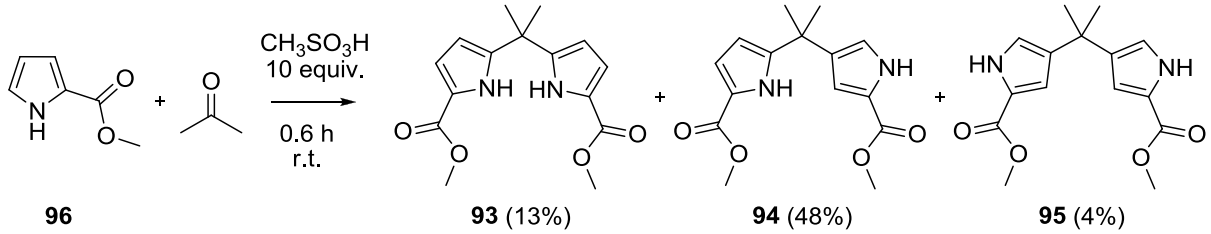

Scheme 77. Synthesis of the N-confused dipyrromethane **94**. The GC analysis showed the following product distribution: **93** : **94** : **95** = 15 : 64 :16. The separation by chromatography of **95** was delicate and led to losses

The recovered raw material corresponded to 95% of the added starting material and was analytically clean on TLC and GC showing only the spots and peaks of the three products (see GC spectrum of the crude reaction mixture in Annex part). Three products were isolated by column chromatography in 65% yield and characterized by ^{1}H-NMR spectroscopy. The structure of the asymmetric dipyrromethane **94** was easy to determine, showing four different signals in the pyrrolic region. The structure of compounds **93** and **95** has tentatively been attributed by analogy with the spectra reported by Dolphin and his coworkers[359] for the α,α'-linked and β,β'-linked diformyldipyrromethane. The three structures could be unequivocally determined by X-ray diffraction analyses.[362] Single crystals of the dipyrromethanes **93**, **94** and **95** were grown by slow evaporation of dichloromethane or by recrystallization in ethanol. The molecular structures of the three products are shown in Figure 111.

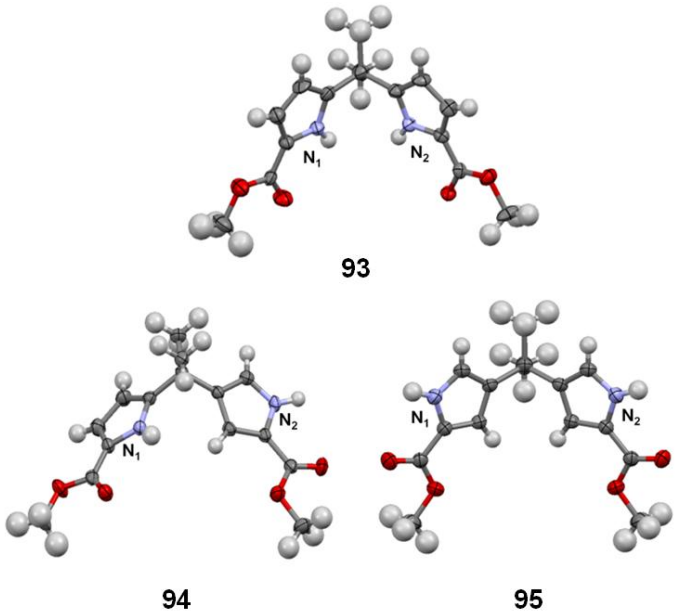

Figure 111. Molecular structure of compound **93a**, **94** and **95** with the thermal ellipsoids drawn at the 30% probability level

To optimize the formation of **94**, we surveyed the influence of the conditions on the ratio between the different regioisomers. The type and quantity of the acid catalysts, the number of equivalents of acetone, the reaction temperature and the reaction time were varied.[363] We started our investigation by reacting pyrrole **96** and acetone in stoechiometric amounts using a catalytic quantity of methanesulfonic acid (Table 22, entry 1). No product formation was observed. Increasing the amount of acid to 10 equivalents (Table 22, entry 2) led to a full conversion into the three products. No trace of degradation or side products was detected by GC and TLC. *N*-confused dipyrromethane **94** was present in the crude, up to 65% and the dipyrromethane **93** and **95** respectively 24% and 4%. The ratio between the α,α'- and the β,β'-product is almost 7:1. Increasing the amount of acetone to 10 equivalents (Table 22, entry 3) after only 40 min the product **94** was present in 64% according to the GC trace. Under these conditions the ratio between the α,α'-linked and the β,β'-linked products has changed to 1:1. Letting run the reaction for an additional 60 min, a small amount of degradation (1.5%) was observed. These conditions were therefore used to perform the reaction in a two grams scale, where the products could be isolated pure in 65%, after careful chromatographic separation (Table 22, entry 3). Neither a significant change in the proportion nor in the yield of the three products was detected. Increasing the temperature to 50 °C using similar concentrations (Table 22, entry 5) did not change the amount of compound **94** formed. The ratio between the dipyrromethane **93** and **95** reached 10:1, a similar value to that observed in entry 2 of Table 22. Increasing the amount of acetone to 50 equivalents, many side reactions were observed and the amount of dipyrromethanes detected by GC dropped to 16%. (Table 22, entry 5). Then, we tested the influence of the type of acid (Table 22, entry 6-10). Using TFA under the conditions successfully applied previously with methanesulfonic acid (Table 22, entry 6), no transformation could be observed. Increasing the amount of TFA to 100 equivalents, we observed in the GC, only 7% conversion of the starting material was transformed to products after 14 h (Table 22, entry 7). After 36 h the reaction stopped at 33% conversion (Table 22, entry 8). Only two regioisomers were detected, increasing the temperature to 50 °C and using 10 equivalents of acetone (Table 22, entry 9). Compound **93** and **95** were obtained in a ratio 35:65 and the conversion reached 59%. Increasing the reaction time led to side reactions and the products **93**, **94** and **95** were present in the crude up to 69% (Table 22, entry 10).

Table 22 Variation of conditions for the Rothemund type reaction between pyrrole **4** and acetone[363]

Entry	Acetone (equiv.)	Acid (equiv.)	Temperature	Time (h)	Conversion of **4** (%) determined by GC	Relative amount (%)[b] Compound **1**	Compound **2**	Compound **3**
1	0.6	CH_3SO_3H (0.5)	r.t.	6	0	0	0	0
2	0.6	CH_3SO_3H (10)	r.t.	14	100	24	65	4
3	10	CH_3SO_3H (10)	r.t.	0.6	100	15/(13)[c]	64/(48)[c]	16/(4)[c]
4	15	CH_3SO_3H (10)	50°C	7	100	25	60	2
5	50	CH_3SO_3H (10)	r.t	7	93	2	11	3
6	0.6	TFA (25)	r.t.	6	0	0	0	0
7	0.6	TFA (100)	r.t.	14	7	2	4	traces
8	10	TFA (100)	r.t.	36	33	9	23	2
9	10	TFA (50)	50°C	7	59	20	38	nd[d]
10	10	TFA (50)	50°C	20	100	26	36	7

[a] Reactions performed in 1.6 mmol scale. [b] Relative amounts were determined by GC. [c] Isolated yields from a two grams scale experiment. [d] No traces of products were detected.

5. MOLECULAR STRUCTURES OF 93, 94, 95

Alkoxycarbonyl-pyrroles have been used in supramolecular chemistry for self assembly and molecular recognition.[364] Our dialkoxycarbonyl-dipyrromethanes represent a unique set of regiochemically differentiated compounds containing the typical framework used in the studies of supramolecular recognition processes reported in literature. The three dipyrromethanes show three distinct and different packings in the crystals. Strong intermolecular H-bond networks are the main feature leading to different supramolecular arrangements of the molecules in the unit cells. The α,α'-linked dipyrromethanes form stable dimers (Figure 112).

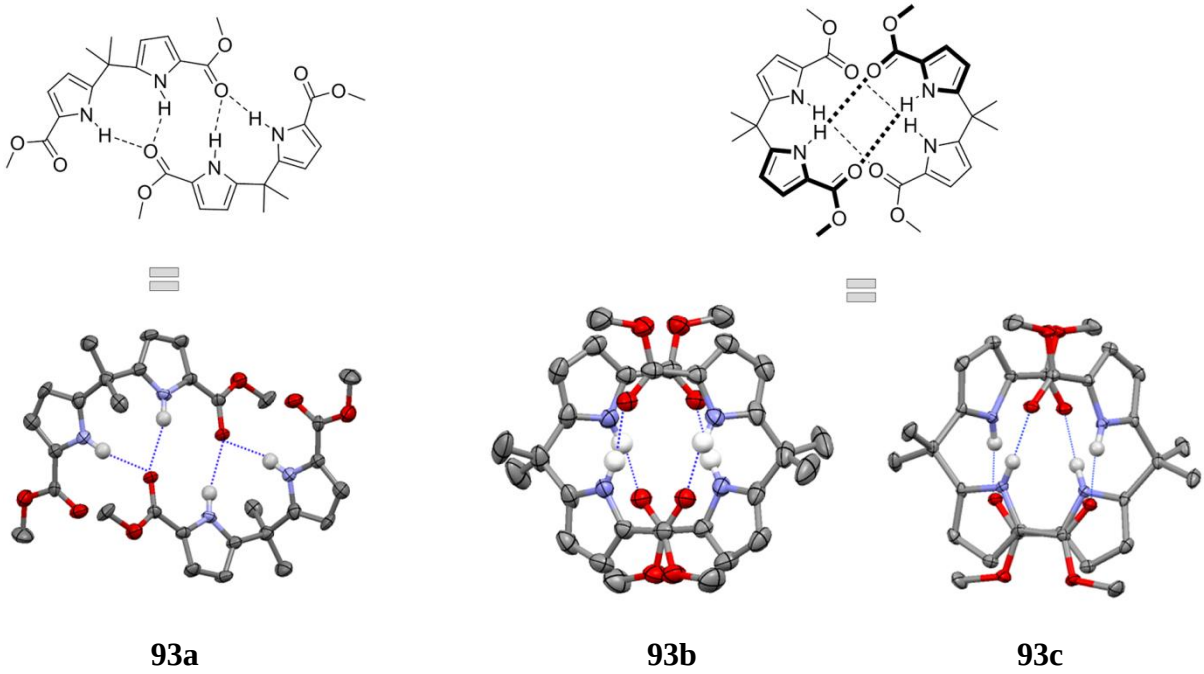

93a **93b** **93c**

Figure 112. Supramolecular assembly of compound **93a**, **93b** and **93c** with the thermal ellipsoids drawn at the 30% probability level (the hydrogens are omitted for clarity). N-H···O hydrogen bonds are shown as blue dashed lines

Three different polymorphs of compound **93** have been obtained and analyzed crystallographically. Compound **93a**, isolated as crystalline impurity from a solution containing mainly **94**, forms a dimer with strong H-bond networks between one carbonyl group of one ester from one molecule and the two pyrroles from the second molecule in the dimer. This arrangement engages the two lone pairs of the carbonyl of one ester in the H-bonding network, whereas the second ester group is not involved in intramolecular

interactions. The two molecules forming the dimer are in an extended, shifted arrangement. The molecular structures of compounds **93b** and **93c** in the crystal are similar to each other and form strong and compact dimers. All the carbonyls of the ester groups are forming a single H-bond with one of the N-H of a pyrrole of the second molecule in the dimeric unit. The structures of **93b** and **93c** are symmetric, which contributes to the dense and esthetically appealing aspect of these two structures. In the crystal of the α,β'-linked dipyrromethane **94** (= *N*-monoconfused) the dimers of the unit cell are held together by a strong H-bond network formed between the carbonyl group of the ester and the N-H bond of the adjacent pyrrole, which is α-linked. The H-bond network is analogous to the network observed for the dimers of carboxylic acids, amides and α-pyridones. The confused pyrrole ring (ring with a β-link) forms a H-bond with two "external" dipyrromethanes by their confused part (Figure 113).

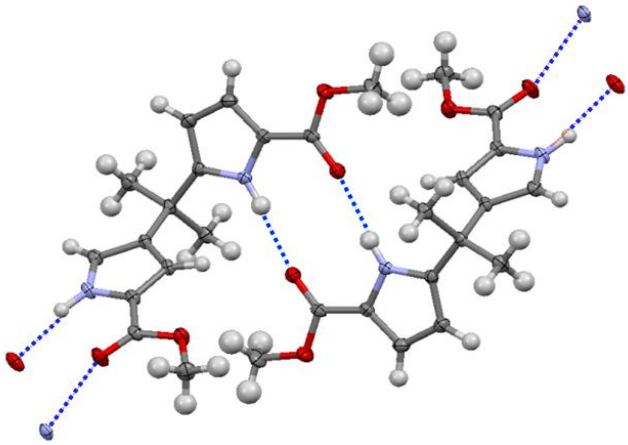

Figure 113. Supramolecular assembly of compound **94** with the thermal ellipsoids drawn at the 30% probability level, N-H···O hydrogen bonds are shown as blue dashed lines

The dimeric unit is in an extended conformation. The two units are even more shifted than in the structure of compound **93a**. In contrast to the structure of **93a**, compound **94** forms dimers, which are further linked to four other symmetry related molecules, thus forming a two-dimensional network. The salient feature of this structure is the clear segregation of the H-bonds between the α-linked units and the H-bonds between the β-linked units. The β,β'-linked dipyrromethane **95** also forms a very stable H-bond two-dimensional network, the four functional groups create H-bonds with four symmetry related dipyrromethanes (Figure 114).

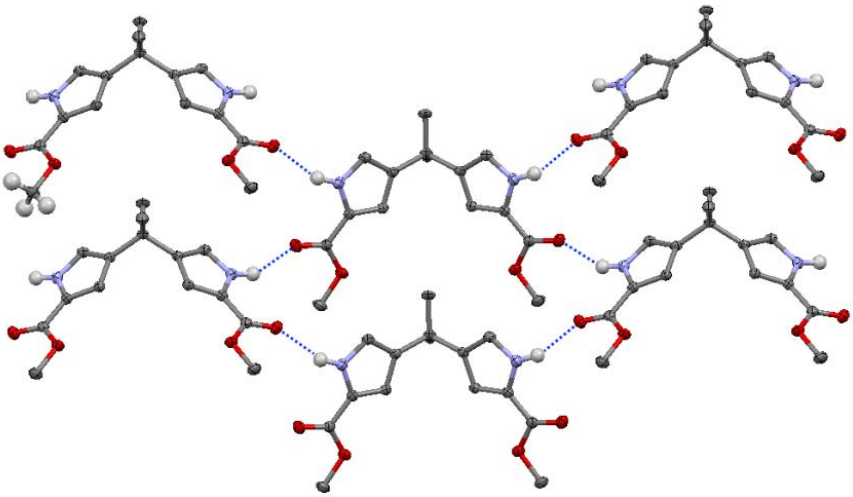

Figure 114. Supramolecular assembly of compound **95** with the thermal ellipsoids drawn at the 30% probability level, N-H···O hydrogen bonds are shown as blue dashed lines

With the exception of the structure of **93a**, the compounds engage all possible partners in the H-bonding. The three structures **93a**, **93b** and **93c** of compound **93** are the only one in which dimmers are present in the crystal. The mono-confused and the bis-confused compound **94** and **95** form networks. In the structure of compound **94** the H-bonds of the α-substituted alkoxycarbonyl-pyrrole unit are forming two H-bonds to the same partner, thereby forming a sort of dimeric subunit. The H-bonds of the β-substituted alkoxycarbonyl-pyrrole unit forms H-bonds to external partners building the network. The DSC analysis of the three dipyrromethane **93**, **94** and **95** disclosed interesting results (Table 23)

Table 23. DSC analysis of **93, 94 and 95**.

Entry	Compound	Melting point (°C)	Freezing point (°C)	ΔH (kJ.mol-1)[a]
1	**93**	191.2	144.2.	37.7
2	**94**	135.4	g[b]	35.1[c]
3	**95**	201.1	140.1	43.5

[a] Determined by DSC on 2nd heating run; [b] Glass transition; [c] Determined by DSC on 1st heating run

Compound **95** showed the highest melting point and the highest fusion enthalpy. The results for compound **93** and **94** are less easy to interpret. Further studies aiming to the understanding of this process are in progress.

6. CONCLUSION

In conclusion, we have established an efficient method for preparing in a single step *N*-confused dipyrromethane **94** in good yield. Two other products the α,α'-linked dipyrromethane **93** and the β,β'-linked dipyrromethane **95** were isolated as side products and fully characterized. The selectivity observed is in accordance with the deactivating electron withdrawing effect of the ester group. Ester groups in the α-position of a pyrrole ring can easily be removed or transformed and are therefore synthetically attractive substituents. The supramolecular arrangement of **93**, **94** and **95** were analyzed by X-ray diffraction and DSC. The structures show a clear segregation between the H-bonds formed between two α-substituted pyrrole units and the H-bonds between β-substituted pyrrole units. The H-bonds between α-substituted pyrroles leads to dimeric association, whereas the β-substituted units lead to the formation of ribbons and networks. The strongest network, measured by its melting point and melting enthalpy, was observed for **95** forming a two dimensional ribbon sheet-like arrangement. The reported method represents a promising route to the preparation of building blocks for *N*-confused macrocycles of the calix[4]pyrrole type. Mechanistic investigations to further characterize the scope and limitation of this approach are currently underway.

7. ANNEX

7.1. GC analysis

Despite the high concentration of acid needed no formation of black degradation products was observed and the GC spectrum of the crude was surprisingly clean (Figure 115).

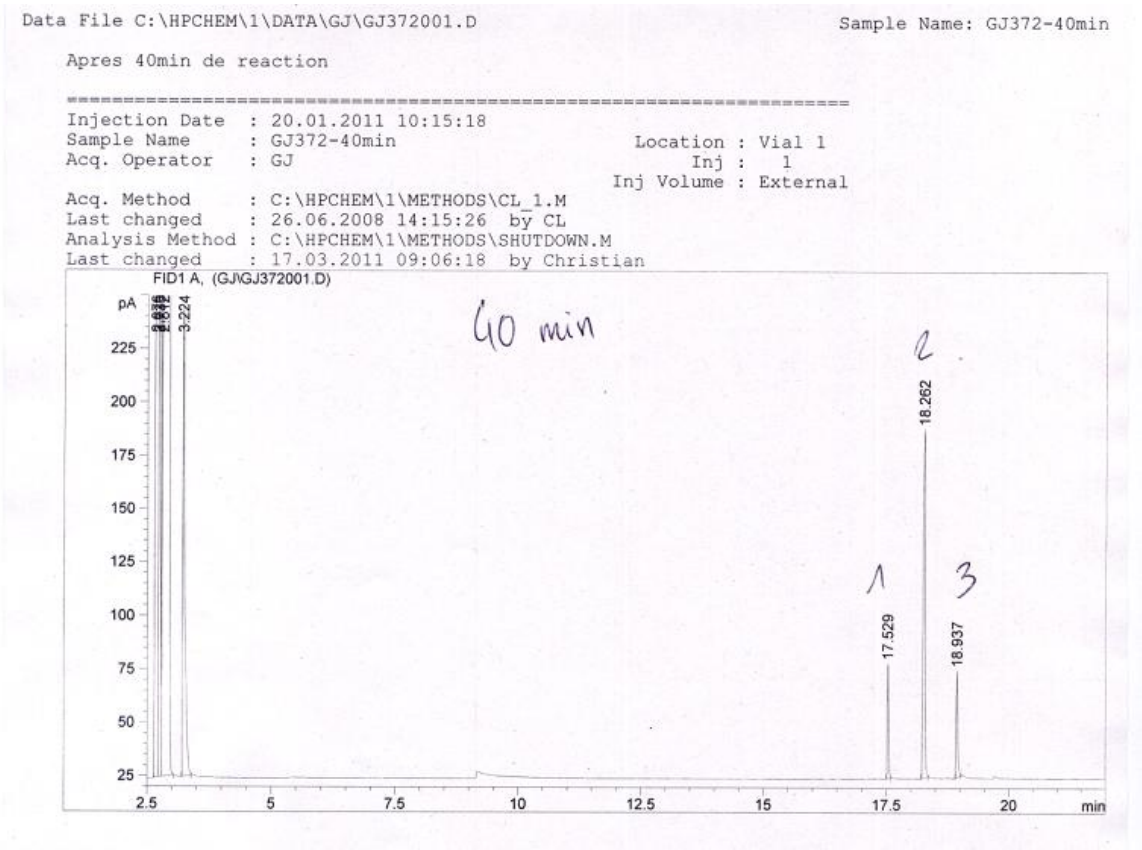

Figure 115. GC spectrum of the crude of reaction using the condition described in Table 22 entry 2

Chapter 6

CONCLUSION AND PERSPECTIVES

1. CONCLUSION

Starting from a simple concept, the hydrogenation of calix[4]pyrrole **1**, we have embarked on a research project which has been full of obstacles and unexpected results. Almost every step was more complicated than anticipated. Most of the time, the obstacles we encountered were not known, which forced us to discover new territory. The adventure has been beautiful and rewarding but strenuous. Detecting new and unprecedented processes and properties has always been a strong motivation for chemists. The interest of discovering and exploring new structures has always been a powerful stimulus. The research project became considerably more complex than what was expected at the beginning. We were lucky as to achieve the partial and then the total hydrogenation of calix[4]pyrrole **1**, a milestone, achieved more than 100 years after the first reported synthesis of this macrocycle. The mechanistic analysis of the postulated mechanism helped to advance and establish a reproducible procedure which allowed the isolation of two diastereoisomers **12a** and **12b** of the partially reduced macrocycle in good yields, using an easy to apply isolation procedure based on the differences of solubility and pH behavior. The yield of the totally reduced calix[4]pyrrolidine **13** has been more than doubled since our first isolation. With the newly developed method we can now obtain the macrocycle **13** in high yields starting from the half reduced compound **12b**. We recently found a condition for the total hydrogenation of calix[4]pyrrole using a large excess of catalyst (10 equivalents). This reaction provided only two fully reduced products,

compound **13**, already isolated from our previous work, and a new isomer of the fully reduced macrocycle, compound **24**. Despite our intensive efforts, the reasons for the use of a huge excess of catalyst to perform the complete hydrogenation of **12b** or calix[4]pyrrole **1** have not been elucidated yet. The relative configurations of the three products from the catalytic hydrogenation of **1** have been assigned through single crystal X-ray diffraction.

In a second project, the hydrogenation of calix[m]furan[n]pyrrole (m+n=4) was explored. This work led to the synthesis and the characterization of 28 macrocyclic products, 18 of them are novel molecules. When the classical analytical methods were not able to provide the relative configuration of the products, their relative configurations were determined by X-ray analysis (15 selected structures measured by Mrs Stoekli that I sincerely thank). Remarkably selective transformations were observed and the structural and chemical factors influencing the diastereoselectivity of the hydrogenation were investigated. As another consequence of this work, the sequence of the catalytic hydrogenation of calix[4]pyrrole was revealed. The synthesized compounds can be seen as mimick of the intermediates in our hydrogenation. As the intermediates are not directly accessible this approach was the best we could do to obtain information on the sequence.

The three years spent attempting to reduce the calix[4]pyrrole **1** completely led to the isolation of a huge amount of half reduced product **12b**. Considering the beauty and the potential of this structure, developing a project focused on its modification was undertaken. The transformation of this readily accessible and symmetric compound into a modified compound, hopefully more valuable structure, in a single step was thus investigated. This work led to the development of suitable conditions for the selective mono- acylation of **12b**. We found that the tight hydrogen bond network of the compound **12b** was responsible for the remarkable reactivity and selectivity pattern toward the acylation. An even stronger hydrogen bond network is formed by the mono-acylated macrocycle. This explains the loss of basicity and of nucleophilicity of this compound. We have successfully applied the optimized condition for the introduction of amino-acid residues under non racemizing condition. A conformational analysis by dynamic NMR spectroscopy coupled to the results of the X-ray diffraction analysis led to the discovery of a ring-flipped conformer of **73** detectable at low temperature. Kinetic and thermodynamic parameters of the amide rotation of compound **73** and **75** and the ring-flip of **73** were extracted from line fitting experiments from a dynamic NMR investigation.

The final project emerged after a lucky discovery in our laboratory. This work led the development of a very efficient method for preparing in a single step *N*-confused dipyrromethane **94** in good yield. Two other products the α,α'-linked dipyrromethane **93** and the β,β'-linked dipyrromethane **95** were isolated as side products and fully characterized. The supramolecular arrangement of **93**, **94** and **95** were extremely interesting showing a dichotomy in their hydrogen bonding in the solid structure analyzed by X-ray diffraction.

2. PERSPECTIVES

The three years spent in the laboratory allowed us to discover interesting chemistry which went beyond our expectations. Quite a few of the projects are not yet finished. We present a few of the possible lines of research for the future.

Experiments in the NMR tube have shown that the macrocycle **12b** forms complexes with palladium. We could show that these complexes are undergoing oxidative transformation in the presence of oxygen. A thorough investigation of the oxidative ability of the palladium complex of **12b** should be undertaken. We can expect interesting results from the careful analysis of this oxidation process.

During our intensive screening in the quest of finding suitable conditions to perform the complete conversion of calix[4]pyrrole **1** into the macrocycle **13**, we made a chance discovery. We tried to perform the hydrogenation of the calix[2]pyrrole[2]pyrrolidine **12b** in formic acid, catalyzed by Pd/C 10%. After the addition of formic acid, we directly observed bubbles of gas suggesting a decomposition of the solvent. A few years ago, Laurenczy et al. described the use of formic acid as a hydrogen-storage material with a homogeneous catalytic system of ruthenium water-soluble complexes (Ru/TPPTS) that selectively decomposed formic acid into H_2 and CO_2.[365] We then realized that we potentially had the same activity than Lauranczy but using a heterogeneous catalyst, which had never been reported so far. We tried to reproduce the reaction without compound **12b** and the reaction did not take place. This result suggests that we formed a kind of complex with **12b** and the heterogeneous Pd/C 10%. This information was extremely interesting for two reasons: 1) if compound **12b** interacts with Pd/C 10% during the reaction the substrate modifies the catalyst in this process. This postulated interaction could be part of the explanation why compound **12b** is so difficult

to reduce. 2) Another interpretation would be, that we created a homogeneous catalyst from a heterogeneous catalyst. The meticulous analysis of the decomposition gazes has not been undertaken yet? A thorough investigation of this process would lead to an interesting new research field.

Other projects could be explored:

- The synthesis of reduced calix[4]pyrrole via reductive amination:

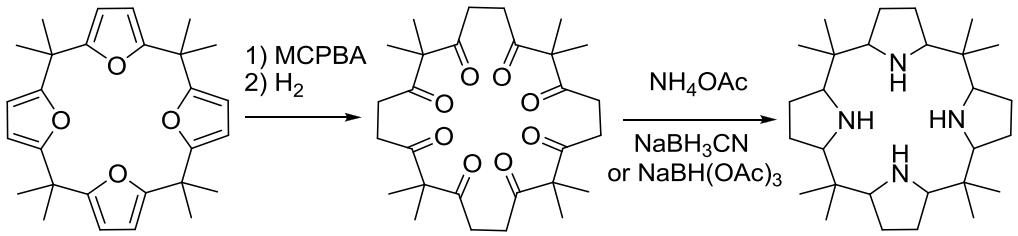

- The synthesis of reduced porphine:

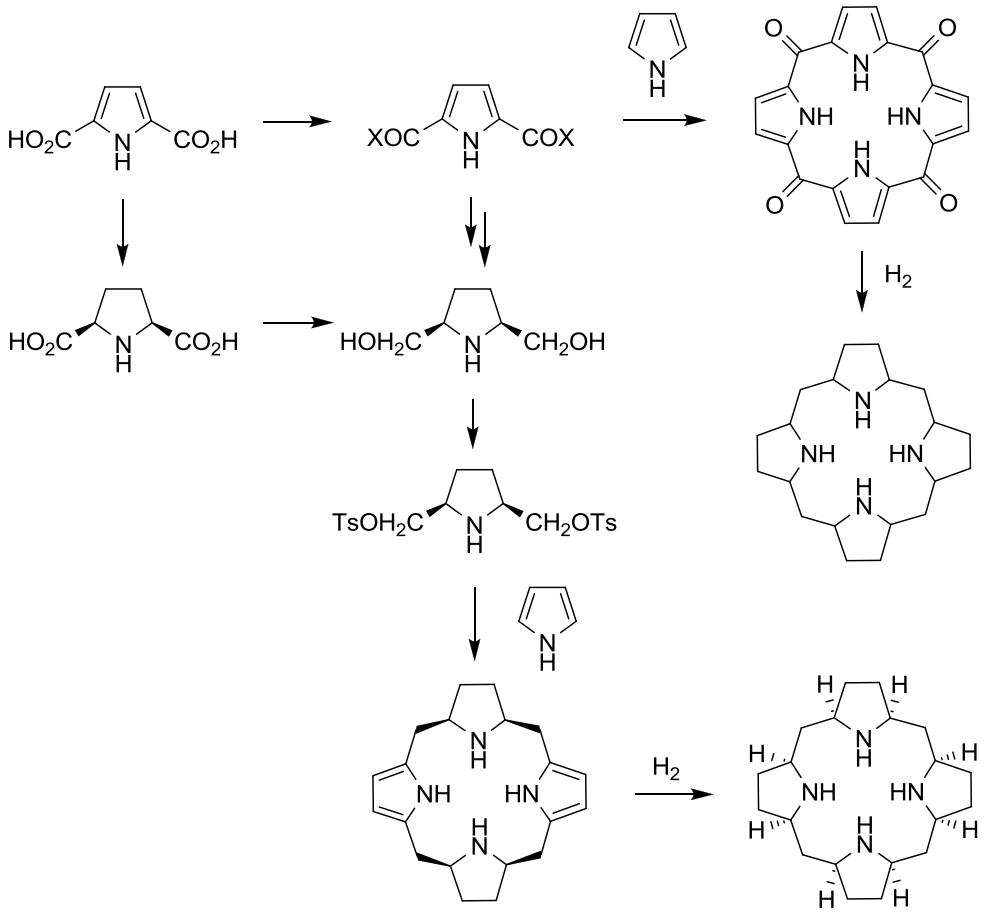

Chapter 7

EXPERIMENTAL PART

1. GENERAL INFORMATION

1.1. Chromatography

1.1.1. Thin layer chromatography (TLC)

Analytical thin layer chromatography was performed on Merck precoated glass-backed TLC plates (silica gel 60 F254) and visualized by UV lamp (254 nm) and potassium permanganate ($KMnO_4$) stain.

1.1.2. Columns chromatography

Columns chromatography were carried out on silica gel 60 Å, 32-63 (Brunschwig) and aluminium oxide Fluka for chromatography, Brockmann activity I. Technical grade solvents were employed, which were distilled prior to use. Concentration under reduced pressure was performed by rotary evaporation at 40 °C at the appropriate pressure. Purified compounds were further dried under high vacuum (0.3 Torr). Yields refer to chromatographically purified and spectroscopically pure compounds, unless stated otherwise.

1.1.3. Gas chromatography (GC)

GC analyses were carried out using an Agilent 6850A, column Agilent Technologies (Part Number 19091Z-413E, Length (m): 30; Diam. (mm): 0.320; film (µm): 0.25). GC method

used (AG7)(injection volume (µL): 1; Inlet Temp. (°C): 280; Inlet Pres. (PSI): 10.32; Flow (mL/min.): 45.6; Detector Temp (°C): 280; Flow (mL/min.): H_2: 40.0, Air: 450, N_2: 45):

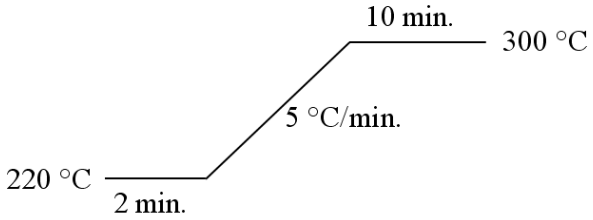

1.1.4. Infrared Spectroscopy (IR)

Perkin Elmer Spectrum One version B FT-IR was used for obtaining IR spectra with the resolution of 2 cm-1. Software used: Spectrum version 5.0.1. The solid substances and thick oil like substances were analyzed by preparing KBr pellet (KBr – Fluka puris p. a). Liquid samples were analyzed as film (sandwich) by applying between two KBr salt plate. The absorption bands between 4000 and 400 cm-1 were measured. The intensity of the spectrum was divided into five equal parts for the abbreviations, *s* (intense), *m* (medium intensity), *w* (weak), *br* (broad).

1.1.5. Nuclear Magnetic Spectroscopy (NMR)

NMR spectra were recorded using a Bruker Avance 400 spectrometer operating at 400.13 MHz (^{1}H) and 100.63 MHz (^{13}C(^{1}H)). The NMR solvents were purchased from Cambridge Isotope Laboratories. ^{1}H NMR spectroscopy chemical shifts are quoted in ppm relative to internal tetramethylsilane TMS (δ= 0.00 ppm) or $CDCl_3$ (δ= 7.26 ppm) or CH_3OH (δ= 3.31 ppm). ^{13}C NMR spectroscopy chemical shifts are quoted in ppm relative to internal tetramethylsilane TMS (δ= 0.00 ppm) or $CHCl_3$ (δ= 77.16 ppm) or CH_3OH (δ= 49.00 ppm). The chemical shift is given in ppm in the descending order and the coupling constant *J* in Hz. The multiplicity of signals were given abbreviations *s* (singlet), *d* (doublet), *t* (triplet), *q* (quartet), *quint* (quintet), *dd* (doublet of doublet), *dt* (doublet of triplet), *br* (broad) and *m* (multiplet).

1.1.6. Mass Spectroscopy (MS)

The mass spectra measurements for ESI (electro-spray ionization) were recorded with a Finnigan LCQ mass spectrometer. The high resolution mass spectroscopy (HRMS) was measured at University of Fribourg (Switzerland) by Mr.F.Nydegger. The instrument used was Bruker FTMS 4.7T BioAPEXII. The ionization used was ESI (electro-spray ionization).

1.1.7. Glassware

For reactions where argon or nitrogen atmosphere was used, the glass apparatus were dried by keeping in the hot oven at 150°C for at least two hours. The apparatus were removed from hot oven and cooled to ambient temperature with argon or nitrogen atmosphere. For reactions at low temperature, ice bath with salt (0°C to -5°C) and acetone/liquid nitrogen bath (-78°C) were used. For heating reactions, oil baths (40-200°C) were used.

1.2. Solvents

1.2.1. Standard solvents

For the purpose of chromatography and extractions, technical grade solvents were distilled over drying agent.

Solvent	Abbreviation used	Drying agent
Chloroform	$CHCl_3$	$CaCl_2$; Molecular sieve 0.4nm
Cyclohexane	Cyclohexane	Molecular sieve 0.4nm
Dichloromethane	CH_2Cl_2	$CaCl_2$; Molecular sieve 0.4nm
Diethyl ether	Et2O	$CaCl_2$
Ethyl acetate	AcOEt	K_2CO_3; Molecular sieve 0.4nm
Methanol	MeOH	CaO

1.2.2. Solvents for reaction

Solvent	Abbreviation used	Quality
Acetic acid glacial	AcOH	Carlo Erba, for analysis
Acetonitrile	ACN	Aldrich, sealed-bottle over molecular sieve (H_2O ≤0.01%), ≥99.5% (GC).
Chloroform	$CHCl_3$	anhydrous, contains amylenes as stabilizer, ≥99%
Dichloromethane	CH_2Cl_2	Acros, 99.8%, extra dry over molecular sieve
Methanol	MeOH	Fluky, puriss. abs., ≥99.5% over molecular sieve (H_2O ≤0.01%),
Tetrahydrofuran	THF	Aldrich, sealed-bottle over molecular sieve (H_2O ≤0.005%), contains ~0.025% 2,6-di-tert-butyl-4-methylphenol as stabilizer, ≥99.5% (GC)
Toluene	toluene	Fluky, puriss. abs., ≥99.7% over molecular sieve (H_2O ≤0.005%),

1.2.3. Reagents

Solvent	Abbreviation used	Quality
(R)-(-)-2-Methylpyrrolidine	(R)-(-)-2-Methylpyrrolidine	Aldrich
3-Chloroperbenzoic acid	*m*CPBA	Aldrich, ≤77%
4,5-Dimethoxy-2-nitrobenzyl chloroformate	4,5-Dimethoxy-2-nitrobenzyl chloroformate	Aldrich, 97%
4-chlorobenzoyl chloride	4-chlorobenzoyl chloride	Aldrich, 99%
4-methoxybenzoyl chloride	4-methoxybenzoyl chloride	Aldrich, 99%
4-nitrobenzoyl chloride	4-nitrobenzoyl chloride	Aldrich, 98%
5-hydroxypentan-2-one	5-hydroxypentan-2-one	Aldrich, mixture of monomer and dimer, 95%
Acetone	Acetone	Aldrich, CHROMASOLV® Plus, for HPLC, ≥99.9%
Acetyl chloride	Acetyl chloride	Aldrich, puriss. p.a., ≥99.0%
Ammonium acetate	$AcONH_4$	Aldrich, for molecular biology, ≥98%
benzoyl bromide	benzoyl bromide	Aldrich, 97%
benzyl bromide	benzyl bromide	Aldrich, reagent grade, 98%
Boron trifluoride diethyl etherate	BF_3OEt_2	Aldrich, purified by redistillation, ≥46.5% BF_3 basis
Butyl Lithium	BuLi	Aldrich, 2.5 M in hexanes
Dimethyl 2,6-pyridinedicarboxylate	Dimethyl 2,6-pyridinedicarboxylate	Aldrich, 99.0%
Furan	Furan	Aldrich, reagent, ≥99.0%
Glutaryl chloride	Glutaryl chloride	Aldrich, 97.0%
Glycine	Glycine	Aldrich, reagent grade, ≥98.5%
Hydrogen	H_2	Carbagaz 45
Iodomethane	CH_3I	Aldrich, purum, ≥99.0% (GC)
L-valine	L-valine	Aldrich, reagent grade, ≥98%
methane sulfonic acid	CH_3SO_3H	Acros, 98%
Methyl 2-pyrrolecarboxylate	Methyl 2-pyrrolecarboxylate	Aldrich, 97.0%
Methyl chloroformate	Methyl chloroformate	Aldrich, puriss. 99%
Methyllithium solution	MeLi	Aldrich, 3.0 M in diethoxymethane
Palladium on carbon (screening catalysts)	Pd/C	See in the text
Palladium on carbon 10%	Pd/C 10%	Aldrich, 10% Pd basis

(for screening conditions)		
Potassium carbonate	K_2CO_3	Aldrich, ACS reagent, ≥99.0%
Potassium permanganate	$KMnO_4$	Aldrich, ACS reagent, ≥99.0%
Propionyl chloride	Propionyl chloride	Aldrich, puriss. p.a., ≥99.0%
p-Toluenesulfonic acid monohydrate	*p*-TSA	Aldrich, ACS reagent, ≥98.5%
p-Toluoyl chloride	*p*-Toluoyl chloride	Aldrich, 98%
Pyrrole	Pyrrole	Aldrich, reagent grade, 98%
Sulfuric acid	H_2SO_4	Carlo Erba, for analysis
thionyl chloride	$SOCl_2$	Aldrich, purum, ≥99.0%
Triethylamine	Et_3N	Aldrich, 99%
Trifluoroacetic acid	TFA	Aldrich, ReagentPlus®, 99%
Zinc dust	Zn	Aldrich, purum, ≥99%, powder

1.3. Remarks

Unless otherwise noted, all reaction mixtures were stirred with a magnetic stir bar in flame-dried glassware and performed under an atmosphere of argon employing standard Schlenk-line techniques. In every case, the assignments of signals were confirmed by ^{1}H, ^{13}C, ^{1}H-COSY, HMBC, HSQC, and DEPT spectra.

2. EXPERIMENTAL PART

Only the description of new products will be fully described. The corresponding compounds will be labeled with a "*" in their title. Compounds already described in literature will be only described by NMR and MS analyses and their literature references.

2.1. General procedure (I) for the *N*-acylation of the *meso*-octamethylcalix-[2]pyrrolidino[2]pyrrole

In a two-necked flask fitted with a gas inlet and containing a stirrer bar was charged *meso*-octamethylcalix[2]pyrrolidino[2]pyrrole (200 mg, 0.46 mmol) and potassium carbonate (138

mg, 1 mmol). The reaction vessel was flushed with argon and sealed with a septum. The mixture of dry THF and ACN was introduced, and the corresponding acyl chloride (2.1 eq.) in THF (1 mL) was added. After 15 min. a precipitate appeared and the reaction mixture was stirred for 2 hours in all at room temperature, under argon. After stirring, 10% sodium carbonate was added and the reaction mixture was extracted with CH_2Cl_2. The organic layer was washed successively with two times 10% sodium carbonate and saturated brine. The organic layer was dried with sodium sulfate, and the solvents were removed under vacuum. The residue was purified by column chromatography.

2.2. General procedure (II) for the formation of acyl chloride

In a round-bottom flask were introduced amino-acid (4.04 mmol) and CH_2Cl_2 (0.08 M), then thionyl chloride (5 mL) was cautiously added. The flask was equipped with a reflux condenser, flushed with argon, and the mixture was stirred at reflux temperature for 2 hours. Then the thionyl chloride was distilled at reduced pressure, and the resulting solid was flashed with CH_2Cl_2 (2 mL) which was removed at reduced pressure to obtain the product which can be used without further purifications.

2.3. Procedure (III) for reactions to perform the kinetic study (Hammett plot)

The five reactions for this study have been done in parallel following the general procedure (I). The reactions have been performed in the same model of glassware for 2 hours (except for reaction using *para*-nitrobenzoyl chloride, 0.5 h). Purifications by column chromatography have been realized in the same model of column with the same amount of silica.

2.4. General procedure for the small-scale hydrogenation reaction (screening)

Calix[4]pyrrole **1** (0.200 g, 0.47 mmol), n-eicosane (0.0266 g, 0.094 mmol), and 10% Pd/C (0.170 g, 0.16 mmol of Pd) were placed in a test tube (125 x 15 mm) containing a small cross stirring bar. AcOH (5 mL) was added and the test tube was placed inside an autoclave vessel containing AcOH (25 mL). The reaction mixture was kept under a hydrogen pressure of 100

atm at 100 °C. After 24 h, the autoclave was cooled to room temperature and the reaction mixture was filtered through a pad of Celite, which was washed with AcOH (2 x 20 mL) and CH_2Cl_2 (3 x 15 mL). The combined filtrate and washings were concentrated under reduced pressure to give a colorless slurry, to which CH_2Cl_2 (25 mL) and 5% aqueous NaOH (15 mL) were added. The resulting mixture was stirred for 5 min. The organic layer was then separated and the aqueous phase was extracted with CH_2Cl_2 (3x20 mL). The collected organic layers were washed with brine (25 mL), dried over K_2CO_3, and concentrated under reduced pressure to give 0.206 g of a white solid. This was redissolved in EtOAc for GC analysis.

2.5. General procedure for the large-scale hydrogenation of calix[4]pyrrole 1

A glass cylinder inside an autoclave vessel was charged with acetic acid (100 mL), calix[4]pyrrole **1** (2.00 g, 4.70 mmol), n-eicosane (0.266 g, 0.94 mmol), and 10% Pd/C (1.70 g, 1.6 mmol of Pd). The autoclave was closed, put under magnetic stirring, filled with hydrogen (100 atm), and heated at 100 °C for 24 h. After cooling to room temperature, the reaction mixture was filtered through Celite and the solid was washed with AcOH (2x20 mL) and CH_2Cl_2 (2x20 mL). The combined filtrate and washings were concentrated to give a slurry residue, which was dried under high vacuum. A small amount of this residue was redissolved in CH_2Cl_2 (5 mL), and this solution was washed with 2M aqueous NaOH (5 mL) prior to GC injection. Addition of CH_2Cl_2 (50 mL) to the stirred reaction product led to the formation of a suspension. The solid was filtered off, then the solid and the solution were treated as appropriate (vide infra) to obtain compounds **12b** from the solid and compounds **13** and **12a** from the solution.

2.6. Synthesis of compound 6

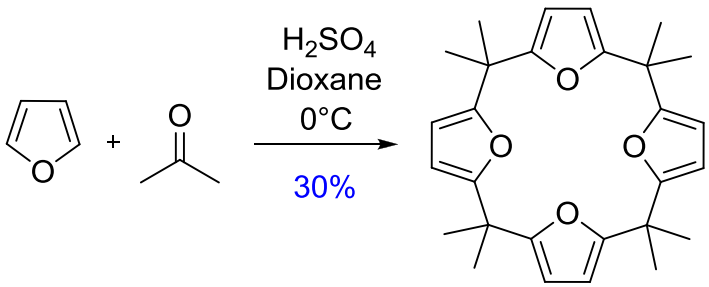

6

A precooled 90.5% sulfuric acid (5 mL) was added dropwise to a stirred precooled (0°C) mixture of acetone (1.46 mL, 20 mmol), furan **(**1.44 mL, 20 mmol), and dioxane (30 mL**).** Upon addition of sulfuric acid, the reaction mixture turned red and some precipitation of product was observed. The reaction mixture was stirred overnight at room temperature, then water (50 mL) was added and the acid was neutralized by a sodium hydroxide aqueous solution (20%). Crude product was filtered off, washed with water (2 x 10 mL**),** methanol (2 x 10 mL) and recrystallized from toluene to give 650 mg (71 % yield) of' colorless needles.

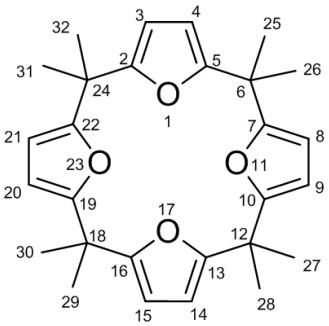

^{1}H NMR ($CDCl_3$, 218K) δ 5.89 (s, 8 H, C-H(3, 4, 8, 9, 14, 15, 20, 21)), 1.48 (s, 24 H, CH_3(25, 26, 27, 28, 29, 30, 31, 32));

^{13}C NMR ($CDCl_3$) δ 158.51 (C(2, 5, 7, 10, 13, 16, 19, 22)), 103.07 (C(3, 4, 8, 9, 14, 15, 20, 21)), 36.55 (C(6, 12, 18, 24)), 25.49 (C(25, 26, 27, 28, 29, 30, 31, 32)).

MS calcd for $C_{35}H_{48}N_4O$ 540.38, found 541.4 (M+H)+,
See additional analyses in "R. Pajewski, R. Ostaszewski and J. Jurczak, *Org. Prep. Proced. Int*. **2000**, *32*, 394".

2.7. Synthesis of macrocycle 12a, 12b and 13

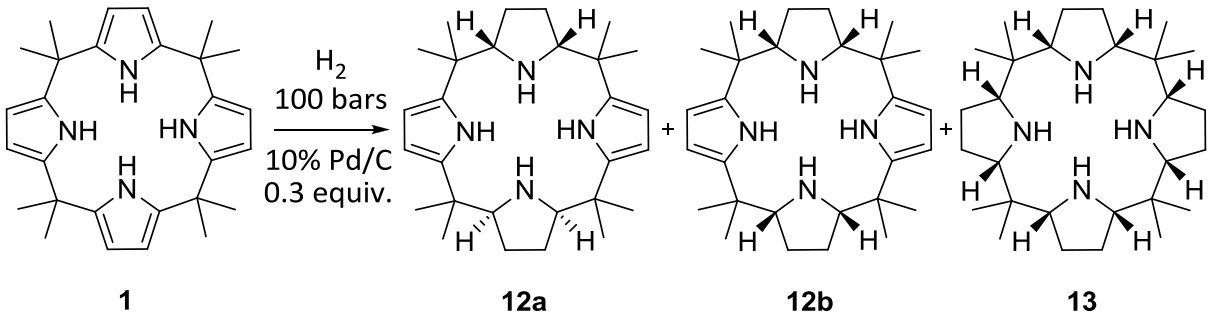

2.7.1. Compound 12b

Compound **12b** was prepared according to the general procedure for the large scale hydrogenation. The precipitate was dissolved in water (30 mL) and NaOH pellets were added until pH 14 was reached, whereupon a white solid was formed. The whole was extracted with CH_2Cl_2 (4 x 30 mL). The organic layers were collected, dried over anhydrous K_2CO_3, and filtered, and then the solvent was evaporated to leave a white solid (0.501 g, 24%), from which 0.489 g (23%) of **12b** was obtained in pure form by crystallization from EtOAc.

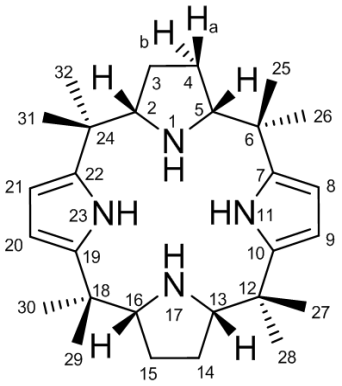

^{1}H NMR ($CDCl_3$, 298K) δ 9.70 (bs, 2 H, N-H(11, 23)), 5.79 (d, ^{4}J(8, 11) = ^{4}J(9, 11) and ^{4}J(20, 23) = ^{4}J(21, 23) = 2.6 Hz, 2 H, pyrrolic-H(8, 9, 20, 21)), 3.11-3.04 (m, 4 H, H(2, 5, 13, 16)), 1.76-1.66 (m, 4 H, CH_2(3a, 4a, 14a, 15a)), 1.66 (bs, 2 H, N-H(1, 17)), 1.58-1.49 (m, 4 H, CH_2(3b, 4b, 14b, 15b)), 1.25 (s, 12 H, CH_3(25, 27, 29, 31)), 1.24 (s, 12 H, CH_3(26, 28, 30, 32));

^{13}C NMR ($CDCl_3$) δ 138.48 (C(7, 10, 19, 22)), 102.64 (C(8, 9, 20, 21)), 68.54 (C(2, 5, 13, 16)), 37.26 (C(6, 12, 18, 24)), 28.28 (C(25, 27, 29, 31)), 26.45 (C(3, 4, 14, 15)), 23.32 (C(26, 28, 30, 32)). MS calcd for $C_{28}H_{44}N_4$ 436.36, found 437.27 (M+H)+.
Additional analysis is available in the thesis of V. Blangy

2.7.2. Compound 12a

Compound **12a** was prepared according to the general procedure for the large scale hydrogenation. The filtered solution obtained following the precipitation of compound **13** (see the above procedure) was concentrated to remove CH2Cl2. Further EtOAc (5 mL) was then added, whereupon compound **12a** precipitated. Alternatively, the previous filtered solution

could be submitted to column chromatography on neutral alumina eluting with a CH2Cl2/MeOH mixture (99:1) to give 80 mg (2%) of pure **12a**.

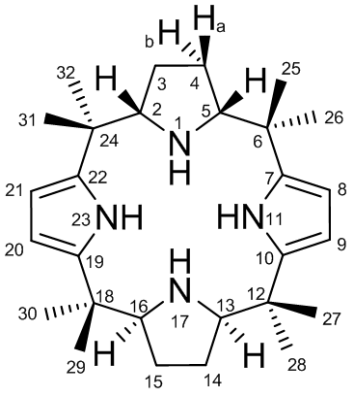

^{1}H NMR (CDCl$_3$, 298K) δ 9.77 (bs, 2 H, N-H(11, 23)), 5.79 (d, ^{4}J(8, 11) = ^{4}J(9, 11) and ^{4}J(20, 23) = ^{4}J(21, 23) = 2.6 Hz, 2 H, pyrrolic-H(8, 9, 20, 21)), 3.11-3.04 (m, 4 H, H(2, 5 ,13, 16)), 1.76-1.66 (m, 6 H, CH(23a, 4a, 14a, 15a)), 1.66 (bs, 2 H, N-H(1, 17)), 1.48-1.39 (m, 4 H, CH(23b, 4b, 14b, 15b)), 1.25 (s, 12 H, CH_3(25, 27, 29, 31)), 1.22 (s, 12 H, CH_3(26, 28, 30, 32));

^{13}C NMR (CDCl3) δ 138.48 (C(7, 10, 19, 22)), 102.64 (C(8, 9, 20, 21)), 68.54 (C(2, 5, 13, 16)), 37.26 (C(6, 12, 18, 24)), 28.28 (C(25, 27, 29, 31)), 26.45 (C(3, 4, 14, 15)), 23.32 (C(26, 28, 30, 32)). MS calcd for $C_{28}H_{44}N_4$ 436.36, found 437.27 (M+H)+.
Additional analysis is available in the thesis of V. Blangy

2.7.3. Compound 13

Compound **13** was prepared according to the general procedure for the large scale hydrogenation. The previously obtained filtered solution was treated with 10% aqueous Na_2CO_3 (4 x 20 mL) and brine (50 mL). Extraction with CH_2Cl_2 (4 x 30 mL) and standard work-up gave a yellow oil, from which a solid precipitated upon addition of EtOAc. Filtration afforded 0.164 g (8%) of compound **13** as a white solid. Alternatively, **13** could be purified by column chromatography on neutral alumina eluting with CH_2Cl_2/EtOAc mixtures (0–100% gradient of CH_2Cl_2).

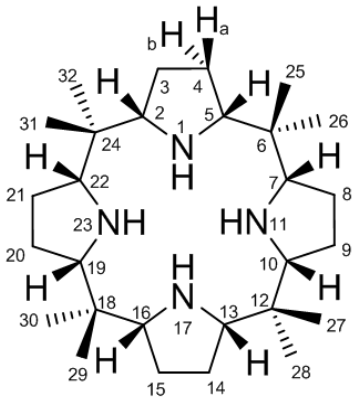

^{1}H NMR ($CDCl_3$, 298K) δ 2.87-2.77 (m, 8 H, C-H(2, 5, 7, 10, 13, 16, 19, 22)), 2.13-2.05 (m, 4 H, N-H(1, 11, 17, 23)), 1.56-1.48 (m, 8 H, CH_2(3a, 4a, 8a, 9a, 14a, 15a, 20a, 21a)), 1.32-1.22 (m, 8 H, CH_2(3b, 4b, 8b, 9b, 14b, 15b, 20b, 21b)), 0.78 (s, 12 H, CH_3(25, 27, 29, 31)), 0.73 (s, 12 H, CH_3(26, 28, 30, 32)).

^{13}C NMR ($CDCl_3$) δ 70.64 (C(2, 5, 7, 10, 13, 16, 19, 22)), 38.47 (C(6, 12, 18, 24)), 26.91 (C(3, 4, 8, 9, 14, 15, 20, 21)), 26.30 (C(25, 27, 29, 31)), 11.31 (C(26, 28, 30, 32)). MS calcd for $C_{28}H_{52}N_4$ 444.42, found 445.5 (M+H)+.
Additional analysis is available in the thesis of V. Blangy

X-ray: Suitable crystals of compound **13** were obtained as colourless rods by slow evaporation of a solution in methanol. The intensity data were collected at 173K on a Stoe Image Plate Diffraction System [1] using MoKα graphite monochromated radiation. Image plate distance 70mm, ϕ oscillation scans 0 - 200°, step Δϕ = 1.0°, exposure time 5 mins, 2θ range 3.27 – 52.1°, d_{min} – d_{max} = 12.45 - 0.81 Å.
The structure was solved by Direct methods using the program SHELXS-97 [2]. The refinement and all further calculations were carried out using SHELXL-97 [2].
The NH H-atoms could not be located in a difference electron-density map and were therefore included in the equatorial position and refined with distance restraints: N-H = 0.88(2) Å and U_{iso}(H) = 1.5U_{eq}(N). The C-bound H-atoms were included in calculated positions and treated as riding atoms using SHELXL default parameters: C-H = 1.0, 0.99 and 0.98 Å for CH, CH_2 & CH_3 H-atoms, respectively, with U_{iso}(H) = k × U_{eq}(C), where k = 1.2 for CH & CH_2, and 1.5 for CH_3, H-atoms. The non-H atoms were refined anisotropically, using weighted full-matrix least-squares on F^2.

An empirical absorption correction was applied using the MulscanABS routine in PLATON [3]; transmission factors: T_{min}/T_{max} = 0.9373/1.1146.

The crystal diffracted very weakly beyond ca. 40° in 2θ, hence in the final cycles of refinement the 2θ limit was restricted to 45°. The high R_{int} and final R values are in part due to the poor quality of the crystal. A small residual electron density peak was observed near a nitrogen atom.

[1] Stoe & Cie (2000). IPDS-I Bedienungshandbuch. Stoe & Cie GmbH, Darmstadt, germany.

[2] G. M. Sheldrick. (2008). Acta Cryst. A64, 112-122.

[3] Spek, A. L. (2003). J. Appl. Cryst. 36, 7-13.

Drawing programs:

ORTEP-3: [3] Farrugia, L. J. (1997). J. Appl. Cryst., 30, 565.

Mercury: [4] Macrae, C. F., Edgington, P. R., McCabe, P., Pidcock, E., Shields, G. P., Taylor, R., Towler, M. & van de Streek, J. (2006). J. Appl. Cryst. 39, 453-457.

PLATON: [5] Spek, A. L. (2003). J. Appl. Cryst. 36, 7-13.

Compound **13** crystallized as a racemate in the centrosymmetric monoclinic space group $P2_1/c$ (No. 14). Two of the pyrrolidine rings, involving atoms N2 and N4, have envelope conformations with the N-atoms at the flap. The other two pyrrolidine rings, involving atoms N1 and N3, have twisted conformations; on bonds C12-N1 and N3-C6, respectively.

2.8. Synthesis of compound 24*

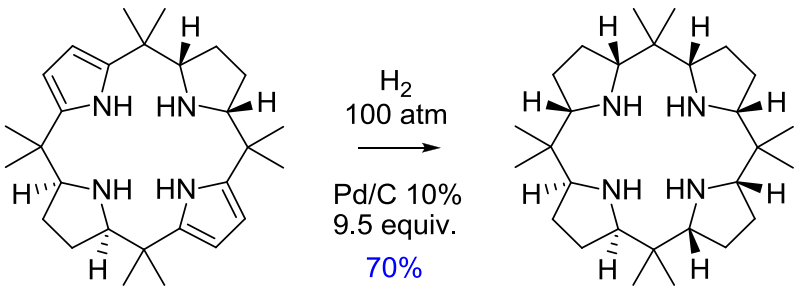

12a **24**

Compound **12a** (50 mg, 0.11 mmol) and 10% Pd/C (1.16 g, 1 mmol of Pd) were placed in an autoclave vessel containing AcOH (25 mL). The reaction mixture was kept under a hydrogen pressure of 100 atm at 100 °C. After 24 h, the autoclave was cooled to room temperature and the reaction mixture was filtered through a pad of celite, which was washed with AcOH (2x20

mL) and CH_2Cl_2 (3 x 25 mL). The combined filtrate and washings were concentrated under reduced pressure to give a colorless slurry, to which CH_2Cl_2 (25 mL) and 5% aqueous NaOH (15 mL) were added. The resulting mixture was stirred for 5 min. The organic layer was then separated and the aqueous phase was extracted with CH_2Cl_2 (3 x 20 mL). The collected organic layers were washed with brine (25 mL), dried over K_2CO_3, and concentrated under reduced pressure. The residue was purified by column chromatography (Al_2O_5, CH_2Cl_2/MeOH, 98/2) to give 35 mg of a white solid.

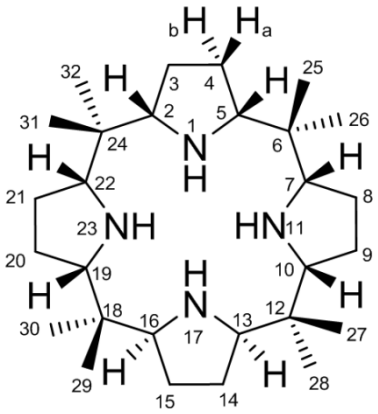

IR (KBr): 2963.1*s*, 2870.6*m*, 1467.0*m*, 1425.0*w*, 1383.7*m*, 1287.0*w*, 1258.0*w*, 1114.1*m*.

^{1}H NMR ($CDCl_3$, 233K) δ 9.21 (bs, 2H, NH), 5.66 (bs, 2H, NH), 4.21 (bs, 2 H, C-H), 3.54 (bs, 2 H, C-H), 2.89 (bs, 2 H, C-H), 2.63 (bs, 2 H, C-H), 2.07-1.94 (m, 8 H, CH_2), 1.77-1.66 (m, 8 H, CH_2), 1.40 (s, 6 H, CH_3), 1.30 (s, 6 H, CH_3), 1.92 (s, 6 H, CH_3), 1.85 (s, 6 H, CH_3);

^{13}C NMR ($CDCl_3$) δ 73.26 (CαN), 71.13 (CαN), 70.07 (CαN), 62.00 (CαN), 38.22 and 37.49 (C(quat.)), 27.52 (CH_3), 27.15 (CH_3), 26.40 (CH_2), 26.00 (CH_2), 24.67 (CH_2), 23.68 (CH_2), 21.75 (CH_3), 12.70 (CH_3).

Melting point: 127°C.

HRMS calcd. for $C_{28}H_{52}N_4H^+$ 445.4265, found 445.4262.

2.9. Synthesis of compound 25*

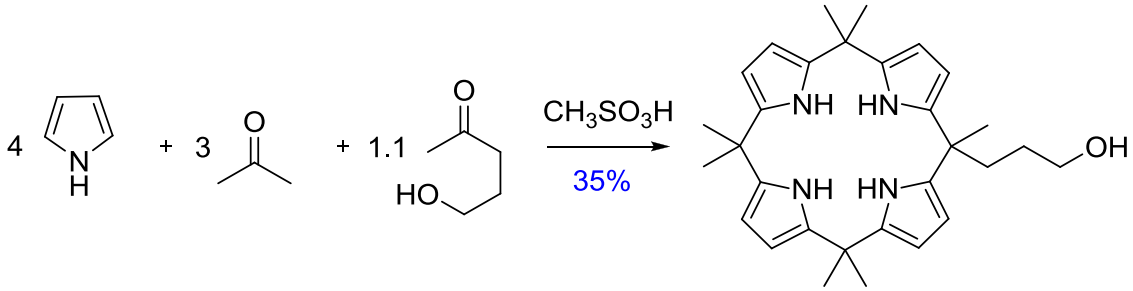

25

In a round-bottom flask were introduced pyrrole (10.3 mL, 0.149 mol), acetone (8.22 mL, 0.112 mol) and 5-hydroxy-2-pentanone (44 mL, 0.035 mol). The flask was equipped with a stirring bar and a reflux condenser. The mixture was stirred for 5 minutes at 0°C, then methane sulfonic acid (0.0745 mL, 11.5 mmol) was added and the mixture was stirred for an additional 15 minutes. After stirring, CH_2Cl_2 was added and the reaction mixture was basified with 5% sodium hydroxide and washed with saturated brine. The aqueous layer was extracted three times with CH_2Cl_2. The combined organic layers were dried with sodium sulfate, and the solvent was removed under vacuum. The residue was purified by column chromatography (SiO_2, Cyclohexane/EtOAc, 7/3) to yield 5.8 g (35%) of colorless powder.

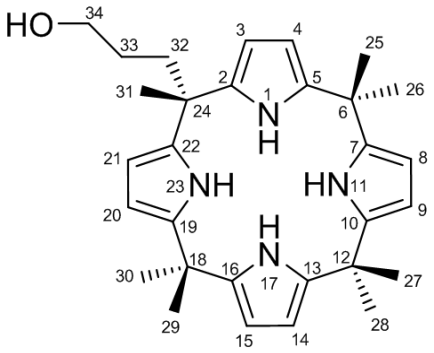

IR (KBr): 3450.6*m*, 3423.1*m*, 3405.0*m*, 3320.0*w*, 2969.2*m*, 2930.1*w*, 2867.59*w*, 768.4*s*. MS calcd for $C_{30}H_{40}N_4O$ 472.66, found 473.3 (M+H+), found 495.3 (M+Na)+.

^{1}H NMR ($CDCl_3$, 298K) δ 7.01 (bs, 4 H, N-H(1, 11, 17, 23)), 5.90 (m, 8 H, pyrrolic-H(3, 4, 8, 9, 14, 15, 20, 21)), 3.52 (td, ^{3}J(34, 33) = 6.3 Hz, ^{3}J(34, OH) = 5.4 Hz, 2 H, CH_2(34)), 1.93-1.89 (m, 2 H, CH_2(32)), 1.51 (s, 12 H, CH_3(25, 26, 29, 30)), 1.50 (s, 6 H, CH_3(27, 28)), 1.45 (s, 3 H, CH_3(31)), 1.43-1.38 (m, 2 H, CH_2(33)), 1.10 (t, ^{3}J(OH, 34) = 5.4 Hz, 1 H, OH);

^{13}C NMR ($CDCl_3$) δ 138.68 and 138.53 (C(5, 7, 10, 13, 16, 19)), 137.26 (C(2)), 137.11 (C(22)), 103.98 and 102.99 (C(3, 4, 8, 9, 14, 15, 20, 21)), 63.28 (C(34)), 38.73 (C(24)), 36.76 (C(32)), 35.35 (C(6, 12, 18)), 29.45 and 29.22 (C(25, 26, 27, 28, 29, 30)), 27.94 (C(33)), 26.48 (C(31)).

Melting point: 228°C.

HRMS calcd. for $C_{30}H_{40}N_4O+Na^+$ 495.3100, found 495.3091.

2.10. Synthesis of compound 21

Compound **21** was isolated as impurity in calix[4]pyrrole by column chromatography (Al_2O_3, Cyclohexane/EtOAc, 9/1).

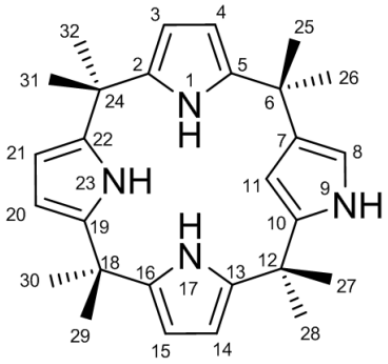

IR (KBr): 3443.9*s*, 2968.1*s*, 2929.8*m*, 2868.1*w*, 1715.6*m*, 1577.3*s*, 1412.9*m*, 1358.8*m*, 1230.4*m*, 1043.4*m*, 962.3*w*, 763.8*s*, 726.5*m*, 699.3*m*, 514.2*w*.

^{1}H NMR (CD_3CN, 298K) δ 8.67 (bs, 1 H, NH9), 8.34 (bs, 1 H, NH(23)), 7.56 (bs, 1 H, NH(1 or 7)), 7.53 (bs, 1 H, NH(1 or 7)), 6.44 (dd, ^{3}J(8, 9) = 2.5 Hz, ^{4}J(8, 11) = 2.0 Hz, 1 H, C-H(8)), 5.86 (dd, ^{3}J(20, 21) = 3.3 Hz, ^{4}J(20, 23) = 2.8 Hz, 1 H, C-H(20 or 21)), 5.84 (dd, ^{3}J(20, 21) = 3.3 Hz, ^{4}J(20, 23) = 2.8 Hz, 1 H, C-H(20 or 21)), 5.79 (dd, ^{3}J = 3.2 Hz, ^{4}J = 2.8 Hz, 1 H, C-H(pyrrole)), 5.74 (m, 3 H, C-H(pyrrole)), 5.18 (dd, ^{3}J(11, 9) = 2.8 Hz, ^{3}J(11, 8) = 1.9 Hz, 1 H, C-H(11)), 1.53 (s, 12 H, CH_3), 1.48 (s, 6 H, CH_3), 1.45 (s, 6 H, CH_3);

^{13}C NMR (CD_3CN) δ 140.70, 139.44 138.85, 138.52, 138.37, 138.07, 137.96 and 132.46 (Cquat), 111.45 (C(8)), 103.27, 103.21, 103.18, 101.89, 101.59, 101.41 and 101.10

(C(pyrrole)), 34.87, 34.79, 34.07 (C(6, 12, 18, 24)), 29.30 (CH_3), 28.44 (CH_3), 28.19 (CH_3), 27.74 (CH_3).

HRMS calcd. for $C_{28}H_{36}N_4Na^+$ 451.2832, found 451.2837.

2.11. Synthesis of compound 27 (4,4-di(1'H-pyrrol-2'-yl)pentan-1-ol)

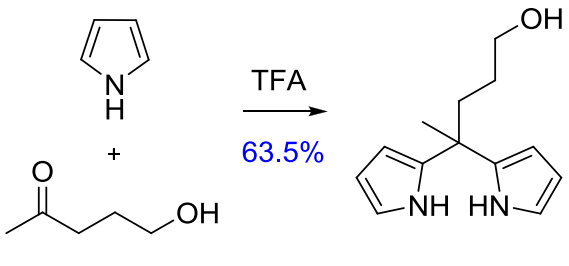

27

In a round-bottom flask were introduced pyrrole (34.88 mL, 0.5 mol) and 5-hydroxypentan-2-one (7.36 mL, 68.5 mmol). The flask was equipped with a stirring bar. The mixture was stirred for 5 minutes, then trifluoroacetic acid (0.52 mL, 6.85 mmol) was added and the mixture was stirred for an additional 15 minutes. After stirring, CH_2Cl_2 was added and the reaction mixture was basified with 5% sodium hydroxide and washed with saturated brine. The aqueous layer was extracted two times with CH_2Cl_2. The combined organic layers were dried with sodium sulfate, and the solvent was removed under vacuum. The residue was purified by column chromatography (SiO_2, Cyclohexane/EtOAc, 1/1) to yield 9.4 g (63.5%) of pale yellow crystals.

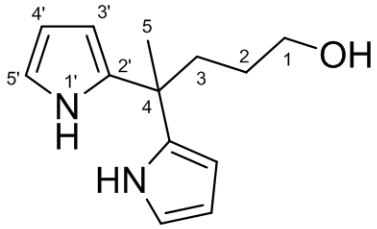

^{1}H NMR ($CDCl_3$, 298K) δ 7.85 (bs, 2 H, N-H(1')), 6.63-6.61 (ddd, ^{3}J(2', 1') = 2.7 Hz, ^{3}J(2', 3') = 2.7 Hz, ^{4}J(2', 4') = 1.6 Hz, 2 H, pyrrolic-H(5')), 6.15-6.13 (ddd, ^{3}J(3', 4') = 3.3 Hz, ^{3}J(2', 3') = 2.7 Hz, ^{4}J(2', 1') = 1.6 Hz, 2 H, pyrrolic-H(4')), 6.10-6.08 (ddd, ^{3}J(4', 3') = 3.3 Hz, ^{3}J(4', 2') = 1.6 Hz, ^{3}J(4', 1') = 1.6 Hz, 2 H, pyrrolic-H(3')), 3.61-3.57 (td, ^{3}J(1, 2) = 6 Hz, ^{3}J(1, OH) = 5 Hz, 2 H, CH_2(1)), 2.07-2.03 (m, 2 H, CH_2(3)), 1.59 (s, 3 H, CH_3(5)), 1.51-1.43 (m, 2 H, CH_2(2)), 1.24-1.20 (t, ^{3}J(1, OH) = 5 Hz, 1 H, OH);

^{13}C NMR ($CDCl_3$) δ 137.97 (C(2')), 117.15 (C(5')), 107.92 (C(4')), 104.77 (C(3')), 63.26 (C(1)), 39.04 (C(4)), 37.35 (C(3)), 28.01 (C(2)), 26.62 (C(5)).
Melting point : 99°C.

MS calcd. for $C_{13}H_{18}N_2O$ 218.14, found 217.13 (M-H)-.

X-ray: Suitable crystals of **27** were obtained as colorless blocks by slow evaporation of a solution in dichloromethane. The intensity data were collected at 173K (-100°C) on a Stoe Mark II-Image Plate Diffraction System [1] equiped with a two-circle goniometer and using MoKα graphite monochromated radiation. Image plate distance 100mm, ω rotation scans 0 - 180° at ϕ 0°, and 0 – 15.0° at ϕ 90°, step Δω = 1.5°, exposures of 1 mins per image,, 2θ range 2.29 – 59.53°, d_{min} – d_{max} = 17.779 – 0.716 Å.
The structure was solved by Direct methods using the program SHELXS [2]. The refinement and all further calculations were carried out using SHELXL-97 [2].
The OH and NH H-aotms, located in difference electron-density maps, were freely refined. The C-bound H-atoms were included in calculated positions and treated as riding atoms using SHELXL default parameters. The non-H atoms were refined anisotropically, using weighted full-matrix least-squares on F^2.
[1] Stoe & Cie (2004). IPDS-I Bedienungshandbuch. Stoe & Cie GmbH, Germany.
[2] Sheldrick, G. M. (2008) Acta Cryst. A64, 112-122.
[3] Spek, A. L. (2009), Acta Cryst. D65, 148-155.
[4] Macrae, C. F., Edgington, P. R., McCabe, P., Pidcock, E., Shields, G. P., Taylor, R., Towler, M. & van de Streek, J. (2006). J. Appl. Cryst. 39, 453-457.
[5] Westrip, S. P. (2010). J. Appl. Cryst. 43, 920-925.
See additional analyses in "D. Yoon, H. Hwang and C. Lee *Angew. Chem. Int. Ed*., **2002**, *41*, 1757".

2.12. Synthesis of compound 39-41

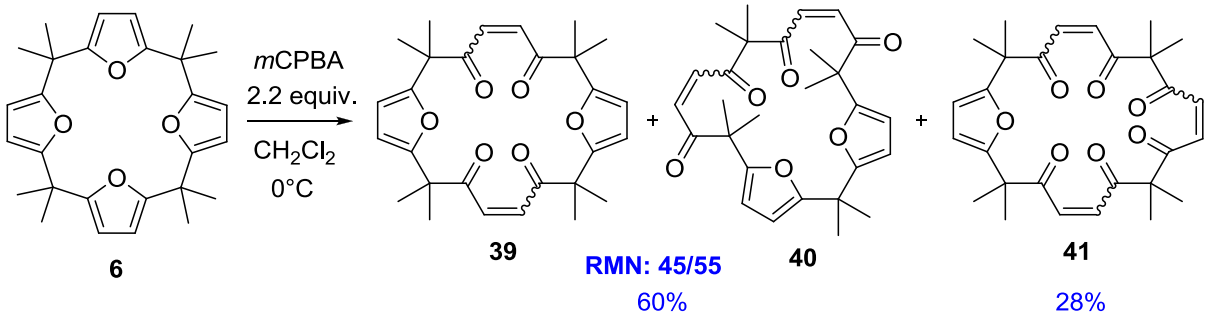

To a magnetically stirred 100-mL round-bottomed flask containing 0.70 g (1.6 mmol) of tetramer **6** dissolved in 45 mL of $CHCl_3$ at 0 °C is added *m*CPBA (0.73 g, 3.52 mmol). The reaction mixture is stirred at 0 °C for 1 h and at 20 °C for an additional 2 h. The crude reaction mixture was extracted with three portions of saturated aqueous $NaHCO_3$, once with saturated aqueous NaCl, and drying of the organic layer anhydrous $NaSO_4$. The solvent is removed in vacuum. The residue was purified by column chromatography (SiO_2, CH_2Cl_2, EtOAc, 9/1) to yield 450 mg (60%) of a mixture containing compound **39** and **40** as yellow crystals, and 219 mg (28%) of compound **41** as yellow crystals.

2.12.1. Compound 39

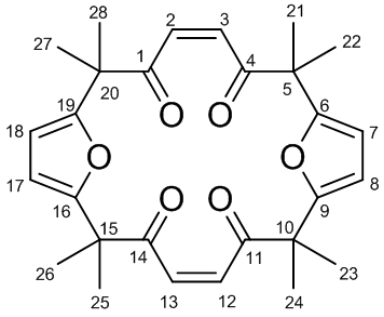

^{1}H NMR ($CDCl_3$, 298K) δ 6.11 (s, 4 H, C-H(7, 8, 17, 18)), 6.08 (s, 4 H, C-H(2, 3, 12, 13)), 1.47 (s, 24 H, CH_3);

^{13}C NMR ($CDCl_3$) δ 202.57 (C(1, 4, 11, 14)), 157.02 (C(6, 9, 16, 19)), 134.29 (C(2, 3, 12, 13)), 107.15 (C(7, 8, 17, 18)), 48.35 (C(5, 10, 15, 20)), 23.25 (CH_3).

MS calcd. for $C_{28}H_{32}O_6$ 464.2, found 487.2 (M+Na)+

See additional analyses in "P. D. Williams and E. LeGoff, *J. Org. Chem.*, 1981, **46**, 4143".

2.12.2. Compound 40

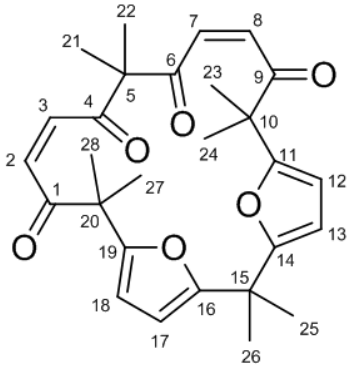

^{1}H NMR ($CDCl_3$, 298K) δ 6.38 (d, ^{3}J(2, 3) = 11.9 Hz, 2 H, C-H(3, 7)), 6.08 (d, ^{3}J(12, 13) and ^{3}J(18, 17) = 3.2 Hz, 2 H, C-H(12, 18)), 5.96 (d, ^{3}J(13, 12) and ^{3}J(17, 18) = 3.2 Hz, 2 H, C-H(13, 17)), 5.79 (d, ^{3}J(2, 3) and ^{3}J(8, 7) = 11.9 Hz, 2 H, C-H(2, 8)), 1.61 (s, 6 H, CH_3(21, 22, or 25, 26)), 1.55 (s, 12 H, CH_3(23, 24, 27, 28)), 1.22 (s, 6 H, CH_3(21, 22, or 25, 26));

^{13}C NMR ($CDCl_3$) δ 206.22 (C(1 or 9)), 197.93 (C(1 or 9)), 159.49 (C(11,19 or 14, 16)), 155.42 (C(11,19 or 14, 16)), 141.37 (C(2, 8 or 3, 7)), 155.42 (C(2, 8 or 3, 7)), 106.70 (C(12, 18 or 13, 17)), 104.53 (C(12, 18 or 13, 17)), 60.68 (C(5 or 15)), 48.88 (C(10, 20)), 37.04 (C(5 or 15)), 29.73 (CH_3), 25.19 (CH_3), 24.07 (CH_3), 20.16 (CH_3).

MS calcd. for $C_{28}H_{32}O_6$ 464.2, found 487.3 (M+Na)+
See additional analyses in "P. D. Williams and E. LeGoff, *J. Org. Chem.*, 1981, **46**, 4143".

2.12.3. Compound 41

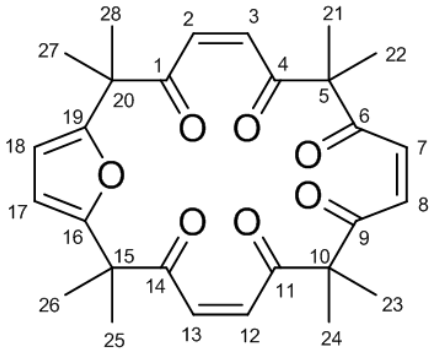

^{1}H NMR ($CDCl_3$, 298K) δ 6.65 (s, 2 H, C-H(7, 8)), 6.50 (d, ^{3}J(2, 3) and ^{3}J(13, 12) = 12.0 Hz, 2 H, C-H(2, 13 or 3, 12)), 6.23 (s, 2 H, C-H(17, 18)), 6.16 (d, ^{3}J(2, 3) and ^{3}J(13, 12) = 12.0 Hz, 2 H, C-H(2, 13 or 3, 12)), 1.46 (s, 12 H, CH_3(21, 22, 23, 24 or 25, 26, 27, 28)), 1.41 (s, 12 H, CH_3(21, 22, 23, 24 or 25, 26, 27, 28));

^{13}C NMR ($CDCl_3$) δ 203.56 (C=O), 202.71 (C=O), 199.78 (C=O), 157.41 (C(16, 19)), 140.20 (C(2, 3 or 12, 13)), 135.13 (C(7, 8)), 128.95 (C(2, 3 or 12, 13)), 107.11 (C(17, 18)), 61.10 (C(5, 10 or 15, 20)), 48.17 (C(5, 10 or 15, 20)), 22.61 (CH_3), 22.33 (CH_3).

MS calcd. for $C_{28}H_{32}O_7$ 580.2, found 503.3 (M+Na)+

See additional analyses in "P. D. Williams and E. LeGoff, *J. Org. Chem.*, 1981, **46**, 4143".

2.13. Synthesis of compound 42 and 43

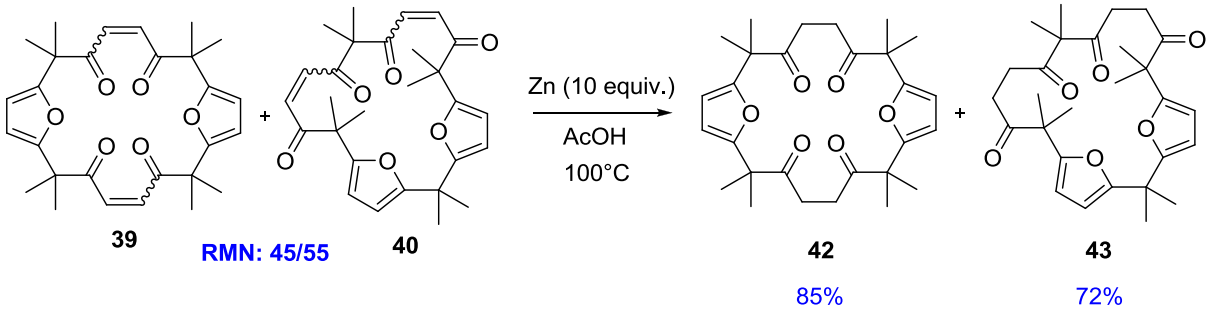

In a 250-mL Erlenmeyer flask is placed 70 mL of glacial acetic acid, in which 1.00 g (2.16 mmol) of a mixture of **39** and **40** is dissolved with heating on a hot plate. The flask is removed from the heat, and while the mixture is still hot, zinc dust (1.4 g, 21.6 mmol) of is added in portions with efficient swirling so as to prevent bumping. The yellow solution turns colorless within seconds, and the contents of the flask are allowed to cool. The excess zinc and precipitated zinc salts are suction filtered and washed with $CHCl_3$. The colorless filtrate is poured into 2 volumes of water, the organic phase removed, and the upper aqueous phase extracted with more $CHCl_3$, (2 x 30 mL). The combined organic layers are washed with water, saturated aqueous $NaHCO_3$, and brine and dried over anhydrous Na_2SO_4. The solvent is removed in vacuum, leaving a colorless solid. The residue was purified by column chromatography (SiO_2, CH_2Cl_2) to yield 927 mg (92%) of a mixture containing compound **42** and **43** as colorless powder. The two compounds were separated by successive washed with 80°C ethanol, yielded 377 mg of **42** (85%) and 400 mg of **43** (72%).

2.13.1. Compound 42

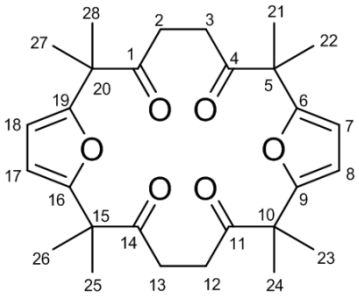

^{1}H NMR ($CDCl_3$, 298K) δ 6.16 (s, 4 H, C-H(7, 8, 17, 18)), 2.45 (s, 8 H, C-H(2, 3, 12, 13)), 1.42 (s, 24 H, CH_3);

^{13}C NMR ($CDCl_3$) δ 209.39 (C(1, 4, 11, 14)), 157.47 (C(6, 9, 16, 19)), 106.44 (C(7, 8, 17, 18)), 48.78 (C(5, 10, 15, 20)), 30.95 (C(2, 3, 12, 13)), 23.05 (CH_3).

MS calcd. for $C_{28}H_{36}O_6$ 468.25, found 491.5 (M+Na)+
See additional analyses in "P. D. Williams and E. LeGoff, *J. Org. Chem.*, 1981, **46**, 4143".

2.13.2. Compound 43

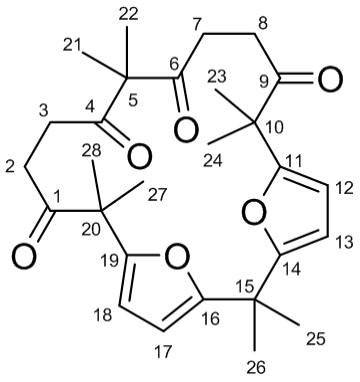

^{1}H NMR ($CDCl_3$, 298K) δ 6.02 (s, 4 H, C-H(12, 13, 17, 18)), 2.58 (m, 4 H, C-H(2, 8 or 3, 7)), 2.43 (m, 4 H, C-H(2, 8 or 3, 7)), 1.54 (s, 6 H, CH_3), 1.42 (s, 12 H, CH_3), 1.29 (s, 6 H, CH_3);

^{13}C NMR ($CDCl_3$) δ 210.04 (C(1, 9, or 4, 6)), 208.15 (C(1, 9, or 4, 6)), 159.18 (C(11, 19 or 14, 16)), 156.10 (C(11, 19 or 14, 16)), 105.99 (C(12, 18 or 13, 17)), 104.40 (C(12, 18 or 13, 17)), 63.4 (C(5)), 48.57 (C(10, 20)), 36.88 (C(15)), 32.14 (C(2, 8 or 3, 7)), 32.11 (C(2, 8 or 3, 7)), 25.76 (CH_3), 23.41 (CH_3), 20.64 (CH_3).

MS calcd. for $C_{28}H_{36}O_6$ 468.25, found 491.5 (M+Na)+

See additional analyses in "P. D. Williams and E. LeGoff, *J. Org. Chem.*, 1981, **46**, 4143".

2.14. Synthesis of compound 35

Compound **35** is poorly described in literature, therefore will be fully characterized here.

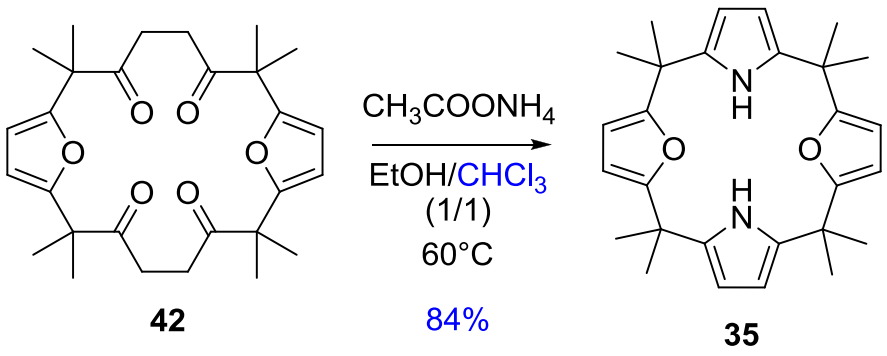

In a round-bottom flask were introduced **42** (440 mg, 0.94 mmol) solubilize in chloroform (10 mL) and ethanol (10 mL). Then, $AcONH_4$ (1.44 g, 18.8 mmol) was added to the solution, and the mixture was heated at 65°C for 24 h. The solvent was partially removed under vacuum and the reaction mixture was filtered off, washed with ethanol and dried under vacuum to yield 340 mg (84%) of **35** as a colorless solid.

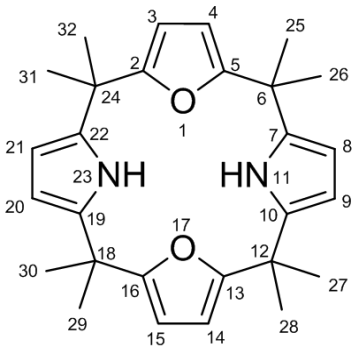

IR (KBr): 3448.3*s*, 2972.7*s*, 2935.4*m*, 1552.9*m*, 1416.8*w*, 1236.3*m*, 1113.4*m*, 1028.0*m*, 954.6*m*, 785.9*m*, 757.6*s*, 725.8*m*, 705.8*s*, 487.1*w*.

^{1}H NMR ($CDCl_3$, 298K) δ 7.19 (bs, 2 H, N-H(11, 23)), 6.04 (s, 4 H, C-H(3, 4, 14, 15)), 5.95 (d, ^{4}J(8, 11) = ^{4}J(9, 11) and ^{4}J(21, 23) = ^{4}J(21, 23) = 2.7 Hz, 4 H, C-H(8, 9, 20, 21)), 1.54 (s, 24 H, CH_3);

^{13}C NMR ($CDCl_3$) δ 159.98 (C(2, 5, 13, 16)), 137.07 (C(7, 10, 19, 22)), 104.25 (C(3, 4, 14, 15)), 102.43 (C(8, 9, 20, 21)), 36.25 (C(6, 12, 18, 24)), 27.90 (CH_3).
Melting point: 231.2°C.

HRMS calcd. for $C_{28}H_{34}N_2O_2Na^+$ 453.2512 found 453.2517

X-ray: Suitable crystals of **35** were obtained as colorless rods by slow evaporation of a solution in dichloromethane. The intensity data were collected at 293K (rt) on a Stoe Image Plate Diffraction System [1] using MoKα graphite monochromated radiation. Image plate distance 70mm, ϕ oscillation scans 0 - 200°, step Δϕ = 1.0°, exposure time 3 mins, 2θ range 3.27 – 52.1°, d_{min} – d_{max} = 12.45 - 0.81 Å. The structure was solved by Direct methods using the program SHELXS-97 [2]. The refinement and all further calculations were carried out using SHELXL-97 [2]. The NH H-atoms were located in a difference Fourier map and freely refined. The C-bound H-atoms were included in calculated positions and treated as riding atoms: C-H = 0.93 and 0.96 Å for CH and CH_3 H-atoms, respectively, with $U_{iso}(H) = k \times U_{eq}(C)$, where k = 1.5 for CH_3 H-atoms, and k = 1.2 for all other H-atoms. The non-H atoms were refined anisotropically, using weighted full-matrix least-squares on F^2. No absorption correction was applied. The crystal diffracted weakly at 2θ greater than 40°.

[1] Stoe & Cie (2004). IPDS-I Bedienungshandbuch. Stoe & Cie GmbH, Germany.
[2] Sheldrick, G. M. (2008) Acta Cryst. A64, 112-122.
[3] Spek, A. L. (2009), Acta Cryst. D65, 148-155.
[4] Macrae, C. F., Edgington, P. R., McCabe, P., Pidcock, E., Shields, G. P., Taylor, R., Towler, M. & van de Streek, J. (2006). J. Appl. Cryst. 39, 453-457.
[5] Westrip, S. P. (2010). J. Appl. Cryst. 43, 920-925.

2.15. Synthesis of compound 36

Compound **36** is poorly described in literature, therefore will be fully characterized here.

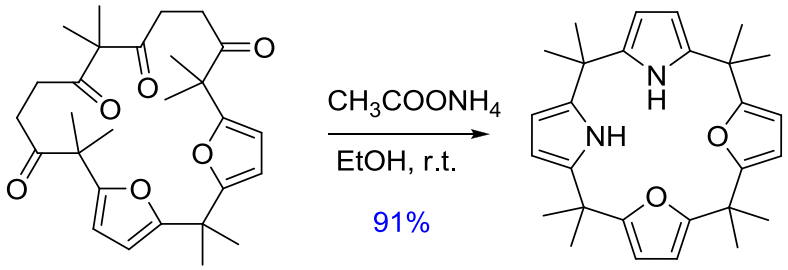

43 **36**

In a round-bottom flask were introduced **43** (500 mg, 0.94 mmol) and ethanol (15 mL). Then, $AcONH_4$ (0.33 g, 4.3 mmol) was added to the slurry, and the mixture was stirred at r.t. for 40 h. The solvent was partially removed under vacuum and the reaction mixture was filtered off, washed with ethanol and dried under vacuum to yield 417 mg (91%) of **36** as a colorless solid.

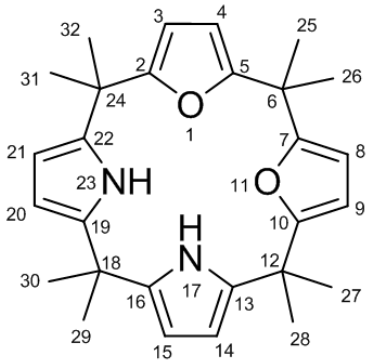

IR (KBr): 3443.1*m*, 2973.2*m*, 2935.1*w*, 1556.4*m*, 1415.2*w*, 1364.1*m*, 1240.4*m*, 1028.4*m*, 954.2*m*, 765.0*m*, 729.8*m*, 706.4*m*.

^{1}H NMR ($CDCl_3$, 298K) δ 6.94 (bs, 2 H, N-H(17, 23)), 5.98 (d, ^{3}J(3, 4) and ^{3}J(9, 8) = 3.1 Hz, 2 H, C-H(3, 9)), 5.95 (d, ^{3}J(4, 3) and ^{3}J(8, 9) = 3.1 Hz, 2 H, C-H(4, 8)), 5.89 (dd, ^{3}J(14, 15) and ^{3}J(21, 20) = 3.0 Hz, ^{4}J(14, 17) and ^{4}J(21, 23) = 2.8 Hz, 2 H, C-H(14, 21)), 5.86 (dd, ^{3}J(15, 14) and ^{3}J(20, 21) = 3.0 Hz, ^{4}J(15, 17) and ^{4}J(20, 23) = 2.8 Hz, 2 H, C-H(15, 20)), 1.50 (s, 24 H, CH_3);

^{13}C NMR ($CDCl_3$) δ 159.08 and 158.94 (C(quat.furan)), 137.97 and 137.82 (C(quat.pyrrole)), 104.37 and 103.58 (C(furan)), 103.09 and 102.00 (C(pyrrole)), 36.73 (C(6 or 18)), 36.08 (C(12, 24)), 35.35 (C(6 or 18)), 29.75 (CH_3), 27.77 (CH_3), 27.61 (CH_3), 25.65 (CH_3).

Melting point: 238.9°C.

MS calcd. for $C_{28}H_{34}N_2O_2$ 430.2, found 453.4 (M+Na)+
HRMS calcd. for $C_{28}H_{34}N_2O_2Na^+$ 453.2512 found 453.2516.

X-ray: Suitable crystals of **36** were obtained as colorless plates by slow evaporation of a solution in dichloromethane. The intensity data were collected at 173K (-100°C) on a Stoe Mark II-Image Plate Diffraction System [1] equiped with a two-circle goniometer and using MoKα graphite monochromated radiation (λ = 0.71073 Å). Image plate distance **140mm,** ω rotation scans 0 - 151° at ϕ 0°, step Δω = 1.0°, exposures of 10 mins per image,
2θ range 1**.64 - 50.53**°, $d_{min} - d_{max}$ = **24.883 - 0.833** Å.

The structure was solved by Direct methods using the program SHELXS-97 [2]. The refinement and all further calculations were carried out using SHELXL-97 [2].
The NH H-atoms were located in difference electron-density maps. In the final cycles of least-squares refinement they was refined with a distance restraint of N-H = 0.87(2) Å and $U_{iso}(H) = 1.2U_{eq}(N)$. The C-bound H-atoms were included in calculated positions and treated as riding atoms: C-H = 0.95 and 0.98 Å for CH(aromatic) and CH_3 H-atoms, respectively, with $U_{iso}(H) = k \times U_{eq}(C)$, where k = 1.2 for CH(aromatic) H-atoms and k = 1.5 for CH_3 H-atoms. The non-H atoms were refined anisotropically, using weighted full-matrix least-squares on F^2. An empirical absorption correction was applied using the MULscanABS routine in PLATON [3]. In the final cycles of refinement, in the absence of significant anomalous scattering effects, the Friedel pairs were merged and Δf ” set to zero.
[1[Stoe & Cie. (2009). *X-Area V1.52 & X-RED32 V1.48 Software*. Stoe & Cie GmbH, Darmstadt, Germany.
[2] Sheldrick, G. M. (2008) Acta Cryst. A64, 112-122.
[3] Spek, A .L. (2009). Acta Cryst. D65, 148-155.
[4] Westrip, S. P. (2010). J. Appl. Cryst. 43, 920-925.

2.16. Synthesis of compound 44*

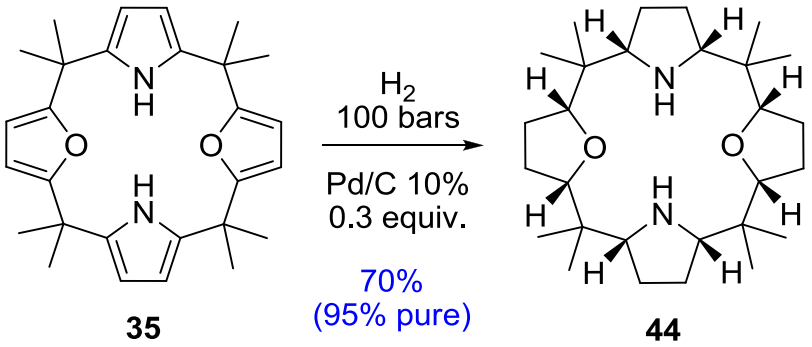

35 **44**

Compound **35** (200 mg, 0.46 mmol) and Pd/C 10% (158 mg, 0.15 mmol) were placed in a test tube (125 x 15 mm) containing a small cross stirring bar. AcOH (5 mL) was added and the test tube was placed inside an autoclave vessel containing AcOH (25 mL). The autoclave was closed, put under magnetic stirring, filled with hydrogen (100 atm), and heated at 100°C for 24 h. After cooling to room temperature, the reaction mixture was filtered through celite and the solid was washed with AcOH (2 x 5 mL) and successively CH_2Cl_2 (5 mL) and EtOAc (5 mL). The combined filtrate and washings were concentrated under reduced pressure to give colorless slurry, to which EtOAc (50 mL) and 5% aqueous NaOH 5% (20 mL) were added. The resulting mixture was stirred for 5 min. The organic layer was then separated and the aqueous phase was extracted with EtOAc (2 x 20 mL). The collected organic layers were washed with brine, dried over K_2CO_3, and concentrated under reduced pressure. The residue was purified first by recrystallization in EtOAc. Then the residue was purified by successive washed with warm THF and finally recrystallized in EtOAc to yield 142 mg (70%) of compound **44**.

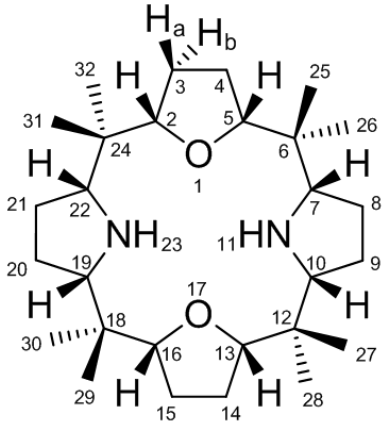

IR (KBr): 3368.3*m*, 2973.5*s*, 2870.4*s*, 2822.5*s*, 2639.8*m*, 1611.4*w*, 1575.0*w*, 1469.0*s*, 1398.6*s*, 1370.2*s*, 1334.5*m*, 1284.7*m*, 1212.1*m*, 1061.6*s*, 932.7*m*, 869.7*m*, 783.4*m*, 529.5*m*.

^{1}H NMR ($CDCl_3$, 218K) δ 3.64 (s, 4 H, C-H(2, 5, 13, 16)), 2.77 (s, 4 H, C-H(7, 10, 19, 22)), 2.32 (m, 2 H, NH(11, 23)), 1.60 (m, 4 H, CH_2(3a, 4a, 14a, 15a)), 1.44 (m, 8 H, CH_2(3b, 4b, 14b, 15b, 8a, 9a, 20a, 21a)), 1.22 (m, 4 H, CH_2(8b, 9b, 20b, 21b)), 0.71 (s, 12 H, CH_3(26, 28, 30, 32)), 0.68 (s, 12 H, CH_3(25, 27, 29, 31));

^{13}C NMR ($CDCl_3$) δ 88.74 (C(2, 5, 13, 16)), 69.97 (C(7, 10, 19, 22)), 38.90 (C(6, 12, 18, 24)), 26.93 (C(3, 4, 14, 15)), 26.52 (C(8, 9, 20, 21)), 25.11 (C(25, 27, 29, 31)), 11.70 (C(26, 28, 30, 32)). ^{1}H NMR ($CDCl_3$, 253K) δ 3.64 (s, 4 H, C-H(2, 5, 13, 16)), 2.79 (s, 4 H, C-H(7, 10, 19, 22)), 2.27 (m, 2 H, NH(11, 23)), 1.63 (m, 4 H, CH_2(3a, 4a, 14a, 15a)), 1.50 (m, 4 H, CH_2(3b, 4b, 14b, 15b)), 1.44 (m, 8 H, CH_2(8a, 9a, 20a, 21a)), 1.26 (m, 4 H, CH_2(8b, 9b, 20b, 21b)), 0.76 (s, 12 H, CH_3(26, 28, 30, 32)), 0.72 (s, 12 H, CH_3(25, 27, 29, 31)); ^{13}C NMR ($CDCl_3$) δ 89.07 (C(2, 5, 13, 16)), 69.82 (C(7, 10, 19, 22)), 38.77 (C(6, 12, 18, 24)), 26.73 (C(3, 4, 14, 15)), 26.08 (C(8, 9, 20, 21)), 25.00 (C(25, 27, 29, 31)), 11.82 (C(26, 28, 30, 32)).

HRMS calcd. for $C_{28}H_{50}N_2O_2H^+$ 447.3945, found 447.3941.

X-ray: Suitable crystals of **44** were obtained as colorless rods by recrystallization from EtOAc. The intensity data were collected at 173K (-100°C) on a Stoe Mark II-Image Plate Diffraction System [1] equiped with a two-circle goniometer and using MoKα graphite monochromated radiation (λ = 0.71073 Å). Image plate distance 130mm, ω rotation scans 0 - 180° at φ 0°, and 0 - 60° at φ = 90°, step Δω = 1.0°, exposures of 10 mins per image, 2θ range 1.76 - 52.59°, d_{min} – d_{max} = 23.107 - 0.802 Å.

The structure was solved by Direct methods using the program SHELXS-97 [2]. The refinement and all further calculations were carried out using SHELXL-97 [2].

Crystal is a non-merohedral TWIN with a 180° rotation about the c axis [batch scale factor, BASF = 0.46390].

The molecule is totally disordered with the N and O positions occupying alternative sites: O1/N3, O2/N4 ,O3/N1 and O4/N2 with occupancies of 0.67295/0.32705, 0.73801/0.26199, 0.68578/0.31422 and 0.711/0.289, respectively.

The NH and CH H-atoms were located in difference Fourier maps and were refined as riding atoms with Uiso(H) = 1.2U_{eq}(N, C). The remainder of the H-atoms were included in calculated positions and treated as riding atoms: C-H = 0.99 and 0.98 Å for CH_2 and CH_3 H

atoms, respectively, with $U_{iso}(H) = 1.2U_{eq}(C)$ for CH_2 H-atoms and = 1.5Ueq(C) for CH_3 H-atoms.

[1] Stoe & Cie. (2009). *X-Area V1.52 & X-RED32 V1.48 Software*. Stoe & Cie GmbH, Darmstadt, Germany.

[2] Sheldrick, G. M. (2008) Acta Cryst. A64, 112-122.

[3] Spek, A .L. (2009). Acta Cryst. D65, 148-155.

[4] Westrip, S. P. (2010). J. Appl. Cryst. 43, 920-925.

2.17. Synthesis of compound 46*

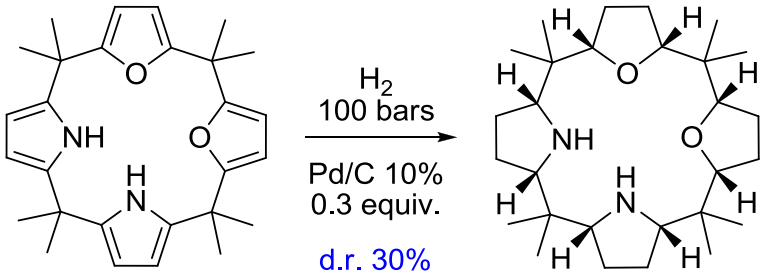

36 **46**

Compound **35** (180 mg, 0.42 mmol) and Pd/C 10% (143 mg, 0.13 mmol) were placed in a test tube (125 x 15 mm) containing a small cross stirring bar. AcOH (5 mL) was added and the test tube was placed inside an autoclave vessel containing AcOH (25 mL). The autoclave was closed, put under magnetic stirring, filled with hydrogen (100 atm), and heated at 100°C for 24 h. After cooling to room temperature, the reaction mixture was filtered through celite and the solid was washed with AcOH (2 x 5 mL) and successively CH_2Cl_2 (5 mL) and EtOAc (5 mL). The combined filtrate and washings were concentrated under reduced pressure to give colorless slurry, to which EtOAc (50 mL) and 5% aqueous NaOH 5% (20 mL) were added. The resulting mixture was stirred for 5 min. The organic layer was then separated and the aqueous phase was extracted with EtOAc (2 x 20 mL). The collected organic layers were washed with brine, dried over K_2CO_3, and concentrated under reduced pressure. The residue was purified by successive recrystallization in EtOAc to yield 21 mg (15%) of compound **46** in 80% purity.

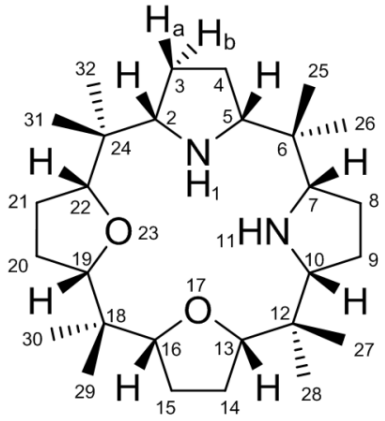

^{1}H NMR ($CDCl_3$, 298K) δ 8.86 (bs, 2 H, NH(1 or 11)), 8.34 (bs, 2 H, NH(1 or 11)), 4.15 (m, 4 H, C-H(13, 16, 19, 22)), 3.39 (m, 4 H, C-H(2, 5, 7, 10)), 2.05 (m, 4 H, CH_2(3a, 4a, 8a, 9a)), 1.95 (m, 4 H, CH_2(3b, 4b, 8b, 9b)), 1.76 (m, 4 H, CH_2(14a, 15a, 20a, 21a)), 1.58 (m, 4 H, CH_2(14b, 15b, 20b, 21b)), 1.36 (s, 12 H, CH_3(26, 28, 30, 32)), 0.86 (s, 12 H, CH_3(25, 27, 29, 31));

^{13}C NMR ($CDCl_3$) δ 85.61 (C(13, 16, 19, 22)), 74.01(C(2, 5, 7, 10)), 39.18 (C(6, 12, 18, 24)), 25.91 (C(14, 15, 20, 21)), 25.67 (C(25, 27, 29, 31)), 23.38 (C(3, 4, 8, 9)), 13.76 (C(26, 28, 30, 32)).

HRMS calcd. for $C_{28}H_{50}N_2O_2H^+$447.3945, found 447.3947 (M+Na)+.

X-ray: Suitable crystals of **46** were obtained as colourless plates by recrystallization from EtOAc. The intensity data were collected at 173K (-100°C) on a Stoe Mark II-Image Plate Diffraction System [1] equiped with a two-circle goniometer and using MoKα graphite monochromated radiation (λ = 0.71073 Å). Image plate distance 130mm, ω rotation scans 0 - 180° at φ 0°, and 0 - 74° at φ 90°, step Δω = 1.0°, exposures of 4 mins per image, 2θ range 1.76 - 52.59°, d_{min} – d_{max} = 23.107 - 0.802 Å.

The structure was solved by Direct methods using the program SHELXS-97 [2]. The refinement and all further calculations were carried out using SHELXL-97 [2].

The NH H-atoms were located in difference Fourier maps and refined with distance restraints (N-H = 0.87(2) Å) and U_{iso}(H) = 1.2U_{eq}(N). The CH H-atoms were also located in a difference Fourier map and were refined isotropically with U_{iso}(H) = 1.2U_{eq}(C). The remainder of the H-atoms were included in calculated positions and treated as riding atoms: C-H = 0.99 and 0.98 Å for CH_2 and CH_3, respectively, with U_{iso}(H) = k × U_{eq}(parent C-atom),

where k = 1.5 for CH_3 H-atoms and k = 1.2 for other H-atoms. The non-H atoms were refined anisotropically, using weighted full-matrix least-squares on F^2.

The molecule is totally disordered with the N and O positions occupying alternative sites: O1/N1, O2/N2 ,O3/N3 and O4/N4 with occupancies of 0.60309/0.39691, 0.55757/0.44243, 0.38804/0.61196 and 0.54532/0.45468, respectively.

[1] Stoe & Cie. (2009). *X-Area V1.52 & X-RED32 V1.48 Software*. Stoe & Cie GmbH, Darmstadt, Germany.

[2] Sheldrick, G. M. (2008) Acta Cryst. A64, 112-122.

[3] Spek, A .L. (2009). Acta Cryst. D65, 148-155.

[4] Westrip, S. P. (2010). J. Appl. Cryst. 43, 920-925.

2.18. Synthesis of compound 7a and 7b

Compound **7a and 7b** are poorly described in literature, therefore they will be fully characterized here.

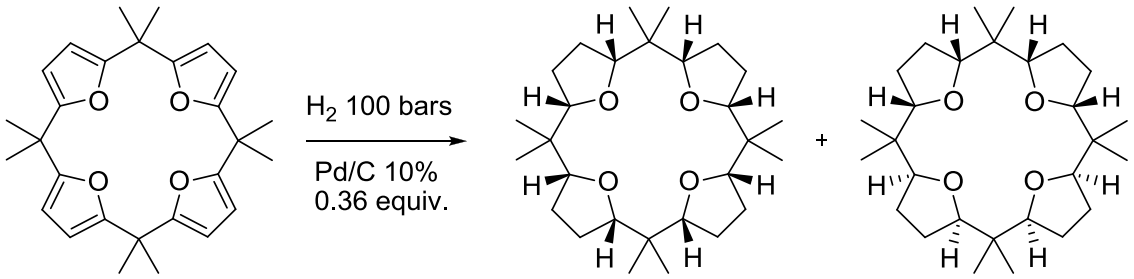

Compound **6** (200 mg, 0.46 mmol) and Pd/C 10% (158 mg, 0.15 mmol) were placed in a test tube (125 x 15 mm) containing a small cross stirring bar. AcOH (5 mL) was added and the test tube was placed inside an autoclave vessel containing AcOH (25 mL). The autoclave was closed, put under magnetic stirring, filled with hydrogen (100 atm), and heated at 100°C for 24 h. After cooling to room temperature, the reaction mixture was filtered through celite and the solid was washed with AcOH (2 x 5 mL) and successively CH_2Cl_2 (2 x 5 mL). The combined filtrate and washings were concentrated under reduced pressure to give colorless slurry, to which CH_2Cl_2 (50 mL) and 5% aqueous NaOH 5% (20 mL) were added. The resulting mixture was stirred for 5 min. The organic layer was then separated and the aqueous phase was extracted with CH_2Cl_2 (2 x 20 mL). The collected organic layers were washed with

brine, dried over K_2CO_3, and concentrated under reduced pressure. The residue was purified by column chromatography (SiO_2, Toluene/cyclohexane 7/3) to yield 68 mg (33%) of compound **7a** and 73 mg (35%) of compound **7b**.

2.18.1. Compound 7a

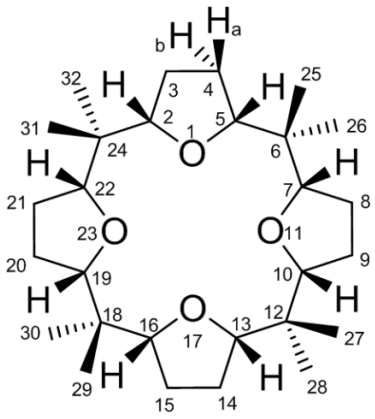

IR (KBr): 2970.7*s*, 2875.5*m*, 2818.7*m*, 1472.5*m*, 1393.3*m*, 1376.0*w*, 1083.8*s*, 1042.5*s*, 980.2*m*, 883.3*m*, 556.3*m*.

^{1}H NMR ($CDCl_3$, 218K) δ 3.95 (m, 4 H, C-H(2, 5, 13, 16)), 3.46 (m, 4 H, C-H(7, 10, 19, 22)), 2.31 (m, 4 H, CH_2(3b, 4b, 14b, 15b)), 1.60 (m, 4 H, CH_2(8a, 9a, 10a, 21a)), 1.56 (m, 4 H, CH_2(3a, 4a, 14a, 15a)), 1.42 (m, 4 H, CH_2(8b, 9b, 10b, 21b)), 0.94 (s, 12 H, CH_3(25, 27, 29, 31)), 0.82 (s, 12 H, CH_3(26, 28, 30, 32));

^{13}C NMR ($CDCl_3$) δ 87.80 (C(7, 10, 19, 22)), 80.47 (C(2, 5, 13, 16)), 39.31(C(6, 12, 18, 24)), 26.69 (C(3, 4, 14, 15)), 26.68 (C(25, 27, 29, 31)), 25.93 (C(8, 9, 10, 21)), 17.55 (C(26, 28, 30, 32)).

Melting point: 191.5.2°C.

HRMS calcd. for $C_{28}H_{48}O_4Na^+$ 471.3445 found 471.3442.

X-ray: Suitable crystals of **7a** were obtained as colorless plates by slow evaporation of a solution in dichloromethane. The intensity data were collected at 173K (-100°C) on a Stoe Mark II-Image Plate Diffraction System [1] equiped with a two-circle goniometer and using MoKα graphite monochromated radiation (λ = 0.71073 Å). Image plate distance 130mm, ω

rotation scans 0 - 180° at ϕ 0° and 0 - 103° at ϕ 90°, step Δω = 1.0°, exposures of 3 mins per image, 2θ range 1.76 - 52.59°, $d_{min} – d_{max}$ = 23.107 - 0.802 Å.

The structure was solved by Direct methods using the program SHELXS-97 [2]. The refinement and all further calculations were carried out using SHELXL-97 [2].

The C-bound H-atoms were included in calculated positions and treated as riding atoms: C-H = 1.0, 0.99, 0.98 Å for CH(methine), CH(methyl) and CH(methylene) H-atoms, respectively, with $U_{iso}(H) = k \times U_{eq}$(parent C-atom), where k = 1.5 for H(methyl) and 1.2 for all other H-atoms. The non-H atoms were refined anisotropically, using weighted full-matrix least-squares on F^2. An empirical absorption correction was applied using the MULscanABS routine in PLATON [3]. The molecular structure and crystallographic numbering scheme are illustrated in Figure 1 (displacement ellipsoids are drawn at the 50% probability level).

[1] Stoe & Cie (2000). IPDS-I Bedienungshandbuch. Stoe & Cie GmbH, Darmstadt, germany.

[2] G. M. Sheldrick. (2008). Acta Cryst. A64, 112-122.

[3] Spek, A. L. (2003). J. Appl. Cryst. 36, 7-13.

[4] Westrip, S. P. (2010). J. Appl. Cryst. 43, 920-925.

Drawing programs:

ORTEP-3: [3] Farrugia, L. J. (1997). J. Appl. Cryst., 30, 565.

Mercury: [4] Macrae, C. F., Edgington, P. R., McCabe, P., Pidcock, E., Shields, G. P., Taylor, R., Towler, M. & van de Streek, J. (2006). J. Appl. Cryst. 39, 453-457.

PLATON: [5] Spek, A. L. (2003). J. Appl. Cryst. 36, 7-13.

2.18.2. Compound 7b

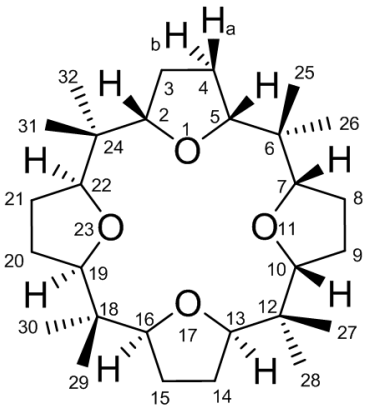

IR (KBr): 2965.7*s*, 2875.0*m*, 2821.6*m*, 1468.9*m*, 1396.4*w*, 1371.3*w*, 1081.6*s*, 995.5*m*, 884.5*m*, 531.5*m*.

^{1}H NMR ($CDCl_3$, 298K) δ 3.74 (dd, ^{3}J(16, 15a) and ^{3}J(7, 8b) = 9.2 Hz, ^{3}J(16, 15b) and ^{3}J(7, 8a) = 6.8 Hz, , 2 H, C-H(7, 16)), 3.57 (dd, ^{3}J(10, 9b) and ^{3}J(13, 14a) = 9.8 Hz, ^{3}J(10, 9a) and ^{3}J(13, 14b) = 6.5 Hz, 2 H, C-H(10, 13)), 3.37 (dd, ^{3}J(19, 20a) and ^{3}J(5, 4b) = 9.4 Hz, ^{3}J(19, 20b) and ^{3}J(5, 4a) = 6.7 Hz, 2 H, C-H(5, 19)), 3.26 (dd, ^{3}J(2, 3b) and ^{3}J(22, 21a) = 11.4 Hz, ^{3}J(2, 3a) and ^{3}J(22, 21b) = 4.2 Hz, 2 H, C-H(2, 22)), 2.31 (m, 2 H, CH_2(20, 4)), 1.97 (quint., ^{3}J(3b, 2) and ^{3}J(21a, 22) = 11.2 Hz, ^{3}J(3b, 3a) and ^{3}J(21a, 21b) = 11.2 Hz, ^{3}J(3b, 4) and ^{3}J(21a, 20) = 11.2 Hz, 2 H, CH_2(3b, 21a)), 1.65 (m, 2 H, CH_2(8, 15)), 1.59 (m, 2 H, CH_2(3a, 21b)), 1.58 (m, 2 H, CH_2(9, 14)), 1.50 (m, 2 H, CH_2(8, 15)), 1.44 (m, 2 H, CH_2(20, 4)), 1.40 (m, 2 H, CH_2(9, 14)), 1.05 (s, 6 H, CH_3(31, 32)), 0.92 (s, 6 H, CH_3(25, 30)), 0.81 (s, 6 H, CH_3(26, 29)), 0.73 (s, 6 H, CH_3(27, 28));

^{13}C NMR ($CDCl_3$) δ 88.12 (C(2, 22)), 87.33 (C(5, 19)), 82.81 (C(10, 13)), 80.22 (C(7, 16)), 38.08 (C(6, 18)), 37.90 (C(24)), 37.82 (C(12)), 27.42 (C(4, 20)), 27.16 (C(31, 32)), 26.27 (C(25, 30)), 26.11 (C(3, 21)), 25.92 (C(8, 15)), 23.93 (C(9, 14)), 17.73 (C(26, 29)), 17.33 (C(27, 28)).

Melting point: 197.4°C.

HRMS calcd. for $C_{28}H_{48}O_4Na^+$ 471.3445 found 471.3443

X-ray: Suitable crystals of **7b** were obtained as colorless plates by slow evaporation of a solution in dichloromethane. The intensity data were collected at 173K (-100°C) on a Stoe Mark II-Image Plate Diffraction System [1] equiped with a two-circle goniometer and using MoKα graphite monochromated radiation (λ = 0.71073 Å). Image plate distance 130mm, ω rotation scans 0 - 180° at ϕ 0° and 0 - 180° at ϕ 90°, step Δω = 1.2°, exposures of 9 mins per image, 2θ range 1.76 - 52.59°, d_{min} – d_{max} = 23.107 - 0.802 Å.

The structure was solved by Direct methods using the program SHELXS-97 [2]. The refinement and all further calculations were carried out using SHELXL-97 [2].

The C-bound H-atoms were included in calculated positions and treated as riding atoms: C-H = 1.0, 0.99, 0.98 Å for CH(methine), CH(methyl) and CH(methylene) H-atoms, respectively, with U_{iso}(H) = k × U_{eq}(parent C-atom), where k = 1.5 for H(methyl) and 1.2 for all other H-atoms. The non-H atoms were refined anisotropically, using weighted full-matrix least-squares on F^2. An empirical absorption correction was applied using the MULscanABS

routine in PLATON [3]. In the final cycles of least-squares refinement the 2θ limit was held at 45˚; the crystal diffracted weakly beyond 20˚ in 2θ, despite exposures of 9 min per image, and for this reason a high R_{int} value > 0.10 was observed.

[1] Stoe & Cie (2000). IPDS-I Bedienungshandbuch. Stoe & Cie GmbH, Darmstadt, germany.

[2] G. M. Sheldrick. (2008). Acta Cryst. A64, 112-122.

[3] Spek, A. L. (2003). J. Appl. Cryst. 36, 7-13.

[4] Westrip, S. P. (2010). J. Appl. Cryst. 43, 920-925.

Drawing programs:

ORTEP-3: [3] Farrugia, L. J. (1997). J. Appl. Cryst., 30, 565.

Mercury: [4] Macrae, C. F., Edgington, P. R., McCabe, P., Pidcock, E., Shields, G. P., Taylor, R., Towler, M. & van de Streek, J. (2006). J. Appl. Cryst. 39, 453-457.

PLATON: [5] Spek, A. L. (2003). J. Appl. Cryst. 36, 7-13.

2.19. Synthesis of compound 47* and 48

Compound **47** is poorly described in literature, therefore it will be fully characterized here.

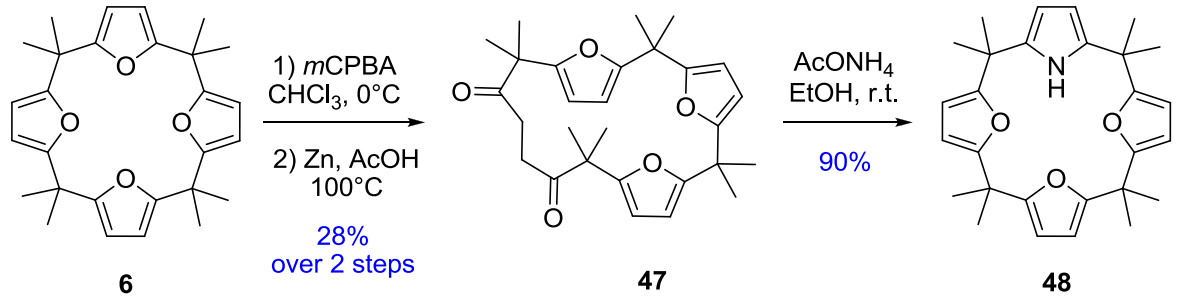

2.19.1. Compound 47*

To a magnetically stirred 100-mL round-bottomed flask containing 0.5 g (1.1 mmol) of tetramer **6** dissolved in 30 mL of $CHCl_3$ at 0 °C is added *m*CPBA (0.57 g, 1.21 mmol). The reaction mixture is stirred at 0 °C for 1 h and at 20 °C for an additional 2 h. The crude reaction mixture was extracted with three portions of saturated aqueous $NaHCO_3$, once with saturated aqueous NaCl, and drying of the organic layer anhydrous $NaSO_4$. The solvent is removed in vacuum. The residue was submitted to the next step without further purification. In a 250-mL Erlenmeyer flask is placed 40 mL of glacial acetic acid, in which the residue is dissolved with heating on a hot plate. The flask is removed from the heat, and while the mixture is still hot, of zinc dust (1 g, 11 mmol) is added in portions with efficient swirling so

as to prevent bumping. The yellow solution turns colorless within seconds, and the contents of the flask are allowed to cool. The excess zinc and precipitated zinc salts are suction filtered and washed with $CHCl_3$. The colorless filtrate is poured into 2 volumes of water, the organic phase removed, and the upper aqueous phase extracted with more $CHCl_3$, (2 x 15 mL). The combined organic layers are washed with water, saturated aqueous $NaHCO_3$, and brine and dried over anhydrous Na_2SO_4. The solvent is removed in vacuum, leaving a colorless solid. The residue was purified by column chromatography (SiO_2, cyclohexane/EtOAc 9/1) to yield 143 mg (28%) of compound **47** as a colorless powder.

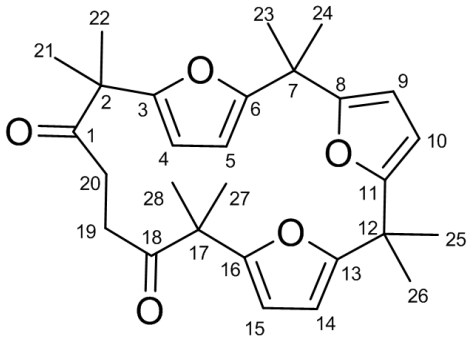

IR (KBr): 3420.6*bs*, 2978.3*m*, 2937.4*m*, 1711.4*s*, 1552.0*m*, 1469.8*m*, 1260.3*m*, 1022.37*m*, 954.6*m*, 778.7*m*, 709.64*w*.

^{1}H NMR ($CDCl_3$, 298K) δ 6.02 (s, 2 H, C-H(furan)), 6.01 (s, 1 H, C-H(furan)), 2.17 (s, 4 H, CH_2(19, 20)), 1.55 (s, 12 H, CH_3(23, 24, 25, 26)), 1.37 (s, 12 H, CH_3(21, 22, 27, 28));

^{13}C NMR ($CDCl_3$) δ 210.44 (C=O), 159.76 (C(quat.furan)), 158.09 (C(quat.furan)), 155.68 (C(quat.furan)), 106.30 (C(furan)), 104.81 (C(furan)), 104.29 (C(furan)), 49.05 (C(meso)), 36.97 (C(meso)), 32.06 (C(19, 20)), 25.76 (C(23, 24, 25, 26)), 22.86 (C(21, 22, 27, 28)).

Melting point: 106.8°C.

MS calcd. for $C_{28}H_{34}O_5$ 450.24, found 473.4 (M+Na)+.
HRMS calcd. for $C_{28}H_{34}O_5Na^+$ 473.2298 found 473.2291(M+Na)+.

2.19.2. Compound 48

In a round-bottom flask were introduced **47** (130 mg, 0.29 mmol) and ethanol (3 mL). Then, $AcONH_4$ (35 mg, 0.43 mmol) was added to the slurry, and the mixture was stirred at r.t. for

40 h. The solvent was partially removed under vacuum and the reaction mixture was filtered off, washed with ethanol and dried under vacuum to yield 112 mg (90%) of **48** as a colorless solid.

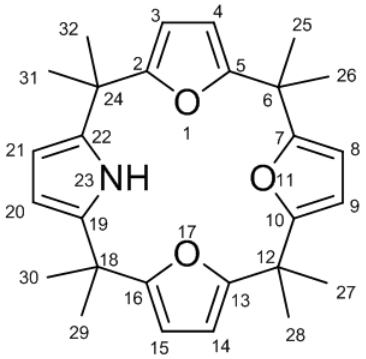

IR (KBr): 3445.5*m*, 2973.2*m*, 2936.4*w*, 1557.3*m*, 1449.8*w*, 1364.1*m*, 1262.8*m*, 1027.9*m*, 955.1*m*, 778.3*m*, 760.0*m*, 731.3*m*, 706.7*m*.

^{1}H NMR ($CDCl_3$, 298K) δ 7.44 (bs, 1 H, N-H(23)), 5.98 (m, 6 H, C-H(furan)), 5.82(d, ^{4}J(20, 23) = ^{4}J(21, 23) = 2.7 Hz, 2 H, C-H(20, 21)), 1.55 (s, 12 H, CH_3), 1.52 (s, 12 H, CH_3);
^{13}C NMR ($CDCl_3$) δ 159.34, 159.26, 158.48 and 137.71 (C(quat.pyrrole)), 104.18, 103.87 and 103.54 (C(furan)), 101.71 (C(20, 21)), 36.96 (C(6, 12 or 18, 24)), 36.22 (C(6, 12 or 18, 24)), 28.15 (CH_3), 26.22 (CH_3).

Melting point : 221.6°C.

MS calcd. for $C_{28}H_{33}NO_3$ 431.2, found 454.4 (M+Na)+.
HRMS calcd. for $C_{28}H_{33}NO_3$+Na^+ 454.2354, found 454.2356.

2.20. Synthesis of compound 49* and 50*

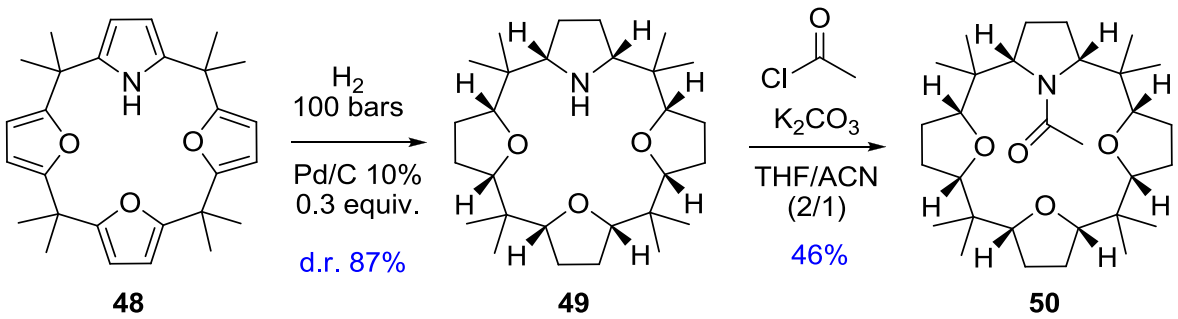

2.20.1. Compound 49*

Compound **48** (77 mg, 0.18 mmol) and Pd/C 10% (68 mg, 0.63 mmol) were placed in a test tube (125 x 15 mm) containing a small cross stirring bar. AcOH (10 mL) was added and the test tube was placed inside an autoclave vessel containing AcOH (25 mL). The autoclave was closed, put under magnetic stirring, filled with hydrogen (100 atm), and heated at 100°C for 24 h. After cooling to room temperature, the reaction mixture was filtered through celite and the solid was washed with AcOH (2 x 5 mL) and successively CH_2Cl_2 (2 x 5 mL). The combined filtrate and washings were concentrated under reduced pressure to give colorless slurry, to which CH_2Cl_2 (50 mL) and 5% aqueous NaOH 5% (20 mL) were added. The resulting mixture was stirred for 5 min. The organic layer was then separated and the aqueous phase was extracted with CH_2Cl_2 (2 x 20 mL). The collected organic layers were washed with brine, dried over K_2CO_3, and concentrated under reduced pressure. The residue was purified first recrystallization in EtOAc to yield 62 mg (78%) of compound **49**.

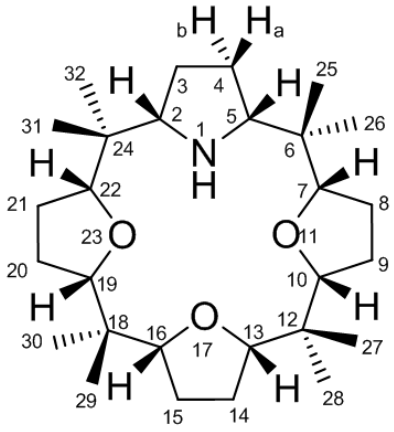

IR (KBr): 2967.5*s*, 2873.5*s*, 2820.2*m*, 2671.4*w*, 1469.9*m*, 1391.9*s*, 1374.6*m*, 1361.0*m*, 1085.2*s*, 1071.5*s*, 1042.2*s*, 999.5*m*, 981.0*m*

^{1}H NMR ($CDCl_3$, 233K) δ 4.02 (m, 2 H, C-H(αO)), 3.91 (m, 1 H, C-H(αO)), 3.51 (m, 1 H, C-H(αO)), 3.43 (m, 2H, C-H(αO)), 3.43 (m, 1H, C-H(αN)), 2.85 (m, 1H, C-H(αN)), 2.33-2.11 (m, 4 H, CH_2), 1.66-1.30 (m, 12 H, CH_2), 0.96 (s, 6 H, CH_3), 0.94 (s, 3 H, CH_3(27, 28)), 0.82 (s, 3 H, CH_3), 0.81 (s, 3 H, CH_3), 0.80 (s, 6 H, CH_3), 0.79 (s, 3 H, CH_3);

^{13}C NMR ($CDCl_3$, 233K) δ 88.12 (C(αO)), 87.83 (C(αO)), 87.77 (C(αO)), 80.89 (C(αO)), 80.03 (C(αO)), 79.86 (C(αO)), 68.43 (C(αN)), 62.06 (C(αN)), 39.32 (C(meso)), 39.30

(C(meso)), 39.15 (C(meso)), 38.76 (C(meso)), 28.94, 27.32, 26.77, 26.74, 26.33, 26.26, 26.13, 26.03, 26.00, 25.85 (CH_2), 18.89, 17.89, 17.71, 17.46 (CH_3).

Melting point: 243°C.

HRMS calcd. for $C_{28}H_{49}NO_3H^+$ 448.3785, found 448.3786.

2.20.2. Compound 50*

The amide **50** was prepared according to the general procedure (I) from compound **49** (62 mg, 1.14 mmol), acetyl chloride (11.8 µL, 0.19 mmol), potassium carbonate (23 mg, 0.16 mmol) in THF (4 mL) and ACN (2 mL). The residue was purified by column chromatography (Al_2O_3, CH_2Cl_2/MeOH, 99/1) to yield 31.2 mg (46%) of compound **50** as a colorless powder.

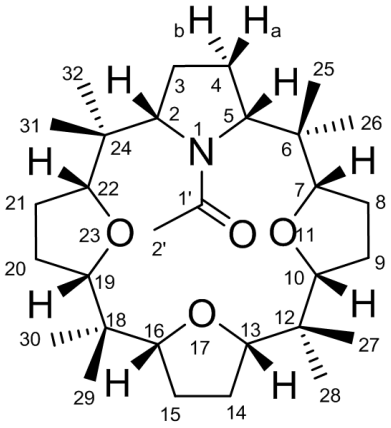

IR (KBr): 3435.6 *broad m*, 2967.4*s*, 2873.7*m*, 2821.0*w*, 1651.1*w*, 1470.0*m*, 1392.1*m*, 1374.6*w*, 1361.8*w*, 1085.2*s*, 1071.6*s*, 1042.8*m*, 999.8*w*, 981.6*w*, 554.4*w*.

^{1}H NMR ($CDCl_3$, 298K) δ 4.02 (dd, ^{3}J(10, 9b) and ^{3}J(19, 20b) = 10.9 Hz, ^{3}J(10, 9a) and ^{3}J(19, 20a) = 4.9 Hz, 2 H, C-H(10, 19)), 3.91 (m, 2 H, C-H(2, 5)), 3.86 (t, ^{3}J(7, 8a) and ^{3}J(22, 21a) = 7.7 Hz, ^{3}J(7, 8b) and 3J(22, 21b) = 7.7 Hz, 2 H, C-H(7, 22)), 3.54 (m, 2 H, C-H(13, 16)), 2.52 (m, 2 H, CH_2(3, 4)), 2.36 (m, 2 H, CH_2(14, 15)), 2.23 (s, 3 H, CH_3(2')), 1.73-1.55 (m, 10 H, CH_2(3, 4, 8, 9,14, 15, 20, 21)), 1.39 (m, 2 H, CH_2), 1.03 (s, 6 H, CH_3(25, 31 or 26, 32)), 1.00 (s, 6 H, CH_3(25, 31 or 26, 32)), 0.99 (s, 6 H, CH_3(27, 29 or 28, 30)), 0.87 (s, 6 H, CH_3(27, 29 or 28, 30));

^{13}C NMR ($CDCl_3$) δ 177.81 (C(1')=O), 87.66 (C(13, 16)), 81.91 (C(7, 22)), 80.69 (C(10, 19)), 70.68 (C(2, 5)), 41.52 (C(6, 24)), 39.24 (C(12, 18)), 28.80 (C(3, 4)), 27.10 (C(27, 29 or

28, 30)), 27.02 (CH_2), 26.02 (CH_2), 25.93 (C(14, 15)), 25.77 (C(2')), 24.13 (C(25, 31 or 26, 32)), 20.88 (C(25, 31 or 26, 32)), 17.30 (C(27, 29 or 28, 30)).

Melting point: 211°C.

HRMS calcd. for $C_{30}H_{51}NO_4Na^+$ 512.3710, found 512.3712.

X-ray: Suitable crystals of **50** were obtained as colorless rods by slow evaporation of a solution in dichloromethane. The intensity data were collected at 173K (-100°C) on a Stoe Mark II-Image Plate Diffraction System [1] equiped with a two-circle goniometer and using MoKα graphite monochromated radiation (λ = 0.71073 Å). Image plate distance 130mm, ω rotation scans 0 - 180° at ϕ 0°, 0 - 17° at ϕ 0°, step Δω = 1.0°, exposures of 5 mins per image, 2θ range 1.76 - 52.59°, d_{min} – d_{max} = 23.107 - 0.802 Å.

The structure was solved by Direct methods using the program SHELXS-97 [2]. The refinement and all further calculations were carried out using SHELXL-97 [2].

The NH H-atom was located in a difference electron-density map and was refined freely. The C-bound H-atoms were included in calculated positions and treated as riding atoms: C-H = 0.95 and 0.98 Å for CH(aromatic) and CH_3, respectively, with $U_{iso}(H) = k \times U_{eq}$(parent C-atom), where k = 1.5 for CH_3 H-atoms and k = 1.2 for all other H-atoms.

The non-H atoms were refined anisotropically, using weighted full-matrix least-squares on F^2.

[1] Stoe & Cie (2000). IPDS-I Bedienungshandbuch. Stoe & Cie GmbH, Darmstadt, germany.

[2] G. M. Sheldrick. (2008). Acta Cryst. A64, 112-122.

[3] Spek, A. L. (2003). J. Appl. Cryst. 36, 7-13.

[4] Westrip, S. P. (2010). J. Appl. Cryst. 43, 920-925.

Drawing programs:

ORTEP-3: [3] Farrugia, L. J. (1997). J. Appl. Cryst., 30, 565.

Mercury: [4] Macrae, C. F., Edgington, P. R., McCabe, P., Pidcock, E., Shields, G. P., Taylor, R., Towler, M. & van de Streek, J. (2006). J. Appl. Cryst. 39, 453-457.

PLATON: [5] Spek, A. L. (2003). J. Appl. Cryst. 36, 7-13.

2.21. Synthesis of compound 51

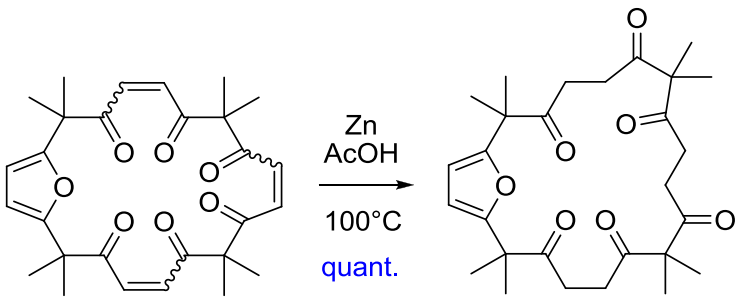

41 **51**

In a 250-mL Erlenmeyer flask is placed 35 mL of glacial acetic acid, in which 300 mg (0.62 mmol) of compound **41** is dissolved with heating on a hot plate. The flask is removed from the heat, and while the mixture is still hot, 0.4 g (10 equiv) of zinc dust is added in portions with efficient swirling so as to prevent bumping. The yellow solution turns colorless within seconds, and the contents of the flask are allowed to cool. The excess zinc and precipitated zinc salts are suction filtered and washed with $CHCl_3$. The colorless filtrate is poured into 2 volumes of water, the organic phase removed, and the upper aqueous phase extracted with more $CHCl_3$, (2 x 15 mL). The combined organic layers are washed with water, saturated aqueous $NaHCO_3$, and brine and dried over anhydrous Na_2SO_4. The solvent is removed in vacuum, leaving 303 mg (quant.) of a colorless solid.

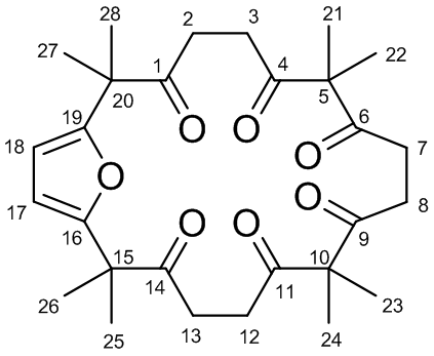

^{1}H NMR ($CDCl_3$, 298K) δ 6.15 (s, 2 H, C-H(17, 18)), 2.66 (s, 4 H, C-H(7, 8)), 2.59 (m, 8 H, C-H(2, 3, 12, 13)), 1.47 (s, 6 H, CH_3(21, 22, 23, 24 or 25, 26, 27, 28)), 1.37 (s, 12 H, CH_3(21, 22, 23, 24 or 25, 26, 27, 28));

^{13}C NMR ($CDCl_3$) δ 210.09 (C=O), 209.46 (C=O), 208.27 (C=O), 157.25 (C(16, 19)), 106.72 (C(17, 18)), 62.01 (C(15, 20)), 48.78 (C(5, 10)), 32.69 (C(7, 8)), 32.05 (C(2, 3, 12, 1)3), 23.44 (CH_3), 20.98 (CH_3).

MS calcd. for $C_{28}H_{38}O_7$ 486.2, found 509.5 (M+Na)+.

See additional analyses in "P. D. Williams and E. LeGoff, *J. Org. Chem.*, 1981, **46**, 4143".

2.22. Synthesis of compound 54*

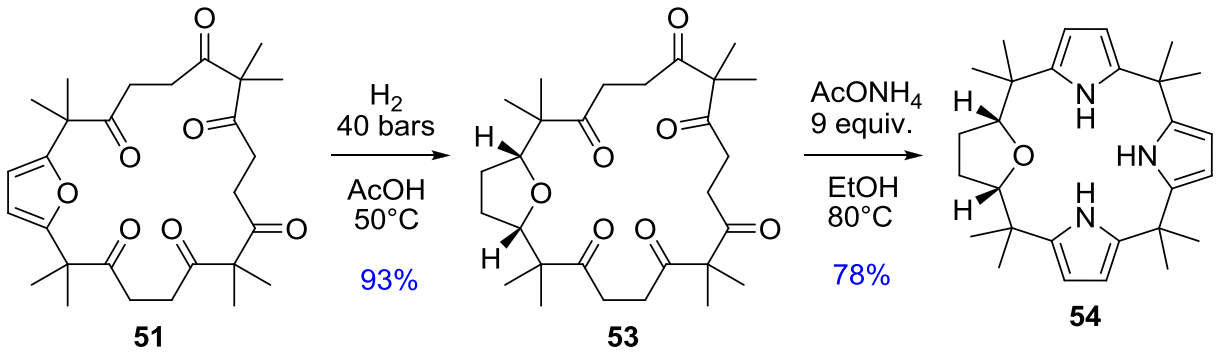

2.22.1. Compound 53*

Compound **51** (200 mg, 0.41 mmol) and Pd/C 10% (35 mg, 0.03 mmol) were placed in a test tube (125 x 15 mm) containing a small cross stirring bar. AcOH (7 mL) was added and the test tube was placed inside an autoclave vessel containing AcOH (25 mL). The autoclave was closed, put under magnetic stirring, filled with hydrogen (40 atm), and heated at 50°C for 6 h. After cooling to room temperature, the reaction mixture was filtered through celite and the solid was washed with AcOH (2 x 5 mL) and successively CH_2Cl_2 (2 x 10 mL). The combined filtrate and washings were concentrated under reduced pressure to give colorless slurry, to which CH_2Cl_2 (50 mL) and 5% aqueous NaOH 5% (20 mL) were added. The resulting mixture was stirred for 5 min. The organic layer was then separated and the aqueous phase was extracted with CH_2Cl_2 (2 x 30 mL). The collected organic layers were washed with brine, dried over K_2CO_3, and concentrated under reduced pressure. The residue was purified by recrystallization in ethanol to yield 187 mg (93%) of compound **53**.

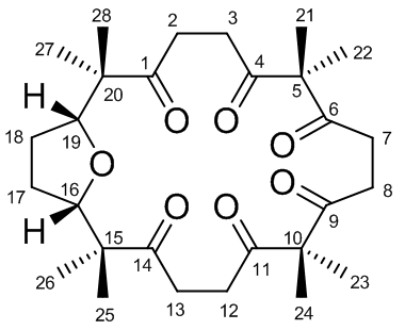

IR (KBr): 2982.3*m*, 2942.1*m*, 2865.6*w*, 1719.3*s*, 1701.0*s*, 1469.7*m*, 1399.5*m*, 1366.3*m*, 1077.0*m*, 1048.3*m*, 579.1*w*.

^{1}H NMR ($CDCl_3$, 298K) δ 3.89 (m, 2 H, C-H(16, 19)), 2.90-2.64 (m, 8 H, CH_2(2, 3, 12, 13)), 2.58 (m, 4 H, CH_2(7, 8)), 1.80 (m, 2 H, CH_2(17, 18)), 1.60 (m, 2 H, CH_2(17, 18)), 1.37 (s, 6 H, CH_3(21, 24 or 22, 23)), 1.36 (s, 6 H, CH_3(21, 24 or 22, 23)), 1.05 (s, 6 H, CH_3(25, 28, or 26, 27)), 1.03 (s, 6 H, CH_3(25, 28, or 26, 27));

^{13}C NMR ($CDCl_3$) δ 213.06 (C (6, 9) =O), 209.31 (C (1, 14 or 4, 11) =O), 208.90 (C (1, 14 or 4, 11) =O), 83.96 (C(16, 19)), 62.06 (C(5, 10)), 49.99 (C(15, 20)), 32.94 (C(7, 8)), 32.45 (C(2, 3, 12, 13)), 25.64 (C(17, 18)), 23.25 (C(25, 28, or 26, 27)), 21.43 (C(21, 24 or 22, 23)), 21.16 (C(21, 24 or 22, 23)), 16.99 (C(25, 28, or 26, 27)).

Melting point: 123.7°C.

HRMS calcd. for $C_{28}H_{42}NaO_7^+$ 513.2823, found 513.2825 .

2.22.2. Compound 54*

In a round-bottom flask were introduced **53** (100 mg, 0.20 mmol) and ethanol (10 mL). Then, $AcONH_4$ (141 mg, 1.8 mmol) was added to the slurry, and the mixture was stirred at 80°C for 6 h. After cooling, CH_2Cl_2 (50 mL) was added and the reaction mixture was basified with 5% sodium hydroxide and washed with saturated brine. The aqueous layer was extracted three times with CH_2Cl_2 (10 mL). The combined organic layers were dried with sodium sulfate, and the solvent was removed under vacuum. The residue was purified by column chromatography (SiO_2, CH_2Cl_2) to yield 69 mg (78%) of colorless powder.

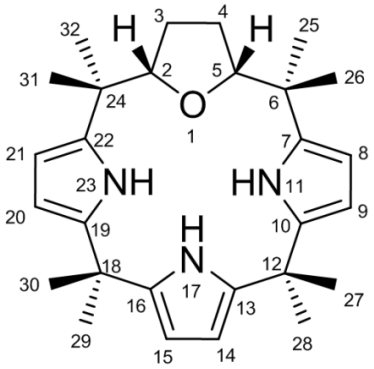

IR (KBr): 3547.0*m*, 3300.4*m*, 2969.3*s*, 2927.8*m*, 2869.2*m*, 1579.7*m*, 1466.2*m*, 1357.1*m*, 1243.9*m*, 1073.8*m*, 1045.4*s*, 767.4*s*, 706.1*m*, 479.8*w*.

^{1}H NMR ($CDCl_3$, 298K) δ 7.70 (bs, 1 H, NH(17)), 7.65 (bs, 2 H, NH(11, 23)), 6.06 (d, ^{4}J(14, 17) and ^{4}J(15, 17) = 2.5 Hz, 2 H, C-H(14, 15)), 5.93 (m, 2 H, C-H(8, 21 or 9, 20)), 5.79 (m, 2 H, C-H(8, 21 or 9, 20)), 3.74 (m, 2 H, C-H(2, 5)), 1.80 (m, 2 H, CH_2(3, 4)), 1.63 (m, 2 H, CH_2(3, 4)), 1.59 (m, 6 H, CH3(27, 30 or 28, 29)), 1.58 (m, 6 H, CH_3(27, 30 or 28, 29)), 1.18 (m, 6 H, CH_3(25, 32 or 26, 31)), 1.05 (m, 6 H, CH_3(25, 32 or 26, 31));

^{13}C NMR ($CDCl_3$) δ 138.91 (C(13, 16)), 138.03 (C(7, 22 or 10, 19)), 137.96 (C(7, 22 or 10, 19)), 103.97 (C(14, 15)), 102.88 (C(8, 21 or 9, 20)), 102.57 (C(8, 21 or 9, 20)), 86.88 (C(2, 5)), 37.42 (C(12, 18)), 35.54 (C(6, 24)), 29.58 (C(27, 30 or 28, 29)), 29.53 (C(27, 30 or 28, 29)), 26.49 (C(3, 4)), 26.20 (C(25, 32 or 26, 31)), 20.74 (C(25, 32 or 26, 31)).

Melting point: 140.2°C.

HRMS calcd. for $C_{28}H_{39}N_3ONa^+$ 456.2985, found 456.2989.

2.23. Synthesis of compound rac-55* and rac-56*

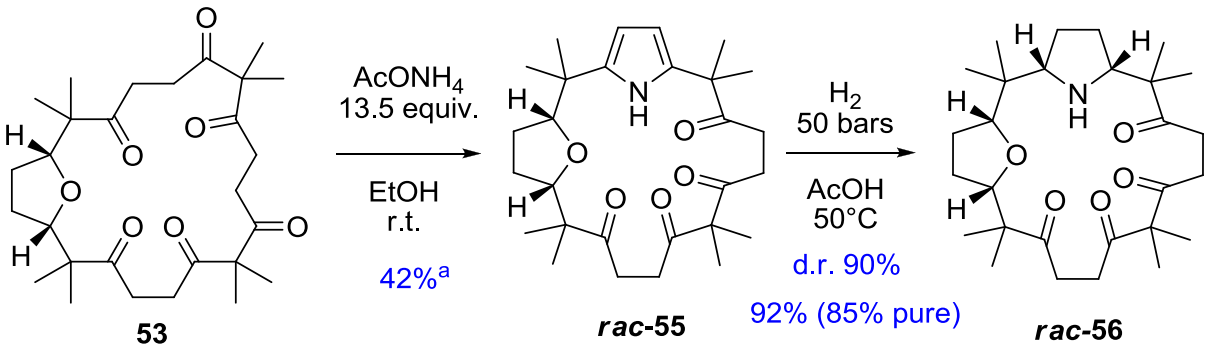

2.23.1. Compound rac-55*

In a round-bottom flask were introduced **53** (558 mg, 1.13 mmol) and ethanol (50 mL). Then, $AcONH_4$ (1.17 g, 15.2 mmol) was added to the slurry, and the mixture was stirred at r.t. for 48 h. After cooling, CH_2Cl_2 (100 mL) was added and the reaction mixture was basified with 5% sodium hydroxide and washed with saturated brine. The aqueous layer was extracted three times with CH_2Cl_2 (50 mL). The combined organic layers were dried with sodium sulfate, and

the solvent was removed under vacuum. The residue was purified by column chromatography (SiO_2, CH_2Cl_2/MeOH, 99/1) to yield 225 mg (42%) of compound **rac-55** as a colorless powder.

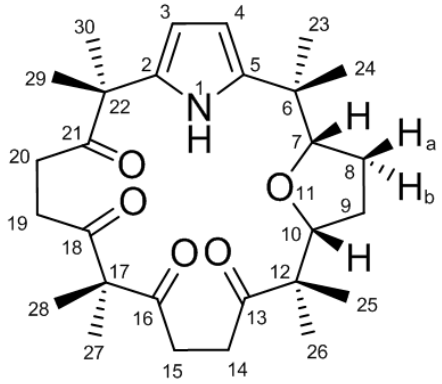

IR (KBr): 3434.2*m*, 2974.4*m*, 2930.3*w*, 2878.1*w*, 1712.9*m*, 1696.4*s*, 1394.3*w*, 1062.9*m*, 777.2*m*, 713.0*w*.

^{1}H NMR ($CDCl_3$, 298K) δ 9.11 (bs, 1H, NH(1)), 5.80 (m, 1 H, C-H(3)), 5.74 (m, 1 H, C-H(4)), 4.31 (m, 1 H, C-H(10)), 3.77 (m, 1 H, C-H(7)), 3.13 (m, 2 H, CH_2(14, 15)), 3.08-3.00 (ddd, ^{2}J(19a, 19b) = 18.8 Hz, ^{3}J(19, 20) = 9.6 Hz, ^{3}J(19, 20) = 2.7 Hz, 1 H, CH_2(19)), 2.95-2.87 (m, 1 H, CH_2(15)), 2.74-2.67 (ddd, ^{2}J(19b, 19a) = 18.8 Hz, ^{3}J(19, 20) = 6.4 Hz, ^{3}J(19, 20) = 2.7 Hz, 1 H, CH_2(19)), 2.66-2.55 (m, 2 H, CH_2(14, 20)), 2.32-2.26 (ddd, ^{2}J(20, 20) = 17.5 Hz, ^{3}J(20, 19) = 6.4 Hz, ^{3}J(20, 19) = 2.8 Hz, 1 H, CH_2(20)), 1.94-1.79 (m, 2 H, CH_2(8, 9)), 1.74-1.59 (m, 2 H, CH_2(8, 9)), 1.53 (s, 3 H, CH_3(29 or 30)), 1.43 (s, 3 H, CH_3(29 or 30)), 1.37 (s, 6 H, CH_3(27, 28)), 1.20 (s, 3 H, CH_3(23 or 24)), 1.17 (s, 3 H, CH_3(25 or 26)), 1.11 (s, 3 H, CH_3(23 or 24)), 1.09 (s, 3 H, CH_3(25 or 26));

^{13}C NMR ($CDCl_3$) δ 213.04 (C(13)=O), 212.72 (C(21)=O), 208.88 (C(16)=O), 207.85 (C(18)=O), 141.60 (C(5)), 133.08 (C(2), 103.11 (C(3)), 101.58 (C(4)), 86.54 (C(7)), 83.53 (C(10)), 63.66 (C(17)), 50.47 (C(12)), 46.39 (C(22)), 37.19 (C(6)), 33.06, 32.92, 32.79 (C(14, 15, 19)), 31.13 (C(20)), 26.42 (C(29 or 30)), 26.32, 25.41 (C(8, 9)), 24.37 (C(23 or 24)), 24.33 (C(29 or 30)), 23.86 (C(25 or 26)), 22.26 (C(23 or 24)), 20.81, 20.64 (C(27, 28)), 16.30 (C(25 or 26)).

Melting point: 155.7°C.

HRMS calcd. for $C_{28}H_{41}NO_5Na^+$ 494.2877, found 494.2875.

2.23.2. Compound rac-56*

Compound **55** (110 mg, 0.23 mmol) and Pd/C 10% (20 mg, 0.02 mmol) were placed in a test tube (125 x 15 mm) containing a small cross stirring bar. AcOH (7 mL) was added and the test tube was placed inside an autoclave vessel containing AcOH (25 mL). The autoclave was closed, put under magnetic stirring, filled with hydrogen (50 atm), and heated at 50°C for 6 h. After cooling to room temperature, the reaction mixture was filtered through celite and the solid was washed with AcOH (2 x 5 mL) and successively CH_2Cl_2 (2 x 10 mL). The combined filtrate and washings were concentrated under reduced pressure to give colorless slurry, to which CH_2Cl_2 (50 mL) and 5% aqueous NaOH 5% (20 mL) were added. The resulting mixture was stirred for 5 min. The organic layer was then separated and the aqueous phase was extracted with CH_2Cl_2 (2 x 30 mL). The collected organic layers were washed with brine, dried over K_2CO_3, and concentrated under reduced pressure. The residue was purified by column chromatography (Al_2O_3, CH_2Cl_2/MeOH, 97/3) to yield 102 mg (92%) of compound **56** (90% pure).

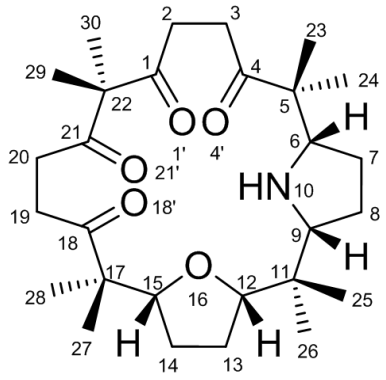

IR (KBr): 3377.1*w*, 2968.8*s*, 2930.0*m*, 2872.1*m*, 1698.2*s*, 1468.2*m*, 1393.1*m*, 1367.0*m*, 1300.0*w*, 1244.0*w*, 1062.7*s*, 1062.7*m*, 1016.9*m*, 980.0*w*.

^{1}H NMR ($CDCl_3$, 298K) δ 4.01 (t, ^{3}J(15, 14a) = 7.2 Hz, ^{3}J(15, 14b) = 7.2 Hz, 1 H, C-H(15)), 3.47 (dd, ^{3}J(12, 13b) = 7.3 Hz, ^{3}J(12, 13a) = 6.5 Hz, 1 H, C-H(12)), 3.11 (bs, 1 H, C-H(6)), 3.00-2.82 (m, 5 H, CH_2(αC=O)), 2.78 (bs, 1 H, C-H(9)), 2.70-2.59 (m, 3 H, CH_2(αC=O)), 2.38 (bs, 1 H, N-H(10)), 1.78-1.67 (m, 2 H, CH_2(13, 14)), 1.56-1.44 (m, 4 H, CH_2(13, 14, 7, 8)), 1.36 (s, 6 H, CH_3(29, 30)), 1.33-1.23 (m, 2 H, CH_2(7, 8)), 1.13 (s, 3 H, CH_3(23 or 24)), 1.10 (s, 3 H, CH_3(27 or 28)), 1.04 (s, 3 H, CH_3(27 or 28)), 1.02 (s, 3 H, CH_3(23 or 24)), 0.69 (s, 6 H, CH_3(25 or 26)), 0.68 (s, 6 H, CH_3(25 or 26));

^{13}C NMR ($CDCl_3$) δ 214.23 and 212.70 (C (4, 18) =O), 209.29 and 208.66 (C (1, 21) =O), 88.89 (C(12)), 83.29 (C(15)), 68.59 (C(9)), 63.29 (C(6)), 63.25 (C(22)), 50.15 (C(5 or 17)), 50.11 (C(5 or 17)), 38.64 (C(11)), 33.07, 32.80 and 32.29 (C(αCO)), 26.35 (C(13 or 14)), 25.81 (C(13 or 14)), 25.44 ((C7 or 8)), 24.66 (C(7 or 8)), 23.82 (CH_3), 23.71 (CH_3), 23.61 (CH_3), 21.15 (C(29 or 30)), 20.93 (C(29 or 30)), 18.26 (CH_3), 17.21 (CH_3), 12.66 (C(25 or 26)).

HRMS calcd. for $C_{28}H_{45}NO_5H^+$ 476.3371, found 476.3376.

X-ray: Suitable crystals of **56** were obtained as colorless rods by slow evaporation of a solution in dichloromethane. The intensity data were collected at 173K (-100°C) on a Stoe Mark II-Image Plate Diffraction System [1] equiped with a two-circle goniometer and using MoKα graphite monochromated radiation (λ = 0.71073 Å). Image plate distance 130mm, ω rotation scans 0 - 180° at φ 0°, and 0 - 91° at φ = 90°, step Δω = 1.0°, exposures of 0.5 mins per image, 2θ range 1.76 - 52.59°, d_{min} – d_{max} = 23.107 - 0.802 Å.

The structure was solved by Direct methods using the program SHELXS-97 [2]. The refinement and all further calculations were carried out using SHELXL-97 [2].

The NH H-atoms were located in difference electron-density maps and were initially freely refined. In the final cycles of least-squares refinement they were refined isotropically with distance restraints: N-H = 0.88(2) Å. The C-bound H-atoms were included in calculated positions and treated as riding atoms: C-H = 1.0, 0.99 and 0.98 Å for CH(methine), CH_2 and CH_3, respectively, with $U_{iso}(H) = k \times U_{eq}$(parent C-atom), where k = 1.5 for CH_3 H-atoms and k = 1.2 for all other H-atoms. The non-H atoms were refined anisotropically, using weighted full-matrix least-squares on F^2. A semi-empirical absorption correction was applied using the MULscanABS routine in PLATON [3].

[1] Stoe & Cie (2000). IPDS-I Bedienungshandbuch. Stoe & Cie GmbH, Darmstadt, germany.
[2] G. M. Sheldrick. (2008). Acta Cryst. A64, 112-122.
[3] Spek, A. L. (2003). J. Appl. Cryst. 36, 7-13.
[4] Westrip, S. P. (2010). J. Appl. Cryst. 43, 920-925.

Drawing programs:

ORTEP-3: [3] Farrugia, L. J. (1997). J. Appl. Cryst., 30, 565.

Mercury: [4] Macrae, C. F., Edgington, P. R., McCabe, P., Pidcock, E., Shields, G. P., Taylor, R., Towler, M. & van de Streek, J. (2006). J. Appl. Cryst. 39, 453-457.
PLATON: [5] Spek, A. L. (2003). J. Appl. Cryst. 36, 7-13.

2.24. Synthesis of compound 58a and 58b*

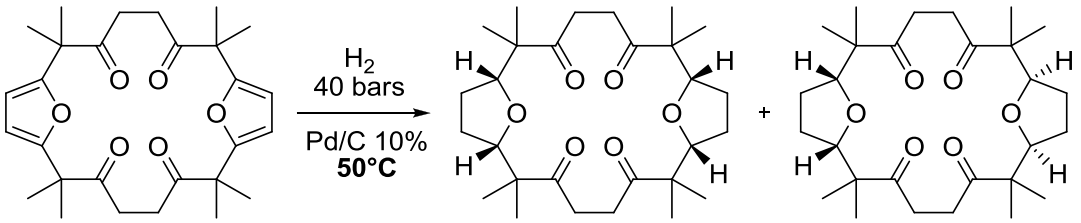

Compound **42** (1.00 g, 2.13 mmol) and Pd/C 10% (360 mg, 0.33 mmol) were placed in a test tube (125 x 15 mm) containing a small cross stirring bar. AcOH (7 mL) was added and the test tube was placed inside an autoclave vessel containing AcOH (25 mL). The autoclave was closed, put under magnetic stirring, filled with hydrogen (40 atm), and heated at 50°C for 24 h. After cooling to room temperature, the reaction mixture was filtered through celite and the solid was washed with AcOH (2 x 10 mL) and successively CH_2Cl_2 (2 x 20 mL). The combined filtrate and washings were concentrated under reduced pressure to give colorless slurry, to which CH_2Cl_2 (100 mL) and 5% aqueous NaOH 5% (40 mL) were added. The resulting mixture was stirred for 5 min. The organic layer was then separated and the aqueous phase was extracted with CH_2Cl_2 (2 x 50 mL). The collected organic layers were washed with brine, dried over K_2CO_3, and concentrated under reduced pressure. The two products were separated by successive recrystallization in EtOAc and ethanol to yield 366 mg (36%) of compound **58a** and 386 mg (38%) of compound **58b**.

2.24.1. Compound 58a*

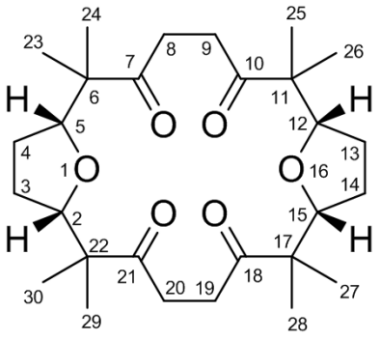

IR (KBr): 2971.8*m*, 2878.6*m*, 1697.8*s*, 1475.6*m*, 1412.7*m*, 1389.6*m*, 1365.2*m*, 1310.2*m*, 1072.9*m*, 1053.5*m*, 980.7*w*.

^{1}H NMR ($CDCl_3$, 298K) δ 3.89 (m, 4 H, C-H(2, 5, 12, 15)), 2.73 (m, 8 H, CH_2(8, 9, 19, 20)), 1.81 (m, 4 H, CH_2(3, 4, 13, 14)), 1.59 (m, 4 H, CH_2(3, 4, 13, 14)), 1.13 (s, 12 H, CH_3), 1.01 (s, 12 H, CH_3);

^{13}C NMR ($CDCl_3$) δ 213.92 (C=O), 84.10 (C(2, 5, 12, 15)), 50.02 (C(6, 11, 17, 22)), 32.78 (C(8, 9, 19, 20)), 25.29 (C(3, 4, 13, 14)), 23.00 (CH_3), 16.45 (CH_3).

Melting point: 181°C.

HRMS calcd. for $C_{28}H_{44}O_6H^+$ 499.3030, found 499.3038.

X-ray: Suitable crystals of **58a** were obtained as colorless blocks by slow evaporation of a solution in dichloromethane. The intensity data were collected at 173 K (-100°C) on a Stoe Mark II-Image Plate Diffraction System [1] equiped with a two-circle goniometer and using MoKα graphite monochromated radiation (λ = 0.71073 Å). Image plate distance 130mm, ω rotation scans 0 - 180° at ϕ 0°, step Δω = 1.0°, exposures of 6 mins per image, 2θ range 1.76 - 52.59°, $d_{min} – d_{max}$ = 23.107 - 0.802 Å.

The structure was solved by Direct methods using the program SHELXS-97 [2]. The refinement and all further calculations were carried out using SHELXL-97 [2].

In the final cycles of least-squares refinement the C-bound H-atoms were included in calculated positions and treated as riding atoms: C-H = 0.99, 0.98 and 0.97 Å

for CH, CH_2 and CH_3, respectively, with $U_{iso}(H) = k \times U_{eq}(C)$, where k = 1.5 for CH_3 H-atoms, and = 1.2 for all other H-atoms.

The non-H atoms were refined anisotropically, using weighted full-matrix least-squares on F^2.

[1] Stoe & Cie (2000). IPDS-I Bedienungshandbuch. Stoe & Cie GmbH, Darmstadt, germany.

[2] G.M. Sheldrick. (2008). Acta Cryst. A64, 112-122.

[3] Spek, A. L. (2003). J. Appl. Cryst. 36, 7-13.

[4] Westrip, S. P. (2010). J. Appl. Cryst. 43, 920-925.

Drawing programs:

ORTEP-3: [3] Farrugia, L. J. (1997). J. Appl. Cryst., 30, 565.

Mercury: [4] Macrae, C. F., Edgington, P. R., McCabe, P., Pidcock, E., Shields, G. P., Taylor, R., Towler, M. & van de Streek, J. (2006). J. Appl. Cryst. 39, 453-457.

PLATON: [5] Spek, A. L. (2003). J. Appl. Cryst. 36, 7-13.

2.24.2. Compound 58b*

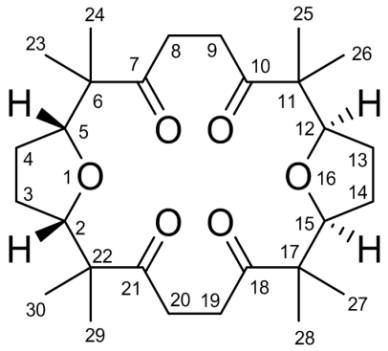

IR (KBr): 2985.2*m*, 2878.9*m*, 1699.0*s*, 1471.9*m*, 1416.7*m*, 1386.7*w*, 1365.8*w*, 1311.5*w*, 1070.6*s*, 1016.3*w*

^{1}H NMR ($CDCl_3$, 298K) δ 3.89 (m, 4 H, C-H(2, 5, 12, 15)), 2.85-2.64 (m, 8 H, CH_2(8, 9, 19, 20)), 1.82 (m, 4 H, CH_2(3, 4, 13, 14)), 1.59 (m, 4 H, CH_2(3, 4, 13, 14)), 1.11 (s, 12 H, CH_3), 1.00 (s, 12 H, CH_3);

^{13}C NMR ($CDCl_3$) δ 213.79 (C=O), 83.91 (C(2, 5, 12, 15)), 49.98 (C(6, 11, 17, 22)), 32.54 (C(8, 9, 19, 20)), 25.26 (C(3, 4, 13, 14)), 23.00 (CH_3), 16.33 (CH_3).

Melting point: 272°C.

HRMS calcd. for $C_{28}H_{44}O_6H^+$ 499.3030, found 499.3038.

2.25. Synthesis of compound 33*

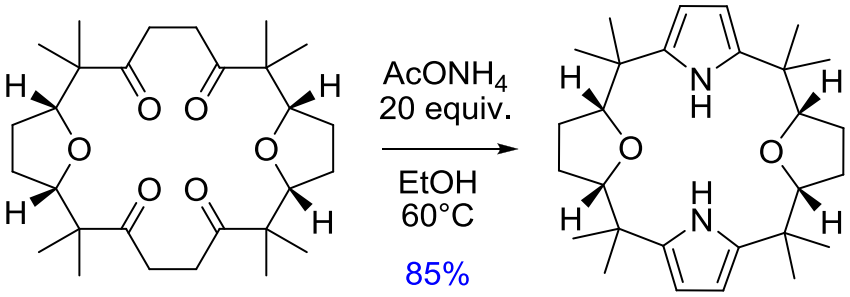

58a **33**

In a round-bottom flask were introduced **58a** (200 mg, 0.42 mmol) and ethanol (30 mL). Then, $AcONH_4$ (646 mg, 8.4 mmol) was added to the slurry, and the mixture was stirred at 60°C for 24 h. After cooling, the solvent was partially removed under vacuum and the reaction mixture was filtered off, washed with ethanol and dried under vacuum to yield 156 mg (85%) of **33** as a colorless solid. The residue could be purified by column chromatography (SiO_2, Cyclohexane/EtOAc, 97/3).

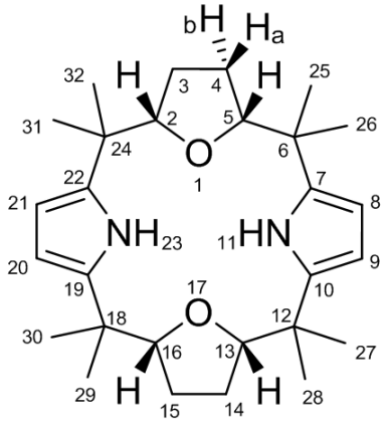

IR (KBr): 3445.8*s*, 2976.4*s*, 2961.5*s*, 2936.8*m*, 2917.3*m*, 2868.1*w*, 1569.1*w*, 1468.0*m*, 1245.80*m*, 1067.6*s*, 1045.3*m*, 1036.3*m*, 1006.7*w*, 955.4*w*, 770.8*s*, 761.4*s*, 511.2*w*

^{1}H NMR (CDCl3, 298K) δ 9.71 (bs, 2 H, NH(11, 23)), 5.85 (d, ^{4}J(8, 11) = ^{4}J(9, 11) and ^{4}J(20, 23) = ^{4}J(21, 23) = 2.6 Hz, 4 H, C-H(8, 9, 20, 21)), 3.93 (m, 4 H, C-H(2, 5, 13, 16)), 1.85 (m, 4 H, CH_2(3a, 4a, 14a, 16a)), 1.64 (m, 4 H, CH_2(3b, 4b, 14b, 16b)), 1.36 (s, 12 H, CH_3), 0.93 (s, 12 H, CH_3);

^{13}C NMR ($CDCl_3$) δ 136.82 (C(7, 10, 19, 22)), 102.94 (C(8, 9, 20, 21)), 87.28 (C(2, 5, 13, 16)), 37.79 (C(6, 12, 18, 24)), 27.14 (C(3, 4, 14, 15)), 26.69 (CH_3), 23.89 (CH_3).

Melting point: 233.5°C.

HRMS calcd. for $C_{28}H_{42}N_2O_2H^+$ 439.3319, found 419.3314.

2.26. Synthesis of compound 59*, 60a* and 60b*

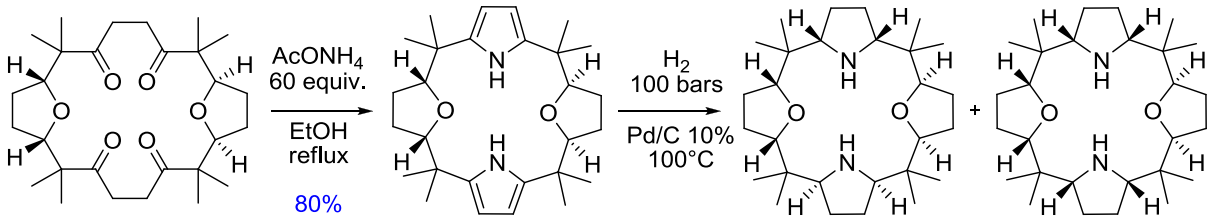

2.26.1. Compound 59*

In a round-bottom flask were introduced **58b** (50 mg, 0.10 mmol) and ethanol (10 mL). Then, $AcONH_4$ (485 mg, 6.30 mmol) was added to the slurry, and the mixture was stirred at 80°C for 3 h. After cooling, CH_2Cl_2 (50 mL) was added and the reaction mixture was basified with 5% sodium hydroxide and washed with saturated brine. The aqueous layer was extracted three times with CH_2Cl_2 (10 mL). The combined organic layers were dried with sodium sulfate, and the solvent was removed under vacuum. The residue was first purified by column chromatography (SiO_2, cyclohexane/EtOAc, 97/3), then by recrystallization in EtOH to yield 37 mg (80%) of colorless powder.

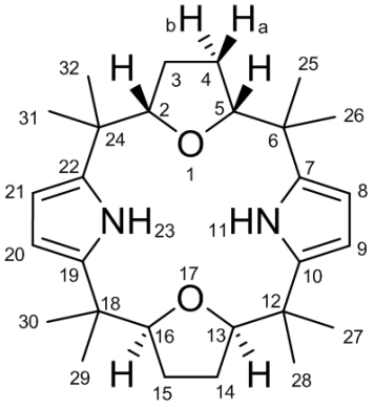

IR (KBr): 3432.1*s*, 3100.9*w*, 2977.4*s*, 2939.5*m*, 2891.0*m*, 2873.4*m*, 2851.5*w*, 1574.6*m*, 1462.0*m*, 1385.6*m*, 1240.2*m*, 1063.6*s*, 1048.4*s*, 970.8*m*, 763.7*s*, 706.5*m*, 591.5*m*, 541.6*w*.

^{1}H NMR ($CDCl_3$, 298K) δ 8.93 (bs, 2 H, NH(11, 23), 5.85 (d, ^{4}J(8, 11) = ^{4}J(9, 11) and ^{4}J(20, 23) = ^{4}J(21, 23) = 2.8 Hz, 4 H, C-H(8, 9, 20, 21)), 3.71 (m, 4 H, C-H(2, 5, 13, 16)), 1.85 (m, 4 H, CH_2(3a, 4a, 14a, 15a)), 1.73 (m, 4 H, CH_2(3b, 4b, 14b, 15b)), 1.31 (s, 12 H, CH_3), 1.15 (s, 12 H, CH_3);

^{13}C NMR ($CDCl_3$) δ 137.90 (C(7, 10, 19, 22)), 101.88 (C(8, 9, 20, 21)), 86.65 (C(2, 5, 13, 16)), 37.18 (C(6, 12, 18, 24)), 26.62 (C(3, 4, 14, 15)), 24.79 (CH_3), 22.34 (CH_3).

Melting point: 182.2°C.

HRMS calcd. for $C_{28}H_{42}N_2O_2+H^+$ 439.3319, found 439.3311.

X-ray: Suitable crystals of **59** were obtained as colorless blocks by recrystallization from ethanol. The crystal was cut to a rod and the intensity data were collected at 173K (-100°C) on a Stoe Mark II-Image Plate Diffraction System [1] equiped with a two-circle goniometer and using MoKα graphite monochromated radiation (λ = 0.71073 Å). Image plate distance 130mm, ω rotation scans 0 - 180° at φ 0°, step Δω = 1.0°, exposures of 3 mins per image, 2θ range 1.76 - 52.59°, d_{min} – d_{max} = 23.107 - 0.802 Å.

The structure was solved by Direct methods using the program SHELXS-97 [2]. The refinement and all further calculations were carried out using SHELXL-97 [2]. The NH H-atom was located in a difference electron-density map and was freely refined. The C-bound H-atoms were included in calculated positions and treated as riding atoms: C-H = 0.95, 0.98, 0.99 and 1.00 Å for CH(aromatic), CH_3, CH_2 and CH(methine) H-atoms, respectively, with U_{iso}(H) = k × U_{eq}(parent C-atom), where k = 1.5 for CH_3 H-atoms and k = 1.2 for all other H-atoms.

The molecule is centrosymmetric possessing C_i symmetry (an inversion center).

[1] Stoe & Cie (2000). IPDS-I Bedienungshandbuch. Stoe & Cie GmbH, Darmstadt, germany.
[2] G. M. Sheldrick. (2008). Acta Cryst. A64, 112-122.
[3] Spek, A. L. (2003). J. Appl. Cryst. 36, 7-13.
[4] Westrip, S. P. (2010). J. Appl. Cryst. 43, 920-925.

Drawing programs:

ORTEP-3: [3] Farrugia, L. J. (1997). J. Appl. Cryst., 30, 565.
Mercury: [4] Macrae, C. F., Edgington, P. R., McCabe, P., Pidcock, E., Shields, G. P., Taylor, R., Towler, M. & van de Streek, J. (2006). J. Appl. Cryst. 39, 453-457.
PLATON: [5] Spek, A. L. (2003). J. Appl. Cryst. 36, 7-13.

2.26.2. Compound 60a* and 60b*

Compound **59** (50 mg, 0.114 mmol) and Pd/C 10% (44 mg, 0.041 mmol) were placed in a test tube (125 x 15 mm) containing a small cross stirring bar. AcOH (5 mL) was added and the test tube was placed inside an autoclave vessel containing AcOH (25 mL). The autoclave was closed, put under magnetic stirring, filled with hydrogen (100 atm), and heated at 100°C for 4 h. After cooling to room temperature, the reaction mixture was filtered through celite and the solid was washed with AcOH (2 x 5 mL) and successively CH_2Cl_2 (2 x 10 mL). The combined filtrate and washings were concentrated under reduced pressure to give colorless slurry, to which CH_2Cl_2 (50 mL) and 5% aqueous NaOH 5% (20 mL) were added. The resulting mixture was stirred for 5 min. The organic layer was then separated and the aqueous phase was extracted with CH_2Cl_2 (2 x 25 mL). The collected organic layers were washed with brine, dried over K_2CO_3, and concentrated under reduced pressure. The two products were separated by column chromatography (Al_2O_3, Toluene/Acetone/Et_3N, 80/19/1) to yield 24 mg (48%) of compound **60a** and 13 mg (25%) of compound **60b**.

2.26.2.1. Compound **60a***

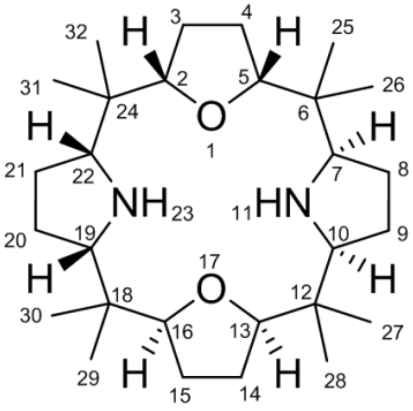

IR (KBr): 2963.7*s*, 2868.3*m*, 2823.5*m*, 2778.7*m*, 2638.6*w*, 1469.7*m*, 1409.8*m*, 1385.5*m*, 1278.3*w*, 1219.6*w*, 1072.7*s*, 1057.3*m*, 1012.6*w*, 545.7*w*

^{1}H NMR ($CDCl_3$, 298K) δ 3.58 (dd, $^{3}J(H\alpha O,CH_2)$ = 7.3 Hz, $^{3}J(H\alpha O,CH_2)$ = 8.1 Hz, 2 H, C-H(2, 5 or 13, 16)), 3.53 (dd, $^{3}J(H\alpha O,CH_2)$ = 5.6 Hz, $^{3}J(H\alpha O,CH_2)$ = 10.7 Hz, 2 H, C-H(2, 5 or 13, 16)), 2.91-2.80 (m, 4 H, C-H(7, 10, 19, 22)), 2.52 (bs, 2 H, N-H(11, 23)), 1.72-1.26 (m, 16 H, CH_2), 0.88 (s, 12 H, CH_3), 0.72 (s, 6 H, CH_3), 0.70 (s, 6 H, CH_3);

^{13}C NMR ($CDCl_3$) δ 87.98 (C(2, 5, 13, 16)), 68.70 and 68.67 (C(7, 10, 19, 22)), 39.34 and 37.79 (C(6, 12, 18, 24)), 26.40 (CH_2), 26.35 (CH_2), 26.23 (CH_2), 25.69 (CH_2), 24.18 (CH_3), 23.75 (CH_3), 22.48 (CH_3), 11.65 (CH_3).

HRMS calcd. for $C_{28}H_{50}N_2O_2H^+$ 447.3945, found 447.3945

X-ray: Suitable crystals of **80a** were obtained as colorless blocks by *slow* evaporation of a solution in acetone. The intensity data were collected at 173K (-100°C) on a Stoe Mark II-Image Plate Diffraction System [1] equiped with a two-circle goniometer and using MoKα graphite monochromated radiation (λ = 0.71073 Å). Image plate distance 130mm, ω rotation scans 0 - 180° at φ 0°, and 0 - 1115° at φ = 90°, step Δω = 1.0°, exposures of 3 mins per image, 2θ range 1.76 - 52.59°, $d_{min} – d_{max}$ = 23.107 - 0.802 Å.

The structure was solved by Direct methods using the program SHELXS-97 [2]. The refinement and all further calculations were carried out using SHELXL-97 [2]. The NH were refined with distances restraints: N-H = 0.88(2) Å, with $U_{iso}(H) = 1.2U_{eq}$(parent N-atom). The C-bound H-atoms were included in calculated positions and treated as riding atoms: C-H = 1.0, 0.99 and 0.98 Å for CH, CH_2 and CH_3, respectively, with $U_{iso}(H) = k \times U_{eq}$(parent C-atom), where k = 1.5 for CH_3 H-atoms and k = 1.2 for all other H-atoms. The non-H atoms were refined anisotropically, using weighted full-matrix least-squares on F^2. A semi-empirical absorption correction was applied using the MULscanABS routine in PLATON [3].

The O and NH atoms are disordered around the ring.

[1] Stoe & Cie (2000). IPDS-I Bedienungshandbuch. Stoe & Cie GmbH, Darmstadt, germany.
[2] G. M. Sheldrick. (2008). Acta Cryst. A64, 112-122.
[3] Spek, A. L. (2003). J. Appl. Cryst. 36, 7-13.
[4] Westrip, S. P. (2010). J. Appl. Cryst. 43, 920-925.

Drawing programs:

ORTEP-3: [3] Farrugia, L. J. (1997). J. Appl. Cryst., 30, 565.

Mercury: [4] Macrae, C. F., Edgington, P. R., McCabe, P., Pidcock, E., Shields, G. P., Taylor, R., Towler, M. & van de Streek, J. (2006). J. Appl. Cryst. 39, 453-457.
PLATON: [5] Spek, A. L. (2003). J. Appl. Cryst. 36, 7-13.

2.26.2.2. Compound **60b***

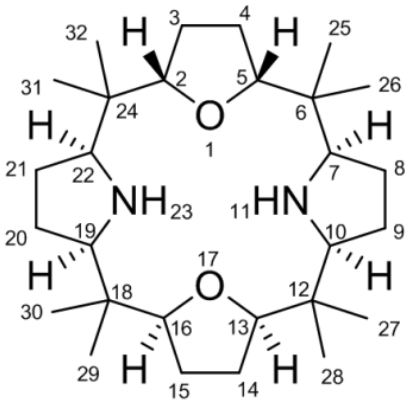

IR (KBr): 2962.6*s*, 2875.4*m*, 2823.5*w*, 1467.6*m*, 1401.5*m*, 1381.8*m*, 1356.6*w*, 1259.1*w*, 1124.3*w*, 1067.1*s*, 1037.7*m*, 970.6*w*, 920.8*w*, 833.6*w*, 646.7*w*, 545.4*w*

^{1}H NMR ($CDCl_3$, 298K) δ 3.58 (dd, $^{3}J(H\alpha O, CH_2)$ = 4.8 Hz, $^{3}J(H\alpha O, CH_2)$= 6.4 Hz, 2 H, C-H(2, 5 or 13, 16)), 3.47 (dd, $^{3}J(H\alpha O, CH_2)$= 5.0 Hz, $^{3}J(H\alpha O, CH_2)$ = 6.1 Hz, 2 H, C-H(2, 5 or 13, 16)), 3.11 (td, $^{3}J(H\alpha N, CH_2)$= 6.5 Hz, $^{3}J(H\alpha N, NH)$ = 6.9 Hz, 2 H, C-H(7, 10 or 19, 22)), 2.95 (td, $^{3}J(H\alpha N, CH_2)$= 5.9 Hz, $^{3}J(H\alpha N, NH)$ = 9.6 Hz, 2 H, C-H(7, 10 or 19, 22)), 2.19 (t, $^{3}J(NH, CH_2)$ = 6.4 Hz , 2 H, N-H(11, 23)), 1.65-1.25 (m, 16 H, CH_2), 0.78 (s, 6 H, CH_3), 0.78 (s, 6 H, CH_3), 0.76 (s, 6 H, CH_3), 0.72 (s, 6 H, CH_3);

^{13}C NMR ($CDCl_3$) δ 89.59 and 82.98 (C(2, 5, 13, 16)), 67.74 and 63.89 (C(7, 10, 19, 22)), 38.37 and 38.16 (C(6, 12, 18, 24)), 27.06 (CH_2), 26.02 (CH_2), 25.42 (CH_2), 25.04 (CH2), 24.80 (CH_3), 20.20 (CH_3), 20.15 (CH_3), 13.08 (CH_3).

HRMS calcd. for $C_{28}H_{50}N_2O_2H^+$ 447.3945, found 447.3941.

X-ray: Suitable crystals of **60a** were obtained as colorless plates by slow evaporation of a solution in acetone. The intensity data were collected at 160 K (-113°C) on an Oxford

Difftaction SuperNova, Dual, Cu at zero, Atlas diffractometer [1], equiped with a SuperNova (Cu) X-ray Source, CuKα mirror monochromated radiation (λ = 1.5418 Å).

The structure was solved by direct methods using the program SHELXS-97 [2]. The refinement and all further calculations were carried out using SHELXL-97 [2]. The NH H-atoms were located in difference Fourier maps and were refined isotropically with a distance restraint: N-H = 0.88(2) Å. The C-bound H-atoms were included in calculated positions and treated as riding atoms: C-H = 1.0, 0.99 and 0.98 Å for CH, CH_2 and CH_3, respectively, with $U_{iso}(H) = k \times U_{eq}$(parent C-atom), where k = 1.5 for CH_3 H-atoms and k = 1.2 for all other H-atoms. The non-H atoms were refined anisotropically, using weighted full-matrix least-squares on F^2. A semi-empirical absorption correction was applied using the SCALE3 ABSPACK scaling algorithm in CrysAlis PRO [1]. The presence of a small satalite on the principal crystal lead to some overlap of reflections, which in turn lead to a higher than usual final R1 vlaue (ca. 9%).

[1] Stoe & Cie (2000). IPDS-I Bedienungshandbuch. Stoe & Cie GmbH, Darmstadt, germany.

[2] G. M. Sheldrick. (2008). Acta Cryst. A64, 112-122.

[3] Spek, A. L. (2003). J. Appl. Cryst. 36, 7-13.

[4] Westrip, S. P. (2010). J. Appl. Cryst. 43, 920-925.

Drawing programs:

ORTEP-3: [3] Farrugia, L. J. (1997). J. Appl. Cryst., 30, 565.

Mercury: [4] Macrae, C. F., Edgington, P. R., McCabe, P., Pidcock, E., Shields, G. P., Taylor, R., Towler, M. & van de Streek, J. (2006). J. Appl. Cryst. 39, 453-457.

PLATON: [5] Spek, A. L. (2003). J. Appl. Cryst. 36, 7-13.

2.27. Synthesis of compound 61a* and 61b*

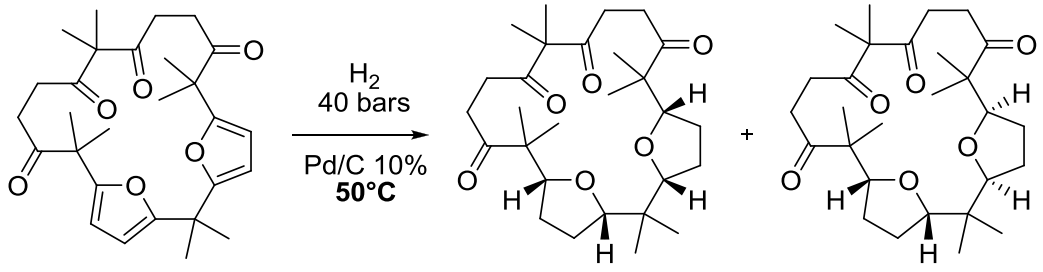

43 → **61a** d.r. 40% 26% + **61b** d.r. 60% 38%

Compound **43** (650 mg, 1.39 mmol) and Pd/C 10% (118 mg, 0.11 mmol) were placed in a test tube (125 x 15 mm) containing a small cross stirring bar. AcOH (10 mL) was added and the test tube was placed inside an autoclave vessel containing AcOH (25 mL). The autoclave was closed, put under magnetic stirring, filled with hydrogen (40 atm), and heated at 50°C for 3 h. After cooling to room temperature, the reaction mixture was filtered through celite and the solid was washed with AcOH (2 x 10 mL) and successively CH_2Cl_2 (2 x 20 mL). The combined filtrate and washings were concentrated under reduced pressure to give colorless slurry, to which CH_2Cl_2 (50 mL) and 5% aqueous NaOH 5% (20 mL) were added. The resulting mixture was stirred for 5 min. The organic layer was then separated and the aqueous phase was extracted with CH_2Cl_2 (2 x 25 mL). The collected organic layers were washed with brine, dried over K_2CO_3, and concentrated under reduced pressure. The two products were first purified from their impurities by column chromatography (silica, 98/2 CH_2Cl_2/EtOAc), then separated by column chromatography (Al_2O_3, Cyclohexane/EtOAc, 92/8). Finally each product is recrystallized in a mixture of EtOH/EtOAc 1/1 to yield 172 mg (26%) of compound **61a** and 250 mg (38%) of compound **61b**.

2.27.1. Compound 61a*

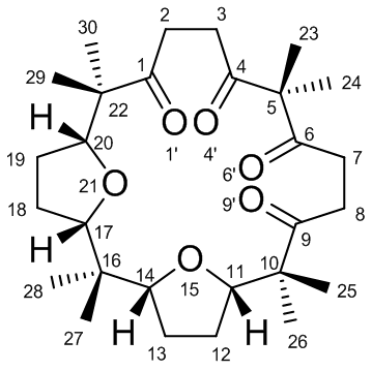

IR (KBr): 2974.8*m*, 2938.0*m*, 2881.3*m*, 1723.3*s*, 1706.7*s*, 1690.4*s*, 1469.2*m*, 1386.1*w*, 1364.6*w*, 1316.3*w*, 1300.2*w*, 1073.5*s*, 1041.6*m*.

^{1}H NMR ($CDCl_3$, 298K) δ 3.72 (dd, ^{3}J(11, 12b) and ^{3}J(20, 19b) = 10.5 Hz, ^{3}J(11, 12a) and ^{3}J(20, 19a) = 5.0 Hz, 2 H, C-H(11, 20)), 3.78 (dd, ^{3}J(14, 13b) and ^{3}J(17, 18b) = 8.0 Hz, ^{3}J(14, 13a) and ^{3}J(17, 18a) = 6.6 Hz, 2 H, C-H(14, 17)), 3.21-3.13 (m, 2 H, CH(22, 8)), 2.85-2.58 (m, 6H, CH_2(2, 8, 3, 7)), 1.85-1.75 (m, 4 H, CH_2(12, 19, 13, 18)), 1.68-1.61 (m, 2 H, CH_2(13, 18)), 1.53-1.43 (m, 2 H, CH_2(12, 19)), 1.48 (s, 3 H, CH_3(23 or 24)), 1.29 (s, 3 H, CH_3(23 or

24)), 1.27 (s, 6 H, CH_3(25, 30 or 26, 29)), 1.04 (s, 6 H, CH_3(25, 30 or 26, 29)), 0.66 (s, 6 H, CH_3(27 or 28)), 0.60 (s, 6 H, CH_3(27 or 28));

^{13}C NMR ($CDCl_3$) δ 213.81 (C(1, 9)=O), 210.21 (C(4, 6)=O), 84.67 (C(11, 20)), 83.04 (C(14, 17)), 61.58 (C(16)), 49.87 (C(10, 22)), 39.94 (C(5)), 34.11 (C(3, 7)), 33.53 (C(2, 8)), 26.22 (C(12, 19)), 24.93 (C(13, 18)), 23.17 (C(25, 30 or 26, 29)), 21.88 (C(23 or 24)), 21.00 (C(23 or 24)), 18.86 (C(25, 29 or 26, 30)), 18.15 (C(27 or 28)), 17.74 (C(27 or 28)).

Melting point: 191°C.

HRMS calcd. for $C_{28}H_{44}O_6Na^+$ 499.3030, found 499.3032.

2.27.2. Compound 61b*

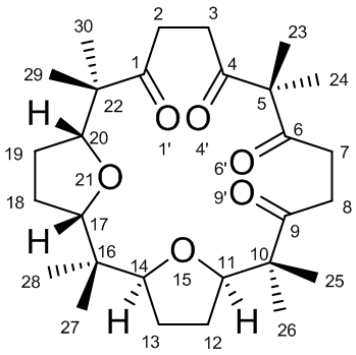

IR (KBr): 2973.5*m*, 2940.4*m*, 2880.3*m*, 1698.8*s*, 1473.9*m*, 1420.4*w*, 1385.6*m*, 1363.8*m*, 1316.1*w*, 1069.9*s*, 1008.7*m*.

^{1}H NMR ($CDCl_3$, 298K) δ 3.94 (dd, ^{3}J(11,20H12a,19a) = 4.9 Hz, ^{3}J(11,20H12b,19b) = 10.5 Hz, 2H, C-H(11, 20)), 3.82 (dd, ^{3}J(14,17H13a,18a) = 6.1 Hz, ^{3}J(14,17H13b,18b) = 7.7 Hz, 2 H, C-H(14, 17)), 2.94-2.85 (m, 2 H, CH_2(2, 8)), 2.80-2.67 (m, 4 H, CH_2(2, 8, 3, 7), 2.52-2.43 (m, 2 H, CH_2(3, 7)), 1.84-1.73 (m, 4 H, CH_2(12, 19, 13, 18)), 1.66-1.59 (m, 2 H, CH_2(13, 18)), 1.48-1.37 (m, 2 H, CH_2(12, 19)), 1.37 (s, 6 H, CH_3(23, 24)), 1.08 (s, 6 H, CH_3(25, 29 or 26, 30)), 1.05 (s, 6 H, CH_3(25, 29 or 26, 30)), 0.66 (s, 6 H, CH_3(27, 28));

^{13}C NMR ($CDCl_3$) δ 212.87 (C(1, 9)=O), 209.20 (C(4, 6)=O), 82.48 (C(11, 20)), 81.50 (C(14, 17)), 63.31 (C(16)), 50.07 (C(10, 22)), 40.04 (C(5)), 33.36 (C(3, 7)), 31.88 (C(2, 8)),

25.99 (C(12, 19)), 25.31 (C(13, 18)), 23.15 ((C25, 29 or 26, 30)), 20.72 (C(23, 24)), 17.27 (C(27, 28)), 16.14 (C(25, 29 or 26, 30)).

Melting point: 167°C.

HRMS calcd. for $C_{28}H_{44}O_6Na^+$ 499.3030, found 499.3028.

X-ray: Suitable crystals of **61b** were obtained as colorless rods by recrystallization from ethyl acetate. The intensity data were collected at 173K (-100°C) on a Stoe Mark II-Image Plate Diffraction System [1] equipped with a two-circle goniometer and using MoKα graphite monochromated radiation (λ = 0.71073 Å). Image plate distance 130mm, ω rotation scans 0 - 180° at φ 0°, step $\Delta\omega$ = 1.0°, exposures of 3 mins per image, 2θ range 1.76 - 52.59°, d_{min} – d_{max} = 23.107 - 0.802 Å.

The structure was solved by Direct methods using the program SHELXS-97 [2]. The refinement and all further calculations were carried out using SHELXL-97 [2].

The C-bound H-atoms were included in calculated positions and treated as riding atoms: C-H = 1.00, 0.99 and 0.98 Å for CH, CH_2 and CH_3, respectively, with $U_{iso}(H) = k \times U_{eq}$(parent C-atom), where k = 1.5 for CH_3 H-atoms and k = 1.2 for all other H-atoms. The non-H atoms were refined anisotropically, using weighted full-matrix least-squares on F^2. A semi-empirical absorption correction was applied using the MULscanABS routine in PLATON [3].

[1] Stoe & Cie (2000). IPDS-I Bedienungshandbuch. Stoe & Cie GmbH, Darmstadt, germany.
[2] G. M. Sheldrick. (2008). Acta Cryst. A64, 112-122.
[3] Spek, A. L. (2003). J. Appl. Cryst. 36, 7-13.
[4] Westrip, S. P. (2010). J. Appl. Cryst. 43, 920-925.

Drawing programs:

ORTEP-3: [3] Farrugia, L. J. (1997). J. Appl. Cryst., 30, 565.

Mercury: [4] Macrae, C. F., Edgington, P. R., McCabe, P., Pidcock, E., Shields, G. P., Taylor, R., Towler, M. & van de Streek, J. (2006). J. Appl. Cryst. 39, 453-457.

PLATON: [5] Spek, A. L. (2003). J. Appl. Cryst. 36, 7-13.

2.28. Synthesis of compound 62*

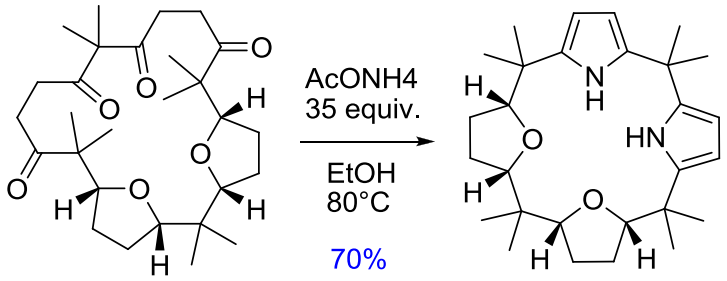

61a **62**

In a round-bottom flask were introduced **61a** (115 mg, 0.24 mmol) and ethanol (20 mL). Then, $AcONH_4$ (650 mg, 8.44 mmol) was added to the slurry, and the mixture was stirred at 80°C for 6 h. After cooling, CH_2Cl_2 (100 mL) was added and the reaction mixture was basified with 5% sodium hydroxide and washed with saturated brine. The aqueous layer was extracted three times with CH_2Cl_2 (20 mL). The combined organic layers were dried with sodium sulfate, and the solvent was removed under vacuum. The residue was first purified by column chromatography (SiO_2, Cyclohexane/EtOAc, 9/1), then by recrystallization in EtOH to yield 74 mg (70%) of colorless powder.

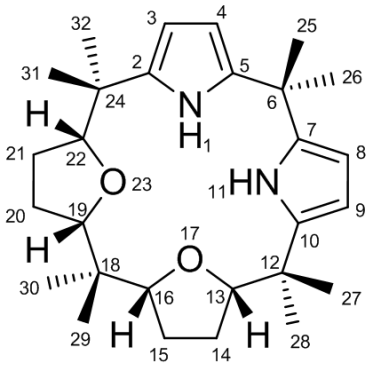

IR (KBr): 3400.2*s*, 2977.9*s*, 2962.0*s*, 2930.2*m*, 2854.7*m*, 1587.2*m*, 1466.1*m*, 1289.6*m*, 1167.0*w*, 1049.3*s*, 1037.9*s*, 962.4*m*, 778.1*s*, 766.3*m*, 530.0*w*.

^{1}H NMR ($CDCl_3$, 298K) δ 8.83 (bs, 2 H, NH(1, 11)), 5.92 (dd, ^{3}J(3, 4) and ^{3}J(9, 8) = 3.2 Hz, ^{4}J(3, 1) and ^{4}J(9, 11) = 3.0 Hz, 2 H, C-H(3, 9)), 5.87 (dd, ^{3}J(4, 3) and ^{3}J(8, 9) = 3.2 Hz, ^{4}J(4, 1) and ^{4}J(8, 11) = 2.6 Hz, 2 H, C-H(4, 8)), 3.74 (m, 4 H, C-H(13, 16, 19, 22)), 1.80 (m, 4 H, CH_2), 1.70 (s, 3 H, CH_3(25 or 26)), 1.59 (s, 3 H, CH_3(25 or 26)), 1.58 (m, 4 H, CH_2), 1.31 (s, 6 H, CH_3(27, 31 or 28, 32)), 1.21 (s, 6 H, CH_3(27, 31 or 28, 32)), 0.82 (s, 3 H, CH_3(29 or 30)), 0.79 (s, 3 H, CH_3(29 or 30));

^{13}C NMR ($CDCl_3$) δ 137.84 (C(5, 7)), 136.71 (C(2, 10)), 103.42 (C(3, 9)), 101.91 (C(4, 8)), 87.55, 87.40 (C(13, 16, 19, 22)), 39.02 (C(6)), 37.46 (C(12, 24)), 35.42 (C(18)), 31.32 (C(25 or 26)), 29.79 (C(25 or 26)), 27.17 (C(27, 31 or 28, 32)), 27.05 (CH_2), 26.15 (CH_2), 23.86 (C(29 or 30)), 23.55 (C(27, 31 or 28, 32)), 13.33 (C(29 or 30)).

Melting point: 196.4°C.

HRMS calcd. for $C_{28}H_{42}N_2O_2Na^+$ 461.3138, found 461.3131.

X-ray: Suitable crystals of **62** were obtained as colourless rods by recrystallization from ethanol. The intensity data were collected at 173K (-100°C) on a Stoe Mark II-Image Plate Diffraction System [1] equiped with a two-circle goniometer and using MoKα graphite monochromated radiation (λ = 0.71073 Å). Image plate distance 130mm, ω rotation scans 0 - 180° at φ = 0°, step Δω = 1.0°, exposures of 3 mins per image, 2θ range 1.76 - 52.59°, d_{min} – d_{max} = 23.107 - 0.802 Å.

The structure was solved by Direct methods using the program SHELXS-97 [2]. The refinement and all further calculations were carried out using SHELXL-97 [2]. All of the H atoms could be located in difference Fourier maps. The NH and the methyl H atoms located about the mirror plane were freely refined, while the remainder were included in calculated positions and treated as riding atoms: C-H = 0.95, 1.00, 0.99 and 0.98 Å for CH(aromatic), CH(methine), CH_2 and CH_3 H atoms, respectively, with $U_{iso}(H) = k \times U_{eq}(C)$, where k = 1.5 for CH_3 H atoms, and k = 1.2 for all other H atoms.

The non-H atoms were refined anisotropically, using weighted full-matrix least-squares on F^2. A semi-empirical absorption correction was applied using the MULscanABS routine in PLATON [3].

The molecule has mirror symmetry, with atoms C5 ,C6, C7, and C15, C16, C17 located in the mirror.

[1] Stoe & Cie (2000). IPDS-I Bedienungshandbuch. Stoe & Cie GmbH, Darmstadt, germany.

[2] G. M. Sheldrick. (2008). Acta Cryst. A64, 112-122.

[3] Spek, A. L. (2003). J. Appl. Cryst. 36, 7-13.

[4] Westrip, S. P. (2010). J. Appl. Cryst. 43, 920-925.

Drawing programs:

ORTEP-3: [3] Farrugia, L. J. (1997). J. Appl. Cryst., 30, 565.

Mercury: [4] Macrae, C. F., Edgington, P. R., McCabe, P., Pidcock, E., Shields, G. P., Taylor, R., Towler, M. & van de Streek, J. (2006). J. Appl. Cryst. 39, 453-457.

PLATON: [5] Spek, A. L. (2003). J. Appl. Cryst. 36, 7-13.

2.29. Synthesis of compound 63*, 64* and 65*

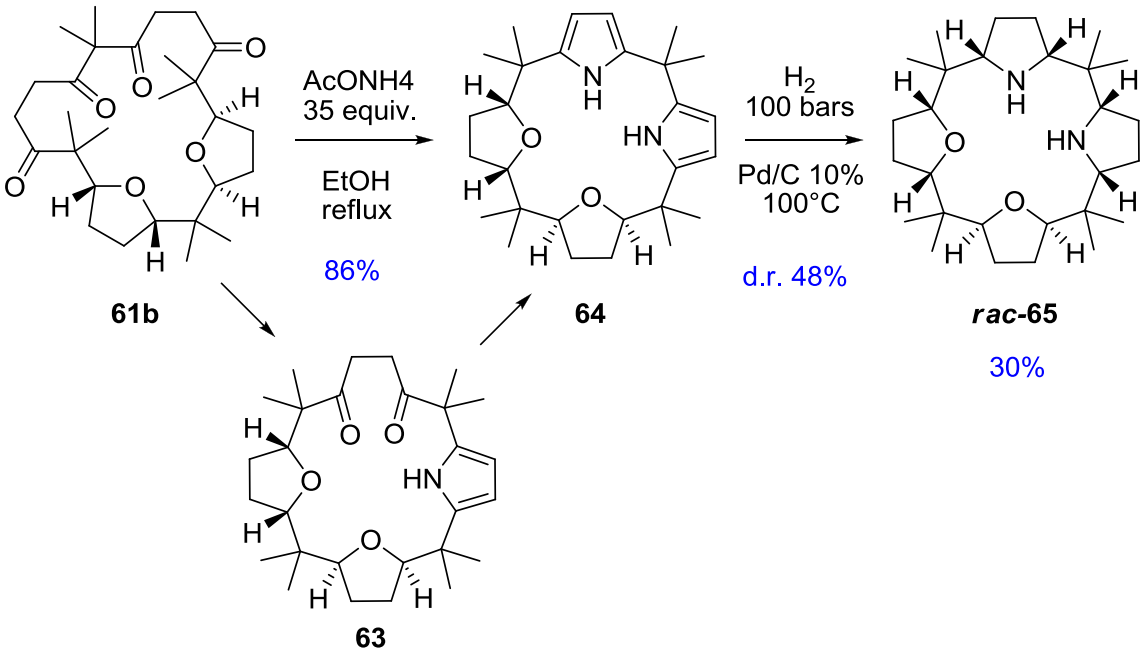

2.29.1. Compound 63* and 64*

In a round-bottom flask were introduced **61b** (273 mg, 0.57 mmol) and ethanol (60 mL). Then, $AcONH_4$ (1.54 g, 20 mmol) was added to the slurry, and the mixture was stirred at 85°C for 12 h. After cooling, CH_2Cl_2 (150 mL) was added and the reaction mixture was basified with 5% sodium hydroxide and washed with saturated brine. The aqueous layer was extracted three times with CH_2Cl_2 (30 mL). The combined organic layers were dried with sodium sulfate, and the solvent was removed under vacuum. The residue was solved in CH_2Cl_2 and purified by filtration through a pad of silica to yield 216 mg (86%) of colorless powder. The reaction could be stopped during the reaction to allow the isolation of compound **63**. After the same treatment than previously described, the residue is purified by column chromatography (SiO_2, CH_2Cl_2).

2.29.1.1. Compound **63***

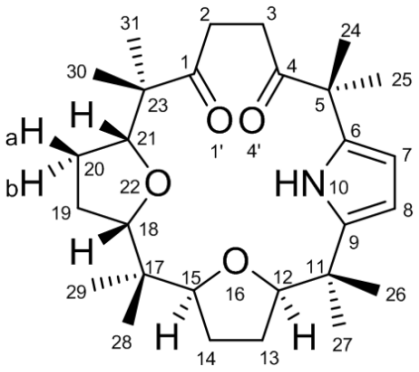

IR (KBr): 3430.5*s*, 2974.8*s*, 2872.2*s*, 1701.9*s*, 1572.3*w*, 1474.4*m*, 1389.5*m*, 1366.0*w*, 1303.3*w*, 1240.4*w*, 1128.6*w*, 1079.4*s*, 1063.8*s*, 765.7*s*, 725.2*w*, 569.3*w*.

^{1}H NMR ($CDCl_3$, 298K) δ 8.74 (bs, 1 H, NH(10)), 5.92 (dd, ^{3}J(7, 8) = 3.2 Hz, ^{4}J(7 or 8, 10) = 3.0 Hz, 1 H, C-H(7 or 8)), 5.84 (dd, ^{3}J(7, 8) = 3.2 Hz, ^{4}J(7 or 8, 10) = 2.5 Hz, 1 H, C-H(7 or 8)), 4.14 (dd, ^{3}J(21, 20b) = 11.1 Hz, ^{3}J(21, 20a) = 4.4 Hz, 1 H, C-H(21)), 4.06 (dd, ^{3}J(18, 19b) = 9.3 Hz, ^{3}J(18, 19a) = 4.5 Hz, 1 H, C-H(18)), 3.96 (t, ^{3}J(15, 14a) = 6.8 Hz, ^{3}J(15, 14b) = 6.8 Hz, 1 H, C-H(15)), 3.56 (dd, ^{3}J(12, 13b) = 10.6 Hz, ^{3}J(12, 13a) = 5.0 Hz, 1 H, C-H(12)), 2.88-2.52 (m, 4 H, CH(22, 3)), 1.97 (m, 1 H, CH_2(THF)), 1.79 (m, 4H, CH_2(THF)), 1.64 (m, 1 H, CH_2(THF)), 1.68-1.44 (m, 2 H, CH_2(THF)), 1.56 (s, 3 H, CH_3(24 or 25)), 1.45 (s, 3 H, CH_3(24 or 25)), 1.25 (s, 3 H, CH_3(26 or 27)), 1.21 (s, 3 H, CH_3(26 or 27)), 1.12 (s, 3 H, CH_3(30 or 31)), 1.11 (s, 3 H, CH_3(30 or 31)), 0.82 (s, 3 H, CH_3(28 or 29)), 0.73 (s, 3 H, CH_3(28 or 29));

^{13}C NMR ($CDCl_3$) δ 214.14 (C(1)=O), 211.57 (C(4)=O), 103.77 and 102.40 (C(pyrrole)), 86.44 (C(12)), 81.82 (C(15)), 81.72 (C(21)), 81.26 (C(18)), 50.33 (C(23)), 48.03 (C(5)), 40.15 (C(17)), 36.59 (C(11)), 33.47 (C(2 or 3)), 32.22 (C(2 or 3)), 26.48 (CH_2(THF)), 26.25 (CH_2(THF)), 25.75 (CH_2(THF)), 25.52 (C(24 or 25)), 25.29 (CH_2(THF)), 23.99 (C(26 or 27)), 23.28 (C(24 or 25)), 21.75 (C(30 or 31)), 21.16 (C(26 or 27)), 17.38 (C(28 or 29)), 17.08 (C(28 or 29)), 16.03 (C(30 or 31)).

Melting point: 214.5°C.

HRMS calcd. for $C_{28}H_{43}NO_4H^+$ 458.3265, found 458.3265.

2.29.1.2. Compound **64***

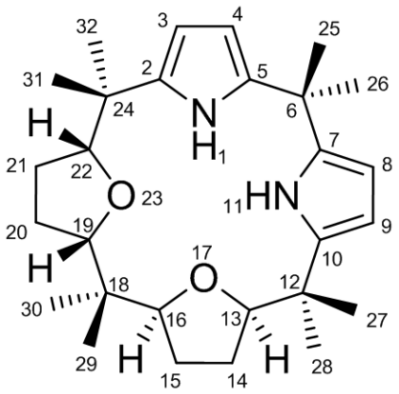

IR (KBr): 3439.4*s*, 2971.6*s*, 2932.4*m*, 2864.0*m*, 1580.5*w*, 1466.3*w*, 1360.4*w*, 1232.1*w*, 1177.8*w*, 1076.7*m*, 1041.3*s*, 963.3*w*, 765.1*s*, 730.9*w*, 718.9*w*.

^{1}H NMR ($CDCl_3$, 298K) δ 8.85 (bs, 2H, NH(1, 11)), 5.84 (dd, ^{3}J(4, 3) and ^{3}J(8, 9) = 3.1 Hz, ^{4}J(4, 1) and ^{4}J(8, 11) = 3.0 Hz, 2 H, C-H(4, 8)), 5.76 (dd, ^{3}J(3, 4) and ^{3}J(9, 8) = 3.0 Hz, ^{4}J(3, 1) and ^{4}J(9, 11) = 2.8 Hz, 2 H, C-H(3, 9)), 3.78 (dd, ^{3}J(13, 14b) and ^{3}J(22, 21b) = 8.1 Hz, ^{3}J(13, 14a) and ^{3}J(22, 21a) = 5.9 Hz, 2 H, C-H(13, 22)), 3.67 (dd, ^{3}J(16, 15b) and ^{3}J(19, 20b) = 10.6 Hz, ^{3}J(16, 15a) and ^{3}J(19, 20a) = 5.3 Hz, 2 H, C-H(16, 19)), 1.84-1.70 (m, 6 H, CH_2), 1.65 (s, 6 H, CH_3(25, 26)), 1.49-1.41 (m, 2 H, CH_2), 1.22 (s, 3 H, CH_3(27, 31 or 28, 32)), 1.10 (s, 6 H, CH_3(27, 31 or 28, 32)), 0.95 (s, 6 H, CH_3(29, 30));

^{13}C NMR ($CDCl_3$) δ 138.36 (C(5, 7)), 138.05 (C(2, 10)), 102.31 (C(3, 9)), 101.16 (C(4, 8)), 86.00 (C(13, 22)), 84.07 (C(16, 19)), 38.31 (C(18)), 37.56 (C(12, 24)), 34.84 (C(6)), 28.79 (CH_2), 26.12 (CH_2), 24.04 (C(27, 31 or 28, 32)), 22.12 (C(27, 31 or 28, 32)), 22.12 (C(29, 30)).

Melting point: 150°C.

HRMS calcd. for $C_{28}H_{43}N_2O_2H^+$ 439.3319, found 439.3321.

2.29.2. Compound 65*

Compound **64** (49 mg, 0.111 mmol) and Pd/C 10% (43 mg, 0.040 mmol) were placed in a test tube (125 x 15 mm) containing a small cross stirring bar. AcOH (5 mL) was added and the test tube was placed inside an autoclave vessel containing AcOH (25 mL). The autoclave was closed, put under magnetic stirring, filled with hydrogen (100 atm), and heated at 100°C for 12 h. After cooling to room temperature, the reaction mixture was filtered through celite and

the solid was washed with AcOH (2 x 5 mL) and successively CH_2Cl_2 (2 x 10 mL). The combined filtrate and washings were concentrated under reduced pressure to give colorless slurry, to which CH_2Cl_2 (25 mL) and 5% aqueous NaOH 5% (10 mL) were added. The resulting mixture was stirred for 5 min. The organic layer was then separated and the aqueous phase was extracted with CH_2Cl_2 (2 x 15 mL). The collected organic layers were washed with brine, dried over K_2CO_3, and concentrated under reduced pressure. The product was purified by column chromatography (Al_2O_3, Tolune/Acetone, 4/1) to yield 15 mg (30%) of compound **65**.

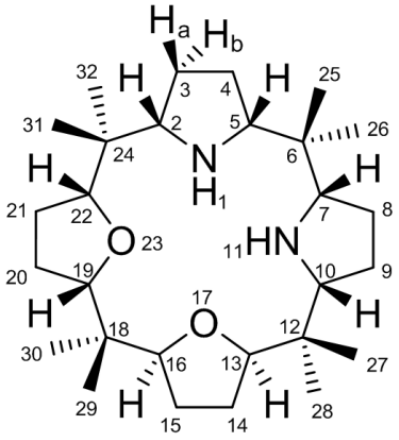

IR (KBr): 2962.0*s*, 2871.3*s*, 2801.12*m*, 2652.5*w*, 1467.1*m*, 1391.3*m*, 1265.5*w*, 1107.7*m*, 1089.1*m*, 1073.0*m*, 1038.5*m*, 1004.9*w*, 971.9*w*, 935.3*w*, 607.6*w*, 561.9*w*.

^{1}H NMR ($CDCl_3$, 298K) δ 3.89 (dd, ^{3}J(HαO,CH_2) = 6.0 Hz, ^{3}J(HαO,CH_2) = 9.6 Hz, 1 H, C-H(αO)), 3.76 (dd, ^{3}J(HαO, CH_2) = 6.8 Hz, ^{3}J(HαO, CH_2) = 9.0 Hz, 1 H, C-H(αO)), 3.60 (m, 1 H, C-H(αO)), 3.41 (m, 1 H, C-H(αO)), 3.20 (dd, ^{3}J(HαN, CH_2) = 7.1 Hz, ^{3}J(HαN, CH_2) = 7.8 Hz, 1 H, C-H(αN)), 3.11 (dd, ^{3}J(HαN, CH_2) = 7.1 Hz, ^{3}J(HαN, CH_2) = 7.6 Hz, 1 H, C-H(αN)), 2.82 (dd, ^{3}J(HαN, CH_2) = 7.6 Hz, ^{3}J(HαN, CH_2) = 7.9 Hz, 1 H, C-H(αN)), 2.68 (dd, ^{3}J(HαN, CH_2) = 5.6 Hz, ^{3}J(HαN, CH_2) = 10 Hz, 1 H, C-H(αN)), 2.08-1.94 (m, 3 H, CH_2(pyrrolidine)), 1.68-1.28 (m, 17 H, CH_2(THF, pyrrolidine, NH), 0.85 (s, 3 H, CH_3), 0.84 (s, 3 H, CH_3), 0.84 (s, 3 H, CH_3), 0.81 (s, 3 H, CH_3), 0.74 (s, 3 H, CH_3), 0.73 (s, 3 H, CH_3), 0.72 (s, 3 H, CH_3), 0.71 (s, 3 H, CH_3);

^{13}C NMR ($CDCl_3$) δ 83.02, 82.63, 81.70 and 80.87 (C(13, 16, 19, 22)), 70.71, 69.27, 64.34 and 62.74 ((C2, 5, 7, 10)), 37.76, 37.73, 37.60 and 37.20 (C(6, 12, 18, 24)), 28.48 (CH_3), 26.68 (CH_3), 26.51 (CH_2), 25.76 (CH_2), 25.73 (CH_2), 25.32 (CH_2), 24.54 (CH_2), 24.50 (CH_2),

23.81 (CH_2), 23.42 (CH_2), 19.13 (CH_3), 18.18 (CH_3), 18.10 (CH_3), 17.83 (CH_3), 17.50 (CH_3), 17.44 (CH3).

HRMS calcd. for $C_{28}H_{50}N_2O_2H^+$ 447.3945, found 447.3943

X-ray: Suitable crystals of **65** were obtained as colourless plates by slow evaporation of a solution in dichloromethane. The intensity data were collected at 173K (-100°C) on a Stoe Mark II-Image Plate Diffraction System [1] equiped with a two-circle goniometer and using MoKα graphite monochromated radiation (λ = 0.71073 Å). Image plate distance 130mm, ω rotation scans 0 - 71° at φ 0°, andstep Δω = 1.0°, exposures of 12 mins per image, 2θ range 1.76 - 52.59°, d_{min} – d_{max} = 23.107 - 0.802 Å.

The structure was solved by Direct methods using the program SHELXS-97 [2]. The refinement and all further calculations were carried out using SHELXL-97 [2].

The NH H-atoms were not located or included in the refinement as it was not possible to be absolutely sure about the positions of the O and N atoms – possible rotational disorder. The C-bound H-atoms were included in calculated positions and treated as riding atoms: C-H = 0.99 and 0.98 Å for CH_2 and CH_3, respectively, with $U_{iso}(H) = k \times U_{eq}$(parent C-atom), where k = 1.5 for CH_3 H-atoms and k = 1.2 for other H-atoms. The non-H atoms were refined anisotropically, using weighted full-matrix least-squares on F^2.

One of the five membered rings is disorded with atoms N1,C27,C28 having an occupancy ratio for the two parts of 0.640(13):0.365(4). The crystal diffracted extremely weakly beyond 24˚ in 2θ [I/σ = 1.1]. In the final cycles of refinemt the 2θ maximum was limited to 42˚ in 2θ.

[1] Stoe & Cie (2000). IPDS-I Bedienungshandbuch. Stoe & Cie GmbH, Darmstadt, germany.
[2] G. M. Sheldrick. (2008). Acta Cryst. A64, 112-122.
[3] Spek, A. L. (2003). J. Appl. Cryst. 36, 7-13.
[4] Westrip, S. P. (2010). J. Appl. Cryst. 43, 920-925.

Drawing programs:

ORTEP-3: [3] Farrugia, L. J. (1997). J. Appl. Cryst., 30, 565.

Mercury: [4] Macrae, C. F., Edgington, P. R., McCabe, P., Pidcock, E., Shields, G. P., Taylor, R., Towler, M. & van de Streek, J. (2006). J. Appl. Cryst. 39, 453-457.

PLATON: [5] Spek, A. L. (2003). J. Appl. Cryst. 36, 7-13.

2.30. Synthesis of compound 67 and 69*

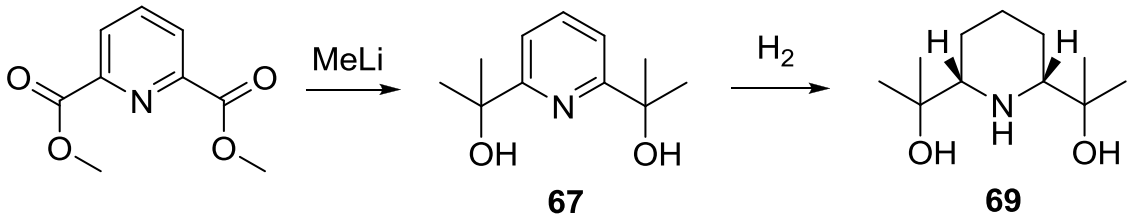

2.30.1. Compound 67 (2,2'-(pyridine-2,6-diyl)dipropan-2-ol)

A 3 M solution of MeLi (29.4 mL, 86 mmol) was added dropwise to dimethyl pyridine-2,6-dicarboxylate (4 g, 20.05 mmol) in THF (100 mL) at -78 °C. After stirring at room temperature for 2 h, the mixture was quenched with an aqueous saturated NH_4Cl solution (100 mL) and extracted with CH_2Cl_2 (3 x 30 mL). The collected organic layers were washed with brine, dried over K_2CO_3, and concentrated under reduced pressure. The product was first purified by chromatography (SiO2, CH_2Cl_2/MeOH, 97/3), then by recrystallization in EtOH to give 2.54 g (65%) of colorless crystals.

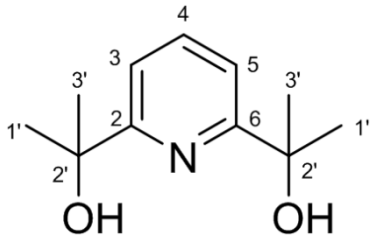

^{1}H NMR ($CDCl_3$, 298K) δ 7.73 (t, ^{3}J(4, 3) = ^{3}J(4, 5) = 33.2 Hz, 1 H, C-H(4)), 7.33 (d, ^{3}J(3, 4) and ^{3}J(5, 4) = 33.4 Hz, 2 H, C-H(3, 5)), 4.17 (s, 2 H, O-H), 1.57 (s, 12 H, CH_3(1', 3')));

^{13}C NMR ($CDCl_3$) δ 165.76 (C(2 or 6)), 164.43 (C(2 or 6)), 138.00 (C(4)), 116.75 (C(3, 5)), 72.23 (C(2')), 30.53 (C(1', 3')).

Ms calcd. for $C_{11}H_{17}NO_2$ 195.12, found 196.2 (M+H)+. Autre ref biblio
See additional analyses in "A. Klein, S. Elmas and K. Butsch *Eur. J. Inorg. Chem.* **2009**, 2271–2281".

2.30.2. Compound 69*

Compound **67** (500 mg, 2.56 mmol) and Pd/C 10% (430 mg, 0.40 mmol) were placed in an autoclave vessel containing a stirring bar and a mixture of AcOH (10 mL) and MeOH (10

mL). The autoclave was closed, put under magnetic stirring, filled with hydrogen (100 atm), and heated at 50°C for 12 h. After cooling to room temperature, the reaction mixture was filtered through celite and the solid was washed with AcOH (2 x 10 mL) and successively CH_2Cl_2 (2 x 10 mL). The combined filtrate and washings were concentrated to give a slurry residue, which was dried under high vacuum. Addition of CH_2Cl_2 (30 mL) to the stirred reaction product led to the formation of a suspension. The solid was filtered off, then the solid was basified by 5% aqueous NaOH 5% (30 mL) and solubilized in CH_2Cl_2 (50 mL). The resulting mixture was stirred for 5 min. The organic layer was then separated and the aqueous phase was extracted with CH_2Cl_2 (2 x 15 mL). The collected organic layers were washed with brine, dried over K_2CO_3, and concentrated under reduced pressure to give 495 mg (96%) of compound **69**.

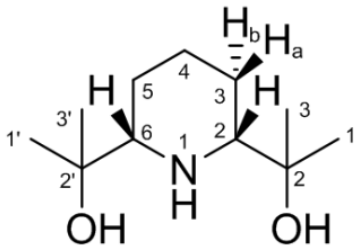

IR (KBr): 3377*bs*, 2982*s*, 2944*s*, 2855*m*, 2782*m*, 2694*w*, 2586*w*, 1456*m*, 1442*m*, 1380*s*, 1130*s*, 931*s*, 822*s*, 537*w*.

^{1}H NMR ($CDCl_3$, 298K) δ 2.88 (bs, 2 H, OH), 2.47 (d, ^{3}J(2, 3b) and ^{3}J(6, 5b) = 11.4 Hz, 2 H, C-H(2, 6)), 1.97 (dquint, ^{3}J(4b, 4a) = 13.3 Hz, ^{3}J(4b, 3b) = ^{3}J(4b, 5b) = 3.3 Hz, ^{3}J(4b, 3a) = ^{3}J(4b, 5a) = 3.3 Hz, 1 H, C-H(4b)), 1.74 (dd, ^{3}J(3a, 3b) and ^{3}J(5a, 5b) = 12.8 Hz, ^{3}J(3a, 4b) and ^{3}J(5a, 4b) = 3.0 Hz, 2 H, C-H(3a, 5a)), 1.45 (qt, ^{3}J(4a, 4b) = 13.0 Hz, ^{3}J(4a, 3b) and ^{3}J(4a, 5b) = 13.0 Hz, ^{3}J(4a, 3a) = ^{3}J(4a, 5a) = 3.7 Hz, 1 H, C-H(4a)), 1.25 (s, 6 H, CH_3), 1.16 (s, 6 H, CH_3), 1.06 (qd, ^{3}J(3b, 2) and ^{3}J(5b, 6) = 12.3 Hz, ^{3}J(3b, 3a) and ^{3}J(5b, 5a) = 12.3 Hz, ^{3}J(3b, 4a) and ^{3}J(5b, 4a) = 12.3 Hz, ^{3}J(3b, 4b) and ^{3}J(5b, 4b) = 3.3 Hz, 2 H, CH_2(3b, 5b));

^{13}C NMR ($CDCl_3$) δ 71.67 (C(2, 2')), 65.45 (C(2, 6)), 27.45 (CH_3), 26.91 (C(3, 5)), 24.69 (C(4)), 24.36 (CH_3).

Melting point: 72.3°C.

HRMS calcd. for [$C_{11}H_{23}NO_2$+H^+] 224.1621, found 224.1621.

X-ray: Suitable crystals of **69** were obtained as colorless blocks by slow evaporation of a solution in dichloromethane. The intensity data were collected at 173K (-100°C) on a Stoe Mark II-Image Plate Diffraction System [1] equiped with a two-circle goniometer and using MoKα graphite monochromated radiation (λ = 0.71073 Å). Image plate distance 130mm, ω rotation scans 0 - 180° at φ 0°, and 0 - 180° at φ = 90°, step Δω = 1.0°, exposures of 2 mins per image, 2θ range 1.76 - 52.59°, d_{min} – d_{max} = 23.107 - 0.802 Å.

The structure was solved by Direct methods using the program SHELXS-97 [2]. The refinement and all further calculations were carried out using SHELXL-97 [2]. The NH and OH H-atoms were located in difference Fourier maps and were refined with distances restraints: O-H = 0.84(2) Å and N-H = 0.88(2) Å, with U_{iso}(H) = 1.5 U_{eq}(parent O/N-atom).

The C-bound H-atoms were included in calculated positions and treated as riding atoms: C-H = 1.0, 0.99 and 0.98 Å for CH, CH_2 and CH_3, respectively, with U_{iso}(H) = k × U_{eq}(parent C-atom), where k = 1.5 for CH_3 H-atoms and k = 1.2 for all other H-atoms. The non-H atoms were refined anisotropically, using weighted full-matrix least-squares on F^2.

The OH H-atoms are disordered over two positions each with an occupancy of 0.5.

[1] Stoe & Cie (2000). IPDS-I Bedienungshandbuch. Stoe & Cie GmbH, Darmstadt, germany.

[2] G. M. Sheldrick. (2008). Acta Cryst. A64, 112-122.

[3] Spek, A. L. (2003). J. Appl. Cryst. 36, 7-13.

[4] Westrip, S. P. (2010). J. Appl. Cryst. 43, 920-925.

Drawing programs:

ORTEP-3: [3] Farrugia, L. J. (1997). J. Appl. Cryst., 30, 565.

Mercury: [4] Macrae, C. F., Edgington, P. R., McCabe, P., Pidcock, E., Shields, G. P., Taylor, R., Towler, M. & van de Streek, J. (2006). J. Appl. Cryst. 39, 453-457.

PLATON: [5] Spek, A. L. (2003). J. Appl. Cryst. 36, 7-13.

2.31. Synthesis of compound 72

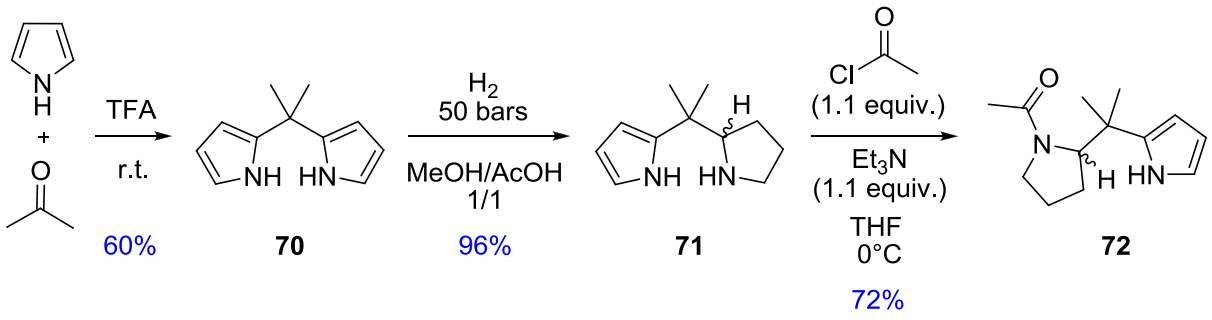

2.31.1. Compound 70 (2,2'-(propane-2'',2''-diyl)bis(1H-pyrrole))

In a round-bottom flask were introduced pyrrole (31.72 mL, 0.459 mol) and acetone (4.21 mL, 57.4 mmol). The flask was equipped with a stirring bar and a reflux condenser. The mixture was stirred for 5 minutes, then trifluoroacetic acid (0.439 mL, 5.74 mmol) was added and the mixture was stirred for an additional 15 minutes. After stirring, CH_2Cl_2 was added and the reaction mixture was basified with 5% sodium hydroxide and washed with saturated brine. The aqueous layer was extracted two times with CH_2Cl_2. The combined organic layers were dried with sodium sulfate, and the solvent was removed under vacuum. The residue was purified by column chromatography (SiO_2, Cyclohexane/EtOAc, 8/2) to yield 6 g (60%) of pale yellow crystals.

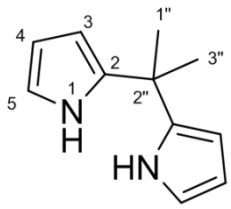

^{1}H NMR ($CDCl_3$, 298K) δ 7.72 (bs, 2 H, N-H(1)), 6.62-6.60 (m, 2 H, pyrrolic-H(5)), 6.15-6.13 (m, 2 H, pyrrolic-H(4)), 6.11-6.09 (m, 2 H, pyrrolic-H(3)), 1.59 (s, 6 H, CH_3(1'', 3''));

^{13}C NMR ($CDCl_3$) δ 139.24 (C(2)), 117.19 (C(5)), 107.91 (C(4)), 103.87 (C(3)), 35.52 (C(2'')), 29.46 (C(1'', 3'')).

MS calcd for $C_{11}H_{14}N_2$: 174.11, found 174.01 (M•).
See additional analyses in "B. J. Littler, M. A. Liller, C. –H. Hung, R. W. Wagner, D. F. O'Shea, P. D. Boyle, J. S. Lindsey, *J. Org. Chem.* **1999**, 64, 1391-1396." and "Andrioletti, B.; Rose, E. *J. Chem. Soc., Perkin Trans. 1* **2002**, 715-716."

X-ray: Suitable crystals of **70** were obtained as colourless blocks by slow evaporation of a solution in cyclohexane/ethyl acetate [4:1]. The intensity data were collected at 173K (-100°C) on a Stoe Mark II-Image Plate Diffraction System [1] equiped with a two-circle goniometer and using MoKα graphite monochromated radiation. Image plate distance 100mm, ω rotation scans 0 - 180° at ϕ 0°, and 0 – 103.0° at ϕ 90°, step Δω = 1.0°, exposures of 3 mins per image, 2θ range 2.29 – 59.53°, d_{min} – d_{max} = 17.779 – 0.716 Å.

The structure was solved by Direct methods using the program SHELXS [2]. The refinement and all further calculations were carried out using SHELXL-97 [2].

The NH H.-atoms were located in an electron density difference map and were freely refined. The C-bound H-atoms were included in calculated positions and treated as riding atoms using SHELXL default parameters. The non-H atoms were refined anisotropically, using weighted full-matrix least-squares on F^2.

The compound crystallized with two independent molecules per asymmetric unit.

[1] Stoe & Cie. (2009). *X-Area V1.52 & X-RED32 V1.48 Software*. Stoe & Cie GmbH, Darmstadt, Germany.

[2] Sheldrick, G. M. (2008) Acta Cryst. A64, 112-122.

[3] Farrugia, L. J. (1997). J. Appl. Cryst., 30, 565.

[4] Macrae, C. F., Edgington, P. R., McCabe, P., Pidcock, E., Shields, G. P., Taylor, R., Towler, M. & van de Streek, J. (2006). J. Appl. Cryst. 39, 453-457.

[5] Spek, A .L. (2009). Acta Cryst. D65, 148-155.

2.31.2. Compound 71* (2'-(2''-(pyrrolidin-2-yl)propan-2''-yl)-1'H-pyrrole)

In an autoclave vessel were introduced dipyrrane **4** (5.00 g, 29 mmol), 10% Pd/C (1.30 g), MeOH (20 mL) and acetic acid (2 mL). The reaction was kept under hydrogen (50 atm) and stirred at room temperature for 20 h. After stirring, the reaction was filtered through a pad of celite and washed three times with CH_2Cl_2. The solution was concentrated under vacuum to give yellow slurry. The slurry was solved in CH_2Cl_2 and washed with 5% sodium hydroxide and the mixture was stirred for 5 minutes. The organic layer was separated and the aqueous layer was extracted three times with CH_2Cl_2. The combined organic layers were washed with brine, dried with sodium sulfate and concentrated under vacuum. The residue was purified by column chromatography (SiO_2, EtOAc/MeOH/trifluoroacetic acid, 95/5/1) to yield 5.0 g (96%) of colorless crystals.

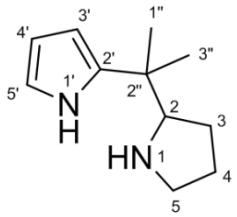

IR (KBr): 3150.4*m*, 3080.7*m*, 2965.8*m*, 2966.5*s*, 2871.8*s*, 1688.4*w*, 1566.6*m*, 1422.9*s*, 879.8*m*, 714.2*s*.

^{1}H NMR ($CDCl_3$, 298K) δ 10.23 (bs, 1 H, N-H(1')), 6.67 (m, 1 H, pyrrolic-H(5')), 6.09 (m, 1 H, pyrrolic-H(4')), 5.92 (m, 1 H, pyrrolic-H(3')), 3.09 (t, ^{3}J(2, 3) = 7.9 Hz, 1 H, CH(2)), 2.90-2.87 (m, 2 H, CH2(5)), 1.87 (bs, 1 H, N-H(1)), 1.78-1.70 (m, 1 H, CH_2(3)), 1.67-1.51 (m, 2 H, CH_2(4)), 1.31 (s, 3H, CH_3(1'')), 1.23 (s, 3 H, CH_3(3'')), 1.22-1.12 (m, 1 H, CH_2(3));

^{13}C NMR ($CDCl_3$) δ 139.65 (C(2')), 116.15 (C(5')), 106.58 (C(4')), 103.97 (C(3')), 69.08 (C(2)), 46.87 (C(5)), 37.43 (C(2'')), 29.62 (C(1'')), 27.10 (C(3)), 26.03 (C(4)), 25.00 (C(3'')).

Melting point: 79.2°C.

MS calcd for $C_{11}H_{18}N_2$: 178.15, found 179.3 (M+H)+.

X-ray: Suitable crystals of **71** were obtained as colorless blocks by recrystallization in ethanol. The intensity data were collected at 173K on a Stoe Image Plate Diffraction System [1] using MoKα graphite monochromated radiation. Image plate distance 70mm, ϕ oscillation scans 0 - 200°, step Δϕ = 1°, exposures of 3 min, 2θ range 4.3 – 51.8°, d_{min} – d_{max} = 12.45 - 0.81 Å. The structure was solved by Direct methods using the program SHELXS-97 [2]. The refinement and all further calculations were carried out using SHELXL-97 [2]. The H-atoms were located from difference electron-density maps and freely refined. The non-H atoms were refined anisotropically, using weighted full-matrix least-squares on F^2.

The compound crystallizes with two independent molecules (A and B) in the asymmetric unit. They differ only slightly, as seen in the auto-fit diagram, Figure 3 [5].

In the crystal they are linked to one another via N-H…N interactions forming a compact rectangular arrangement.

[1] Stoe & Cie. (2009). *X-Area V1.52 & X-RED32 V1.48 Software*. Stoe & Cie GmbH, Darmstadt, Germany.

[2] Sheldrick, G. M. (2008) Acta Cryst. A64, 112-122.

[3] Farrugia, L. J. (1997). J. Appl. Cryst., 30, 565.

[4] Macrae, C. F., Edgington, P. R., McCabe, P., Pidcock, E., Shields, G. P., Taylor, R., Towler, M. & van de Streek, J. (2006). J. Appl. Cryst. 39, 453-457.

[5] Spek, A .L. (2009). Acta Cryst. D65, 148-155.

See X-ray structure "Journot, G., Neier, R.; Stoeckli-Evans, H. *Acta Cryst., Section C.* **2012**, *C68*, o119."

2.31.3. Compound 72* (1''-(2-(2'''-(1'H-pyrrol-2'-yl)propan-2'''-yl)pyrrolidin-1-yl)ethanone

By the way **A**: The amide **72** was prepared according to the general procedure (I) from **71** (100 mg, 0.56 mmol), acetyl chloride (83.8 uL, 1.17 mmol), potassium carbonate (163 mg, 1.17 mmol) in THF (5 mL) and ACN (2.5 mL). The residue was purified by column chromatography (SiO_2, CH_2Cl_2/MeOH, 90/10) or by recrystallisation in ethanol to yield 119 mg (96%) of colorless crystals. By way **B**: In a round-bottom flask were introduced **71** (100 mg, 0.56 mmol) and Et_3N (164.3 uL, 1.17 mmol) in THF (10 mL) at 0°C. Then acetyl chloride (83.8 uL, 1.17 mmol) in THF (1 mL) was added. The reaction mixture was stirred for 1 hour at 0°C, under argon. After stirring, CH_2Cl_2 was added and the reaction mixture was washed successively with two times 10% ammonium chloride and saturated brine. The organic layer was dried with sodium sulfate, and the solvent was removed under vacuum. The residue was purified by column chromatography (SiO_2, CH_2Cl_2/MeOH, 90/10) or by recrystallization in ethanol to yield 89.9 mg (72%) of colorless crystals.

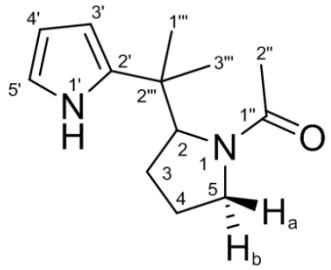

IR (KBr): 3235.4*m*, 2974.8*m*, 1613.7*s*, 1564.1*w*, 1478.1*w*, 1422.4*m*, 1388.9*w*, 722.5*m*.

^{1}H NMR ($CDCl_3$, 298K) δ 8.31 (m, 1 H, N-H(1')), 6.71 (m, 1 H, pyrrolic-H(5')), 6.12 (m, 1 H, pyrrolic-H(4')), 5.95 (s, 1 H, pyrrolic-H(3')), 4.41 (dd, ^{3}J(2, 3) = 8.2 Hz, ^{3}J(2, 3) = 2.4 Hz, 1 H, H(2)), 3.37 (td, ^{3}J(5b, 4) = 10.1 Hz, ^{1}J(5b, 5a) = 7.99 Hz, 1 H, H(5b)), 3.09 (ddd, ^{3}J(5a, 4) = 9.93 Hz, ^{1}J(5a, 5b) = 8.9 Hz, ^{1}J(5a, 4) = 6.61 Hz, 1H, H(5a)), 2.12 (s, 3 H, CH3(2'')), 1.76 (m, 1 H, H(3)), 1.69 (m, 1 H, H(3)), 1.59 (m, 1 H, H(4)), 1.32 (s, 6 H, CH_3(1''', 3''')), 1.00 (m, 1 H, H(4));

^{13}C NMR ($CDCl_3$) δ 171.79 (C(1'')=O), 137.23 (C(2')), 116.75 (C(5')), 108.11 (C(4')), 105.18 (C(3')), 64.18 (C(2)), 49.18 (C(5)), 40.16 (C(2''')), 26.90 (C(3)), 26.57 (C(1''')), 26.40 (C(3''')), 23.83 (C(4)), 23.61 (C(2'')).

Melting point: 158°C.

HRMS calcd. for $C_{13}H_{20}N_2O+Na^+$ 243.1468, found 243.1469.

X-ray: Suitable crystals of **72** were obtained as colourless blocks by slow evaporation of a solution in dichloromethane. The intensity data were collected at 173K (-100°C) on a Stoe Mark II-Image Plate Diffraction System [1] equiped with a two-circle goniometer and using MoKα graphite monochromated radiation. Image plate distance 130 mm, ω rotation scans 0 - 180° at ϕ 0°, and 0 - 83° at ϕ 90°, step Δω = 1.0°, exposures of 2 mins per image, 2θ range 1.76 - 52.59°, $d_{min} – d_{max}$ = 23.107 - 0.802 Å.

The structure was solved by Direct methods using the program SHELXS-97 [2]. The refinement and all further calculations were carried out using SHELXL-97 [2]. The NH H-atoms was locate in a difference fourier map and freely refined. The C-bound H-atoms were included in calculated positions and treated as riding atoms using SHELXL default parameters. The non-H atoms were refined anisotropically, using weighted full-matrix least-squares on F^2. A semi-empirical absorption correction was applied using the MULscanABS routine in PLATZON [3].

[1] Stoe & Cie (2000). IPDS-I Bedienungshandbuch. Stoe & Cie GmbH, Darmstadt, Germany.

[2] G. M. Sheldrick. (2008). Acta Cryst. A64, 112-122.

[3] Spek, A. L. (2003). J. Appl. Cryst. 36, 7-13.

Drawing programs:

ORTEP-3: [3] Farrugia, L. J. (1997). J. Appl. Cryst., 30, 565.

Mercury: [4] Macrae, C. F., Edgington, P. R., McCabe, P., Pidcock, E., Shields, G. P., Taylor, R., Towler, M. & van de Streek, J. (2006). J. Appl. Cryst. 39, 453-457.

PLATON: [5] Spek, A. L. (2003). J. Appl. Cryst. 36, 7-13.

2.32. Synthesis of compound 73* and 74*

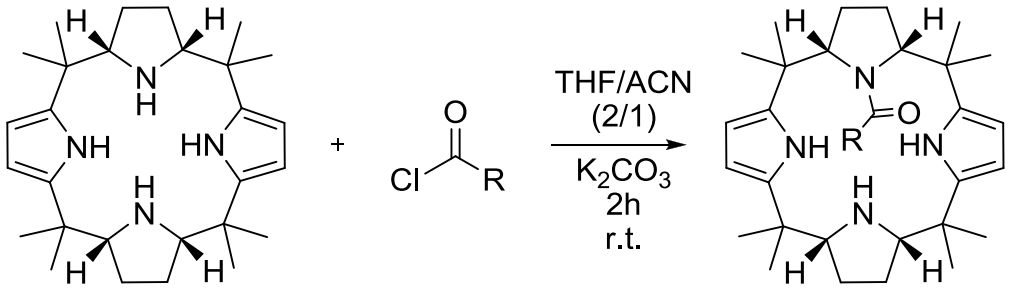

2.32.1. Compound 73*

The amide **73** was prepared according to the general procedure (I) from *meso*-octamethylcalix[2]-pyrrole[2]pyrrolidine (1 g, 2.29 mmol), acetyl chloride (342 µL, 4.81 mmol), potassium carbonate (665 mg, 4.81 mmol) in THF (50 mL) and ACN (25 mL). The residue was purified by washing with cold ethanol to yield 1.085g (99.4%) of colorless powder. The resulting powder can be recrystallized in ethanol.

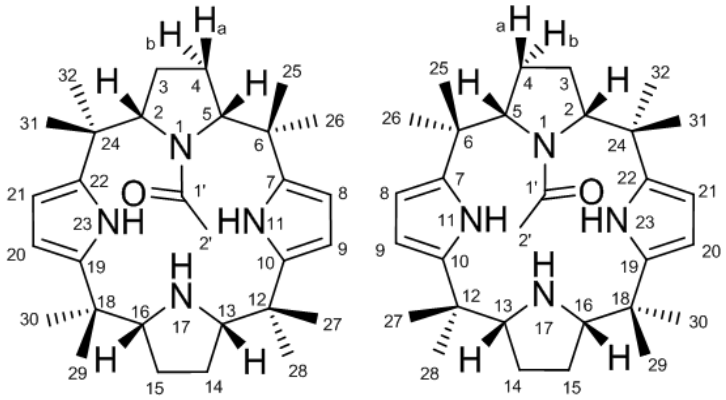

Compound **73** is described as a racemate mixture.

IR (KBr): 3463.2*m*, 3363.3*m*, 3266.8*s*, 2964.8*s*, 2863.2*s*, 1647.4*s*, 1572.8*w*, 1451.3*m*, 1366.7*m*, 1319.3*m*, 1099.1*m*, 1051.0*m*, 765.9*s*, 711.0*w*.

^{1}H NMR ($CDCl_3$, 218K) δ 9.03 (s, 1 H, N-H(23)), 8.77 (s, 1 H, N-H(11)), 5.89 (s, 2 H, pyrrolic-H(20, 21)), 5.69 (s, 2 H, pyrrolic-H(8, 9)), 4.20 (t, ^{3}J(2, 3b) = 9.1 Hz, ^{3}J(2, 3a) = 9.1 Hz, 1 H, H(2)), 3.55 (d, ^{3}J(5, 4) = 8.7 Hz, 1 H, H(5)), 3.19 (bs, 1 H, H(13)), 2.89 (bs, 1 H, H(16)), 2.40 (bs, 1 H, N-H(17)), 2.37 (m, 1 H, CH_2(3b)), 2.11-2.06 (m, 1 H, CH_2(3a)), 1.89-1.86 (m, 1 H, CH_2(4b), 1.67 (m, 2 H, CH_2(4a, 14a)), 1.53 (m, 1 H, CH_2(15a)), 1.47 (s, 3 H, CH_3(31)), 1.33 (s, 3 H, CH_3(28)), 1.30 (s, 3 H, CH_3(32)), 1.25 (s, 3 H, CH_3(29)), 1.22 (s, 3 H,

CH_3(30)), 1.19 (s, 3 H, CH_3(25)), 1.18 (s, 3 H, CH_3(27)), 1.10 (s, 3 H, CH_3(2')), 0.89 (m, 2 H, CH_2(14b, 15b)), 0.03 (s, 3 H, CH_3(26));

^{13}C NMR ($CDCl_3$) δ 179.63 (C(1')=O), 138.51 (C(10)), 137.39 (C(7)), 135.59 (C(19)), 135.02 (C(22)), 106.86 (C(20 or 21)), 106.07 (C(20 or 21)), 103.44 (C(8 or 9)), 101.43 (C(8 or 9)), 71.64 (C(5)), 70.52 (C(16)), 67.02 (C(2)), 66.07 (C(13)), 40.50 (C(24)), 37.50 (C(6)), 37.44 (C(12)), 36.55 (C(18)), 32.89 (C(29)), 30.66 (C(32)), 29.17 (C(31)), 28.16 (C(28)), 27.46 (C(25)), 26.99 (C(3)), 26.69 (C(4)), 26.51 (C(15)), 26.28 (C(27)), 25.80(C(14)), 25.52 (C(30)), 22.01 (C(2')), 19.6 (C(26)).

Melting point: 223.6°C.

MS calcd for $C_{30}H_{46}N_4O$ 478.37, found 479.7 (M+H)+.
HRMS calcd. for $C_{30}H_{46}N_4O+H^+$ 479.3744, found 479.3742.

X-ray: Suitable crystals of **73** were obtained as colourlessblocks by by slow evaporation of a solution in ethanol. The intensity data were collected at 173K (-100°C) on a Stoe Mark II-Image Plate Diffraction System [1] equiped with a two-circle goniometer and using MoKα graphite monochromated radiation. Image plate distance 100 mm, ω rotation scans 0 - 180° at ϕ 0°, and 0 - 103° at ϕ 90°, step Δω = 1.0°, with an exposure time of 3 mins per image, 2θ range 2.29 – 59.53°, d_{min} – d_{max} = 17.779 – 0.716 Å.
The structure was solved by Direct methods using the program SHELXS [2]. The refinement and all further calculations were carried out using SHELXL-97 [2]. All the H-atoms could be located in difference electron-density maps. The NH H-atoms were freely refined, while the C-bound H-atoms were included in calculated positions and treated as riding atoms using SHELXL default parameters. The non-H atoms were refined anisotropically, using weighted full-matrix least-squares on F^2.
The compound is a racemate, crystallizing in the centrosymmetric trigonal space group R-3, with 18 molecules per unit cell.
There is very small cavity in the unit cell, which is estimated to be occupied by only 11 electrons, for a volume of 373 Å^3 which is 3% of the total volume of the unit cell. No correction was made for this.
[1] Stoe & Cie (2000). IPDS-I Bedienungshandbuch. Stoe & Cie GmbH, Darmstadt, germany.

[2] G. M. Sheldrick. (2008). Acta Cryst. A64, 112-122.

[3] Spek, A. L. (2003). J. Appl. Cryst. 36, 7-13.

2.32.2. Compound 74*

The amide **74** was prepared according to the general procedure (I) from *meso*-octamethylcalix[2]pyrrole[2]pyrrolidine (700 mg, 1.60 mmol), propionyl chloride (280 uL, 3.2 mmol), potassium carbonate (442 mg, 3.2 mmol) in THF (30 mL) and ACN (15 mL). The residue was purified by column chromatography (SiO_2, cyclohexane/EtOAc, 6/4) to yield 758 mg (96%) of colorless crystals.

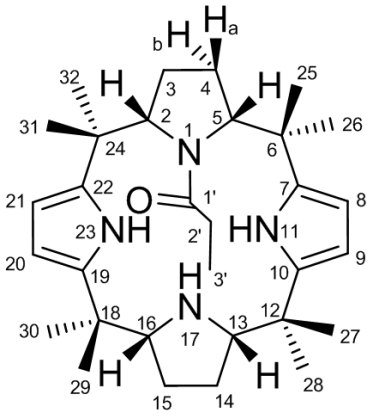

IR (KBr): 3435.6*m*, 2968.4*m*, 2926.3*m*, 1647.1*s*, 1494.0*m*, 1215.5*s*, 1050.7*m*, 752.6*s*, 668.4*m.*

^{1}H NMR ($CDCl_3$ 218K) δ 9.02 (s, 1 H, N-H(23)), 8.73 (s, 1 H, N-H(11)), 5.88 (s, 2 H, pyrrolic-H(20, 21)), 5.68 (s, 2 H, pyrrolic-H(8, 9)), 4.21 (dd, ^{3}J(2, 3b) = 9.5 Hz, ^{3}J(2, 3a) = 9.0 Hz, 1 H, H(2)), 3.57 (d, ^{3}J(5, 4) = 8.8 Hz, 1 H, H(5)), 3.18 (bs, 1 H, H(13)), 2.88 (bs, 1 H, H(16), 2.40 (bs, 1 H, N-H(17)), 2.35 (m, 1 H, CH_2(3b)), 2.06 (m, 1 H, CH_2(3a)), 1.86 (m, 1 H, CH_2(4b)), 1.67 (m, 1 H, CH_2(2')), 1.65 (m, 1 H, CH_2(4a)), 1.62 (m, 1 H, CH_2(14a)), 1.50 (m, 1 H, CH_2(15a)), 1.48 (s, 3 H, CH_3(32)), 1.29 (s, 6 H, CH_3(28, 31)), 1.25 (s, 3 H, CH_3(29)), 1.22 (s, 3 H, CH_3(30)), 1.18 (s, 3 H, CH_3(25)), 1.16 (s, 3 H, CH_3(27)), 0.86 (m, 2 H, CH_2(14b, 15b)), 0.77 (t, ^{3}J(2', 3') = 7.0 Hz, 3 H, CH_3(3')), 0.49 (m, 1 H, CH_2(2')), 0.00 (s, 3 H, CH_3(26));

^{13}C NMR ($CDCl_3$) δ 182.62 (C(1')=O), 138.36 (C(7)), 137.44 (C(10)), 135.63 (C(22)), 134.98 (C(19)), 106.82 (C(20 or 21)), 105.92 (C(20 or 21)), 103.33 (C(9)), 101.28 (C(8)), 70.95 (C(5)), 70.40 (C(16)), 67.50 (C(2)), 65.96 (C(13)), 40.50 (C(24)), 37.40 (C(6)), 36.47

(C(12, 18)), 32.90 (C(29)), 30.91 (C(31)), 29.26 (C(32)), 28.35 (C(28)), 27.50 (C(25)), 26.66 (C(3)), 26.58 (C(4)), 26.48 (C(15)), 26.36 (C(2')), 26.28 (C(27)), 25.74 (C(14)), 20.35 (C(30)), 19.47 (C(26)), 10.24 (C(3')).

MS calcd for $C_{31}H_{48}N_4O$ 492.38, found 493.4 (M+H)+, 515.4 (M+Na)+.
HRMS calcd. for $C_{31}H_{48}N_4O+H^+$ 493.3901, found 493.3904.

X-ray: Suitable crystals of **74** were obtained as colorless blocks by a slow evaporation of a solution in dichloromethane. The intensity data were collected at 173K (-100°C) on a Stoe Mark II-Image Plate Diffraction System [1] equiped with a two-circle goniometer and using MoKα graphite monochromated radiation (λ = 0.71073 Å). Image plate distance 130mm, ω rotation scans 0 - 180° at ϕ 0°, and 0 – 64.0° at ϕ 90°, step Δω = 1.2°, exposures of 5 mins per image, 2θ range 1.76 - 52.59°, $d_{min} – d_{max}$ = 23.107 - 0.802 Å.
The structure was solved by Direct methods using the program SHELXS-97 [2]. The refinement and all further calculations were carried out using SHELXL-97 [2].
The NH H-atoms were located in difference electron-density maps. In the final cycles of least-squares refinement H-atom N3H was refined with a distance restraint of N-H = 0.88(2) Å and $U_{iso}(H) = 1.2U_{eq}(N)$. The other NH H-atoms and the C-bound H-atoms were included in calculated positions and treated as riding atoms: N-H = 0.87 Å, C-H = 0.99, 0.98 and 0.97 Å for CH, CH_2 and CH_3, respectively, and 0.94 Å for CH-allyl and CH-aromatic, with $U_{iso}(H) = k \times U_{eq(}N,C)$, where k = 1.5 for CH_3 H-atoms, and = 1.2 for all other H-atoms.
The non-H atoms were refined anisotropically, using weighted full-matrix least-squares on F^2. An empirical absorption correction was applied using the MULscanABS routine in PLATON [3].
The crystal, a dichloromethane solvate, diffracted very weakly beyond 40˚ in 2θ, despite exposures of 5 min per image. Due to the large number of very weak reflections the R_{int} value was relatively high. In the final cycles of refinement the data were restricted to 22.5˚ in θ; consequently the R_{int} value was lower but still > 0.12.
[1] Stoe & Cie (2000). IPDS-I Bedienungshandbuch. Stoe & Cie GmbH, Darmstadt, germany.
[2] G. M. Sheldrick. (2008). Acta Cryst. A64, 112-122.
[3] Spek, A. L. (2003). J. Appl. Cryst. 36, 7-13.

2.33. Synthesis of compound 75* and 76*

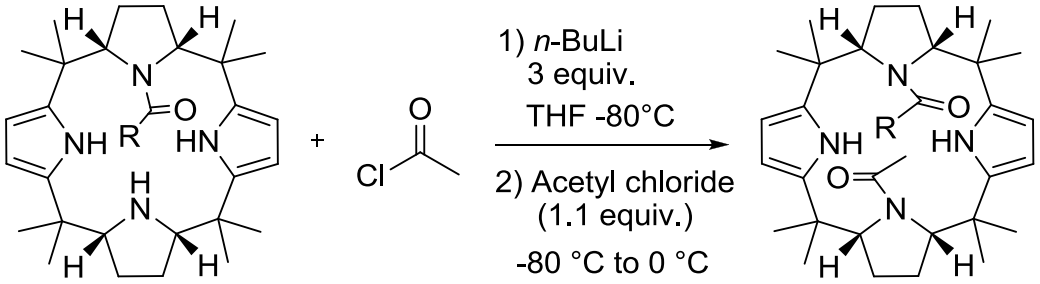

73: R = CH_3
74: R = C_2H_5

75: R = CH_3, 7%
76: R = C_2H_5, 12%

2.33.1. Compound 75*

To a solution of amide **73** (1 g, 2.03 mmol) in THF (40 mL) at -78°C was added a 1.6 M solution of *n*-butyllithium in hexanes (3.92 mL, 6.09 mmol) over 10 minutes. The reaction mixture was stirred for 30 minutes at this temperature and then a solution of acetyl chloride (149.2 µL, 2.03 mmol) in THF (5 mL) was slowly added. The resulting solution was stirred at -78°C for 30 minutes then allows warming to room temperature (additional 30 min). After stirring, 100 mL of 10% sodium carbonate was added and the reaction mixture was extracted with CH_2Cl_2 (3 x 50 mL). The aqueous layer was extracted by 40 mL of EtOAc followed by 40 mL of CH_2Cl_2. The organic layer was washed saturated brine. The organic layer was dried with sodium sulfate, and the solvents were removed under vacuum. The residue was solved in CH_2Cl_2/MeOH (9/1) and filtered through a pad of aluminum oxide. The solvents were removed under vacuum and the residue purified by column chromatography (SiO2, Cyclohexane/EtOAc, 6/4) to yield 76.1 mg (7%) of white powder.

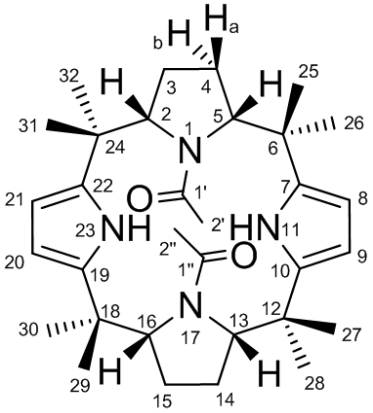

IR (KBr): 3457.6*m*, 2965.8*m*, 2926.7*w*, 1675.8*s*, 1392.4*m*, 1360.9*m*, 1311.9*m*, 1287.9*s*, 770.9*m*.

^{1}H NMR ($CDCl_3$, 218K) δ 9.33 (s, 2 H, N-H(11, 23)), 5.87 (s, 2 H, pyrrolic-H(9, 21)), 5.83 (s, 2 H, pyrrolic-H(8, 20)), 4.30 (t, ^{3}J(2, 3b) and ^{3}J(13, 14b) = 9.3 Hz, ^{3}J(2, 3a) and ^{3}J(13, 14a) = 9.3 Hz, 2 H, H(2, 13)), 3.90 (d, ^{3}J(5, 4b) and ^{3}J(16, 15b) = 8.5 Hz, 2 H, H(5, 16)), 2.05 (m, 4 H, CH_2(3, 14)), 1.83 (m, 2 H, CH_2(4b)), 1.73 (s, 6 H, CH_3(2')), 1.69 (m, 2 H, CH_2(4a)), 1.45 (s, 6 H, CH_3(28, 32)), 1.33 (m, 6 H, CH_3(27, 31)), 1.21 (s, 6 H, CH_3(25, 29)), 0.02 (s, 6 H, CH_3(26, 30));

^{13}C NMR ($CDCl_3$) δ 179.32 (C(1')=O), 138.71 (C(7, 19)), 134.49 (C(10, 22)), 106.85 (C(9, 21)), 104.57 (C(8, 20)), 70.04 (C(5)), 67.84 (C(2)), 40.71 (C(12, 24)), 37.33 (C(6, 18)), 29.94 (C(28, 32)), 29.18 (C(27, 31)), 28.64 (C(25, 29)), 27.70 (C(3, 14)), 27.31 (C(4, 15)), 25.26 (C(2')), 24.80 (C(26, 30)).

MS calcd for $C_{32}H_{48}N_4O_2$ 520.38, found 543.8 (M+Na)+.

X-ray: Suitable crystals of **75** were obtained as colourless rods by a slow evaporation of a solution in dichloromethane. The intensity data were collected at 173K (-100°C) on a Stoe Mark II-Image Plate Diffraction System [1] equiped with a two-circle goniometer and using MoKα graphite monochromated radiation. Image plate distance 130 mm, ω rotation scans 0 - 180° at ϕ 0°, step Δω = 1.3°, exposures of 9 mins per image, 2θ range 1.76 - 52.59°, d_{min} – d_{max} = 23.107 - 0.802 Å. The structure was solved by Direct methods using the program SHELXS-97 [2]. The refinement and all further calculations were carried out using SHELXL-97 [2]. The H-atoms were included in calculated positions and treated as riding atoms using SHELXL default parameters. The non-H atoms were refined anisotropically, using weighted full-matrix least-squares on F^2. An empirical absorption correction was applied using the multi-scan routine available in PLATON (Sepk, 2009).

The crystal diffracted weakly beyond 40° in 2θ, and this is responsable for the high R_{int} value of 0.19. Only ca. 35% of the data can be considered to be observed [$I > 2\sigma(I)$].

[1] Stoe & Cie (2000). IPDS-I Bedienungshandbuch. Stoe & Cie GmbH, Darmstadt, germany.
[2] G. M. Sheldrick. (2008). Acta Cryst. A64, 112-122.
[3] Spek, A. L. (2003). J. Appl. Cryst. 36, 7-13.

2.33.2. Compound 76*

To a solution of amide **8** (930 mg, 1.89 mmol) in THF (20 mL) at -78°C was added a 2 M solution of *n*-butyllithium in hexanes (2.83 mL, 5.66 mmol) over 10 minutes. The reaction mixture was stirred for 30 minutes at this temperature and then a solution of acetyl chloride (135.36 µL, 1.89 mmol) in THF (1 mL) was slowly added. The resulting solution was stirred at -78°C for 5 minutes then allows warming to room temperature (additional 30 min). After stirring, 100 mL of 10% sodium carbonate was added and the reaction mixture was extracted with CH_2Cl_2 (3 x 50 mL). The aqueous layer was extracted by 40 mL of EtOAc followed by 40 mL of CH_2Cl_2. The organic layer was washed saturated brine. The organic layer was dried with sodium sulfate, and the solvents were removed under vacuum. The residue was solved in CH_2Cl_2/MeOH (9/1) and filtered through a pad of aluminum oxide. The solvents were removed under vacuum and the residue purified by column chromatography (Al_2O_3, Cyclohexane/ EtOAc, 80/20) to yield 121 mg (12%) of white powder.

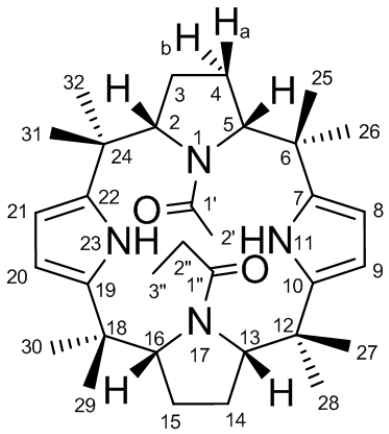

IR (KBr): 3451.42*m*, 2976.92*m*, 1674.24*s*, 1389.8*m*, 1359.96*m*, 765.13*m*, 706.26*w*.

^{1}H NMR ($CDCl_3$ 223K) δ 9.33 (s, 1 H, N-H(23)), 9.24 (s, 1 H, N-H(11)), 5.89 (s, 1 H, pyrrolic-H(20)), 5.86 (s, 2 H, pyrrolic-H(9, 21)), 5.81 (s, 1 H, pyrrolic-H(8)), 4.31 (dd, ^{3}J(13, 14b) = 10.2 Hz, ^{3}J(13, 14a) = 8.5 Hz, 1 H, H(13)), 4.25 (dd, ^{3}J(2, 3b) = 10.0 Hz, ^{3}J(2, 3a) = 8.6 Hz, 1 H, H(2)), 3.94 (d, ^{3}J(16, 15) = 8.5 Hz, 1 H, H(16)), 3.84 (d, ^{3}J(5, 4) = 8.6 Hz, 1 H, H(5)), 2.16 (m, 1 H, CH_2(2'')), 2.03 (m, 4 H, CH_2(3, 14)), 1.83 (m, 2 H, CH_2(4a, 15a)), 1.69 (m, 2 H, CH_2(4b, 15b)), 1.69 (m, 1 H, CH_2(2'')), 1.69 (s, 3 H, CH_3(2')), 1.45 (m, 3 H, CH_3(28)), 1.42 (s, 3 H, CH_3(32)), 1.34 (s, 3 H, CH_3(27)), 1.32 (s, 3 H, CH_3(31)), 1.22 (s, 3 H,

CH_3(29)), 1.19 (s, 3 H, CH_3(25)), 0.98 (t, ^{3}J(3'', 2'') = 7.2 Hz, 3 H, CH_3(3'')), 0.02 (s, 3 H, CH_3(30)), -0.05 (s, 3 H, CH_3(26));

^{13}C NMR ($CDCl_3$) δ 182.09 (C(1'')=O), 178.97 (C(1')=O), 138.75 (C(19)), 138.31 (C(7)), 134.23 (C(10 or 22)), 134.14 (C(10 or 22)), 106.69 (C(20)), 106.35 (C(9 or 21)), 104.40 (C(9 or 21)), 103.91 (C(8)), 69.72 (C(5)), 68.91 (C(16)), 68.12 (C(13)), 67.46 (C(2)), 40.34 (C(12 or 24)), 40.32 (C(12 or 24)), 37.10 (C(18)), 36.96 (C(6)), 30.07 (C(2'')), 29.82 (C(28)), 29.71 (C(32)), 29.06 (C(27 or 31)), 28.95 (C(27 or 31)), 28.66 (C(29)), 28.18 (C(25)), 27.34 and 27.21 and 27.13 and 27.07 (C(3, 4, 14, 15)), 25.52 (C(2')), 24.61 (C(30)), 24.10 (C(26)), 10.28 (C(3'')). MS calcd for $C_{33}H_{50}N_4O_2$ 534.39, found 535.4 (M+H)+.

Melting point: 269°C.

HRMS calcd. for $C_{33}H_{50}N_4O_2$+Na^+ 557.3826, found 557.3827.

2.34. Synthesis of compound 77-81*

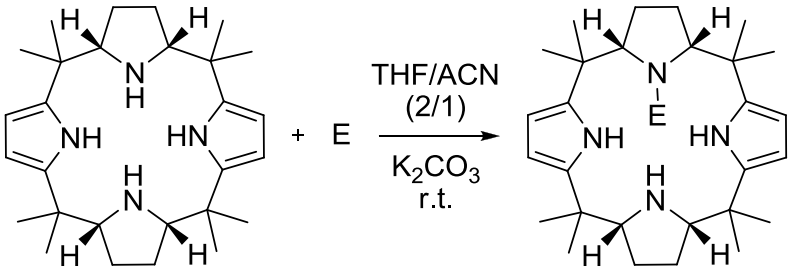

12b

2.34.1. Compound 77*

The amide **77** was prepared according to the general procedure (I) from *meso*-octamethylcalix[2]pyrrole[2]pyrrolidine (100 mg, 0.23 mmol), benzoyl bromide (57.7 µL, 0.48 mmol), potassium carbonate (70 mg, 0.48 mmol) in THF (10 mL) and ACN (5 mL). The residue was washed with cold ethanol to yield 123.8 mg (quant.) of colorless solid.

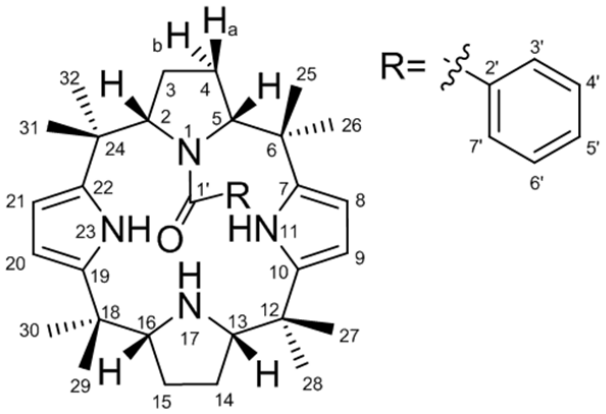

IR (KBr): 3393.8*m*, 3274.9*m*, 2966.2*m*, 1631.5*s*, 1348.1*s*, 1097.9*w*, 952.5*m*, 769.23*m*, 699.0*m*.

^{1}H NMR ($CDCl_3$ 218K) δ 9.19 (s, 1 H, N-H(23)), 8.74 (s, 1 H, N-H(11)), 7.15 (bs, 1 H, H(5')), 7.07 (bs, 2 H, H(3', 7')), 6.24 (bs, 2 H, H(4', 6')), 5.91 (s, 2 H, pyrrolic-H(20, 21)), 5.73 (bs, 1 H, pyrrolic-H(9)), 5.14 (bs, 1 H, pyrrolic-H(8)), 4.50 (bs, 1 H, H(2)), 3.74 (bs, 1 H, H(5)), 3.22 (bs, 1 H, H(13)), 2.93 (bs, 1 H, H(16)), 2.55 (m, 1 H, CH_2(3b)), 2.44 (bs, 1 H, N-H(17)), 2.17 (m, 1 H, CH_2(3a)), 1.82 (m, 1 H, CH_2(4b)), 1.68 (m, 1 H, CH_2(4a)), 1.66 (m, 1 H, CH_2(14a)), 1.66 (s, 3 H, CH_3(32)), 1.55 (m, 1 H, CH_2(15a)), 1.48 (s, 3 H, CH_3(34)), 1.39 (s, 3 H, CH_3(31)), 1.28 (s, 3 H, CH_3(29)), 1.25 (s, 3 H, CH_3(27)), 1.25 (s, 3 H, CH_3(30)), 0.92 (s, 3 H, CH_3(31)), 0.92 (m, 2 H, CH_2(14b, 15b)), 0.00 (s, 3 H, CH_3(26));

^{13}C NMR ($CDCl_3$) δ not detected (C(1')=O, 2', 10, 7, 19, 22)), 128.0 (C(3', 7')), 127.8 (C(5')), 125.4 (C(4', 6')), 107.10 (C(20, 21)), 105.15 (C(9)), 103.71 (C(8)), 71.60 (C(5)), 70.82 (C(16)), 68.82 (C(2)), 66.65 (C(13)), not detected (C(24, 18 12, 6)) , 33.17 (C(29)), 32.30 (C(31)), 29.29 (C(28)), not detected (C(25)), 26.91 (C(32)), not detected (C(3, 27, 4, 15)), 26.12 (C(30)), not detected (C(14)), 20.50 (C(26)).

Melting point: 265°C.

MS calcd for $C_{35}H_{48}N_4O$ 540.38, found 541.4 (M+H)+, 563.4 (M+Na)+.
HRMS calcd. for $C_{35}H_{48}N_4O+H^+$ 541.3901, found 541.3907.

X-ray: Suitable crystals of **77** were obtained as thin colorless plates by a slow evaporation of a solution in dichloromethane. The intensity data were collected at 233K (-40°C) on a Stoe Mark II-Image Plate Diffraction System [1] equiped with a two-circle goniometer and using

MoKα graphite monochromated radiation (λ = 0.71073 Å). Image plate distance 130mm, ω rotation scans 0 - 180° at ϕ 0°, and 0 – 75.0° at ϕ 90°, step Δω = 1.0°, exposures of 9 mins per image, 2θ range 1.76 - 52.59°, d_{min} – d_{max} = 23.107 - 0.802 Å.

The structure was solved by Direct methods using the program SHELXS-97 [2]. The refinement and all further calculations were carried out using SHELXL-97 [2].

The NH H-atoms were located in difference electron-density maps. In the final cycles of least-squares refinement H-atom N3H was refined with a distance restraint of N-H = 0.88(2) Å and U_{iso}(H) = 1.2U_{eq}(N). The other NH H-atoms and the C-bound H-atoms were included in calculated positions and treated as riding atoms: N-H = 0.87 Å, C-H = 0.99, 0.98 and 0.97 Å for CH, CH_2 and CH_3, respectively, and 0.94 Å for CH-allyl and CH-aromatic, with U_{iso}(H) = k × $U_{eq(}$N,C), where k = 1.5 for CH_3 H-atoms, and = 1.2 for all other H-atoms.

The non-H atoms were refined anisotropically, using weighted full-matrix least-squares on F^2. An empirical absorption correction was applied using the MULscanABS routine in PLATON [3]. The crystal diffracted very weakly beyond 35˚ in 2θ, despite exposures of 9 min per image. Due tothe large number of very weak reflections the R_{int} value was relatively high. In the final cycles of refinement the data were restricted to 22.5˚ in θ; consequently the R_{int} value was lower but still > 0.12.

[1] Stoe & Cie (2000). IPDS-I Bedienungshandbuch. Stoe & Cie GmbH, Darmstadt, germany.

[2] G. M. Sheldrick. (2008). Acta Cryst. A64, 112-122.

[3] Spek, A. L. (2003). J. Appl. Cryst. 36, 7-13.

2.34.2. Compound 78*

The carbamate **11** was prepared according to the general procedure (I) from *meso*-octamethylcalix[2]pyrrole[2]pyrrolidine (100 mg, 0.23 mmol), methyl chloroformate (37.5 uL, 0.48 mmol), potassium carbonate (70 mg, 0.48 mmol) in THF (5 mL) and ACN (2.5 mL). The residue was washed with cold ethanol to yield 113.8 mg (99%) of colorless solid.

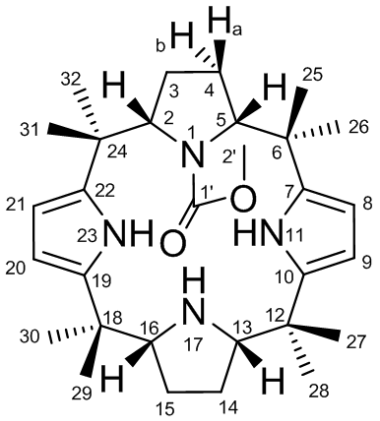

IR (KBr) : 3415(*m*), 2963(*s*), 2869(*m*), 1708(*s*), 1574(*w*), 1439(*m*), 1319(*s*), 1296(*s*), 1249(*w*), 1207(*m*), 1100(*m*), 925(*m*), 772(*m*), 759(*s*), 711(*m*), 526(*w*).

^{1}H NMR ($CDCl_3$ 223.2 K) δ 9.01 (s, 1 H, N-H(23)), 8.71 (s, 1 H, N-H(11)), 5.90 (s, 2 H, pyrrolic-H(20, 21)), 5.68 (bs, 1 H, pyrrolic-H(9)), 5.63 (bs, 1 H, pyrrolic-H(8)), 3.86 (bs, 1 H, H(2)), 3.66 (bs, 1 H, H(5)), 3.18 (s, 3 H, CH_3(2')), 3.17 (bs, 1 H, H(13)), 2.88 (bs, 1 H, H(16)), 2.39 (bs, 1 H, N-H(17)), 2.29 (m, 1 H, CH_2(3a)), , 2.06 (m, 1 H, CH_2(3b)), 1.73 (m, 1 H, CH_2(4a)), 1.65 (m, 1 H, CH_2(14a)), 1.63 (m, 1 H, CH_2(4b)), 1.51 (m, 1 H, CH_2(15a)), 1.50 (s, 3 H, CH_3(32)), 1.29 (s, 3 H, CH_3(28)), 1.25 (s, 3 H, CH_3(30)), 1.24 (s, 3 H, CH_3(31)), 1.20 (s, 3 H, CH_3(29)), 1.15 (s, 3 H, CH_3(27)), 1.13 (s, 3 H, CH_3(25)), 0.88 (m, 2 H, CH_2(14b, 15b)), -0.02 (s, 3 H, CH_3(26));

^{13}C NMR ($CDCl_3$) δ 162.0 (C(1')=O), 138.6 (C(7)), 136.8 (C(10)), 135.8 (C(19)), 134.3 (C(22)), 106.8 (C(20 or 21)), 105.7 (C(21 or 20)), 102.5 (C(9)), 99.6 (C(8)), 72.1 (C(5)), 70.3 (C(16)), 68.9 (C(2)), 66.2 (C(13)), 52.9 (C(2')), 40.3 (C(24)), 37.3 (C(12)), 37.1 (C(6)), 36.4 (C(18)), 33.5 (C(30)), 29.7 (C(32)), 28.9 (C(28)), 27.4 (C(3)), 26.9 (C(27)), 26.7 (C(25)), 26.4 (C(14)), 26.3 (C(15)), 25.9 (C(31)), 25.6 (C(4)), 25.2 (C(29)), 18.9 (C(26)).

^{1}H NMR ($CDCl_3$ 298 K) δ 8.87 (s, 2 H, N-H(11, 23)), 5.77 (dd, ^{3}J(8, 9) and ^{3}J(20, 21) = 6.8 Hz, ^{4}J(8 or 9, NH) and ^{4}J(20 or 21, NH) = 2.6 Hz, 4 H, pyrrolic-H(20, 21, 8, 9)), 3.87 (dd, ^{3}J(2, 3b) and ^{3}J(5, 4b) = 7.9 Hz, ^{3}J(2, 3a) and ^{3}J(5, 4a) = 5.1 Hz , 2 H, H((2, 5)) , 3.29 (s, 3H, CH_3(2')), 3.05 (bs, 2 H, H(13,16)) , 2.15 (bs, 1 H, N-H(17)), 1.98 (bs, 2 H, CH_2(4a, 3a)), 1.80 (bs, 2 H, CH_2(4b,3b)), 1.63 (m, 2 H, CH_2(14a, 15a)), 1.33 (s, 6 H, CH_3(meso)), 1.30 (s, 6 H, CH_3(meso)), 1.20 (s, 6 H, CH_3(meso)), 1.11 (m, 2 H, CH_2(14b, 15b)), 0.83 (bs, 6 H, CH_3(meso));

^{13}C NMR ($CDCl_3$) δ 161.4 (C(1')=O), 137.1 (C(7, 10)), 136.7 (C(19, 22)), 104.6 (C(8, 9, 20, 21)), 71.2 (C(2, 5)), 68.9 (C(13, 16)), 52.8 (C(2')), 38.9 (C(12, 24)), 37.2 (C(6, 18)), 30.0 (CH_3), 28.0 (CH_3), 27.2 (C(3, 4)), 26.3 (C(4, 15)), 25.4 (CH_3).

MS calcd for $C_{30}H_{46}N_4O_2$ 494.3, found 495.4 $(M+H)^+$;
HRMS calcd for $C_{30}H_{46}N_4O_2H^+$ 495.3693, found 495.36982.

2.34.3. Compound 79*

The carbamate **79** was prepared according to the general procedure (I) from *meso*-octamethylcalix[2]pyrrole[2]pyrrolidine (100 mg, 0.23 mmol), 6-nitroveratryl chloroformate (132.2 mg, 0.48 mmol), potassium carbonate (70 mg, 0.48 mmol) in THF (5 mL) and ACN (2.5 mL). The residue was washed with cold ethanol to yield 155.0 mg (99%) of colorless crystals.

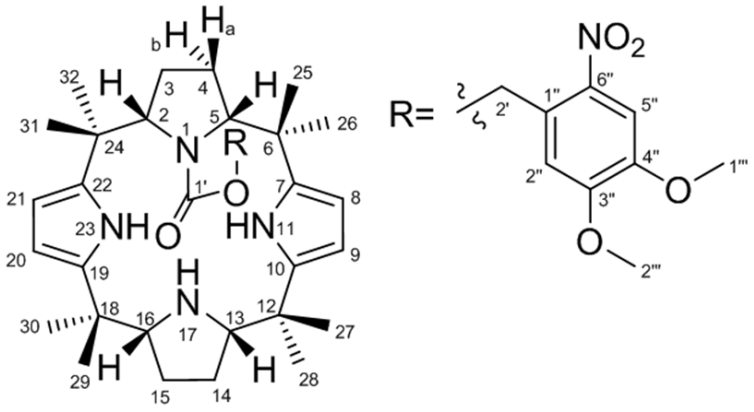

IR (KBr): 3436(*m*), 2966(*s*), 2871(*m*), 1703(*m*), 1580(*w*), 1523(*s*), 1463(*w*), 1332(*m*), 1277(*s*), 1220(*m*), 1099(*w*), 1064(*w*), 915(*w*), 760(*w*), 731(*w*), 712(*w*), 602(*w*).

^{1}H NMR ($CDCl_3$ 223.2 K) δ 9.09 (s, 1 H, N-H(23)), 8.72 (s, 1 H, N-H(11)), 7.67 (s, 1H, H(5'')), 6.63 (s, 1H, H(2'')), 5.90 (s, 2 H, pyrrolic-H(20, 21)), 5.47 (m, 1 H, CH_2(2'a or 2'b)), 5.43 (s, 1 H, pyrrolic-H(9)), 5.31 (s, 1 H, pyrrolic-H(8)), 4.47 (m, 1 H, CH_2(2'b or 2'a)), 3.97 (s, 6H, CH_3(1''',2''')), 3.90 (bs, 1 H, H(5)), 3.81 (bs, 1 H, H(2)), 3.16 (bs, 1 H, H(13)), 2.89 (bs, 1 H, H(16)), 2.39 (m, 1 H, CH_2(3a)), 2.38 (bs, 1 H, N-H(17)), 2.11 (m, 1 H, CH_2(3b)), 1.83 (m, 1 H, CH_2(4a)), 1.74 (m, 1 H, CH_2(4b)), 1.63 (m, 1 H, CH_2(14a)), 1.52 (s, 3 H, CH_3(32)), 1.51 (m, 1 H, CH_2(15a)), 1.37 (s, 3 H, CH_3(28)), 1.26 (s, 3 H, CH_3(29)), 1.25 (s, 3

H, CH_3(30)), 1.21 (s, 3 H, CH_3(31)), 1.13 (s, 3 H, CH_3(25)), 1.08 (s, 3 H, CH_3(27)), 0.80 (m, 2 H, CH_2(14b, 15b)), 0.08 (s, 3 H, CH_3(26));

^{13}C NMR ($CDCl_3$) δ 160.4 (C(1')=O), 152.9 (C(3'')), 147.5 (C(4'')), 139.5 (C(1'')), 138.4 (C(7)), 137.3 (C(10)), 136.7 (C(19)), 134.9 (C(22)), 128.9 (C(6'')), 109.6 (C(2'')), 107.7 (C(5'')), 107.4 (C(21 or 20)), 106.5 (C(20 or 21)), 103.2 (C(8)), 100.7 (C(9)), 72.3 (C(5)), 70.9 (C(16)), 69.9 (C(2)), 66.7 (C(13)), 65.5 (C(2')), 56.4 (C(1''', 2''')), 40.8 (C(24)), 37.7 (C(12)), 37.3 (C(6)), 36.9 (C(18)), 33.3 (C(30)), 31.0 (C(29)), 29.7 (C(32)), 29.2 (C(28)), 28.0 (C(3)), 27.3 (C(25)), 26.9 (C(15)), 26.8 (C(27)), 26.3 (C(4)), 26.0 (C(14)), 25.7 (C(31)), 19.5 (C(26)).

^{1}H NMR ($CDCl_3$ 298 K) δ 8.92 (s, 2 H, N-H(11, 23)), 7.65 (s, 1 H, H(5'')), 6.75 (s, 1 H, H(2'')), 5.68 (bs, 4 H, pyrrolic-H(8, 9, 20, 21), 5.10 (bs, 2 H, H(2')), 3.97 (s, 6H, CH_3(1''', 2''')) and (bs, 2 H, H(2, 5)), 3.06 (bs, 2 H, H(13,16)) 2.04 (m, 1 H, CH_2(3a, 4a)), 2.17-2.0 (bs, 1 H, N-H(17)), 1.84 (bs, 2 H, CH_2(3b,4b)), 1.62 (bs, 2 H, CH_2(14a,15a)), 1.32-1.28 (s, 12 H, CH_3(meso)), 1.22 (s, 6 H, CH_3(meso)), 1.17 (bs, 2 H, CH_2(14b, 15b)), 0.88 (bs, 6 H, CH_3(meso));

^{13}C NMR ($CDCl_3$) δ 160.2 (C(1')=O), 153.1 (C(3'')), 147.1 (C(4'')), 140.1 (C(1'')), 136.9 (C(7, 10, 19, 22)), 128.9 (C(6'')), 110.5 (C(2'')), 108.1 (C(5'')), 104.7 (C(8, 9, 20, 21)), 71.5 (C(2, 5)), 68.9 (C(13, 16)), 65.0 (C(2')), 56.4 (C(1''', C2''')), 39.1 (C(12, 24)), 37.2 (C(6, 18)), 30.2 (CH_3(meso)), 29.3 (CH_3(meso)), 28.3 (C(3, 4)), 28.2 (C(14, 15)), 27.4 (CH_3(meso)).

MS calcd for $C_{38}H_{53}N_5O_6$ 675.4, found 676.7 $(M+H)^+$, 698.7 $(M + Na)^+$;
HRMS calcd for $C_{38}H_{53}N_5O_6H^+$ 676.4068, found 676.4065

2.34.4. Compound 80*

In a two-necked flask fitted with a gas inlet and containing a stirrer bar was charged *meso*-octamethylcalix[2]pyrrole[2]pyrrolidine (400 mg, 0.92 mmol) and potassium carbonate (280 mg, 2 mmol). The reaction vessel was flushed with argon and sealed with a septum. THF (20 mL) and ACN (10 mL) was introduced, and then benzyl bromide (237 µL, 2 mmol) was added. The reaction mixture was stirred for 2 hours in all at room temperature, under argon. After stirring, 10% sodium carbonate was added and the reaction mixture was extracted with

CH_2Cl_2. The organic layer was washed successively with two times 10% sodium carbonate and saturated brine. The organic layer was dried with sodium sulfate, and the solvents were removed under vacuum. The residue was purified by column chromatography (Al_2O_3) to yield 48.2 mg (10%) of colorless crystals.

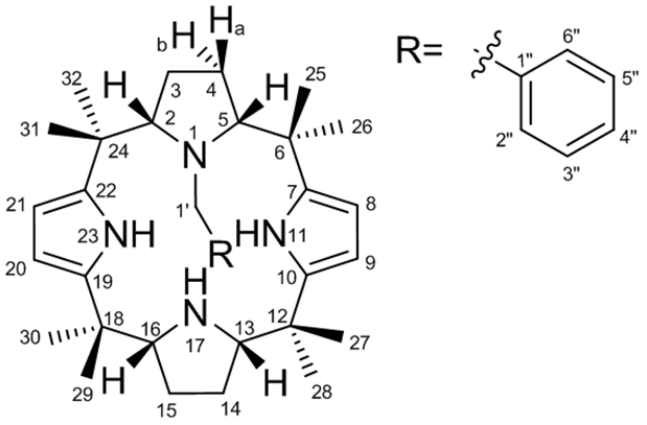

IR (KBr): 3450*m*, 2962*s*, 2872*m*, 2347*w*, 1718*w*, 1571*m*, 1491*w*, 1466*w*, 1379*m*, 1355*m*, 1279*m*, 1240*m*, 1104*m*, 1070*m*, 1040*m*, 763*s*, 707*s*, 624*w*, 526*w*, 468*w*.

^{1}H NMR ($CDCl_3$ 223.2 K) δ 8.73 (s, 2 H, N-H(11, 23)), 7.21 (m, 3 H, H(3'', 5'')), 6.98 (m, 2 H, H(2'',6'')), 5.98 (s, 2 H, pyrrolic-H(8, 9)), 5.82 (s, 2 H, pyrrolic-H(20, 21)), 3.16 (bs, 2 H, H(2, 5)), 2.99 (bs, 2 H, H(13,16)), 1.83 (bs, 2 H, CH_2(1')), 1.67 (m, 4 H, CH_2(3b, 4b,1 4b, 15b)), 1.53 (m, 4 H, CH_2(3a, 4a, 14a, 15a)), 1.42 (s, 3 H, CH_3(32)), 1.36 (s, 6 H, CH_3(28, 30)), 1.29 (s, 6 H, CH_3(27, 29)), 1.24 (s, 3 H, CH_3(25)), 1.21 (s, 3 H, CH_3(31)), 0.85 (s, 3 H, CH_3(26));

^{13}C NMR ($CDCl_3$) δ 139.4 (C(19, 22)), 138.7 (C(7, 10)), 136.0 (C(1'')), 131.9 (C(2'', 6'')), 127.4 (C(3'', 5'')), 126.6 (C(4'')), 102.4 (C(20, 21)), 102.2 (C(8, 9)), 70.1 (C(2, 5)), 67.7 (C(13, 16)) , 53.5 (C(1')), 38.2 (C(6)), 37.7 (C(24)), 37.2 (C(12)), 35.9 (C(18)), 30.1 (C(32)), 27.5 (C(25)), 26.6 (C(14, 15)), 26.1 (C(3,4)), 26.4 (C(31)), 20.4 (C(28, 30)),19.4 (C(27, 29)), 14.3 (C(26)).

^{1}H NMR (CD_2Cl_2 183.4 K) δ 8.63 (s, 2 H, N-H(11, 23)), 7.12 (s, 3 H, C-H(3'',4'', 5'')), 6.87 (m, 2 H H(2'', 6'')), 5.85 (s, 2 H, pyrrolic-H(8, 9)), 5.70 (s, 2 H, pyrrolic-H(20, 21)), 3.03 (s, 2 H, H(13, 16)), 2.89 (s, 2 H, H(2, 5)), 2.10 (bs, 1 H, N-H(17)), 1.67 (s, 2 H, H(1')) 1.58-1.40 (m, 8 H, CH_2), 1.26 (s, 6 H, CH_3(meso)), 1.21 (s, 3 H, CH_3(meso)), 1.13 (s, 6 H, CH_3(meso)), 1.11 (s, 6 H, CH_3(meso)) 0.80 (s, 3 H, CH_3(meso));

^{13}C NMR ($CDCl_3$) δ 138.7 (C(22, 19)), 138.0 (C(8, 9)), 135.5 (C(1'')), 131.2 (C(2'', 6'')), 126.7 (C(3'', 5'')), 126.0 (C(4'')), 101.9 (C(7, 10)), 101.7 (C(20, 21)), 69.2 (C(2, 5)), 67.2 (C(13, 16)) , 52.6 (C(1')), 36.9 (C(12, 24)), 36.4 (C(6, 18)), 26.6 (CH_3(meso)), 25.9 (CH_3(meso)), 25.8 (C(3, 4)), 25.5 (C(14, 15)), 19.6 (CH_3meso)), 18.7 (CH_3(meso)).

MS calcd for $C_{35}H_{51}N$ 526.4, found 527.8 (M+H)+, 549.7 (M+Na)+;
HRMS calcd for $C_{35}H_{51}N_4H^+$ 527.4108, found 527.4116.

2.34.5. Compound 81*

In a two-necked flask fitted with a gas inlet and containing a stirrer bar was charged *meso*-octamethylcalix[2]pyrrole[2]pyrrolidine (400 mg, 0.92 mmol) and potassium carbonate (280 mg, 2 mmol). The reaction vessel was flushed with argon and sealed with a septum. THF (20 mL) and ACN (10 mL) was introduced, and then methyl iodine (144 µL, 1.84 mmol) was added. The reaction mixture was stirred for 2 hours in all at room temperature, under argon. After stirring, 10% sodium carbonate was added and the reaction mixture was extracted with CH_2Cl_2. The organic layer was washed successively with two times 10% sodium carbonate and saturated brine. The organic layer was dried with sodium sulfate, and the solvents were removed under vacuum. The residue was purified by column chromatography (Al_2O_3, CH_2Cl_2) to yield 297 mg (60%) of colorless crystals.

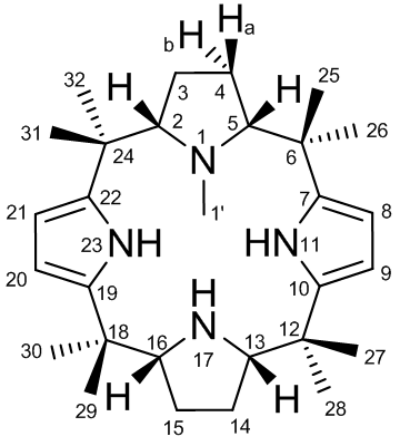

IR (KBr): 3447.4*m*, 2965.8*s*, 2873.1*s*, 1569.9*w*, 1467.5*w*, 1380.8*m*, 758.9*s*, 704.9*m*.

^{1}H NMR ($CDCl_3$, 218 K) δ 8.88 (s, 1 H, N-H(23)), 5.78 (m, 4 H, pyrrolic-H(8, 9, 20, 21)), 3.05 (m, 2 H, C-H(13, 16)), 2.43 (m, 2 H, H(2, 5)), 1.81 (m, 2 H, CH_2(3, 4)), 1.71 (m, 4 H,

CH_2(3, 4, 14, 15)), 1.57 (bs, 1 H, N-H(17)), 1.52 (m, 2 H, CH_2(14, 15)), 1.27 (s, 6 H, CH_3), 1.26 (s, 6 H, CH_3), 1.25 (s, 6 H, CH_3), 1.21 (s, 3 H, CH_3), 1.20 (s, 3 H, CH_3(1')));

^{13}C NMR ($CDCl_3$) δ 139.14 and 138.84 (C(pyrrolic quat.)), 102.51 (C(8, 9 or 18, 19)), 102.26 (C(8, 9 or 18, 19)), 79.99 (C(2, 5)), 68.65 (C(12, 15)), 46.70 (C(6, 11, 16, 21)), 27.26 (CH_3), 26.94 (CH_3), 26.71 (C(3, 4)), 26.57 (C(13, 14)), 21.61 (CH_3), 20.93 (CH_3).

Melting point: 165°C.

MS calcd for $C_{35}H_{48}N_4O$ 540.38, found 541.4 (M+H)+, 563.4 (M+Na)+.
HRMS calcd. for $C_{29}H_{46}N_4$+H^+ 451.3795, found 451.3794.

2.35. Synthesis of compound 83*

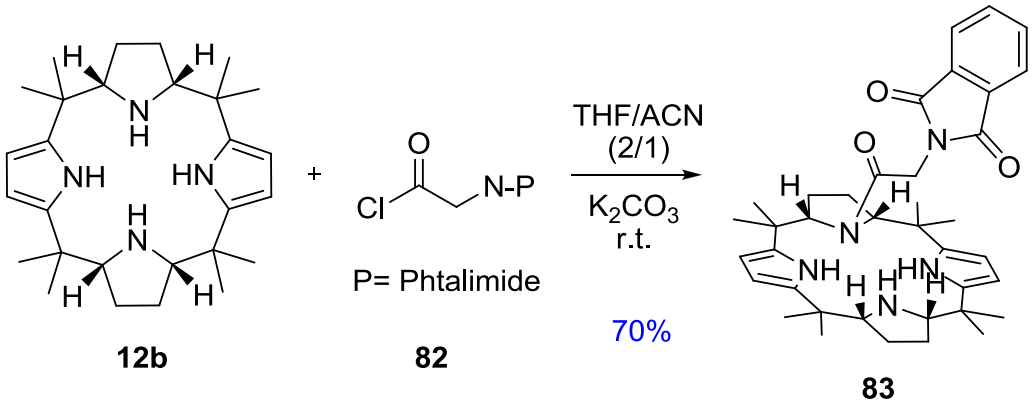

N-phtaloyl glycinoyl chloride was prepared according to the general procedure (II) from N-phtaloyl glycine (197 mg, 0.962 mmol), dichloromethane (1 mL), and thionyl chloride (1 mL), which can be used without further purifications. Then the amide **20** was prepared according to the general procedure (I) from *meso*-octamethylcalix[2]pyrrole[2]pyrrolidine (200 mg, 0.46 mmol), N-phtaloyl glycinoyl chloride (255 mg, 0.96 mmol), potassium carbonate (140 mg, 1 mmol) in THF (10 mL) and ACN (5 mL). The residue was purified by column chromatography (Al_2O_3, CH_2Cl_2/MeOH, 98/2) to yield 200 mg (70%) of colorless solid.

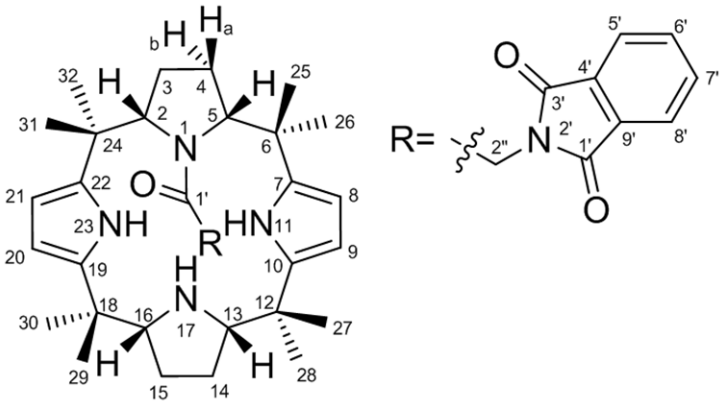

IR (KBr): 2965.9*m*, 2926.3*m*, 2863.1*m*, 1793.7*w*, 1720.0*s*, 1664.2*m*, 1495.3*m*, 1417.3*m*, 1405.3*m*, 1050.8*m*, 873.7*w*, 824.2*m*, 757.3*s*, 714.9*m*, 605.0*w*.

^{1}H NMR ($CDCl_3$, 218K) δ 8.98 (s, 1 H, N-H(23)), 8.91 (s, 1 H, N-H(11)), 7.78 (m, 2 H, C-H(5', 8')), 7.68 (m, 2 H, C-H(6', 7')), 5.91 (s, 2 H, pyrrolic-H(20, 21)), 5.75 (s, 2 H, pyrrolic-H(8, 9)), 4.29 (dd, ^{3}J(2, 3b) = 9.7 Hz, ^{3}J(2, 3a) = 9.4 Hz, 1 H, H(2)), 3.99 (d, ^{3}J(5, 4) = 8.7 Hz, 1 H, H(5)), 3.80 (d, ^{3}J(2'', 2'') = 17.3 Hz, 1 H, H(2'')), 3.22 (bs, 1 H, H(13)), 2.89 (bs, 1 H, H(16)), 2.89 (d, ^{3}J(2'', 2'') = 17.2 Hz, 1 H, H(2'')), 2.45 (bs, 1 H, N-H(17)), 2.40 (m, 1 H, CH_2(3b)), 2.11 (m, 1 H, CH_2(3a)), 1.96 (m, 1 H, CH_2(4b)), 1.90 (m, 1 H, CH_2(4a)), 1.69 (m, 1 H, CH_2(14a)), 1.60 (s, 3 H, CH_3(28)), 1.57 (m, 1 H, CH_2(15a)), 1.41 (s, 3 H, CH_3(32)), 1.25 (s, 3 H, CH_3(27, 29, 30, 31)), 0.93 (m, 2 H, CH_2(15b)), 0.83 (m, 2 H, CH_2(14b)), 0.06 (s, 3 H, CH_3(26));

^{13}C NMR ($CDCl_3$) δ 175.23 (C(1'')=O), 168.33 (C(1', 3')=O), 139.32 (C(10)), 136.31 (C(7)), 135.63 (C(19)), 134.66 (C(22)), 134.12 (C(6', 7')), 131.67 (C(4', 9')), 123.35 (C(5', 8')), 107.18 (C(20 or 21)), 106.33 (C(20 or 21)), 104.48 (C(8 or 9)), 102.58 (C(8 or 9)), 71.59 (C(5)), 70.36 (C(16)), 67.53 (C(2)), 66.42 (C(13)), 40.50 (C(24)), 37.78 (C(6)), 37.58 (C(12)), 37.03 (C(2'')), 36.64 (C(18)), 32.84 (C(27 or 29 or 30 or, 31)), 30.92 (C(27 or 29 or 30 or, 31)), 28.62 (C(32)), 28.36 (C(28)), 27.57 (C(27 or 29 or 30 or, 31)), 26.89 (C(4)), 26.53 (C(3, 15, 27 or 29 or 30 or, 31)), 25.55 (C(14)), 19.47 (C(26)).

HRMS calcd for $C_{38}H_{49}N_5O_3H$+ 624.3914, found 624.3910 (M+H)+.

2.36. Synthesis of compound 84, 85, 86* and 87*

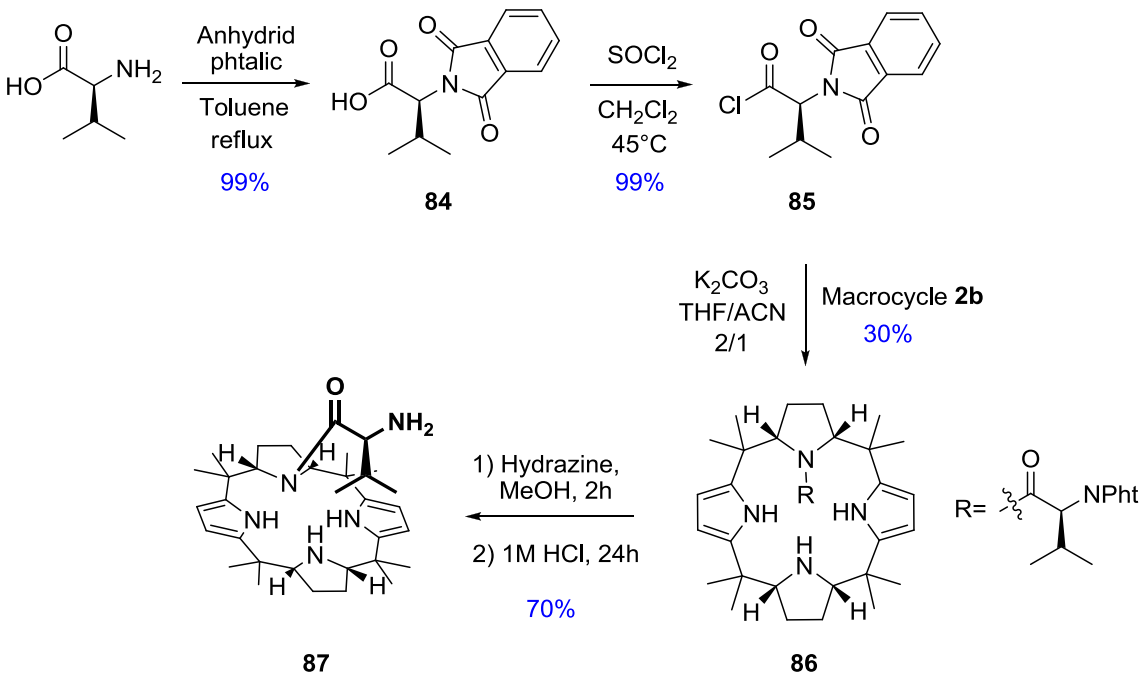

2.36.1. Compound 84 ((S)-2'-(1,3-dioxoisoindolin-2-yl)-3'-methylbutanoic acid)

In a round-bottom flask were introduced L-valine (1 g, 8.53 mmol), phtalic anhydride (1.26 g, 8.53 mmol), Et_3N (1.19 mL, 8.53 mmol) and toluene (80 mL). The flask was equipped with a stirring bar, a Dean-Stark trap and a reflux condenser. The mixture was heated to reflux temperature and stirred for further 6 hours with azeotropic removal of water. After completion of the reaction the solvent was removed under vacuum. The resulting solid was solved in CH_2Cl_2 and washed with 10% HCl. The organic layer was dried with sodium sulfate, and the solvents were removed under vacuum to yield 2.08 g (99%) of white powder which can be used without further purifications (>99% pure).

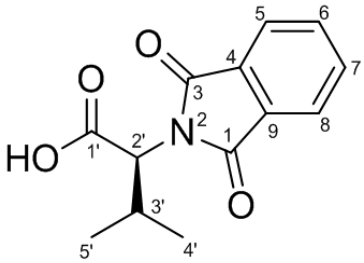

^{1}H NMR ($CDCl_3$, 298K) δ 7.87 (m, 2 H, H(5, 8)), 7.74 (m, 2 H, H(6, 7)), 4.64 (d, ^{3}J(2', 3') = 8.5 Hz, 1 H, H(2')), 2.76 (dsept, ^{3}J (2', 3') = 8.2 Hz, ^{3}J(3', 4', 5') = 6.7 Hz, 1 H, H(3')), 1.17 (d, ^{3}J(4', 3') = 6.7 Hz, 3 H, CH_3(4')), 0.92 (d, ^{3}J(5', 3') = 6.7 Hz, 3 H, CH_3(5'));

^{13}C NMR ($CDCl_3$) δ 173.86 (C(1')=O), 167.77 (C(1,3)=O), 134.32 (C(6, 7)), 131.63 (C(4, 9)), 123.69 (C(5, 8)), 57.66 (C(2')), 28.46 (C(3')), 20.90 (C(4')), 19.53 (C(5')).

MS calcd for $C_{13}H_{13}NO_4$: 247.08, found 220.16 (M+H)+.
See additional analyses in "Casimir, J. R.; Guichard, G.; Briand, J. P. *J. Org. Chem.* **2002**, *67*, 3764-3768".

2.36.2. Compound 85 ((S)-2'-(1,3-dioxoisoindolin-2-yl)-3'-methylbutanoyl chloride)

The acyl chloride **85** was prepared according to the general procedure (II) from N-phtaloyl L-valine (1 g, 4.04 mmol), CH_2Cl_2 (5 mL), thionyl chloride (5 mL) to yield 1.06 g (99%) of white solid which can be used without further purifications (purity 85%).

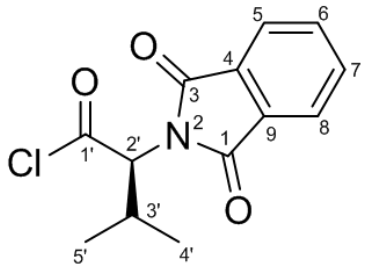

^{1}H NMR ($CDCl_3$, 298K) δ 7.92 (m, 2 H, H(5, 8)), 7.82 (m, 2 H, H(6, 7)), 4.72 (d, ^{3}J(2', 3') = 8.4 Hz, 1 H, H(2')), 2.76 (dsept, ^{3}J(2', 3') = 8.5 Hz, ^{3}J(3', 4', 5') = 6.8 Hz, 1 H, H(3')), 1.17 (d, ^{3}J(4', 3') = 6.7 Hz, 3 H, H(4')), 0.92 (d, ^{3}J(5', 3') = 6.7 Hz, 3 H, H(5'));

^{13}C NMR ($CDCl_3$) δ 204.34 (C(1')=O), 169.8 (C(1 or 3)=O), 167.77 (C(1 or 3)=O), 134.65 (C(6, 7)), 131.37 (C(4, 9)), 123.98 (C(5, 8)), 66.37 (C(2')), 29.18 (C(3')), 20.40 (C(4')), 19.06 (C(5')).

MS calcd for $C_{13}H_{12}ClNO_3$: 265.05, found 265.97 (M+H)+.
See additional analyses in "Wixey, J. S., Ward, B. D., *Chem. Commun.*, **2011,** 47(19), 5449-5451".

2.36.3. Compound 86*

The amide **86** was prepared according to the general procedure (I) from *meso*-octamethylcalix[2]pyrrole[2]pyrrolidine (200 mg, 0.46 mmol), N-phtaloyl L-valinoyl chloride

(255 mg, 0.96 mmol), potassium carbonate (140 mg, 1 mmol) in THF (10 mL) and ACN (5 mL). The residue was purified by recrystallization in MeOH or by column chromatography (Al_2O_3, CH_2Cl_2/MeOH, 95/5) to yield 91.5 mg (30%) of white solid.

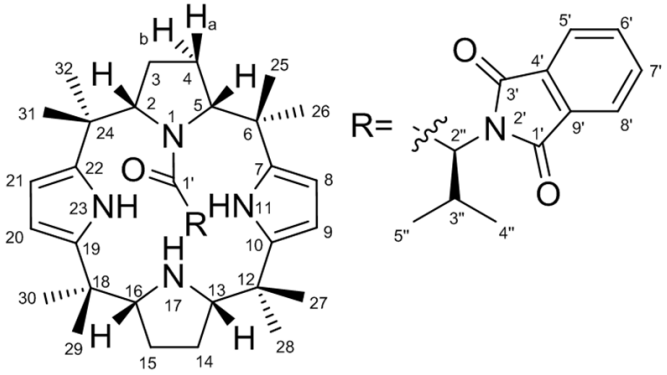

IR (KBr): 2966.3*m*, 2926.6*s*, 2863.1*m*, 1719.3*s*, 1664.1*w*, 1607.0*w*, 1494.0*s*, 1452.6*m*, 1378.9*m*, 875.8*w*, 824.3*s*, 757.9*m*, 605.0*w*.

^{1}H NMR ($CDCl_3$, 298K) δ 9.14 (bs, 1 H, N-H(11 or 23)), 8.89 (bs, 1 H, N-H(11 or 23)), 7.82 (m, 2 H, H(5',8'')), 7.73 (m, 2 H, H(6',7'')), 6.28 (bs, 1 H, pyrrolic-H(8)), 5.91 (bs, 1 H, pyrrolic-H(20 or 21)), 5.86 (bs, 1 H, pyrrolic-H(9)), 5.82 (bs, 1 H, pyrrolic-H(20 or 21)), 4.59 (d, ^{3}J(2'', 3'') = 7.9 Hz, 1 H, H(2'')), 4.37 (m, 1 H, H(2)), 4.00 (m, 1 H, H(5)), 3.17 (bs, 1 H, H(13)), 2.94 (bs, 1 H, H(16)), 2.65 (bs, 1 H, H(3'')), 2.52 (bs, 1 H, CH_2(3b)), 2.35 (bs, 1 H, NH(17)), 1.98 (bs, 1 H, CH_2(3a)), 1.74 (bs, 1 H, CH_2(4b)), 1.67 (bs, 1 H, CH_2(14a)), 1.66 (bs, 1 H, CH_2(15a)), 1.61 (s, 3 H, CH_3(32)), 1.35 (bs, 1 H, CH_2(4a)), 1.34 (s, 3 H, CH_3(31)), 1.33 (s, 6 H, CH_3(28)), 1.26 (s, 3 H, CH_3(29)), 1.25 (s, 3 H, CH_3(25 or 30)), 1.25 (s, 3 H, CH_3(25 or 30)), 1.22 (s, 3 H, CH_3(27)), 1.16 (bs, 1 H, CH_2(15b)), 0.97 (bs, 1 H, CH_2(14b)), 0.64 (d, ^{3}J(4'', 3'') = 6.6 Hz, 3 H, CH_3(4'')), 0.51 (d, ^{3}J(5'', 3'') = 5.6 Hz, 3 H, CH_3(5'')), 0.09 (s, 3 H, CH_3(26));

^{13}C NMR ($CDCl_3$) δ 173.39 (C(1'')=O), 167.99 (C(1, 3)=O), 137.61 (C(10)), 136.53 (C(7)), 135.80 (C(22)), 135.12 (C(19)), 134.04 (C(6', 7')), 131.33 (C(4', 9')), 123.33 (C(5', 8')), 107.68 (C(20 or 21)), 106.82 (C(20 or 21)), 105.25 (C(8, 9)), 70.71 (C(16)), 68.95 (C(2)), 68.29 (C(13)), 67.17 (C(5)), 59.28 (C(2'')), 40.68 (C(24)), 38.99 (C(6)), 37.80 (C(12)), 36.99 (C(18)), 32.62 (C(29)), 32.41 (C(31)), 29.68 (C(25 or 30)), 29.33 (C(28)), 28.12 (C(3'')), 27.42 (C(4)), 27.11 (C(27, 32)), 26.58 (C(3, 15)), 25.49 (C(25 or 30)), 25.37 (C(14)), 20.18 (C(26)), 19.59 (C(5'')), 18.31 (C(4'')).

HRMS calcd for $C_{41}H_{56}N_5O_3+H^+$ 666.4383, found 666.4378 (M+H)+.

2.36.4. Compound 87*

In a round-bottom flask were introduced **86** (120 mg, 0.180 mmol), MeOH (2 mL) and 1M hydrazine in THF (1.8 mL, 1.80 mmol). The resulting solution was stirred at room temperature for 2 hours. After stirring, CH_2Cl_2 was added and the reaction mixture was washed successively with two times 10% sodium carbonate and saturated brine. The organic layer was dried with sodium sulfate, and the solvents were removed under vacuum. The resulting solid was solved in MeOH (10 mL) and 1M HCl (20 mL) and the mixture were stirred for an additional 24 hours at room temperature and the solution become light pink. After stirring, the reaction mixture was washed with CH_2Cl_2 and the resulting aqueous layer was basified with 10% sodium carbonate and the resulting suspension was solved in CH_2Cl_2 and washed with two times 10% sodium carbonate. The organic layer was dried with sodium sulfate, and the solvents were removed under vacuum. The residue was purified by column chromatography (Al_2O_3, CH_2Cl_2/MeOH, 99/1) to yield 67.5 mg (70%) of white solid.

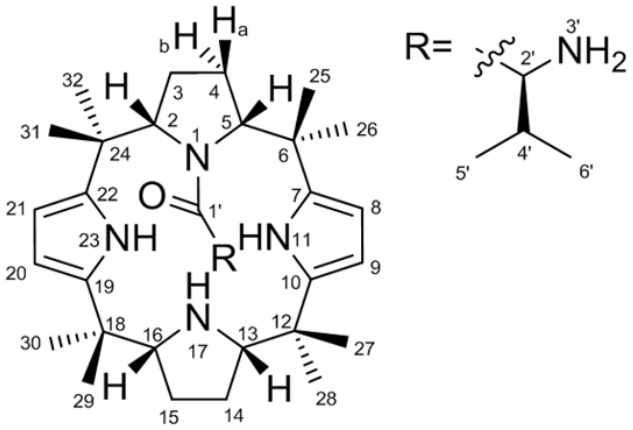

IR (KBr): 3019.3*s*, 2968.4*m*, 2928.4*m*, 2863.1*m*, 1644.5*s*, 1494.0*m*, 1452.6*m*, 1213.9*s*, 1050.8*s*, 874.7*w*, 824.2*m*, 773.7*s*, 670.2*m*, 605.1*w*.

^{1}H NMR ($CDCl_3$, 223K) δ 9.15 (s, 1 H, N-H(11)), 8.86 (s, 1 H, N-H(23)), 5.90 (s, 2 H, pyrrolic-H(19, 20)), 5.88 (s, 1 H, pyrrolic-H(8)), 5.82 (s, 1 H, pyrrolic-H(9)), 4.14 (dd, ^{3}J(2, 3b) = 9.4 Hz, ^{3}J(2, 3a) = 9.0 Hz, 1 H, H(2)), 3.76 (d, ^{3}J(5, 4) =8.9 Hz, 1 H, H(5)), 3.17 (bs, 1 H, H(13)), 2.88 (bs, 1 H, H(16)), 2.77 (bs, 1 H, H(2')), 2.50 (m, 1 H, CH_2(3b)), 2.41 (bs, 1 H,

N-H(17)), 2.11 (m, 1 H, CH_2(3a)), 1.85 (m, 1 H, CH_2(4b)), 1.64 (m, 1 H, CH_2(4a)), 1.64 (m, 1 H, CH_2(14a)), 1.56 (m, 1 H, CH_2(15a)), 1.54 (s, 3 H, CH_3(32)), 1.42 (m, 1 H, H(4')), 1.31 (s, 3 H, CH_3(31)), 1.31 (s, 3 H, CH_3(28)), 1.26 (s, 3 H, CH_3(29)), 1.23 (s, 3 H, CH_3(30)), 1.19 (s, 3 H, CH_3(25)), 1.15 (s, 3 H, CH_3(27)), 0.94 (m, 1 H, CH_2(15b)), 0.83 (d, ^{3}J(5', 4') = 6.2 Hz, 3 H, CH_3(5')), 0.83 (d, ^{3}J(4', 6') = 6.6 Hz, 3 H, CH_3(6')), 0.73 (m, 1 H, CH_2(14b)), 0.01 (s, 3 H, CH_3(26));

^{13}C NMR ($CDCl_3$) δ 184.15 (C(1')=O), 137.44 (C(10)), 137.38 (C(7)), 135.60 (C(19)), 134.90 (C(22)), 107.47 (C(20 or 21)), 106.28 (C(20 or 21)), 105.24 (C(8)), 102.97 (C(9)), 70.46 (C(16)), 68.80 (C(5)), 68.03 (C(2)), 66.83 (C(13)), 58.07 (C(2')), 40.82 (C(24)), 38.01 (C(6)), 37.60 (C(12)), 36.57 (C(18)), 32.94 (C(29)), 31.88 (C(4')), 31.71 (C(28)), 28.73 (C(32)), 28.68 (C(31)), 28.19 (C(25)), 26.68 (C(3)), 26.52 (C(27)), 26.52 (C(15)), 26.38 (C(4)), 25.42 (C(30)), 25.42 (C(14)), 20.21 (C(5')), 19.19 (C(26)), 17.87 (C(4')).

HRMS calcd for $C_{33}H_{53}N_5O+H^+$: 536.4328, found 536.4328 (M+H)+.

2.37. Synthesis of compound 87a*

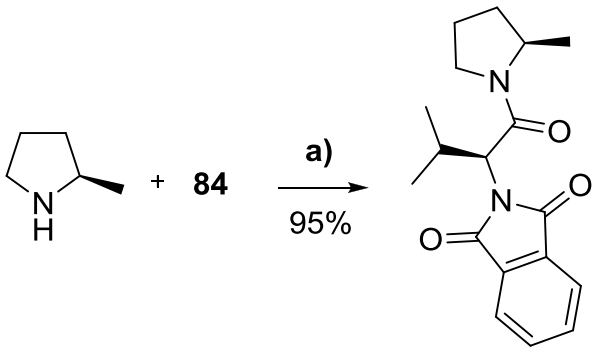

87a

2-((S)-3''-methyl-1''-((R)-2'-methylpyrrolidin-1'-yl)-1''-oxobutan-2''-yl)isoindoline-1,3-dione **87a** was prepared according to the general procedure (I) from (R)-(-)-2-Methylpyrrolidine (287 mg, 3.37 mmol), N-phtaloyl L-valinoyl chloride (1.78 g, 6.74 mmol), potassium carbonate (930 mg, 6.74 mmol) in THF (40 mL) and ACN (20 mL). The residue was purified by column chromatography (SiO_2, CH_2Cl_2/MeOH, 97/3) to yield 1 g (95%) of colorless crystals (purity 90%).

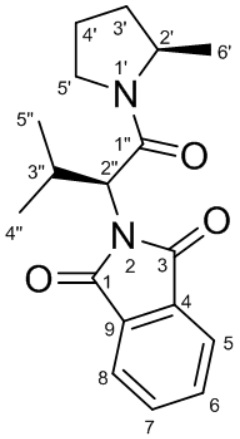

IR (KBr): 3018.9*m*, 2970.5*m*, 2928.4*m*, 2873.7*w*, 1768.4*w*, 1717.0*s*, 1641.6*m*, 1493.8*m*, 1447.3*m*, 1383.3*m*, 1215.8*m*, 1071.8*m*, 824.3*m*, 757.9*s*.

^{1}H NMR ($CDCl_3$, 298K) δ 7.84 (m, 2 H, H(5, 8)), 7.73 (m, 2 H, H(6, 7)), 4.58 (d, ^{3}J(2'', 3'') = 10.8 Hz, 1 H, H(2'')), 4.19 (m, 1 H, H(2')), 3.71 (m, 1 H, CH_2(4')), 3.62 (m, 1 H, CH_2(4')), 3.26 (dsept, ^{3}J(3'', 2'') = 10.8 Hz, ^{3}J(3'', 4'',5'') = 6.6 Hz, 1 H, H(3'')), 2.00 (m, 1H, CH_2(5')), 1.92 (m, 1 H, CH_2(3')), 1.86 (m, 1 H, CH_2(5')), 1.56 (m, 1 H, CH_2(3')), 1.25 (d, ^{3}J(2', 6') = 6.3 Hz, 3 H, CH_3(6')), 1.06 (d, ^{3}J(5'', 3'') = 6.7 Hz, 3 H, CH_3(5'')), 0.92 (d, ^{3}J(4'', 3'') = 6.6 Hz, 3 H, CH_3(4''));

^{13}C NMR ($CDCl_3$) δ 167.28 (C(1, 3)=O), 168.34 (C(1'')=O), 134.16 (C(6, 7)), 131.84 (C(4, 9)), 123.51 (C(5, 8)), 59.81 (C(2'')), 53.70 (C(2')), 47.34 (C(4')), 31.93 (C(3')), 27.49 (C(3'')), 24.32 (C(5')), 19.90 (C(4'', 5'')), 19.22 (C(6')).

MS calcd for $C_{18}H_{22}N_2O_3$: 314.16, found 313.99 (M+•), 315.3 (M+H)+, 337.2 (M+Na)+. **HRMS** calcd for $C_{18}H_{22}N_2O_3$+Na^+ 337.1523, found 337.1521 (M+Na)+.

X-ray: Suitable crystals of *GJ249* were obtained as colourless rods by a slow evaporation of a solution in dichloromethane. The intensity data were collected at 233K (-40°C) on a Stoe Mark II-Image Plate Diffraction System [1] equiped with a two-circle goniometer and using MoKα graphite monochromated radiation (λ = 0.71073 Å). Image plate distance 130mm, ω rotation scans 0 - 180° at ϕ 0°, and 0 – 90.0° at ϕ 90°, step Δω = 1.3°, exposures of 5 mins per image, 2θ range 1.76 - 52.59°, d_{min} – d_{max} = 23.107 - 0.802 Å.

The structure was solved by Direct methods using the program SHELXS-97 [2]. The refinement and all further calculations were carried out using SHELXL-97 [2].

Two carbon atoms in the pyrrole ring (C3 & C4) are disordered over two positions: A / B with refined occupanies of 0.457(15) / 0.543(15). The H-atoms were included in calculated positions and treated as riding atoms: C-H = 0.95 – 1.0 Å with $U_{iso}(H) = k \times U_{eq}(C)$, where k = 1.5 for CH_3 H-atoms, and = 1.2 for all other H-atoms.

In the final cycles of refinement, in the absence of significant anomalous scattering effects, 1337 Friedel pairs were merged and \Df " set to zero. The non-H atoms were refined anisotropically, using weighted full-matrix least-squares on F^2.

[1] Stoe & Cie (2000). IPDS-I Bedienungshandbuch. Stoe & Cie GmbH, Darmstadt, germany.

[2] G. M. Sheldrick. (2008). Acta Cryst. A64, 112-122.

[3] Spek, A. L. (2003). J. Appl. Cryst. 36, 7-13.

2.38. Synthesis of compound 88-91*

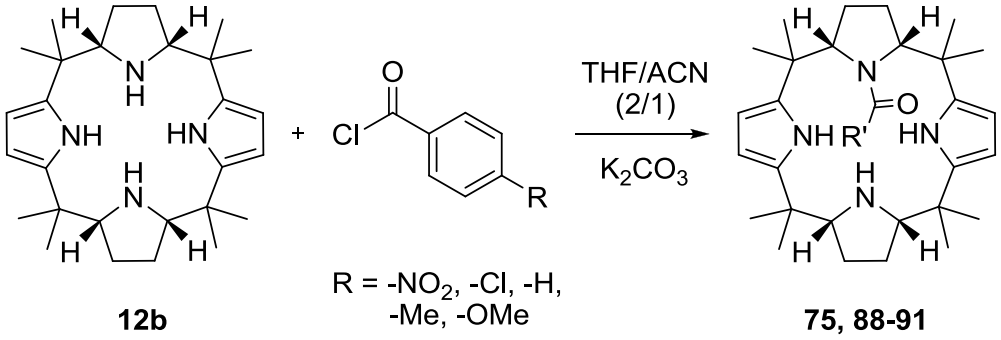

12b **75, 88-91**

2.38.1. Compound 88*

The amide **88** was prepared according to the procedure (III) from *meso*-octamethylcalix[2]pyrrole[2]pyrrolidine (100 mg, 0.23 mmol), 4-nitrobenzoyl chloride (89.24 µL, 0.48 mmol), potassium carbonate (70 mg, 0.48 mmol) in THF (5 mL) and ACN (2.5 mL). The residue was purified by column chromatography (SiO_2, CH_2Cl_2/MeOH, 97/3) to yield 134.1 mg (81%) of yellow crystals.

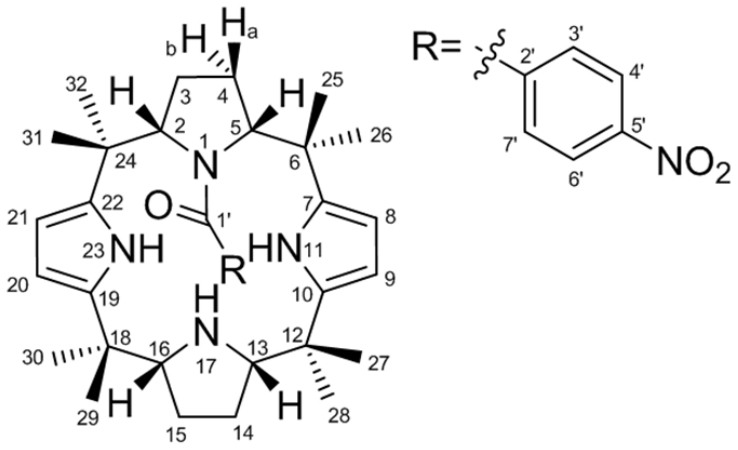

IR (KBr): 3413.1*m*, 3319.5*s*, 2966.7*m*, 1630.8*s*, 1524.6*s*, 1341.1*s*, 775.6*m*, 712.5*m*.

^{1}H NMR ($CDCl_3$ 218K) δ 9.11 (s, 1 H, N-H(23)), 8.81 (s, 1 H, N-H(11)), 7.95 (d, ^{3}J(3', 4') and ^{3}J(7', 6') = 8.4 Hz, 2 H, H(3', 7')), 6.42 (bs, 2 H, H(4', 6')), 5.93 (s, 2 H, pyrrolic-H(20, 21)), 5.72 (s, 1 H, pyrrolic-H(9)), 5.05 (s, 1 H, pyrrolic-H(8)), 4.47 (dd, ^{3}J(2, 3b) = 9.5 Hz, ^{3}J(2, 3a) = 9.3 Hz, 1 H, H(2)), 3.64 (d, ^{3}J(5, 4) = 8.4 Hz, 1 H, H(5)), 3.24 (bs, 1 H, H(13)), 2.92 (bs, 1 H, H(16)), 2.58 (m, 1 H, CH_2(3b)), 2.46 (bs, 1 H, N-H(17)), 2.23 (m, 1 H, CH_2(3a)), 1.89 (m, 1 H, CH_2(4b)), 1.74 (m, 1 H, CH_2(4a)), 1.68 (m, 1 H, CH_2(14a)), 1.64 (s, 3 H, CH_3(32)), 1.55 (m, 1 H, CH_2(15a)), 1.51 (s, 3 H, CH_3(28)), 1.40 (s, 3 H, CH_3(31)), 1.29 (s, 3 H, CH_3(29)), 1.27 (s, 3 H, CH_3(27)), 1.24 (s, 3 H, CH_3(30)), 0.90 (s, 3 H, CH_3(25)), 0.88 (m, 2 H, CH_2(14b, 15b)), -0.02 (s, 3 H, CH_3(26));

^{13}C NMR ($CDCl_3$) δ 177.24 (C(1')=O), 146.14 (C(5)'), 144.56 (C(2')), 138.52 (C(10)), 136.76 (C(7)), 135.74 (C(19)), 134.89 (C(22)), 126.25 (C(4', 6')), 123.49 (C(7', 3')), 107.78 (C(20 or 21)), 106.87 (C(20 or 21)), 105.51 (C(9)), 104.02 (C(8)), 71.73 (C(5)), 70.80 (C(16)), 69.10 (C(2)), 66.86 (C(13)), 40.46 (C(24)), 38.07 (C(6)), 37.96 (C(12)), 36.90 (C(18)), 33.09 (C(29)), 32.20 (C(31)), 29.27 (C(28)), 29.08 (C(25)), 27.92 (C(32)), 27.78 (C(4)), 27.00 (C(27)), 26.77 (C(3)), 26.77 (C(15)), 25.84 (C(30)), 25.78 (C(14)), 20.35 (C(26)).

Melting point: 260°C.

MS calcd for $C_{35}H_{47}N_5O_3$ 585.37, found 584.4 $(M-H)^-$.

HRMS calcd. for $C_{35}H_{47}N_5O_3+H^+$ 586.3752, found 586.3752.

X-ray : Suitable crystals of **88** were obtained as yellow plates by a slow evaporation of a solution in dichloromethane. The intensity data were collected at 233K (-40°C) on a Stoe Mark II-Image Plate Diffraction System [1] equiped with a two-circle goniometer and using MoKα graphite monochromated radiation (λ = 0.71073 Å). Image plate distance 130mm, ω rotation scans 0 - 180° at ϕ 0°, and 0 – 50.0° at ϕ 90°, step Δω = 1.0°, exposures of 3 mins per image, 2θ range 1.76 - 52.59°, d_{min} – d_{max} = 23.107 - 0.802 Å.

The structure was solved by Direct methods using the program SHELXS-97 [2]. The refinement and all further calculations were carried out using SHELXL-97 [2].

The NH H-atoms were located in difference electron-density maps. In the final cycles of least-squares refinement H-atom N3H was refined with a distance restraint of N-H = 0.88(2) Å and $U_{iso}(H) = 1.2U_{eq}(N)$. The other NH H-atoms and the C-bound H-atoms were included in calculated positions and treated as riding atoms: N-H = 0.87 Å, C-H = 0.94 – 0.99 Å, with $U_{iso}(H) = k \times U_{eq(}N,C)$, where k = 1.5 for CH_3 H-atoms, and = 1.2 for all other H-atoms.

The non-H atoms were refined anisotropically, using weighted full-matrix least-squares on F^2. An empirical absorption correction was applied using the MULscanABS routine in PLATON [3].

The O-atoms of the NO_2 group are disordered over two positions with refined occupancies of A/B = 0.376(15) / 0.624(15).

[1] Stoe & Cie (2000). IPDS-I Bedienungshandbuch. Stoe & Cie GmbH, Darmstadt, Germany.

[2] G. M. Sheldrick. (2008). Acta Cryst. A64, 112-122.

[3] Spek, A. L. (2003). J. Appl. Cryst. 36, 7-13.

Drawing programs:

ORTEP-3: [3] Farrugia, L. J. (1997). J. Appl. Cryst., 30, 565.

Mercury: [4] Macrae, C. F., Edgington, P. R., McCabe, P., Pidcock, E., Shields, G. P., Taylor, R., Towler, M. & van de Streek, J. (2006). J. Appl. Cryst. 39, 453-457.

PLATON: [5] Spek, A. L. (2003). J. Appl. Cryst. 36, 7-13.

2.38.2. Compound 89*

The amide **89** was prepared according to the procedure (III) from *meso*-octamethylcalix[2]pyrrole[2]pyrrolidine (100 mg, 0.23 mmol), 4-chlorobenzoyl chloride (53.61 µL, 0.48 mmol), potassium carbonate (70 mg, 0.48 mmol) in THF (5 mL) and ACN

(2.5 mL). The residue was purified by column chromatography (SiO_2, CH_2Cl_2/MeOH, 97/3) to yield 131.6 mg (75.6%) of colorless crystals.

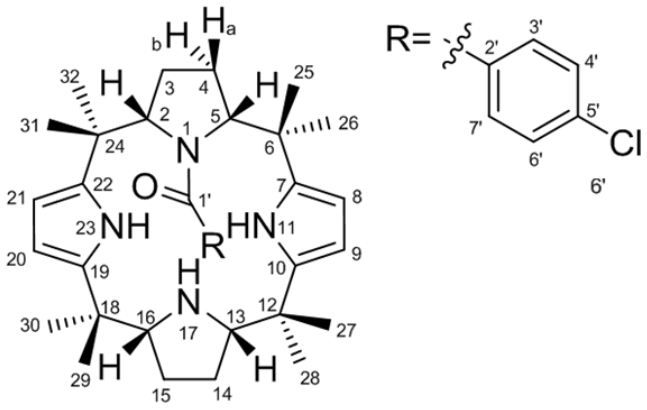

IR (KBr): 3410.9*m*, 3318.2*s*, 2966.1*m*, 1629.7*s*, 1346.4*s*, 1091.6*w*, 775.1*m*, 758.7*m*, 711.7*w*.

^{1}H NMR ($CDCl_3$ 218K) δ 9.15 (s, 1 H, N-H(23)), 8.74 (s, 1 H, N-H(11)), 7.04 (d, ^{3}J(3', 4') and ^{3}J(7', 6') = 7.7 Hz, 2 H, H(3', 7')), 6.10 (bs, 2 H, H(4', 6')), 5.91 (s, 2 H, pyrrolic-H(20, 21)), 5.76 (s, 1 H, pyrrolic-H(9)), 5.21 (s, 1 H, pyrrolic-H(8)), 4.49 (dd, ^{3}J(2, 3b) = 8.9 Hz, ^{3}J(2, 3a) = 8.6 Hz, 1 H, H(2)), 3.63 (d, ^{3}J(4, 5) = 7.7 Hz, 1 H, H(5)), 3.22 (bs, 1 H, H(13)), 2.92 (bs, 1 H, H(16)), 2.54 (m, 1 H, CH_2(3b)), 2.44 (bs, 1 H, N-H(17)), 2.18 (m, 1 H, CH_2(3a)), 1.85 (m, 1 H, CH_2(4b)), 1.67 (m, 1 H, CH_2(4a)), 1.65 (m, 1 H, CH_2(14a)), 1.63 (s, 3 H, CH_3(32)), 1.54 (m, 1 H, CH_2(15a)), 1.45 (s, 3 H, CH_3(28)), 1.38 (s, 3 H, CH_3(31)), 1.28 (s, 3 H, CH_3(29)), 1.24 (s, 3 H, CH_3(27)), 1.24 (s, 3 H, CH_3(30)), 0.93 (s, 3 H, CH_3(25)), 0.88 (m, 2 H, CH_2(14b, 15b)), -0.01 (s, 3 H, CH_3(26));

^{13}C NMR ($CDCl_3$) δ Not detected (C1'=O), Not detected (C(5')), (C(2')), (C(10)), (C(7)), (C(19)), (C(22)), 128.12 (C(4', 6')), 126. 39 (C(7', 3')), 107.61 (C(20) or (21)), 106.61 (C(20) or (21)), 105.30 (C(9)), 104.17 (C(8)), 71.79 (C(5)), 68.85 (C(16)), 66.70 (C(2)), 62.71 (C(13)), 40.32 (C(24)), 38.11 (C(6)), 37.98 (C(12)), 36.87 (C(18)), 33.06 (C(29)), 32.25 (C(31)), 29.18 (C(28)), 29.05 (C(25)), 27.81 (C(32)), 27.72 (C(4)), 27.02 (C(27)), 26.83 (C(3)), 26.83 (C(15)), 25.94 (C(14)), 25.81 (C(30)), 20.71 (C(26)).
Melting point: 228°C.

MS calcd for $C_{37}H_{45}ClN_4O$ 574.34, found 575.3 (M+H)+, 597.3 (M+Na)+.
HRMS calcd. for $C_{35}H_{47}ClN_4O$+H+ 575.3511, found 575.3510.

X-ray: Suitable crystals of **89** were obtained as colorless blocks by a slow evaporation of a solution in dichloromethane. The intensity data were collected at 233K (-40°C) on a Stoe Mark II-Image Plate Diffraction System [1] equiped with a two-circle goniometer and using MoKα graphite monochromated radiation (λ = 0.71073 Å). Image plate distance 130mm, ω rotation scans 0 - 180° at ϕ 0°, and 0 – 106.0° at ϕ 90°, step Δω = 1.0°, exposures of 3 mins per image, 2θ range 1.76 - 52.59°, d_{min} – d_{max} = 23.107 - 0.802 Å.

The structure was solved by Direct methods using the program SHELXS-97 [2]. The refinement and all further calculations were carried out using SHELXL-97 [2].

The NH H-atoms were located in difference electron-density maps. In the final cycles of least-squares refinement H-atom N3H was refined with a distance restraint of N-H = 0.88(2) Å and U_{iso}(H) = 1.2U_{eq}(N). The other NH H-atoms and the C-bound H-atoms were included in calculated positions and treated as riding atoms: N-H = 0.87 Å, C-H = 0.94 – 0.99 Å, with U_{iso}(H) = k × $U_{eq(}$N,C), where k = 1.5 for CH_3 H-atoms, and = 1.2 for all other H-atoms.

The non-H atoms were refined anisotropically, using weighted full-matrix least-squares on F^2. An empirical absorption correction was applied using the MULscanABS routine in PLATON [3].

[1] Stoe & Cie (2000). IPDS-I Bedienungshandbuch. Stoe & Cie GmbH, Darmstadt, Germany.

[2] G. M. Sheldrick. (2008). Acta Cryst. A64, 112-122.

[3] Spek, A. L. (2003). J. Appl. Cryst. 36, 7-13.

Drawing programs:

ORTEP-3: [3] Farrugia, L. J. (1997). J. Appl. Cryst., 30, 565.

Mercury: [4] Macrae, C. F., Edgington, P. R., McCabe, P., Pidcock, E., Shields, G. P., Taylor, R., Towler, M. & van de Streek, J. (2006). J. Appl. Cryst. 39, 453-457.

PLATON: [5] Spek, A. L. (2003). J. Appl. Cryst. 36, 7-13.

2.38.3. Compound 90*

The amide **90** was prepared according to the procedure (III) from *meso*-octamethylcalix[2]pyrrole[2]pyrrolidine (100 mg, 0.23 mmol), 4-methylbenzoyl chloride (63.37 µL, 0.48 mmol), potassium carbonate (70 mg, 0.48 mmol) in THF (5 mL) and ACN (2.5 mL). The residue was purified by column chromatography (SiO_2, CH_2Cl_2/MeOH, 97/3) to yield 127.04 mg (54.3%) of colorless crystals.

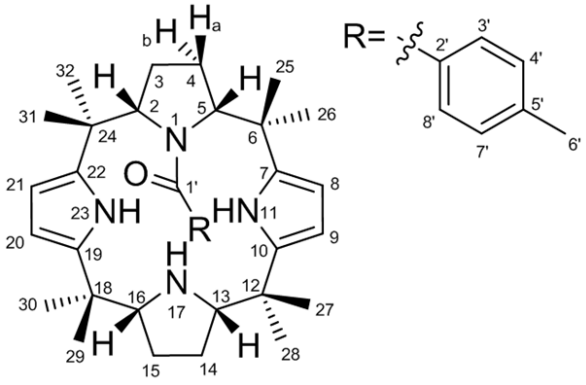

IR (KBr): 3412.1*s*, 2965.3*s*, 2865.7*m*, 1631.0*s*, 1348.9*s*, 773.6*m*, 755.6*s*, 711.5*m*, 607.9*w*.

^{1}H NMR ($CDCl_3$ 218K) δ 9.21 (s, 1 H, N-H(23)), 8.71 (s, 1 H, N-H(11)), 6.86 (m, 2 H, H(3', 8')), 6.06 (bs, 2 H, H(4', 7')), 5.90 (s, 2 H, pyrrolic-H(20, 21)), 5.77 (s, 1 H, pyrrolic-H(9)), 5.23 (bs, 1 H, pyrrolic-H(8)), 4.51 (bs, 1 H, H(2)), , 3.70 (bs, 1 H, H(5)), 3.22 (bs, 1 H, H(13)), 2.92 (bs, 1 H, H(16)), 2.52 (m, 1 H, CH_2(3b)), 2.42 (bs, 1 H, N-H(17)), 2.26 (s, 3 H, CH_3(6')), 2.15 (m, 1 H, CH_2(3a)), 1.83 (m, 1 H, CH_2(4b)), 1.68 (m, 1 H, CH_2(14a)), 1.65 (s, 3 H, CH_3(32)), 1.63 (m, 1 H, CH_2(4a)), 1.54 (m, 1 H, CH_2(14a)), 1.45 (s, 3 H, CH_3(28)), 1.38 (s, 3 H, CH_3(31)), 1.27 (s, 3 H, CH_3(29)), 1.25 (s, 3 H, CH_3(27)), 1.20 (s, 3 H, CH_3(30)), 0.94 (s, 3 H, CH_3(25)), 0.94 (m, 1 H, CH_2(14b)), 0.89 (m, 1 H, CH_2(15b)), 0.00 (s, 3 H, CH_3(26);

^{13}C NMR ($CDCl_3$) δ Not detected (C(1')=O, 5', 2', 10, 7, 19, 22)), 128.7 (C(4', 7')), 125. 6 (C(3', 8')), 107.0 (C(20, 21)), 105.1 (C(9)), 103.8 (C(8)), 71.7 (C(5)), 71.0 (C(16)), 67.8 (C(2)), 66.8 (C(13)), not detected (C(24, 6, 12 18)), 33.2 (C(29)), 32.2 (C(31)), 29.1 (C(28)), 29.0 (C(25)), 27.2 (C(32)), not detected (C(4)), 26.8 (C(27)), not detected (C(3, 15, 14)), 25.5 (C(30)), 21.4 (C(6')), 20.5 (C(26)).

Melting point: 233°C.

MS calcd for $C_{36}H_{50}N_4O$ 554.40, found 555.5 (M+H)+, 577.5 (M+Na)+.
HRMS calcd. for $C_{36}H_{50}N_4O+H^+$ 555.4057, found 555.4049.

X-ray: Suitable crystals of **90** were obtained as thin colorless plates by a slow evaporation of a solution in dichloromethane. The intensity data were collected at 233K (-40°C) on a Stoe Mark II-Image Plate Diffraction System [1] equiped with a two-circle goniometer and using

MoKα graphite monochromated radiation (λ = 0.71073 Å). Image plate distance 130mm, ω rotation scans 0 - 180° at ϕ 0°, step Δω = 1.0°, exposures of 7 mins per image, 2θ range 1.76 - 52.59°, $d_{min} - d_{max}$ = 23.107 - 0.802 Å.

The structure was solved by Direct methods using the program SHELXS-97 [2]. The refinement and all further calculations were carried out using SHELXL-97 [2].

The NH H-atoms were located in difference electron-density maps. In the final cycles of least-squares refinement H-atom N3H was refined with a distance restraint of N-H = 0.862(16) Å and $U_{iso}(H) = 1.2U_{eq}(N)$. The other NH H-atoms and the C-bound H-atoms were included in calculated positions and treated as riding atoms: N-H = 0.87 Å, C-H = 0.99, 0.98 and 0.97 Å for CH, CH_2 and CH_3, respectively, and 0.94 Å for CH-allyl and CH-aromatic, with $U_{iso}(H) = k \times U_{eq(}N,C)$, where k = 1.5 for CH_3 H-atoms, and = 1.2 for all other H-atoms.

The non-H atoms were refined anisotropically, using weighted full-matrix least-squares on F^2. An empirical absorption correction was applied using the MULscanABS routine in PLATON [3]. The crystal diffracted very weakly beyond 45˚ in 2θ, despite exposures of 7 min per image. Despite the large number of very weak high angle reflections the R_{int} value was relatively low. In the final cycles of refinement the data were restricted to 23˚ in θ.

[1] Stoe & Cie (2000). IPDS-I Bedienungshandbuch. Stoe & Cie GmbH, Darmstadt, Germany.

[2] G. M. Sheldrick. (2008). Acta Cryst. A64, 112-122.

[3] Spek, A. L. (2003). J. Appl. Cryst. 36, 7-13.

Drawing programs:

ORTEP-3: [3] Farrugia, L. J. (1997). J. Appl. Cryst., 30, 565.

Mercury: [4] Macrae, C. F., Edgington, P. R., McCabe, P., Pidcock, E., Shields, G. P., Taylor, R., Towler, M. & van de Streek, J. (2006). J. Appl. Cryst. 39, 453-457.

PLATON: [5] Spek, A. L. (2003). J. Appl. Cryst. 36, 7-13.

2.38.4. Compound 91*

The compound **91** was prepared according to the procedure (III) from *meso*-octamethylcalix[2]pyrrole[2]pyrrolidine (100 mg, 0.23 mmol), 4-methoxybenzoyl chloride (64.93 µL, 0.48 mmol), potassium carbonate (70 mg, 0.48 mmol) in THF (5 mL) and ACN (2.5 mL). The residue was purified by column chromatography (SiO_2, CH_2Cl_2/MeOH, 97/3) to yield 64.0 mg (49%) of colorless crystals.

The amide **26** was prepared according to the general procedure (I) *meso*-octamethylcalix[2]pyrrole[2]pyrrolidine (100 mg, 0.23 mmol), 4-methoxybenzoyl chloride (64.93 µL, 0.48 mmol), potassium carbonate (70 mg, 0.48 mmol) in THF (5 mL) and ACN (2.5 mL). The residue was purified by column chromatography (SiO_2, CH_2Cl_2/MeOH, 97/3) to yield 117.0 mg (90%) of colorless crystals.

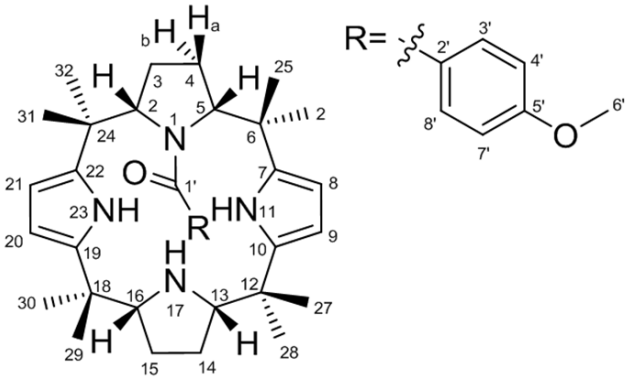

IR (KBr): 3411.2*m*, 3319.4*w*, 2963.2*m*, 1627.1*s*, 1341.0*s*, 1247.3*s*, 1039.7*m*, 772.3*w*, 754.3*w*.

^{1}H NMR ($CDCl_3$ 218K) δ 9.20 (s, 1 H, N-H(23)), 8.72 (s, 1 H, N-H(11)), 6.56 (m, 2 H, H(3', 8')), 6.08 (bs, 2 H, H(4', 7')), 5.90 (s, 2 H, pyrrolic-H(20, 21)), 5.78 (s, 1 H, pyrrolic-H(9)), 5.29 (bs, 1 H, pyrrolic-H(8)), 4.54 (bs, 1 H, H(2)), 3.77 (s, 3 H, CH_3(6')), 3.66 (bs, 1 H, H(5)), 3.22 (bs, 1 H, H(13)), 2.92 (bs, 1 H, H(16)), 2.53 (m, 1 H, CH_2(3b)), 2.44 (bs, 1 H, N-H(17)), 2.15 (m, 1 H, CH_2(3a)), 1.83 (m, 1 H, CH_2(4b)), 1.68 (m, 1 H, CH_2(14a)), 1.64 (s, 3 H, CH_3(32)), 1.63 (m, 1 H, CH_2(4a)), 1.55 (m, 1 H, CH_2(15a)), 1.44 (s, 3 H, CH_3(28)), 1.38 (s, 3 H, CH_3(31)), 1.27 (s, 3 H, CH_3(29)), 1.25 (s, 3 H, CH_3(27)), 1.20 (s, 3 H, CH_3(30)), 0.95 (s, 3 H, CH_3(25)), 0.95 (m, 1 H, CH_2(14b)), 0.86 (m, 1 H, CH_2(15b)), 0.01 (s, 3 H, CH_3(26));

^{13}C NMR ($CDCl_3$) δ 180.16 (C(1')=O), 158.47 (C(5')), 138.14 (C(10)), 136.96 (C(7)), 135.40 (C(19)), 135.03 (C(22)), 131.01 (C(2')), 127.04 (C(4', 7')), 112.59 (C(3', 8')), 107.11 (C(20 or 21)), 106.19 (C(20 or 21)), 104.78 (C(9)), 103.81 (C(8)), 71.65 (C(5)), 70.50 (C(16)), 68.49 (C(2)), 66.34 (C(13)), 55.24 (C(6')), 39.88 (C(24)), 37.82 (C(6)), 37.70 (C(12)), 36.54 (C(18)), 32.81 (C(29)), 31.93 (C(31)), 28.81 (C(28)), 28.65 (C(25)), 27.54 (C(4)), 27.32 (C(32)), 26.57 (C(27)), 26.44 (C(3)), 25.69 (C(15)), 25.48 (C(30, 14)), 20.71 (C(26)).

Melting point: 215°C.

MS calcd for $C_{36}H_{50}N_4O_2$ 570.4, found 571.4 (M+H)+, 593.4 (M+Na)+.
HRMS calcd. for $C_{36}H_{50}N_4O_2+H^+$ 571.4007, found 571.3993.

X-ray: Suitable crystals of **91** were obtained as colorless blocks by a slow evaporation of a solution in dichloromethane. The intensity data were collected at **173K (-100°C)** on a Stoe Mark II-Image Plate Diffraction System [1] equiped with a two-circle goniometer and using MoKα graphite monochromated radiation (λ = 0.71073 Å). Image plate distance 130mm, ω rotation scans 0 - 180° at ϕ 0°, 0 - 108° at ϕ 90°, step Δω = 1.0°, exposures of 3 mins per image, 2θ range 1.76 - 52.59°, $d_{min} – d_{max}$ = 23.107 - 0.802 Å.
The structure was solved by Direct methods using the program SHELXS-97 [2]. The refinement and all further calculations were carried out using SHELXL-97 [2].
The NH H-atoms were located in difference electron-density maps. In the final cycles of least-squares refinement H-atom N3H was refined with a distance restraint of N-H = 0.924(18) Å and $U_{iso}(H) = 1.2U_{eq}(N)$. The other NH H-atoms and the C-bound H-atoms were included in calculated positions and treated as riding atoms: N-H = 0.88 Å, C-H = 1.0, 0.99 and 0.98 Å for CH, CH_2 and CH_3, respectively, and 0.95 Å for CH-allyl and CH-aromatic, with $U_{iso}(H) = k \times U_{eq(}N,C)$, where k = 1.5 for CH_3 H-atoms, and = 1.2 for all other H-atoms.
The non-H atoms were refined anisotropically, using weighted full-matrix least-squares on F^2. An empirical absorption correction was applied using the MULscanABS routine in PLATON [3].
[1] Stoe & Cie (2000). IPDS-I Bedienungshandbuch. Stoe & Cie GmbH, Darmstadt, Germany.
[2] G. M. Sheldrick. (2008). Acta Cryst. A64, 112-122.
[3] Spek, A. L. (2003). J. Appl. Cryst. 36, 7-13.
Drawing programs:
ORTEP-3: [3] Farrugia, L. J. (1997). J. Appl. Cryst., 30, 565.
Mercury: [4] Macrae, C. F., Edgington, P. R., McCabe, P., Pidcock, E., Shields, G. P., Taylor, R., Towler, M. & van de Streek, J. (2006). J. Appl. Cryst. 39, 453-457.
PLATON: [5] Spek, A. L. (2003). J. Appl. Cryst. 36, 7-13.

2.39. Synthesis of compound 93-95*

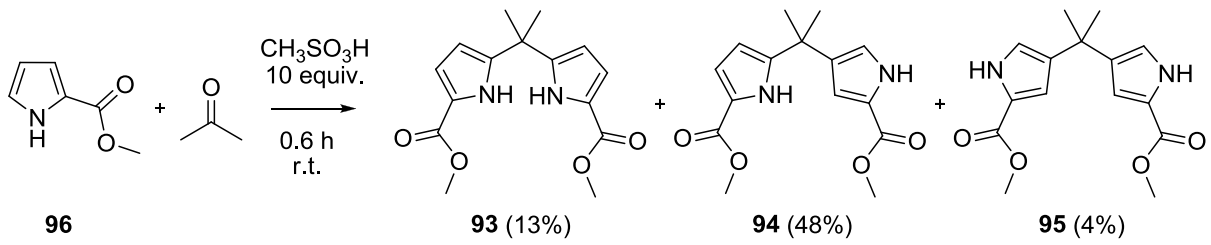

Methyl 2-pyrrolecarboxylate **4** (2 g, 16 mmol) and acetone (12 mL, 0.16 mol) in dry CH_2Cl_2 (200 mL) were stirred at room temperature for 5 min. Then, methanesulfonic acid (10.3 mL, 0.16 mol.) was added at room temperature and stirred further 40 min. After stirring, 10% sodium carbonate was added and the reaction mixture was extracted with dichloromethane. The organic layer was washed successively with two times 10% sodium carbonate and saturated brine. The organic layer was dried with sodium sulfate, and the solvents were removed under vacuum. The colorless residue was submitted to GC analysis and then was purified by column chromatography (SiO_2, Cyclohexane/EtOAc/MeOH, 80/18/2). The first fraction (Rf = 0.36) afforded 312 mg (13%) of compound **93** as a clear white solid (*R*=13%). The second fraction (Rf = 0.163) afforded 1.12 g (48%) of compound **94** as a white solid (*R*=48%). The third fraction (Rf = 0.139) gave 80 mg (4%) of compound **95** as a clear white solid (*R*=3.4%).

2.39.1. Compound 93* (Dimethyl 5,5-(propane-2',2'-diyl)bis(1H-pyrrole-2-carboxylate)

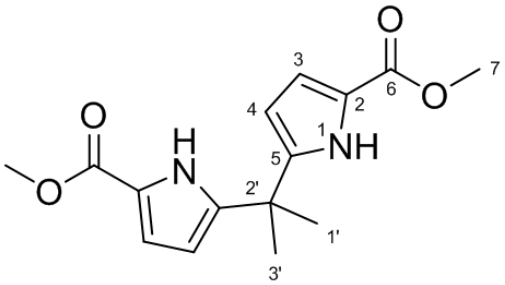

IR (KBr): 3358.8*m*, 3269.8*m*, 2948.0*w*, 1698.4*s*, 1660.8*s*, 1485.5*s*, 1326.2*m*, 1235.2*s*, 1002.5*m*, 797.3*w*, 767.3*m.*

^{1}H NMR ($CDCl_3$, 298K) δ 9.99 (bs, 1 H, NH(1)), 6.70 (m, 2 H, C-H(3)), 6.07 (m, 2 H, C-H(4)), 3.76 (s, 6H, O-CH_3(7)), 1.64 (s, 6 H, CH_3(1', 3'));

^{13}C NMR ($CDCl_3$) δ 162.12 (C=O), 144.30 (C(5)), 121.72 (C(2)), 115.47 (C(3)), 106.46 (C(4)), 51.27 (C(7)), 36.22 (C(2')), 29.41 (C(1', 3')).

Melting point: 196°C.

HRMS calcd. for $C_{15}H_{18}N_2O_4H^+$ 291.1339, found 291.1336.

X-ray: Suitable crystals of **1a, 1b**, **1c**, **2** and **3** were obtained as colorless rods. Slow evaporation of a solution of **1** in dichloromethane afforded two kinds of crystals **1a** and **1b** having different morphology; 2) Crystal of **1c** has been isolated as impurity in the middle of other crystals of **2** (with different shape) after a recrystallization of a solution of **2** in ethanol; 5) Recrystallization of a solution of **3** in ethanol. The intensity data were collected at 173K (-100°C) on a Stoe Mark II-Image Plate Diffraction System [1] equipped with a two-circle goniometer and using MoKα graphite monochromated radiation (λ = 0.71073 Å). The structures were solved by direct methods using the program SHELXS-97 [2]. The refinement and all further calculations were carried out using SHELXL-97 [2]. The NH H-atoms were located in difference Fourier maps and were freely refined. The C-bound H-atoms were included in calculated positions and treated as riding atoms: C-H = 0.95 and 0.98 Å for CH and CH_3, respectively, with $U_{iso}(H) = k \times U_{eq}$(parent C-atom), where k = 1.5 for CH_3 H-atoms and k = 1.2 for all other H-atoms. The non-H atoms were refined anisotropically, using weighted full-matrix least-squares on F^2. The figures were drawn using the program Mercury [3].

[1] Stoe & Cie (2000). IPDS-I Bedienungshandbuch. Stoe & Cie GmbH, Darmstadt, Germany.

[2] G. M. Sheldrick. (2008). Acta Cryst. A64, 112-122.

[3] Spek, A. L. (2003). J. Appl. Cryst. 36, 7-13.

Drawing programs:

ORTEP-3: [3] Farrugia, L. J. (1997). J. Appl. Cryst., 30, 565.

Mercury: [4] Macrae, C. F., Edgington, P. R., McCabe, P., Pidcock, E., Shields, G. P., Taylor, R., Towler, M. & van de Streek, J. (2006). J. Appl. Cryst. 39, 453-457.

PLATON: [5] Spek, A. L. (2003). J. Appl. Cryst. 36, 7-13.

2.39.2. Compound 94* (Methyl 4-(2'-(5'-(methoxycarbonyl)-1'H-pyrrol-2'-yl)propan-2''-yl)-1H-pyrrole-2-carboxylate)

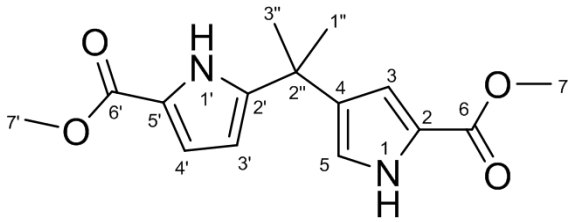

IR (KBr): 3355.0*m*, 3311.9*m*, 2947.0*w*, 1685.9*s*, 1568.3*w*, 1485.35*m*, 1440.3*m*, 1382.5*m*, 1236.0*m*, 766.3*m* cm^{-1}.

^{1}H NMR ($CDCl_3$, 298K) δ 9.24 (bs, 1 H, NH(1')), 8.73 (bs, 1 H, NH(1)), 6.82 (m, 1 H, C-H(4')), 6.77 (m, 1H, C-H(3)), 6.73 (m, 1 H, C-H(5)), 6.07 (m, 1 H, C-H(3')), 3.83 (s, 3 H, O-CH_3(7')), 3.79 (s, 3 H, O-CH_3(7)), 1.62 (s, 6 H, CH_3(1'', 3'')).

^{13}C NMR ($CDCl_3$) δ 161.73 (C=O), 161.56 (C=O), 146.54 (C(2')), 133.77 (C(4)), 122.76 (C(2)), 121.00 (C(5')), 119.67 (C(5)), 115.71 (C(4')), 113.22 (C(3)), 106.34 (C(3')), 51.52 (C(7 or 7')), 51.52 (C(7 or 7')), 34.91 (C(2'')), 30.14 (C(1'', 3'')).

Melting point: 134°C.

HRMS calcd. for $C_{15}H_{18}N_2O_4H^+$ 291.1339, found 291.1336.

X-ray: See above

2.39.3. Compound 95* (Dimethyl 4,4-(propane-2',2'-diyl)bis(1H-pyrrole-2-carboxylate)

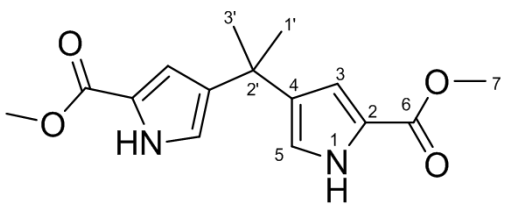

IR (KBr): 3352.3*m*, 2958.0*w*, 1682.7*s*, 1478.2*w*, 1440.3*w*, 1393.6*m*, 1231.6*m*, 1125.43*m*, 769.4*m* cm^{-1}.

^{1}H NMR ($CDCl_3$, 298K) δ 8.88 (bs, 2 H, NH(1)), 6.80 (m, 2 H, C-H(3)), 6.72 (m, 2 H, C-H(5)), 3.83 (s, 6H, O-CH_3(7)), 1.58 (s, 6 H, CH_3(1', 3'));

^{13}C NMR ($CDCl_3$) δ 161.57 (C=O), 136.77 (C(4)), 122.19 (C(2)), 119.34 (C(5)), 113.41 (C(3)), 51.38 (C(7)), 33.61 (C(2')), 31.28 (C(1', 3')).

Melting point: 199°C.

HRMS calcd. for $C_{15}H_{18}N_2O_4H^+$ 291.1339, found 291.1336.

X-ray: See above

Chapter 8

REFERENCES AND NOTES

1. G. H. Daub, A. A. Leon, I. R. Silverman, G. W. Daub and S. B. Walker, *Aldrichimica Acta,* 1984, **17**, 13.
2. A. Eschenmoser, *Helv. Chim. Acta,* **93**, 1439.
3. A. Baeyer and V. Drewsen, *Ber. Dtsch. Chem. Ges.,* 1882, **15**, 2856.
4. O. Wallach, *Liebigs Ann. Chem.,* 1889, **252**, 106.
5. E. Fischer, *Ber. Dtsch. Chem. Ges.,* 1890, **23**, 799.
6. R. G. Ault, D. K. Baird, H. C. Carrington, W. N. Haworth, R. Herbert, E. L. Hirst, E. G. V. Percival, F. Smith and M. Stacey, *J. Chem. Soc.,* 1933, 1419.
7. R. G. Ault, W. N. Haworth and E. L. Hirst, *J. Chem. Soc.,* 1934, 1722.
8. D. K. Baird, W. N. Haworth, R. W. Herbert, E. L. Hirst, F. Smith and M. Stacey, *J. Chem. Soc.,* 1934, 62.
9. W. N. Haworth, E. L. Hirst, J. K. N. Jones and F. Smith, *J. Chem. Soc.,* 1934, 1192.
10. P. Karrer and K. Schopp, *Helv. Chim. Acta,* 1932, **15**, 745.
11. P. Karrer, B. von Euler and H. von Euler, *Ark. Kemi, Mineral. Geol.,* 1928, **10B**, 6 pp.
12. H. Wieland and F. Weil, *Z. physiol. Chem.,* 1913, **80**, 287.
13. A. Butenandt, *Trends Biochem. Sci. (Pers. Ed.),* 1979, **4**, 215.
14. K.-H. Altmann, J. Buchner, H. Kessler, F. Diederich, B. Krautler, S. Lippard, R. Liskamp, K. Muller, E. M. Nolan, B. Samori, G. Schneider, S. L. Schreiber, H. Schwalbe, C. Toniolo, C. A. A. van Boeckel, H. Waldmann and C. T. Walsh, *ChemBioChem,* 2009, **10**, 16.
15. A. Eschenmoser, *Angew. Chem.,* 1988, **100**, 5.
16. A. Eschenmoser, *Tetrahedron,* 2007, **63**, 12821.
17. B. Kraeutler and S. Ostermann, "in The Porphyrin Handbook". In Vol. 11 (Eds.: K. M. Kadish, K. M. Smith, R. Guilard): 2003; p 229.
18. B. Kraeutler, *Chimia,* 1987, **41**, 277.
19. B. Kraeutler, *Biochem. Soc. Trans.,* 2005, **33**, 806.
20. H. Scheer, *Adv. Photosynth. Respir.,* 2006, **25**, 1.
21. H. Scheer, *Compr. Ser. Photochem. Photobiol. Sci.,* 2008, **8**, 101.
22. H. Scheer, *Wiley Encycl. Chem. Biol.,* 2009, **1**, 341.
23. W.-D. Woggon, *Chimia,* 1999, **53**, 234.
24. W.-D. Woggon, *Acc. Chem. Res.,* 2005, **38**, 127.
25. W.-D. Woggon, *Met. Ions Life Sci.,* 2007, **3**, 27.
26. A. R. Battersby and E. McDonald, *Acc. Chem. Res.,* 1979, **12**, 14.

27. A. R. Battersby, C. J. R. Fookes, G. W. J. Matcham and E. McDonald, *Nature (London),* 1980, **285**, 17.
28. A. R. Battersby, *Nat. Prod. Rep.,* 2000, **17**, 507.
29. A. R. Battersby, *Acc. Chem. Res.,* 1986, **19**, 147.
30. P. M. Jordan, *Ciba Found. Symp.,* 1994, **180**, 70.
31. A. I. Scott and C. A. Roessner, *Biochem Soc Trans,* 2002, **30**, 613.
32. E. K. Jaffe, *Open Conf. Proc. J.,* **1**, 1.
33. E. K. Jaffe, *Bioorg. Chem.,* 2004, **32**, 316.
34. A. R. Battersby and F. J. Leeper, *Top. Curr. Chem.,* 1998, **195**, 143.
35. H.-J. Kwon, C. Smith Wyatt, A. J. Scharon, H. Hwang Sung, J. Kurth Mark and B. Shen, *Science,* 2002, **297**, 1327.
36. A. I. Scott, *J. Org. Chem.,* 2003, **68**, 2529.
37. S. S. Lamb and G. D. Wright, *PNAS,* 2005, **102**, 519.
38. F. Stauffer, E. Zizzari, C. Soldermann-Pissot, J.-P. Faurite and R. Neier, *Chimia,* 2001, **55**, 314.
39. P. Bobal and R. Neier, *Trends Org. Chem.,* 1997, **6**, 125.
40. C. P. Soldermann, R. Vallinayagam, M. Tzouros and R. Neier, *J. Org. Chem.,* 2008, **73**, 764.
41. R. Neier, *Adv. Nitrogen Heterocycl.,* 1996, **2**, 35.
42. D. Mauzerall, *J. Am. Chem. Soc.,* 1960, **82**, 2605.
43. D. Mauzerall, *J. Am. Chem. Soc.,* 1960, **82**, 2601.
44. G. R. Geier, III and J. S. Lindsey, *J. Chem. Soc., Perkin Trans. 2,* 2001, 687.
45. F. Li, K. Yang, J. S. Tyhonas, K. A. MacCrum and J. S. Lindsey, *Tetrahedron,* 1997, **53**, 12339.
46. J. S. Lindsey, V. Chandrashaker, M. Taniguchi and M. Ptaszek, *New J. Chem.,* **35**, 65.
47. J. S. Lindsey, M. Ptaszek and M. Taniguchi, *Origins Life Evol. Biospheres,* 2009, **39**, 495.
48. P. M. Shoolingin-Jordan, *Vitamin B12 B12-Proteins, Lect. Eur. Symp., 4th,* 1998, 101.
49. P. M. Shoolingin-Jordan and K.-M. Cheung, *Compr. Nat. Prod. Chem.,* 1999, **4**, 61.
50. D. Jacoby, C. Floriani, A. Chiesi-Villa and C. Rizzoli, *J. Chem. Soc., Chem. Commun.,* 1991, 790.
51. D. Jacoby, S. Isoz, C. Floriani, A. Chiesi-Villa and C. Rizzoli, *J. Am. Chem. Soc.,* 1995, **117**, 2805.
52. D. Jacoby, S. Isoz, C. Floriani, A. Chiesi-Villa and C. Rizzoli, *J. Am. Chem. Soc.,* 1995, **117**, 2793.
53. J. Jubb, D. Jacoby, C. Floriani, A. Chiesi-Villa and C. Rizzoli, *Inorg. Chem.,* 1992, **31**, 1306.
54. L. Bonomo, E. Solari, R. Scopelliti and C. Floriani, *Chemistry,* 2001, **7**, 1322.
55. C. Floriani and R. Floriani-Moro, '*in The Porphyrin Handbook,*' ed. by K. M. Kadish, K. M. Smith, R. Guilard, Vol. 3, San Diego, 2000, p.
56. C. Floriani, *Chem. Commun.,* 1996, 1257.
57. C. Angst, M. Kajiwara, E. Zass and A. Eschenmoser, *Angew. Chem.,* 1980, **92**, 139.
58. A. Eschenmoser, *Nova Acta Leopold.,* 1982, **55**, 47 pp.
59. A. Eschenmoser, *Ann. N. Y. Acad. Sci.,* 1986, **471**, 108.
60. R. Schwesinger, R. Waditschatka, J. Rigby, R. Nordmann, W. B. Schweizer, E. Zass and A. Eschenmoser, *Helv. Chim. Acta,* 1982, **65**, 600.
61. R. Waditschatka, C. Kratky, B. Jaun, J. Heinzer and A. Eschenmoser, *J. Chem. Soc., Chem. Commun.,* 1985, 1604.
62. N. Fotinos, M. A. Campo, F. Popowycz, R. Gurny and N. Lange, *Photochem.*

Photobiol., 2006, **82**, 994.
63. A. E. O'Connor, W. M. Gallagher and A. T. Byrne, *Photochem. Photobiol.*, 2009, **85**, 1053.
64. M. Studer, A. Riesen and T. A. Kaden, *Helv. Chim. Acta*, 1989, **72**, 1253.
65. E. Kimura, Y. Kodama, M. Shionoya and T. Koike, *Inorg. Chim. Acta*, 1996, **246**, 151.
66. P. S. Bryan and J. C. Dabrowiak, *Inorg. Chem.*, 1975, **14**, 296.
67. Z. Guo and P. J. Sadler, *Angew. Chem. Int. Ed.*, 1999, **38**, 1512.
68. R. Hage, J. E. Iburg, J. Kerschner, J. H. Koek, E. L. M. Lempers, R. J. Martens, U. S. Racherla, S. W. Russell and T. Swarthoff, *Nature*, 1994, **369**, 637.
69. D. De Vos and T. Bein, *Chem. Commun.*, 1996, 917.
70. J. T. Groves and T. E. Nemo, *J. Am. Chem. Soc.*, 1983, **105**, 5786.
71. B. Meunier, E. Guilmet, M. E. De Carvalho and R. Poilblanc, *J. Am. Chem. Soc.*, 1984, **106**, 6668.
72. W. Nam, R. Ho and J. S. Valentine, *J. Am. Chem. Soc.*, 1991, **113**, 7052.
73. M. R. Bukowski, K. D. Koehntop, A. Stubna, E. L. Bominaar, J. A. Halfen, E. Muenck, W. Nam and L. Que, Jr., *Science*, 2005, **310**, 1000.
74. F. Tiago de Oliveira, A. Chanda, D. Banerjee, X. Shan, S. Mondal, L. Que, Jr., E. L. Bominaar, E. Muenck and T. J. Collins, *Science*, 2007, **315**, 835.
75. Y. Kang, H. Chen, Y. J. Jeong, W. Lai, E. H. Bae, S. Shaik and W. Nam, *Chem.-Eur. J.*, 2009, **15**, 10039.
76. Y. Gao, T. Akermark, J. Liu, L. Sun and B. Akermark, *J. Am. Chem. Soc.*, 2009, **131**, 8726.
77. A. J. McGown, W. D. Kerber, H. Fujii and D. P. Goldberg, *J. Am. Chem. Soc.*, 2009, **131**, 8040.
78. M. C. White, A. G. Doyle and E. N. Jacobsen, *J. Am. Chem. Soc.*, 2001, **123**, 7194.
79. A. L. Gavrilova and B. Bosnich, *Chemical Reviews*, 2004, **104**, 349.
80. K. Nehru, S. J. Kim, I. Y. Kim, M. S. Seo, Y. Kim, S.-J. Kim, J. Kim and W. Nam, *Chem. Commun.*, 2007, 4623.
81. J. England, M. Martinho, E. R. Farquhar, J. R. Frisch, E. L. Bominaar, E. Munck and L. Que, Jr., *Angew. Chem. Int. Ed.*, 2009, **48**, 3622.
82. M. S. Chen and M. C. White, *Science*, 2007, **318**, 783.
83. J. M. Ready and E. N. Jacobsen, *Angew. Chem. Int. Ed.*, 2002, **41**, 1374.
84. J. M. Lehn, *Pure Appl. Chem.*, 1979, **51**, 979.
85. J. M. Lehn, '*Supramolecular Chemistry: Concepts and Perspectives*,' ed. by Vol. 1995.
86. C. J. Pederson, J. M. Lehn and D. J. Cram, *Resonance*, 2001, **6**, 71.
87. R. J. Geue, T. W. Hambley, J. M. Harrowfield, A. M. Sargeson and M. R. Snow, *J. Am. Chem. Soc.*, 1984, **106**, 5478.
88. J. M. Harrowfield, A. J. Herlt, P. A. Lay, A. M. Sargeson, A. M. Bond, W. A. Mulac and J. C. Sullivan, *J. Am. Chem. Soc.*, 1983, **105**, 5503.
89. P. M. Angus, A. M. T. Bygott, R. J. Geue, B. Korybut-Daszkiewicz, A. W. H. Mau, A. M. Sargeson, M. M. Sheil and A. C. Willis, *Chem.-Eur. J.*, 1997, **3**, 1283.
90. T. J. Hubin, *Coord. Chem. Rev.*, 2003, **241**, 27.
91. J. C. Timmons and T. J. Hubin, *Coord. Chem. Rev.*, 2010, **254**, 1661.
92. A. Baeyer, *Ber. Dtsch. Chem. Ges.*, 1886, 2184.
93. V. V. Chelintzev, B. V. Tronov and S. G. Karmanov, *J. Russ. Chem. Soc.*, 1916, **48**, 1210.
94. P. Rothemund and C. L. Gage, *J. Am. Chem. Soc.*, 1955, **77**, 3340.
95. P. A. Gale, J. L. Sessler, V. Kral and V. Lynch, *J. Am. Chem. Soc.*, 1996, **118**, 5140.

96. P. A. Gale. and J. L. Sessler, ed. by K. M. Kadish, K. M. Smith, R. Guilard, Vol. 6, San Diego, 2000, p 257.
97. H. Miyaji, P. Anzenbacher, Jr., J. L. Sessler, E. R. Bleasdale and P. A. Gale, *Chem. Commun.*, 1999, 1723.
98. P. A. Gale, L. J. Twyman, C. I. Handlin and J. L. Sessler, *Chem. Commun.*, 1999, 1851.
99. H. Adalsteinsson and T. C. Bruice, *J. Am. Chem. Soc.*, 1998, **120**, 3440.
100. J. Jubb, D. Jacoby, C. Floriani, A. Chiesi-Villa and C. Rizzoli, *Inorg. Chem.*, 1992, **31**, 1306.
101. W. E. Allen, P. A. Gale, C. T. Brown, V. M. Lynch and J. L. Sessler, *J. Am. Chem. Soc.*, 1996, **118**, 12471.
102. J. L. Sessler, A. Andrievsky, P. A. Gale and V. Lynch, *Angew. Chem., Int. Ed. Engl.*, 1997, **35**, 2782.
103. D. Jacoby, C. Floriani, A. Chiesi-Villa and C. Rizzoli, *J. Chem. Soc., Chem. Commun.*, 1991, 220.
104. M. Van Beylen, B. Roland, G. S. D. King and J. Aerts, *J. Chem. Res., M.*, 1985, 4201.
105. B. R. Kusche, A. E. Smith, M. A. McGuirl and N. D. Priestley, *J. Am. Chem. Soc.*, 2009, **131**, 17155.
106. E. Vogel, P. Roehrig, M. Sicken, B. Knipp, A. Herrmann, M. Pohl, H. Schmickler and J. Lex, *Angew. Chem.*, 1989, **101**, 1683.
107. M. Ahmed and O. Meth-Cohn, *Tetrahedron Lett.*, 1969, 1493.
108. G.-A. Lee, W.-C. Wang, M. Shieh and T.-S. Kuo, *Chem. Commun.*, **46**, 5009.
109. A. Nagarajan, J. W. Ka and C. H. Lee, *Tetrahedron*, 2001, **57**, 7323.
110. G.-A. Lee, W.-C. Wang, M. Shieh and T.-S. Kuo, *Chem. Commun* , 2010, **46**, 5009.
111. K. E. Wiegers and S. G. Smith, *J. Org. Chem.*, 1978, **43**, 1126.
112. R. G. Ackman, W. H. Brown and G. F. Wright, *J. Org. Chem.*, 1955, **20**, 1147.
113. R. E. Beals and W. H. Brown, *J. Org. Chem.*, 1956, **21**, 447.
114. W. H. Brown, B. J. Hutchinson and M. H. MacKinnon, *Can. J. Chemistry*, 1971, **49**, 4017.
115. W. J. Hale, W. D. McNally and C. J. Pater, *Amer. Chem. J.*, 1906, **35**, 68.
116. M. Chastrette and F. Chastrette, *J. Chem. Soc., Chem. Commun.*, 1973, 534.
117. M. Chastrette, F. Chastrette and J. Sabadie, *Org. Synth.*, 1977, **57**, 74.
118. M. de Sousa Healy and A. J. Rest, *J. Chem. Soc., Perkin Trans. 1*, 1985, 973.
119. Y. Kobuke, K. Hanji, K. Horiguchi, M. Asada, Y. Nakayama and J. Furukawa, *J. Am. Chem. Soc.*, 1976, **98**, 7414.
120. A. J. Rest, S. A. Smith and I. D. Tyler, *Inorg. Chim. Acta*, 1976, **16**, L1.
121. M. Van Beylen, B. Roland, G. S. D. King and J. Aerts, *J. Chem. Res., Synop.*, 1985, 388.
122. B. Roland, M. Van Beylen and J. Smid, *Journal of Physical Chemistry*, 1994, **98**, 4707.
123. L. A. R. Pioda, A. H. Wachter, R. E. Dohner and W. Simon, *Helv. Chim. Acta*, 1967, **50**, 1373.
124. J. L. Pierre and H. Handel, *Tetrahedron Lett.*, 1974, 2317.
125. H. Handel and J. L. Pierre, *Tetrahedron*, 1975, **31**, 997.
126. H. Handel and J. L. Pierre, *Tetrahedron Lett.*, 1976, 2029.
127. W. Bird, '*Comprehensive Heterocyclic Chemistry*,' ed. by Vol. 4 chap. 3.01 page 29.
128. K. M. J. A. Joule, '*Heterocyclic Chemistry*,' ed. by Blackwell Publishing oxford, 2007, page 8.
129. G. Journot, C. Letondor, R. Neier, H. Stoeckli-Evans, D. Savoia and A. Gualandi,

Chem.-Eur. J., 2010, **16**, 4224.
130. V. Blangy, C. Heiss, V. Khlebnikov, C. Letondor, H. Stoeckli-Evans and R. Neier, *Angew. Chem. Int. Ed.*, 2009, **48**, 1688.
131. F. Bruyneel, C. Letondor, B. Bastürk, A. Gualandi, A. Pordea, H. Stoeckli-Evans and R. Neier, *Adv. Synth. Cat., in press*, 2011.
132. H. Scheer, '*Chlorophylls*,' ed. by CRC Press Boca Raton, 1991, p.
133. J. G. V. D. Voet, '*Biochemistry*,' New York, 1990.
134. J. C. Timmons and T. J. Hubin, *Coord. Chem. Rev.*, 2010, **254**, 1661.
135. *C. Heiss, Diploma work 2000, M. Schmid, Progress report, summarized in V. Blangy, Ph.D. of the University of Neuchatel, 2007*.
136. G. Lunn, *J. Org. Chem.*, 1987, **52**, 1043.
137. C. G. Overberger, L. C. Palmer, B. S. Marks and N. R. Byrd, *J. Am. Chem. Soc.*, 1955, **77**, 4100.
138. G. Journot, C. Dalvit and R. Neier, *submitted to JACS*, 2012.
139. D. Savoia, C. Trombini and A. Umani-Ronchi, *Pure Appl. Chem.*, 1985, **57**, 1887.
140. V. G. Albano, A. Gualandi, M. Monari and D. Savoia, *J. Org. Chem.*, 2008, **73**, 8376.
141. G. Falini, A. Gualandi and D. Savoia, *Synthesis*, 2009, 2440.
142. D. Savoia, C. Trombini, A. Umani-Ronchi and G. Verardo, *J. Chem. Soc., Chem. Commun.*, 1981, 540.
143. A. Kamal, M. Sandbhor and A. Ali Shaik, *Bioorg. Med. Chem. Lett.*, 2004, **14**, 4581.
144. See further informations in the experimental part.
145. Thesis of Valeria Blangy, Université de Neuchâtel, **2007**. In Neuchâtel: Neuchâtel, 2007.
146. S. Depraetere, M. Smet and W. Dehaen, *Angew. Chem. Int. Ed.*, 1999, **38**, 3359.
147. Y. Kang, H. Chen, Y. J. Jeong, W. Lai, E. H. Bae, S. Shaik and W. Nam, *Chemistry--A European Journal*, 2009, **15**, 10039.
148. R. Irie, Y. Ito and T. Katsuki, *Synlett*, 1991, 265.
149. J. P. Collman, T. Kodadek, S. A. Raybuck and B. Meunier, *PNAS*, 1983, **80**, 7039.
150. A. Takahashi, T. Kurahashi and H. Fujii, *Inorganic Chemistry*, 2009, **48**, 2614.
151. J. A. Kovacs and L. M. Brines, *Acc. Chem. Res.*, 2007, **40**, 501.
152. W. Nam, M. H. Lim, S.-Y. Oh, J. H. Lee, H. J. Lee, S. K. Woo, C. Kiem and W. Shin, *Angew. Chem. Int. Ed.*, 2000, **39**, 3646.
153. J. A. A. W. Elemans, E. J. A. Bijsterveld, A. E. Rowan and R. J. M. Nolte, *Eur. J. Org. Chem.* 2007, 751.
154. S. P. de Visser, J. S. Valentine and W. Nam, *Angew. Chem. Int. Ed.*, 2010, **49**, 2099.
155. F. Bruyneel, C. Letondor, B. Bastuerk, A. Gualandi, A. Pordea, H. Stoeckli-Evans and R. Neier, *Adv. Synth. & Cat.*, 2012, **354**, 428.
156. C. H. Lee, *Bull. Kor. Chem. Soc.*, 2011, **32**, 768.
157. V. K. Jain and H. C. Mandalia, *Heterocycles*, 2007, **71**, 1261.
158. P. A. Gale, J. L. Sessler and V. Kral, *Chem. Commun.*, 1998, 1.
159. P. A. Gale, P. Anzenbacher, Jr. and J. L. Sessler, *Coord. Chem. Rev.*, 2001, **222**, 57.
160. D.-W. Yoon, H. Hwang and C.-H. Lee, *Angew. Chem. Int. Ed.*, 2002, **41**, 1757.
161. G. Journot, R. Neier and H. Stoeckli-Evans, *Acta Crystallographica E*, 2010, **E66**, o393.
162. G. Journot, H. Stoeckli and R. Neier, *Manuscript in preparation*, 2012.
163. D. J. Cram and F. A. A. Elhafez, *J. Am. Chem. Soc.*, 1952, **74**, 5828.
164. M. Cherest, H. Felkin and N. Prudent, *Tetrahedron Lett.*, 1968, 2199.
165. M. Heitbaum, F. Glorius and I. Escher, *Angew. Chem. Int. Ed.*, 2006, **45**, 4732.
166. A. Tungler and G. Fogassy, *J. Mol. Cat. A* 2001, **173**, 231.

167. A. Tungler, E. Sipos and V. Hada, *ARKIVOC*, 2004, 223.
168. M. S. Pavlin Hydrogenation of α-pinene to cis-pinane. 1980-2150334310714, 19801210., 1982.
169. L. A. Canova Selective hydrogenation of α-pinene to cis-pinane. 1976-6905584018842, 19760527., 1977.
170. H. W. Thompson, E. McPherson and B. L. Lences, *J. Org. Chem.*, 1976, **41**, 2903.
171. J. C. Sheehan and R. E. Chandler, *J. Am. Chem. Soc.*, 1961, **83**, 4795.
172. I. N. Lisichkina, A. I. Vinogradova, B. O. Tserevitinov, M. B. Saporovskaya, V. K. Latov and V. M. Belikov, *Tetrahedron: Asymmetry*, 1990, **1**, 567.
173. U. Schmidt, S. Kumpf and K. Neumann, *J. Chem. Soc., Chem. Commun.*, 1994, 1915.
174. N. Izumiya, S. Lee, T. Kanmera and H. Aoyagi, *J. Am. Chem. Soc.*, 1977, **99**, 8346.
175. N. Ikemoto, D. M. Tellers, S. D. Dreher, J. Liu, A. Huang, N. R. Rivera, E. Njolito, Y. Hsiao, J. C. McWilliams, J. M. Williams, J. D. Armstrong, III, Y. Sun, D. J. Mathre, E. J. J. Grabowski and R. D. Tillyer, *J. Am. Chem. Soc.*, 2004, **126**, 3048.
176. D. G. Melillo, R. J. Cvetovich, K. M. Ryan and M. Sletzinger, *J. Org. Chem.*, 1986, **51**, 1498.
177. M. Prashad, Y. Liu, H.-Y. Kim, O. Repic and T. J. Blacklock, *Tetrahedron: Asymmetry*, 1999, **10**, 3479.
178. F. Glorius, N. Spielkamp, S. Holle, R. Goddard and C. W. Lehmann, *Angew. Chem. Int. Ed.*, 2004, **43**, 2850.
179. B. Scheiper, F. Glorius, A. Leitner and A. Fuerstner, *PNAS*, 2004, **101**, 11960.
180. K. Nasar, F. Fache, M. Lemaire, J. C. Beziat, M. Besson and P. Gallezot, *J. Mol. Catal.*, 1994, **87**, 107.
181. M. Besson, S. Neto and C. Pinel, *Chem. Commun.*, 1998, 1431.
182. M. Besson and C. Pinel, *Topics in Catalysis*, 1998, **5**, 25.
183. W. H. Brown and W. N. French, *Can. J. Chemistry*, 1958, **36**, 371.
184. A. Corsini and J. M. Panoyan, *J. Inorg. Nucl. Chem.*, 1977, **39**, 1449.
185. Y.-S. Jang, H.-J. Kim, P.-H. Lee and C.-H. Lee, *Tetrahedron Lett.*, 2000, **41**, 2919.
186. S. M. Lim, H. J. Chung, K.-J. Paeng, C.-H. Lee, H. N. Choi and W.-Y. Lee, *Analytica Chimica Acta*, 2002, **453**, 81.
187. K. S. Park, S. O. Jung, I. Yoon, K.-M. Park, J. Kim, S. S. Lee and J. S. Kim, *J. Inclusion Phenom. Macro.*, 2001, **39**, 295.
188. J. L. Sessler, D. An, W.-S. Cho, V. Lynch, D.-W. Yoon, S.-J. Hong and C.-H. Lee, *J. Org. Chem.*, 2005, **70**, 1511.
189. C. A. Teixeira dos Santos and A. L. Magalhaes, *J. Mol.Struc.*, 2010, **956**, 50.
190. P. D. Williams and E. LeGoff, *J. Org. Chem.*, 1981, **46**, 4143.
191. G. Cafeo, F. H. Kohnke, G. L. La Torre, A. J. P. White and D. J. Williams, *Angew. Chem. Int. Ed.*, 2000, **39**, 1496.
192. R. Pajewski, R. Ostaszewski and J. Jurczak, *Org. Prep. Proced. Int.*, 2000, **32**, 394.
193. H. Ahlbrecht, G. Bringmann and J. M. Brown, '*Stereoselective synthesis*,' ed. by Vol. E 21a, New York, 1995.
194. V. Kral, P. A. Gale, P. Anzenbacher, Jr., K. Jursikova, V. Lynch and J. L. Sessler, *Chem. Commun.*, 1998, 9.
195. J. Liu, E. Muth, U. Floerke, G. Henkel, K. Merz, J. Sauvageau, E. Schwake and G. Dyker, *Adv. Synth. & Cat.*, 2006, **348**, 456.
196. A. Klein, S. Elmas and K. Butsch, *Eur. J. Inorg. Chem.*, 2009, 2271.
197. J. L. Sessler, W.-S. Cho, V. Lynch and V. Kral, *Chemistry--A European Journal*, 2002, **8**, 1134.
198. G. Van Koten, *Pure Appl. Chem.*, 1989, **61**, 1681.

199. M. Albrecht and G. van Koten, *Angew. Chem. Int. Ed.*, 2001, **40**, 3750.
200. H. Hofmeier and U. S. Schubert, *Chem. Soc. Rev.*, 2004, **33**, 373.
201. Y. Li, J. C. Huffman and A. H. Flood, *Chem. Commun.*, 2007, 2692.
202. D. Y. Lee and J. C. Martin, *J. Am. Chem. Soc.*, 1984, **106**, 5745.
203. O. Brucher and J. Hartung, *ACS Catalysis*, 2011, **1**, 1448.
204. E. Gomez, R. Flores, G. Huerta, C. Alvarez-Toledano, R. A. Toscano, V. Santes, N. Nava and P. Sharma, *J. Organomet. Chem.*, 2003, **672**, 115.
205. S. Shimada, M. L. N. Rao and M. Tanaka, *Organometallics*, 2000, **19**, 931.
206. C. R. Goldsmith and T. D. P. Stack, *Inorg. Chem.*, 2006, **45**, 6048.
207. T. Mino, T. Hasegawa, Y. Shirae, M. Sakamoto and T. Fujita, *J. Organomet. Chem.*, 2007, **692**, 4389.
208. E. Gomez, V. Santes, V. de la Luz and N. Farfan, *J. Organomet. Chem.*, 2001, **622**, 54.
209. S. Bellemin-Laponnaz, K. S. Coleman, P. Dierkes, J.-P. Masson and J. A. Osborn, *Eur. J. Inorg. Chem.*, 2000, 1645.
210. G. Journot, R. Neier and H. Stoeckli-Evans, *Acta Crystallographica E*, 2012, **E68**, o857.
211. J. Hartung, G. Stapf and U. Bergstraesser, *Acta Crystallographica E*, 2007, **E63**, o2586.
212. B. M. Cole, K. D. Shimizu, C. A. Krueger, J. P. A. Harrity, M. L. Snapper and A. H. Hoveyda, *Angew. Chem., Int. Ed. Engl.*, 1996, **35**, 1668.
213. H. Groeger, J. Wilken and A. Berkessel, *Org. Synth. Highlights V*, 2003, 178.
214. K. D. Shimizu, B. M. Cole, C. A. Krueger, K. W. Kuntz, M. L. Snapper and A. H. Hoveyda, *Angew. Chem. Int. Ed.*, 1997, **36**, 1704.
215. A. G. Doyle and E. N. Jacobsen, *Chem. Rev.*, 2007, **107**, 5713.
216. C. Grutter, E. Alonso, A. Chougnet and W.-D. Woggon, *Angew. Chem. Int. Ed.*, 2006, **45**, 1126.
217. C. A. Krueger, K. W. Kuntz, C. D. Dzierba, W. G. Wirschun, J. D. Gleason, M. L. Snapper and A. H. Hoveyda, *J. Am. Chem. Soc.*, 1999, **121**, 4284.
218. M. S. Sigman and E. N. Jacobsen, *J. Am. Chem. Soc.*, 1998, **120**, 4901.
219. S. Taylor Mark and N. Jacobsen Eric, *Angew. Chem. Int. Ed.*, 2006, **45**, 1520.
220. P. Rothemund, *J. Am. Chem. Soc.*, 1935, **57**, 2010.
221. P. J. Stang and B. Olenyuk, *Acc. Chem. Res.*, 1997, **30**, 502.
222. S. R. Seidel and P. J. Stang, *Acc. Chem. Res.*, 2002, **35**, 972.
223. J. K. Whitesell, *Chemical Reviews*, 1989, **89**, 1581.
224. P. Anzenbacher, Jr., K. Jursikova, V. M. Lynch, P. A. Gale and J. L. Sessler, *J. Am. Chem. Soc.*, 1999, **121**, 11020.
225. P. Anzenbacher, Jr., A. C. Try, H. Miyaji, K. Jursikova, V. M. Lynch, M. Marquez and J. L. Sessler, *J. Am. Chem. Soc.*, 2000, **122**, 10268.
226. R. Custelcean, L. H. Delmau, B. A. Moyer, J. L. Sessler, W.-S. Cho, D. Gross, G. W. Bates, S. J. Brooks, M. E. Light and P. A. Gale, *Angew. Chem. Int. Ed.*, 2005, **44**, 2537.
227. P. A. Gale, J. L. Sessler, V. Kral and V. Lynch, *J. Am. Chem. Soc.*, 1996, **118**, 5140.
228. P. A. Gale, L. J. Twyman, C. I. Handlin and J. L. Sessler, *Chem. Commun.*, 1999, 1851.
229. H. Miyaji, P. Anzenbacher, Jr., J. L. Sessler, E. R. Bleasdale and P. A. Gale, *Chem. Commun.*, 1999, 1723.
230. H. Miyaji, W. Sato and J. L. Sessler, *Angew. Chem. Int. Ed.*, 2000, **39**, 1777.
231. J. L. Sessler, D. E. Gross, W.-S. Cho, V. M. Lynch, F. P. Schmidtchen, G. W. Bates,

M. E. Light and P. A. Gale, *J. Am. Chem. Soc.*, 2006, **128**, 12281.
232. S. K. Kim, J. L. Sessler, D. E. Gross, C.-H. Lee, J. S. Kim, V. M. Lynch, L. H. Delmau and B. P. Hay, *J. Am. Chem. Soc.*, 2010, **132**, 5827.
233. C.-H. Lee, J.-S. Lee, H.-K. Na, D.-W. Yoon, H. Miyaji, W.-S. Cho and J. L. Sessler, *J. Org. Chem.*, 2005, **70**, 2067.
234. H. Miyaji, H.-K. Kim, E.-K. Sim, C.-K. Lee, W.-S. Cho, J. L. Sessler and C.-H. Lee, *J. Am. Chem. Soc.*, 2005, **127**, 12510.
235. H. Miyaji, W. Sato, J. L. Sessler and V. M. Lynch, *Tetrahedron Lett.*, 2000, **41**, 1369.
236. K. A. Nielsen, W.-S. Cho, J. Lyskawa, E. Levillain, V. M. Lynch, J. L. Sessler and J. O. Jeppesen, *J. Am. Chem. Soc.*, 2006, **128**, 2444.
237. R. Nishiyabu and P. Anzenbacher, Jr., *J. Am. Chem. Soc.*, 2005, **127**, 8270.
238. R. Nishiyabu, M. A. Palacios, W. Dehaen and P. Anzenbacher, Jr., *J. Am. Chem. Soc.*, 2006, **128**, 11496.
239. P. Piatek, V. M. Lynch and J. L. Sessler, *J. Am. Chem. Soc.*, 2004, **126**, 16073.
240. J. L. Sessler, D. An, W.-S. Cho and V. Lynch, *Angew. Chem. Int. Ed.*, 2003, **42**, 2278.
241. J. L. Sessler, P. Anzenbacher, Jr., K. Jursikova, H. Miyaji, J. W. Genge, N. A. Tvermoes, W. E. Allen, J. A. Shriver, P. A. Gale and V. Kral, *Pure Appl. Chem.*, 1998, **70**, 2401.
242. J. L. Sessler, P. Anzenbacher, Jr., H. Miyaji, K. Jursikova, E. R. Bleasdale and P. A. Gale, *Ind. Eng. Chem. Res.*, 2000, **39**, 3471.
243. J. L. Sessler, S. K. Kim, D. E. Gross, C.-H. Lee, J. S. Kim and V. M. Lynch, *J. Am. Chem. Soc.*, 2008, **130**, 13162.
244. E. Valeur and M. Bradley, *Chem. Soc. Rev.*, 2009, **38**, 606.
245. Y. S. Klausner and M. Bodansky, *Synthesis*, 1972, 453.
246. L. A. Carpino, M. Beyermann, H. Wenschuh, Bienert and Michael, *Acc. Chem. Res.*, 1996, **29**, 268.
247. C. Bissantz, B. Kuhn and M. Stahl, *J. Med. Chem.*, 2010, **53**, 5061.
248. Testa Bernard, van de Waterbeemd Han, Folkers Gerd and G. Richard, '*Hydrogen Bonding: The Last Mystery in Drug Design?*,' ed. by Bernard Testa, Han van de Waterbeemd, Gerd Folkers, Richard Guy, Vol. Verlag Helvetica Chimica Acta, 2007, p 513-524.
249. M. W. Hosseini, *Coord. Chem. Rev.*, 2003, **240**, 157.
250. M. C. Etter, Z. Urbanczyk-Lipkowska, P. A. Fish, T. W. Panunto, P. W. Baures and J. S. Frye, *J. Cryst. Spec.*, 1988, **18**, 311.
251. P. Chaudhary, R. A. Shank, T. Montina, J. T. Goettel, N. A. Foroud, P. Hazendonk and F. Eudes, *Toxins*, 2011, **3**, 1310.
252. M. L. DeRider, S. J. Wilkens, M. J. Waddell, L. E. Bretscher, F. Weinhold, R. T. Raines and J. L. Markley, *J. Am. Chem. Soc.*, 2002, **124**, 2497.
253. R. Improta, C. Benzi and V. Barone, *J. Am. Chem. Soc.*, 2001, **123**, 12568.
254. S. M. S. Chauhan and S. Mishra, *Molecules*, 2011, **16**, 7256.
255. G. Journot, R. Neier and H. Stoeckli-Evans, *Acta Cryst. Sect. E*, 2010, **E66**, 392.
256. G. V. Zyryanov, T. H. Kinstle and P. Anzenbacher, Jr., *Synlett.*, 2008, 1171.
257. G. Journot, R. Neier and H. Stoeckli-Evans, *Acta Crystallographica C*, 2012, **C68**, o119.
258. C. A. G. N. Montalbetti and V. Falque, *Tetrahedron*, 2005, **61**, 10827.
259. F. I. Luknitskii and B. A. Vovsi, *Usp. Khim.*, 1969, **38**, 1072.
260. H. J. Bestmann, G. Schmid and D. Sandmeier, *Angew. Chem.*, 1976, **88**, 92.
261. K. Chow and H. W. Moore, *Tetrahedron Lett.*, 1987, **28**, 5013.
262. S. Yildirir and H. Senoz, *Marmara Univ. Fen Bilimleri Derg.*, 1989, **6**, 201.

263. V. Patinec, J. J. Yaouanc, J. C. Clement, H. Handel and H. de Abbayes, *Tetrahedron Lett.,* 1995, **36**, 79.
264. M. Suchy and R. H. E. Hudson, *Eur. J. Org. Chem.* 2008, 4847.
265. S. K. Verma, R. Ghorpade, A. Pratap and M. P. Kaushik, *Green Chem.,* 2012, **14**, 326.
266. C. Pena, I. Alfonso and V. Gotor, *Eur. J. Org. Chem.* 2006, 3887.
267. J. Massue, S. E. Plush, C. S. Bonnet, D. A. Moore and T. Gunnlaugsson, *Tetrahedron Lett.,* 2007, **48**, 8052.
268. K. Pappas, X. Zhang and S. Fang, *Letters in Organic Chemistry,* 2010, **7**, 539.
269. W. Tang and S. Fang, *Tetrahedron Lett.,* 2008, **49**, 6003.
270. J. A. Bender, N. A. Meanwell and T. Wang, *Tetrahedron,* 2002, **58**, 3111.
271. D. W. Lee, H.-J. Ha and W. K. Lee, *Synth. Commun.,* 2007, **37**, 737.
272. L. Zhang, X.-J. Wang, J. Wang, N. Grinberg, D. K. Krishnamurthy and C. H. Senanayake, *Tetrahedron Lett.,* 2009, **50**, 2964.
273. B. Lygo, *e-EROS Encycl. Reagents Org. Synth.,* 2001.
274. L. A. Carpino, A. El-Faham and F. Albericio, *J. Org. Chem.,* 1995, **60**, 3561.
275. R. Chinchilla, D. J. Dodsworth, C. Najera and J. M. Soriano, *Tetrahedron Lett.,* 2000, **41**, 2463.
276. F. Albericio, J. M. Bofill, A. El-Faham and S. A. Kates, *J. Org. Chem.,* 1998, **63**, 9678.
277. V. Dourtoglou, J. C. Ziegler and B. Gross, *Tetrahedron Lett.,* 1979, 4371.
278. V. Dourtoglou, B. Gross, V. Lambropoulou and C. Zioudrou, *Synthesis,* 1984, 572.
279. S. A. Jadhav, *Synlett,* 2010, 1287.
280. K. Pudhom and T. Vilaivan, *Synth. Commun.,* 2001, **31**, 61.
281. H. Qu, X. Gu, B. J. Min, Z. Liu and V. J. Hruby, *Org. Lett.,* 2006, **8**, 4215.
282. S.-Y. Han and Y.-A. Kim, *Tetrahedron,* 2004, **60**, 2447.
283. L. A. Carpino and A. El-Faham, *Tetrahedron,* 1999, **55**, 6813.
284. W. Konig and R. Geiger, *Chem Ber,* 1970, **103**, 788.
285. J. Coste, D. Le-Nguyen and B. Castro, *Tetrahedron Lett.,* 1990, **31**, 205.
286. J. M. Humphrey and A. R. Chamberlin, *Chem. Rev.,* 1997, **97**, 2243.
287. A. J. Pearson, W. R. Roush and Editors, '*Handbook of Reagents for Organic Synthesis: Activating and Agents and Protecting Groups,*' ed. by Vol. 1999.
288. T. W. Green, '*Protective Groups in Organic Synthesis,*' ed. by Vol. 1999, p 564-566, 740-743.
289. A. L. Van Geet, *Analytical Chemistry,* 1970, **42**, 679.
290. A. Williams, *Acc. Chem. Res.,* 1989, **22**, 387.
291. M. Zhong and J. I. Brauman, *J. Am. Chem. Soc.,* 1999, **121**, 2508.
292. M. Adler, S. Adler and G. Boche, *J. Phys. Org. Chem.,* 2005, **18**, 193.
293. V. M. Vlasov, *New J. Chem.,* 2009, **33**, 501.
294. W. P. Jencks and M. Gilchrist, *J. Amer. Chem. Soc.,* 1968, **90**, 2622.
295. E. A. Castro, M. Cubillos and J. G. Santos, *J. Org. Chem.,* 2001, **66**, 6000.
296. I.-H. Um, J.-S. Min, J.-A. Ahn and H.-J. Hahn, *J. Org. Chem.,* 2000, **65**, 5659.
297. I.-H. Um and A. R. Bae, *J. Org. Chem.,* 2011, **76**, 7510.
298. E. A. Castro, D. Millan, R. Aguayo, P. R. Campodonico and J. G. Santos, *J. Chem. Kinet.,* 2011, **43**, 687.
299. D. Stefanidis, S. Cho, S. Dhe-Paganon and W. P. Jencks, *J. Am. Chem. Soc.,* 1993, **115**, 1650.
300. A. Williams, *Chem. Soc. Rev.,* 1994, **23**, 93.
301. B. D. Song and W. P. Jencks, *J. Am. Chem. Soc.,* 1989, **111**, 8479.

302. T. W. Bentley, G. Llewellyn and J. A. McAlister, *J. Org. Chem.*, 1996, **61**, 7927.
303. T. W. Bentley and H. C. Harris, *J. Chem. Soc., Perkin Trans. 2*, 1986, 619.
304. D. N. Kevill and C. B. Kim, *J. Chem. Soc., Perkin Trans. 2*, 1988, 1353.
305. I. Lee, C. K. Kim, H. G. Li, C. K. Sohn, C. K. Kim, H. W. Lee and B.-S. Lee, *J. Am. Chem. Soc.*, 2000, **122**, 11162.
306. J. F. Blake and W. L. Jorgensen, *J. Am. Chem. Soc.*, 1987, **109**, 3856.
307. J. M. Fox, O. Dmitrenko, L.-A. Liao and R. D. Bach, *J. Org. Chem.*, 2004, **69**, 7317.
308. A. C. Regan and C. I. F. Watt, *J. Phys. Org. Chem.*, 2007, **20**, 180.
309. Z. H. Ryu, S. H. Shin, J. P. Lee, G. T. Lim and T. W. Bentley, *J. Chem. Soc., Perkin Trans. 2*, 2002, 1283.
310. B. D. Song and W. P. Jencks, *J. Am. Chem. Soc.*, 1989, **111**, 8470.
311. E. A. Castro, A. Hormazabal and J. G. Santos, *J. Chem. Kinet.*, 1998, **30**, 267.
312. F. Ruff and O. Farkas, *J. Phys. Org. Chem.*, 2011, **24**, 480.
313. U. Ragnarsson and L. Grehn, *Acc. Chem. Res.*, 1998, **31**, 494.
314. A. P. Rajput and R. P. Gore, *Pharma Chemica*, 2011, **3**, 409.
315. L. Pauling, '*The Nature of the Chemical Bond*,' ed. by 3rd, Vol. Cornell University Press: Ithaca, NY, 1960.
316. G. A. Jeffrey and W. Saenger, '*Hydrogen Bonding in Biological Structures*,' ed. by Vol. Springer-Verlag: Berlin, 1991.
317. G. A. Jeffrey, '*An Introduction to Hydrogen Bonding*,' ed. by Vol. Oxford University Press: New York, 1997.
318. G. R. Desiraju and T. Steiner, '*The Weak Hydrogen Bond in Structural Chemistry and Biology*,' ed. by Vol. Oxford University Press Inc.: New York, 1999.
319. S. Scheiner, '*Intermolecular Interactions-From Van der Waals to Strongly Bound Complexes*,' ed. by Vol. Wiley: New York, 1997.
320. G. R. Desiraju, *Acc. Chem. Res.*, 2002, **35**, 565.
321. E. A. Meyer, R. K. Castellano and F. Diederich, *Angew. Chem. Int. Ed.*, 2003, **42**, 1210.
322. W. W. Cleland and M. M. Kreevoy, *Science*, 1994, **264**, 1887.
323. P. A. Frey, S. A. Whitt and J. B. Tobin, *Science*, 1994, **264**, 1927.
324. J. A. Gerlt, M. M. Kreevoy, W. W. Cleland and P. A. Frey, *Chemistry & Biology*, 1997, **4**, 259.
325. S.-o. Shan, S. Loh and D. Herschlag, *Science*, 1996, **272**, 97.
326. N. J. Pienta and R. J. Kessler, *J. Am. Chem. Soc.*, 1993, **115**, 8330.
327. Y. Otani, O. Nagae, Y. Naruse, S. Inagaki, M. Ohno, K. Yamaguchi, G. Yamamoto, M. Uchiyama and T. Ohwada, *J. Am. Chem. Soc.*, 2003, **125**, 15191.
328. C. R. Kemnitz and M. J. Loewen, *J. Am. Chem. Soc.*, 2007, **129**, 2521.
329. M. O. Senge, *Angew. Chem. Int. Ed.*, 2011, **50**, 4272.
330. H. Furuta, T. Asano and T. Ogawa, *J. Am. Chem. Soc.*, 1994, **116**, 767.
331. P. J. Chmielewski, L. Latos-Grazynski, K. Rachlewicz and T. Glowiak, *Angew. Chem. Int. Ed.*, 1994, **33**, 779.
332. H. Furuta, H. Maeda and A. Osuka, *Chem. Commun.* , 2002, 1795.
333. R. Gu, S. Depraetere, J. Kotek, J. Budka, E. Wagner-Wysiecka, J. F. Biernat and W. Dehaen, *Org. Biom. Chem.*, 2005, **3**, 2921.
334. Y. Ishikawa, I. Yoshida, K. Akaiwa, E. Koguchi, T. Sasaki and H. Furuta, *Chemistry Letters*, 1997, 453.
335. C.-H. Hung, S.-L. Wang, J.-L. Ko, C.-H. Peng, C.-H. Hu and M.-T. Lee, *Org. Lett.*, 2004, **6**, 1393.
336. H. Furuta, T. Ishizuka, A. Osuka and T. Ogawa, *J. Am. Chem. Soc.*, 1999, **121**, 2945.

337. H. Furuta, T. Ishizuka, A. Osuka and T. Ogawa, *J. Am. Chem. Soc.*, 2000, **122**, 5748.
338. T. Ishizuka, H. Yamasaki, A. Osuka and H. Furuta, *Tetrahedron*, 2007, **63**, 5137.
339. H. Furuta, T. Ishizuka, A. Osuka, Y. Uwatoko and Y. Ishikawa, *Angew. Chem. Int. Ed.*, 2001, **40**, 2323.
340. H. Furuta, T. Ishizuka and A. Osuka, *Inorg. Chem. Commun.*, 2003, **6**, 398.
341. X. Li, P. J. Chmielewski, J. Xiang, J. Xu, Y. Li, H. Liu and D. Zhu, *Org. Lett.*, 2006, **8**, 1137.
342. B. Y. Liu, C. Brueckner and D. Dolphin, *Chem. Commun.*, 1996, 2141.
343. T. D. Lash, D. T. Richter and C. M. Shiner, *J. Org. Chem.*, 1999, **64**, 7973.
344. M. Toganoh and H. Furuta, *Chem. Commun.(DOI: 10.1039/c1cc14633e)*, 2011.
345. A. Srinivasan and H. Furuta, *Acc. Chem. Res.*, 2005, **38**, 10.
346. M. Toganoh, Y. Kawabe and H. Furuta, *J. Org. Chem.*, 2011, **76**, 7618.
347. H. Maeda, A. Osuka, Y. Ishikawa, I. Aritome, Y. Hisaeda and H. Furuta, *Org. Lett.*. 2003, **5**, 1293.
348. H. Furuta, H. Maeda and A. Osuka, *J. Am. Chem. Soc.*, 2000, **122**, 803.
349. T. D. Lash, A. D. Lammer and G. M. Ferrence, *Angew. Chem. Int. Ed.*, 2011, **50**, 9718.
350. C. Bruckner, J. J. Posakony, C. K. Johnson, R. W. Boyle, B. R. James and D. Dolphin, *J.Porphyrins Phthalocyanines*, 1998, **2**, 455.
351. B. Dolensky, J. Kroulik, V. Kral, J. L. Sessler, H. Dvorakova, P. Bour, M. Bernatkova, C. Bucher and V. Lynch, *J. Am. Chem. Soc.*, 2004, **126**, 13714.
352. J. K. Laha, S. Dhanalekshmi, M. Taniguchi, A. Ambroise and J. S. Lindsey, *Org. Process Res. Dev*, 2003, **7**, 799.
353. E. Pacholska, L. Latos-Grazynski, L. Szterenberg and Z. Ciunik, *J. Org. Chem.*, 2000, **65**, 8188.
354. S. M. S. Chauhan, B. Garg and T. Bisht, *Molecules*, 2007, **12**, 2458.
355. B. J. Littler, M. A. Miller, C.-H. Hung, R. W. Wagner, D. F. O'Shea, P. D. Boyle and J. S. Lindsey, *J. Org. Chem.*, 1999, **64**, 1391.
356. C. S. Beshara and A. Thompson, *J. Org. Chem.*, 2005, **70**, 10607.
357. M. L. Murat-Onana, C. Berini, F. Minassian, N. Pelloux-Leon and J.-N. Denis, *Org. Biomol. Chem.*. 2010, **8**, 2204.
358. T. Tsuchimoto, K. Hatanaka, E. Shirakawa and Y. Kawakami, *Chem. Commun.*, 2003, 2454.
359. Z. Zhang, J.-Y. Shin and D. Dolphin, *J. Org. Chem.*, 2008, **73**, 9515.
360. Z. Zhang and D. Dolphin, *Chem. Commun.*, 2009, 6931.
361. P. E. Sonnet, *J. Org. Chem.*, 1971, **36**, 1005.
362. CCDC 865719, 865720, 865721, 865722 and 865723 contain the supplementary crystallographic data for **1a**, **1b**, **1c**, **2**, and **3**, respectively. These data can be obtained free of charge at http://www.ccdc.cam.ac.uk/conts/retrieving.html, or from the Cambridge Crystallographic Data Center, 12 Union Road, Cambridge CB2 1EZ, UK (fax: 0044 1223 336 033; e-mail: deposit@ccdc.cam.ac.uk). In.
363. Reactions monitored by GC. In.
364. C. Schmuck, *Synlett*, 2011, 1798.
365. C. Fellay, P. J. Dyson and G. Laurenczy, *Angew. Chem. Int. Ed.*, 2008, **47**, 3966.